

*NASA Conference Publication 3310*

# **1995 Shuttle Small Payloads Symposium**

*Edited by*  
Frann Goldsmith  
*NASA Goddard Space Flight Center*  
*Greenbelt, Maryland*

Frances L. Mosier  
*Interstel, Inc.*  
*Beltsville, Maryland*

Proceedings of a symposium  
held at Camden Yards  
Baltimore, Maryland  
September 25-28, 1995



National Aeronautics  
and Space Administration

**Goddard Space Flight Center**  
Greenbelt, Maryland 20771

**1995**

This publication is available from the NASA Center for AeroSpace Information,  
800 Elkridge Landing Road, Linthicum Heights, MD 21090-2934, (301) 621-0390.



## CONTENTS

		Page
1.	<b>FLIGHT TESTING OF THE CAPILLARY PUMPED LOOP FLIGHT EXPERIMENT</b> Dan Butler, Laura Ottenstein, and Jentung Ku .....	1
2.	<b>THE CRYOGENIC TEST BED EXPERIMENTS</b> Lee Thienel and Chuck Stouffer .....	21
3.	<b>EXPERIMENTAL RESULTS FROM THE THERMAL ENERGY STORAGE-1 (TES-1) FLIGHT EXPERIMENT</b> Lawrence W. Wald, Carol Tolbert, and David Jacqmin .....	31
4.	<b>ON THE HITCHHIKER ROBOT OPERATED MATERIALS PROCESSING SYSTEM EXPERIMENT DATA SYSTEM</b> Semion Kizhner and Del Jenstrom .....	39
5.	<b>DESIGN AND DEVELOPMENT OF HIGH VOLTAGE (DC) SOURCES FOR THE SOLAR ARRAY MODULE PLASMA INTERACTION EXPERIMENT</b> Irene K. Bibyk and Lawrence W. Wald .....	51
6.	<b>TELESCIENCE OPERATIONS WITH THE SOLAR ARRAY MODULE PLASMA INTERACTION EXPERIMENT</b> Lawrence W. Wald and Irene K. Bibyk .....	59
7.	<b>THE PHOTOGRAMMETRIC APPENDAGE STRUCTURAL DYNAMICS EXPERIMENT</b> Michael G. Gilbert, Sharon S. Welch, and Christopher L. Moore .....	73
8.	<b>SHUTTLE LASER ALTIMETER (SLA)</b> Jack Bufton, Bryan Blair, John Cavanaugh, James Garvin, David Harding, Dan Hopf, Ken Kirks, David Rabine, and Nita Walsh .....	83
9.	<b>HELPFUL HINTS TO PAINLESS PAYLOAD PROCESSING</b> Terry Terhune and Maggie Carson .....	91
10.	<b>SPACE EXPERIMENT MODULE -- A NEW LOW-COST CAPABILITY FOR EDUCATION PAYLOADS</b> Theodore C. Goldsmith and Ruthan Lewis .....	101
11.	<b>CRYOGENIC TWO-PHASE FLIGHT EXPERIMENT; RESULTS OVERVIEW</b> T. Swanson, M. Buchko, P. Brennan, M. Bello, and M. Stoyanof .....	111
12.	<b>STANDARD GAS HARDWARE</b> Stan Spencer .....	125
13.	<b>G-399 AND G-178: LESSONS LEARNED</b> Michael Dobeck .....	133

## CONTENTS (CONTINUED)

		Page
14.	<b>DESCRIPTION OF AND PRELIMINARY TESTS RESULTS FOR THE JOINT DAMPING EXPERIMENT (JDX)</b> Jeffrey G. Bingham and Steven L. Folkman .....	139
15.	<b>THE GROWTH OF SOLAR RADIATED YEAST</b> Tyrone Kraft .....	149
16.	<b>NON-GRAVITATIONAL EFFECTS ON GENUS PENICILLIUM</b> MacKenzie Loup .....	151
17.	<b>THE EFFECTS OF SOLAR RADIATION ON PLANT GROWTH</b> Joslyn Agard .....	153
18.	<b>PRELIMINARY RESULTS AND POWER ANALYSIS OF THE UAH SEDS G503 GAS CAN</b> Lyle B. Jalbert, Steven Mustaikis II, and Philip Nerren .....	163
19.	<b>G254: USU STUDENT PAYLOAD FLOWN ON STS-64 IN SEPTEMBER, 1994</b> Tumkur Raghuram, Oscar A. Monje, Brett Evans, Matt Droter, Mark Lemon, Kristen Redd, Tina Hubble, Mark Wilkinson, Michael Wilkinson, Dan Tebbs, Casey Hatch, Brandon Lobb, Kent Altsuler, R. Gilbert Moore, Jan J. Sojka, and Prent Klag .....	171
20.	<b>MEASUREMENTS OF THE STS ORBITER'S ANGULAR STABILITY DURING IN-ORBIT OPERATIONS</b> Werner M. Neupert, Gabriel L. Epstein, James Houston, and Andrew Zarechnak .....	183
21.	<b>ACOUSTIC MODAL PATTERNS AND STRIATIONS (AMPS) EXPERIMENT G-325, NORFOLK PUBLIC SCHOOLS</b> Joy W. Young .....	193
22.	<b>CONSTRUCTION OF THE GAMCIT GAMMA-RAY BURST DETECTOR (G-056)</b> Michael H. Coward, John M. Grunsfeld, Benjamin J. McCall, and Albert Ratner .....	203
23.	<b>PHOTOGRAPHING THE EARTH</b> <b>G324, THE CAN DO GEOCAM PAYLOAD</b> James H. Nicholson, Thomas J. O'Brien, and Carol A. Tempel .....	213
24.	<b>THE VORTEX RING TRANSIT EXPERIMENT (VORTEX) GAS PROJECT</b> Sven G. Bilen, Lynn S. Langenderfer, Rebecca D. Jardon, Hansford H. Cutlip, Alexander C. Kazerooni, Amber L. Thweatt, Joseph L. Lester, and Luis P. Bernal .....	221
25.	<b>G 301: THE FLYING FALCON GEOLOGICAL REMOTE SENSING EXPERIMENT</b> Robert K. Vincent, Curtis Birnbach, and Arthur H. Mengel .....	231

## CONTENTS (CONTINUED)

		Page
26.	<b>CONSTRUCTION MATERIAL PROCESSED USING LUNAR SIMULANT IN VARIOUS ENVIRONMENTS</b> Stan Chase, Bridget O'Callaghan-Hay, Ralph Housman, Michael Kindig, John King, Kevin Montegrando, Raymond Norris, Ryan Van Scotter, Jonathan Willenborg, Harry Staubs, Michael Petran, Ed Tate, Tim Williams, Phong Chen, Campbell Dinsmore, Lincoln Le, Gautam Shah, and Phat Vu . . . . .	241
27.	<b>NEUTRONS, GAMMA RAYS, AND BETA PARTICLES INTERACTIONS WITH IIaO FILMS FLOWN ON ASTRO I AND ASTRO II AND COMPARISON WITH IIaO FLOWN ON THE GET AWAY SPECIAL STS-7</b> Ernest C. Hammond, Jr., Kevein Peters, and Kevin Boone . . . . .	247
28.	<b>CHARACTERIZATION OF FLUID PHYSICS EFFECTS ON CARDIOVASCULAR RESPONSE TO MICROGRAVITY (G-572)</b> George M. Pantalos, Thomas E. Bennett, M. Keith Sharp, Stewart Woodruff, Sean O'Leary, Kevin Gillars, Mark Lemon, and Jan Sojka . . . . .	255
29.	<b>DOES SOLAR RADIATION AFFECT THE GROWTH OF TOMATO SEEDS RELATIVE TO THEIR ENVIRONMENT?</b> Kristi Holzer . . . . .	257
30.	<b>SMALL PASSIVE STUDENT EXPERIMENTS ON G324</b> <b>261 INDIVIDUAL QUESTS FOR STUDENT KNOWLEDGE</b> James H. Nicholson, Carol A. Tempel, Ruth Ashcraft-Truluck, and. . . . . Robin Rutherford	259
31.	<b>HITCHHIKER MISSION OPERATIONS</b> <b>PAST, PRESENT AND FUTURE</b> Kathryn Anderson, Agustin J. Alfonzo, Georgeann Brophy, Victor Gehr, Brian Murphy, and Francis Wasiak . . . . .	265
32.	<b>APPLICATION OF SPACE SHUTTLE PHOTOGRAPHY TO STUDIES OF UPPER OCEAN DYNAMICS</b> Quanan Zheng, Vic Klemas, Xiao-Hai Yan, and Zongming Wang . . . . .	275
33.	<b>COLLISION MANAGEMENT UTILIZING CCD AND REMOTE SENSING TECHNOLOGY</b> Harvey E. McDaniel, Jr. . . . .	285
34.	<b>SPARTNIK: ENGINEERING CATALYST FOR GOVERNMENT AND INDUSTRY</b> James D. Prass, Thomas C. Romano, and Jeanine M. Hunter . . . . .	289
35.	<b>THE FAILURE ANALYSIS, REDESIGN, AND FINAL PREPARATION OF THE BRILLIANT EYES THERMAL STORAGE UNIT FOR FLIGHT TESTING</b> T. Lamkin and Brian Whitney . . . . .	295

## CONTENTS (CONTINUED)

	<b>Page</b>
<b>36. AN ADAPTABLE PRODUCT FOR MATERIAL PROCESSING AND LIFE SCIENCE MISSIONS</b>	
Gregory Wassick and Michael Dobbs . . . . .	<b>303</b>
<b>37. IJEMS</b>	
<b>IOWA JOINT EXPERIMENT IN MICROGRAVITY SOLIDIFICATION</b>	
Richard A. Hardin, John R. Bendle, and Steven J. Mashl . . . . .	<b>317</b>

FLIGHT TESTING OF  
THE CAPILLARY PUMPED LOOP FLIGHT EXPERIMENT

Dan Butler  
Laura Ottenstein  
Jentung Ku  
NASA Goddard Space Flight Center

ABSTRACT

The Capillary Pumped Loop Flight Experiment (CAPL) employs a passive two-phase thermal control system that uses the latent heat of vaporization of ammonia to transfer heat over long distances. CAPL was designed as a prototype of the Earth Observing System (EOS) instrument thermal control systems. The purpose of the mission was to provide validation of the system performance in micro-gravity, prior to implementation on EOS. CAPL was flown on STS-60 in February, 1994, with some unexpected results related to gravitational effects on two-phase systems. Flight test results and post flight investigations will be addressed, along with a brief description of the experiment design.

INTRODUCTION - EXPERIMENT DESCRIPTION

CAPL was developed as a follow-on to the initial Capillary Pumped Loop (CPL) Get Away Special (GAS) and Hitchhiker flight experiments that were flown in 1985 and 1986 [1]. These small-scale experiments were highly successful and demonstrated the feasibility of using capillary pumped loop (CPL) technology in micro-gravity. CAPL was a much larger experiment and was a prototype of the EOS-AM instrument thermal control systems. EOS has six separate CPL's to provide redundant thermal control of three of its instruments [2]. The original CAPL experiment is now designated as "CAPL 1" to differentiate it from the redesigned "CAPL 2", planned for flight in July 1995. Additional detailed descriptions of the original CAPL experiment are given in references 3 and 4.

Experiment Structure - The CAPL experiment measures 1.57 m by 2.54 m by 0.36 m deep (62" by 100" by 14") and weighs approximately 181 kg (400 pounds). The experiment components were sandwiched between the CAPL radiator and a Hitchhiker mounting plate that was used to mount CAPL to the GAS bridge aboard the Space Shuttle (see Figures 1 and 2)

Capillary Evaporators - CAPL 1 had two capillary evaporator plates (cold plates) that were an approximate simulation of the cold plates that will be used on the EOS-AM spacecraft. Each plate contained two small diameter (1.38 cm outer diameter, 0.545 in.) capillary evaporators (see Figure 3). Instrument power dissipation was simulated with heaters located on top of the plates, with up to 600 Watts of heater power on each plate.

Heat Pipe Heat Exchangers (HPHX's) - The vapor traveled through an eight-meter long, 1.27 cm (1/2 in) O.D. vapor line to four heat pipe heat exchangers which condensed the ammonia vapor and

transferred the heat to the radiator via eight heat pipes. This method of heat rejection has been selected for EOS (and CAPL) instead of a direct condensation radiator because it greatly reduces the vulnerability to meteoroids since the cold plate fluid loop is separated from the radiator fluid loop. The HPHX utilized spiral grooved channels machined into a heavy wall heat pipe to accomplish vapor condensation and heat transport to the radiator [9]. An external flow regulator provided flow balancing between parallel HPHXs and trapped non-condensable gases in the flow.

Subcooler - The ammonia liquid returned to the cold plates via an eight-meter long 0.64 cm (1/4 in) O.D. liquid line which was attached to a separate radiator to insure that the liquid was subcooled below its saturation temperature prior to entering the capillary pumps.

Reservoir - A two-phase temperature controlled reservoir was used to establish the loop operating or saturation temperature and to automatically maintain the proper liquid inventory in the loop. A new reservoir design was employed for the CAPL experiment. It utilized a combination of wall screens, porous polyethylene flow tubes, and a sintered stainless steel vapor barrier for fluid management and temperature control [10].

Starter pump - A capillary starter pump, vapor line heaters, and cold plate vapor header heaters were used to prime the cold plates and ready the system for start-up. The capillary starter pump is similar in design to the evaporator pumps, however, its liquid core is plumbed in series to the reservoir to insure that it stays primed during the start-up process.

Mechanical Pumps - The experiment also included a pair of mechanical pumps and associated valving. The mechanical pumps were included as a back-up for start-up and repriming operations, and were also used to test hybrid (mechanical pump assisted) loop operation.

Instrumentation - CAPL was instrumented with a variety of sensors, including 180 thermistors which were used to measure temperatures throughout the experiment. In addition, there was a differential pressure transducer to measure the pressure rise in the cold plates, and another to measure the pressure drop along the vapor line. An absolute pressure transducer measured the saturation pressure at the reservoir. There was also a thermal flowmeter in the liquid transport line to measure ammonia flow rates.

Electronics - CAPL utilized the Temperature Control System (TCS) electronics, in conjunction with the Hitchhiker avionics and standard Shuttle services for power, data, and command of the experiment. Real time data monitoring and control of CAPL was accomplished from the Hitchhiker control center at NASA Goddard via commercial 486PC computers with specialized software. This capability allowed for modifications to the power profiles and startup techniques during the mission.

## PREFLIGHT TESTING

The CAPL experiment underwent an extensive functional test program before flight which included prototype development and

testing, flight component testing, system level ambient functional testing, and thermal vacuum testing. This testing has been documented in numerous reports and papers, with the Thermal Vacuum test results and the Flight Component Test Results given in References 4 and 5 respectively.

The ground test program showed that the HPHXs and reservoir exceeded their design requirements. However, the cold plates were found to be more temperamental than many capillary pumps that have been tested to date. Pump depriming occurred during power reduction from high power levels or when the power level was low enough to allow liquid condensation in the vapor lines. Also, start-ups were initially very difficult and usually ended with pump depriming until start-up procedures were developed that cleared the vapor lines and pump vapor grooves of liquid prior to start-up. The start-ups were then very reliable - IN ONE G. Once the pumps were started, they generally performed well and exceeded the EOS requirements for power levels and temperature stability.

START-UP PROCESS - (Refer to CAPL flow schematic, figure 4). The first step in starting the loop is to apply power to the reservoir to establish the loop saturation temperature and to insure that the capillary pumps have liquid for priming. For a fully flooded or "stressful" start-up, the entire loop is filled with liquid when heat is applied to the capillary pumps. Nucleate boiling then occurs in the capillary pump vapor grooves after the saturation temperature is exceeded. The liquid must "superheat" before boiling is initiated as defined by the Clausius-Clapeyron equation (see Figure 5, excerpted from reference 6). The onset of boiling is a highly dynamic transient event that results in a pressure spike and the rapid formation of vapor (figure 6). Vapor can be forced through the pump wick and into the core of the pump, and a deprime can occur if the vapor bubble is large enough to block the flow of liquid to the wick.

Pump Diameter - One of the reasons for the start-up difficulty with the CAPL 1 pumps has been traced to the pump diameter. Due to EOS weight considerations, the pumps used on CAPL 1 were 1.27 cm (1/2 in) in diameter versus 2.54 cm (1 in) for those used on the first CPL ground test loops and flight experiments (see Figure 7). The smaller diameter pump has a much thinner wick and smaller inner core, making these pumps much more susceptible to vapor penetration and blockage of the core. The larger diameter pumps start more readily than the smaller pumps from a fully flooded condition, although there has been some evidence of vapor penetration of the core of the larger diameter pumps as well.

Vapor Line Heaters - A solution to the start-up problem was developed that relies on clearing the grooves and vapor lines of liquid prior to pump start-up. This resulted in essentially zero superheat since a vapor space was created that eliminated nucleate boiling during pump start-up (see Figure 8). One way of achieving the clearing process involved the use of heaters on the vapor line and a heater on the vapor header of the cold plates. When these heaters were powered, they would vaporize the liquid in the vapor lines and vapor would be forced into the pump grooves. At this point, power was applied to the cold plates and a "non-stressful" start-up of the system was accomplished - IN ONE G. Once the loop

was started, it then operated normally for a variety of power levels, saturation temperatures, and sink conditions.

Starter Pump - Another method of clearing the liquid from the vapor lines and pump grooves was also employed on CAPL. This involved the use of a capillary starter pump (see Figure 9). The starter pump is a standard large diameter capillary pump with a bayonet tube inserted into the core, which is then plumbed in a series connection to the reservoir (refer to Figure 4). For start-up, power is applied directly to the starter pump with the loop in a fully flooded condition. As the starter pump generates vapor, liquid displaced from the vapor line must pass through the pump core before it enters the reservoir. This clears vapor bubbles that may have penetrated the wick and provides a repriming action that results in a highly reliable start-up process for the starter pump. Once the starter pump is running, the vapor it creates clears the liquid from the vapor lines and pump vapor grooves and leads to a "non-stressful" startup for the cold plates - IN ONE G. The starter pump, in combination with the vapor header heater, led to highly reliable start-ups and ground testing showed that CAPL met all of the EOS transport requirements. Further details on capillary pumped loop start-up issues can be found in reference 7.

Thermal Vacuum Tests - A mission operations plan was developed pre-flight to run a number of tests, with up to 145 hours of on orbit operations planned. The majority of the tests were initially conducted in a thermal vacuum chamber to provide a one-g data base for comparison to the flight data. The primary tests were the EOS power profiles that simulated EOS instrument power dissipations, with power levels ranging from 100 to 200 watts per cold plate. Other tests included high and low power, asymmetric loading, subcooling limit, saturation temperature transitions, mechanical pump assist, and induced deprime/reprime. Further details of these tests can be found in reference 4. Again, the start-up procedures entailed the use of the vapor line and vapor header heaters or the use of the starter pump with the vapor header heaters to clear the grooves of the evaporator pumps prior to cold plate activation.

Ground Start-up - The groove clearing process was easily verified by monitoring the thermistor data during the tests. A typical ground start-up for evaporator pump #4 is shown in figure 10 from the thermal vacuum testing. The saturation temperature was first set by energizing the reservoir heaters at hour 19.1. The cold plate heaters were also used briefly to pre-heat the plate (hour 19.5), but its temperature was not allowed to reach the saturation temperature. The vapor line heaters were then used to clear the vapor lines of liquid, followed by the vapor header heater which was used to clear the pump grooves. This was evidenced by the pump body temperature (E4 PB3), which reached the saturation temperature shortly after the vapor header heater was activated (hour 20.25), thus indicating the presence of vapor in the pump grooves. Fifty watts of power was then applied to the plate (hour 20.3) and its temperature remained near the saturation temperature with little or no superheat, thus demonstrating normal priming and temperature control.



## FLIGHT RESULTS

Flight - The CAPL experiment was flown on the Space Shuttle Discovery in February 1994 (STS-60). The first startup attempt was not successful, although conflicts with other experiments for commanding capability interfered with timely heater activations. However, subsequent attempts were only partially successful, and there was no start-up in which all four evaporator pumps started simultaneously. Table 1 summarizes the various start-up attempts and shows which pumps started, if any. NONE of the start-ups were successful in clearing the pump grooves, even though this had been done routinely on the ground. Various startup methods were attempted, although it was obvious after the first few attempts that clearing the grooves would not be possible on-orbit with the CAPL 1 design.

Flight Start-up - Figure 11 shows a typical failed start-up from the flight. In this case the pump outlet (E4 Outlet) was cleared of liquid with the vapor header heater as evidenced by a temperature higher than the reservoir temperature (hour 8.75). However, the pump body (E4 PB3) temperature remained below saturation thus showing that the grooves were filled with liquid, even though the vapor header heater and the starter pump had been activated and left on for some time. Nonetheless, a startup was attempted at hour 9 with the application of 36 watts to the cold plate. The pump then experienced approximately 1.5 degrees of superheat as seen by E4 PB3 temperature at hour 9.1. When boiling started, the pump temperature dropped to saturation for a few minutes indicating possible priming and inspiring false hope to the test conductor. However, once the liquid in the pump was vaporized, the pump temperature rose quickly since there was no pumping action to provide additional liquid, thus showing a pump deprime.

FLIGHT OPERATION - As seen in Table 1, many start-ups were partially successful with two or three of the four pumps primed. In all of these cases, the pumps experienced some superheat, but started nonetheless. For these cases, either no vapor was forced into the core at the onset of nucleate boiling, or the amount of vapor in the core was not severe enough to cause a deprime. A successful start-up of pump #1 is shown in Figure 12, which is the same system startup shown in Figure 11 where pump #4 deprimed. Shortly after 36 W was applied to the plate at hour 9, the pump body temperature (E1 PB3) increased and exhibited approximately 1 degree C of superheat before boiling was initiated. At this point, the pump temperature dropped quickly to the saturation temperature and remained there, indicating a primed pump. At hour 9.5, power was increased to 125 watts, yet the pump temperature stayed near saturation, indicating a good prime. The pump continued to operate normally for the remainder of the test.

Four of the startups resulted in 2 primed pumps on one of the cold plates. This allowed the planned flight testing to continue and a number of tests were performed that demonstrated the proper operation of the loop in microgravity. In one case, after two pumps were primed, a reservoir pressure prime was successful in bringing all four pumps on-line for approximately 9 hours until the

loop had to be shut down for other shuttle experiments. In all cases, the loop performed well and exceeded the EOS requirements for heat transport and temperature control, with no unexpected pump depriming once the loop was started. Figure 13 shows the results for a typical EOS instrument power profile. The pump temperature stayed near the saturation temperature even though the power was varied from 125 watts to 250 watts and back to 125 watts, thus demonstrating proper thermal control and loop operation.

Component Testing - Flight testing confirmed the proper operation of the reservoir, heat pipe heat exchangers, and starter pump in microgravity. In addition, the loop electronics and instrumentation performed well, and hybrid operation with the mechanical pumps was accomplished. The performance of all of these components exceeded their design requirements. Additional details of the CAPL 1 flight will be available when the flight report is published.

Starter Pump - The starter pump performance was particularly encouraging in that it started on every attempt (25 times), even under adverse conditions. A typical starter pump activation is shown in Figure 14. The pump temperature increased rapidly after power was applied just prior to hour 19.6, and actually exceeded the reservoir temperature by several degrees, indicating a highly stressful start-up. This continued while liquid was being purged from the vapor line and forced into the reservoir. Once this process was complete near hour 19.7, the starter pump temperature dropped to the saturation temperature and the pump operated normally. The starter pump never deprimed because it was plumbed directly to the reservoir feed line. As the vapor line was cleared, the liquid displaced from it had to pass through the core of the starter pump before entering the reservoir. This kept the pump primed and eliminated any adverse effects caused by vapor bubbles that may have penetrated the wick. The starter pump always started successfully, even at a -8 degree C saturation temperature, which is more stressful than warmer levels due to the change in the thermodynamic properties of ammonia with temperature.

## POST FLIGHT INVESTIGATIONS

Post flight testing of CAPL showed that its behavior on the ground was the same after the mission as it was before flight, thus eliminating the possibility of a severe anomaly such as a large loss of ammonia or a transport line blockage. This confirmed that the start-up difficulties were due to gravitational effects. Figure 15 is a diagram based on temperature data, comparing the approximate location of the liquid/vapor interface in the pump for microgravity and one-g. In one-g, gravity pulled the liquid from the top grooves of the pump as a vapor space was created by the vapor header heater. This provided the needed clearing of the grooves for a successful pump start-up. In microgravity, there was vertical stratification of the liquid/vapor interface and the grooves remained flooded, even when the vapor header heater was allowed to run to its thermostat limit of 50 degrees C. The best on-orbit conditions were obtained when the starter pump was used in conjunction with the vapor header heater to develop a pressure head

on the vapor side of the loop. While this did succeed in pushing the liquid/vapor interface into the pump outlet, the pump grooves remained flooded and "non-stressful" start-ups were not possible.

"Heat Pipe Effect" - The evaporator pumps are constructed by inserting a wick into a heat pipe extrusion, with the grooves acting as vapor channels and the wick acting as the pump. However, the grooves themselves have a pumping capability based on the equation:

$$P = 2 \sigma / R$$

where P is the pumping pressure,  $\sigma$  is the surface tension of the ammonia, and R is the pumping radius based on the groove geometry. Calculations for CAPL yield a groove pumping capability of approximately 98 Pascal at 25 C, which is sufficient to keep the grooves flooded in microgravity, even with the vapor lines clear. This pumping effect was easily overcome on the ground by gravitational forces. The HPHX's were located 8.9 cm (3.5 in) lower than the evaporator cold plates, representing a 520 Pascal gravitational pressure rise (pumping head) in ground tests. Thus, the vapor generated by the starter pump preferentially cleared the vapor grooves in the cold plate evaporators before flowing to the HPHX's, resulting in a "non-stressful" start-up. In microgravity, there was no gravitational pressure head to overcome, and therefore the vapor flowed to the condenser rather than clearing the pump grooves. This kept the grooves flooded and led to "stressful" start-ups that often led to pump depriming. Analysis comparing the one-g and microgravity cases is shown in Figure 16. Unfortunately, the effects of this phenomena were not realized before the mission, and the difficulties experienced in microgravity were totally unexpected.

## CAPL 2 FLIGHT VERIFICATION

Discussion of a CAPL reflight was started even before the CAPL 1 flight was completed. Initial redesign efforts focused on revised vapor outlet heater locations, increased starter pump power, and higher vapor line pressure drop to clear the pump grooves in microgravity. This effort was continued through a Reflight Design Review, which was held in June, 1994. One of the recommendations at the review (made by Mr. Brent Cullimore) was to replace the traditional CPL with a loop that utilizes only a single starter pump [8]. A heat pipe imbedded in the cold plate would be used to provide the required isothermalization of the plate and carry heat to the starter pump. This intriguing suggestion led to the construction of a prototype Starter Pump Cold Plate (SCP). Testing of this design was very encouraging and the Starter Pump System is now baselined for EOS and CAPL-2 (see Figure 17). This system is very robust, always starts from a fully flooded condition without groove clearing, and can withstand conditions that would deprime a traditional CPL. The success of the starter pump on CAPL 1 also lends credence to this design.

CAPL 2 has been designed to more accurately reflect the EOS design and to serve as a microgravity verification of the EOS CPL

loops. The starter pump cold plate is the same size as the EOS plate and the liquid and vapor line lengths and diameters have been changed to more accurately reflect the current EOS design. CAPL 2 is scheduled for a flight in July 1995 on the Space Shuttle Endeavor. Results of that mission will be published as they become available.

## CONCLUSION

The CAPL 1 flight reinforces the need for microgravity flight verification of gravitationally sensitive systems prior to their implementation on spacecraft. Even though the performance of CAPL 1 could have been anticipated and corrected before the mission, it is very difficult to anticipate the effects of microgravity from a one-g environment. A successful flight of CAPL 2 will demonstrate the operation of the starter pump system in microgravity and will lead to its use on EOS and other space based systems.

## REFERENCES

1. Ku, J., Kroliczek, E., Butler, D., McIntosh, R., and Schweickart, R., "Capillary Pumped Loop GAS and Hitchhiker Flight Experiments," Paper 86-1249, AIAA/ASME 4th Joint Thermophysics and Heat Transfer Conference, Boston, MA, June, 1986.
2. EOS-AM Critical Design Review, Thermal Subsystems Technical Audit, Martin Marietta Corporation, Princeton NJ, January 1995.
3. Butler, D. and Hoang, T., "The Capillary Pumped Loop Flight Experiment (CAPL), A Pathfinder for EOS," Space Shuttle Small Payloads Symposium, New Carrollton, MD, October 1992.
4. Ottenstein, L., Ku, J., Butler, D., "Thermal Vacuum Testing of the Capillary Pumped Loop Flight Experiment," SAE Paper 941599, 24th ICES Conference, Friedrichshafen, Germany, June, 1994.
5. Ottenstein, L., Ku, J., Butler, D., "Testing of Flight Components for the Capillary Pumped Loop Flight Experiment," SAE Paper 932235, 23rd ICES Conference, Colorado Springs, CO, July, 1993.
6. Capillary Pumped Loop (CAPL 2) Flight Verification Reflight Design Review (RDR), NASA Goddard Space Flight Center, June, 1994.
7. Ku, J., "Start-up Issues of Capillary Pumped Loops," Ninth International Heat Pipe Conference, Albuquerque, NM, May, 1995.
8. Sherman, A., "Action Items and Review Team Recommendations from the CAPL 2 Reflight Design Review (RDR)," NASA Goddard Space Flight Center Memorandum, July, 1994.

9. Ku, J., Yun, S., "A Prototype Heat Pipe Heat Exchanger for the Capillary Pumped Loop Flight Experiment," AIAA Paper 92-2910, AIAA 27th Thermophysics Conference, Nashville, TN, July 1992.
10. Wolf, D., "Design and Development of a Two-Phase Reservoir for the Capillary Pumped Loop (CAPL) Flight Experiment," SAE Paper 921405, 22nd ICES, Seattle, WA, July, 1992.

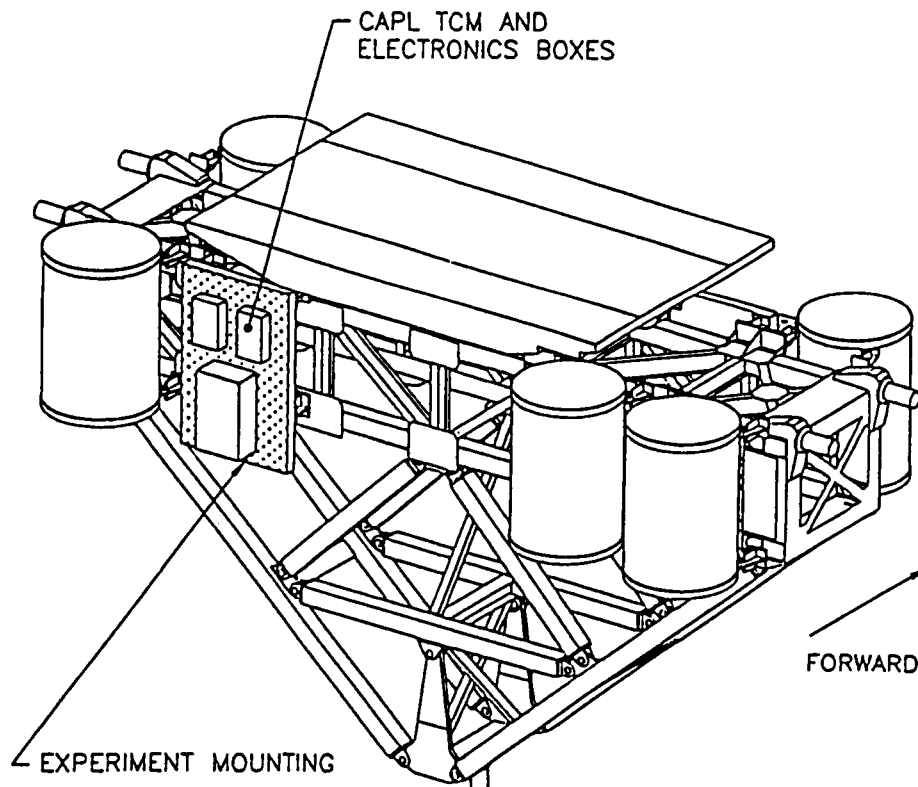
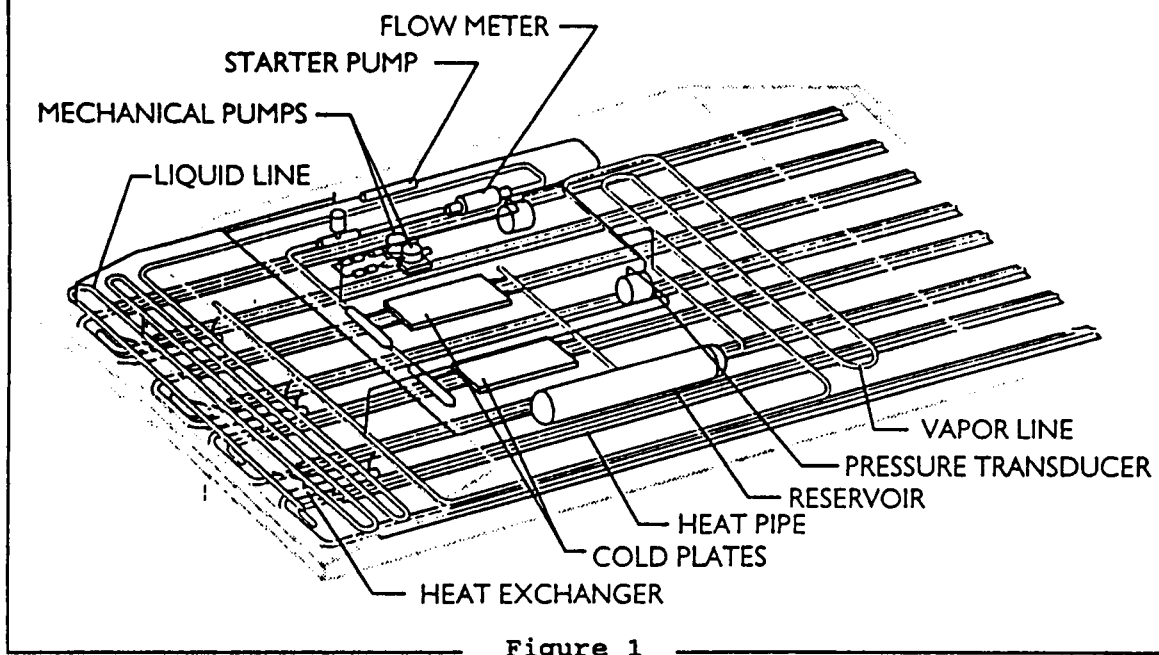
Table 1: CAPL Flight Start-Up Conditions

Start-up #	Starter Pump Power (W)	Vapor Header Power (W)	Vapor Line Power (W)	Cold Plate Power		Capillary pumps started				Saturation Temperature (C)	average Radiator Temperature (C)	REPRIME METHOD	
				Plate 1 (W)	Plate 2 (W)	E1	E2	E3	E4			(before start) pressure	mech pump
1		33-off	54-off	126	124			?		25	-7	N/A	N/A
2	145	33-off		126	124					28	3	X	
3	145			64	63		?			25	-19		X
4	145	33-off		126	124		X	X	X	14	0	X	X
5		33-off	56-off	127	124	X		X		16.9	2	X	X
6	145	33		35	36	X	X			19	5	X	X
7		33-off	104-off	35	36	X			X	21	1	X	X
8	145	33-off		35	36		X			20	1	X	X
9	145	33-off?		35	36	X		X		-10.1	-40	X	X
10	145	33		34	35	X		X	X	-2	-36	X	X
11		33	54-off	35	35	X				7.9	-13	X	X
12	145	33		35	36	X				11	-8	X	X
13	145	33		35	36		X		X	10	-2	?	X
14	145	33-off		126	126	?				18	-2	X	X
15	145			125	36/96				?	18	-4	X	X
16	145	33		35	36		X		X	14	-1	X	X
17	145			122	123					16.9	1	X	X
18	145	33-off		32	32					22	1	X	X
19	145	33		32	32		X	X		5	-5		X
20	145			32	32	X				10	-7	X	X
21				125	125	X	X		X	25	0		X

X indicates that the pump operated successfully

## - off indicates that the heater was used, but that it was off when cold plate power was applied

# CAPILLARY PUMPED LOOP EXPERIMENT (CAPL)



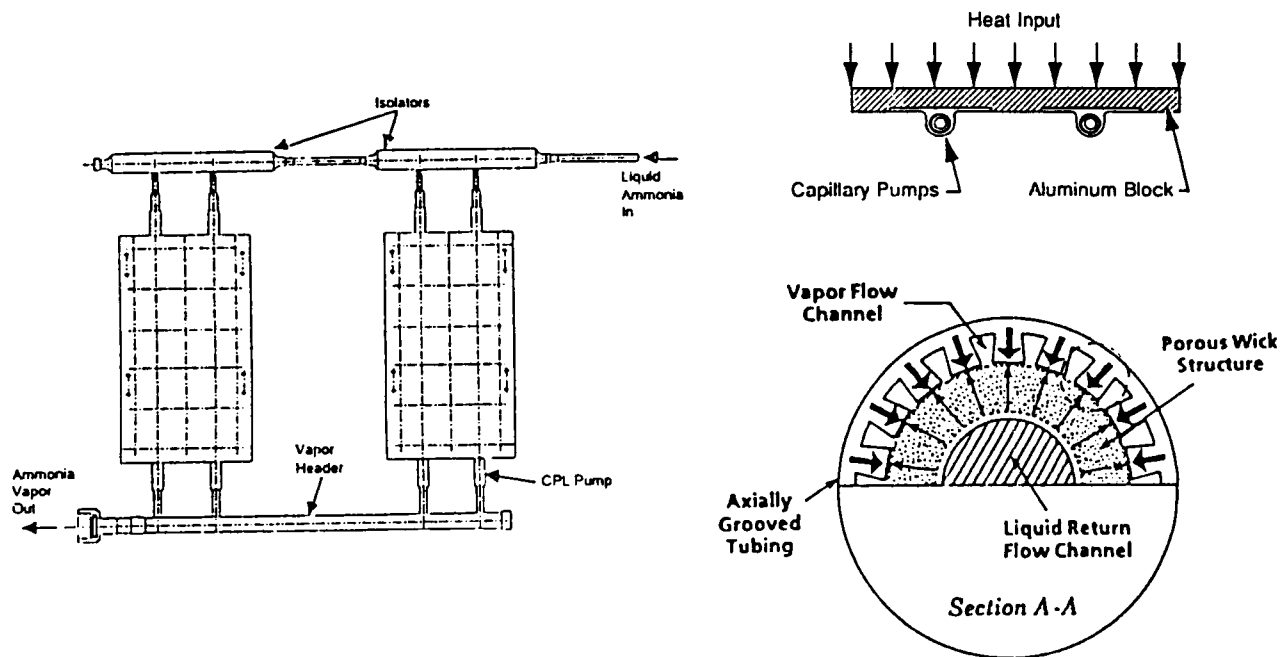


Figure 3 Capillary Evaporator Plates

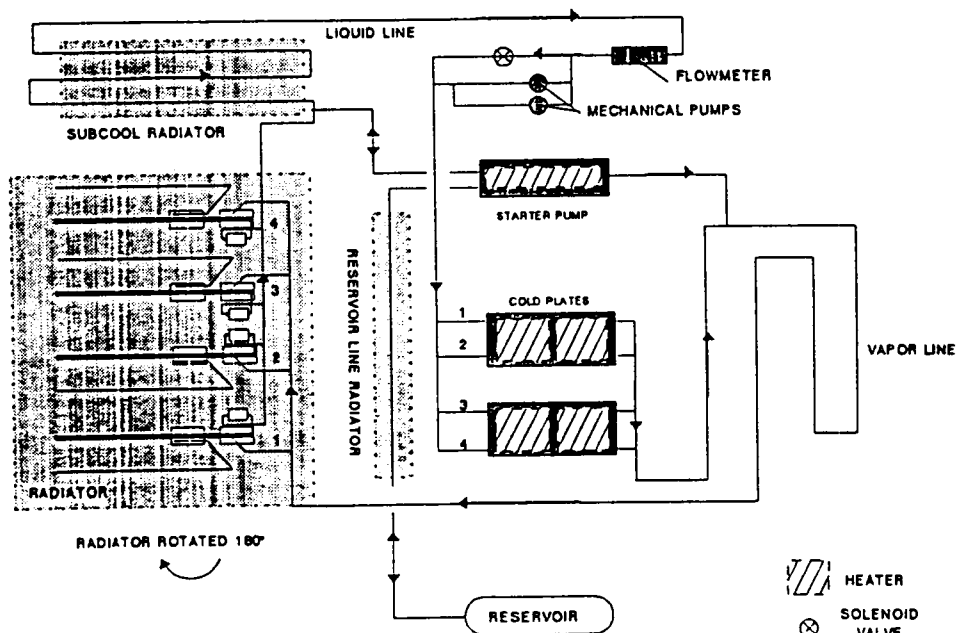


Figure 4 CAPL Flow Schematic



# NUCLEATE BOILING THEORY

## ● CLAUSIUS-CLAPEYRON EQUATION

$$T_L - T_{RES.} \cong \frac{RT_{RES.}^2}{\lambda P_{RES.}} \left( \frac{2\sigma}{r} \right) \quad \text{where } T_L = T_v \text{ and } P_L = P_{RES.}$$

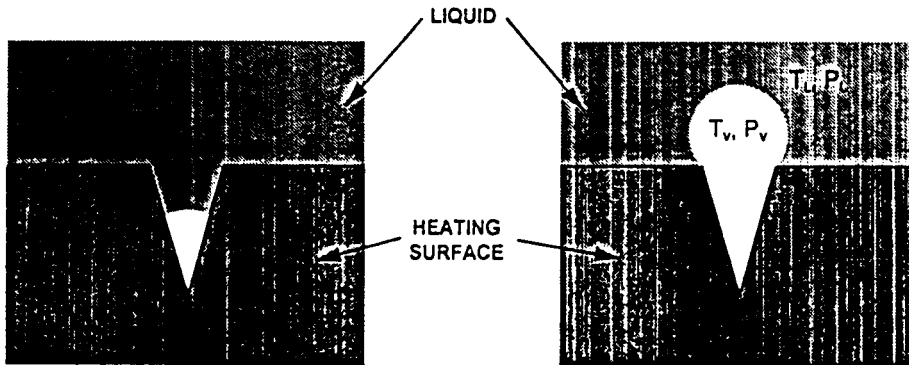


Figure 5

## PRESSURE DROP AND TEMPERATURES DURING START-UP WITH HIGH SUPERHEAT

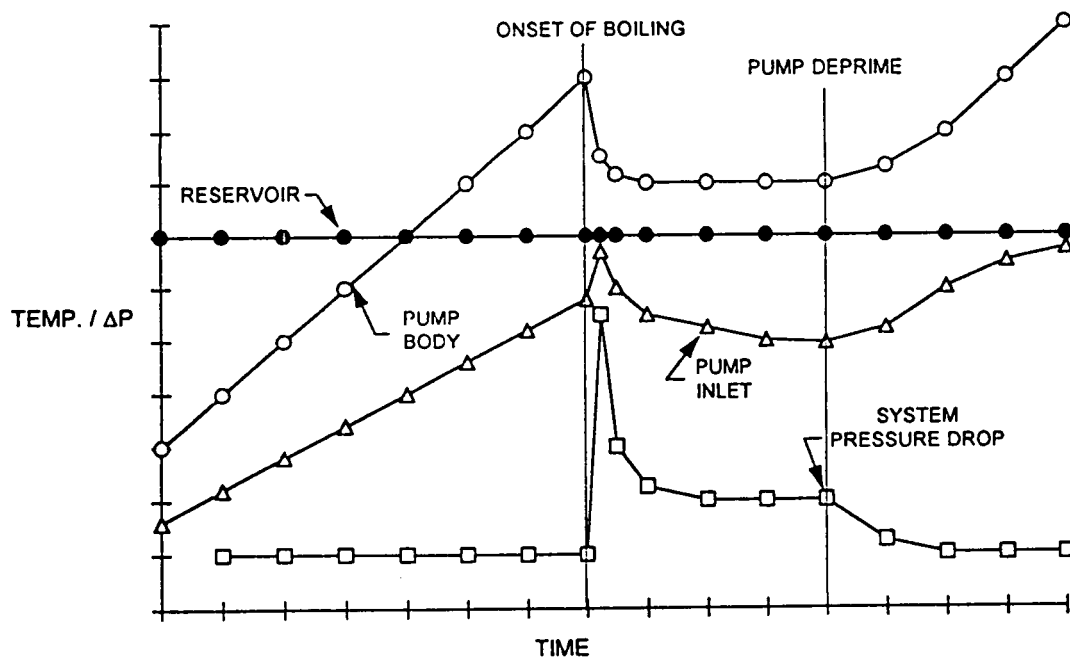


Figure 6

## THREE EVAPORATOR PUMP DESIGNS

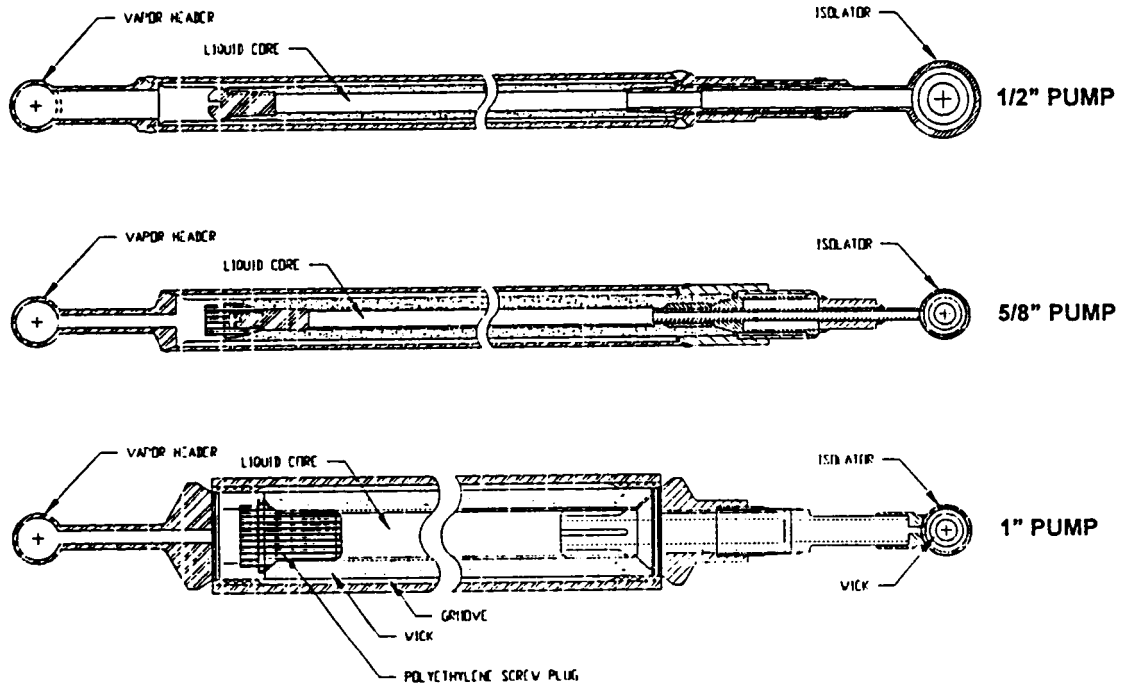


Figure 7

## PRESSURE DROP AND TEMPERATURES DURING START-UP WITHOUT SUPERHEAT

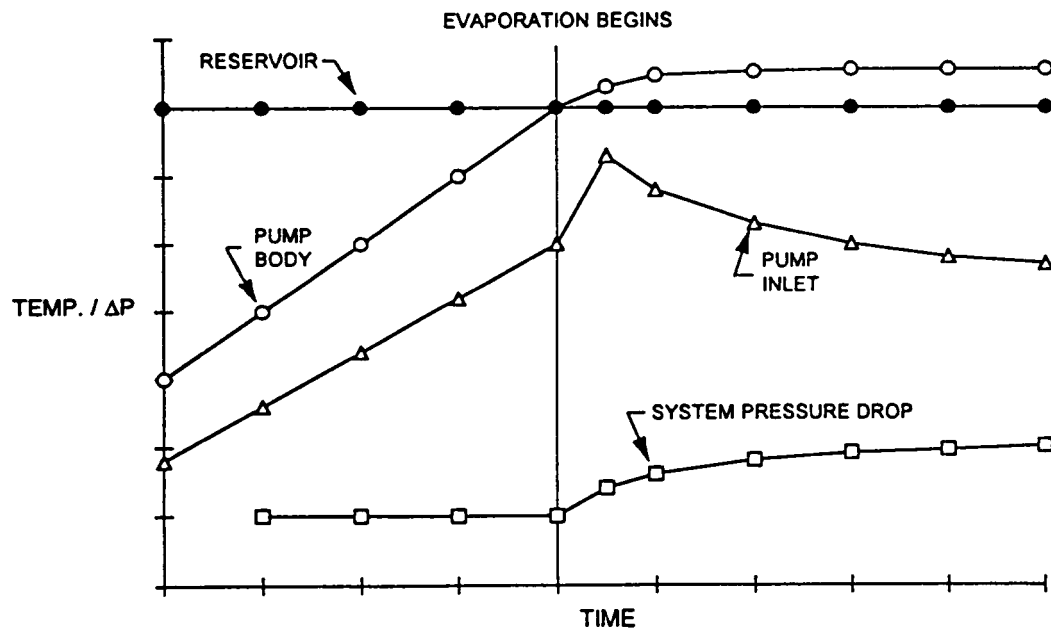


Figure 8

# SCHEMATIC OF A CAPILLARY STARTER PUMP

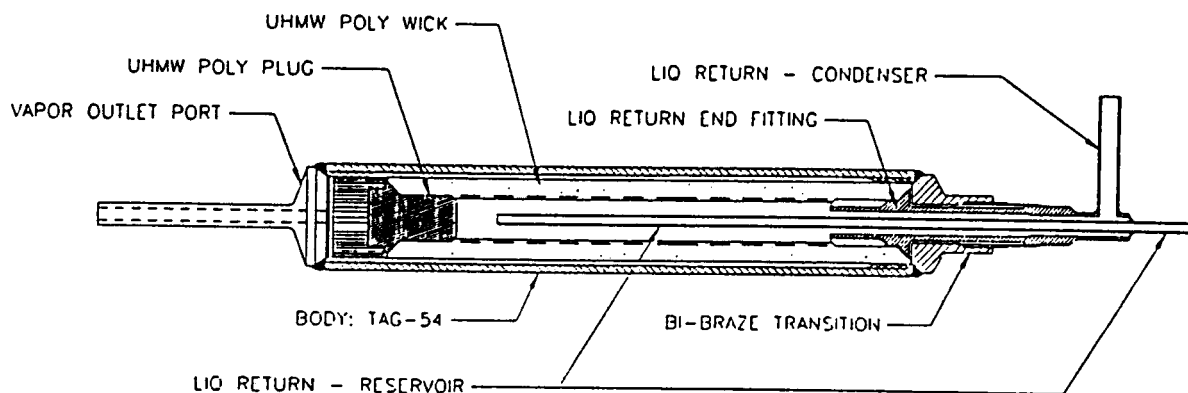


Figure 9

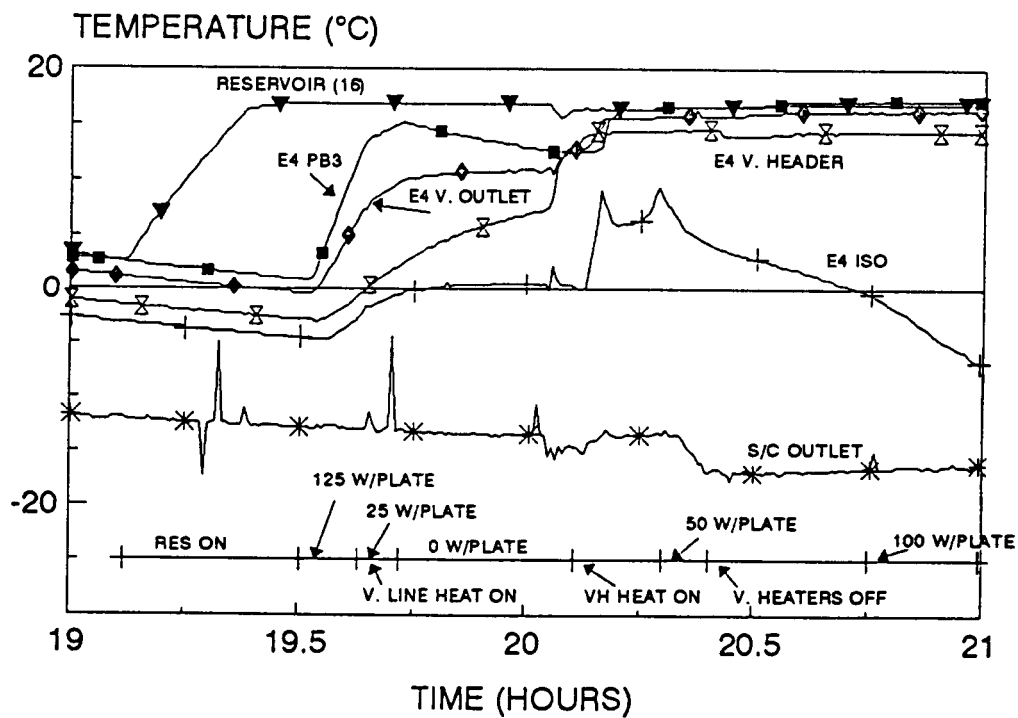


Fig 10: Start-Up #4, Thermal Vacuum

(5/15/93; filter = 5)

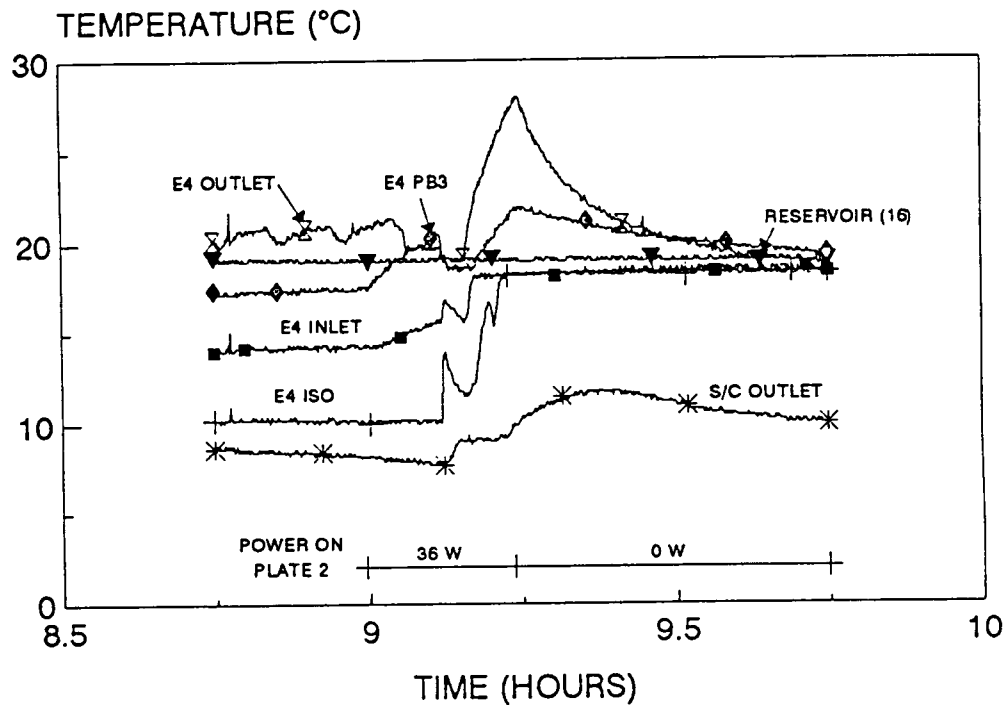


Figure 11: CAPL start-up # 6, FLIGHT  
Evaporator #4, failure  
(2/4/94, no filler)

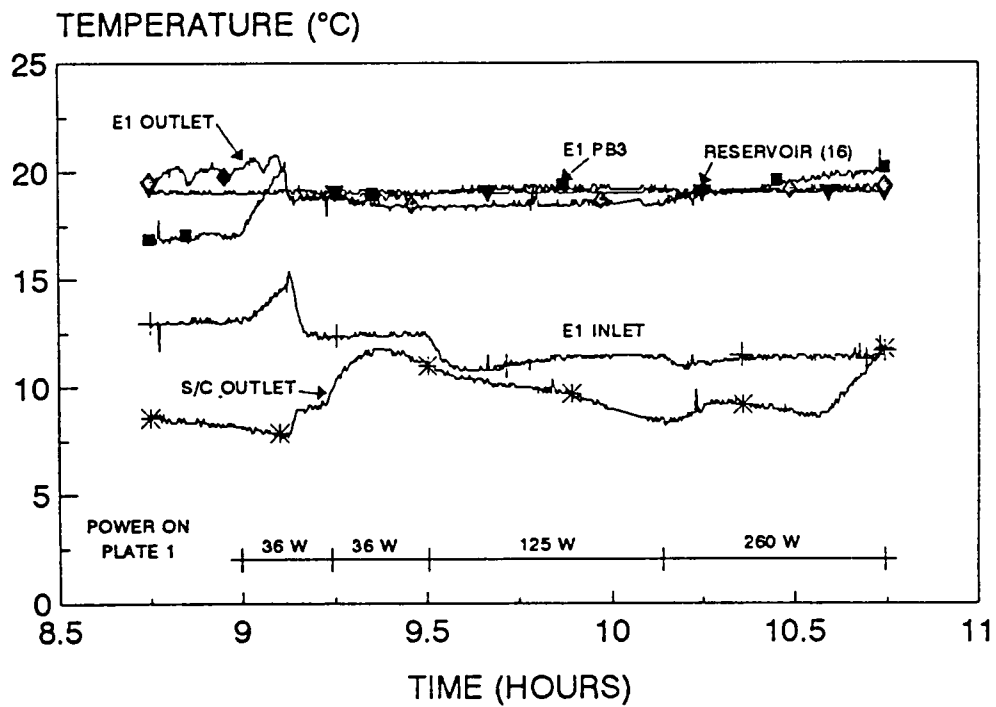


Figure 12: EOS start-up # 6, FLIGHT  
Evaporator #1, successful  
(2/4/94, filter = 2)

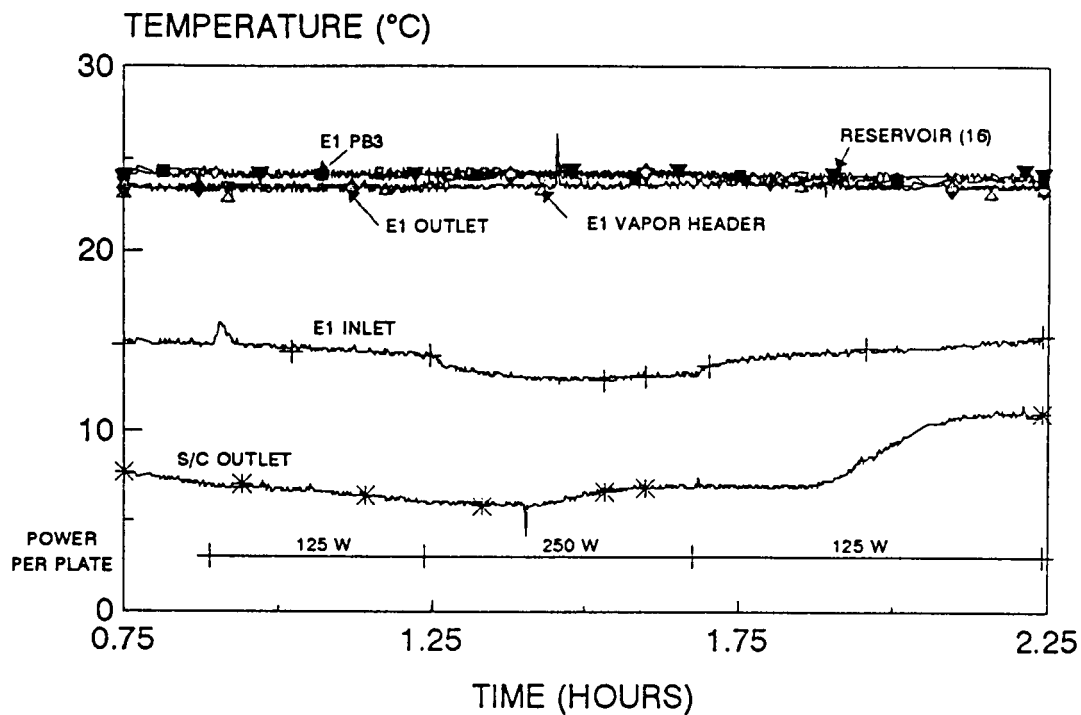


Figure 13: EOS Profile B1 - flight  
Evaporator 1, Successful  
(2/5/94, no filter)

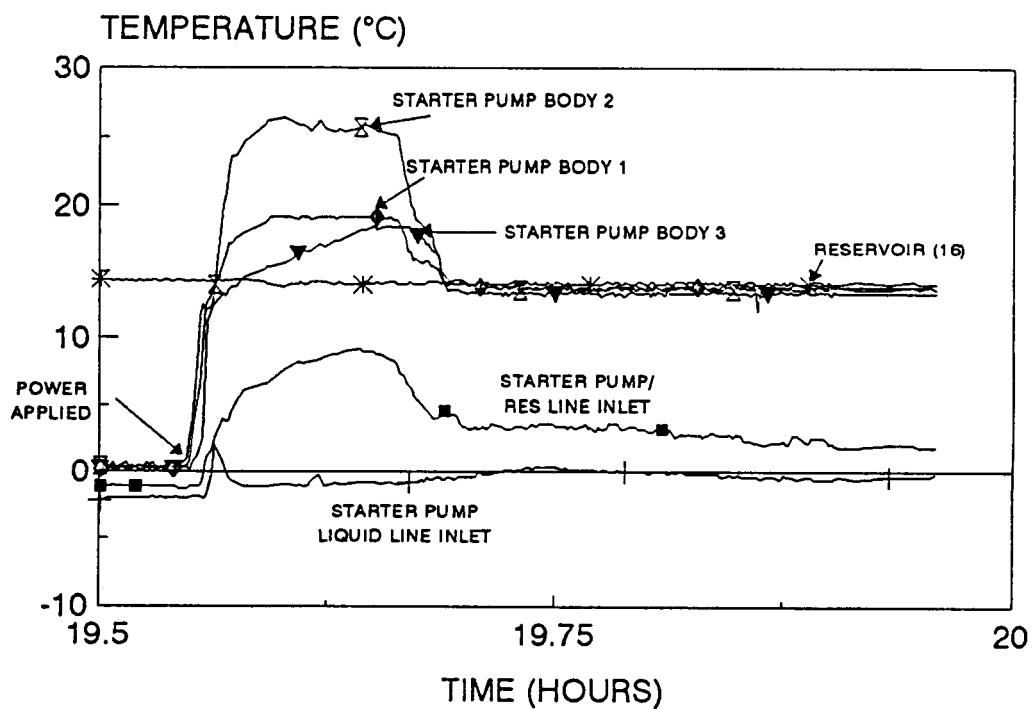
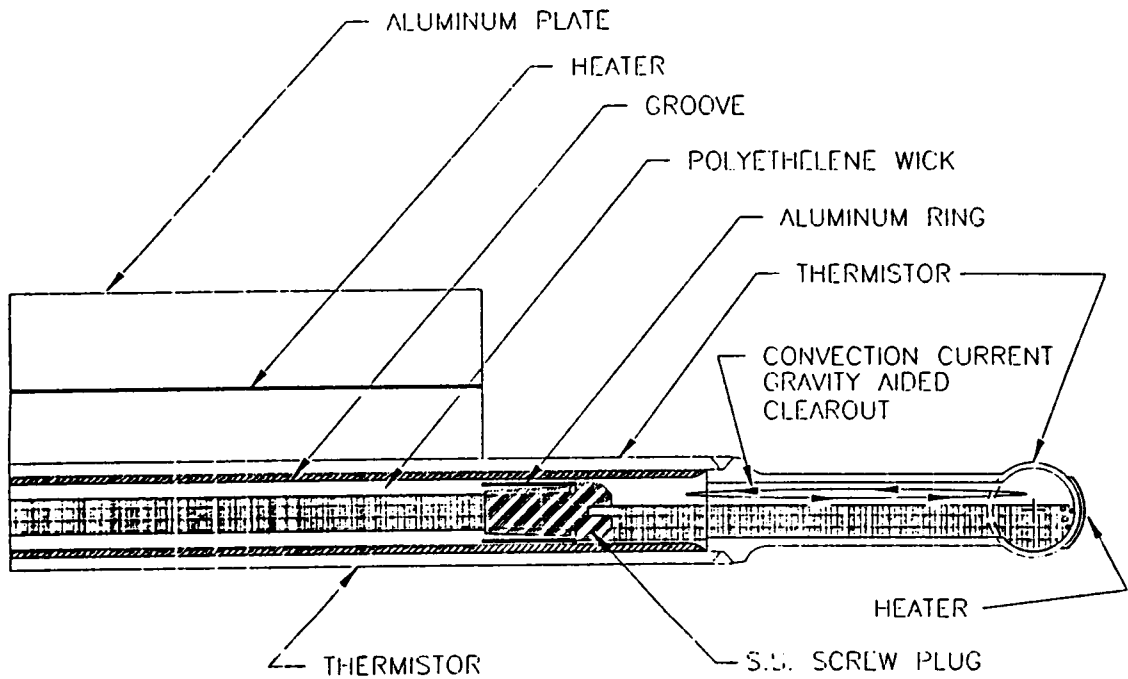


Figure 14: Starter Pump Start-Up - flight  
150 W on starter pump  
(2/3/94)

## GRAVITY INFLUENCED START-UP



## START-UP IN MICRO-GRAVITY

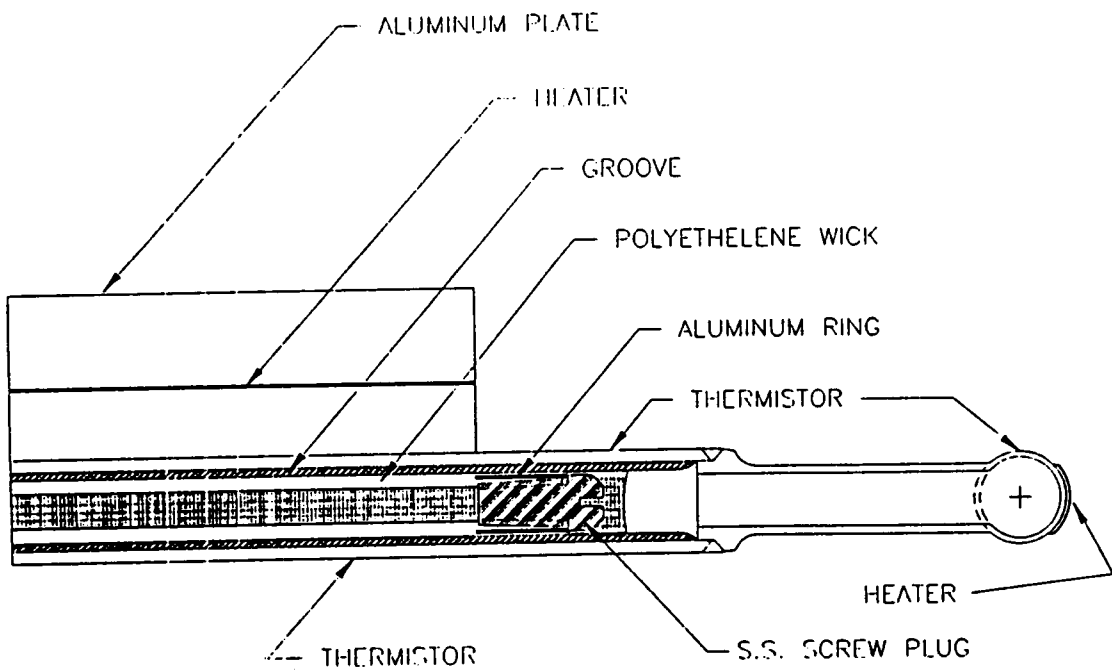
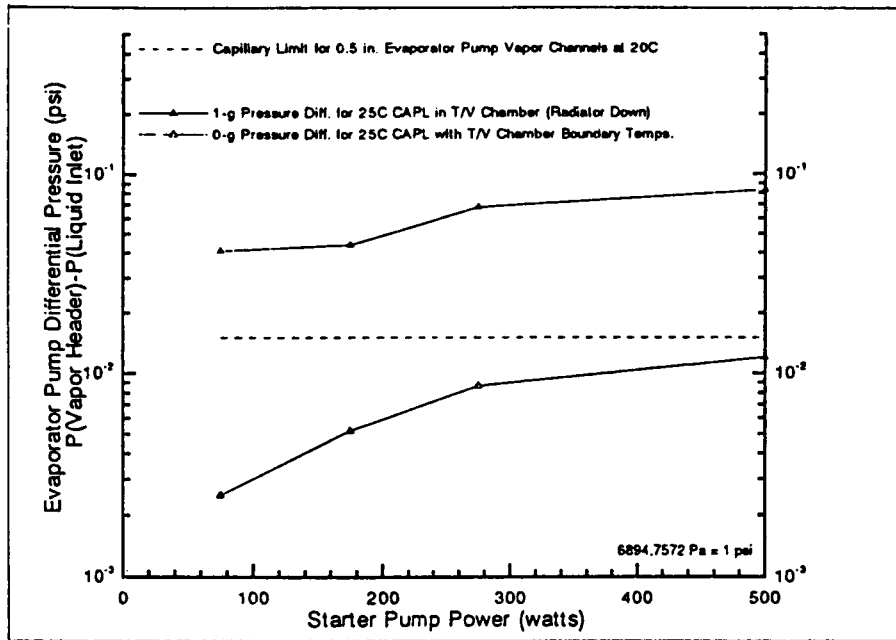


Figure 15



**Available CAPL-1 starter pump heater power of ~150 watts is insufficient to clear the evaporator pump vapor channels in 0-g, but is adequate in 1-g.**

Figure 16

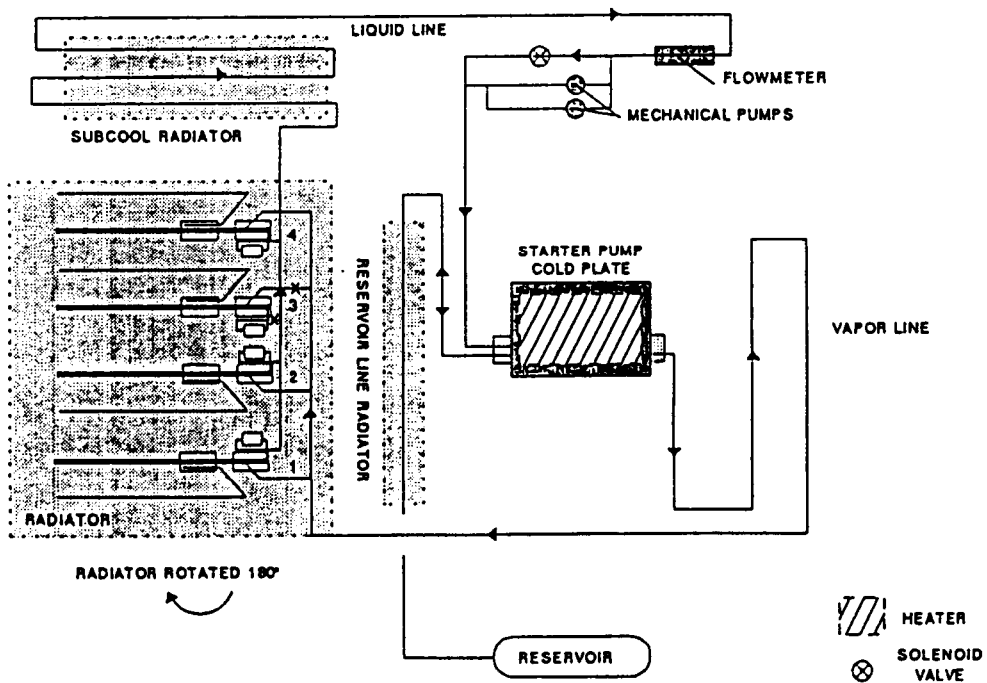


Figure 17 CAPL 2 FLOW SCHEMATIC  
STARTER PUMP COLD PLATE

**The Cryogenic Test Bed Experiments**  
Cryogenic Heat Pipe Flight Experiment CRYOHP (STS-53)  
Cryogenic Two Phase Flight Experiment CRYOTP (STS-62)  
Cryogenic Flexible Diode Flight Experiment CRYOFD

Lee Thienel  
Jackson and Tull  
Albuquerque, NM

Chuck Stouffer  
OAO Corporation  
Lanham, MD

## **ABSTRACT**

This paper presents an overview of the Cryogenic Test Bed (CTB) experiments including experiment results, integration techniques used, and lessons learned during integration, test and flight phases of the Cryogenic Heat Pipe Flight Experiment (STS-53) and the Cryogenic Two Phase Flight Experiment (OAST-2, STS-62). We will also discuss the Cryogenic Flexible Diode Heat Pipe (CRYOFD) experiment which will fly in the 1996/97 time frame and the fourth flight of the CTB which will fly in the 1997/98 time frame. The two missions tested two oxygen axially grooved heat pipes, a nitrogen fibrous wick heat pipe and a 2-methylpentane phase change material thermal storage unit. Techniques were found for solving problems with vibration from the cryo-coolers transmitted through the compressors and the cold heads, and mounting the heat pipe without introducing parasitic heat leaks. A thermally conductive interface material was selected that would meet the requirements and perform over the temperature range of 55 to 300 K. Problems are discussed with the bi-metallic thermostats used for heater circuit protection and the S-Glass suspension straps originally used to secure the BETSU PCM in the CRYOTP mission. Flight results will be compared to 1-g test results and differences will be discussed.

## **INTRODUCTION**

An objective of the Cryogenic Heat Pipe Flight Experiment (CRYOHP) was to develop a reusable Cryogenic Test Bed (CTB) for use in joint NASA/USAF flight experiments. In the process of fulfilling this objective several techniques were developed to integrate the test articles with the experiment and lessons were learned from efforts that did not produce the expected/desired results. The Cryogenic Two Phase Flight Experiment (CRYOTP) was the first re-flight of the CTB. More was learned and is still being learned about the CTB and implementation of the various cryogenic experiments after the second flight and as preparations are being started for the third flight of the CTB. The third flight will test two cryogenic flexible diode heat pipes (one charged with oxygen and the other charged with methane) and is currently planned for late 1996. The fourth flight of the CTB will test a 60 Kelvin thermal storage unit.



## CTB Description

The CTB was developed for NASA's Goddard Space Flight Center (GSFC) and the USAF's Wright Laboratory. Figure 1 shows the CTB configuration and major components (this configuration shows the heat pipes flown on CRYOHP). The CTB is designed to test two cryogenic thermal devices, each on a separate cryogenic system using tactical cryogenic coolers (providing 3.5 W of cooling at 80 K each). The coolers have a Coefficient of Performance (CoP) of 25 to 30. One test article is cooled with three coolers and the other is cooled with two coolers. The Hitchhiker (HH) canister is fitted with a modified Upper End Plate (UEP) having an additional 40 Kg of thermal mass and increased surface area to allow for up to 12 hours continuous operation while maintaining the cryogenic cooler compressor bodies below 80°C with up to 320 watts of heat dissipation.

The test articles are supported by a stainless steel support structure which is thermally de-coupled from the UEP by G-10 spacers inserted in the vertical legs of the support structure. The cryogenic coolers are coupled to the test articles using vibration isolation mounts and thermal shunts to couple the multiple cryogenic coolers, provide thermal mass, and to span the vertical distance from the cold heads to the test article.

Graphite foil conductive interfaces and G-10 isolators are used throughout the experiment as necessary to either minimize the  $\Delta T$  (graphite foil) or the heat flow across the interface (G-10). Individual components and assemblies were wrapped with multi-layer insulation (MLI) blankets as necessary to minimize radiation heat leaks (parasitic heat loads).

Power (for electronics and experiment heaters), command and telemetry interfaces are provided by the CTB electronics control module (CECM) and the power and control for the cryo-coolers are controlled by the power distribution box (PDB). The CRYOHP mission was a side mount experiment and four sets of HH power and signal lines were available for the CRYOHP (3 for the experiment and one for the lower end plate (LEP)). The CRYOTOP mission was a bridge mount, and only three sets of power and signal lines were available.

We had to modify the PDB for the CRYOTOP mission to require fewer pulse commands for experiment control. The original design had twelve pulse commands:

- CECM ON/OFF (2 commands)
- CRYO-Cooler ON/OFF (2 each for 5 coolers = 10 commands)

Only ten commands were available for the CRYOTOP flight. Since it was not part of the mission plan to run both sides of the CTB at any time it would be possible to have commands that turn off two cryo-coolers (1 on each side) since both would never be on. We modified the PDB circuitry so that one command would turn off the #1 coolers on each side of the experiment and another would turn off both #2 coolers.

Each test article and its associated hardware (thermal shunt, cryo-cooler cold heads, etc.) are instrumented with 13 platinum resistance thermometers (PRTs) providing accurate temperature data over the range of 50 to ~200 K. Thermistors were used for temperature measurements in the range of 200 - 350 K.

## BI-METALLIC THERMOSTATS

Shuttle safety requirements led us to a heater circuit design based on a tri-series redundant thermostat system with one thermostat on the return leg of the heater (if different set points are used on the same circuit the lowest set point is used on the return leg).

The thermostats preferred for space applications (based on our knowledge and resources) are not rated for cryogenic applications. We found that the set point of the thermostat dropped dramatically after exposure to cryogenic temperatures. This phenomenon was observed during testing with the CRYOHP experiment. Figure 2 shows data for a thermostat of the type used with a specified open on rise temperature of  $58 \pm 2^\circ\text{C}$ , and an original open temperature of  $57.4^\circ\text{C}$ . As shown in

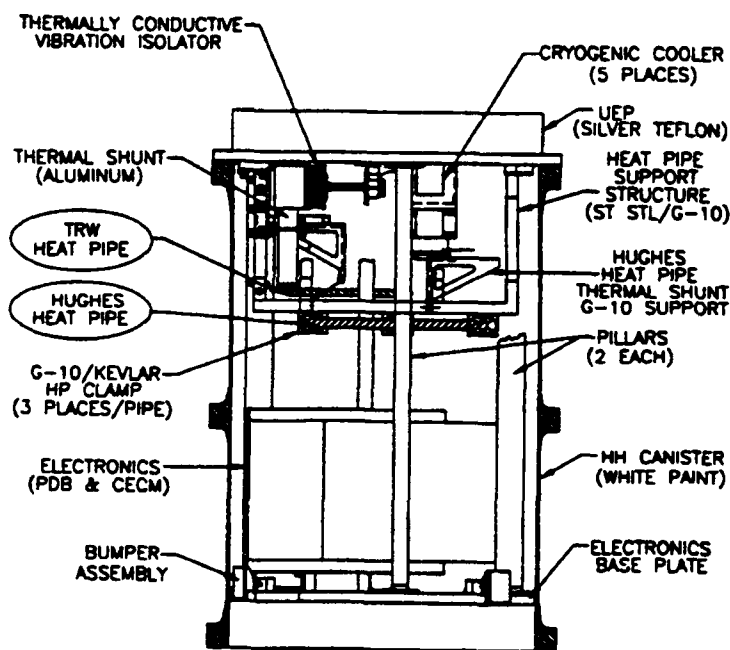


Figure 1. CTB Configuration

Figure 2, the set point moved to  $\sim 3^{\circ}\text{C}$  after exposure to liquid nitrogen ( $\text{LN}_2$ ) temperatures. This unit (still in its test set-up) was retested after more than 18 months of storage at room temperature. Repeated testing revealed that the unit's set point had not changed. There was some concern that, after time, the set point may start to return to its original value. If the set point drifted during storage one may have to prove that it would never rise above its original value to satisfy Space Shuttle (NSTS) safety requirements.

Less formal observations indicate that as units flown on CRYOHP were exposed to temperatures below  $\text{LN}_2$  the set point dropped even lower. We have taken this series of thermostat to temperatures in the range of 60 K without any failures. The issue does not seem to be that a unit might fail but rather that the set point will drop to a

temperature below  $0^{\circ}\text{C}$  or close enough to  $0^{\circ}\text{C}$  that it is not possible to use the experiment heaters to warm up the test articles during thermal vacuum testing. This is undesirable because it is time consuming and costly to wait for the experiment to warm up on its own in a vacuum. Some of the units that we used on the first flight had set points specified as low as  $30^{\circ}\text{C}$  and they drifted to approximately  $-20^{\circ}\text{C}$  after exposure to cryogenic temperatures.

## TESTING WITH HH

When the experiments were delivered to GSFC for flight as HH payloads they underwent a series of testing. The sequence of tests was the same for both the CRYOHP and CRYOTP missions.

The first test run after delivery to HH was a post ship functional. We delivered our ground support equipment (GSE) with the experiment to allow for performance of the post ship functional and any future stand alone testing that circumstances might have required. The post ship functional tests were straight forward, and no problems were encountered.

The next test to be performed was an interface verification test (IVT). The purpose of this test is to perform a safe-to-mate test followed by verification of the power interface. The IVT is designed to verify that the experiment will not damage the HH avionics. We also performed a safe-to-mate test on the avionics and flight harness with the measurements being made at the LEP. The only anomaly that we found was on the LEP where two of the HH signal connectors are mislabeled.

After power interface verification the experiment was mated with the HH and the command and telemetry interfaces were verified. The only problem encountered in the IVT was on CRYOHP, there was a bad integrated circuit on the RS422 interface and only one side of the differential signals was present (the other was floating). The problem did not show up during experiment level testing because the experiment RS422 interface was tied to a commercial RS422/RS232 converter. It turned out that the converter used would still work with only one side of the differential RS422 signal. After replacing the chip, no other problems were encountered.

After the IVTs were performed for all of the experiments, the HH and the experiments were taken to the Electromagnetic Interference (EMI)/Electromagnetic Compatibility (EMC) test facility at GSFC. We experienced two problems in EMI/EMC, the first was that the coolers had high in-rush characteristics that were deemed allowable (the coolers have in-line EMI filters). The other problem we experienced was a susceptibility to conducted emissions in the range of 1-50 MHz. We ran diagnostic tests to determine the levels at which CTB became susceptible. We determined that it was unlikely that we would encounter noise at levels that would cause problems for us (the experiment was not susceptible at the STS/HH ICD levels). During both flights of the CTB we only had noise in the telemetry due to internal circuits controlling experiment heater power levels.

CRYOTP emissions were too high in a frequency range which could have interfered with the Shuttle crews intercom system (used by some crews to communicate between compartments). When Johnson Space Center (JSC) was contacted it was discovered that there was revised data for the intercom system which increased the level of noise that could be present without impacting the intercom system and the experiment met this new specification.

## BRILLIANT EYES THERMAL STORAGE UNIT (BETSU)

During the flight qualification of the CRYOTP Flight Experiment the S-Glass suspension System that was used to support the BETSU canister failed under vibration. The following summary describes the BETSU design, failure event and the corrective action taken to qualify and successfully fly the experiment.

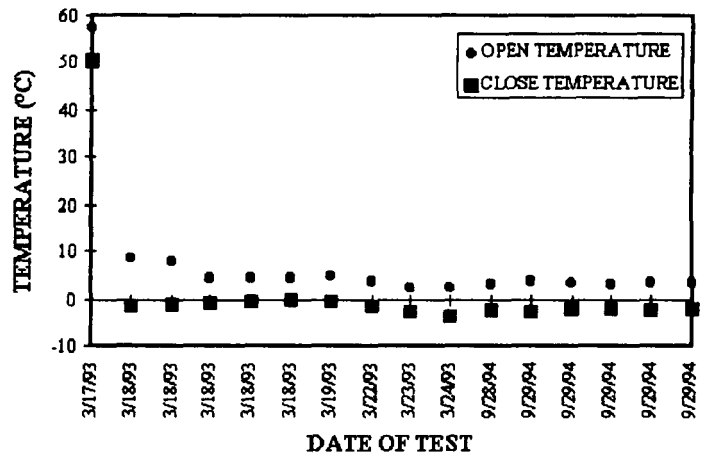


Figure 2. Thermostat Test Data

The structural configuration of the BETSU experiment consisted of an internal PCM canister suspended from the outer shell as illustrated in Figure 3. Due to the small envelope available, the cable system was designed with very short cable lengths. The system was designed using six S-Glass fixed loops; each being approximately 1" long. S-Glass material has a very small linear stretch under tension, and therefore the system was designed with a very short stroke for adjusting tension in the cable.

The experiment was tested in the HH canister at protoflight random vibration levels. The input levels and the levels observed by the BETSU due to transmissivity of the HH canister mounts are shown in Table 1. During the post vibration evaluation it was apparent the S-Glass straps had failed leaving the lacing cord back-up straps completely supporting the internal BETSU canister. A failure evaluation was performed with the BETSU unit including segmented vibration testing and inspections to determine the failure modes. During this evaluation a microscopic inspection of the fractured straps revealed two failure modes for these straps, wearing on the internal radius and stress cracks in the radius. A study was performed to evaluate alternative strap types and/or materials that could be used for this application. The following parameters were used as a baseline for the study:

- Thermal conductance
- Envelope constraints
- Short length of straps that the BETSU can accommodate
- Tension adjustment 15 mm (0.6") maximum
- No linear take-up mechanism to accommodate cable stretch

The study included fabrication and testing of materials such as, s-glass, aramid (braid and weave), stainless steel and titanium wire.

Aramid (braid and weave) was eliminated as a option due to its stretch under tension which could not be accommodated in this application. Stainless Steel was eliminated as a option due to problems maintaining structural integrity during construction of the fixed loop system. Titanium wire welded in a fixed loop was selected due to its low stretch under tension and the reliability and high strength during tension testing. Even with its small stretch under load, the straps still required pre stretching prior to installation to meet this application. Although the titanium straps have a higher thermal conductivity than the S-Glass Straps they represent a negligible parasitic impact to the canister as verified in thermal vacuum tests and in flight. The straps were installed in the BETSU and retested to protoflight levels without a failure.

The BETSU design caused significant difficulty to qualify the flight experiment. The following lessons learned are issues that should be considered when developing a cable tension system:

- Envelope Constraints:  
The design should be user friendly and required a minimum effort for cable installation.  
The tensioning method should be easily accessible and have ample travel.

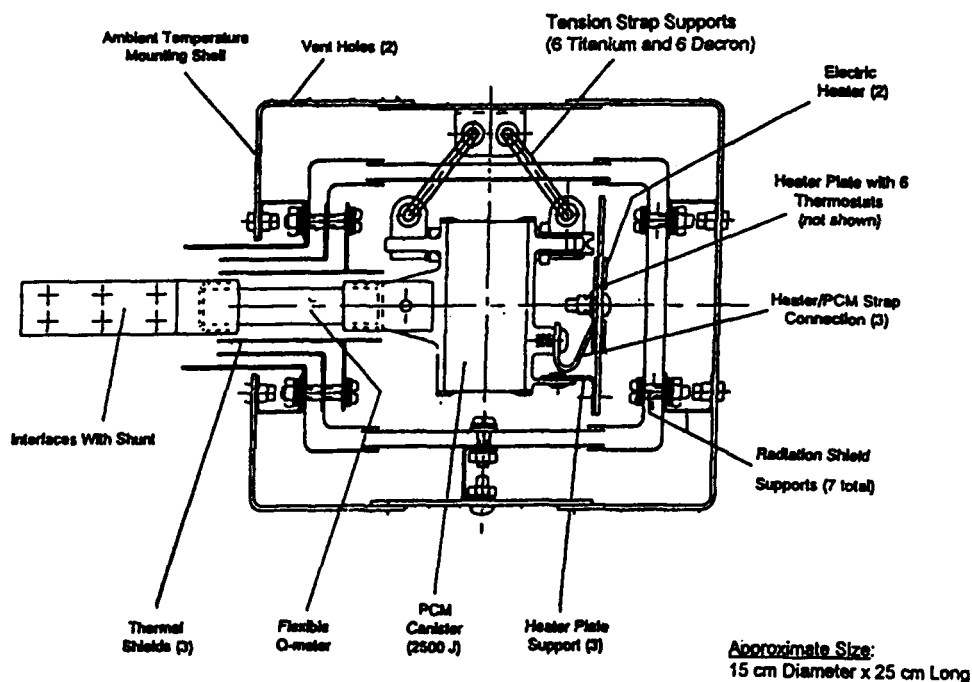


Figure 3. BETSU Structural Design

Table 1  
CRYOTP Vibration Test Levels

Test #1 7-28-93			
Test	Input #1	Input #2	Outside Canister
Z-Axis Sine Burst	12.02	12.37	-2.24, -2, 15.15
Y-Axis Sine Burst	12.12	-12.44	-16.19, 3.67, -3.21
X-Axis Sine Burst	15.31	-14.19	-5.11, -19.21, 3.70
Z-Axis Random	5.523	4.105	7.92, 9.85, 12.12
Y-Axis Random	4.782	4.38	6.74, 6.84, 10.97
X-Axis Random	4.69	3.156	5.49, 4.90, 3.23

Allow access for inspection methods during qualification testing.

- **Short Cable Length:**

The length of the cable from centerline to centerline of the fixed ends should allow for stretch or give in cables.

- **Linear Take-up Mechanism:**

From our successful experience with the CTB heat pipe clamps we understand the benefit in having a mechanism to maintain tension under cable elongation. A spring type device, (convex washers) should be used in the tensioning mechanism to maintain tension of the cable when it elongates under load.

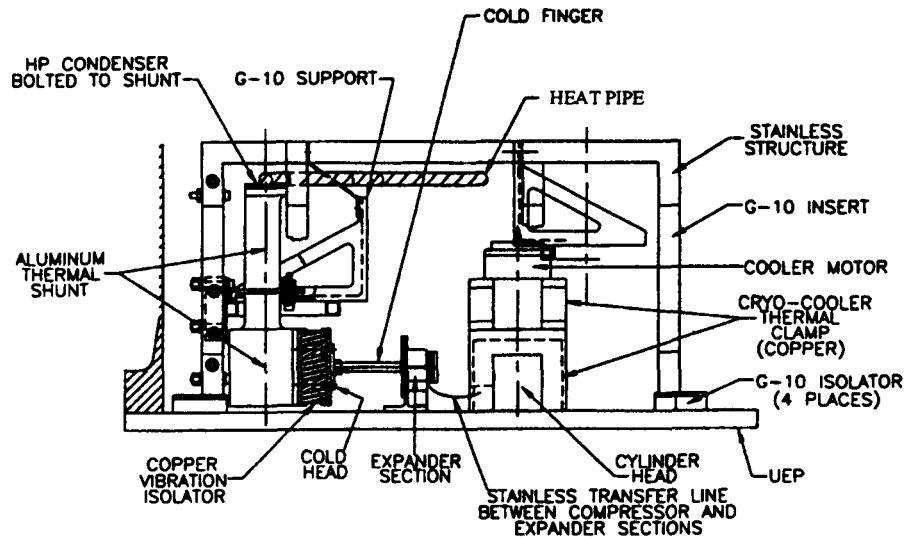


Figure 4. CTB Assembly

## ARAMID CORD HEAT PIPE SUSPENSION

An aramid cord retention system was used as the primary means of support for the cryogenic heat pipes on the CRYOHP and CRYOTP flight experiments. This system was implemented to support the heat pipes during launch and landing loads and minimize the parasitic heat loads induced into the heat pipe. To fully understand the heat pipe support structure we will first describe the structural buildup to the heat pipes and then the heat pipe clamps themselves.

The rigid support of the UEP is transferred to the heat pipe location in the test bed by the heat pipe support structure (HPSS) as shown in Figure 4. This support structure is constructed of 19 mm (0.75") square stainless steel tubing welded in a truss structure with four base mounting pads. Thermal isolation between the UEP and the HPSS is provided by milled G-10 isolation pads between the mounting pads of the HPSS and the UEP and G-10 tubing inserts installed in the vertical legs of the HPSS. The HPSS is structurally attached by a fail safe attachment utilizing 1/4-20 hardware.

G-10 heat pipe support bodies shown in Figure 5 provide the rigid support for the cable attachment to the heat pipe and are attached to the HPSS by stainless steel hardware. The contact between the heat pipe support body and the HPSS is minimized by the low surface area of the body base in contact with the HPSS.

The cable attachment of the heat pipe is a wrap around method with locking pins to maintain tension in the required directions and a continuous load to keep the heat pipe from translating around its center line. Two parallel wrapped cables constructed of a 3 mm (0.12") diameter aramid weave are positioned perpendicular to the heat pipe, located 19 mm (0.75") apart forming a truss to the body attachment. The cable is installed by attaching the fixed end of the cable to the body and then wrapped around the heat pipe in the V-grooved rings epoxied to the heat pipe around the locking pins. The free end is brought through the body for tension screw attachment. Tension on the cable is adjusted by the tension screw located at the free end

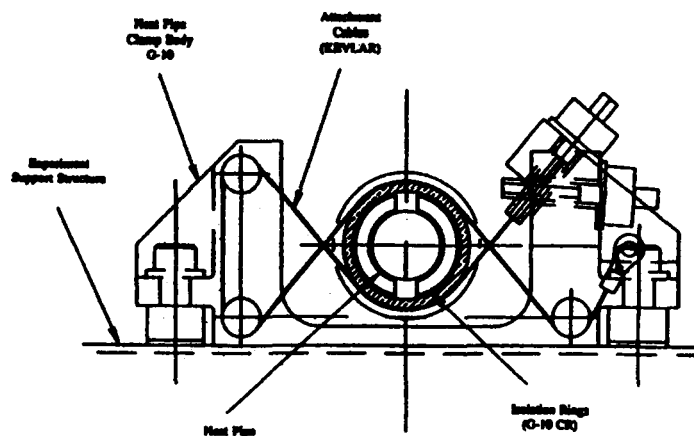


Figure 5. Heat Pipe Attachment and Isolation Support

of the cable. The tension setting for flight qualification is 25 lbs. Tension on the cable is maintained by self locking hardware between the body and the tension screw.

Two unexpected problems occurred during the development of the design:

- If the cable is continuous without locking at the pin locations the heat pipe could translate within the G-10 bodies.
- The tensioning system must have the ability to accommodate stretch in the cable due to the tension over time.

The continuous cable problem was eliminated by installing locking pins at the body pin locations and fixing the cable after final tensioning.

Accommodating the stretch in the cable due to tension over time was performed by using convex washers in the tension mechanism. The convex washers were stacked in an opposing orientation between the locking hardware of the tension screw and the heat pipe support bodies.

Course positioning of the heat pipe in the x-y coordinates of the experiment was accomplished by loosening the cables at the tension screws and physically locating the pipe at the correct level. The tension screw was then torqued to the proper tension and the cable was secured by tightening the locking pins. It is important to understand that the transitional stretch and adjustment of the cable is performed over time with periodic checks before locking down the pins. Fine elevation adjustment for the heat pipe is then provided by stainless steel shims between the HPSS and the heat pipe support body.

## CRYO-COOLER VIBRATION ISOLATION MOUNT

The CTB flight experiments contained five tactical cryogenic split Stirling cycle coolers. These coolers were installed in the CTB experiments in the configuration as illustrated in Figure 6. The heat conductance and structural support coincide in this mounting configuration. The major portion of the heat is dissipated from the coolers in three locations: the compressor body, the cylinder head of the compressor, and the expander body. The compressor bodies and cylinder heads are heat sunk and rigidly mounted to the oversized, UEP by solid copper mounts on the three cooler side of the test bed and aluminum mounts on the two cooler side (aluminum was utilized to reduce mass and was possible due to the lower heat load 200 vs. 300 W) and the expander body is heat sunk and rigidly mounted to the UEP by gold plated mounts. All body mounting locations used graphite foil as a thermal interface material. The coolers are configured on the UEP as illustrated in Figure 6. This configuration optimizes the amount of coolers and provides two independent test beds.

These coolers produce a vibration due to their internal working system. As illustrated in Figure 7 the vibration induced from the coolers originates from three locations in the system; the

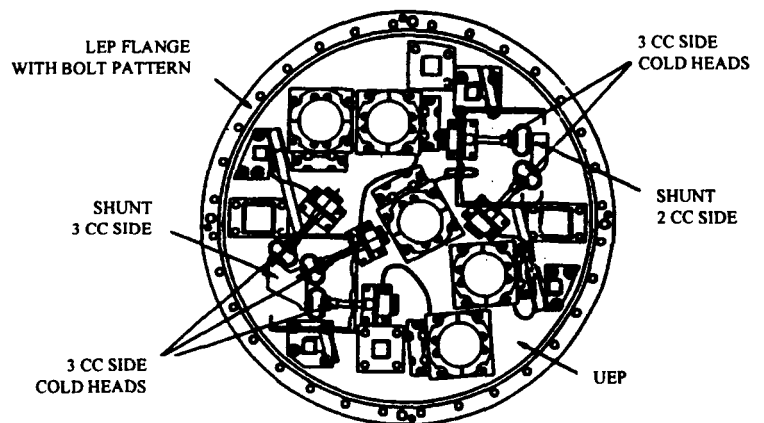


Figure 6. CTB Cry-Cooler Configuration

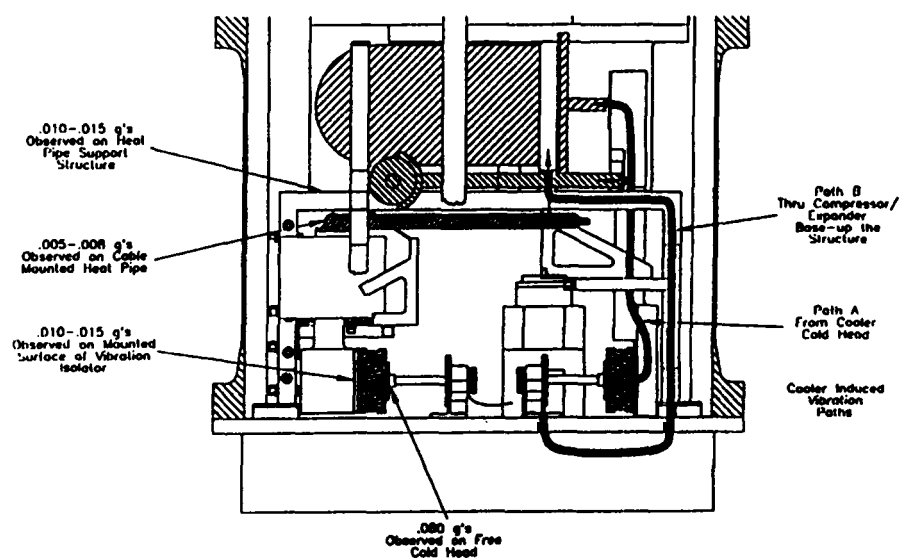


Figure 7. CTB Cry-Cooler Induced Vibration

compressor body, the expander body and the cold head of the expander. The expander and compressor bodies were hard mounted to the UEP and vibration loads are transmitted up to the experiment area through the heat pipe support structure. The majority of the vibration is induced by the piston in the expander tube and is applied at the cold head of the coolers. This induced vibration is translated directly to the test articles through the thermal shunt.

During the development of the mounts, tests were performed to characterize the vibration induced at the cold head of the coolers. A cooler was mounted on the UEP in the flight configuration. The base of the compressor and expander bodies were rigidly mounted with graphite foil between the interface to reflect the flight configuration. This test set-up was fully instrumented providing vibration readings across the UEP and on the cold head of the cooler. The most severe vibration was emitted in line with the expansion tube perpendicular to the cold head having a magnitude of approximate 80 milli-g's. The result was consistent across the several tests performed.

The development of the vibration isolation system between the cold head and the experiment interface required a design study to evaluate the following parameters:

- thermal conductance
- vibration isolation
- load, induced on the cold head
- envelope available
- cost

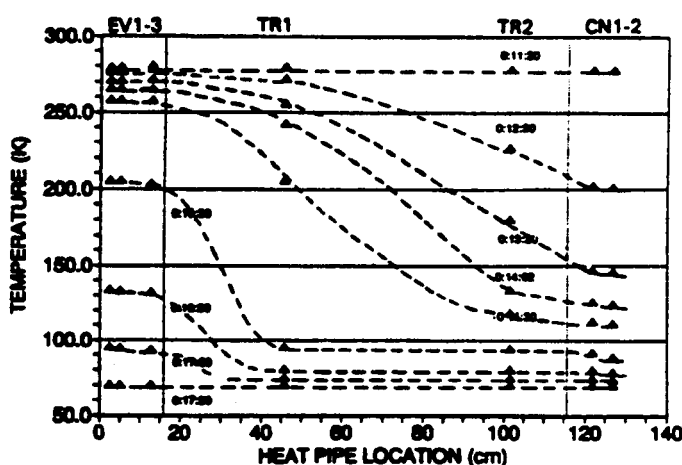
The design team developed a simple copper braided vibration isolation mount to be mounted between the individual cold plate head of the coolers and the thermal shunt. This thermally conductive vibration isolator is constructed of copper braid sandwiched between two copper plates at each end. Epoxy was used to bond the copper plates with the braid.

Tests were run with full instrumentation mapping the test bed including a sample heat pipe. The results of the total assembly are illustrated in Figure 7. The resulting conductance across the mounts was approximately 2 W/°C and the mounts in the configuration of the test bed reduced the vibration across the isolation mounts to .010-.015 milli-g's and at the heat pipe to .005 to .008 - Milli-g's.

It is important to understand the test bed configuration, the oversized UEP and aramid cable heat pipe mount in combination with the vibration isolators, achieved the results.

### CRYOHP (CTB I)

The first flight of the CTB tested two axially grooved oxygen heat pipes. Heat Pipe #1 was 11.2 mm in diameter and had a special groove geometry that was intentionally degraded so that its transport capacity could be tested within the limits of the CTB's cooling capacity (~ 5 watts net at 80 K). Heat Pipe #2 was 15.9 mm in diameter and had a transport capacity that exceeded the capacity of the CTB permitting demonstration of priming from the super critical state and transport but not transport limit verification or recovery demonstration.. These heat pipes provided the first available flight data



for cryogenic heat pipes that operate below 100 K.

## Heat Pipe #1

The first cooldown of Heat Pipe #1 started at mission elapsed time (MET) 11:22. Figure 8 shows the axial temperature profile for the first transient cooldown of Heat Pipe #1. The cooldown took approximately 6 hours. The heat pipe condenser was cooled to the critical point of oxygen in two hours marking the beginning of condensation. The cooldown was performed three times and all were essentially identical. Figure 9 compares the flight performance of the heat pipe with the pre-flight ground testing. The flight data has been adjusted by an equivalent 0.45 watts evaporator heat load to adjust for a 0.8 watt parasitic heat load. The flight data is in reasonably good agreement with the groove analysis program (GAP) predictions. The flight performance is consistently 0.4 to 0.6 watts below the GAP predictions which was used to improve the model.

## Heat Pipe #2

The first cooldown of Heat Pipe #2 started at MET 22:18. Figure 10 shows the axial temperature profile for the first transient cooldown of Heat Pipe #2. The cooldown took approximately 6.5 hours, the increased time compared to Heat Pipe #1 is due to decreased cooling capacity of the two cooler side of the experiment. The heat pipe condenser was cooled to the critical point of oxygen in 3.25 hours marking the beginning of condensation. The cooldown was performed twice and both were essentially identical. Figure 11 compares the flight performance of the heat pipe with the pre-flight ground testing. The flight data has been adjusted by an equivalent 0.64 watts evaporator heat load to adjust for a 1.14 watt parasitic heat load. The flight data is in good agreement with the GAP predictions.

We attempted a third flight cool down of the heat pipe however the cryo-coolers did not perform well. The UEP was at 332 K (59°C) when we turned them on and the cold heads were at 277 K (4°C). Post flight testing and discussions with the manufacturer has led us to believe that the high cooler temperatures had driven all system moisture to the cooler cold heads where it froze when the cold heads reached 0°C. The units had fully recovered after time and performed nominally during post flight testing.

## CRYOTP (CTB II)

The second flight of the CTB tested the BETSU and a nitrogen heat pipe (NHP). The BETSU is a phase change material (PCM) canister using 35 grams of

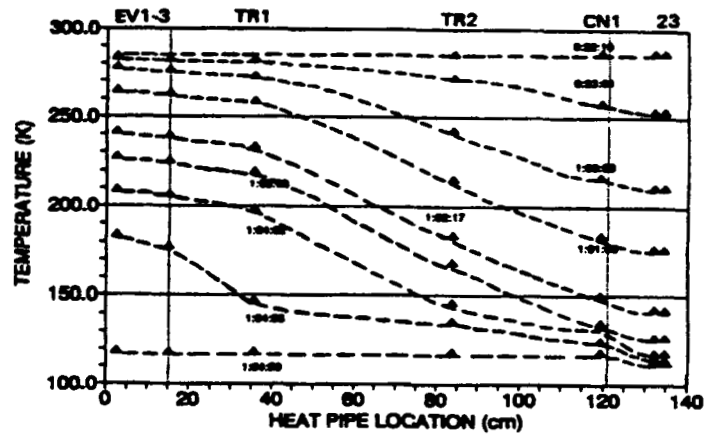


Figure 10. Axial Profile of Heat Pipe #2 Transient Cooldown

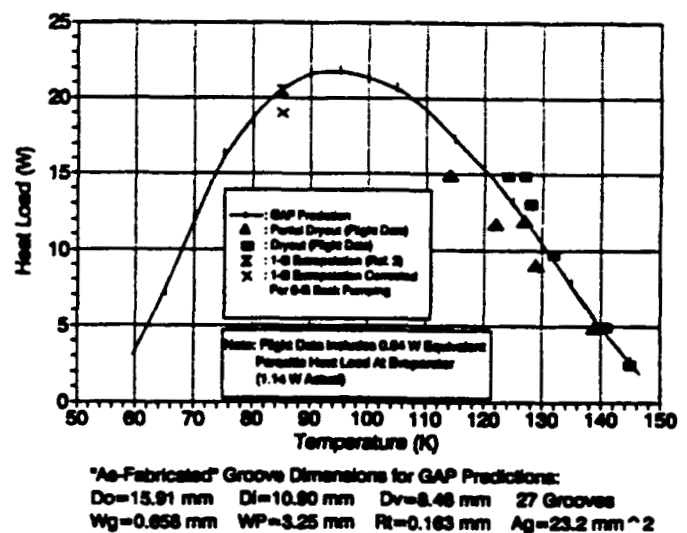


Figure 11. Heat Pipe #2 Transport Capability  
(PCM Hot Side)

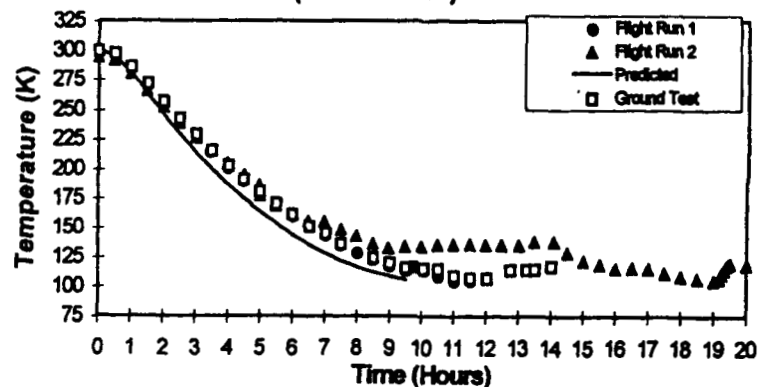


Figure 12. Comparison of BETSU Ground and Flight Transient Cooldowns

2-methylpentane with 3% acetone added. The BETSU provides 2500 Joules of energy storage with a freeze/thaw point at 120 K. The NHP was fabricated from titanium - Ti-6Al-4V (ELI), has a 15 mm diameter and is charged with 24.1 grams of nitrogen.

## BETSU

The assembly of the BETSU is shown in Figure 3. The first BETSU cooldown started approximately 23 hours MET. Figure 12 presents the cooldown data for two flight cycles and compares them to ground and predicted data. On the first cooldown cycle the PCM did not freeze until it was cooled to 105 K and the temperature climbed to 117.5 K as the heat of fusion was released. The second cycle was nearly the same with supercooling occurring at 105.4 K and freezing at 119.8 K. More than 200 hours of on-orbit data consisting of fifty-five freeze/thaw cycles and 26 steady state calibrations were completed. Results from ground and flight tests show that virtually all of the stored energy (2472 J) is realized during the phase cycling. Temperature control at  $119 \pm 1.5$  K was demonstrated with a one watt heating rate.

## NHP

The cooldown of the NHP was initiated within minutes of CRYOTP turn on. Figure 13 shows the axial profile of the transient cool down. A second cycle was performed on day 6 of the mission. The NHP did not isothermalize in either cycle. Both cycles had similar cool down profiles. The anomaly was initially attributed to an excessive liquid slug, however, further analysis has been performed and a paper was presented on this topic at the International Heat Pipe Conference in Albuquerque in 1995. That paper points to design issues that need to be addressed when designing cryogenic heat pipes to prevent the anomaly that the NHP demonstrated on orbit.

## CRYOFD (CTB III)

The third flight of the CTB will test two cryogenic flexible diode heat pipes. One heat pipe will be an oxygen pipe and the other will be charge with methane. The oxygen heat pipe will be tested over the temperature range of 60 - 100 K and the methane heat pipe will have a nominal operating temperature of 120 K. The flexible nature of the CFDHPs will allow for differential thermal contraction and expansion for large temperature gradients and dissimilar materials. The diode operation will isolate an instrument from redundant (or failed) cryo-coolers, or a hot radiator.

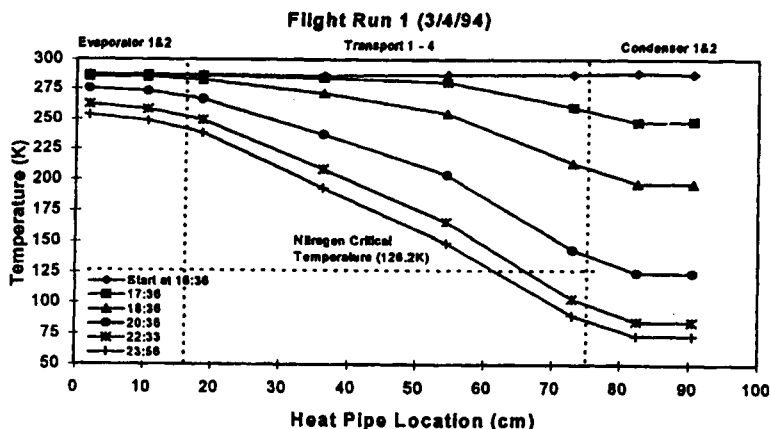


Figure 13. Axial Profile of NHP Cooldown

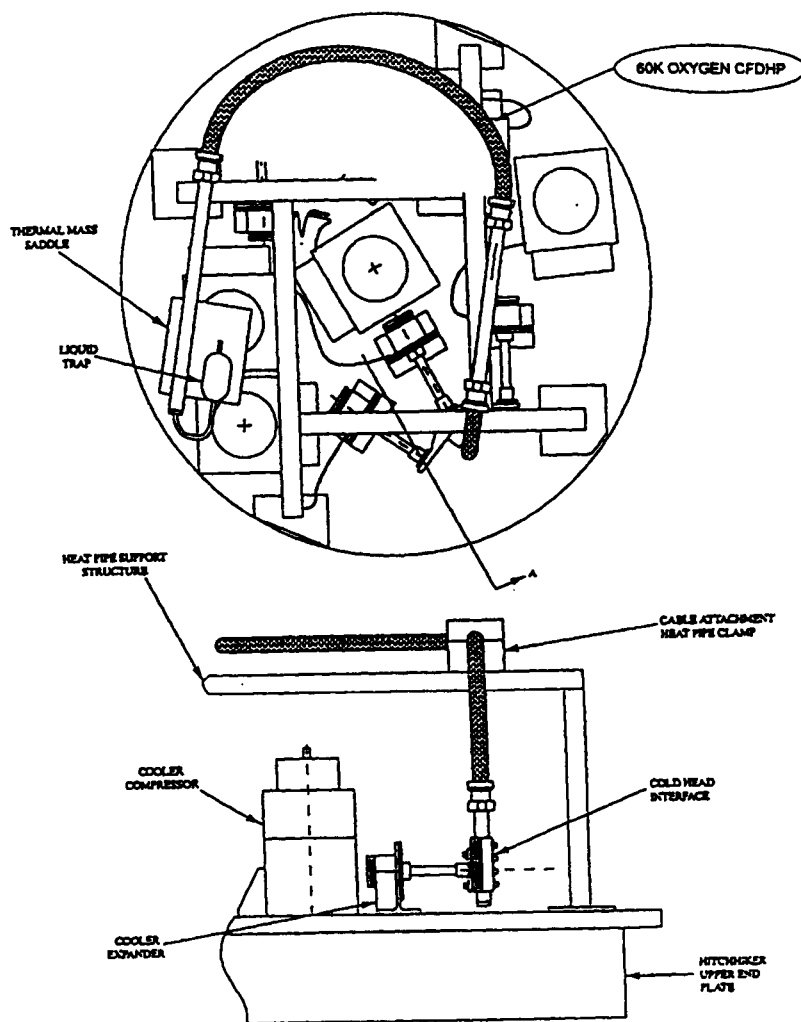


Figure 14. CRYOFD Configuration



## Acronyms:

BETSU	Brilliant Eyes Thermal Storage Unit	IVT	Interface Verification Test
CECM	CTB Electronics Control Module	JSC	Johnson Space Center
CoP	Coefficient of Performance	K	Kelvin(s)
CRYOFD	Cryogenic Flexible Diode Experiment	LEP	Lower End Plate (of a HH canister)
CRYOHP	Cryogenic Heat Pipe Experiment	LN <sub>2</sub>	Liquid Nitrogen
CRYOTP	Cryogenic Two Phase Experiment	MET	Mission Elapsed Time
CTB	Cryogenic Test Bed	MLI	Multi Layer Insulation
EMC	Electromagnetic Compatibility	NHP	Nitrogen Heat Pipe
EMI	Electromagnetic Interference	NSTS	National Space Transportation System
GAP	Groove Analysis Program	PCM	Phase Change Material
GSE	Ground Support Equipment	PDB	Power Distribution Box
GSFC	Goddard Space Flight Center	PRT	Platinum Resistance Thermometer
HH	Hitchhiker	UEP	Upper End Plate
HPSS	Heat Pipe Support Structure		

## References:

1. Brennan, P., Stouffer, C., Thienel, L., and Morgan, M., "Performance of the Cryogenic Heat Pipe Flight Experiment" SAE Technical Paper Series number 921408, July 1992.
2. Brennan, P., Thienel, L., Swanson, T., and Morgan, M., "Flight Data for the Cryogenic Heat Pipe (CRYOHP) Experiment" AIAA Paper number 93-2735, July 1993.
3. Brennan, P., Thienel, L., Stoyanof, M., Bello, M., "Design and Performance of the Cryogenic Two Phase Flight Experiment" SAE Technical Paper Series number 941474, June 1994.
4. Brennan, P., Thienel, L., "Cryogenic Heat Pipe Technology" NASA/GSFC Capillary Pumped Loop Workshop IV, September 1994.
5. Thienel, L., Stouffer, C., Brennan, P., "The Cryogenic Test Bed, A Discussion of Techniques Used and Lessons Learned Through Two Shuttle Flights (STS-53 and STS-62)" 1st Annual Spacecraft Thermal Control Symposium, 16 - 18 November 1994, Albuquerque, New Mexico.

## **EXPERIMENTAL RESULTS FROM THE THERMAL ENERGY STORAGE-1 (TES-1) FLIGHT EXPERIMENT**

Lawrence W. Wald, Carol Tolbert, and Dr. David Jacqmin

NASA Lewis Research Center

### **ABSTRACT**

The Thermal Energy Storage-1 (TES-1) is a flight experiment that flew on the Space Shuttle Columbia (STS-62), in March 1994, as part of the OAST-2 mission. TES-1 is the first experiment in a four experiment suite designed to provide data for understanding the long duration microgravity behavior of thermal energy storage fluoride salts that undergo repeated melting and freezing. Such data have never been obtained before and have direct application for the development of space-based solar dynamic (SD) power systems. These power systems will store solar energy in a thermal energy salt such as lithium fluoride or calcium fluoride. The stored energy is extracted during the shade portion of the orbit. This enables the solar dynamic power system to provide constant electrical power over the entire orbit.

Analytical computer codes have been developed for predicting performance of a space-based solar dynamic power system. Experimental verification of the analytical predictions is needed prior to using the analytical results for future space power design applications. The four TES flight experiments will be used to obtain the needed experimental data. This paper will focus on the flight results from the first experiment, TES-1, in comparison to the predicted results from the Thermal Energy Storage Simulation (TESSIM) analytical computer code.

The TES-1 conceptual development, hardware design, final development, and system verification testing were accomplished at the NASA Lewis Research Center (LeRC). TES-1 was developed under the In-Space Technology Experiment Program (IN-STEP), which sponsors NASA, industry, and university flight experiments designed to enable and enhance space flight technology. The IN-STEP Program is sponsored by the Office of Space Access and Technology (OSAT).

### **INTRODUCTION**

The Thermal Energy Storage (TES) experiments are designed to provide data for understanding the long-duration microgravity behavior of thermal energy storage fluoride salts that undergo repeated melting and freezing. Such data have never been obtained before and have direct application to using space-based solar dynamic power systems. These power systems will store solar energy in a thermal energy salt such as lithium fluoride (LiF) or a eutectic of lithium fluoride/calcium difluoride (LiF-CaF<sub>2</sub>). The energy is stored as the latent heat of fusion when the salt is melted by absorbing solar thermal energy. The stored energy is then extracted during the shade portion of the orbit, enabling the solar dynamic power system to provide constant electrical power over the entire orbit.

The principal investigator of the TES-1 experiment was David Namkoong, of the Space Power Technology Division at the NASA Lewis Research Center (LeRC), Cleveland Ohio. Project management for the experiment was performed by Andrew Szaniszló, of the LeRC Space Experiments Division. Task work was accomplished by an in-house project team consisting of LeRC and NYMA Technology, Inc., engineers and technicians. The project was supported by the NASA Headquarters Office of Space Access and Technology.

## BACKGROUND

An advanced solar dynamic power system utilizing either a Brayton or Stirling Power Conversion System has the potential for high efficiency with weight, cost, and area advantages over other solar power systems. When operating in a low earth orbit (LEO), the power system will experience a sun/shade cycle which is on the order of 60 minutes sun and 34 minutes shade. Delivery of continuous electric power over the entire orbit requires a method of storing energy during the sun cycle for use during the shade cycle. An efficient method of accomplishing this is to utilize the high heat-of-fusion associated with TES phase change materials. These TES materials possess the physical properties that are desirable in advanced solar dynamic heat receiver designs. Such properties include high values of the heat-of-fusion, very low toxicity and are generally non-corrosive. However, they also possess properties of low thermal conductivity, low density, and most significantly, high specific-volume change with phase change. This last characteristic leads to formation of a void, or voids, that can degrade heat-receiver energy transfer performance by the formation of local hot spots on the container wall or local distortion of the wall. Since void formation and location are strongly influenced by gravitational forces, it is necessary to be able to understand and predict this phenomenon in the on-orbit microgravity environment in order to achieve optimum design for the heat receiver canisters. This is especially important since the canister and heat receiver are significant elements of the overall weight and cost of a SD power system.

Dr. David Jacqmin, of the LeRC Internal Fluid Mechanics Division, has developed the TESSIM (Thermal Energy Storage Simulation) computer code. TESSIM can predict the migration of voids and the resulting thermal behavior of SD receiver canisters. It is currently useful as a qualitative design tool but requires further experimental validation before it can be reliably used for critical design decisions. Once thoroughly validated, the code will be invaluable in the detailed design of lighter, more efficient solar dynamic receivers.

## PROJECT OBJECTIVE

The objective of this flight project work is to develop and flight-test long-duration microgravity experiments for obtaining data that characterize the void behavior in TES fluoride salts. This project is the first in which TES materials will be subjected to an extended microgravity environment during a number of phase change cycles.

## EXPERIMENT APPROACH

Four experiments are needed to provide the necessary data to validate the TESSIM computer code. The first two flight experiments, TES-1 and TES-2, were developed to obtain data on PCM behavior in cylindrical canisters. The TES-1 and TES-2 experiments are identical except for the fluoride salts to be characterized; TES-1 uses lithium fluoride (LiF) salt which melts at 1121 °K, and TES-2 uses a fluoride eutectic salt (LiF/CaF<sub>2</sub>) which melts at 1042 °K. Both experiments use a sealed cylindrical canister fabricated from Haynes-188 steel to contain the salts. Flight data are stored in the random access memory of each payload. A postflight tomographic scan of each TES canister will provide data on void location, size, and distribution for comparison with preflight predictions.

The final two experiments, TES-3 and TES-4, currently under development, will obtain data on PCM behavior in wedge-shaped canisters. TES 3 will use LiF salt, with a canister interior that is wetting to the salt. TES 4 will use the same LiF salt with a canister interior that is non-wetting to the salt.

## FLIGHT HARDWARE

The TES-1 payload consists of the three hardware subsystems (Fig. 1). The top section, or the experiment section (Fig. 2), is made up of a cylindrical canister assembly, a two-zone radiant heater, high-temperature multilayer insulation (MLI), and an MLI shutter and drive mechanism. The entire canister assembly is enclosed within the MLI and MLI shutter. The primary components of the canister assembly are the Haynes-188 canister, the boron nitride radiant heater, and the thermal radiator disc. The canister has an annular cross section with a solid conductor rod of Haynes-188 in the center of the annulus. The purpose of the rod is to conduct heat away from the inside of the canister to the radiator disk, simulating the thermal response of a SD power system. The annular cylindrical volume contains the TES salt. The canister is welded closed in a vacuum after the salt is loaded into the canister. The experiment section also includes

temperature measurement instrumentation, consisting of swaged 20-mil, type K thermocouples at many different locations in the section.

Thermal energy needed to melt the TES salt in each canister is provided by the two-zone radiant heater. The cylindrical heater material consists of boron nitride with a graphite conductive path. Two radiant heater zones create a temperature difference in the salt resulting in buoyancy forces in the molten salt which are large compared to the low gravitational forces present during space flight. In general the buoyancy forces cause any void to move towards the high-temperature zone of the heater. Prior to launch the void is preferentially located by melting the salt in the canister, with the canister in the desired orientation in a 1-g field.

During the freeze portion of the cycle the MLI shutter mechanism opens the shutter doors (2) to allow the radiator disk to transfer heat to the top of the GAS can lid. At the completion of the freeze cycle the mechanism closes the shutter doors in preparation for the next heating cycle or at the completion of the experiment.

The middle section of the TES-1 payload is occupied by the data acquisition and control system (DACS), which controls heater power levels and the MLI shutter operation. The DACS also periodically records the instrumentation output signals. An 80386SX central processing unit is used in the DACS to provide the needed data collection speed and processing. Solid state memory is used for on-orbit data storage of temperatures and experiment engineering data. In addition to the DACS, independent high-temperature control units are located in this section in order to provide added control for maintaining a safe maximum temperature level associated with these 1200 °K temperature level experiments.

The bottom section consists of a battery box that contains 23 silver-zinc cells which provide all the electrical energy required for the two-zone radiant heater and the DACS. Each cell contains a potassium hydroxide electrolyte. The initial electrical energy level provided by the battery box for each payload prior to placement in the shuttle is about 6300 Wh., which accounts for any battery degradation over time. The energy expected to be used on-orbit by each experiment is about 3400 Wh.

The TES-1 experiment was mounted on a HH-M bridge, along with the other OAST-2 experiments, and placed within the payload bay of the shuttle. TES-1 occupied roughly 0.14 m<sup>3</sup> (5 ft.<sup>3</sup>) and had a mass of roughly 110 kg prior to placement in the GAS payload container.

## OPERATION SEQUENCE

The operations sequence for TES-1 is shown in Fig. 3. Upon launch, the GAS Payload container is vented into the payload bay and ultimately to space. After a minimum of 24 hours, which provides for an adequate vacuum environment to be achieved in the payload, the experiment is activated by an astronaut and begins a 5-hr heatup phase. After the heatup phase the on-orbit melt-and-freeze thermal cycles begin. A total of four thermal cycles over a 10-hr period are needed for characterizing the void behavior of the TES salt in a 10<sup>-3</sup> g environment.

The desired time for the experiment heating cycle was 60 minutes, which would simulate the solar heating period for a typical LEO SD power system. The actual heating cycle time was about 80 minutes, due to the requirement to minimize thermal gradients and hence thermal stress of the Haynes 188 canister. The circumferential heater was designed from ground test data to provide the necessary heating to transition the salt from the incipient melt state to the fully molten condition within the 80 minute period.

The freeze or solidification phase of a thermal cycle is initiated when heater power is turned off and the MLI shutter is opened. This period was desired to be roughly 30 minutes but the experimental time was about 60 minutes, due to the design of the experiment section. Thermal energy dissipation needed to freeze the salt is achieved by conducting the thermal energy out of the salt into the solid rod in the center of the canister, and from the rod to the thermal radiator disc. The disc radiates the stored thermal energy (latent heat of fusion for the salt) to the GAS payload container upper end-plate. This plate in turn radiates the thermal energy out to space. At the end of the freeze phase, the MLI shutter is then closed and the next melt cycle begins.

Flight data is recorded at 5-min. intervals and primarily consists of the time variation of temperatures and heater power during the heatup to incipient melt, melt-and-freeze, and cool-down phases of the experiment. Other data include the time elapsed from the startup of the experiment, time of each data sample, power level, and estimated electrical energy remaining in the battery cells. After the thermal cycles are completed and the experiment section cools down to approximately 750 °K, the experiment is deactivated by the crew. At this point, a vent valve in the GAS payload container is closed to seal off the GAS container prior to the shuttle de-orbit.

## FLIGHT DATA AND RESULTS

TES-1 was flown on STS-62 in March 1994. TES-1 was activated by the crew 48 minutes prior to the desired time of activation. This moved part of the first melt/freezing cycle into a time that coincided with astronaut activity and subsequently some higher level of environmental g forces. The remaining three melt/freezing cycles did coincide with the desired low g period of crew pre-sleep and sleep activities. TES-1 operated for roughly 14 hours in space.

From the data collected on-orbit Fig. 4 shows one set of thermocouple locations and the temperatures from the canister recorded during the four melt/freezing cycles of the LiF salt. The first melt cycle shows some erratic behavior when compared to the remaining three melt/freezing cycles. This was believed to be caused by migration of the void and/or by the g forces present during this period. In general, after the first melt/freezing cycle, the temperatures show repeatability from cycle to cycle at each location.

After the data was downloaded from the experiment, TES-1 was partially disassembled and the canister removed. Computer-Aided Tomographic (CAT) scanning was performed on the canister in order to record the final location and distribution of the voids in the canister. Figure 5 [ref. 1.] shows the tomographic data taken on the TES-1 canister for nine "stations" along the length of the canister along with the predicted results from TESSIM. Salt locations are shown in black. In general, TESSIM appears to have predicted void behavior accurately, as is evidenced by comparing the tomographic images with the TESSIM images. These initial results from TES-1, of high-temperature fluoride salt melting and freezing under microgravity, do not absolutely validate TESSIM, but the comparison of the predictions with the data establishes a basic confidence in the code. Future experiments such as TES-2, 3 and 4 will contribute to further validation of TESSIM.

## CONCLUSIONS

The TES-1 flight experiment has provided the first experimental data on the long duration effects on TES salts used for space-based solar dynamic power systems. Good correlation between the predicted on-orbit characteristics of the salt and the actual flight data indicate that, for the configuration tested, the TESSIM code is basically sound. The additional flight experiments in the four experiment suite will provide the opportunity for the complete validation of the TESSIM code. The flight experiments will provide data from different canister configurations and both wetting and non-wetting interfaces for the TES salts. In addition, the effect of heat leakage will be studied more closely.

## REFERENCES

1. David Namkoong, David Jacqmin, and Andrew Szaniszló: "Effect of Microgravity on Material Undergoing Melting and Freezing-The TES Experiment" NASA TM 106845, Lewis Research Center, Cleveland Ohio. Presented at the 33 Aerospace Sciences Meeting and Exhibit, sponsored by the American Institute of Aeronautics and Astronautics, Reno, Nevada, January 1995.

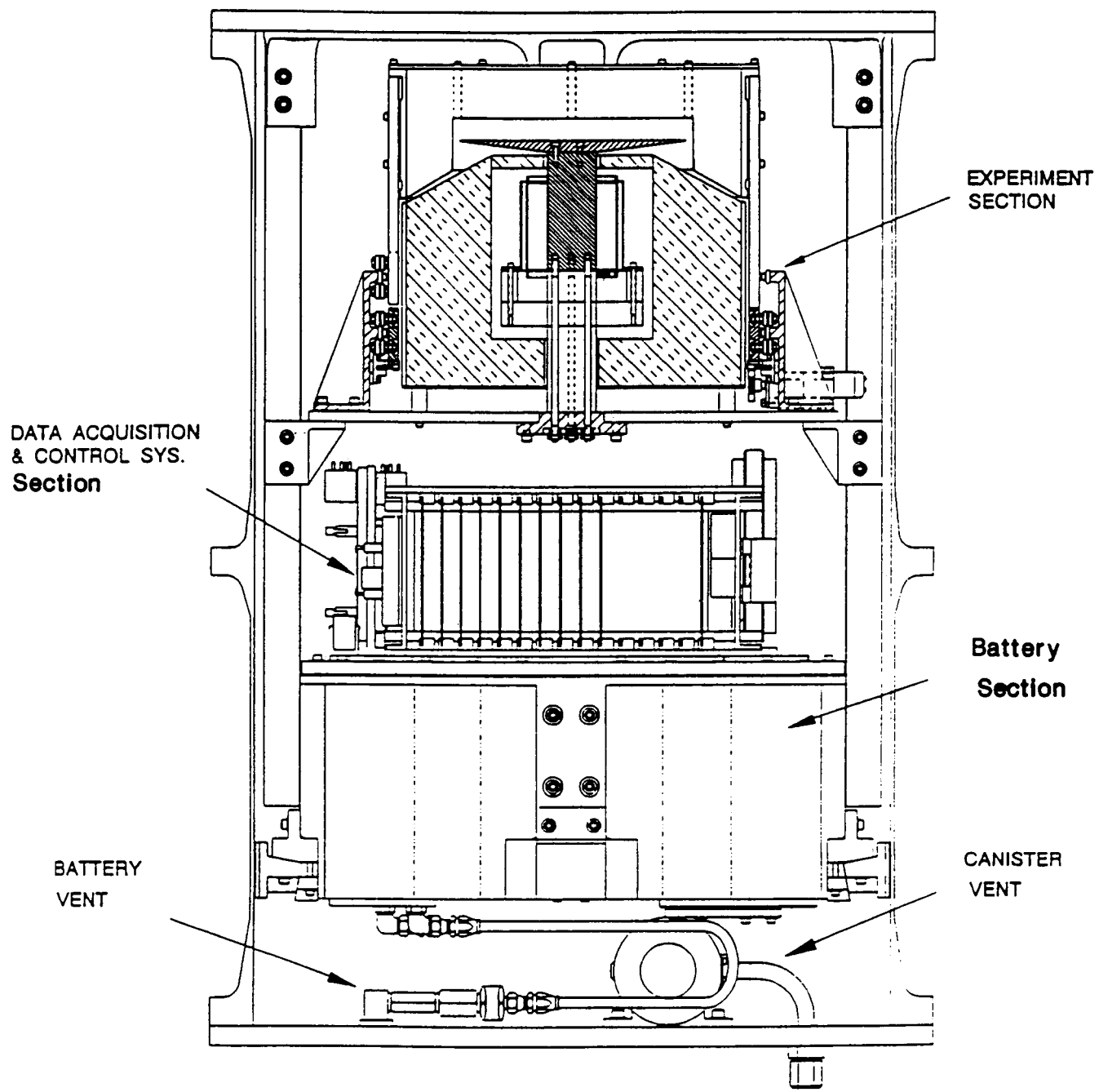
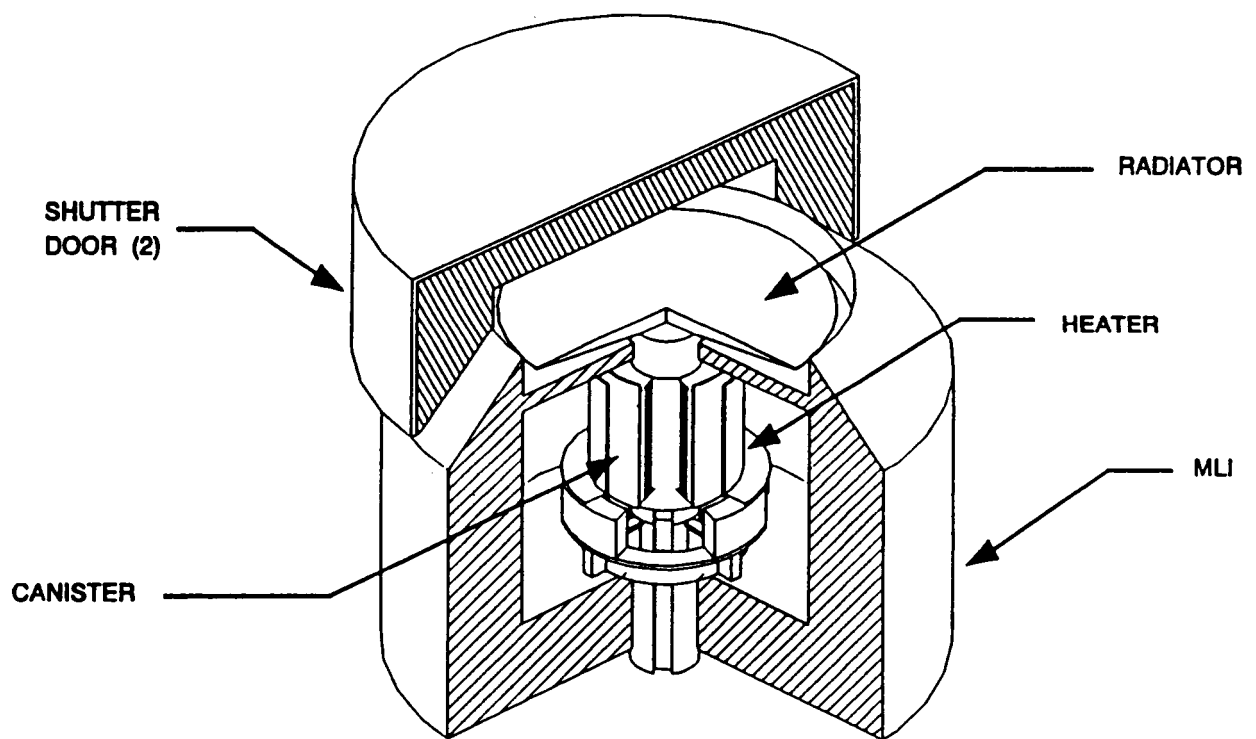


Fig. 1 TES-1 Payload



**Fig. 2 TES-1 Experiment Section**

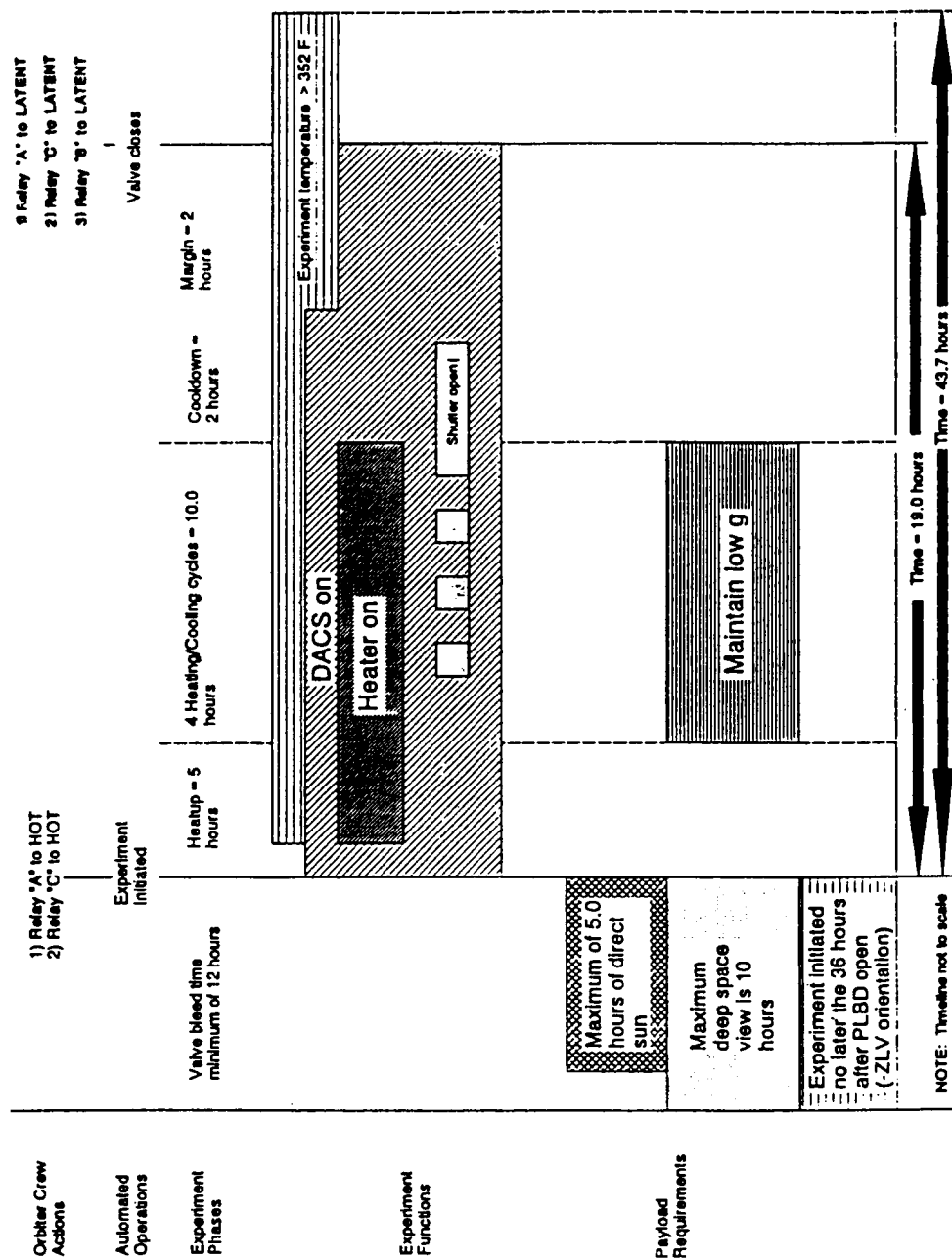


Fig. 3 TES-1 On-Orbit Operations Timeline



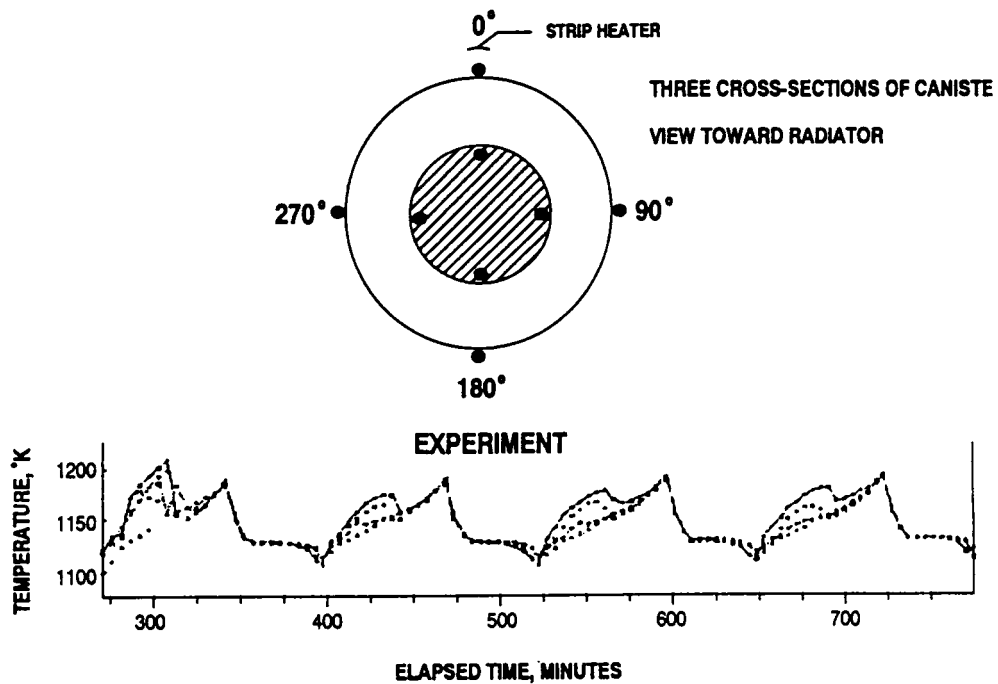


Fig. 4 Canister Temperatures vs. Time

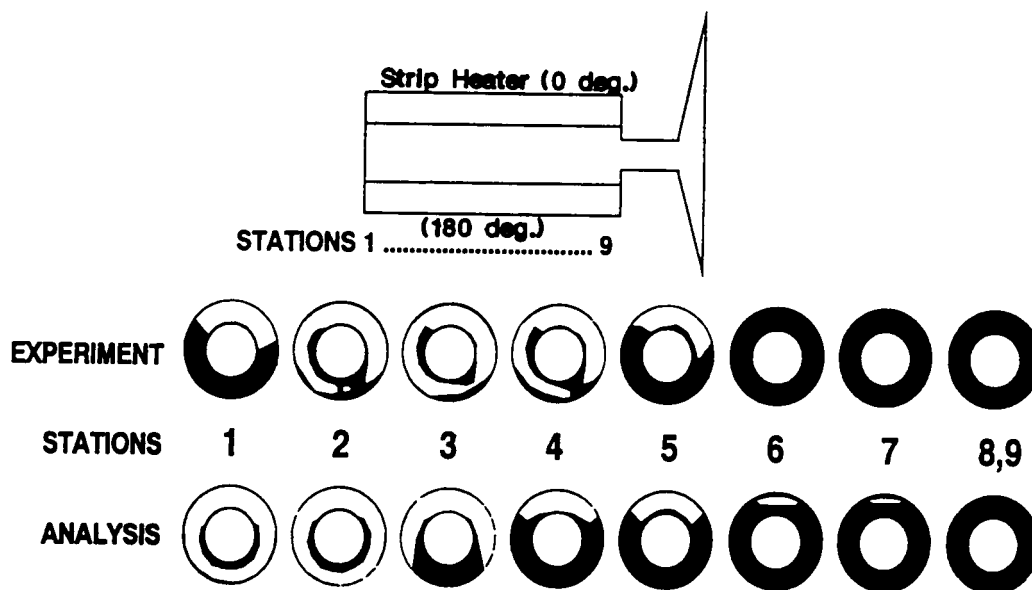


Fig. 5 Comparison of Void Location  
Between TESSIM and Flight Data

# ON THE HITCHHIKER ROBOT OPERATED MATERIALS PROCESSING SYSTEM EXPERIMENT DATA SYSTEM

Semion Kizhner and Del Jenstrom  
NASA Goddard Space Flight Center, Greenbelt MD

## ABSTRACT

The Space Shuttle Discovery STS-64 mission carried the first American autonomous robot into space, the Robot Operated Materials Processing System (ROMPS). On this mission ROMPS was the only Hitchhiker experiment and had a unique opportunity to utilize all Hitchhiker space carrier capabilities. ROMPS conducted rapid thermal processing of one hundred semiconductor material samples to study how micro gravity affects the resulting material properties. The experiment was designed, built and operated by a small GSFC team in cooperation with industry and university based principal investigators who provided the material samples and data interpretation. ROMPS' success presents some valuable lessons in such cooperation, as well as in the utilization of the Hitchhiker carrier for complex applications. The motivation of this paper is to share these lessons with the scientific community interested in attached payload experiments. ROMPS has a versatile and intelligent material processing control data system. This paper uses the ROMPS data system as the guiding thread to present the ROMPS mission experience. It presents an overview of the ROMPS experiment followed by considerations of the flight and ground data subsystems and their architecture, data products generation during mission operations, and post mission data utilization. It then presents the lessons learned from the development and operation of the ROMPS data system as well as those learned during post-flight data processing.

## ROMPS OVERVIEW

The Space Shuttle Discovery STS-64 mission carried the first American autonomous robot into space, ROMPS, in September of 1994. The ROMPS Hitchhiker experiment goal was to demonstrate commercial methods of processing semiconductor materials in a microgravity environment, namely rapid thermal processing of 100 thin film semiconductor material samples in space to improve the properties of the materials. The basis for this experiment is the fact that the performance of most semiconductor materials is dependent on their crystalline structure. Gravity driven convection and sedimentation, which disturb crystal formation, can be eliminated in the micro gravity of space. The crystal structures of material samples are reformed by ROMPS in heating and cooling cycles. The material processing was facilitated by an autonomous 4-degrees of freedom cylindrical robot (ref. 1).

ROMPS required two Space Shuttle sidewall mounted Get Away Special(GAS) cans, one containing the two furnaces, material samples, the robot, the furnace controller, and drive electronics; the other containing control electronics. Both cans were backfilled with one atmosphere of dry nitrogen to allow for the use of commercial grade and other non-vacuum rated components. The Hitchhiker avionics system provided ROMPS with power and with the communication channels for commands and telemetry.

The thermal-time processing profile for each material sample was parameterized by the Principal Investigators. These parameters were uploaded during the mission. The power to the halogen lamp parabolic focusing furnace was servoed using the parameters to cause the prescribed thermal-time profile at the furnace focus where a material sample is positioned by the robot. The material samples were housed in sample holders on individual pallets. The pallets were stored in six racks each capable of holding approximately 25 pallets. The job of sample pallet removal from a rack, placing the pallet into the furnace, holding for the duration of the

sample thermal-time profile, removal from furnace and returning to the rack was performed by the ROMPS robot.

ROMPS had several calibration samples representing each of the nine types of material samples. All calibration samples were processed first and actual temperature-time profiles were observed at the Payload Operations Control Center (POCC) using real time telemetry. The flight calibration data was compared with laboratory data obtained preflight. A calibration sample pallet has two thermocouples which contact the furnace spring leads when the sample is placed and held in contact with the furnace by the robot for the duration of processing. Thus the actual temperature was measured and telemetered to the POCC. The processing temperature profiles could then be adjusted by ground commands in the event that furnace lamp performance varied from preflight measurements.

ROMPS autonomous processing was organized into small sets of material samples. Each set was preceded and followed by processing of a corresponding material calibration sample to provide a frequent record of furnace performance. The processing of a set of material samples was initiated and controlled by ground commands, and telemetry was used in real time to monitor progress. The ROMPS experiment was capable of processing the entire compliment of material samples on-board without ground intervention once initiated. However, autonomously processing only small sets of samples at a time afforded several benefits; 1) processing during the frequent predictable telemetry outages could be avoided, 2) experiment performance could be analyzed prior to proceeding to the next set of samples, and 3) it was insured that processing took place only during designated ROMPS experiment operating periods. The processed samples were removed from the experiment after landing and studied at Principal Investigators (PI) laboratories to determine any resulting beneficial properties.

An experiment called the Capaciflector proximity sensor was added to the ROMPS robot for a flight demonstration of this sensing technology. After all material processing activities had been completed, the Capaciflector sensor was successfully used to demonstrate sensor-based robot control by guiding the robot to align and mate a material pallet to the processing furnace. Performance was monitored and verified by using the robot's own optical position encoders.

The entire ROMPS experiment and mission were facilitated and controlled by the ROMPS data system. The data system was developed primarily by the Space Automation and Robotics Center (SpARC) at the Environmental Research Institute of Michigan (ERIM), a NASA Center for the Commercial Development of Space (NASA CCDS), in conjunction with its commercial partners Interface and Control Systems, Inc. (ICS) and Zymark Corporation, under contract to the ROMPS project. Other portions of the data system were developed by ITE, Inc. of Laurel, MD., or they were developed in house at the NASA Goddard Space Flight Center (GSFC). The ROMPS data system consideration is used in this paper as the guiding thread to describe the ROMPS mission experience.

## **DATA SYSTEM DESIGN METHODOLOGY**

In keeping with the commercial orientation and goals of the ROMPS mission and the ERIM/SpARC NASA CCDS, the ROMPS data system was built around a number of commercially available products. This greatly influenced the design that emerged. Combining a commercial spacecraft control software package along with a commercial robot controller eliminated much of the low level system design and development typically required to build a control system, and resulted in a highly capable and flexible system. However, significant effort was expended tackling compatibility, interface, and reliability issues, and resulted in a hierarchical design of significant complexity.

Requirements for the data system were functionally partitioned into several groups for implementation - experiment control computer requirements, robot controller requirements, furnace controller requirements, and ground station requirements (ref. 2, 3). Functional partitioning is a contemporary structured design methodology. This methodology, along with current availability of commercial software and hardware technologies that can support this design methodology, allowed fast prototyping and development of the ROMPS data system. This approach also provided flexibility. For example, a few months before delivery of the ROMPS experiment a new experiment, the Capaciflector, was added to the configuration. The same methodology was used to rapidly change the ROMPS data system to include the Capaciflector telemetry and commands.

Significant use was made of commercial electronic boards. All commercial boards were properly supported, heat sunk, staked, and coated, using NHB-5300 as a guideline (ref. 6). Custom made boards used military grade parts where available. All hardware and software were thoroughly tested, including environmentally testing each electronic box prior to integrated testing with the rest of the experiment.

For reliability and safety reasons, each processor was equipped with a watchdog timer that would reboot the processor into a benign state should its software fail. A hardware watchdog override was also installed using one of the Hitchhiker discrete commands in the event that a watchdog timer failed, preventing operation of the system. In addition, due to safety concerns with the furnace, temperatures and lamp on-time were monitored in several different computers, and hardware/software interlocks were designed to prevent inadvertent lamp operation.

A Hitchhiker Carrier hardware emulator was developed by the ROMPS project. The emulator was configured in a single mobile rack and was used at different sites at GSFC and the Kennedy Space Center (KSC) for ROMPS payload development, integration and test (I&T), and post-mission payload checkout.

## **FLIGHT SYSTEM ARCHITECTURE OVERVIEW**

The flight data system consists of 4 computers as shown in Figure 1. Each are described below.

### **Spacecraft Command Language Computer (SCC)**

**Hardware:** Single Board 80286 equivalent 10MHz CPU, A/D converter and multiplexer boards.

**Function:** SCC ran a VERTEX operating system and two tasks, DataIO and Spacecraft Command Language (SCL), both commercial products of Interface and Control Systems, Inc. (ref. 4). The DataIO and SCL tasks were used as a command and telemetry interface to Hitchhiker avionics over an RS-422 1200 baud interface. The ROMPS telemetry downlink originated from 150 telemetry data sources at 1 or 30 second intervals. The SCC collected 48 discrete inputs, about 50 analog inputs, and actuated 16 discrete commands. It also derived many telemetry points that reported process parameters and status. SCC commanded the ROMPS robot by executing stored scripts or forwarding ground serial asynchronous commands. Commands to the robot were sent to the Easylab Computer over an RS-232-C 1200 baud serial asynchronous interface.

### **Easylab Computer (EZC)**

**Hardware:** Two board 80386 equivalent 20MHz CPU and quad serial board.

**Function:** EZC ran the Easylab System V Controller software, a commercial product of Zymark Corporation, which stored the high level functions and positions for the ROMPS robot

and furnace controller. It effected robot moves by sending commands to the XPC Controller over an RS-232-C 1200 baud interface. It effected furnace operation by sending furnace commands to the furnace controller over an RS-422 interface, and a single bi-level furnace enable control signal.

### **XP Computer (XPC)**

Hardware: Modified and repackaged Zymark Corporation XP controller based on 80C188 processor.

Function: XPC operated as a slave device to the above described EZC over its RS-232-C 1200 baud interface. The XPC provided low level servo control functions for the ROMPS robot.

### **Furnace Controller**

Hardware: 80C188 controller with assorted custom electronics.

Function: The furnace controller was connected to the EZC over an RS-422 interface to receive serial asynchronous commands that specify the temperature profile. It was also connected to EZC by a single bi-level voltage line. When this line was commanded high the furnace was turned ON and the thermal profile stored in the furnace controller was started; when the line was commanded low the furnace was turned OFF.

### **FLIGHT SOFTWARE**

SCC software was developed on a PC and tested on the developers SCC prototype card. The tested flight software was loaded into flight system RAM for testing and flight PROMs for I&T completion and the mission. The EZC was programmed on the ground development system prototype and loaded into EZC from SCC for ground tests. For flight configurations EZC PROMS were prepared and installed. The SCC ran the on-board SCL task with its database and the SCL run time engine for processing ROMPS scripts and rules. It also ran the DataIO task for data commutation and downlink, received commands from the HH avionics, and distributed the commands throughout the ROMPS flight data system (ref. 3). The software was developed incrementally and organized in five deliveries. The data system development was placed under strict configuration control three months prior to delivery of the payload to KSC, and frozen approximately 2 months prior to delivery.

### **FLIGHT SYSTEM/GROUND SYSTEM COMMUNICATIONS**

The telemetry and command rates were both 1200 baud. The experiment telemetry frame was 110- bytes long and the telemetry frame cycle was 1 second. The experiment housekeeping data frame was 50-bytes long on a 30-second cycle. Flight-ground dialog text messages were down linked in telemetry frames of variable length. During the ROMPS mission 90 Mbytes of telemetry were collected and 1600 command blocks were uplinked. The command and telemetry communication channels were provided by the Hitchhiker project.

### **GROUND SYSTEM ARCHITECTURE OVERVIEW**

The ground system requirements could most likely have been met using one powerful workstation. However, the ground system was implemented as a distributed system using several Macintosh computers. This distributed system was chosen for reasons of cost and compatibility with Spacecraft Command Language software. Its features included fast Ethernet interface of the computers into a 4-computer network, a copy of the ROMPS database on each computer, and database synchronization over the network. The primary ground system architecture is shown in Figure 2.

Once the primary ground system was integrated and tested in the POCC approximately 6 months prior to launch, the need to control that configuration required that it not be removed for travel to KSC for shuttle integration activities. Recognizing that this situation would occur, a second 2-computer ground system was developed that was used for activities at KSC. In addition, this system was used as a backup during flight operations. In parallel with the primary system, it received and archived ROMPS telemetry, and was available for payload commanding should the primary system go down.

## **GROUND SOFTWARE**

The four computers of the primary ground system were labeled RGSEA1 through RGSEA4. RGSEA1 ran the DataIO task. This task received telemetry from the HH Customer/Carrier Ground Support Equipment (CCGSE) and displayed the flight system dialog messages on the computer screen. It searched the raw telemetry stream for the ROMPS telemetry frame synchronization pattern (SYNC) and, when SYNC was found, DataIO checked the frame Cyclic Redundancy Code(CRC). When both the SYNC and CRC were correct, DataIO archived the telemetry frame to the archive data set. DataIO then updated the computer database and sent database updates to two of the downstream computers, the Display computer RGSEA2 and the Command computer RGSEA3. DataIO also encoded the symbolic commands received from the RGSEA3 Command computer into HH-format commands, wrote them to the archive file and then sent them to the CCGSE.

The Display computer RGSEA2 ran a DataIO task to receive database updates from RGSEA1 and synchronize its database with RGSEA1, and a LabVIEW task to graphically display ROMPS telemetry. The LabVIEW task retrieved items from the database using a specially developed SCL interface task.

The Command computer RGSEA3 ran the ground SCL task with its database and the SCL intelligent expert system run time engine for processing ROMPS scripts and rules. These were ground equivalents of corresponding flight software tasks. RGSEA3 also ran the SCL ROMPS Project Version 3.0. and the DataIO task to update its database. Commands to the flight experiment entered at this terminal were automatically forwarded by DataIO to RGSEA1 for reformatting and transmission to the HH CCGSE.

The RGSEA4 computer was used for off-line data processing. Updates to material processing parameter tables and processing schedule scripts were developed on RGSEA4. These updates were copied to the command computer through the 4-computer Ethernet for uploading to the flight system. RGSEA4 was also used for near-real-time processing of data products such as generating graphs of furnace performance.

## **OPERATIONAL PROCEDURES AND DATA ARCHIVES**

Thorough documentation is invaluable for maintaining control of and insuring efficient use of a data system. A complete set of ROMPS documentation was planned and systematically developed including software operators guides, a ground system user's guide, and a data products generation guide. These documents were used to develop operations procedures and served as main reference documents for ROMPS experiment I&T, flight operations, and post mission data processing.

ROMPS experiment operations were structured and controlled by developing a set of ROMPS operational procedures for each of four areas of ground operations competence: principal investigator (the team leader of a given ROMPS operating shift), lead operator (the single person on a given operating shift responsible for every command sent to the payload), operator (assistant to the lead operator in monitoring payload health and command generation),

and technical support (science principle investigators and other personnel with specific technical competence). In the lead operator's procedures, every command planned for the nominal mission was listed in order along with an estimated time required to implement each command. This proved to be invaluable for insuring that the proper commands got sent in the proper order, especially during the first few days of the mission when everyone was excited. This list was also very useful for planning which commands could be executed within each command window allocated to the ROMPS experiment throughout the mission.

In addition to individually outlining the responsibilities of each of the four positions, these procedures required that each individual manually record all significant events in a logbook designated to each position. These logbooks have provided redundant written records of mission events that have proven to be extremely useful in archive data interpretation.

The archive data sets automatically generated by the RGSEA1 DataIO task consisted of symbolic command log files (92K bites), ASCII files of dialog messages from the flight system (2.4 M bytes), and the main telemetry data set (approximately 90 M bytes). Similar archives of these last two data sets were also compiled by the backup ground system. The backup system did not archive commands since no commands were sent from it.

During the mission, the archived data sets were used to produce graphs of calibration sample temperature versus time. These were necessary to verify furnace performance prior to processing of actual material samples. Graphs of other flight system parameters were produced at various times during the mission, as well.

## **POSTMISSION DATA UTILIZATION**

Virtually all forms of data that were archived during the mission have since been used to analyze different aspects of the mission. The hand written logbooks have been used to make initial estimates of total flight operating time, total sample processing time, total functional test time, and total Capaciflector experiment time. Entries in these logbooks have also been used as guides for sifting through the hundreds of archive data files.

The symbolic command log files have been used to identify the time when each material sample was processed. This time ordered list was then used as a guide for extracting data from the telemetry archives to produce graphs of furnace power versus time for every material sample and sample temperature versus time for every calibration sample. These graphs are now being used to analyze system performance during the flight as compared to pre- and post-flight test performance - the ultimate goal being to determine if any correlations can be made to the samples that were processed on-orbit. In the case of three sample runs, data from the backup archives were used to produce the graphs because the primary archive files were incomplete due to intermittent problems with the primary system during the mission.

In addition to analyzing furnace performance, archive data has also been used for evaluation of on-orbit robot performance and experiment thermal performance (ref. 5).

## **KEY ASPECTS OF ROMPS DATA SYSTEM DEVELOPMENT AND OPERATIONS**

### **1) Rapid Telemetry and Command System Development**

A notable aspect of this complex NASA sponsored commercially oriented experiment was its rapid pace of development: critical design review to shuttle integration took less than 18 months. The novel methodology of arranging system requirements by function and use of commercial hardware and software allowed fast prototyping and data system development.

## **2) Highly Flexible Control System**

The ROMPS multilevel control system provided selectable degrees of autonomy - from highly interactive to totally autonomous. The principal investigators' ability to interact with their experiment in real time from the ground was a breakthrough in the ROMPS experiment.

## **3) Ground Station Based On Local Network of Macintosh Computers**

Use of the Macintosh computer's fastest interface available, Ethernet instead of LocalTalk, in a distributed ground system computer network resolved the largest part of inter-system performance throughput problems.

## **4) Encoding Of HH Command Issuance Timing Separation Formula**

Encoding of the HH format command issuance timing separation formula for uplink of long command sequences was needed to avoid HH Carrier command system overflow. During the mission, it was used to upload 10 Mbytes of the temperature-profile parameters and schedules. No command system overflows occurred.

## **5) Archive Telemetry Stream Delineated With HH Format Archived Commands**

The archive file of real time telemetry frames was also archiving uplinked commands in hexadecimal format. This archive of commands was in addition to the symbolic command archive. This facilitated the telemetry analysis of what happened as a result of one command issuance until the next command issuance. This form of command archiving was also useful because archived commands could be displayed in hexadecimal form and used to debug the HH format commands during the system development phase of the ROMPS project.

## **6) Leasing of Backup Ground System Computers**

The backup ground system computers were leased to reduce cost and provide computer delivery in a few days. It allowed the use of a separate system for I&T and prevented the break up of the primary system that was already at the POCC.

## **7) ROMPS Data System Hardware And Software Reusability**

In addition to using the ROMPS data system to re-fly the ROMPS experiment, the system might also be reused to support other GSFC Hitchhiker payloads due to its highly flexible design and proven performance.

## **LESSONS LEARNED**

**Lesson 1-** There is always at least one more customer on the mission besides you, namely the HH Carrier itself. HH Carrier designates three ID's for the HH Avionics commands issued by the carrier ground system. Because of this, you must always negotiate early with the HH Project for your needs and priorities, even when you think you are the only customer on your mission. All other non-Hitchhiker payloads during the mission also share with you the command channel and the low rate telemetry downlink, and compete for its bandwidth.

**Lesson 2-** CCGSE Command and Link packets are very useful during customer system development and I&T to verify the CGSE/CCGSE command and telemetry interface. These are not often used with a price paid in time lost during I&T and interface debugging.



**Lesson 3-** Verify that all advertised HH Carrier features are provided in your mission and use them whenever possible for development and I&T benefits.

**Lesson 4-** In planning your system development, plan for at least 5 software deliveries in increments of complexity. There will be a reduction in the number of change requests following acceptance testing of each delivery. This will insure that you are not overwhelmed at the last moment.

**Lesson 5-** Plan for contingencies during the mission by leaving some of your designated command windows empty of commands.

**Lesson 6-** Commercial software is not generally tested to the degree that custom designed space flight software is. Plan to diligently test every single feature and parameter of commercial software in the configuration planned for flight and then do not upgrade to newer versions. Beware of incompatibility between commercial packages. Remember that testing can show presence of errors but not absence of errors.

**Lesson 7-** Throughput limitation is a common problem. Do the most to insure that your ground system can handle the required data throughput multiplied by at least a factor of 2.

**Lesson 8-** Expect downlink communication channel data errors that cause short data dropouts during POCC operations that may not be recoverable. Generally, such short data dropouts (those less than a few minutes) are not treated as gaps and cannot be counted on being recovered in postmission playback requests. Such dropouts can wreak havoc with time scales when graphing flight data using commercial spreadsheet programs. Plan to either preprocess the data to restore lost time points or else devise a method to identify regions of missing data in the graphs.

**Lesson 9-** Expect some duplicate time stamps on successive one second telemetry frames. This is due to different frames occurring within the same second boundary and receiving the same time stamp. This is especially true of time stamps issued within the user's ground station due to the irregular flow of telemetry from the CCGSE.

**Lesson 10-** Your command channel throughput does not mean that you can continuously pump commands at the assigned channel rate. It just means that such a channel is there. Expect additional throughput limitations for non-sparse commanding.

**Lesson 11-** Sometimes there is a need to upload long serial asynchronous command sequences. For such cases, carefully plan the command sequence timing and inter-command delay to insure that the commands will not overrun the CCGSE command buffers and other HH carrier elements. Load as much as you can pre-flight into the flight system's nonvolatile memory because it can be very difficult to upload them at the POCC during the mission. It is likely you will run out of a command window or an error will occur during transmission, forcing you to repeat the upload, perhaps many times.

**Lesson 12-** Plan to provide the Hitchhiker project with the full commanding profile for your nominal mission. Within the profile, account for the time required for your payload to execute each command. This will force you to fully plan your mission and help to avoid last minute command design errors. In addition, KSC will require hexadecimal codes for all commands planned for the CITE test during shuttle integration. Test these codes repeatedly with your flight and ground system prior to providing the codes, and again prior to shipment of your payload to KSC. This will assure no codes have changed during late software modifications, thereby avoiding embarrassing and frustrating delays during shuttle integration testing.

**Lesson 13-** Operations simulations and training sessions are designed to insure you are prepared for mission operations. Do not trivialize their value and do not ignore or underestimate their significance. It will be much easier for you at the POCC during mission operations if you take full advantage of such events.

**Lesson 14-** Operations personnel at the POCC have participated in many missions while this is probably your first, and perhaps the last time, at the POCC. Listen to the advice of Operations personnel very carefully and attempt to follow it.

**Lesson 15-** At times your GSE will be required to support different activities at different sites - integration and testing at I&T facilities, simulations at the POCC, and shuttle integration tests at KSC. If possible, develop two ground systems, primary and backup, and use the backup system at all remote locations. This will avoid needless wear and tear on the primary system, eliminate worries over breaking up the primary system once it is at the POCC and tested, and provide a backup system during mission operations. Leasing the backup system may be attractive in terms of both cost and schedule.

**Lesson 16-** Sometimes advanced hardware features, like a computer's 32-bit addressing mode, cannot be fully utilized because the commercially delivered software was developed on an older system and does not run unless the advanced feature is turned off. Make sure that commercial software does not require superseded modes of operation and thus force you to underutilized the resources you paid for, like computer memory.

**Lesson 17-** Some basic tools like a telemetry frame generator must be required as part of a system delivery. A telemetry frame generator can be a hardware telemetry generator in a flight prototype board with a software module supplying telemetry source values or a ground based software telemetry frame generator.

**Lesson 18-** In ground systems based on networked computers with local databases, think in advance how you will insure that all databases remain synchronized, especially if change-only telemetry is being sent to downstream computers. Similarly, think about how you will set your GSE computers' clock to the POCC panel GMT time.

**Lesson 19-** Verify that time counter registers are implemented in sufficient size to avoid a rollover condition. I&T tests may not discover an error because the I&T activities are shorter than actual mission processing schedules.

**Lesson 20-** It is necessary to preserve the previous mission configuration for a re-fly mission and only change to accommodate new requirements. The environment present at the time of ROMPS1 mission completion in September of 1994 must be preserved. Commercial vendors must be notified to save and deliver to GSFC the system development environment and latest source code version. This will be needed to re-fly the ROMPS payload. All computer configurations must be frozen and no upgrades allowed for a mission re-fly unless new requirements emerge.

**Lesson 21-** The ROMPS mission resulted in a large amount of data to be processed and analyzed. Consider how you will process all of you data post-flight. The mission is not over until all necessary information has been extracted and sufficiently analyzed. Do not underestimate the amount of work involved in this. An object oriented data base for data products generation may be appropriate.

**Lesson 22-** In addition to automatically archived data, organize a method for all operations personnel to maintain written logs of events that occur during the mission. Insure that the time of each entry is listed. These logs will be of great assistance in evaluating data post-flight, especially when anomalies occur.

## **RESULTS AND CONCLUSIONS**

ROMPS was one of the most complex Hitchhiker payloads flown to date. The mission was very successful with all of its goals fully attained. Its data system was based on a number of commercial products that resulted in a highly capable and flexible control system that provided selectable degrees of automation and graphical presentation of telemetry at the ground station. A number of very good lessons were learned while developing and operating the ROMPS experiment and these have been shared above.

## **TRADEMARK NOTICES**

Spacecraft Command Language is a registered trademark of Interface and Control Systems, Inc. EasyLab and System V are registered trademarks of Zymark Corporation.

Apple, LocalTalk, Macintosh, and Macintosh Quadra are registered trademarks of Apple Corporation.

LabVIEW is a registered trademark of National Instruments Corporation.

Bernoulli is a registered trademark of Iomega Corporation.

## **REFERENCES**

1. Voellmer, G. M., "The ROMPS Robot in Hitchhiker", Shuttle Small Payloads Symposium, October 22, 1992
2. Olsztyn, P., Dobbs, M., Dickerhoof, G., Dorrance, P., "A Space-Based Laboratory Automation Architecture for Material Processing Experimentation", National Symposium on Laboratory Automation and Robotics, October 17-20, 1993, Boston, MA
3. Olsztyn, P., Dobbs, M., Conrad, D., "A Distributed Architecture For On-Orbit Laboratory Automation And Robotics Using COTS Components", AIAA 94-4506, 1994 AIAA Space Programs and Technologies Conference
4. *The Spacecraft Command Language Software System*, Interface & Control Systems, Inc., 1993
5. Bugby, D. C., "ROMPS Thermal Analysis Final Report", Swales & Associates Inc., Technical Report No. SAI-RPT-015, October 15, 1994
6. *Reliability, Maintainability, and Quality Assurance Manual*, NHB 5300.4, NASA Headquarters, Washington, DC

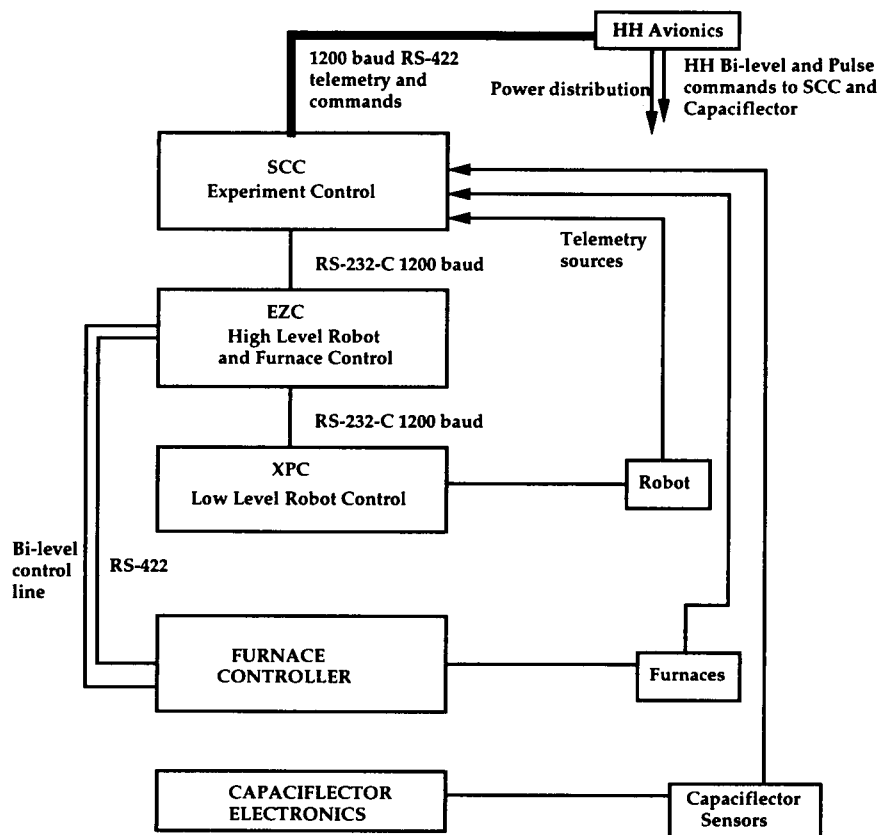


Figure 1: ROMPS Flight Data System Diagram

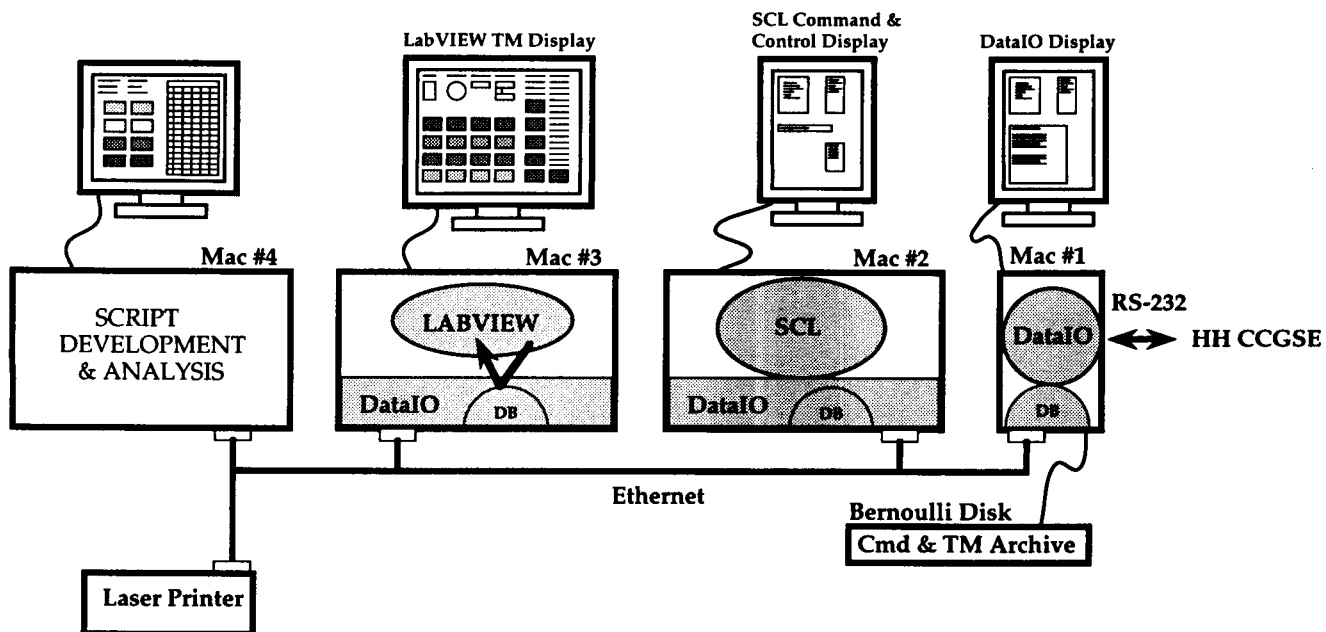


Figure 2: ROMPS Ground Station Hardware and Software

# **DESIGN AND DEVELOPMENT OF HIGH VOLTAGE (DC) SOURCES FOR THE SOLAR ARRAY MODULE PLASMA INTERACTION EXPERIMENT**

Irene K. Bibyk and Lawrence W. Wald  
NASA Lewis Research Center

## **ABSTRACT**

Two programmable, high voltage DC power supplies were developed as part of the flight electronics for the Solar Array Module Plasma Interaction Experiment (SAMPIE). SAMPIE's primary objectives were to study and characterize the high voltage arcing and parasitic current losses of various solar cells and metal samples within the space plasma of low earth orbit (LEO). High voltage arcing can cause large discontinuous changes in spacecraft potential which lead to damage of the power system materials and significant Electromagnetic Interference (EMI). Parasitic currents cause a change in floating potential which lead to reduced power efficiency.

These primary SAMPIE objectives were accomplished by applying artificial biases across test samples over a voltage range from -600 VDC to +300 VDC. This paper chronicles the design, final development, and test of the two programmable high voltage sources for SAMPIE. The technical challenges to the design for these power supplies included vacuum, space plasma effects, thermal protection, Shuttle vibrations and accelerations.

## **INTRODUCTION**

The Solar Array Module Plasma Interaction Experiment (SAMPIE) was a flight experiment that flew on the Space Shuttle Columbia (STS-62) in March 1994, as part of the OAST-2 mission. SAMPIE and OAST-2 were sponsored by the Office of Space Access and Technology (OSAT) as part of the In-Space Technology Experiments Program (IN-STEP). The SAMPIE conceptual development, hardware design, and system verification for Shuttle flight were accomplished at the Lewis Research Center (LeRC) in Cleveland, Ohio, with support from NYMA engineers. The technology requirements and experiment definition were developed by Principal Investigators (PIs), Dr. Dale Ferguson and Dr. G. Barry Hillard, of the LeRC Space Power Technology Division. The experiment required two high voltage power supplies which were developed by American High Voltage (AHV), to meet SAMPIE performance specifications.

The two programmable, high voltage DC power supplies provide voltages from -600 VDC to +300 VDC with respect to Shuttle ground. These biases were applied to experiment samples, solar cells and metal/insulator materials. High Voltage Power Supply #1 (HVPS#1) was a complex and unique design that could bias test samples from -600 VDC to +300 VDC. In addition, HVPS#1 provided electrical isolation, output overcurrent protection, and isolated logic voltages to the precision current measurement circuitry on the SAMPIE Electrometer Board. High Voltage Power Supply #2 (HVPS#2) was a 0 to -500 VDC programmable voltage source that was a commercial, off-the-shelf (COTS) item.

## **DESIGN AND OPERATION**

### **SAMPIE Technology Background**

A detailed description of the experiment may be found in Ref. 1 and will not be discussed in this paper, but a general overview of the hardware and science may be helpful to understand the

function of the two high voltage power supplies. The main objective of SAMPIE was to collect data to quantify and investigate high voltage interactions on solar cells and power system materials. The results will be vital to the design and construction of future high voltage space power systems. Flying SAMPIE in space is needed in order to subject the various components to the space plasma environment and thereby to understand the space plasma interaction effects as a function of spacecraft orientation in the ram and wake. The ram orientation is achieved when the Shuttle velocity vector is coincident with the line normal to and out of the shuttle payload bay. The wake orientation is 180 degrees away from ram. Also, the flight results will validate analytical predictions based on ground experiments.

## **SAMPIE Hardware Overview**

SAMPIE consisted of an aluminum box that contained the Main Electrical Unit (MEU) with an experiment plate fixed on the top surface. Solar cell and material samples were mounted on the outside of the experiment plate, as shown in Fig. 1. The MEU was mounted to a 2.54 cm thick aluminum base plate for both thermal and structural support. Inside the aluminum box and bolted to the base plate was a card cage that contained several printed circuit boards and instrument boxes. To measure plasma environment, SAMPIE had a Langmuir probe to monitor plasma density and temperature and a V-body probe to monitor Orbiter potential with respect to the ionosphere.

A simple description of the experiment is that each test sample is biased to a series of voltages ranging from +300 VDC to - 600 VDC. Some electrical functions are as follows:

- When samples are negatively biased, the circuitry will detect and measure the arc rates as a function of bias voltage.
- For both negative and positive bias voltages, current collection versus bias voltage measurements are made. Current collection from the samples is measured by the Electrometer Board with a sensitivity of +/- 1 nanoamps.
- One relay board is located between each high voltage power supply output and the test samples. Relay Board #1 is connected to HVPS #1 and contains eighteen reed relays with high isolation resistance and low contact resistance. These characteristics are vital so that the Electrometer Board can measure currents down to the nanoamp level. Relay Board #2 is connected to HVPS #2 and contains fourteen reed relays.

The Data Acquisition System (DAS) controls the sequence of sample selection, voltage selection, data collection and storage, and uplink/downlink communications.

## **High Voltage Power Supply #1**

A custom high voltage power supply made by American High Voltage provided a programmable bias voltage to one sample set. Controlled by the DAS, the HVPS #1 generated an output voltage that varied from -600 VDC to +300 VDC. In addition to the programmable bias voltage, the supply features included:

- Electrical isolation between high voltage output and experiment ground.
- Output overcurrent protection, whereby the supply shuts down if output current exceeds 50 milliamperes.
- Switching frequency of 50 kHz, common with the other switching power supplies used in SAMPIE. A common frequency was used to minimize EMI.

- Electrical isolation of the +5 VDC and the  $\pm 15$  VDC logic power supplies provided to the Electrometer Board.

HVPS #1 is mounted on a circuit card (Fig. 2) that includes the Electrometer Board and other housekeeping electronics. The critical areas for space flight development will be described in the next section.

## High Voltage Power Supply #2

High Voltage Power Supply #2 provided programmable voltages to a second set of samples connected to a second relay board. For the experiment, the output voltage varied from 0 to -500 VDC and was also controlled by the DAS. HVPS #2 was made by American High Voltage (AHV), the same company that made the custom HVPS #1. One major difference in the two supplies is that HVPS #1 was a unique design, specifically made for SAMPIE and HVPS #2 was a COTS item, space-qualified by LeRC for this application. HVPS #2 was also mounted on a circuit card as shown in Fig. 3.

## DEVELOPMENT FOR SPACE-FLIGHT ENVIRONMENT

### Thermal Control for HVPS #1

Since HVPS #1 was required to operate in a vacuum, convection heat transfer could not be accomplished and conduction was the primary heat transfer mechanism. Complicating this issue is the fact that electrical insulation must be maintained, thus preventing the metal to metal contact which is ideal for conductive heat transfer. Therefore, thermal issues for components were resolved with a combination of solutions. Heat sinks were attached to high power components and the heat sinks were attached to the power supply case. Thermal conduction, without electrical conduction, was achieved by using a material called Co-therm, applied between the heat sinks and case. Co-therm is an electrical insulation material that has good thermal transfer characteristics. Active components, such as the Field Effect Transistors (FETs), were attached to the power supply case, and the case acted as a heat sink.

HVPS #1 was potted to provide resistance to vibration and to maintain an acceptable thermal profile during operation. Potting the units with the standard material used by AHV was not adequate for the thermal profile of HVPS #1, because the material had a low thermal conductivity. SAMPIE engineering personnel found a material from Nusil (CV2946), which had a higher thermal conductivity, for use in HVPS #1.

To evaluate the effectiveness of these thermal design accommodations, a test unit was constructed with thermocouples attached to several critical areas in the unit. The unit was subjected to 8 hours of high voltage, full load operation in a vacuum chamber. Temperatures stayed within their specified limits during the test.

To provide a thermal path from the power supplies to the SAMPIE base plate the supplies were mounted on printed circuit cards (PC) which used thermal planes, also known as heat ladders (see Fig. 2 & 3). Between each power supply case and the thermal plane, 30 mil silver foil was used to enhance the thermal conductivity. Other foils were considered but were not chosen because of their expense. On the PC card edges, wedge-lock card guides were used to conduct the heat from the thermal plane to the aluminum card cage. The card cage was bolted to the base plate; the base plate provided the thermal mass needed for conducting the heat from the electronics. One risk with thermal planes in a vacuum environment is the possibility of high voltage arcing or dielectric breakdown; therefore, conformal coating was applied after the power supplies were mounted to their respective PC cards.

The use of potting material and conformal coating is a trade-off. The benefits for space use are thermal conductivity for improved thermal control, structural stability for improved vibration resilience and electrical isolation for improved control with high voltage applications in a vacuum. The disadvantages for space use are additional weight, cost and the difficulty with component re-work, if necessary.

### **HVPS #1 Transformer Integration/Packaging**

Transformer encapsulation is necessary to withstand the vibration and maintain an acceptable thermal profile during operation. Five transformers are used in HVPS #1. The standard encapsulation techniques used by AHV were inadequate for HVPS #1 because of packaging constraints. AHV used several hybrid techniques to encapsulate the transformers to provide the required structural stability to meet vibration and thermal requirements. The major concern with the transformer packaging was that the wires used in the transformers do not break from stress due to vibration and/or thermal mismatch at the wire connection points. Thermal shrink tubing over the wire at the interface between the hybrid encapsulation and the wire was used to relieve the stress at that point.

### **HVPS #1 EMI Control**

For Shuttle experiments, electromagnetic interference (EMI) is always a concern, especially radiated emissions from high frequency power components. Standard practices were used to decrease the radiated emissions from the two power supplies. For HVPS #1, input filters were used and a "snubber-resistor" was placed across a switching circuit to absorb power spikes as FETs switched at 50 kHz. Preliminary EMI testing at Lewis Research Center showed that the power supply operated within the limits that were necessary for shuttle applications. At the Goddard Space Flight Center (GSFC), the SAMPIE payload was tested for EMI compliance to the General Environmental Verification Specification (GEVS) document for STS payloads. Among the suite of tests performed by the GSFC personnel were the narrow band conducted emissions tests (CE01/CE03), from 30 Hz to 50 MHz, broadband conducted emissions (CE03), from 20 kHz to 50 MHz, and the radiated emissions tests (RE02 and RE04), from 30 Hz up to 18 GHz. The SAMPIE passed these tests with no problems or necessary re-work.

### **Flight Operation**

SAMPIE's primary mission objectives were to collect arcing measurements as a function of negative voltages and current measurements as a function of both positive and negative voltages. The SAMPIE measurements were taken on test samples that were identified by the PIs to support Space Station and other future high voltage power systems for space applications. One set of measurements were needed in the bay-to-ram orientation, the worst-case condition for plasma effects, and another set was planned for the bay-to-wake orientation. The essential engineering data was not the entire planned mission timeline, but a subset which contained current collection and arcing measurements on all samples in a bay-to-ram orientation, with voltage ranges of particular interest for space applications. Therefore, the minimum success criteria for SAMPIE was defined as this essential engineering data and these experiments were performed at the start of the planned mission timeline.

Both high voltage power supplies operated as designed throughout the entire flight, with SAMPIE collecting the data needed to meet its minimum success criteria and collecting nearly all of its planned flight data. All SAMPIE mission objectives, in both orientations, were met except for approximately 10% of the high voltage timeline (voltages ranging from -400 VDC to -600



VDC) in the bay-to-ram orientation. Therefore, the collected data in the bay-to-ram orientation included all current and arcing measurements on all samples with bias voltages ranging from -300 VDC to +300 VDC. During the bay-to-ram orientation and high voltage arcing at -600 VDC, a voltage breakdown occurred between the case of a component on the Electrometer Board and the thermal plane on the Electrometer Board. This resulted in an overcurrent condition seen by HVPS #1, which caused HVPS#1's high voltage output to shut down. The high voltage breakdown on the Electrometer Board caused a component to fail, which precluded any further collection current measurements.

HVPS#2 operated as designed throughout SAMPIE's entire flight. In addition, HVPS#2 continued to operate after HVPS#1 shut down due to the overcurrent condition. Therefore, all test samples that were connected to HVPS#2 were not affected by the anomaly and SAMPIE continued to collect useful arcing measurements, with bias voltage ranging from 0 VDC to -500 VDC.

## RECOMMENDATIONS

The high voltage power supplies were a challenge for space flight development and most engineering efforts were spent on thermal, high voltage and packaging developments. Accordingly, high voltage DC engineering recommendations from the experience on SAMPIE are listed as follows:

1. Conformal coating and potting material must be applied following manufacturer's procedures to preclude the formation of any voids or bubbles in the material, especially for high voltage operations. These voids may be the site of partial outgassing, which, due to Pailson's Breakdown Effects, may allow inadvertent arcing to occur in a circuit. These recommended procedures usually include the proper preparation of the surface, degassing the conformal coating or potting material in a vacuum bell jar prior to application, a bake-out of the boards and components to minimize any moisture, and curing the conformal/potting material in a vacuum, possibly also at elevated temperatures.
2. Thermal planes on circuit cards are highly effective for thermal conduction on components which are located on the cards. The sides of the card can also be used as a thermal path as illustrated on Figs. 2 and 3. The sides have wedge-lock card guides to ensure good thermal contact to the card cage. The card cage is then bolted to the base plate to add more conductive paths in order to transfer heat from the electronics.
3. Conformal coating and potting materials are good for thermal conduction, but one should use a material that can easily be removed in case of the need for rework.
4. Before operating high voltages in a vacuum, the electronic unit should be given time to outgas by sitting for a predetermined time in the vacuum environment. The outgassing time is dependent on the package volume, temperature, moisture content, and mean free path length for any trapped gas molecules.

## REFERENCES

1. Lawrence Wald and Dr. G. Barry Hillard: "The Solar Array Module Plasma Interaction Experiment". Presented at the 26th IECEC Conference, in Boston, Massachusetts, August, 1991.

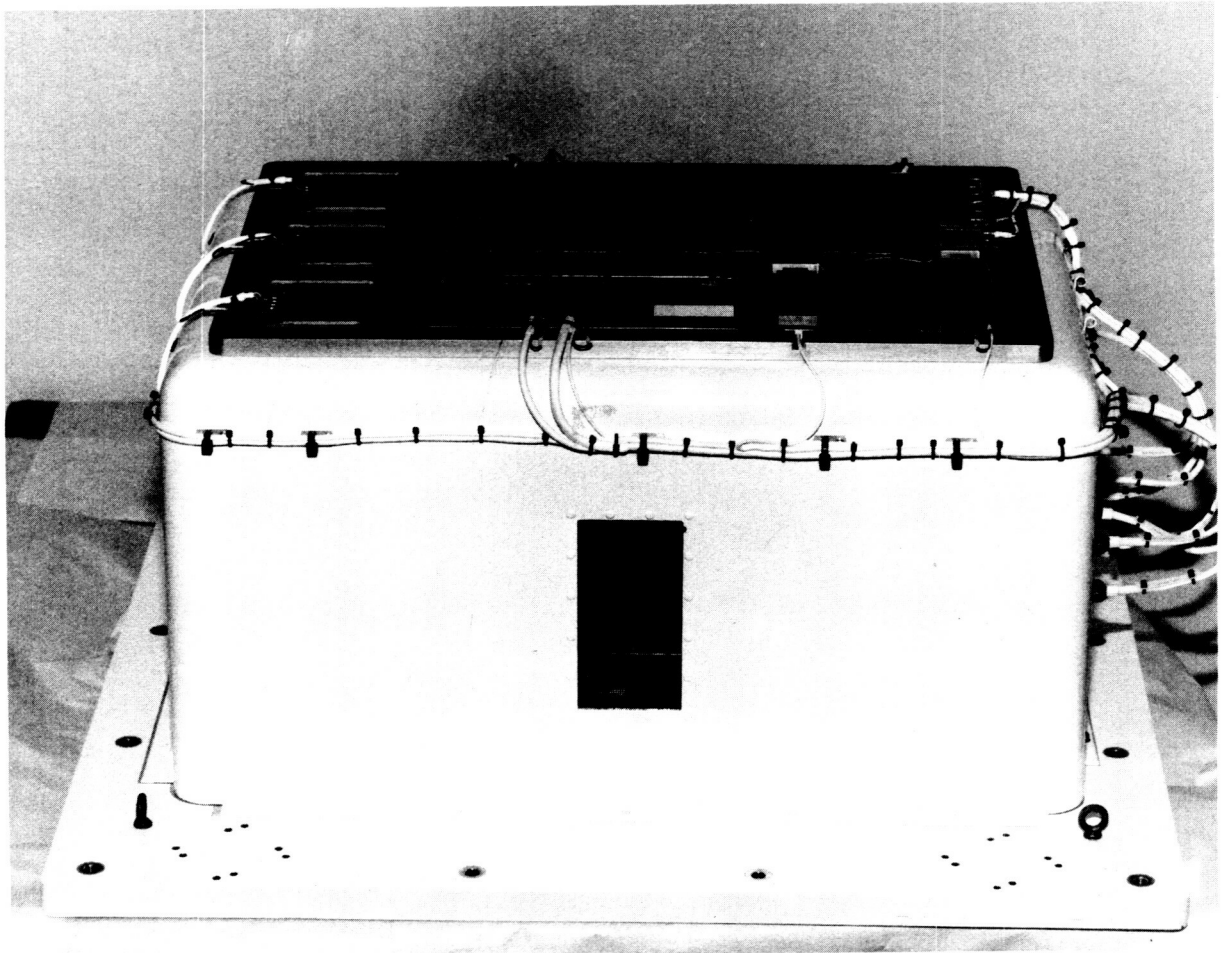


**Figure 1.** The SAMPIE main electrical assembly, an aluminum box with an experiment plate fixed on the top surface.

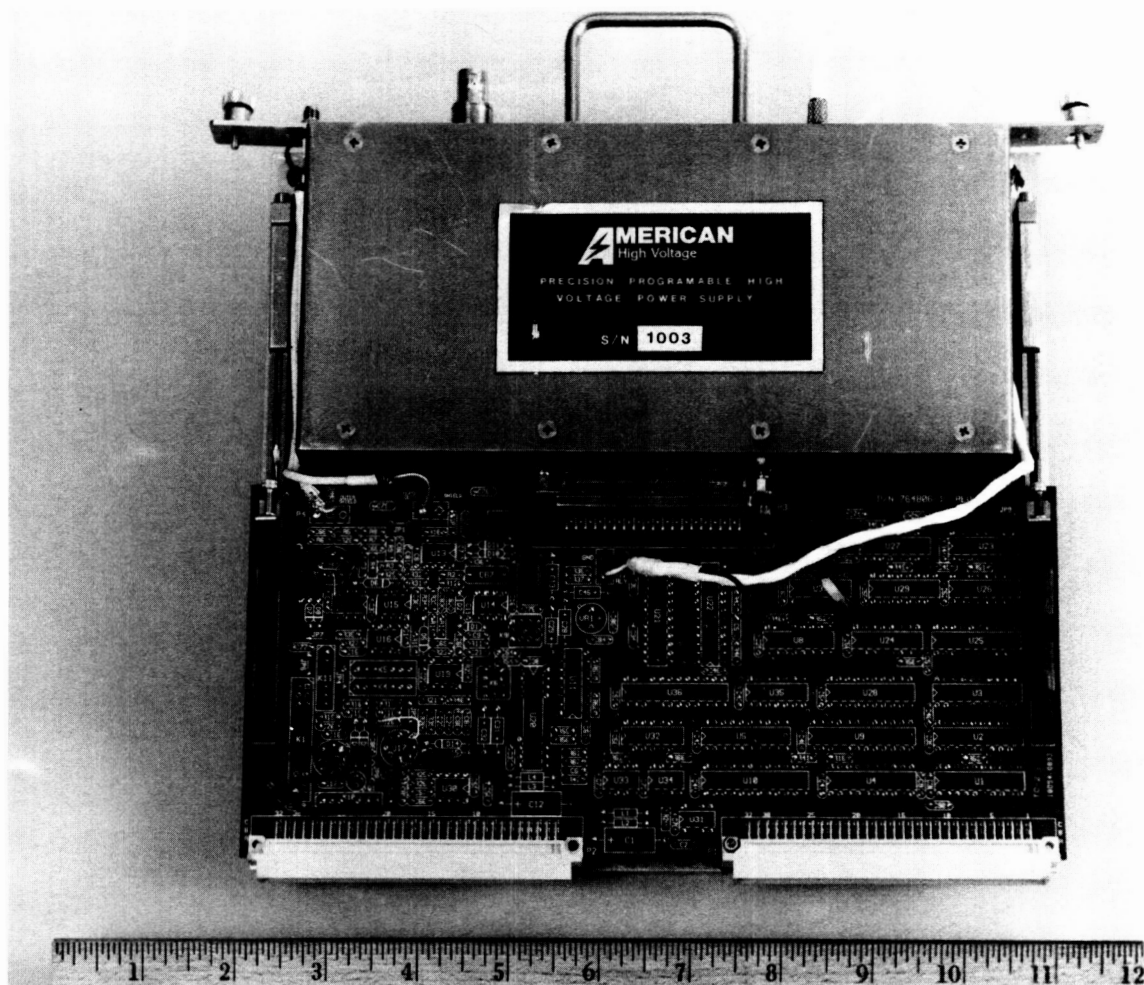


**Figure 2.** The High Voltage Power Supply #1 (HVPS#1) by American High Voltage mounted on a printed circuit card with a thermal plane and wedge-lock card guide.

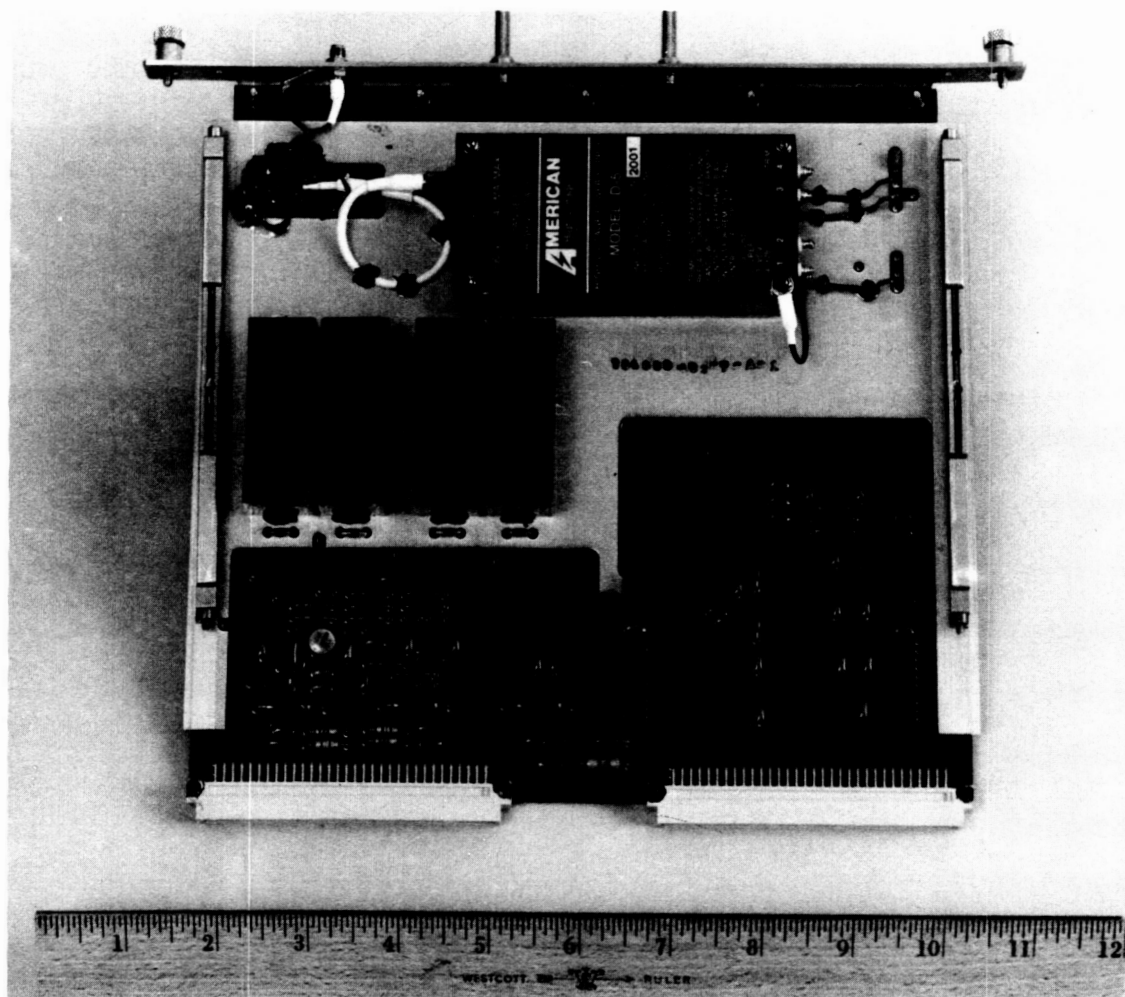


**Figure 3.** The High Voltage Power Supply #2 (HVPS#2) by American High Voltage mounted on a printed circuit card with a thermal plane and wedge-lock card guide.

# **TELESCIENCE OPERATIONS WITH THE SOLAR ARRAY MODULE PLASMA INTERACTION EXPERIMENT**

**Lawrence W. Wald and Irene K. Bibyk**

**NASA Lewis Research Center**

## **ABSTRACT**

The Solar Array Module Plasma Interactions Experiment (SAMPIE) is a flight experiment that flew on the Space Shuttle Columbia (STS-62) in March 1994, as part of the OAST-2 mission. The overall objective of SAMPIE was to determine the adverse environmental interactions within the space plasma of low earth orbit (LEO) on modern solar cells and space power system materials which were artificially biased to high positive and negative direct current (DC) voltages. The two environmental interactions of interest included high voltage arcing from the samples to the space plasma and parasitic current losses. High voltage arcing can cause physical damage to power system materials and shorten expected hardware life. Parasitic current losses can reduce power system efficiency because electric currents generated in a power system drain into the surrounding plasma via parasitic resistance.

The flight electronics included two programmable high voltage DC power supplies to bias the experiment samples, instruments to measure the surrounding plasma environment in the STS cargo bay, and the on-board data acquisition system (DAS). The DAS provided in-flight experiment control, data storage, and communications through the Goddard Space Flight Center (GSFC) Hitchhiker flight avionics to the GSFC Payload Operations Control Center (POCC). The DAS and the SAMPIE POCC computer systems were designed for telescience operations; this paper will focus on the experiences of the SAMPIE team regarding telescience development and operations from the GSFC POCC during STS-62.

The SAMPIE conceptual development, hardware design, and system verification testing were accomplished at the NASA Lewis Research Center (LeRC). SAMPIE was developed under the In-Space Technology Experiment Program (IN-STEP), which sponsors NASA, industry, and university flight experiments designed to enable and enhance space flight technology. The IN-STEP Program is sponsored by the Office of Space Access and Technology (OSAT).

## **INTRODUCTION**

Contemporary satellites and spacecraft have evolved in size, weight and sophistication to the point that they now require space power systems which operate at higher operating voltages than current spacecraft. This demand creates a new challenge for spacecraft designers to contend with the interaction of space plasma with materials and systems.

The Solar Array Module Plasma Interactions Experiment (SAMPIE) is a Space Shuttle experiment designed by NASA LeRC to investigate and quantify high voltage plasma interactions. The objective of SAMPIE was to determine the environmental effects of the low earth orbit (LEO) space plasma environment on modern solar cells and space power system materials artificially biased to high plus and minus DC voltages. The two environmental effects of interest included high voltage arcing from the samples to the space plasma, which can cause physical damage to power system materials, and parasitic current losses, in which electric currents generated in a power system drain into the surrounding plasma via parasitic resistance. These parasitic losses reduce power system efficiency. SAMPIE results will play a key role in the design and construction of high voltage space power systems.

The Principal Investigators (PI's) of the SAMPIE experiment were Dr. Dale Ferguson and Dr. G. Barry Hillard, both of the LeRC Space Power Technology Division. The Project Manager (PM) for the experiment was Lawrence W. Wald. Irene K. Bibyk was Deputy to Mr. Wald. Task work was accomplished by an in-house project team consisting of LeRC and NYMA Technology, Inc., engineers and technicians. The project was supported by the NASA Headquarters Office of Space Access and Technology.

## **BACKGROUND**

Numerous ground and flight experiments have shown that there are two basic interactions with the space plasma when spacecraft surfaces are biased at high potentials relative to it.

First, conducting surfaces whose electrical potential is highly negative with respect to the plasma undergo arcing - damaging the material and resulting in current disruptions, significant Electromagnetic Interference (EMI), and large discontinuous changes in potential.

Second, solar arrays or other surfaces whose potential is positive with respect to the plasma collect electrons from the plasma, resulting in a parasitic loss of power to the power system and a change in the floating potential of the system.

## **PROJECT OBJECTIVE**

The overall objective of SAMPIE is to minimize adverse environmental interactions by investigating the arcing and current collection behavior of materials and geometries likely to be exposed to the Low Earth Orbit (LEO) plasma on high voltage space power systems [Ref. 1]. There are seven specific objectives of the experiment:

1. For selected solar cell technologies, determine the arcing threshold, arc rates, and magnitude of arc current.
2. For these sample arrays, measure plasma current collection versus applied bias.
3. Design and test an arc mitigation strategy; i.e., modifications to standard design which may significantly improve the arcing threshold.
4. Design and test simple metal/insulator mock-ups to allow the dependence of current collection on exposed areas to be studied with all other relevant parameters controlled.
5. Design and fly an experiment to determine the dependence of arcing threshold, arc rates, and arc strengths on the choice of metal with all other relevant parameters controlled.
6. Design and fly controlled experiments to study arcing from anodized aluminum using alloys and anodization processes typical of ones being considered for use on large space structures.
7. Measure a basic set of plasma parameters to permit data reduction and analysis.

## **EXPERIMENT APPROACH**

The SAMPIE flight experiment is shown in Fig. 1. Mounted to the top side of the experiment is the Experiment Plate, which contains the experimental samples. The samples include modern solar cells, samples used to verify program elements of the Space Station program, sample items of modern power system materials, and samples used to collect data to verify numerical simulation computer codes. A diagram of the Experiment Plate is shown in Fig. 2; a short description of each sample is listed below.

### ***SPACE STATION CELLS***

A four-cell coupon of 8-cm by 8-cm space station cells having copper interconnects on the reverse side will allow a test of this technology. Arcing is expected to occur from the cell edges and there is considerable interest in arc rate versus bias curves as well as in the arcing threshold for these cells. Current collection from these cells will perhaps be even more interesting, as it can dramatically affect the floating potential of spacecraft.

### ***APSA***

A twelve-cell coupon of 2-cm by 4-cm Advanced Photovoltaic Solar Array (APSA) cells will test the behavior of this relatively new, very thin (60  $\mu\text{m}$ ) technology. For use in LEO, the sample blanket will use germanium-coated Kapton for protection from atomic oxygen attack. Ground tests have shown that the use of such material, which is a weak conductor, leads to increased plasma current collection under some conditions.

### ***STANDARD SILICON***

By including a coupon of traditional 2-cm by 2-cm silicon solar cells, a baseline for comparison is provided by including the technology that has been used exclusively in the U. S. space program to date. Second, computer codes that predict the results of plasma interactions are now mature though largely unvalidated. A key feature of such codes is the ability to predict current collection for solar arrays. Unfortunately, plasma sheath effects make scaling the current collection to large arrays highly nonlinear and very difficult to predict. We have devised an experiment to study this effect. Data is taken from a four-cell coupon of 2-cm by 2-cm silicon solar cells wired as a series string. A second independent series string of 12 cells surrounds the inner four. a third series string of 20 cells, also independent, surrounds the entire assembly. By biasing these strings independently in various combinations, these scaling effects will be studied.

### ***MULTIPLE BREAKDOWN TEST***

The samples tested on this plate will explore the hypothesis that negative potential arcing is a special case of the classical vacuum arc. With geometry and test conditions controlled, only the composition of the metal will be varied. Two different types of measurements of five different pure metals - gold, silver, copper, aluminum, and tungsten - will be made.



## ***SNAPOVER***

To study current collection and snapover (a condition where an entire surrounding surface, normally an insulator, behaves like a conductor), we include six 1 cm diameter copper disks covered with 3-mil-thick Kapton. Each has a pinhole in the center with hole sizes tentatively chosen as 1 mil, 5 mil, 10 mil, 15 mil, 20 mil, and 30 mil. the use of such simple geometry will enable computer modeling of the essential physics without the complications introduced by geometrical complexities inherent in solar cells. The resulting family of current versus applied bias curves will be compared with computer predictions and other theoretical treatments.

## ***MODIFIED SPACE STATION***

On the bottom of the experiment plate are three coupons of four cells. These are space station cells reduced from the normal 8-cm by 8-cm size to 4-cm by 4-cm. This size reduction is necessary to increase the number of experiments that can be done in the limited area provided by the experiment plate. The data returned from the selected experiments will not be impacted by the scaling. Several factors in the cell design are now known to significantly affect plasma interactions. The three coupons to fly are designed to study several of these factors.

## ***SINGLE BREAKDOWN TEST***

The single breakdown test consists of a sample of anodized aluminum. There is considerable concern that this material undergoes dielectric breakdown and arcing when biased to high voltages. The particular alloy and sulfuric acid anodization process are chosen to be identical with that currently baselined for the space station main truss structure.

## ***FLIGHT HARDWARE***

The SAMPIE main electronics unit (MEU), is shown in an exploded view in Fig. 3. The package consists of a 2.54 cm baseplate to which a card cage for printed circuit boards (PCB's) and various instrument boxes are attached. Most of the instruments and electrical subsystems are on PCB's mounted within the card cage. The enclosure cover is a one piece case which provides a mounting surface for the experiment plate. Two electrical probes - a Langmuir probe to monitor plasma density and temperature and a V-body probe to monitor Shuttle potential with respect to the ionosphere - are part of the package. Since SAMPIE will significantly disturb the ionosphere within an area estimated to be about 1 m. in all directions, these probes are positioned on a side mount on the Hitchhiker-M carrier, about 2 m. away, from the SAMPIE MEU, as shown in Fig. 4.

A microprocessor is used to control the experiment and record the data. Data is stored on board in flash memory cards and will be transferred to PC as soon as possible after flight. A minimum subset of experiment data and housekeeping information will be downlinked in real time. Data analysis will be performed in-house at LeRC.

The Data Acquisition System (DAS) consists of a 25 MHz 68030 based single board computer (DMV-141), a custom made I/O Board, two Flash Memory Boards (DMV-540), and two A/D Boards (DMV-666). In general, the DAS provides the following: 1) Executes instructions in firmware to operate each experiment contained within SAMPIE's timeline; 2) Collects data from and controls the operation of other electronic boards/modules within SAMPIE's electrical system; 3) Interface to the outside world (GSE) via an RS422 interface. Specifications of each board that makes up the DAS are discussed below:

**CPU Board:** 68030 based board, 512 Kbytes of static ram (SRAM), 512 Kbytes of flash memory, two RS-232 ports (only one is required on SAMPIE), two 8-bit timers, and VMEBus interface circuitry. Located in VME Backplane slot one.

**Memory Boards:** Each card contains 4 MBytes of Flash Memory, write protection, VME interface, and Built-In-Test (BIT). Located in VME Backplane slots two and three.

**A/D Board:** Analog to Digital Converter, 12-bit resolution and 20  $\mu$ S conversion time, 16-single ended inputs or 8 differential inputs, Inputs configurable to  $\pm 40$  VDC,  $\pm 10$  VDC, 0-20 mA with programmable gain control. Located in VME Backplane slots five and six.

## **FLIGHT OPERATIONS**

In a simplified description of the experiment, one sample is biased to a particular voltage for a preset time while all remaining samples are held at ground potential. The power supply will bias the solar cell samples and other experiments to dc voltages as high as +300 V and -600 V with respect to shuttle ground. When biased negative, suitable instruments will detect the occurrence of arcing and measure the arc rate as a function of bias voltage. For both polarities of applied bias, measurements will be made of current collection versus voltage. A set of plasma diagnostics measurements is then taken and the procedure repeated at the other bias voltages. Diagnostic measurements consist of background pressure, plasma density and pressure, and the potential of the Shuttle with respect to the plasma.

The flight electronics included two programmable, high voltage DC power supplies to provide voltages from -600 VDC to +300 VDC to the samples. A transient current detector detected arcs and measured arc-rates as a function of negative DC

voltages for each sample. An electrometer, a precision DC current measuring device, measured parasitic current collection versus voltage for both positive and negative DC voltages. A plasma diagnostic instrument suite collected data on the plasma environment during operation of the experiment. The on-board data acquisition system (DAS) recorded the flight data, stored the information on nonvolatile memory, controlled the flight experiment, and provided communications capability to SAMPIE team members located in the Payload Operations Control Center at the Goddard Space Flight Center during the mission.

Vehicle orientation with respect to its velocity vector is critical since ram and wake effects are known to be significant. SAMPIE's operations plan will request control of Shuttle orientation such that one entire set of measurements is made with the payload bay held in the ram direction and a second set with the bay in the wake. The experiment timeline is expected to require approximately 25 hours of bay-to-ram and about 15 hours of bay-to-wake.

A team of LeRC and NYMA engineers and scientists were to be at the GSFC POCC for on-orbit operations during the mission. The total on-orbit time would be around 40 hours, which would require several shifts of support staff. POCC personnel would control the experiment operation by sending commands from the POCC to SAMPIE via uplink telemetry. Command acknowledgment, experiment data, and health & welfare data for the experiment would, in turn, be sent to the POCC from the experiment. The data received in the POCC was to be a subset of the on-orbit data; it would allow the engineers and scientists to monitor the environmental effects and if necessary, certain experiments could be repeated by sending the appropriate commands to the experiment.

After the OAST-2 mission is completed, the SAMPIE payload will be removed from the Hitchhiker-M carrier and returned to the Lewis Research Center. The data stored on-board the experiment will be copied to floppy disk media for the Principal Investigator and Project Scientist to study and analyze. The SAMPIE experiment will then be inspected, re-furbished as necessary, and safely stored in preparation for future flight opportunities.

## **FLIGHT DATA AND RESULTS**

The SAMPIE flight experiment was flown on STS-62 from March 4-19, as part of the OAST-2 payload. During the mission, project personnel located at the GSFC POCC participated in the on-orbit operations of the experiment, sending commands to and receiving downlinked data from the payload. From the data received in the POCC, the SAMPIE experiment provided a number of "firsts" to the investigation of modern solar arrays and power system materials. These include the first data ever taken on actual Space Station flight solar cells and Advanced Photovoltaic Solar Array (APSA) cells. SAMPIE is also the first high voltage plasma interaction

experiment ever retrieved after its in-space operations were completed. Along with the data collected for each experiment sample a set of plasma diagnostic data was collected, providing information on the payload bay environment.

SAMPIE completed its mission objectives in a comprehensive manner. The minimum success criteria and all planned plasma current collection measurements were completed in the bay-to-ram and bay-to-Earth orientations. The bay-to-Earth measurements were obtained in the wake of the Extended Investigation of Spacecraft Glow (EISG) experiment, and were representative of bay-to-wake measurements. All planned low voltage (to -300 VDC) arcing measurements were completed in the bay-to-ram orientation. Approximately three quarters of all desired high voltage (-400 V and higher) arcing measurements were also completed in a bay-to-ram orientation.

During bay-to-ram orientation, high voltage arcing on the APSA array, a large arc at -600 VDC caused one of SAMPIE's two high voltage power supply circuits to eventually cease operation. This limited subsequent arcing measurements to the arc mitigation samples, the metal samples, and the space station anodized aluminum samples and precluded any further current collection data. By that time, however, good high voltage arcing data had already been obtained for the APSA, space station, standard silicon, and Z-93 samples. Because all current collection and arcing measurements on all samples had already been completed under worst case (bay-to-ram) conditions throughout their anticipated useful voltage range, no essential engineering data were lost.

Subsequent to the power supply anomaly, several sets of true bay-to-wake high voltage arcing data were obtained for approximately half of the SAMPIE samples.

Throughout SAMPIE operation data was obtained on the payload bay neutral pressure, plasma density and temperature, Shuttle potential, and temperatures within the SAMPIE enclosure. This data will enable full analysis of the current collection and arcing data, so they can be used directly to confirm or require modification of analytical models used for spacecraft power system and charging analysis.

LeRC personnel received the downlink data in real time at Lewis, in Cleveland, Ohio, in the User Operation Facility (UOF). This enabled a larger group of scientists to view the flight results first hand.

SAMPIE also took pressure data in support of and in conjunction with the EISG experiment. SAMPIE measured high voltage arcing characteristics and payload bay pressures in a bay-to-ram orientation, low altitude (140 nm) circular orbit and later in an extremely elliptical orbit with a perigee of 105 nm.

## TELESCIENCE LESSONS LEARNED

A written mission plan should be completed prior to departure from LeRC to the mission POCC. The mission plan for the experiment details the following: the success criteria for the experiment, the on-orbit experiment milestones and their nominal time of occurrence, and the nominal command plan for the experiment. The plan should be written by the PM and/or the PI. An electronic copy should be in the POCC for reference and mission time updates. POCC personnel must be familiar with the mission plan prior to on-orbit operations. POCC personnel should be familiar with the expected on orbit thermal performance and electrical requirements of the experiment in order to determine nominal operation

8 hour fixed shifts are recommended and staff each shift with at least 2 people. Allow experiment personnel to pick their shifts (if possible). The day shift is very important for public affairs reasons and either the PI or the PM should be assigned to this shift.

POCC personnel must be prepared to answer a variety of questions from mission management personnel in the areas of experiment function, success criteria, environmental limits, etc..

During the 18 day mission of STS-62, SAMPIE collected data on environmental interactions during several periods. Our observations regarding telescience operations are as follows:

- Real time changes in the experiment timeline can be accommodated as necessitated by any of the following reasons:
  - 1) Significant experiments may be repeated a number of times in order to collect as much flight data as possible.
  - 2) Accommodation of unforeseen changes in the shuttle operation during flight may be made. An experimenter may choose not to operate during water dumps, shuttle maneuvers, or the loss of on-orbit communication capability.
- Project personnel provided real time data on the density of the space plasma to another experiment on OAST-2 which enhanced their science return during their primary on-orbit operations.
- Scientists and engineers in the UOF POCC were able to see the downlinked data in real time and make recommendations to the primary POCC team at the GSFC

## CONCLUSIONS

The Columbia was launched on March 4, 1994 and landed at KSC on March 19, 1994. During the 16 day mission SAMPIE operated over 70 hours in space. The primary set of required measurements were taken with the Columbia payload bay oriented in the "ram" direction (coincident with the velocity vector). In this orientation all planned current collection data at DC voltages to +300 VDC was collected, all low voltage arcing data (at voltages down to - 300 VDC) were collected, and 90% of the high voltage DC data (at voltages down to -600 V) was collected.

In the other required attitude orientation, known as the "wake" direction (with the payload bay oriented 180 away from the velocity vector) the planned low voltage (to +300 VDC) current collection measurements were not taken due to on-orbit problems with the high voltage bias line of one of the power supplies. The other high voltage power supply was used to collect high voltage arcing data in the wake. This was not in the original plan due to the pre-flight assumption that there would be no arcing in the wake due to the low plasma density. In fact, arcing was seen on several samples in the wake, providing unexpected information to the SAMPIE team. During both shuttle attitudes the plasma diagnostic instruments collected high fidelity data on plasma temperature, plasma turbulence, and shuttle vehicle potential. This data will be used to "normalize" the arcing and current collection data, removing variations due only to plasma variations.

Currently the flight data is being analyzed by the SAMPIE PI, Dr. Dale Ferguson. The PI has already used the flight data to validate the design of the ISSA plasma contactor program. The flight data will also be used to help validate computer modeling codes that have been developed at Lewis in support of space power system design. The SAMPIE flight hardware is currently in bonded storage at the LeRC awaiting another flight opportunity.

## References

1. G. Barry Hillard and Dale C. Ferguson: "The SAMPIE Flight Experiment Final Technical Requirements Document", NASA TM 106224, June 1993.

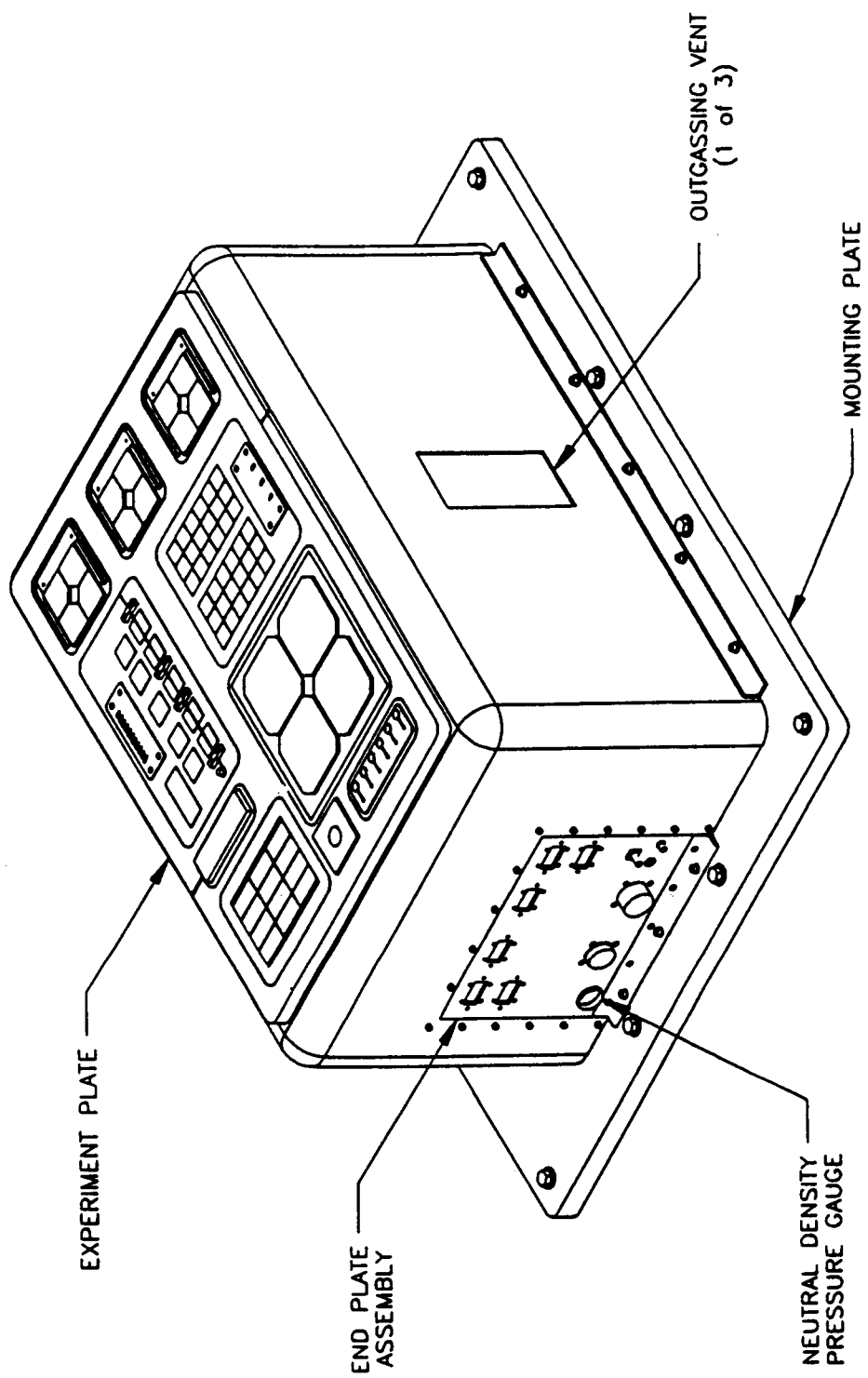


**Fig. 1 SAMPLE Payload**

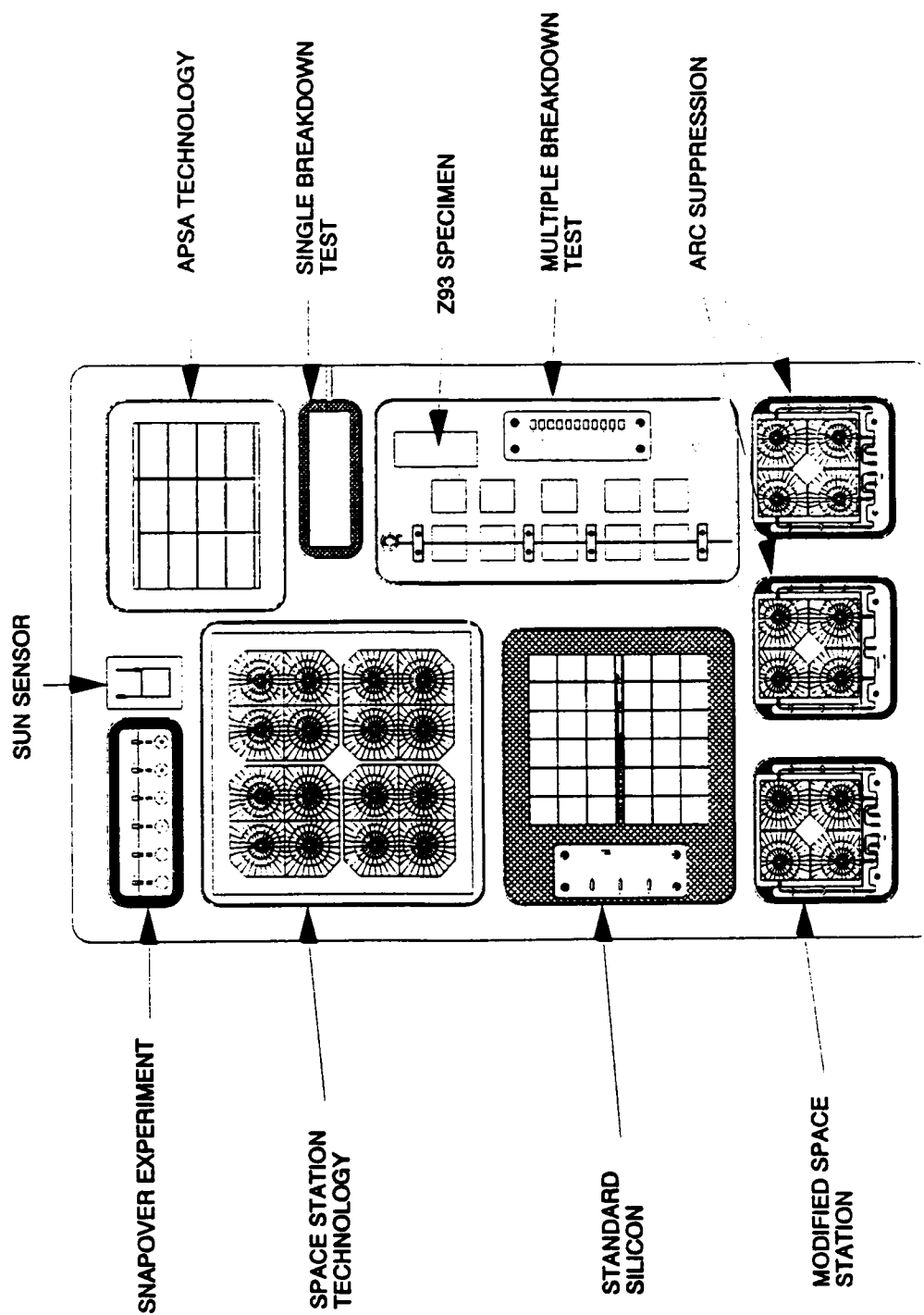
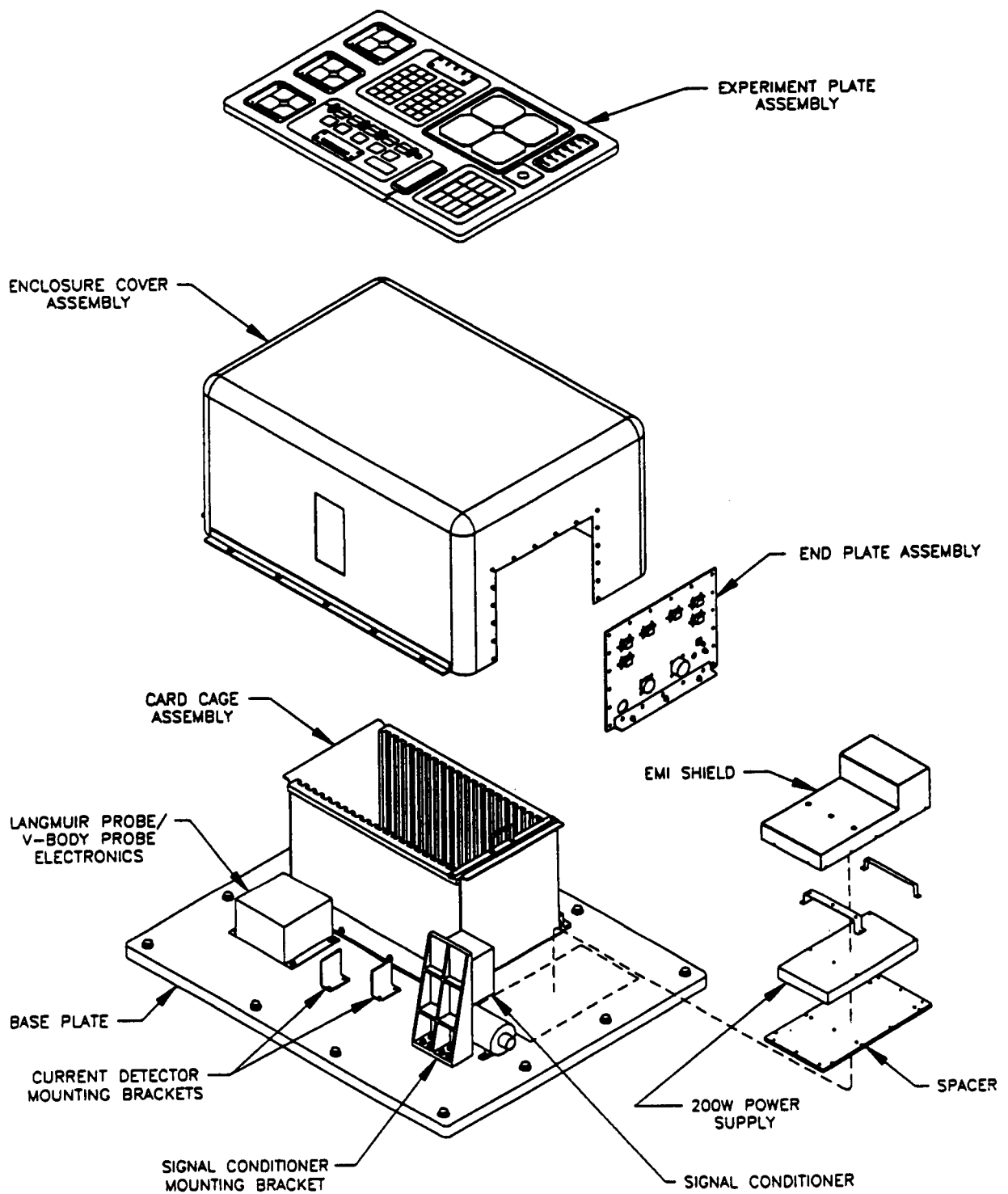


Fig. 2 SAMPLE Experiment Plate





**Fig. 3 SAMPIE Payload (Exploded View)**

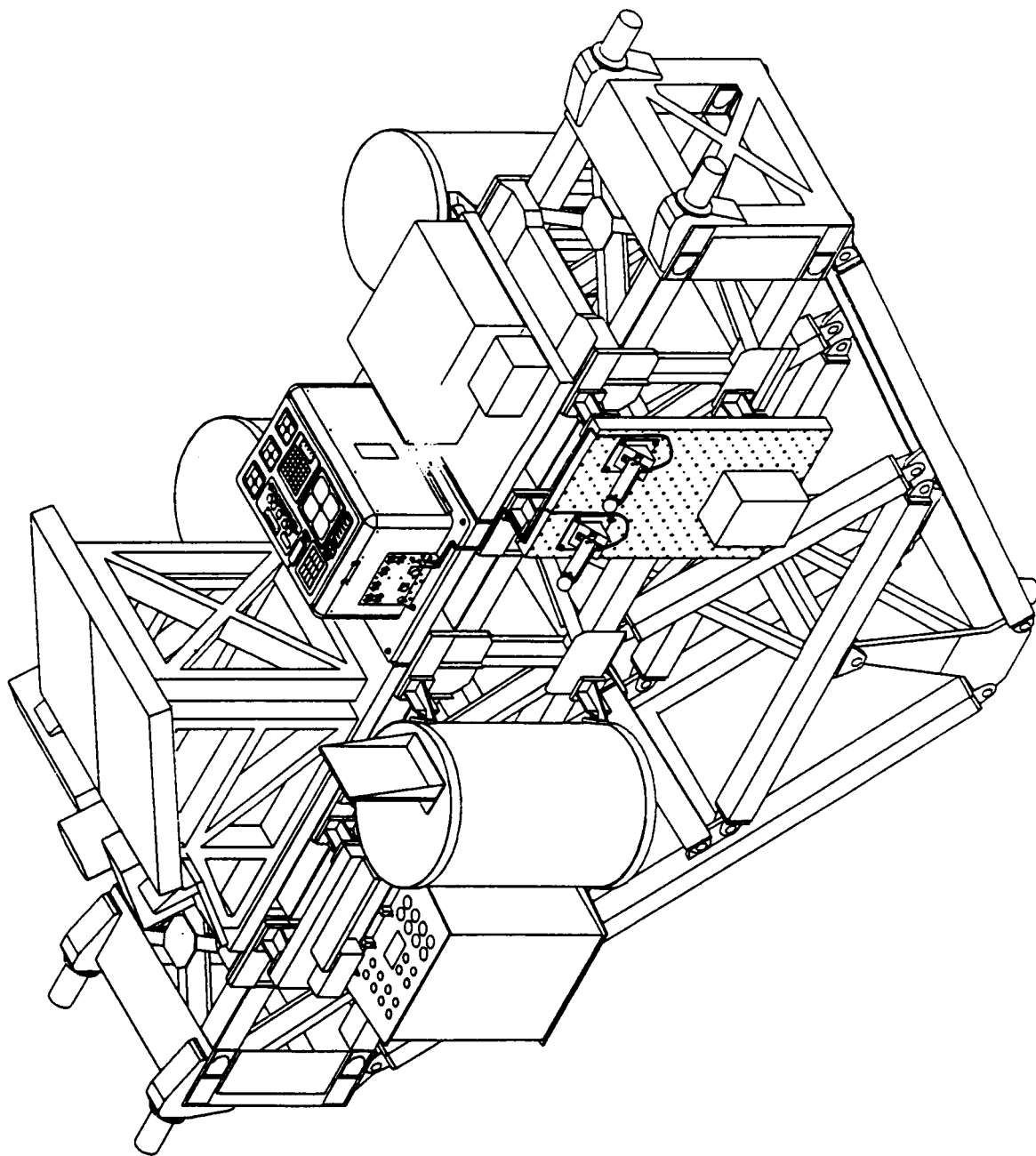


Fig. 4 SAMPLE Mounted on the Hitchhiker-M Carrier (OAST-2)

# **The Photogrammetric Appendage Structural Dynamics Experiment**

Dr. Michael G. Gilbert, Sharon S. Welch, & Dr. Christopher L. Moore  
NASA Langley Research Center  
Hampton, VA. 23681-0001

## **Abstract**

The Photogrammetric Appendage Structural Dynamics Experiment (PASDE) is a Hitchhiker payload scheduled to fly as part of the International Space Station (ISS) Phase-I flight program to the Russian Space Station Mir. The objective of the first flight of PASDE on STS-74 is to obtain video images of the Mir Kvant-II solar array response to various structural dynamic excitation events. This experiment will demonstrate the use of photogrammetric techniques for on-orbit structural dynamics measurements. Photogrammetric measurements will provide a low cost alternative to appendage mounted accelerometers to the ISS program. The PASDE experiment hardware consists of three instruments each containing two video cameras, two video tape recorders, a modified video signal time inserter, and associated avionics boxes. The instruments were designed and built at the NASA Langley Research Center, and are integrated into standard Hitchhiker canisters at the NASA Goddard Space Flight Center. The Hitchhiker canisters are then installed into the Space Shuttle cargo bay in locations selected to achieve good video coverage and photogrammetric geometry. The measurement resolution of the instruments is expected to be on the order of 0.25 cm (0.1 in.).

## **Introduction**

The Photogrammetric Appendage Structural Dynamics Experiment (PASDE) is an experiment to mitigate technical risk and cost associated with passive, on-orbit, measurement of spacecraft appendage structural response for the International Space Station (ISS) program. The experiment will demonstrate a photogrammetric method for making appendage structural measurements, provide engineering data on solar arrays designs expected to be used on the ISS, and verify that routine on-orbit spacecraft operational events provide sufficient excitation for structural response testing.

On-orbit measurements of spacecraft structural response are often desired or necessary for structural verification and loads prediction validation. Typically, acceleration response time-history data is collected and processed on the ground. From this data, structural dynamic characteristics (structural mode frequencies, damping, and mode shapes) can be determined using parametric identification algorithms such as the Eigensystem Realization Algorithm (ERA) [1].

The use of photogrammetric measurements is a low cost alternative to dedicated accelerometer-based structural response measurement systems, especially when measurements are required for articulating or rotating spacecraft components such as solar arrays or thermal radiators. Elimination of accelerometers, wiring, signal conditioning and digital conversion electronics, etc., can greatly simplify the spacecraft electrical design and integration, with corresponding reduction in spacecraft cost.

For the International Space Station (ISS), Figure 1, on-orbit structural response measurements are required for loads validation and verification of structural mathematical models. Currently, accelerometer-based measurements of the US. primary truss and modules are being planned, however, accelerometer measurement of the US. solar arrays are not being considered because of cost and resource impacts. Since the current ISS design calls for numerous video

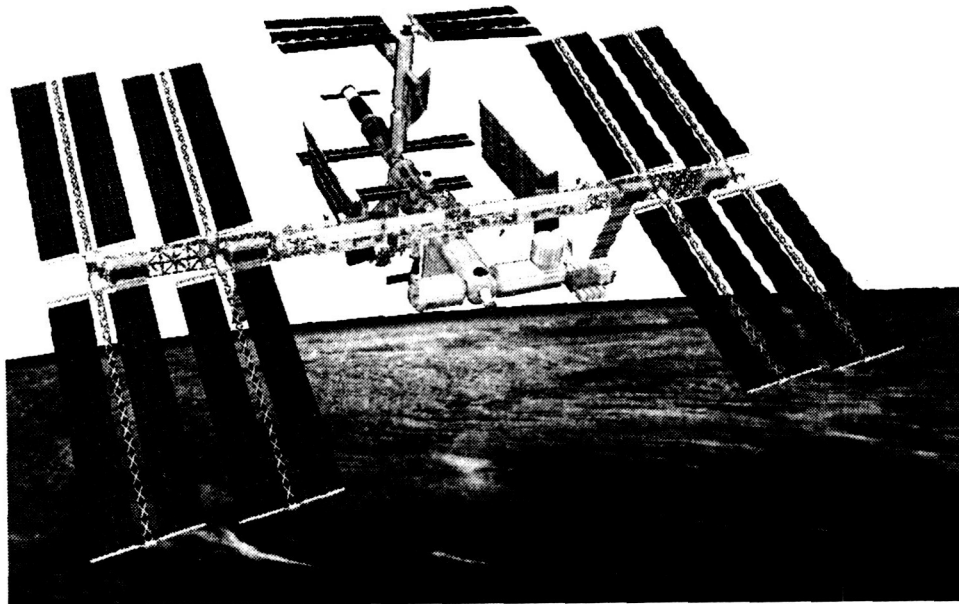


Figure 1 - International Space Station (ISS)

cameras mounted at various external points, photogrammetric measurements of solar array structural responses is a potential alternative.

The PASDE experiment will verify that photogrammetric measurements can provide measurement resolution and accuracy sufficient for ISS structural verification purposes. It is manifested as part of the ISS Phase I Risk Mitigation Program. ISS Phase I involves seven flights of the U. S. Space Shuttle to the orbiting Russian Space Agency Mir space station. Current plans call for PASDE to fly twice as part of the Phase I program.

NASA Langley Research Center (LaRC) is funded by NASA Headquarters Code X for development and first flight of PASDE. PASDE hardware will be flown as a Class D, NASA Goddard Space Flight Center (GSFC) Hitchhiker payload. On STS-74, the second Space Shuttle flight to Mir, PASDE will fly along with the Glo-4 experiment [2] as the Hitchhiker Glo-4/PASDE or GPP payload. On STS-86, the seventh mission of Shuttle to Mir, PASDE hardware will be used to obtain measurements as part of the Mir Structural Dynamics Experiment (MiSDE) Risk Mitigation Experiment. Funding for the STS-86 flight of PASDE is provided by the ISS Phase-I program.

The remainder of this paper is organized as follows. The concept of photogrammetric structural response measurements is discussed first, followed by specific measurement requirements for the PASDE experiment. The design and fabrication of hardware to meet the measurement requirements is covered next, followed by the STS-74 mission science objectives and planned operations.

### **Photogrammetric Structural Response Measurement**

Photogrammetry is defined as "the science of making reliable measurements by the use of photographs..." [3]. In the case of a single photograph or image, certain precise measurements of an object in the image, such as geometrical size, can be made under appropriate conditions. With several images of an object, again under appropriate conditions, the orientation and/or position of

the object with respect to the positions of the cameras can be determined using a triangulation process [4]. The precision of the position or orientation determination is dependent on the quality and number of images. At least two independent images are required for triangulation, with more images leading to higher precision. If the object of interest is moving, determination of the position or orientation as a function of time requires a sequence or series of images from each camera location and triangulation at each time of interest. Measurement of time-varying structural response, which is of interest here, is an example of this third type of photogrammetric measurement.

The measurement of structural dynamic response using photographic cameras has previously been limited by costs of film and film processing, alignment of photographic frames in time, and the significant manual processing inherent in using photographs for triangulation. The recent advent of low-cost, charge-coupled-device (CCD) video cameras, video recorder systems, and digital image processing techniques have eliminated most of these limitations.

Several efforts at measuring structural response by photogrammetric methods have been made [e.g. 5,6]. In the 1984 Solar Array Flight Experiment (SAFE) for example, photogrammetric measurements of a solar array cantilevered from the cargo bay of the Space Shuttle were made from video recorded by the Shuttle's on-board camera systems. The position of the array in the cargo bay was fixed with respect to the Shuttle camera system in this experiment. As shown in Figure 2, the motion recorded in the SAFE video images was directly proportional to the structural deformation of the array as it responded to various structural excitation sources.

For the case of the International Space Station solar arrays, there will be relative, rigid-body motion of the solar array with respect to the positions of the photogrammetric cameras. This motion is due to articulation and/or rotation of the array as it tracks the sun in Earth orbit. Thus the motion measured by a photogrammetric system for ISS solar arrays will consist of combined rigid-

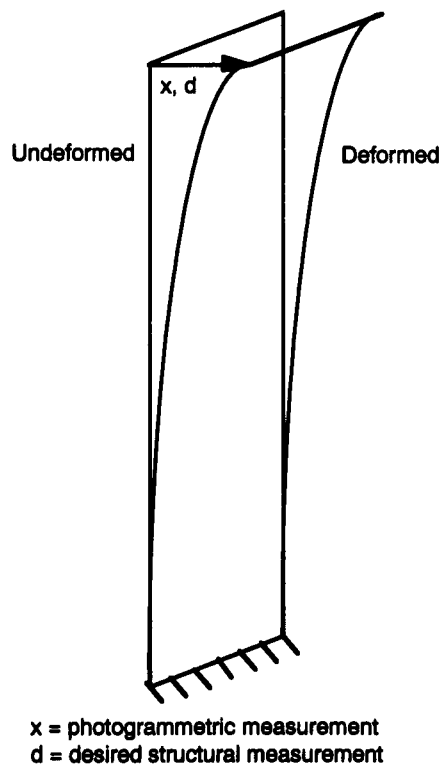


Figure 2 - Solar Array Flight Experiment (SAFE) structural measurement.

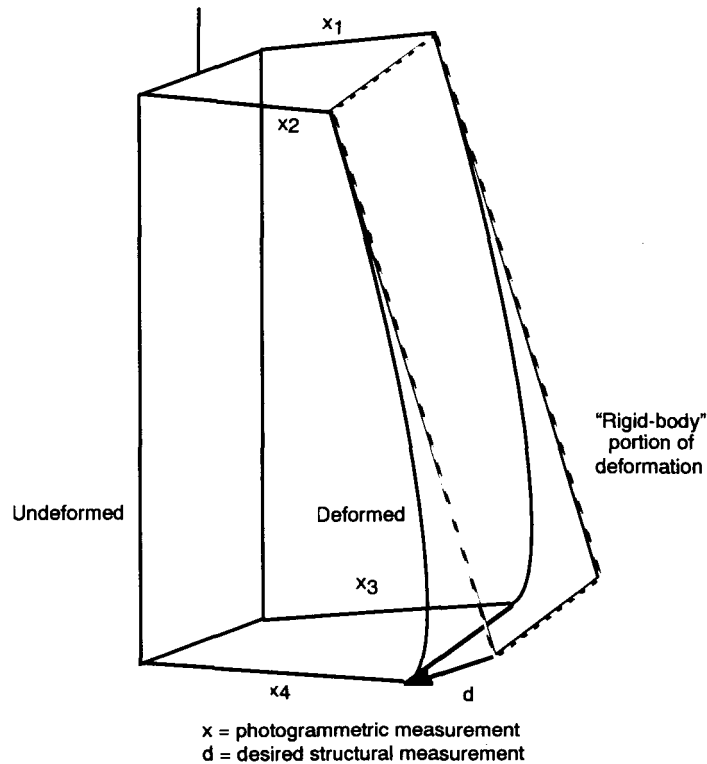


Figure 3 - Relative motion case structural measurement.

body and structural deformations, as shown in Figure 3. To extract the structural motion from the combined motion, the apparent "rigid-body" motion component must be determined. This can be accomplished by determining the motion of points on the solar array which can reasonably be expected to have little structural deformation (such as near the root), and using this measurement to predict a "rigid-body" orientation and position of the array from known array geometry. Subtracting the predicted "rigid-body" motion from the total measured motion leaves an estimate for the structural deformation.

The PASDE experiment was designed to make relative motion structural measurements as defined in Figure 3. Use of the latest technologies in CCD cameras and digital image processing enables the extraction of minute structural motions from video images of spacecraft solar arrays and other flexible, articulating components. The hardware requirements to make these measurements are described in the next section.

### PASDE Measurement Requirements

The hardware requirements for on-orbit photogrammetric spacecraft structural response measurements are dependent on the size and orientation of the appendage(s) of interest, the lighting conditions, the distances and three dimensional relationship of the imaging devices, and the number of desired mode parameter sets (frequencies, damping, and shapes) desired.

For the PASDE hardware development, a general sense of potential flight opportunities and possible targets and geometry was used to generate a set of design requirements. These potential flight opportunities involved imaging solar arrays on the Russian Mir space station during Space Shuttle docking flights. For these opportunities, photogrammetric distances ranging from 10 to 20 meters (30 to 60 feet) were expected, measuring from 2 or 3 Shuttle cargo bay locations. Identification of the first 3 or 4 solar array mode parameter sets was desired, leading to the hardware design requirements listed in Table 1.

Table 1 - PASDE hardware design requirements.

Item	Requirement
Resolution	Measure 0.1" motions of the array tip
# of Array Measurements	Minimum of 6 needed to extract motion and determine modes shapes
Data Recording	1-2 minutes prior/during excitation 3-5 minutes following excitation
Time Correlation	Video data time tagged to Shuttle events consistently for all events
Sample Rate	10 Hz. or greater

From analytical finite element structural models of the coupled (docked) Shuttle/Mir spacecraft, solar array responses to expected on-orbit excitation events were computed. These results in conjunction with solid-body viewing models and likely Shuttle payload bay locations led to the PASDE requirement to resolve 0.25 cm (0.1 inch) motions at the expected viewing distances. To identify both bending and torsion mode parameters while extracting relative array motions, a minimum of six time history data points are required. Desired ranges of locations for the six minimum points were defined, and target regions for pointing the cameras were established, as illustrated in Figure 4. In Figure 4, the arrows and dimensions establish the six approximate locations, indicated by small circles, with respect to the length and width of the array. The larger viewing circles indicate the desired viewing areas for the cameras, which encompass the minimum number of time history points. Actual data points for flight data analysis will be determined after the flight based on the obtained images, contrast, identifiable features, etc. It is expected that time history data will be obtained for more than the minimum number of points.

The other requirements listed in Table 1 were defined qualitatively, accounting for the typical types of data characteristics needed for good identification of structural modes. These included the amount of free decay response following excitation, the time correlation of the video

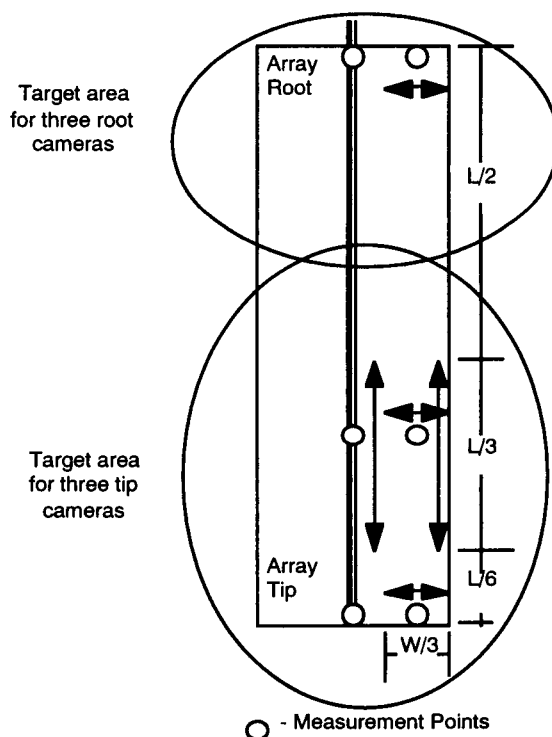


Figure 4 - Definition of minimum number and location of measurement points.

images with each other, and the sampling rate. The minimum 10 Hertz sampling rate provides a 10 to 1 frequency ratio with respect to the highest frequency mode that can reasonably be expected to be identified. Standard video data is 30 Hertz.

### **Hardware Design**

Based on the length of the Mir solar arrays and the viewing geometries possible in the Shuttle payload bay, a PASDE design incorporating six video cameras in three Hitchhiker canisters located in the Shuttle payload bay was selected. Two cameras are in each Hitchhiker canister, one aimed and focused at the root of the array, and the other at the tip of the array. It was also decided that the PASDE hardware for each canister would be identical, with adjustable mounting arrangements for the cameras to allow for individual pointing. A photo of an assembled flight unit is shown in Figure 5, prior to installation into a Hitchhiker canister.

Pulnix Model TM-9701 monochrome video cameras with CCD array sizes of 764 x 486 pixels were selected. Each camera has a Schneider 50 millimeter focal length lens with a motor driven iris to adjust for lighting conditions. Lens focus is adjusted on the ground prior to flight and cannot be changed on-orbit. The camera/lens combination has a  $\pm 5$  degree field-of-view. Associated with each camera is a Teac Model V-80AB-F Hi8 video tape recorder providing two hours of video recording time. A single modified IRIG-B time inserter from Sekai, a single Power Conversion and Distribution Unit (PCDU) from Vicor, and a single Langley designed and built Interface and Control Unit (ICU) were used for each set of flight hardware. The IRIG-B time inserters convert time code from the Shuttle into a video format and add the result to the video signal prior to recording. This ensures that the six recorded video signals can be time correlated to within a single video frame. The ICU provides the interface between the PASDE hardware and the

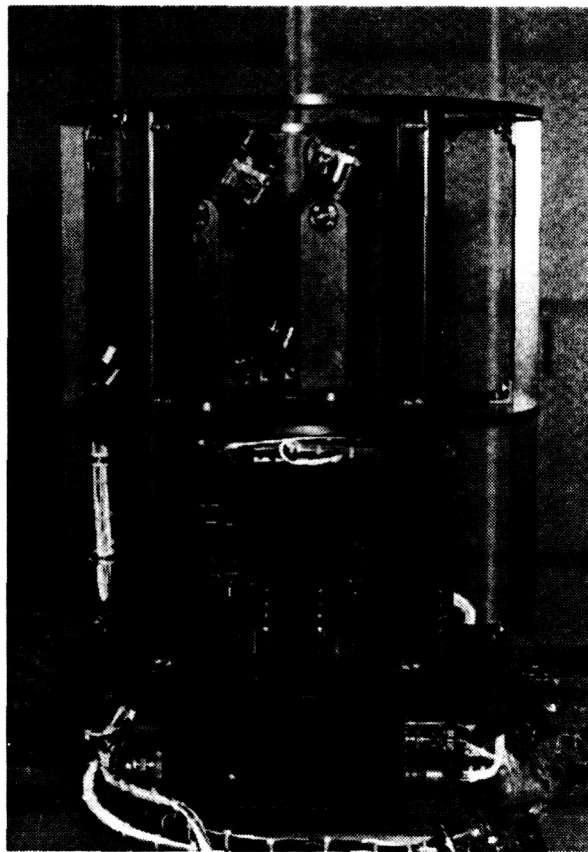


Figure 5 - PASDE flight hardware prior to Hitchhiker canister integration.



standard Hitchhiker avionics. It processes 8 different bi-level commands from the Hitchhiker to activate the hardware, initiate and stop recording, and to establish lens iris positions.

A supporting structure to mount two cameras, two recorders, and the avionics boxes to fit inside a standard Hitchhiker payload canister was designed. In addition, a 3 degree-of-freedom camera/lens mount gimbal was designed to allow each camera to be individually pointed. The gimbal is fixed prior to flight and is not adjustable on on-orbit.

Three sets of identical flight hardware were fabricated, assembled, and tested at the NASA Langley Research Center. Each unit was subjected to acceptance level vibration, EMI, thermal-vacuum, and functional tests. The units were then shipped to GSFC for integration with the Hitchhiker canisters and further EMI testing. Once integrated, the canisters were sealed with a large aperture window upper endplate and pressurized with dry nitrogen.

### STS-74 Mission Science Objectives

The measurement objective for the PASDE experiment on the STS-74 mission is the lower, Kvant-II solar array as shown in Figure 6. During the docked portions of the combined Shuttle/Mir mission, this array will be outboard on the port side of the Shuttle, slightly ahead of the wing. The three Hitchhiker canisters containing the PASDE flight hardware will be located aft of the Kvant-II array in Shuttle cargo bays 6 (port side), bay 7 (starboard side), and bay 13 (port side). The expected camera images (for one orientation of the array with respect to Mir) for each PASDE canister tip and root camera are shown in Figures 7 and 8 respectively.

Excitation and structural deformation of the lower Kvant-II array is expected from a variety of events planned for the mission. These include the actual docking, a series of Shuttle Primary Reaction Control System (PRCS) jet firings, day/night and night/day orbital transitions, and solar array rotational slews for sun tracking. Data for each of these events will be collected (i.e. tape recorded) and stored for post-flight analysis.

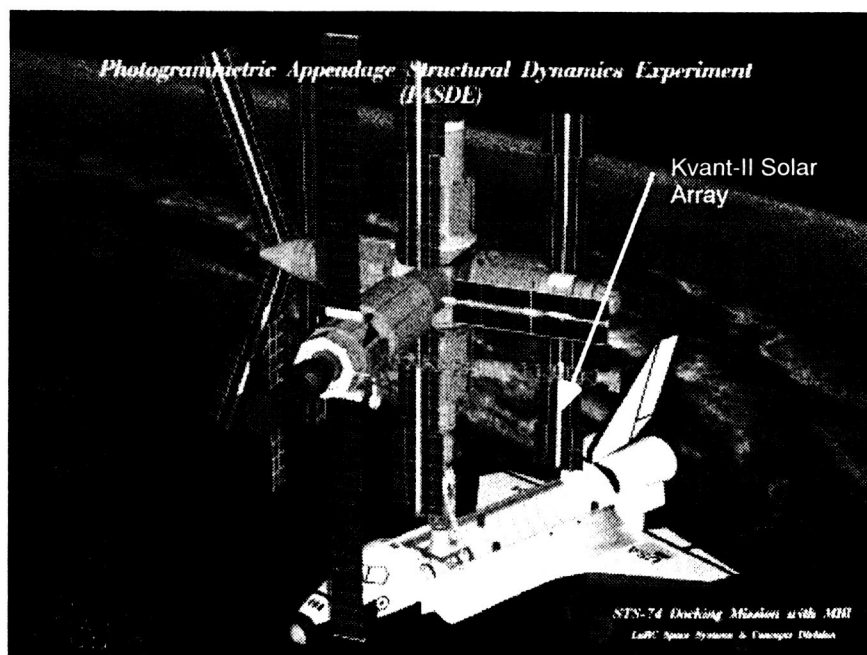


Figure 6 - STS-74 Shuttle/Mir configuration.

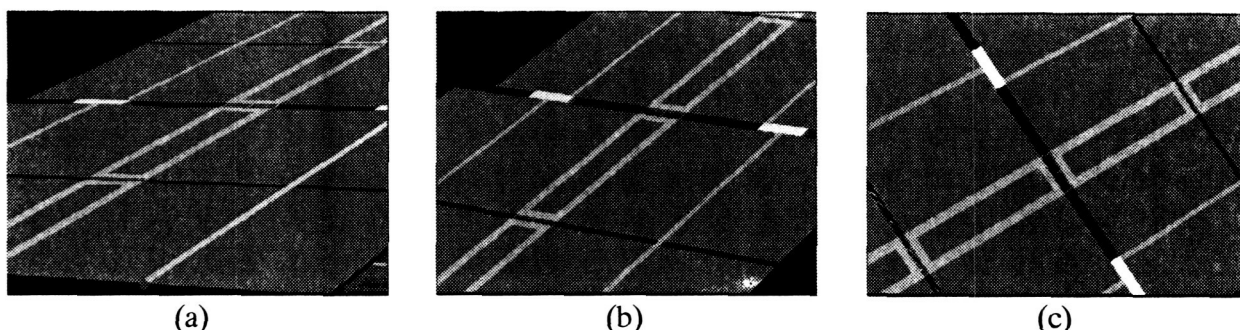


Figure 7 - Tip camera views of Kvant-II solar array: (a) Bay 6, (b) Bay 7, and (c) Bay 13

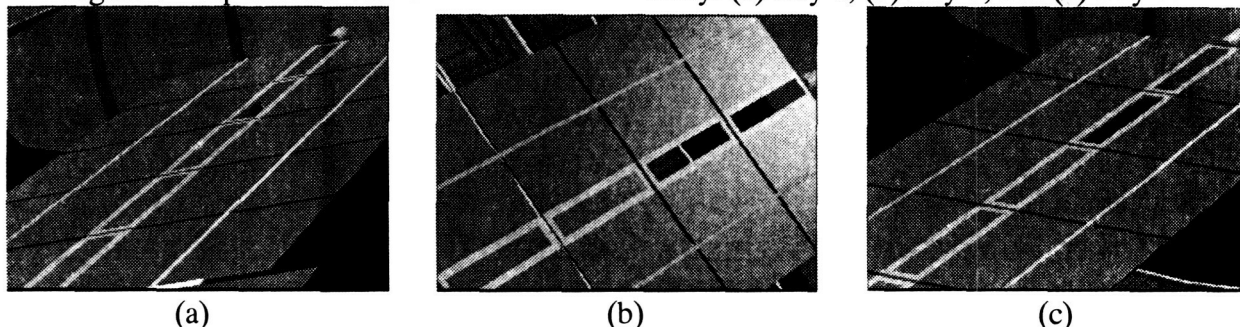


Figure 8 - Root camera views of Kvant-II solar array: (a) Bay 6, (b) Bay 7, and (c) Bay 13

Post-flight, the recorded video data will be digitized frame-by-frame and high contrast features in the images will be identified. Advanced digital image processing algorithms will be applied to precisely locate the high contrast features with respect to the focal planes of the individual cameras. A triangulation process will then be used to determine the three dimensional position of features appearing in multiple views with respect to the Shuttle coordinate system. Processing of the images in sequential time order will provide a three-dimensional time history record of motion at various points on the array.

The time history data describing the motion of points on the array will be further processed to determine the relative "rigid-body" motion of the array with respect to the camera system. With this information, the structural deformation and modal parameters can be determined. The final data will satisfy the following three science objectives:

- 1) Verification that photogrammetric measurements techniques can be used for passive on-orbit measurement of structural response sufficient to determine structural mode parameter sets for appendages which may have non-structural relative motion with respect to the cameras.
- 2) Direct determination of the response of Mir Kvant-II solar arrays to day/night and night/day thermal transitions.
- 3) Verification that normal on-orbit dynamic events provide sufficient excitation for determination of structural mode parameters.

Satisfaction of objective 1) will be enhanced by accelerometer data collected on the Mir space station and from the Inertial Measurement Units (IMU) on the Space Station. Mir has 22 accelerometers located at various points inside the modules which will collect data during some of the expected on-orbit events.

## STS-74 Mission Operations

PASDE mission operations will be conducted during the STS-74 mission from the Hitchhiker Payload Operations Control Center (POCC) at NASA Goddard. The PASDE hardware will be commanded to set camera iris positions and start and stop recording directly from the POCC. Within the POCC, PASDE will have a limited capability to downlink a video signal from any one of the six cameras in real or near-real time.

During the mission, the first PASDE operations will occur prior to docking when a calibration of the camera iris settings is undertaken. The Shuttle Remote Manipulator System (RMS) end effector will be positioned in the approximate location of the tip of the Kvant-II solar array, and the Shuttle attitude will correspond to an expected post-docking orientation. Direct downlink of video images from the tip cameras for various lens iris settings will be compared with ground based data to update iris settings for later data collection activities.

The first actual data collection event will be the Shuttle/Mir docking. Table 2 lists the expected recording time and solar array motion for this event. Based on current mission timelines, several hours following the docking the Shuttle will undertake a series of PRCS jet firings for confirmation of Shuttle flight control system parameters. The solar array response to each of these jet firings will also be recorded. A second iris calibration period and a second PRCS jet firing sequence may be scheduled following the first jet firings events. Recording of day/night and night/day transitions will occur later in the docked portion of the mission, with several different lens iris settings. Multiple recordings will be made, dependent on remaining available tape, to mitigate the effects of the rapidly changing lighting conditions for these events. Of the 120 minutes of available tape recording time, 100 minutes is currently scheduled so as to provide tape margin for contingencies and "event-of-opportunity" data collection.

Table 2 - STS-74 excitation events and data collection periods.

Event	Time	Expected Motion (0-Peak)
STS/Mir Docking	30	> 2"
PRCS Jet Firings	40	≤ 0.8"
Day/Night	15	?
Night/Day	15	?

## Concluding Remarks

The ISS Phase-I PASDE Risk Mitigation experiment is being developed by NASA Langley Research Center and flown as a NASA Goddard Space Flight Center Hitchhiker attached payload. The PASDE flight hardware has been fabricated, assembled, tested, and integrated for first flight on STS-74, currently scheduled for launch in October 1995. Planning and operational training for the first flight is underway. Data from the experiment will provide confidence to the ISS program that photogrammetric measurement methods can provide sufficient resolution and accuracy to meet appendage structural verification measurement requirements.

## References

- [1] Pappa, R. S.; Eigensystem Realization Algorithm User's Guide for VAX/VMS Computers. NASA TM 109066, May 1994.
- [2] Glo Experiment/Photogrammetric Appendage Structural Dynamics Experiment Payload, Payload Integration Plan (PIP) Basic, NASA Johnson Space Center Document NSTS 21316, February 1995.

- [3] Webster's Ninth New Collegiate Dictionary, Merriam-Webster Inc., Springfield, MA. 1990.
- [4] Slama, C. C., Theurer, C., and Henriksen, S. W.; Manual of Photogrammetry, Fourth Edition, Published by American Society of Photogrammetry, Falls Church, VA. 1980.
- [5] Brumfield, M. L., Pappa, R. S., Miller, J. B., and Adams, R. R.; Orbital Dynamics of the OAST-1 Solar Array Using Video Measurements. Presented at the AIAA/ASME/ASCE/AHS 26<sup>th</sup> Structures, Structural Dynamics, and Materials Conference, Orlando, FL., April 15-17, 1985. AIAA Paper 85-0758-CP.
- [6] Byrdsong, T. A., Adams, R. R., and Sandford, M. C.; Close-Range Photogrammetry Measurement of Static Deflections for an Aeroelastic Supercritical Wing. NASA TM-4194, December 1990.

## **SHUTTLE LASER ALTIMETER (SLA)**

### **A Pathfinder for Space-Based Laser Altimetry & Lidar**

**Jack Bufton, Bryan Blair, John Cavanaugh, James Garvin,  
David Harding, Dan Hopf, Ken Kirks, David Rabine, & Nita Walsh**

**Laboratory for Terrestrial Physics  
Goddard Space Flight Center  
Greenbelt, MD 20771  
301-286-8671**

## **INTRODUCTION**

The Shuttle Laser Altimeter (SLA) is a Hitchhiker experiment now being integrated for first flight on STS-72 in November 1995. Four Shuttle flights of the SLA are planned at a rate of about a flight every 18 months. They are aimed at the transition of the Goddard Space Flight Center airborne laser altimeter and lidar technology to low Earth orbit as a pathfinder for operational space-based laser remote sensing devices. Future laser altimeter sensors such as the Geoscience Laser Altimeter System (GLAS), an Earth Observing System facility instrument, and the Multi-Beam Laser Altimeter (MBLA), the land and vegetation laser altimeter for the NASA TOPSAT (Topography Satellite) Mission, will utilize systems and approaches being tested with SLA.

The SLA Instrument measures the distance from the Space Shuttle to the Earth's surface by timing the two-way propagation of short ( $\sim 10$  nsec) laser pulses. Laser pulses at 1064 nm wavelength are generated in a laser transmitter and are detected by a telescope equipped with a silicon avalanche photodiode detector. The SLA data system makes the pulse time interval measurement to a precision of about 10 nsec and also records the temporal shape of the laser echo from the Earth's surface for interpretation of surface height distribution within the 100 m diam. sensor footprint. For example, tree height can be determined by measuring the characteristic double-pulse signature that results from a separation in time of laser backscatter from tree canopies and the underlying ground. This is accomplished with a pulse waveform digitizer that samples the detector output with an adjustable resolution of 2 nsec or wider intervals in a 100 sample window centered on the return pulse echo. The digitizer makes the SLA into a high resolution surface lidar sensor. It can also be used for cloud and atmospheric aerosol lidar measurements by lengthening the sampling window and degrading the waveform resolution. Detailed test objectives for the STS-72 mission center on the acquisition of sample data sets for land topography and vegetation height, waveform digitizer performance, and verification of data acquisition algorithms.

The operational concept of SLA is illustrated in Fig. 1 where a series of 100 m footprints stretch in a profile of Earth surface topography along the nadir track of the Space Shuttle. The location of SLA as a dual canister payload on the Hitchhiker Bridge Assembly in Bay 12 of the Space Shuttle Endeavor can also be noted in this figure. Full interpretation of the SLA range measurement data set requires a 1 m knowledge of the Orbiter trajectory and better than  $0.1^\circ$  knowledge of Orbiter pointing angle. These ancillary data sets will be acquired during the STS-72 mission with an on-board Global

positing System (GPS) receiver, K-band range and range-rate tracking of the Orbiter through TDRSS, and use of on-board inertial measurement units and star trackers. Integration and interpretation of all these different data sets as a pathfinder investigation for accurate determination of Earth surface elevation is the overall science goal of the SLA investigation.

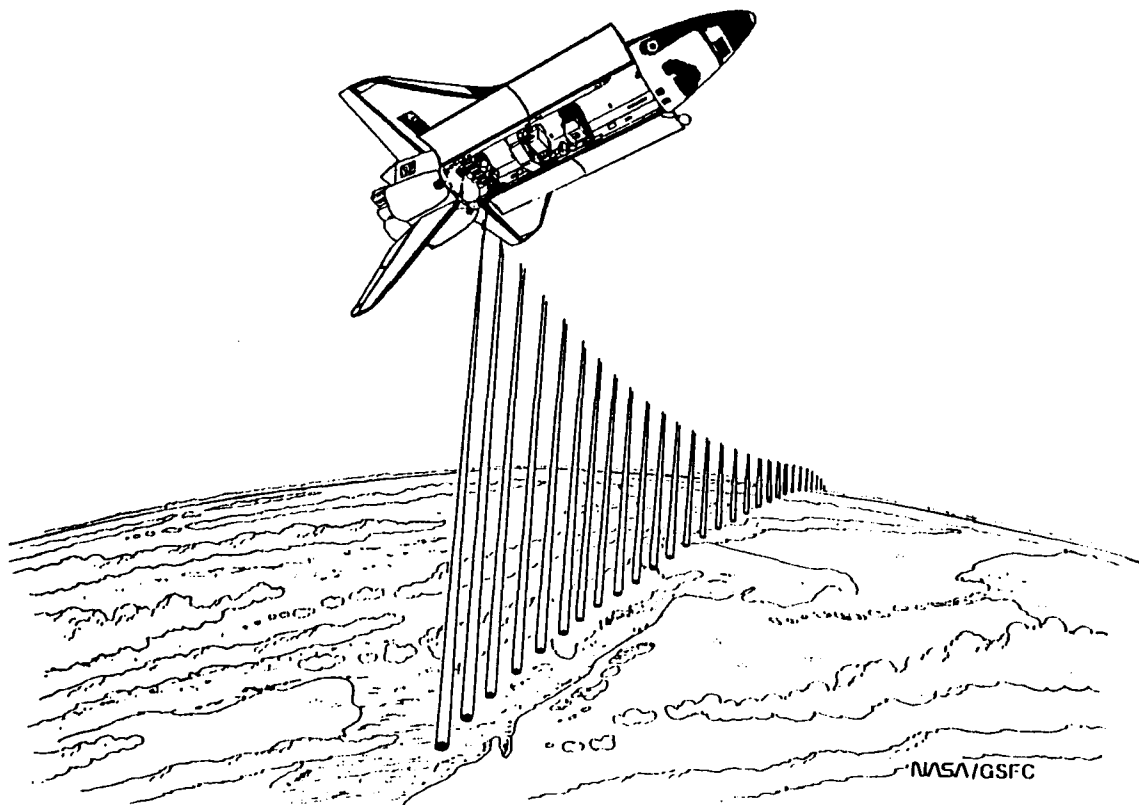


Fig. 1  
Global Topography Measurements with the Shuttle Laser Altimeter

## INSTRUMENT DESCRIPTION

The SLA works by generation of short ( $\sim 10$  nsec duration) laser pulses at a 1064 nm near-infrared wavelength on the Space Shuttle and reception of weak backscattered laser radiation from the Earth. The pulsed laser source is a Nd:YAG device that pulses at a fixed, continuous rate of 10 pps throughout the SLA operational periods. A silicon PIN diode receives  $\sim 1\%$  of the outgoing laser pulse and provides a "START" signal for the pulse timing and data acquisition. In the optically clear atmosphere essentially all the initial laser pulse energy reaches the surface where it is spread into a 100 m diameter spot. Distance between laser spots on the Earth is approximately 740 m due to the laser pulse rate and the Shuttle orbital velocity. Reflection from this spot is typically diffuse which results in spreading of the incident laser light into a full hemisphere. Only a very small fraction of the reflected laser pulse can thus be collected by the SLA receiver telescope back on the Shuttle. The SLA telescope is a gold-plated aluminum, parabolic mirror with a relatively large (for a Hitchhiker canister) 0.38 m diam. aperture. Some twelve orders-of-magnitude separate the received signal (femtojoule) from the initial laser pulse energy ( $\sim 40$  millijoule). A sensitive silicon avalanche photodiode (APD) with 40% quantum efficiency at 1064 nm is used to detect this weak laser pulse at

the telescope mirror prime focus and produce an electronic “STOP” signal. An optical bandpass filter and focusing lenses in the mirror focal plane assist the detector by reducing broadband optical noise due to daytime solar illumination and reduce the size of the image spot to fit it on the 0.8 mm APD.

The SLA Instrument design requires the use of two adjacent, Hitchhiker instrument canisters with nominal 5 ft<sup>3</sup> capacity that are connected by an interconnecting cable for data transmission between the canisters as shown in the general arrangement concept of Fig. 2. The two assemblies are the Laser Altimeter Canister (LAC) and the Altimeter Support Canister (ASC), each of which is separately connected to the Hitchhiker avionics through the signal and power ports. The transmitter and receiver sub-assemblies of the laser altimeter instrument are located in the LAC canister which is equipped with a Hitchhiker motorized door assembly (HMDA) and a 1 inch thick optical window for operation of the laser altimeter instrument in a pressurized environment at the full, clear aperture size of 15.375 inch (0.38 m) diam. Both canisters are pressurized with dry nitrogen; the LAC to 1/2 atmosphere and the ASC to 1 atmosphere. Three-dimensional assembly views of the contents of the two canisters that comprise the SLA are shown in Figs. 3 and 4. Major sub-assemblies of the both canisters are labeled in these drawings.

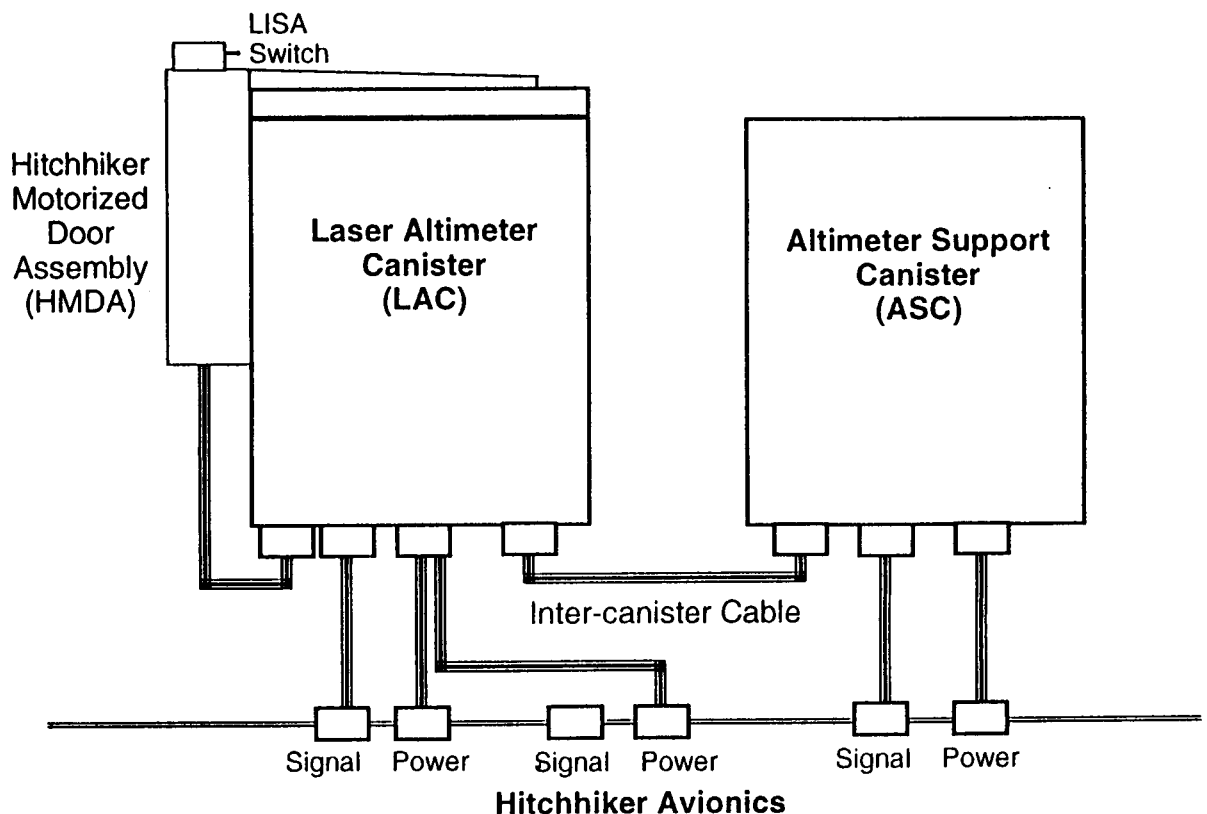
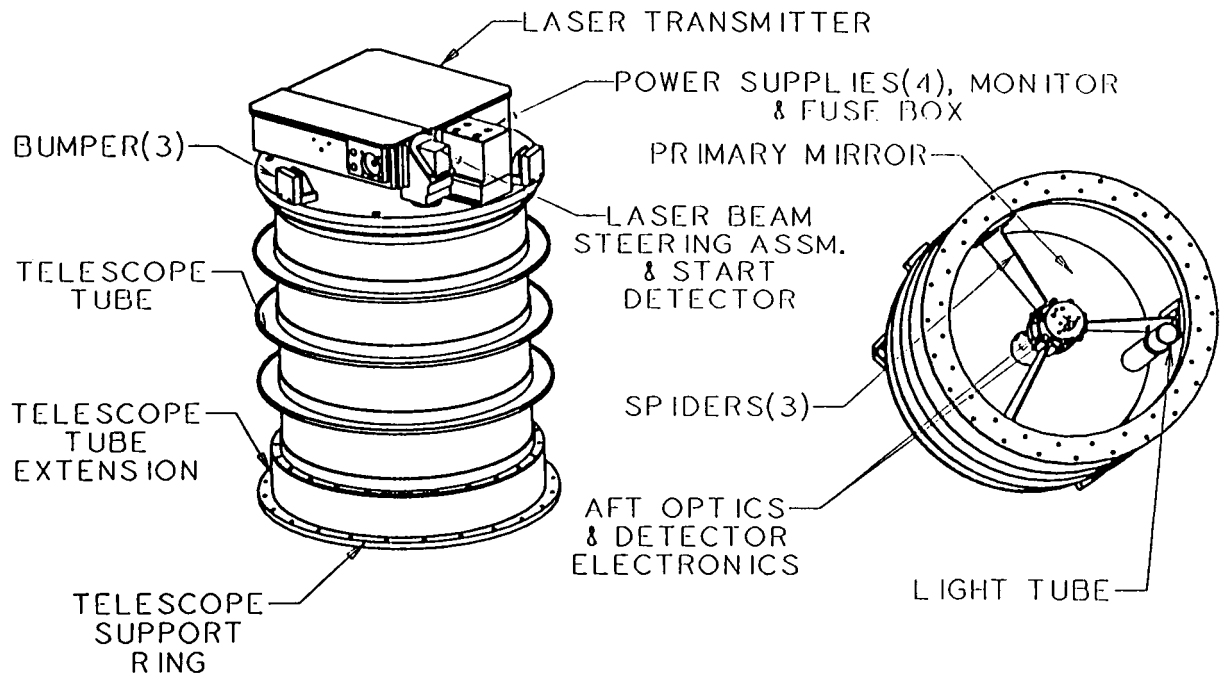
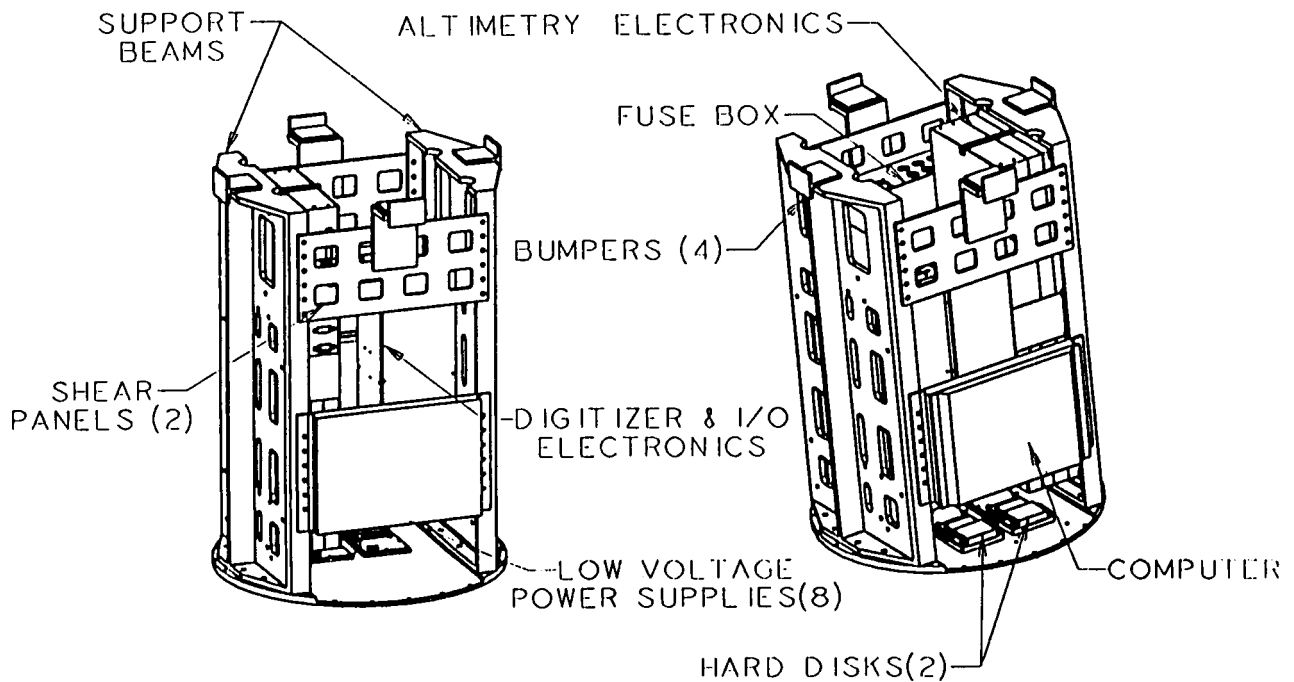


Fig. 2  
Shuttle Laser Altimeter Dual Canister Configuration



**Fig. 3**  
**Laser Altimeter Canister**



**Fig. 4**  
**Altimeter Support Canister**



A functional block diagram of the SLA showing the relationship of the contents of both canisters is presented in Fig. 5. Notable in this figure are the presence of the diode-pumped Nd:YAG laser transmitter in the LAC along with the diamond-turned aluminum parabola telescope mirror and focal plane detector that serve as the optical receiver. The outgoing laser pulse is turned 90° at the output after emerging from the laser source and passes through a Risley prism pair that is adjusted to impart a co-boresight (i.e. alignment) of the laser beam to the fixed pointing (i.e. staring) receiver telescope. The laser source, built by McDonnell Douglas in St. Louis, MO was originally designed for the Mars Observer Laser Altimeter (MOLA) Project. This device weighs only 13 lb. and consumes only 15 W of + 28 vdc electrical power. Power converter and monitor electronics in the LAC serve to provide a source of  $\pm 5$  vdc and  $\pm 12$  vdc for the detector packages. The main APD detector was also originally designed for MOLA Project and was a flight spare.

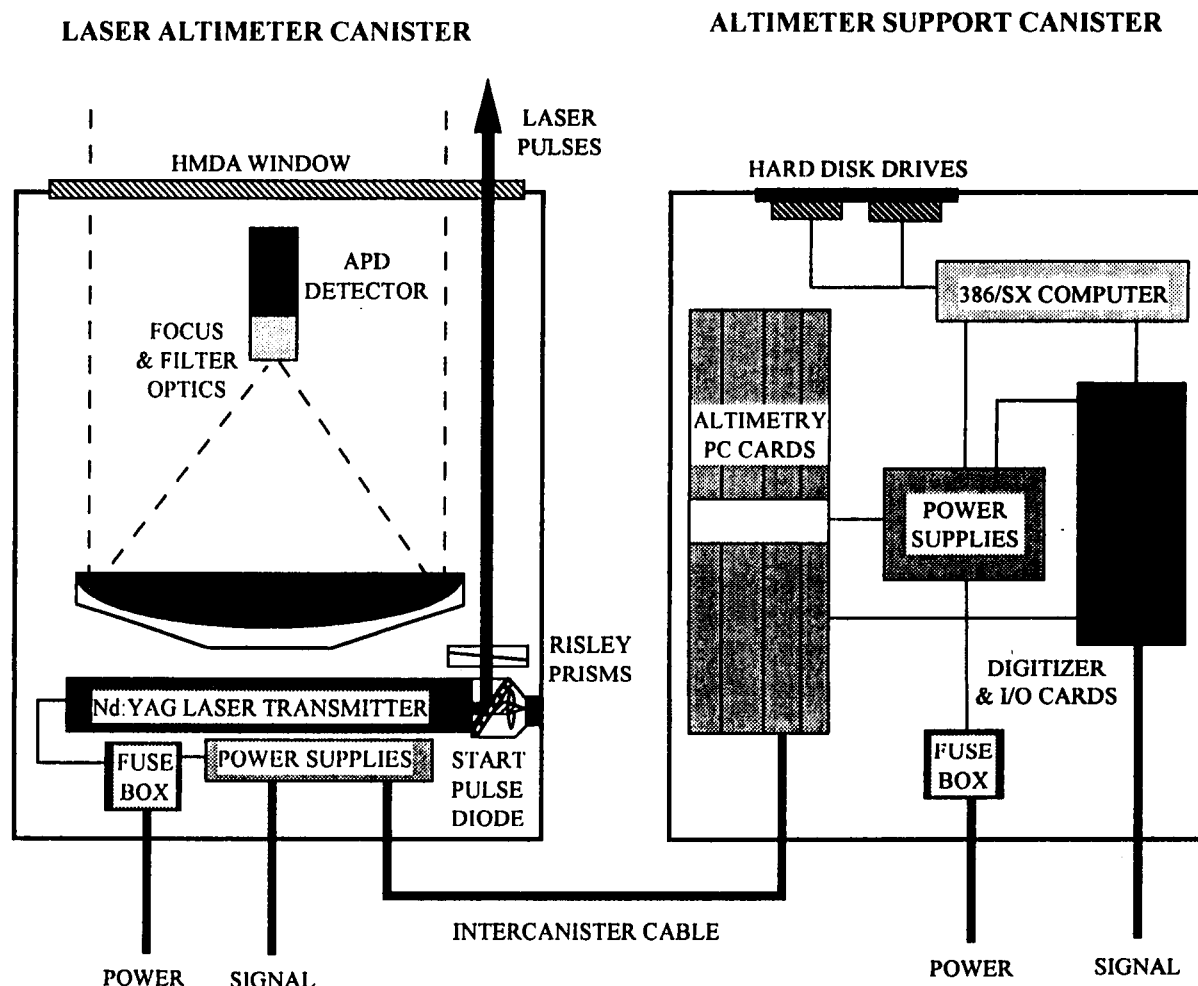


Fig. 5  
Shuttle Laser Altimeter Functional Block Diagram

Principal systems contained in the ASC and their connections are evident in Fig. 5. All the pulse timing, pulse energy, power & temperature monitoring measurements are provided by the altimetry electronics which are composed of five 8x10 inch printed wiring boards and interconnects. These

boards are mounted in aluminum trays or slices that are assembled in an electronics box. Four of these boards were constructed of MIL-SPEC or space-rated EEE parts that were spares from the MOLA Project. Their design is the MOLA design for 4-channel matched-filter laser pulse timing, but does include a clock-pulse interpolation circuit to increase timing resolution to 5 nsec (i.e. provide sub-meter range resolution). Also the fourth (lowest bandwidth) channel of pulse energy is replaced with a channel 1 pulsewidth measurement. Channel 1 has a Gaussian filter detection bandwidth of 16.6 MHz which is signal-to-noise ratio optimized for detection of a 20 nsec pulse. The computer, a 386/SX single board device with a single 512 Kbyte EPROM and 2 Kbyte of RAM, and most low voltage power converters are located in two trays (i.e. slabs) that mount across the support frames of the ASC assembly. The AT computer bus is actually a ribbon cable which extends to an aluminum housing containing the three expander cards necessary for pulse waveform digitization, parallel I/O operations with the altimetry electronics, and the all-important serial I/O communication card extending RS-422 and RS-232 connections to the Hitchhiker avionics for commands and data. The digitizer is capable of 500 Megasample-per-sec (i.e. 2 nsec sample intervals) operation and has an on-board memory of 8 K samples. It is potentially a very power hungry device that would like to use 25 W or more when operating continuously. A key innovation of the SLA Instrument design is power cycling of this device that turns in on for only 5 msec when it is needed, i.e. when the laser pulse is transmitted, flies to Earth, returns and is analyzed. The digitizer duty cycle is thus 5% (5 msec every 100 msec based on the 10 pps laser pulse rate). Separate dc-to-dc converters supply the +5 vdc and +12 vdc required by the three expander cards and are mounted inside the card housing. A summary of the mass and power parameters for the both canisters is given in Table 1.

PAYLOAD ASSEMBLY	MASS (KG)	MASS (LB)	POWER AVERAGE (W)	HEATER POWER (W)	PEAK POWER (W)	ENERGY AVERAGE* (KWH/DAY)
LASER ALTIMETER CANISTER (instrument)	48	105.7	20	60	90	0.6
HMDA CANISTER/ with WINDOW	117.3	258.3	-	-		-
SUB-TOTAL (LAC):	165.3	364	20	60	90	0.6
ALTIMETER SUPPORT CANISTER (instrument)	51.1	99.9	34	60	105	0.77
STANDARD HITCHHIKER CANISTER (5 cubic ft.)	45.4	153.8	-	-		-
SUB-TOTAL (ASC):	96.5	253.6	34	60	105	0.77
HITCHHIKER AVIONICS & ADAPTER PLATE (1/3)	27.7	61	42	0		1.01
TOTAL (SLA):	289.5	678.6	96	120	195	2.38

Table 1  
Mass and power summary for the Shuttle Laser Altimeter Instrument.

\* Assumes: 50% operations duty cycle & replacement heaters to maintain LAC & ASC at minimum operating temp.

The LAC and ASC canister electronics are connected by a special purpose cable that is separate from the Hitchhiker power and signal interface cables. This multi-conductor (41) interconnecting cable contains coaxial cables for transfer of data pulses from the LAC to the ASC, #22 AWG twisted pair wires for connection of the various temperature sensor lines and digital I/O lines from the LAC to the ASC, and transmission of the TTL laser fire pulses from the ASC to the LAC.

## **HITCHHIKER PAYLOAD OPERATIONS**

An initial on-orbit cool-down period of a minimum of 24 hrs. prior to SLA activation is planned in order to achieve optimum operation (the generation of maximum laser pulse energy) of the laser altimeter transmitter in the LAC at 0 C. During this period thermostatically-controlled replacement heaters will activate if the LAC falls below -5 C or the ASC falls below +5 C. The first step in activation of the SLA occurs when astronauts activate the laser power enabling Standard Switch Panel (SSP) switches S16 & S22 and the Hitchhiker motorized door assembly (HMDA) for the Laser Altimeter Canister is opened by ground control. With an open door and acceptable operating temperatures in both the LAC and the ASC, the power-on command will be given to the ASC in order to initiate SLA operation for a verification of medium and low rate telemetry and commanding capability. Activation of the LAC canister shall be permitted only when the Orbiter is in the -ZLV orientation, SLA instrument power is on, and the HMDA door lid is fully open. Laser transmitter operation shall not be permitted during crew EVA or any spacecraft retrieval operations. The potential eye safety hazard to the crew from reflection of SLA laser radiation; either from a partially open HMDA door lid or objects in the near-space environment of the Orbiter will be controlled by three independent inhibits to SLA laser operation. These are as follows:

- (1) a relay in the LAC that switches +28 vdc electrical input power to the laser;
- (2) a relay in the LAC that switches the +28 vdc return of electrical power to the laser; and
- (3) ground commanding through the ACCESS computer.

Inhibits (1) and (2) are respectively controlled by astronaut activated switches S22 and S16. A door interlock switch, called the LISA switch, is in series with inhibit (2) and prevents laser operation until the door is fully open (95° rotation). Computer commands from the Hitchhiker Payload Operations Control Center (POCC) are required to operate the HMDA door, activate the ASC and LAC, and generate laser fire pulses from the ASC which go by intercanister cable to the LAC and its laser transmitter.

The data acquisition configuration of SLA Instrument operations is controlled by several commands and 38 individual parameters that can be updated through the parameter command. The SLA data system command instructions flow to the SLA on-board 386/SX computer where they modify the pre-programmed EPROM flight software operational modes and default parameter values. When first activated, the on-board SLA computer boots from the EPROM and enters the flight software in a "SAFE" (i.e. standby) mode in which both medium-rate and low-rate telemetry packets are generated, but no laser pulses are generated. Upon receipt of the "FIRE" command, the laser transmitter pulses at 10 pulses per sec, pulse data from laser radiation backscattered by the Earth's surface are collected and processed, and the altimetry and housekeeping data are formatted and recorded on-board on hard disk drives and sent by both telemetry channels to the ground for SLA GSE monitoring and recording. All laser altimeter data are acquired and stored on the twin 260 Mbyte hard disk drives in the ASC and a summary of laser altimeter ranging, waveform, and housekeeping data are sent over the HH 1200 baud low-rate telemetry channel. The flight hard drives are VIPER™ drives manufactured by Integral, Inc. and have excellent shock/vibrations specifications

(150 G operating, 750 G non-operating). The complete data set is continuously sent to the HH medium-rate data channel at 19.2 Kbaud and reaches the ground when that link is available. The ASC computer program operates the laser altimeter instrument in the LAC continuously until the "SAFE" (i.e. laser off) command is issued. The SLA payload operations will typically continue for 10 to 15 hours, nominally centered on the crew sleep periods after mission day 2. The total planned data take for STS-72 is about 100 hours. The minimum operational cycle length requested is two orbits (about 3 hours). After laser transmitter operation is secured and SLA payload power is removed, the HMDA door on the LAC is closed to complete payload operations.

Pointing control for SLA is required to be within  $\pm 5^\circ$  (3 sigma in roll & pitch) with respect to the Orbiter local nadir (-ZLV) for successful payload operation. The Flight Plan for STS-72 indicates a nominal pointing control deadband of  $1^\circ$  supplemented by two observational periods later in the Mission with  $0.1^\circ$  pointing control deadband. This high-quality pointing control will permit collection of SLA data at the Orbiter nadir direction resulting minimizes laser pulse spreading due to off-axis pointing effects. Data quality for the SLA Experiment is also highly dependent on nominal (full power) operation of the pulsed laser transmitter and maintenance of a clear, unobstructed line-of-sight for the SLA telescope aperture. In the hazy or cloudy atmospheres the laser pulse is scattered before reaching the Earth's surface and the laser altimeter measurement may be triggered by the top surface of the cloud, haze, or aerosol layer. Actual operations of the SLA in space will encounter a continuum of atmospheric conditions ranging from the extremes of cloudy to clear providing a good operational test for the laser altimetry technique. Not only do these conditions impart a great variability on the amplitude of the received laser pulse but result in a highly variable solar backscatter "noise" component. The SLA data acquisition algorithm can accommodate a variable noise level by an automatic threshold tracking loop. In this loop the continuous monitoring of APD detector noise level in a noise pulse counter is used to adjust a voltage threshold up or down to "track" the once-per-sec noise count. This loop provides a stable false-alarm-pulse-rate and maximizes the probability-of-detection of the weak laser pulses that are returned from the surface; hence maximizing the Earth surface data. Performance of this loop in space is a key engineering objective of the STS-72 Mission opportunity for SLA.

## ACKNOWLEDGMENTS

In addition to all the many long hours contributed by each of the named co-authors, we wish to recognize the contributions of many individuals in the Experimental Instrumentation Branch, the Laboratory for Terrestrial Physics, the Earth Sciences Directorate, the Engineering Directorate at the GSFC, and the Observational Sciences Branch at the Wallops Flight Facility (WFF) for their many contributions over the years to the development, testing, and delivery of the Shuttle Laser Altimeter Instrument. Notable among these is work by Paul Weir (retired), Bill Schaefer, James Fitzgerald, James C. Smith, Glenn Staley (retired), and Dick Aldridge at the GSFC and Gerry McIntire at the WFF. Special thanks to Vernon Muffaletto (now deceased; Muffalletto Optics, Baltimore, MD) and Bill Clark (Optical Filter Crop., Keene New Hampshire) for the SLA telescope and Greg Speno, Steve Monroe, Gary Gaither and the rest of the laser development team at McDonnell Douglas in St. Louis for the SLA laser transmitter and the APD detector hybrid. Finally, this effort could not have been possible without the foresight of Henry Price (former Chief Engineer at the GSFC), funding by the GSFC Director's Discretionary Fund, and by all the altimetry and detector electronics design, spare parts, algorithms, experience, and continued support provided by the Mars Observer Laser Altimeter Team at the GSFC.

## **HELPFUL HINTS TO PAINLESS PAYLOAD PROCESSING**

presented by

Terry Terhune  
McDonnell Douglas Aerospace Space & Defense Systems  
Goddard Resident Office, Kennedy Space Center, FL

Author

Maggie Carson  
UNISYS Corporation  
Goddard Resident Office, Kennedy Space Center, FL

### **ABSTRACT**

The helpful hints herein describe, from a system perspective, the functional flow of hardware and software. The flow will begin at the experiment development stage and continue through build-up, test, verification, delivery, launch and deintegration of the experiment. An effort will be made to identify those interfaces and transfer functions of processing that can be improved upon in the new world of "Faster, Better, and Cheaper." The documentation necessary to ensure configuration and processing requirements satisfaction will also be discussed. Hints and suggestions for improvements to enhance each phase of the flow will be derived from extensive experience and documented lessons learned. Charts will be utilized to define the functional flow and a list of "lessons learned" will be addressed to show applicability. In conclusion, specific improvements for several areas of hardware processing, procedure development and quality assurance, that are generic to all Small Payloads, will be identified.

### **INTRODUCTION**

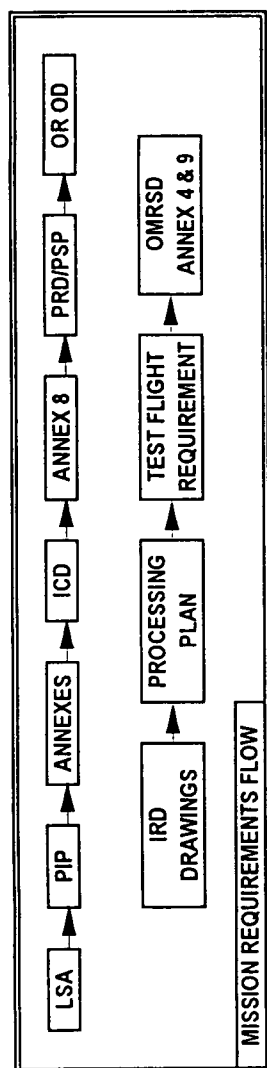
The opportunity to test theory in space is often the culmination of many years of research and dedication of this nations finest educators, scientists, and research teams. The process from experiment concept through launch and mission operations to experiment results is exciting, rewarding, and often overwhelming. This paper is intended not only to present to the experimenter the overall scope of the process requirements (Figure 1-2), but more importantly to encourage the utilization of the valuable resources available and consider integrating certain disciplines within the experiment life-cycle that have been discovered from lessons learned. The lessons learned experience base from which this information is derived covers over 130 flight experiments aboard 27 shuttle missions.

### **THE NASA TECHNICAL MONITOR (NTM) AND LAUNCH SITE SUPPORT MANAGER (LSSM)**

The two individuals responsible for ensuring a smooth transition between critical milestones are your NTM and LSSM. Following the submission of your Payload Accommodation Requirements (PAR) an NTM will be selected for your mission. The NTM has the tremendous task of planning and verifying that all of your documentation, experiment requirements, support needs and schedules are in place and maintained particularly during the first half of the experiment processing effort. Once your experiment reaches the launch site, the LSSM assumes this task with direct input and support from the NTM. Their contribution to the success of flight experiments in the past is invaluable. To effectively manage the various aspects of preparation, integration, and support, it is crucial that you remain in close contact with your NTM.

# HITCHHIKER

CONCEPT



- ◆ Experiment to GSFC
- ◆ Experiment/Carrier Integration Complete
- ◆ Payload to KSC
- ◆ Payload in Orbiter

- ◆ Customer Payload Requirements
- ◆ RFA (Form 1628)

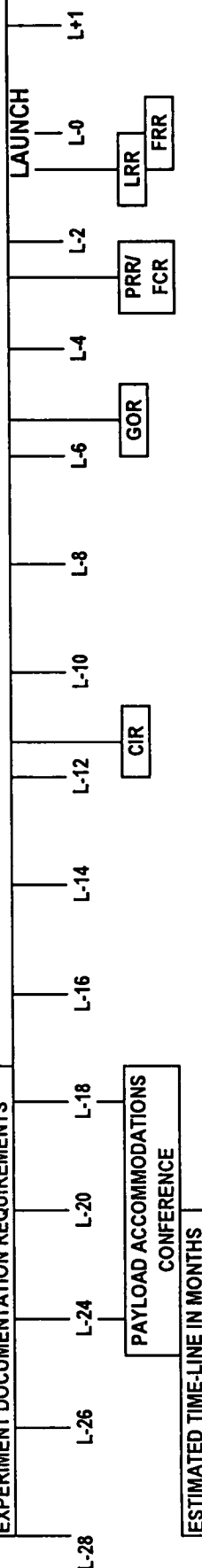
- ◆ Hazard Analysis
- ◆ Hazard Matrix
- ◆ Hazard Report

- ◆ Preliminary Safety Data Package
- ◆ Structural Integrity Verification Plan

- ◆ Structural Integrity Verification Report

- ◆ Final Safety Data Package
- ◆ Hazardous Procedures to KSC
- ◆ Safety Certification

EXPERIMENT DOCUMENTATION REQUIREMENTS



- ◆ Design Requirements
- Structural Integrity
- Limit Acceleration Load Factors
- Vibration Frequency Constraints
- Acoustic Noise and Random Vibration

- Materials
- Design Envelope
- Non-Metallic Materials
- Thermal Blanket Attachment

- ◆ Analysis Requirements
- Fracture Control
- Pressure Profile
- Structural Analysis
- Structural Modeling

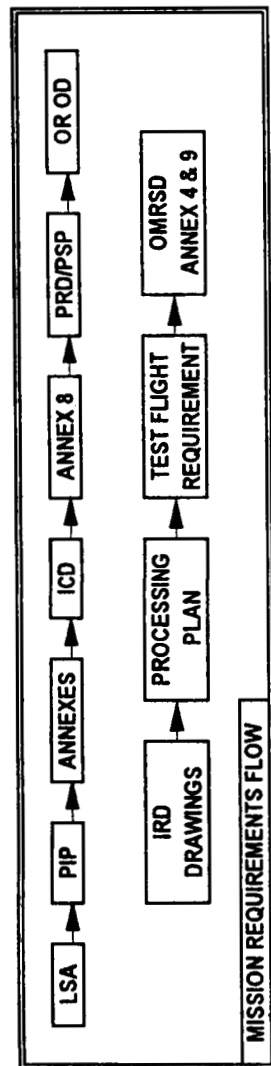
- ◆ Test Requirements
- Structural Test
- Natural Frequency Verification
- ◆ Electrical Requirements
- ◆ Thermal Requirements

EXPERIMENT DEVELOPMENT REQUIREMENTS/CONSIDERATIONS

Figure 1.

# Get-Away Special

CONCEPT



◆ GSFC Ships Shipping Container (after Phase 3)

◆ Payload to KSC

◆ Payload in Orbiter

◆ GSFC Ships Experiment Mounting Plate, Electrical Interface Connector and Dummy Battery Turret (if applicable) (after FSDP)

◆ Flight Reservation

◆ Payload Definition and Design Concept

◆ Preliminary LSA

◆ PAR

◆ Preliminary Payload Design

◆ Payload Final Design

◆ Final Safety Data Package

◆ Launch Services Addendum

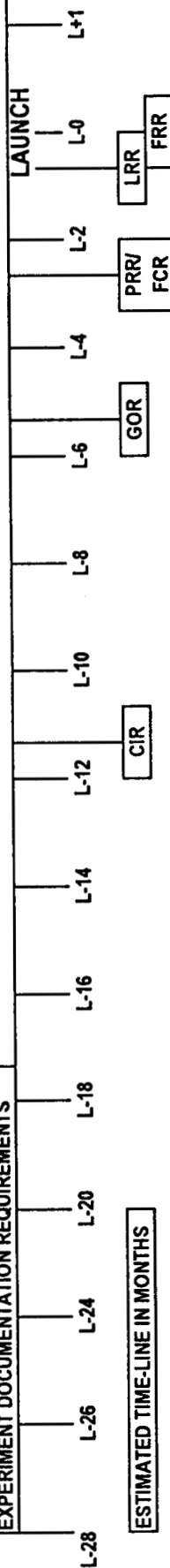
◆ As-Built Verification

◆ Safety Verification

◆ Phase 3 Safety

◆ Safety Certification

EXPERIMENT DOCUMENTATION REQUIREMENTS



◆ Design Requirements

- Structural Integrity
- Materials
- Design Envelope

◆ Design Considerations

- Acceleration Load Factors
- Acoustic Noise and Random Vibration

◆ Thermal Considerations

- Orbit Inclination Angle
- Orbiter Attitude Timeline
- Top Surface of Payload Container
- Internal Heat
- Payload Thermal Conduction and Isolation

◆ Test Requirements

- Payload to GAS Control Electrical Interface
- Malfunction Inputs to Payload Power Contactor (PPC)
- Relay Operation

EXPERIMENT DEVELOPMENT REQUIREMENTS/CONSIDERATIONS

Figure 2.

## **DESIGN PHASE**

Based on Lessons Learned, there are particular aspects of hardware and software design and development that are sometimes overlooked. Early consideration of these factors can prevent late-stage work-arounds that are time consuming and can dramatically affect the level of integrity of the hardware and/or mission success.

### **Replacement/Back-up Parts/Hardware**

During the design and development of your experiment, consider retaining a small stock of critical parts or sub-components vital to experiment function that could easily replace failed units. Long-lead or custom items should be procured with spares in mind. Ensure that the spares have been tested and are qualified for flight. Remember also to bring them with you to the launch-site for contingency use.

### **Access to Serviceable Components**

Access to serviceable or system-critical components should be the primary focus in the design of the hardware. The location of batteries, cryogen and pressure ports, film transports, data storage units, drive mechanisms, and thermal control units, are some of the areas of critical failure that could determine the fate of the experiment if there should be a delay in the launch schedule or your experiment fails post-ship functional testing at the launch site.

### **Flight Environment VS Test Environment and Vibration & Thermal Effects**

The mission environment can present a host of unforeseen impacts to the proper function of the experiment. Obvious considerations include launch-induced vibrations, and hot and cold-case attitudes, which have been contributors to numerous experiment failures in the past. The orientation of the experiment during launch can cause vibration-induced failures of support structures, component housings, actuators and drive-mechanisms. There are additional aspects of the mission cycle that are rarely anticipated. Events such as crew activity on-orbit can produce micro-gravity upsets that may affect the processing of materials. The experiment may be affected by virtue of its location relative to co-manifested payloads. Thermal extremes may occur as a result of shadowing from larger payloads. Unusual occurrences which have affected previous experiments include the South Atlantic Anomaly which can interrupt and/or corrupt critical data and telemetry functions. While not all impacts can be foreseen, giving thoughtful consideration to certain extremes may provide you with the opportunity to incorporate certain safe-guards within your design to protect your experiment from such events.

### **Ground Support Equipment (GSE) Operating Parameters**

A vital component of experiment function is the integrity of the GSE. Having a thorough understanding of its electrical or mechanical influence on the experiment can reduce or eliminate your support hardware as a contributor in hard failures or unexplained anomalies in testing. A primary performance function of electrical GSE is accurate signal generation. Grounding schemes within the support equipment and flight experiment can significantly affect signal quality. Troubleshooting efforts during previous launch site processing operations ultimately resulted in signal spikes, or timing incompatibilities produced by the Electrical Ground Support Equipment (EGSE).

### **Limited Life Items**

When selecting certain items for your experiment, determine the survivability of that item under conditions such as the time-lag between final installation and the end of mission. Under normal circumstances, that duration could last as long as 3 months depending upon your installation date of that item. O-rings, valves, seals, film, lubricants, etc. could suffer severe degradation or ultimate failure if installed too soon or schedule slips force a launch delay.

### **Weight/Volume Limitations**

Keep in mind the importance of maintaining your estimated payload weight. The experiment directly affects the overall weight and Center of Gravity (CG) of the carrier and could violate requirements established in the Interface Control Document/Information Requirements Document (ICD/IRD) which constrain both the carrier and launch vehicle. The volume of your experiment must also remain within the requirements established by your carrier hardware. Design modifications may contribute to both weight and volume exceedances.



### **On-Orbit Input Requirements**

During the design stage of your experiment development, be aware of the extent of maintenance or operational processes that would be required during the mission to ensure proper function and health of your experiment. It may be possible for you to incorporate "self-check and correct" features within your system that would automatically provide protection to your experiment without the assistance of the flight or ground crews.

### **Experiment Structural Support**

When designing the experiment support structure it is imperative to verify that it can withstand launch-induced vibration and shock loads in their respective orientations. A vertical support strut will be horizontal at launch and must withstand launch-mode effects without compromise in this orientation.

### **Drawings/Historical Traceability**

There is no substitute for documentation that accurately reflects the configuration and history of experiment performance, specifically when an anomaly occurs. During off-line processing it's an invaluable tool for assisting in troubleshooting, oftentimes reducing the extent of tear-down to reveal the source of a failure. But more so, it is a tremendous time-saver in that historical performance patterns often reflected in the data are ordinarily impossible to detect through troubleshooting efforts. Traceability of testing results and configuration also becomes more valuable as your experiment moves through the integration processes with the carrier and ultimately to the launch vehicle. On-line experiment failures involve numerous organizations including co-manifested payload organizations, flow managers and directors, and other NASA centers responsible for mission operations or orbiter integrity. Being able to provide or access accurate and complete data of your experiment will not only expedite the troubleshooting effort for the launch site community but also produce a level of confidence within that community that the experiment integrity has been maintained through a tracking discipline.

### **Payload Integration Plan (PIP) and Interface Control Document (ICD) Input**

The top-level controlling documents for shuttle payloads are the PIP and the ICD. Requirements unique to your experiment should be provided to your NTM for consideration and/or incorporation into these top level documents. Special servicing, handling, monitoring, and accessing requirements will be addressed and an implementation approach developed within the constraints of these documents.

## **EXPERIMENT DEVELOPMENT & TEST PHASE**

The integrity of the experiment resides in the workmanship afforded it, the level of testing performed, and the strict control of configuration.

### **Ensure As-Built Compliance to PAR, Drawings and Safety Package**

The largest contributor to the loss of flight-worthy configuration is design modifications. Most changes are likely to occur during the experiment development phase. Ordinarily by this time the PAR has been established and understood, the preliminary design has been issued, and build-up efforts are underway in the development of the final safety data package. As design changes occur it is imperative that they be evaluated against the requirements documents to ensure that the experiment remains within the specified limits of acceptability for flight.

### **Materials (Compatibility, Acceptability)**

When selecting materials both for flight and ground support use, special attention should be given to the following situations. Several regulating documents exist that control the level of incompatibility and hazard of materials used for space flight. However, there are instances when materials used independently or combined within your experiment may produce unfavorable conditions for sensitive instruments and systems. Verify that the location, containment and compatibility of your materials will not adversely affect your experiment or the carrier hardware both in ambient and flight environments. Another area of caution when utilizing materials is during on-line operations. Materials used for lens covers, support structures, transport containers, etc., must also meet the

stringent cleanliness requirements imposed on flight hardware. Off-gassing fluids and materials that are incompatible with the orbiter or co-manifested payloads will be prohibited. In preparing your ground support equipment and remove-before-flight items, keep in mind the environment in which that it will be used. You may find yourself being denied access to your experiment until your support equipment is bagged, cleaned, encapsulated, or any number of time-consuming corrections are made.

#### **Payload Orientation Effects During Launch Processing**

Fluid distribution and containment systems, batteries, low-viscosity materials, etc., must withstand a 90 degree change in orientation from the payload vertical axis following installation into the orbiter. It will remain in that orientation until a successful launch is achieved. Nominally the time of orbiter rotation to launch is approximately 5 weeks. However, launch delays and in rare cases orbiter roll-back could extend that duration up to 2 months or longer.

#### **Detailed Test Objectives/Detailed Science Objectives (DTO/DSO)**

Definitive test objectives should be established during the development and test phase for incorporation into launch-site procedures. A clear go/no-go criteria for experiment performance will eliminate the need to interpret performance data real-time and aid in defining success and failure criteria during carrier and launch vehicle testing.

### **CARRIER INTEGRATION & TEST PHASE AT GODDARD SPACE FLIGHT CENTER (GSFC)**

#### **Simulate/Verify Flight Configuration of Hardware and Software**

Once your experiment has reached this stage, there will be a noticeable acceleration of the schedule toward launch. Now is the time to simulate complete command and control capability and verify integrated systems compatibility. An interface verification test will be performed validating system integrity. Within that process, the software utilized at this phase of your experiment testing should also result in the final version for flight.

#### **Perform Fit Checks**

Non-standard interfaces should be verified through fit checks. Conditions such as the build-up of tolerances can ultimately result in the improper fit, form or function upon final integration.

#### **Procedure Development**

As the experiment moves into the carrier integration phase of the launch flow, there should be a verification process by which to ensure that experiment unique requirements such as special handling, ESD precautions, or other restrictions are addressed correctly within the working documentation. Involvement in the review process is highly encouraged and could prevent an inadvertent oversight by support personnel who are less familiar with your particular experiment.

#### **Experiment/Carrier Interface Verification Test (IVT)**

The experiment/carrier IVT is the most critical phase of pre-flight processing. This is the stage of the flow that offers a sufficient margin within the schedule and resource limitations of processing for discovering and recovering from any system failures. It is also the final opportunity to sufficiently test your experiment and its crucial interface with the carrier. Once this phase of testing has been accomplished, there should be few, if any, unexpected "occurrences" following shipment to the launch site.

### **CARRIER INTEGRATION & TEST PHASE AT KENNEDY SPACE CENTER (KSC)**

#### **Access to Launch-Site Facilities**

The Launch Site Support Plan (LSSP) is a baseline document that is customized for each mission incorporating inputs provided by your NTM and the LSSM. It is a valuable guide to the processing environment at the launch site and covers requirements for such things as training, security, support, and safety.

**Launch-Site Support Capabilities/Limitations**

In preparation for launch-site processing the experiment should be at or near flight configuration. However, post-ship functional and integration activities may warrant minor adjustments and securing for final integration into the orbiter. It is best to assume that materials and equipment that you may require will be difficult to provide. So if at all possible add them to your shipment of GSE. In the event of an experiment failure in the field, real-time support for equipment and supplies has been provided in the past, but is difficult to arrange in short notice, so plan for contingencies.

**Impact/Affect of External Operations**

Inform your NTM of experiment sensitivities early. Following payload installation into the orbiter, literally hundreds of separate and distinct operations will occur in preparing the orbiter for flight. Generally the payloads are protected from orbiter activity, but there are instances when routine operations have been a cause of concern for experiments within the cargo bay. Operations such as main engine x-rays at the launch pad generated an experimenter request to install a lead blanket between his flight hardware and the aft bulkhead of the orbiter. Co-manifested payloads conducting pre-flight operations may also inadvertently affect your experiment. These issues are ordinarily discussed and agreed upon early in the ground operations planning meetings, but it is always advisable to clarify instrument sensitivities.

**Instrument/Carrier Testing With Simulated Orbiter Power/Signal**

It is crucial to establish an accurate test simulation of the orbiter supplied power and signal generation to verify complete system compatibility. This would include video cabling and monitor or other unique interfaces that will be utilized during the mission.

**Maintain Configuration**

Once the experiment/carrier testing has been accomplished at GSFC, maintain configuration of both flight hardware and GSE. Annoying subtleties between duplicate equipment can cause deviations in the expected results and this can easily be avoided through diligent control of the validated system. This would also include your validated software version.

**Procedures Hazardous VS Non-Hazardous**

Keep in mind that the later in the processing flow that operations are deferred the more difficult they are to get approved. Personnel safety constraints are a large part of the difficulty in requesting late-stage operations. There are firm and heavily enforced requirements in place at the launch-site regarding hazardous operations. The long-pole of the process is obtaining procedure approval which stands at a 45-day minimum prior to first use. Hazardous operations are clearly defined in the KHB 1700.7 and it is recommended that the experimenter familiarize himself with the differentiation between hazardous and non-hazardous operations.

**Contingency Landing Site (CLS), Launch Delay/Slip**

Within the realm of possibilities is post-mission landing at an alternate site. Special thought must be given to the precautionary measures to be taken in stabilizing your experiment, if applicable, and whether equipment and/or support personnel would be required to perform safing operations upon landing.

Launch delays are not uncommon. Any number of factors can prevent the shuttle from an on-time launch. Under this condition, your experiment should be able to sustain relatively minor delays without special consideration. However, in the eventuality that the delay has slipped the launch to several days or even weeks, it may be necessary for you to access or service your experiment. Prepare for the eventuality of late-breaking changes. They are, in more moderate doses, a commonality in this business.

## **ORBITER INTEGRATION & TEST PHASE**

### **Interface Verification Test (IVT)**

The final system validation occurs with orbiter power and signal following payload installation. This is the final test-

hurdle that will verify full-up integrity for mission success. It is also when problems can occur if there was not sufficient testing of the experiment and carrier during off-line operations.

### **Remove-Before-Flight Items**

When designing instrument covers, be advised that the removal operations ordinarily occur following installation into the orbiter and therefore requires all tools and equipment to be tethered upon installation or removal from the cargo bay. Designing in a simple handle or eye-let through which a tether could be secured prevents make-shift rigging that may compromise the success of the removal operations.

### **Payload Stand-Alone Operations**

Stand-alone operations is a term given to payload autonomous activity once "on-line". As private and comforting as that may sound, it is far from either. Any operations occurring within the orbiter are highly visible, carefully monitored, and generally cumbersome particularly when access support such as buckets or platforms are required.

### **Payload Documentation Closure**

It is advisable that prior to launch the experimenter ensure that all discrepancies, failures and action items have been adequately addressed and/or resolved. A brief documentation review provides an additional level of assurance that nothing has been overlooked. It is not uncommon to become consumed in pre-flight operations to the extent of losing sight of some of the details. Through comprehensive planning efforts and periodic checks of hardware, software and documentation status' your attention can stay focused on the more rewarding aspects of flight processing, specifically your experiment.

## **POST-FLIGHT DEINTEGRATION PHASE**

### **Post-Flight Payload Access**

Generally, payload removal from the orbiter occurs a week after orbiter arrival. At that time, depending on the carrier, your experiment may be available to you within the following week. Under certain circumstances, it may be possible to perform an initial visual inspection of the flight hardware shortly after cargo bay doors are opened. This is ordinarily an option if anomalous conditions are suspected.

### **Safing Requirements**

Depending on the complexity of your experiment, there may or may not be a requirement to perform safing operations post-landing. This is generally reserved for payloads carrying ordinance, or require flight battery circuit deactivation. If your experiment requires early access, be sure to negotiate options early in your agreement planning phase.

### **Shipping and Storage Details**

The concern in packaging for shipment is with hazardous materials. Items that are flammable, corrosive, or toxic, radiation or ignition sources, or other commodities that require protective handling must be packaged and labeled correctly for shipment. They must also be utilized in compliance with KSC Safety, Health Physics and Occupational Safety and Health Administration (OSHA) regulations while at the launch site. Be aware of what qualifies as a hazardous material and the restrictions over their use. This data is available from your LSSM.

### **Data Retrieval and Integrity Maintenance**

As important as it is to have developed a flight-worthy experiment that successfully completes its mission, it is

equally important that the experiment results are protected properly after flight. Too often in the rush of accessing mission results, there is a tendency to forgo precautionary measures in the handling, tear-down, shipping, or storage process that can degrade or destroy critical experiment results. Define your protective requirements prior to the launch. Someone else may have the responsibility to deintegrate your payload and ship your data/GSE.

## **CONCLUSION**

A successful processing effort can be achieved by maintaining control of the hardware, software, and GSE configuration, ensuring compliance to flight and processing requirements, and communicating regularly with the NTM. Items for consideration in formulating processing objectives are summarized for use by the experimenter in Figure 3. The degree of attention provided in each phase of experiment processing builds upon and proportionately translates into a smoother interface and transfer effort. It is evidenced through the lessons learned that when sound processing discipline is installed there is a marked improvement in experiment performance and mission results.

## **REFERENCES**

1. NASA Kennedy Space Center, "Kennedy Space Center Operations", KSC FORM 4-607, Revision 1/88.
2. McDonnell Douglas Payload Ground Operations Contractor, "Launch Site Accommodations Handbook for Payloads", NASA K-STSM-14.1 Revision G, August 1992.
3. Rex W. Ridenoure, "Space Shuttle Get away Special Experiment Performance Summary for Missions Through 1991", Ecliptic Astronautics Company Report TR92-002, October 20, 1992.
4. NASA Goddard Space Flight Center Special Payloads Division, "Get Away Special (GAS) Small Self-Contained Payloads Experimenter Handbook", 1991.

# Helpful Hints for Experimenters

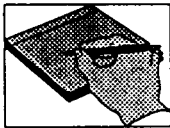
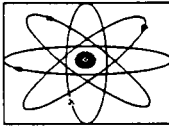
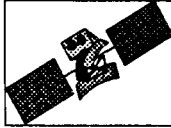
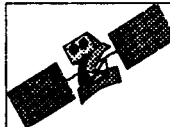
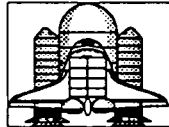

DESIGN	DEVELOPMENT & TEST	CARRIER I & T (GSFC)
		
<b>PLANNING</b>		
<ul style="list-style-type: none"> <li>◆ Replacement/back-up parts/hardware</li> <li>◆ Access to Serviceable Components</li> <li>◆ Flight VS Test Environment</li> <li>◆ GSE Operating Parameters</li> <li>◆ Limited Life Items</li> <li>◆ Weight/Volume Limitations</li> <li>◆ Vibration &amp; Thermal Effects</li> <li>◆ On-Orbit Input Requirements</li> <li>◆ Experiment Power, Heat, Data, etc.</li> <li>◆ Carrier Mounting Interfaces</li> <li>◆ Battery Selection</li> <li>◆ Experiment Structural Support</li> </ul>	<ul style="list-style-type: none"> <li>◆ Understand Operating Parameters of Purchased Components</li> <li>◆ Ensure As-Built Compliance to PAR, Drawings &amp; Safety Data Package</li> <li>◆ Materials(Compatability,Acceptability)</li> <li>◆ Payload Orientation Effects During Launch Processing</li> </ul>	<ul style="list-style-type: none"> <li>◆ Simulate/Verify Flight Configuration</li> <li>◆ Contingency in Schedule for Problems/Failures</li> <li>◆ Perform Fit Checks</li> </ul>
<b>DOCUMENTATION</b>		
<ul style="list-style-type: none"> <li>◆ Payload Accommodation Requirements</li> <li>◆ Flight Reservation</li> <li>◆ Launch Services Agreement (LSA)</li> <li>◆ Hazard Assessment</li> <li>◆ Hazard Control Verification</li> <li>◆ Preliminary Safety Data Package</li> <li>◆ Final Safety Data Package</li> <li>◆ Flight Certification</li> <li>◆ PIP/ICD Input</li> </ul>	<ul style="list-style-type: none"> <li>◆ Complete Safety Data Package</li> <li>◆ Materials (MUA, Shipping, MSDS)</li> <li>◆ DTO/DSO</li> <li>◆ As-Built Verification For Phase 3 Safety</li> <li>◆ LSA Addendum</li> <li>◆ Input to PIP Annexes</li> </ul>	<ul style="list-style-type: none"> <li>◆ Experiment Carrier IVT</li> </ul>
CARRIER I & T (KSC)	ORBITER I & T	POST-FLIGHT DEINTEGRATION
		
<b>PLANNING</b>		
<ul style="list-style-type: none"> <li>◆ Access to Launch-Site Facilities</li> <li>◆ Launch-Site Support Capabilities/ Limitations</li> <li>◆ Impact/Affect of External Operations</li> <li>◆ Instrument/Carrier Testing With Simulated Orbiter Power/Signal</li> <li>◆ Maintain Configuration</li> </ul>	<ul style="list-style-type: none"> <li>◆ Remove-Before-Flight Items</li> <li>◆ External Impacts: Temperature, Humidity, Welding, X-Rays, etc.</li> <li>◆ Payload Servicing</li> </ul>	<ul style="list-style-type: none"> <li>◆ Post-Flight Payload Access</li> <li>◆ Safing Requirements</li> <li>◆ Shipping and Storage Details</li> <li>◆ Data Retrieval &amp; Integrity Maintenance</li> </ul>
<b>DOCUMENTATION</b>		
<ul style="list-style-type: none"> <li>◆ Procedures Hazardous VS Non</li> <li>◆ EEOM,TAL,DFRF,Launch Delay/Slip</li> </ul>	<ul style="list-style-type: none"> <li>◆ Payload Stand-Alone Operations</li> <li>◆ Payload Documentation Closure</li> </ul>	<ul style="list-style-type: none"> <li>◆ Payload Special Handling Instructions</li> <li>◆ Shipper Including Special Instructions</li> </ul>

Figure 3.

# **SPACE EXPERIMENT MODULE -- A NEW LOW-COST CAPABILITY FOR EDUCATION PAYLOADS**

**Theodore C. Goldsmith and Ruthan Lewis  
NASA Goddard Space Flight Center**

## **INTRODUCTION**

The Space Experiment Module (SEM) concept is one of a number of education initiatives being pursued by the NASA Shuttle Small Payloads Project (SSPP) in an effort to increase educational access to space by means of Space Shuttle Small Payloads and associated activities. In the SEM concept, NASA will provide small containers ("modules") which can accommodate small zero-gravity experiments designed and constructed by students. A number, (nominally ten), of the modules will then be flown in an existing Get Away Special (GAS) carrier on the Shuttle for a flight of 5 to 10 days. In addition to the module container, the NASA carrier system will provide small amounts of electrical power and a computer system for controlling the operation of the experiments and recording experiment data.

This paper describes the proposed SEM carrier system and program approach.

### **SEM Objectives**

The objectives of the SEM program are to provide increased U.S. educational access to space especially for K-12 participants and increase educational use of the Shuttle and GAS Program.

As a goal, the cost to the experimenter organization for development and space flight of a SEM experiment should be reduced by at least 90 percent relative to GAS.

SEM should be reasonably equally available nationwide and not depend on the experimenter's proximity to a NASA installation or other locality dependent aspect.

The SEM program should provide a reasonable number of flight opportunities such that students from a wide number of localities may participate in the flight program. The system should allow for a larger number of students to participate in experiment design exercises.

The SEM system should provide easy access to design information and information on previously developed student experiments via internet or other public means.

The SEM system design should minimize the recurring cost to the government involved in processing, supporting, and flying SEM experiments.

### **Get Away Special (GAS)**

The GAS Program has been operating since 1982 and has currently flown over 110 payloads. Each payload is housed in a NASA provided canister which can hold customer equipment of up to 5 cubic feet (142 L) in a volume measuring 19.75 inches (50 cm) in diameter and 28.25 inches (72 cm) in height. Up to 200 lb. (91 Kg) of customer equipment can be accommodated. GAS payloads and contents typically wait as much as 3 months between the last access opportunity and flight. GAS payloads are controlled by the Shuttle astronauts using a laptop class computer keyboard and display.

The GAS carrier will be used to carry the Space Experiment Module System.

## **Space Experiment Module (SEM) Overview**

In the GAS Student Space Experiment Module concept NASA will provide a small enclosed module which can contain approximately 300 cubic inches (4.9 L) of experimenter apparatus weighing up to approximately 6 lb. (2.7 Kg.). After installation of the experimenter's equipment up to 10 modules will be housed in a pressurized GAS canister which will have NASA supplied equipment for providing electrical power and means for recording simple data such as temperatures, pressures, etc. A control system for activating user apparatus according to a preset time sequence devised by the user will also be provided.

Following the mission the experiment hardware and SEM mounting plate will be returned to and retained by the customer. A computer diskette containing experiment measurement data taken during the flight will also be sent to the experimenter. NASA supplied software can be used by the experimenter to generate printed plots and other displays of the experiment data.

Because power, data system, software, and most of the required mechanical structure is provided, and because of the smaller size, the cost and effort to the end user is dramatically reduced relative to a full GAS payload. The remaining effort is more concentrated in areas germane to the actual experiment being performed.

Experiments selected for flight will be delivered to NASA approximately 4 months prior to the assigned Shuttle mission and returned approximately three weeks after the mission.

SEM modules and flight service will be provided to domestic educational institutions at a cost to be determined. Recipients will be selected by means of a procedure to be determined.

## **Space Experiment Module Technical Implementation**

The following is a preliminary plan for implementing the SEM hardware and software.

The module system will be designed to fly in a standard GAS carrier and consists of :

A battery compartment containing 12 volt batteries. Fuses and cables will be provided to connect power to each module. Power will be turned on near the beginning of the mission by the flight crew and turned off near the end of the mission using the existing GAS relay system.

Experiment modules containing a sealed compartment and a separate electronics compartment. The sealed experimenter compartment is designed to accept an experiment mounting plate with attached experiment hardware. The modules are integrated to the GAS carrier with a simple attachment scheme to minimize integration effort.

A Module Electronics Unit (MEU) for each module provides for programmed sequencing of the experiment operation and acquisition and storage of experiment data.

A ground version of the MEU for use at the experimenter's location. The GMEU will be a small unit which simulates the operation of the module electronics at the experimenter's location. The GMEU requires the use of an experimenter supplied IBM type computer and 12 volt power supply, and will probably be implemented as an electronics card to be installed in the experimenter's computer. Initially, a stand-alone version which connects to the experimenter's computer with a cable will also be developed.

## **Experiment Development and Test Scenario**

In order to develop and test a space experiment the following experimenter (user) and NASA supplied items will be involved:



#### NASA Supplied Items:

Experiment Mounting Plate  
Module Electronics Unit (ground version)  
Ground Software  
Documentation  
Internet Data Base

#### Experimenter Supplied Items:

Experiment hardware to be mounted to mounting plate  
Power Supply (12 Volt, Radio Shack No. 22-120 for 2.5 A or less)  
IBM PC compatible computer with:

Microsoft DOS and Windows 3.1  
Modem and serial port if required by modem, or other internet access  
Printer  
Two card slots for GMEU  
Access to internet (at least E-mail)

#### SEM Participation

Three levels of participation are anticipated; the design phase, hardware phase, and flight phase.

In the **design phase**, experimenters will perform a paper design of an experiment. NASA supplied documentation and electronic data base will provide support to this activity including examples, tips, etc. The NASA supplied software running in an experimenter supplied computer will prompt the experimenter to "fill-in-the-blanks" in the Experiment Data File (EDF). The EDF will contain information describing the experimenters and experiment including addresses, phone numbers, purpose, method, components, parts, materials, etc. The EDF will also contain the experimenter's scenario or timeline for sending control commands from the module electronics to the experiment apparatus and for sampling and recording experiment data such as temperatures, pressures, etc.

The supplied software will provide for printing the experimenter information on an experimenter supplied printer for making reports or papers. The EDF or printed report will form the basis for an application to the hardware phase.

The software and documentation can be widely distributed allowing any number of participants in the design phase.

Participants selected for the **hardware phase** will receive a NASA experiment mounting plate and Ground Module Electronics Unit. Experimenter supplied components will be mounted on the mounting plate, drilling screw holes as necessary. The experiment hardware is then connected to the GMEU which will simulate the functions of the flight MEU. Trial runs of the experiment can then be conducted according to the chosen timeline. Experiment data from the trial runs is recorded in a Measurement Data File (MDF) on the experimenter's computer and can be printed or plotted using the supplied software. The electronic or paper version of the experimenter's report from the hardware phase is used as part of an application for the flight phase.

The number of participants in the hardware phase will be limited by the number of available Ground Module Electronics Units but could be extensive. The GMEU is being designed to be as inexpensive as possible and could be shared by several experimenter groups.

Experimenters selected for participation in the **flight phase** will submit their experiments (on mounting plates) and data files to NASA/SSPP to be installed in modules. The timeline data in the experimenter's EDF will be loaded into the module processor. Following flight of the module, the mounting plate and experiment hardware will be returned to the experimenter with a copy of the measurement data from the module processor.

### **Shuttle Flight Manifesting**

Modules selected for flight will be accommodated as part of the existing Get Away Special Program.

### **MODULE TECHNICAL CHARACTERISTICS**

The following are preliminary technical characteristics for the Space Experiment Module system. Specifications are for each module unless otherwise stated:

#### **Mechanical Specifications:**

Mounting plate surface: Approximately 85 in<sup>2</sup> (550 cm<sup>2</sup>) (see drawing)  
Depth of Experiment compartment below mounting plate: 3.5 inches (8.8 cm)  
Maximum weight of experimenter hardware: 6 lb. (2.7 Kg.)

Experiment hardware to be attached to the mounting plate using supplied 6/32 screws, nuts, and sealing washers.

#### **Electrical Specifications:**

The module will have a D type 37 pin connector socket (D37S) on the side of the experiment compartment. The experimenter will provide a 37 pin plug connector (D37P) and the necessary wires to connect any desired components to the provided electrical services. Outputs to Experiment:

One, timeline controlled 12 Volt (10V to 12.6 V depending on battery charge and temperature) output, 5 amps peak maximum, (P1)

Eight, individually timeline controlled 12 Volt outputs, 1 Amp peak maximum (P2 - P9)

Total simultaneous current from all the outputs P1 through P9 together must not exceed 5 Amps.

Experimenter components to be connected to the programmed power outputs typically include heaters, electric valves for fluid control, fans, pumps for fluid circulation, motors, or camera actuators. All connections to the P1 - P9 or PWRRET pins to be made by means of size #20 stranded copper wire, teflon insulated.

Sensor power, regulated 5.0 volts, 10 milliampere maximum. The sensor power is turned on only when the processor is making a measurement and can be used to power an experiment sensor which works on a voltage divider (potentiometer) principle such as a pressure gauge or linear position sensor.

The energy drawn from all of the five experimenter power lines together cannot exceed 60 Watt Hours during the flight. This corresponds to a current-time product of 5 ampere hours at the nominal 12 V battery voltage.

As instructed by the timeline, the module processor will sample the voltage on any or all of the six input data lines, convert the voltage into a digital number, and store the number in a memory. The memory can hold at least 16,000 measurements. The digital number will be ten bits in length which means that there are only 1024 possible numbers and that the corresponding voltage between 0 and 5.12 volts can only be

determined to a precision of approximately one part in 1024 or about .1 percent. Actual accuracy will be somewhat lower. Experiment information to be stored must be converted into a voltage between zero and +5.12 volts by components in the experiment and connected to one of the six data input lines designated I7 - I12. These inputs each have an input resistance of not less than 1 megohm.

Three additional inputs, designated I1 - I3 are special and are designed to be connected to a NASA supplied temperature sensor. The sensor is a small bead (.1 inches (2.5 mm) in diameter) which can be glued to the component whose temperature is to be measured and wired to one of the temperature inputs. This sensor is designed to measure temperatures in the range of -40 degrees C to + 80 degrees C. The sensor will continue to work between -50 degrees C and +110 degrees C but with reduced accuracy. The sensor has two wires. One must be connected to a temperature input and the other connected to SIGGND. The temperature sensor, known as a thermistor, has an electrical resistance which varies with temperature. The special inputs I1 - I3 are the same as the I7 - I12 inputs except for a resistor (10K ohms) connected to 5.00 volts.

Three of the processor inputs, I4, I5, and I6 are prewired in the MEU to measure module processor temperature, battery voltage, 5.00 V supply voltage.

### **Electrical grounds and returns**

Current flowing from the +12 V power lines must be returned to the battery on the wires designated power return (PWRRET).

The wire designated signal ground (SIGGND) is the reference point for measurement of voltage for the input signals. One side of all temperature sensors and other sensors should be connected to SIGGND. SIGGND should have no connection to any power line or power return line.

The experimenter should provide a wire connecting the plate ground pin on the connector (PLTGND) to the mounting plate.

### **Experiment Operations Timeline**

Power to the module system will be turned on several hours after launch by a crew command. Following activation, the computer in each module will follow its unique experiment program to activate control functions and acquire data samples as a function of time. Analog circuitry and the 5.00 volt supply will only be turned on during sampling of data to conserve power.

The timeline data is ultimately converted to binary and downloaded to the experiment control microprocessor. Only three simple commands are currently possible: turn on (set) a power line, turn off (reset) a power output, and begin sampling a data channel at one of the allowed sampling rates. Sampling of a data channel can be stopped by setting its sample rate to zero.

The experiment clock is started at the time the experiment system is turned on by the astronaut crew and increments at 0.1 second intervals. Experiment time is specified as days, hours, minutes seconds and tenths of second since turn-on. Time range is 00D 00H 00M 00.0S to 19D 23H 59M 59.9S. Successive times in the timeline file must be the same or greater than previous statements.

Power outputs are designated P1 to P9. A set (SET) command turns on the specified output to allow power to flow to the experimenter components connected to that output. The power remains on until reset (RES) command is sent.

Data sampling for the various data channels is initially set to zero or no sampling. A rate (RATE) command sets the sample rate for the specified channel which is then sampled at the specified rate until the rate is set again. Each data sample requires two bytes in the data storage memory. Software will check the specified timeline to insure that data memory capacity will not be exceeded.

Data channels are as follows:

Channel #	ID	Description
I0	PROC	Processor internal status
I1	TEMP1	Experimenter temperature sensor #1
I2	TEMP2	Experimenter temperature sensor #2
I3	TEMP3	Experimenter temperature sensor #3
I4	TEMP4	Module internal temperature sensor
I5	BATTV	Battery voltage (12v) monitor
I6	500V	Sensor power (5.00v) voltage
I7	EXPD1	Experimenter data input #1
I8	EXPD2	Experimenter data input #2
I9	EXPD3	Experimenter data input #3
I10	EXPD4	Experimenter data input #4
I11	EXPD5	Experimenter data input #5
I12	EXPD6	Experimenter data input #6

Data sample rates are as follows:

Rate #	Rate ID	Description	Measurements (per hour)
0	ZERO	No sampling	-
1	ONCE	Sample once only	-
2	10MIN	Sample every 10 minutes	6
3	5MIN	Sample every 5 minutes	12
4	1MIN	Sample every minute	60
5	10SEC	Sample every 10 seconds	360
6	5SEC	Sample every 5 seconds	720
7	1SEC	Sample every second	3600
8	.2SEC	Sample 5 times per second	18000
9	.1SEC	Sample 10 times per second	36000

Timeline command statements in the experiment data file will have the format shown below. A comment can be provided on each line. Software will prompt the experimenter to enter the timeline data, insert the data into the format shown, and perform checks on entries. Software will also compute energy usage, and memory usage, and will flag any attempt to exceed the allowable parameters.

```

00D 00H 00M 00.0S RATE TEMP3 10MIN  Start sampling temperature
00D 00H 00M 00.0S RATE BATTV 10MIN  and battery voltage
00D 00H 50M 00.0S RATE EXPD1 1SEC   Start sampling pressure sensor
00D 01H 00M 00.0S SET P1             Turn on solenoid valve
00D 01H 00M 14.5S RES P1             Valve off after 14.5 sec
00D 01H 15M 00.0S RATE EXPD1 10SEC  Reduce rate for pressure sensor

```

## **SEM Experimenter Software**

The SEM experimenter software will be available at no cost to anyone wishing to design a SEM experiment. The software is designed to run on a PC type computer running Microsoft DOS 5.0 or later and Microsoft Windows 3.1 or later. A preliminary partial version of the software is available by anonymous FTP to: [sspp.gsfc.nasa.gov/pub/software/](ftp://sspp.gsfc.nasa.gov/pub/software/) file: semxx.zip where xx is the version number.

The SEM software will perform the following functions:

The Experiment Data File Editor will allow entry and editing of the various parts of the Experiment Data File (EDF) which includes narrative data, timeline, electrical information, parts list, and materials list. Printed reports can be made of each section.

The Experiment Data File Analyzer reads a completed or partly completed EDF and generates a printed report. The analyzer flags missing data, determines the electrical power and energy required by the timeline, and determines the amount of data memory consumed. Plots can also be made of power and energy vs time and the times that various outputs are "on".

The Module Operations Program will download the timeline data to a flight or ground version of the SEM module processor. Following a ground test run or flight the program will upload the measurement data and create a Measurement Data File.

The Measurement Data Processor program will read data from a Measurement Data File and produce a variety of printed plots and tabular lists of flight or test data.

## **Environmental Conditions**

During launch, payloads are subjected to vibration from the Shuttle rocket engines. Additional information to be supplied.

At launch, when the solid rocket boosters are fired, payloads are subjected to a substantial shock force. A second shock force is encountered at landing. These shock events can involve momentary accelerations of the payload of as much as 11 times the force of gravity or 11 "Gs". Additional information to be supplied.

SEMs will be flown in GAS canisters with insulation on all exterior surfaces. At launch, payloads are normally at a temperature of 65 - 70 degrees F (18 -21 degrees C). During flight the payload temperature gradually changes depending on the orientation of the Shuttle with respect to the ground and sun. Usually temperatures fall during the flight, sometimes to below zero degrees C. Additional information to be supplied.

## **Safety Considerations**

All experiments flown in SEMs must meet Shuttle safety requirements. In order to satisfy this requirement the experimenter must supply a list of all components and materials used in construction of the experiment as part of the Experiment Data File. Highly toxic, flammable, corrosive, or explosive materials may not be used.

All experiments will be inspected by NASA prior to installation into modules.

The Project will develop and maintain a list of acceptable materials and components in the data base.

## **Typical Experiments**

Experiments to be flown could include investigations in the following areas:

### **Behavior of liquids**

- Bubbles
- Surface tension
- Immiscible fluids
- Fluid management in microgravity

### **Bacteria growth**

### **Crystal growth from liquids**

### **Crystal formation from melting/freezing**

### **Plant behavior**

## **Certificate of Space Flight**

Experiments returned to experimenters following flight will be accompanied by a certificate certifying the flight on a specific mission.

## **Art and Decoration**

The experimenters may decorate the surfaces of the mounting plate with art or decorations except that inks or paints should be from an approved list to avoid contamination of the carrier.

## **Restrictions on Resale**

NASA regulations prohibit commercial use of SEM experiments including resale for profit of flown items such as the experiment or mounting plate.

## **Internet Data Base**

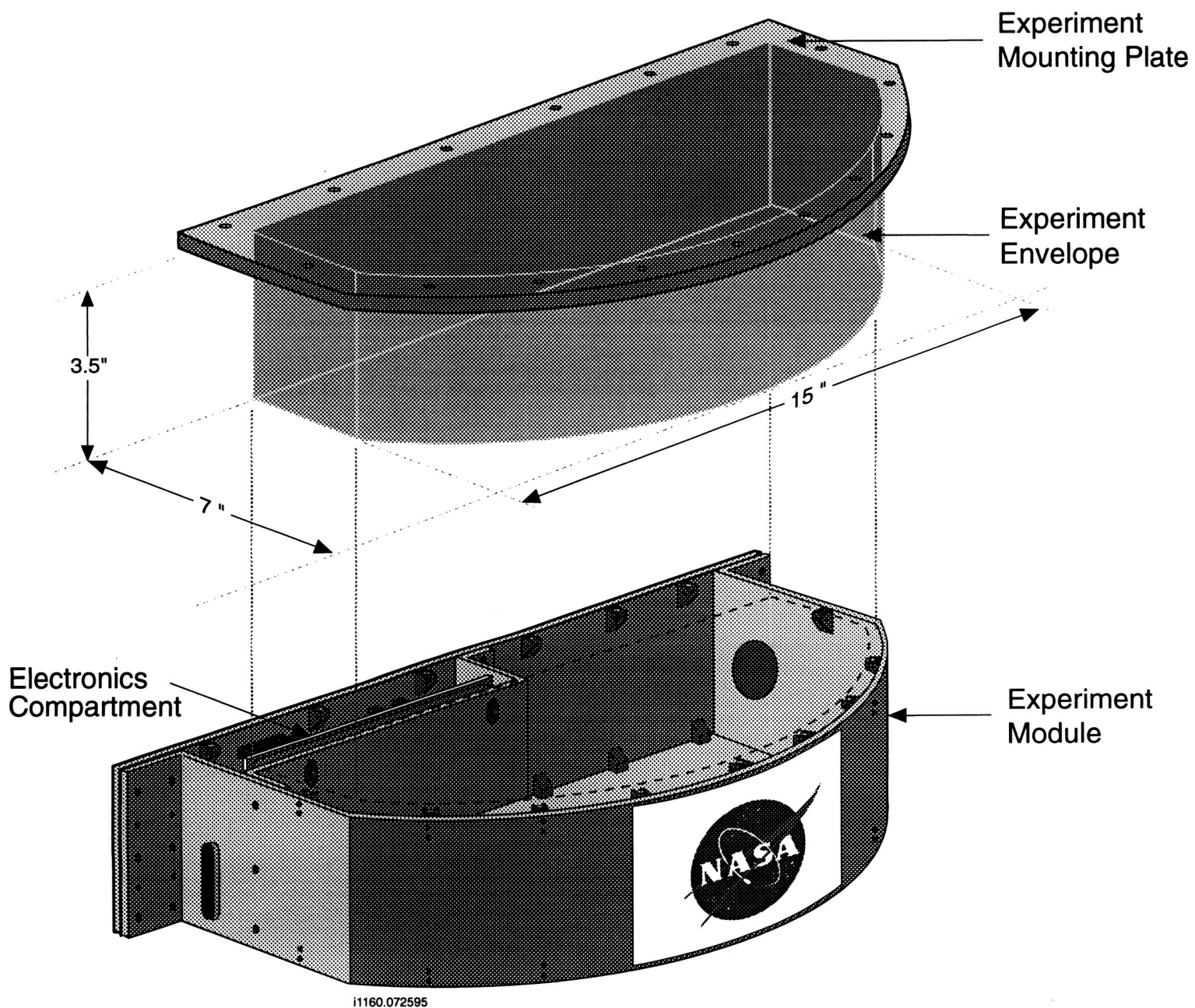
The Project will develop and maintain a data base of information for those interested in the SEM program and other SSPP activities. An E-mail mailing list and/or newsgroup will also be provided for those interested in SEM. The data base is accessible by E-mail by sending a message to [Majordomo@sspp.gsfc.nasa.gov](mailto:Majordomo@sspp.gsfc.nasa.gov) with the word help in the body of the message. A return message will automatically be sent giving instructions. The E-mail service may be accessed by anyone having access to Compuserve, Prodigy, America On-line, or other similar information service. Internet users can also access the Project data using FTP, Gopher, or WWW at: [sspp.gsfc.nasa.gov](http://sspp.gsfc.nasa.gov).

It is very important that participants contribute to the data base to help future participants. Experiment data files submitted to NASA will be put in the data base unless the experimenter requests that this not be done.

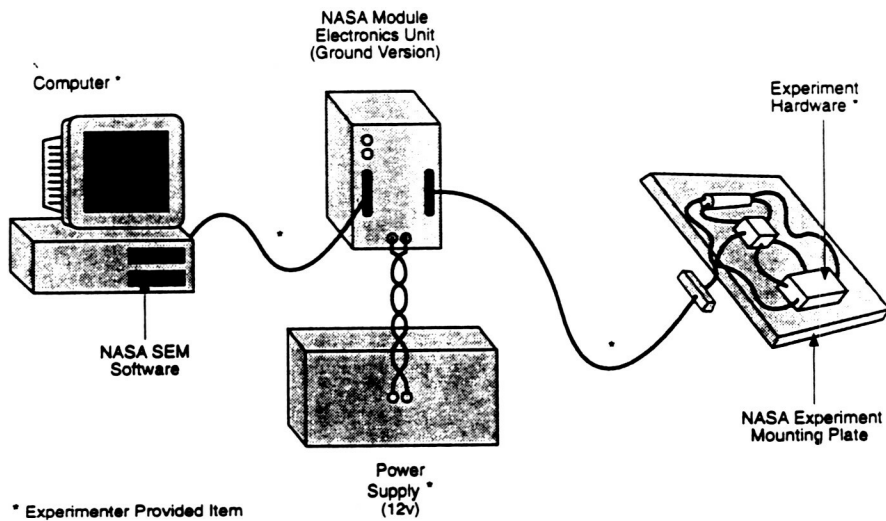
## **Project Contacts**

Contact T. Goldsmith or R. Lewis for more information.  
(301) 286-8799 or (301) 286-2060  
[tcg@sspp.gsfc.nasa.gov](mailto:tcg@sspp.gsfc.nasa.gov) or [ruthan\\_lewis@ccmail.gsfc.nasa.gov](mailto:ruthan_lewis@ccmail.gsfc.nasa.gov)

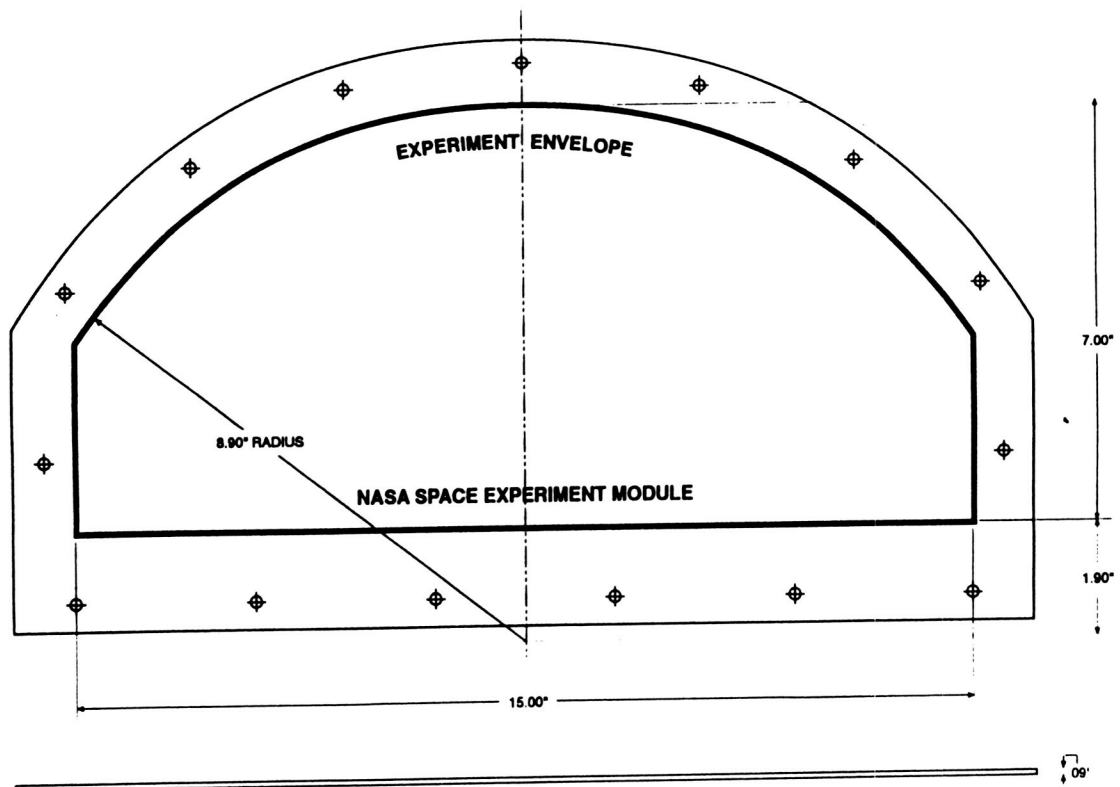
## SPACE EXPERIMENT MODULE (Experiment Envelope)



## EXPERIMENT DEVELOPMENT CONFIGURATION



## SEM EXPERIMENT MOUNTING PLATE





## CRYOGENIC TWO-PHASE FLIGHT EXPERIMENT; RESULTS OVERVIEW

T. Swanson and M. Buchko, NASA Goddard Space Flight Center  
P. Brennan, OAO Corporation  
M. Bello, The Aerospace Corporation  
M. Stoyanof, Phillips Laboratory

### Abstract

This paper focuses on the flight results of the Cryogenic Two-Phase Flight Experiment (CRYOTP), which was a Hitchhiker based experiment that flew on the space shuttle Columbia in March of 1994 (STS-62). CRYOTP tested two new technologies for advanced cryogenic thermal control; the Space Heat Pipe (SHP), which was a constant conductance cryogenic heat pipe, and the Brilliant Eyes Thermal Storage Unit (BETSU), which was a cryogenic phase-change thermal storage device. These two devices were tested independently during the mission. Analysis of the flight data indicated that the SHP was unable to start in either of two attempts, for reasons related to the fluid charge, parasitic heat leaks, and cryocooler capacity. The BETSU test article was successfully operated with more than 250 hours of on-orbit testing including several cooldown cycles and 56 freeze/thaw cycles. Some degradation was observed with the five tactical cryocoolers used as thermal sinks, and one of the cryocoolers failed completely after 331 hours of operation. Post-flight analysis indicated that this problem was most likely due to failure of an electrical controller internal to the unit.

### Introduction

The Cryogenic Two-Phase Flight Experiment (CRYOTP) was designed to flight test two new, thermal control cryogenic test articles; the Space Heat Pipe (SHP) and the Brilliant Eyes Thermal Storage Unit (BETSU). CRYOTP was flown as a Hitchhiker-based experiment aboard the space shuttle Columbia on STS-62 in March of 1994 as part of the Office of Advanced Science and Technology (OAST-2) primary payload. The SHP was a constant conductance nitrogen cryogenic heat pipe designed to operate from

approximately 80K to 110K. While oxygen heat pipes were successfully flown on the Cryogenic Heat Pipe Flight Experiment (CRYOHP) mission in December of 1992, the SHP marked the first flight test of a nitrogen heat pipe. Perceived advantages of the SHP included use of a non-flammable working fluid (nitrogen) and a high performance wick design. The SHP employed a titanium tube for pressure containment and five parallel fibrous copper wicks for axial fluid transport. Cryogenic working fluids like liquid nitrogen have relatively poor liquid transport factors and low static wicking heights. The fibrous wick employed in the SHP alleviated this problem by providing significantly better capillary pumping height ( $> 25$  mm) than the axially grooved CRYOHP heat pipes. The SHP was provided to the NASA Goddard Space Flight Center (GSFC) through a Small Business Innovative Research (SBIR) Phase II contract. Reference 1 describes this test article in detail.

The BETSU test article is a 2500 joule thermal storage device utilizing 2-methylpentane as a Phase Change Material (PCM). The PCM has a nominal liquid/solid phase change at 120 K. This type of device would be very useful for providing a totally quiescent, heat absorbing environment for a sensor, optics, or shroud. The BETSU was provided to the CRYOTP experiment by the US Air Force/Phillips Laboratory. Reference 2 describes the BETSU test article in detail.

In order to meet very stringent budget and schedule constraints, the cryogenic test bed from CRYOHP was reused. The two oxygen heat pipes tested in this experiment were removed and replaced with the SHP and BETSU test articles. GSFC was responsible for overall program management and integration of the CRYOTP experiment. This included refurbishment of

the cryogenic test bed from the previous experiment, integration of the two test articles, systems verification, and delivery to the Hitchhiker (HH) carrier. GSFC also functioned as the Principal Investigator (PI) for SHP. Aerospace Corporation acted as PI for BETSU.

The CRYOTP experiment had a number of technical and programmatic objectives. These were as follows:

- Demonstrate startup of the SHP from a supercritical condition in microgravity.
- Determine the SHP's heat transport characteristics in microgravity.
- Employ SHP flight data to update and validate analytical predictions..
- Demonstrate the steady-state and transient performance of the BETSU test article in a microgravity environment.
- Validate the analytical predictions for BETSU.
- Determine the correlation between the ground and flight data for both test articles.
- Demonstrate the feasibility of reusing an existing test bed for minimal cost (10% of the original) and quick turnaround (1 year).

All of the above objectives were achieved except for the first two. The SHP failed to start during flight operations. Two cooldowns were attempted from an initial temperature of 270 - 300K. Failure to start can be attributed to the relationship between the length of the liquid slug at the condenser end, the parasitic heat leaks on the transport and evaporator sections, and the available cooling capacity. The BETSU testing was a complete success, and a total of about 250 hours of data was acquired over the 14 day mission. Flight data correlated very well with predictions, and the feasibility of the PCM concept was fully demonstrated. Some interesting science on subcooling effects was also observed.

The following sections provide a more complete description of the CRYOTP test bed and the SHP and BETSU test articles. Flight results are then summarized and compared with analytical predictions. The cryocooler failure is also briefly addressed.

### Test Bed Description

The CRYOTP test bed (Figure 1) utilized much of the hardware used in the CRYOHP Flight Experiment flown in December of 1992 aboard STS-53. The CRYOHP experiment is described in detail in References 3 and 4. Each of the CRYOTP test articles was operated independently with its own set of cryogenic refrigerators as shown in Figure 2. The cryogenic refrigerators are tactical cryocoolers (Hughes Model No. 7044H) and were selected because they provide approximately 3.5 watts of cooling capacity at 80K with a power draw of approximately 100 watts. Vibration isolators consisting of multiple braided copper straps connected in parallel were used to interface each cryocooler to one of two aluminum thermal shunts. One thermal shunt was connected to an individual test article, as shown in Figure 2. The vibration isolators effectively dampened vibration transmission from the cold heads while providing a thermal conductance of approximately 2 W/°C. Tests conducted in the CRYOHP program showed that although there are acceleration levels of approximately  $70 \times 10^{-3}$  g's at the cryocooler cold heads, the vibration level at the heat pipe was less than  $2 \times 10^{-3}$  g.

Three cryocoolers were dedicated to the SHP to permit tests near the freezing point of nitrogen (63.1K) and to demonstrate up to 5 watts transport at 80K. The BETSU device was integrated with the two cryocoolers. Ground and flight operations consisted of operating only one test article at a time because of HH electrical power constraints and limited CRYOTP radiative heat dissipation.

### SHP Description

The SHP is a "U" shaped titanium/aluminum alloy (Ti-6Al-4V, ELI) nitrogen heat pipe that used six parallel fibrous copper cables to form the capillary wick structure. The porous metal cables are held against the interior wall surface with a beryllium-copper spring. The individual cables run the length of the heat pipe and are equally spaced around the inner circumference. Titanium/aluminum end caps are electron beam welded to the evaporator and condenser ends, and a titanium (CP-2) fill tube is welded to the evaporator end cap. Titanium (CP-2) saddles were clamped to the evaporator and condenser ends to provide a flat mounting surface for the thermal shunt and electrical heaters. Graphite foil was used as a filler material to provide a thermally conductive interface between the saddles and the heat pipe. Primary and redundant

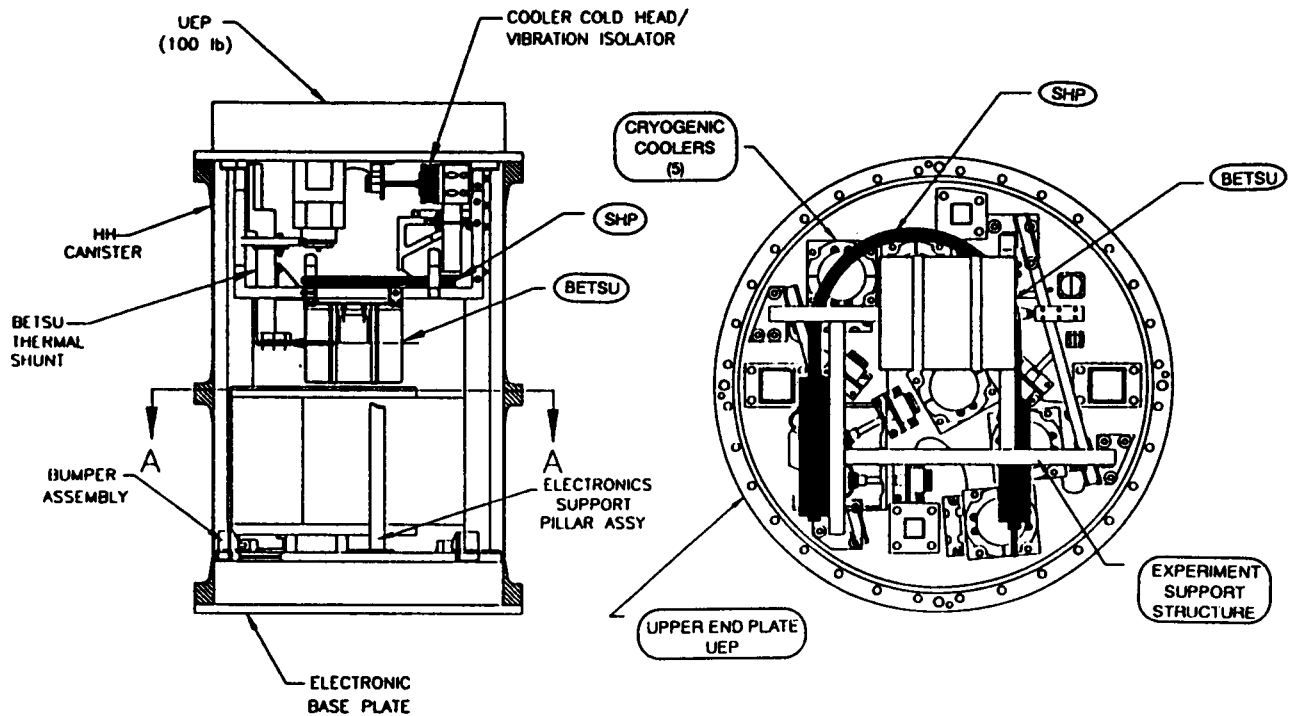


Figure 1. CRYOTP Flight Experiment

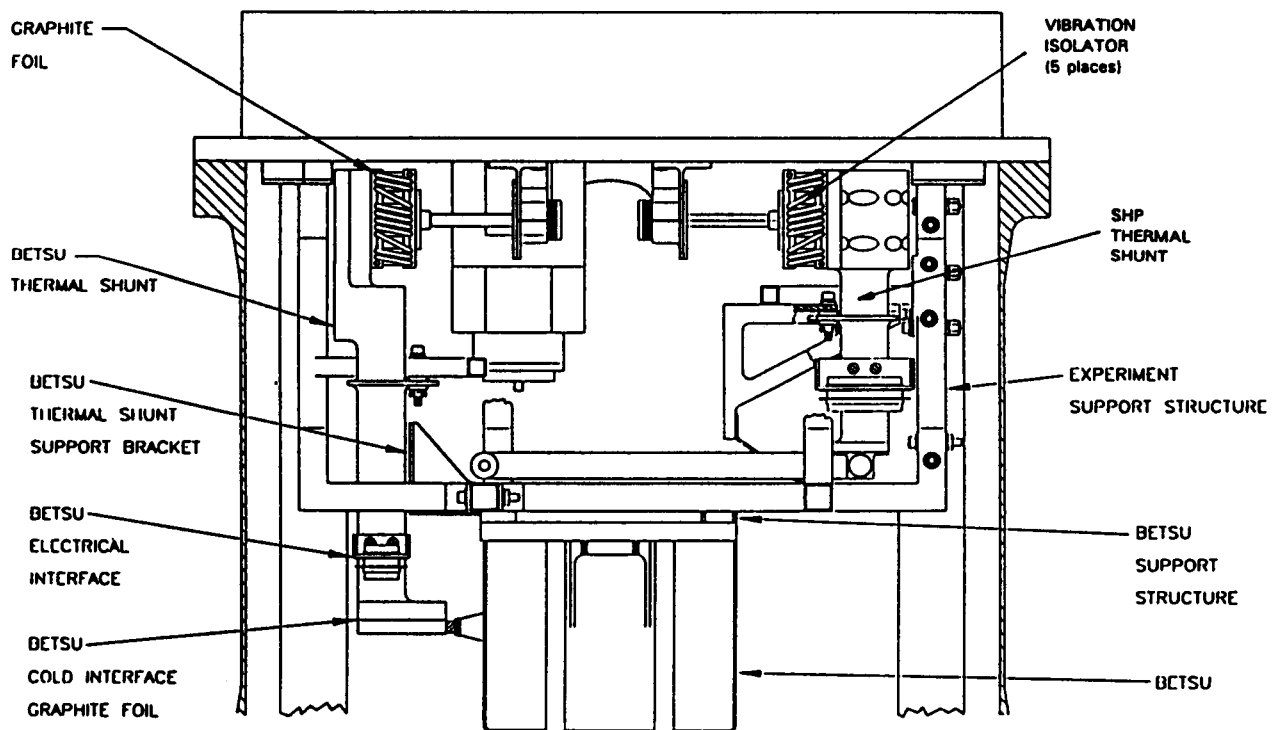


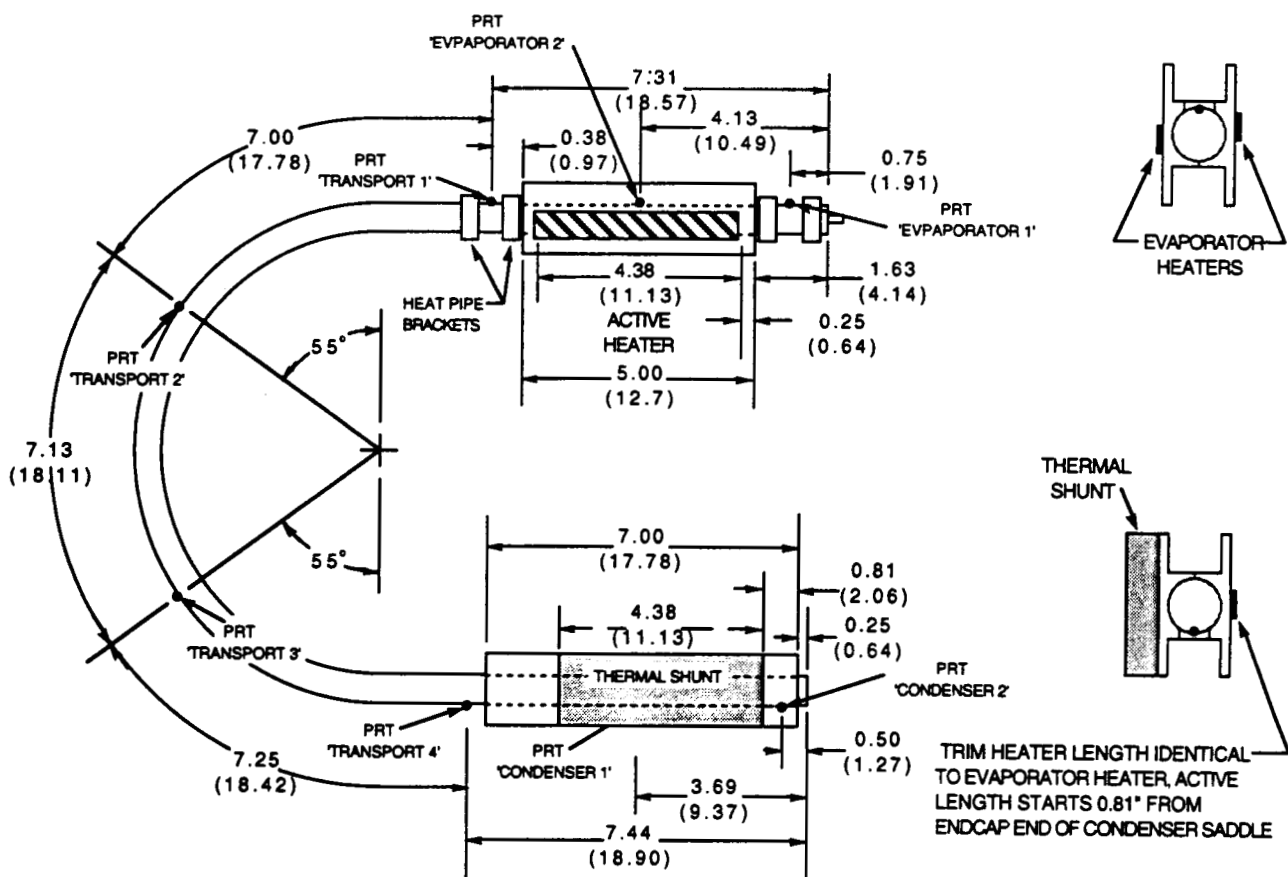
Figure 2. Test Article Integration

Kapton foil heaters and thermostats were epoxied to the both saddles. Eight (8) Platinum Resistance Thermometers (PRTs) were used to measure temperatures along the 91.8 cm long heat pipe at the locations shown in Figure 3. The design of the SHP is summarized in Table 1. Four additional PRTs were located on the SHP thermal shunt and cryocooler cold heads.

Thermal vacuum ground tests consisted of cooling the SHP down to and below the nitrogen critical point (126.2K) until the heat pipe was isothermalized. The SHP was typically cooled to 80K for conducting heat transport tests at various tilts. These tests consisted of applying heat to the evaporator section in 0.5 watt increments until evaporator dryout was indicated. The cooling capacity of the cryocoolers is a constant at a given temperature, so a trim heater on the condenser end of the SHP was used to balance the cooling load and maintain the desired operating temperature during the transport tests.

Table 1  
Space Heat Pipe (SHP) Design

Dimensions/Specifications	
Heat Pipe Total Length	91.8 cm
Evaporator Length	12.7 cm
Condenser Length	17.8 cm
Wall Outer Diameter	1.5 cm
Wall Inner Diameter	1.026 cm
Geometry	U-Shaped
Total Mass	549 grams
Wick Material	6 fibrous copper cables 3.2 mm dia. held against the ID
Heat Pipe Tube Material	Ti-6Al-4V (ELI)
Working Fluid	24.1 grams pure nitrogen



### BETSU Description

The BETSU consisted of a PCM canister surrounded by gold-plated aluminum radiation shields and mounted inside an aluminum shell enclosure. Schematics of the BETSU are presented in Figures 4 and 5 and the PCM's canister design is summarized in Table 2. An aluminum plate with redundant Kapton foil heaters was attached to one face of the PCM canister using flexible copper straps. A large flexible copper strap was attached to the opposite face of the canister and extended beyond the enclosure to the aluminum thermal shunt to thermally couple the PCM to two cryocoolers. This strap, referred to as the Q-Meter, was used to determine the heat flow from the PCM based on the measured temperature drop across the strap. The Q-meter conductance was approximately 0.25 W/°C. The PCM canister weighed less than 0.34 Kg including instrumentation and the Q-Meter. Conductive heat leaks were minimized by suspending the PCM canister within the BETSU enclosure using six titanium wire tension straps (and six dacron braid straps as backup).

The PCM canister was a welded aluminum cylinder with aluminum fins vacuum-brazed to the two flat internal faces. The fins were in an 'accordion' configuration and were perforated to permit cross-flow of the melted PCM. Approximately 35 grams of 2-methylpentane with 3% acetone was used to provide approximately 2500 Joules of energy storage at a freeze/thaw temperature of 120K. The acetone was present to minimize sub-cooling effects that tend to extend the freezing temperature range, which results in less precise or potentially unacceptable temperature control. BETSU flight and thermal vacuum ground tests consisted of cooling down the PCM canister to 120K and then conducting multiple freeze/thaw cycles at different cooling and heating rates. Heat was applied to the PCM canister at discrete levels to vary the rate at which the PCM thawed, and to determine the total energy that was stored. A commandable trim heater and fixed 4 and 6 watt boost heaters are attached to the BETSU thermal shunt to provide precise control of the rate at which heat was removed from the PCM canister. A total of 14 PRTs were used to monitor the temperature across the BETSU and the cryocoolers. Calibration tests were conducted at approximately 135K and 110K to permit an accurate determination of parasitic heat inputs.

Table 2  
Design Summary for BETSU PCM Canister

Phase Change Material	2-Methylpentane & 3% acetone
Theoretical Capacity Available	2,500 joules
Maximum Pressure at 80°C	3.81 Bars
Nominal Void Volume at 120K	33%
Maximum $\Delta T$ in PCM @ 1w	0.3 K
Volume Percent Metal Fin	24%
Inside Diameter, cm	6.1
Inside Length, cm	2.9
L/D	0.48
PCM Weight, grams	35.3
Canister Total Weight, grams	136
Canister Wall Thickness, mm	0.254
PCM to Wall Conductance Ratio	18
PCM to Fin Conductance Ratio	16
Fin Thickness, mm	0.2
Fin Density, fins per cm	11.9
Canister Material	6061-T6 Aluminum
Fin Material	3003-0 Aluminum

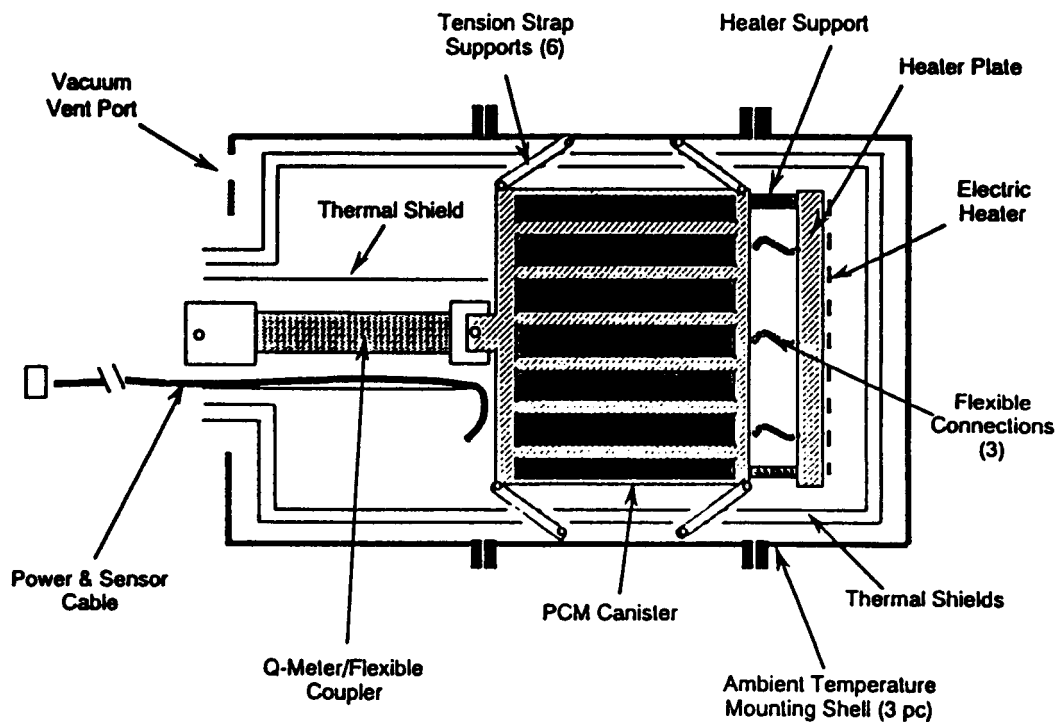


Figure 4. BETSU Thermal Structure

Approximate size: 6" Diameter by 10" Long (1.7 lbs)

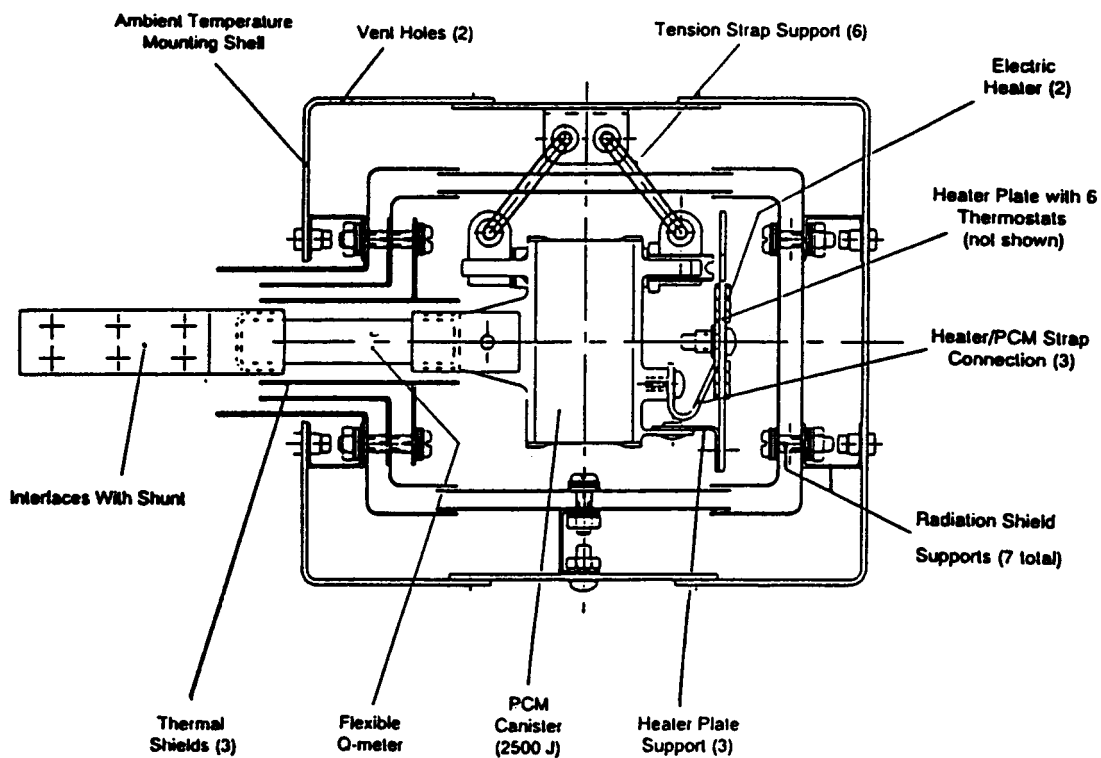


Figure 5. BETSU Mechanical Assembly

### CRYOTP Integration

The CRYOTP experiment was installed within a HitchHiker-G canister for flight aboard the Space Shuttle. The SHP and BETSU test articles were mounted to a common stainless steel support structure and shared the same CRYOTP Electronics Control Module (CECM) and Power Distribution Box (PDB). The experiment structure and the coolers were mounted directly to the canister's Upper End Plate (UEP). The standard UEP was modified for the CRYOHP experiment to increase both its thermal mass (by approximately 40 kg) and its heat rejection area. The increased UEP heat capacity permitted continuous operation for 12 hours or more with cryocooler compressor body temperatures of less than 70°C. Up to 320 watts of heat could be dissipated while in an earth viewing or colder environment. The SHP was suspended from the stainless steel structure using three Kevlar wire/G-10 fiberglass sub-assemblies to minimize thermal conduction losses and induced vibration levels (shown in Figure 6). Graphite foil thermal interfaces and G-10 isolators were used throughout the experiment as necessary. The heat pipe, thermal shunts, and the cryocooler cold head vibration isolators were wrapped with Multi-Layer Insulation (MLI) blankets to minimize radiation heat leaks.

Thermistors were used throughout the experiment for housekeeping temperature measurements. Primary and redundant kapton foil heaters were used to provide heat input to each test article and to permit control at a specific operating temperature. Real-time series commands were used to apply incremental heater power to the test articles. The SHP's heaters could be incremented in 0.5 watt steps from 0 to 7.5 watts. The BETSU's input heater power could be varied in 0.25 watt increments between 0 and 4 watts. Three series thermostats were used with each heater to provide a two-fault tolerance against a runaway heater failure.

After the final ground testing of the BETSU and SHP were complete, the CRYOTP experiment was delivered to the Hitchhiker OAST-2 carrier for integration. Power, commands and telemetry for the experiment were provided by the Hitchhiker avionics mounted adjacent to CRYOTP on the OAST-2 bridge. Real-time telemetry was downloaded to the Payload Operations Control Center (POCC) at GSFC. Commands were forwarded from the POCC to permit real-time control of the experiment.

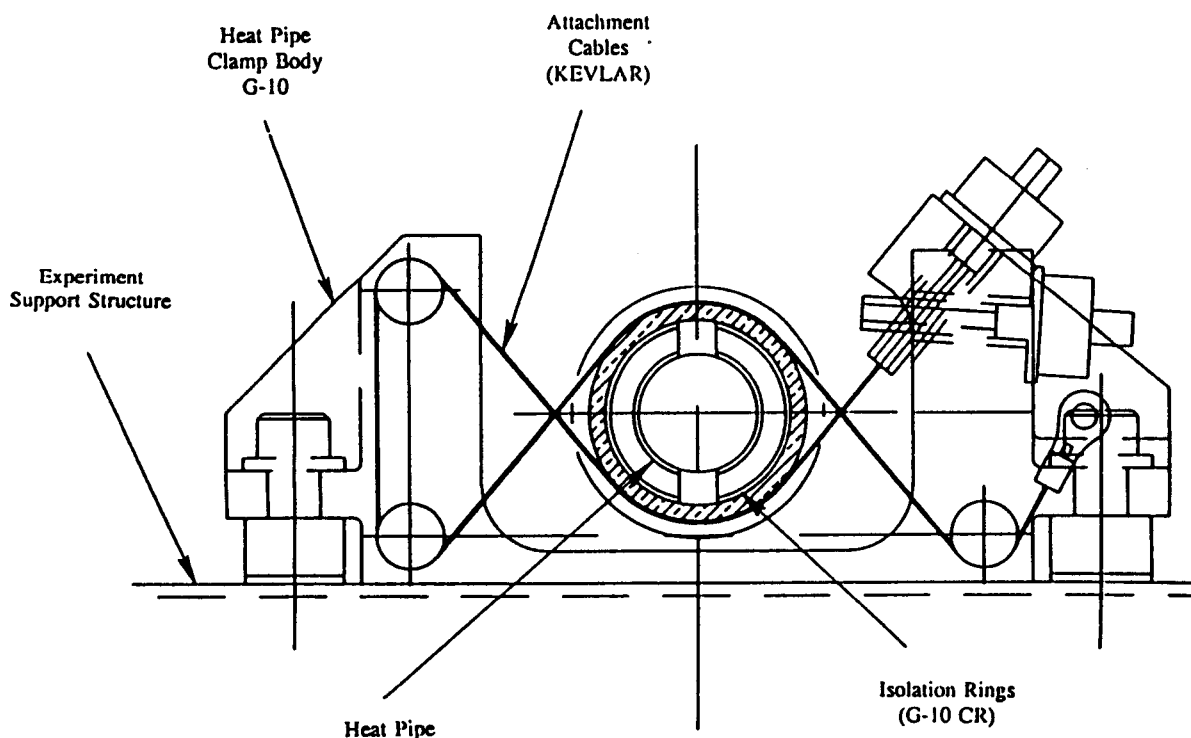


Figure 6. SHP Attachment and Isolation Supports (3 Places)

### Flight Results

The CRYOTP experiment was activated approximately 9 hours after launch and tests were performed continuously over the following thirteen days. The experiment was deactivated on flight day fourteen just prior to shuttle deorbit.

### SHP Test Results

The cooldown of the SHP was initiated within minutes of the CRYOTP activation. The transient cooldown temperatures of the heat pipe's condenser and evaporator sections are shown in Figure 7 along with cryocooler #2's cold head temperature for the two flight test cycles. The second cooldown cycle was conducted on flight day six of the mission. Heat pipe axial temperature profiles are shown for the first cooldown cycle in Figure 8; similar profiles were experienced in the second cycle. The SHP did not isothermize in either cooldown cycle, but rather reached a non-operational near steady-state condition in which the evaporator temperature remained well above the critical point of nitrogen. The axial temperature profiles indicate that only the last 30 cm of the heat pipe cooled below the critical temperature, a result one would expect if the heat pipe had lost its fluid charge. However, when the SHP was de-integrated from the CRYOTP test bed post-flight the nitrogen was vented and measured to be design charge of 24.1 grams. In the liquid state this mass represents more than 40% of the internal volume of the heat pipe at 80K. The cooldown and startup of the SHP during CRYOTP thermal vacuum ground tests is compared to Flight Cycle #1 in Figure 9. Ground tests were conducted with the SHP at a slight adverse tilt ( $\sim 1$  mm). Startup and isothermization were accomplished at about 85K within seven hours from the start of cooldown.

The failure of the SHP to startup and isothermize in microgravity is attributed to supercritical startup limit not readily observable in ground tests. The SHP never cooled sufficiently to drop the internal pressure of the heat pipe below the critical pressure of nitrogen, and therefore the wick could not be primed. Since the condenser section was well below the critical temperature a large liquid slug was formed. This liquid slug extended into the transport section of the SHP and effectively blocked the condenser, separating the evaporator from the cooling source. At this point no convective heat transfer could take place within the heat pipe. The heat pipe essentially reached a steady-state condition in which the parasitic heat load along the pipe

was equal to the cooling rate available by axial conduction through the heat pipe wall. This operating condition can only be reached in microgravity. During ground testing heat pipes are capillary-limited to small angles of adverse elevation, and the liquid slug forms a puddle along the bottom of the heat pipe. Startup is thus aided by gravity-assisted liquid return and natural convection, along with axial heat conduction.

In fairness it must be noted that the SHP might have eventually started if given enough time. The transport section was slowly cooling (although much slower than in ground tests) but both cooldown attempts had to be terminated due to operational constraints. The first attempt was terminated to allow BETSU testing to begin. The second cooldown cycle was ended when one of the cryocoolers (Hughes tactical cryogenic refrigerator, Model No. 7044H) used as a heat sink failed. At this point the parasitics through the failed cryocooler were large enough that further cooling of the pipe was impossible. Despite these problems, significant observations of cryogenic heat pipe behavior were gained from the SHP tests; the vapor-to-liquid volume ratio should be maximized, allowance must be made for the size of the liquid slug (a reservoir could provide this), a low thermal conductivity wall material such as titanium is a disadvantage for startup (although beneficial for diode action and pressure containment), and the relationship between cooling capacity and parasitics is especially important.

### BETSU Test Results

The first BETSU cooldown cycle was initiated upon termination of the SHP's first test cycle, approximately 23 hours into the mission. Transient data for the heat input side of the PCM canister is presented in Figure 10 for both BETSU cooldowns. In each of these cycles supercooling occurred because the PCM was being cooled from a totally melted state. In the first cycle the PCM did not start to freeze until it reached a temperature about 112K, and was further supercooled to 105K. In following freeze/thaw cycles freezing occurred at about 117K. The plateau shown in the second cooldown cycle at 135K is due to the application of heater power during a calibration test. The PCM was supercooled to 105K in this case, and subsequent freezing occurred around 120K. Figure 11 presents a comparison of flight cooldown cycle #1 with the thermal vacuum ground test data. The temperature profiles are nearly identical with supercooling and freezing occurring at the points for both the flight and ground tests.



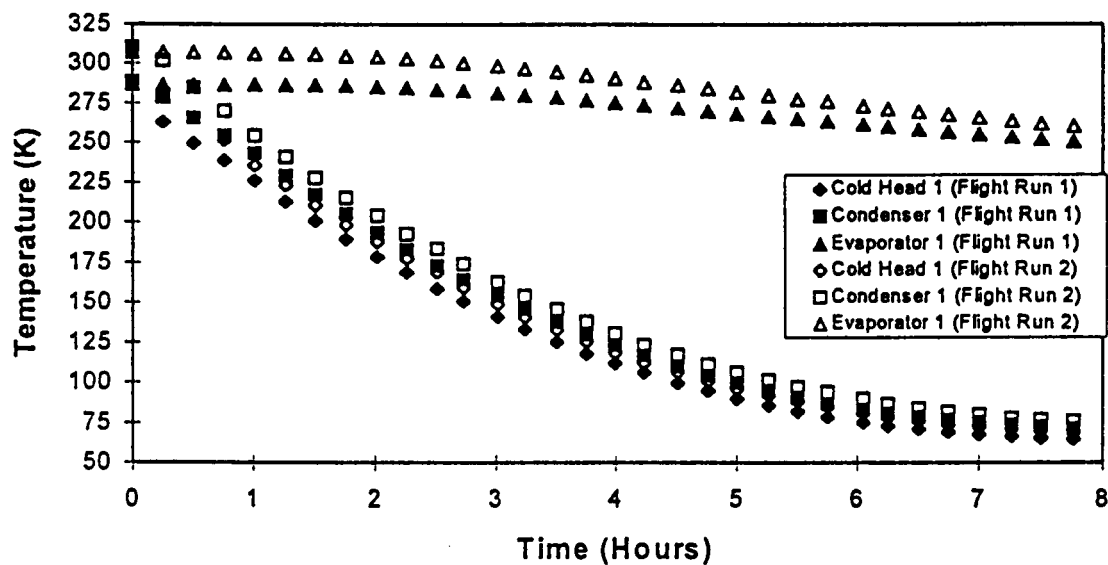


Figure 7. SHP Transient Cooldown Cycles 1 and 2

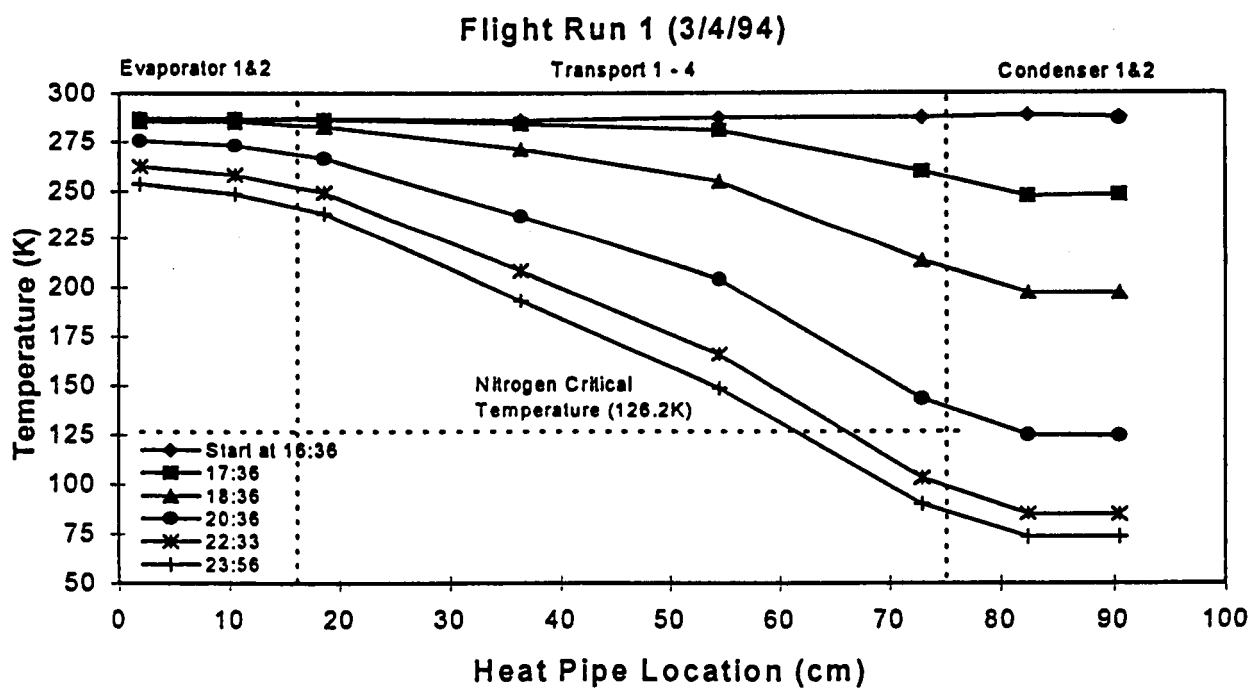


Figure 8. SHP Axial Temperature Profiles During Cooldown

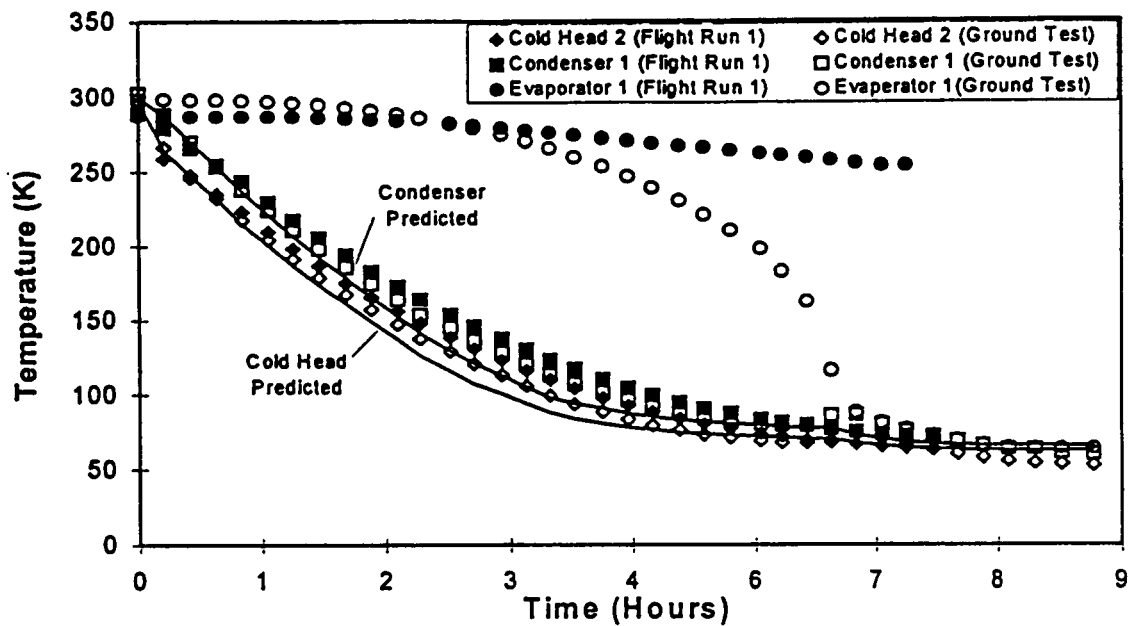


Figure 9. Comparison of SHP Ground and Flight Transient Cooldowns

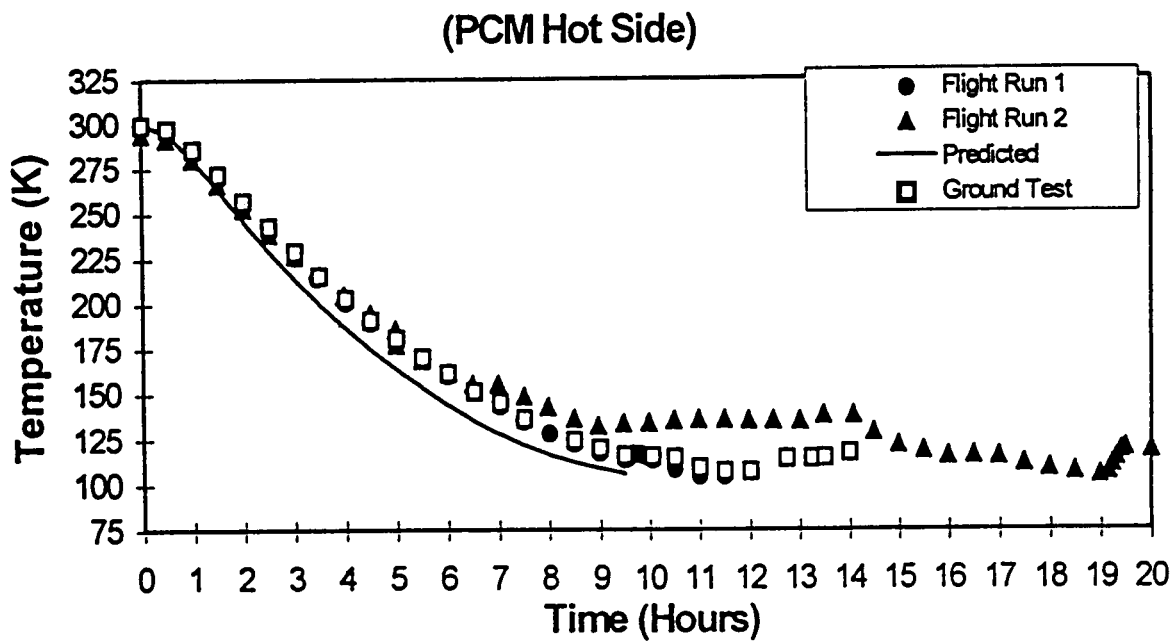


Figure 10. Comparison of BETSU Ground and Flight Transient Cooldowns

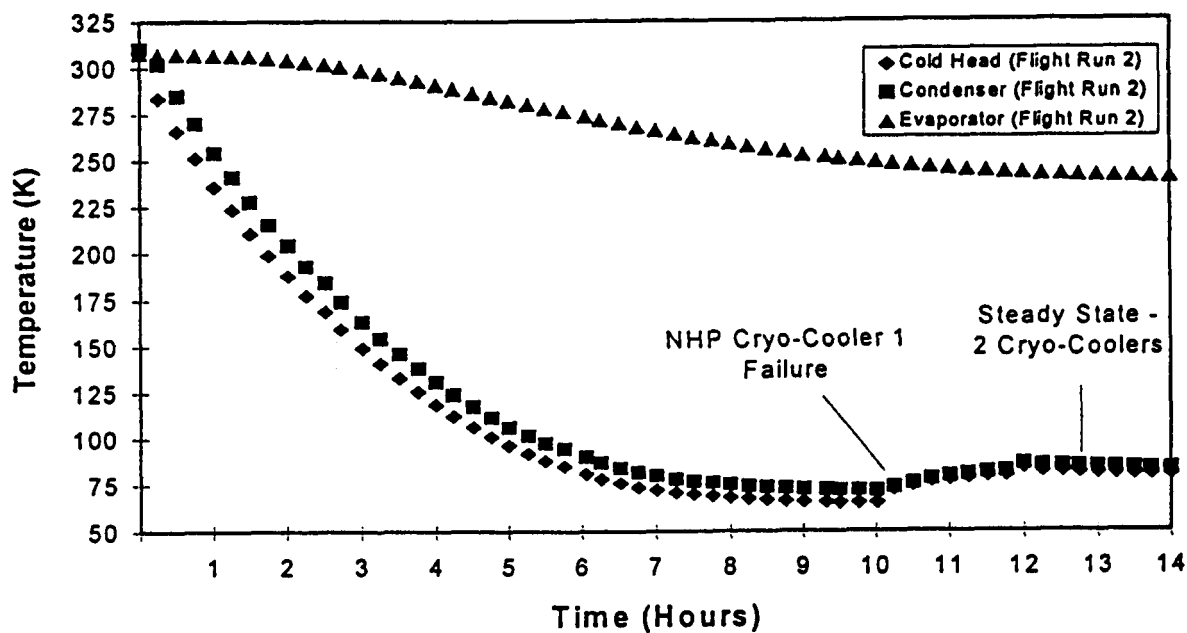


Figure 11. SHP Cryocooler Failure

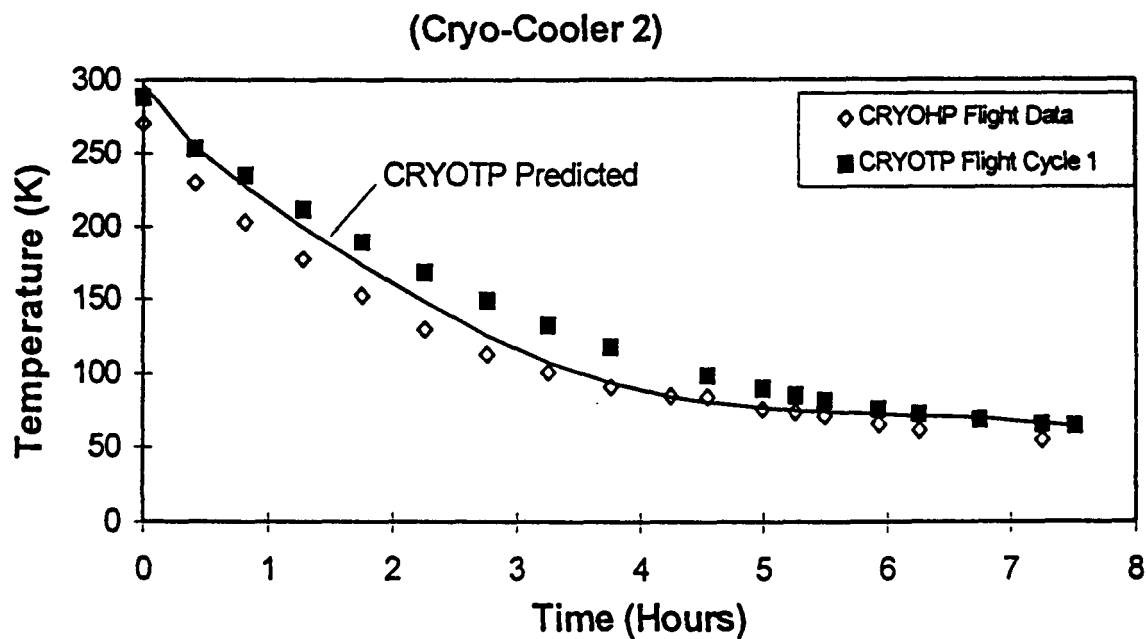


Figure 12. Comparison of Three-Cooler Cold Head Transient Cooldown for CRYOHP and CRYOTP Missions

More than 250 hours of on-orbit test data consisting of 56 freeze/thaw cycles and 26 steady-state calibrations were completed. Supercooling was acceptable ( $< 3^{\circ}\text{C}$  at a 1 watt cooling rate) as long as the PCM was never completely melted. The solid particles in the liquid/solid mixture apparently provide nucleation sites for freezing that minimize the supercooling effect. Results of the ground and flight tests show that virtually all of the stored energy (2472 J) is released during two-phase cycling with temperature control at  $119\text{K} \pm 1.5\text{K}$  and with a 1 watt heating or cooling rate. The  $3^{\circ}\text{C}$  difference is primarily caused by two-phase subcooling that is difficult to totally eliminate. Test results show that the supercooling effect was more pronounced as the cooling rate was increased. This implies that increasing the PCM canister's internal thermal conductance and effective heat transfer surfaces (decreasing the cooling flux) is a potential method for providing tighter temperature control.

#### Cryocooler Performance

CRYOTP represented the second flight of the five tactical cryocoolers. These cryocoolers were all procured in the spring of 1992 for the CRYOHP flight. Total operational time for these cryocoolers is shown in Table 3. The manufacturer indicated that these cryocoolers should have a nominal time to failure of 2000 hours. However, as previously mentioned, the SHP cryocooler #1 failed after only 331 hours of operation. Interestingly, this was the cryocooler with the lowest total operational time. Failure was indicated by a sudden increase in cold head temperature and a reduction in the net cooling effect on the SHP test article. No warning of impending failure was evident. Several unsuccessful attempts were made to recover the the cryocooler by cycling the power on and off. With

only two cryocoolers working the SHP condenser came to a steady-state temperature of about 81.5K. The resulting parasitic heat leak through the non-functional cryocooler was estimated to be about 1 W. Additional in-flight and post-flight testing indicated that this cryocooler could not recover its cooling capacity. The cryocooler appeared to draw the same amount of power post-failure, and there was no evidence for frictional heating at the cold head. Loss of the helium working fluid was suspected, but post-flight testing revealed that this was not the problem. Failure of an electrical controller internal to the unit is now the suspected culprit. Confirmation will require that the cooler be disassembled, which has not yet been performed due to funding constraints.

In addition, comparisons of the flight data from CRYOHP and CRYOTP appears to show that the three cryocoolers servicing the SHP side of the experiment may have experienced some minor degradation prior to the CRYOTP flight (Figure 12). Data from the BETSU testing also indicates that the net cooling capacity for the two cryocoolers on this side of the experiment degraded at about 1K per day during the CRYOTP flight. Post-flight testing suggested that this reduction was not due to a change in cryocooler capacity (unless performance was recovered over time). An increase in parasitics during flight may have been the cause of the apparent degradation in performance. At cryogenic temperatures the system is very sensitive to contaminants that would reduce the effectiveness of the multi-layer insulation.

	BETSU1	BETSU2	SHP1	SHP2	SHP3
Pre CRYOHP Flight	43	38	135	207	286
Post CRYOHP Flight	126	125	202	266	358
Pre CRYOTP Flight	296	254	311	378	469
Post CRYOTP Flight	559	518	331	421	512
Total Flight Time	346	351	87	101	115

### Conclusions

The flight of the CRYOTP experiment in March of 1994 demonstrated the effectiveness of two new cryogenic test articles in a microgravity environment. The SHP test article was not able to start within the available time and operational constraints, but valuable lessons were learned from this experience. A new startup criteria regarding the relationship between fluid inventory and internal volume for cryogenic heat pipes was observed. Other valuable design criteria for cryogenic heat pipes were also obtained. The failure of the SHP to start, despite successful ground testing, once again demonstrated the need for flight testing of two-phase heat transfer systems, since ground testing can be misleading due to gravity effects. A proven transient startup model is also needed to reliably predict heat pipe performance in microgravity.

The BETSU testing was completely successful, with 56 freeze/thaw cycles at 120K accomplished. Precise temperature and thermal calibration data were also obtained. Supercooling and melt/freeze behavior was essentially the same as observed in ground testing, and the analytical model was verified to be accurate.

Failure of one of the five tactical cryocoolers, despite it being far short of its rated lifetime, and the back parasitics associated with this failure demonstrates the need to address cryocooler reliability.

Another major conclusion from the CRYOTP flight was the demonstrated ability to fly a new experiment at modest cost and with a very accelerated schedule. This was made possible through reuse of an existing test bed and a highly experienced team of people. None of the above observations could have been learned from ground testing alone, hence the value of the flight experiment.

### Acknowledgements

The CRYOTP experiment was funded jointly by the U.S. Air Force through Phillips Laboratory and the Space Test Program (STP), and by NASA through the Goddard Space Flight Center.

### References

1. Rosenfeld, J., and Keller, R., "Sintered Powder Artery-Free Cryogenic Heat Pipe", Final Report, Contract No. NAS5-30783, prepared by Thermacore, Inc. for NASA Goddard Space Flight Center, Greenbelt, MD, 1994.
2. Stoyanof, M., and Glaister, D., "Design and Performance of a Two-Phase Thermal Storage Unit at 120 Kelvin", SAE Technical Series Paper No. 94-1155, April, 1994.
3. Brennan, P., Stouffer, C., Thienel, L., Morgan, M., "Performance of the Cryogenic Heat Pipe Experiment (CRYOHP)", SAE Paper No. 92-1408, 22nd Int. Conf. on Environmental Systems, Seattle, WA, July 13-16, 1992.
4. Brennan, P., Thienel, L., Swanson, T., Morgan, M., "Flight Data for the Cryogenic Heat Pipe (CRYOHP) Experiment", AIAA Paper No. 93-2735, AIAA 28th Thermophysics Conf., Orlando, FL, July 6-9, 1993.

## STANDARD GAS HARDWARE

Stan Spencer  
Bright Moments Engineering,  
Sierra College Space Technology Program<sup>1</sup>

### ABSTRACT

The Sierra College Space Technology Program is currently building their third GAS payload in addition to a small satellite. The project is supported by an ARPA/TRP grant. One aspect of the grant is the design of standard hardware for GAS payloads. A standard structure has been designed and work is progressing on a standard battery box and computer.

### INTRODUCTION

Under the direction of Michael Dobeck, Sierra College has successfully flown two GAS payloads aboard the Space Transportation System. Many lessons were learned about the difficulties of building GAS payloads. Considerable time and effort were expended in the design, analysis, and safety-approval process for the structure, battery box, and computer. It was clear that the building of a payload would be greatly simplified if standard flight-qualified hardware existed, and the documentation or actual hardware was readily available. Researchers could then be relieved of much of the work of building a payload and freed to concentrate on developing their experiments. With this in mind, Michael Dobeck wrote a successful grant proposal for Sierra College in the Summer of 1993. One of the major components of the ARPA/TRP grant is the design, construction, and flight qualification of a standard structure, battery box, and computer for GAS experiments. This paper will discuss the progress Sierra College has made toward the development of standard GAS hardware.

### PROGRAM HISTORY

#### Payload G-399

A short overview of the Sierra College Space Technology Program is in order to provide some background for the work currently in progress. The first Sierra GAS payload, G-399, was begun under the direction of Michael Dobeck in 1990. Aerojet

---

<sup>1</sup> The work described in this paper is supported by an ARPA/TRP grant. The grant is managed through the NASA management office at the Jet Propulsion Laboratory in Pasadena, California. The grant number is NAG7-1.

Corporation donated the services of one of their structural engineers, P. J. Krusi, to design an internal structure for the five cubic foot payload. Three shelves were required for the planned experiments, and Mr. Krusi connected the shelves with four tubular columns to form the structure. Figure one shows the basic design.

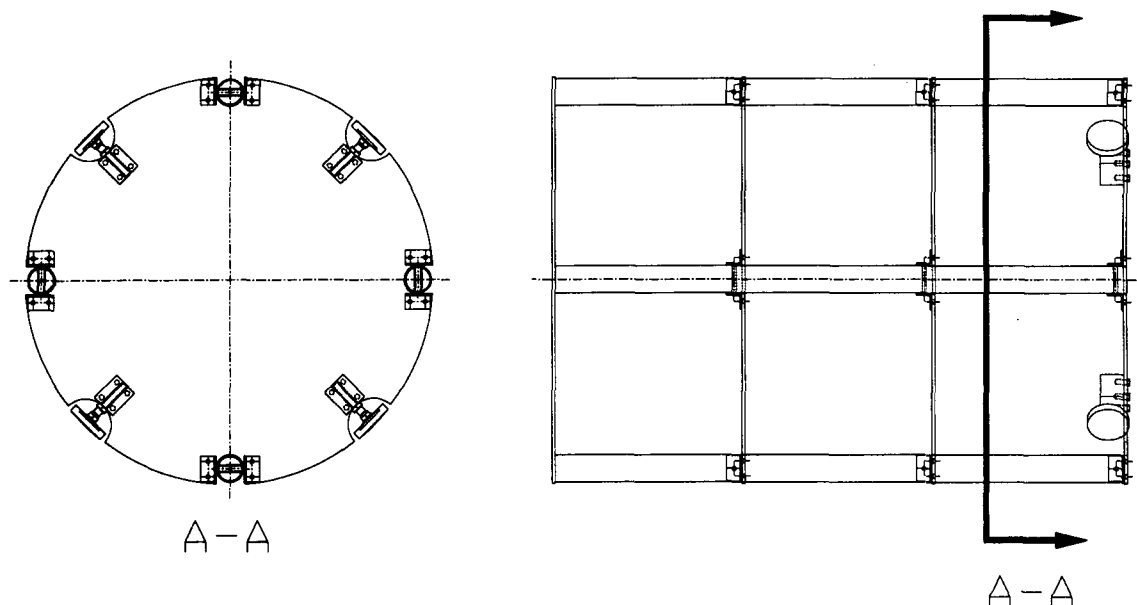


Figure 1: The G-399 internal structure

The columns were built with round tubing to maximize the strength-to-weight ratio of the structure. Small crush tubes were welded through the columns for added strength at the attachment points for the shelves. Four snubbers were required on the bottom shelf to prevent possible deflection of the structure into the walls of the GAS canister.

The design was very successful in meeting the objectives of light weight, high strength, and minimal intrusion into the available canister volume. However, integrating the experiment hardware with the structure revealed a shortcoming of the design -- it was difficult to assemble and disassemble. Additionally, there were some difficulties that arose in the manufacturing process. The welding of the crush tubes in the thin-walled columns required a highly skilled welder, and the welds had to be x-rayed to demonstrate their quality. Nevertheless, the project was completed in three years, flew in June of 1993 aboard the Shuttle Endeavour, and the structure performed flawlessly.

### **Payload G-178**

While G-399 sat in Florida awaiting launch, work had already begun back at Sierra on the second GAS payload, G-178. At the G-399 integration other GAS experiments were observed that were professionally built with budgets into the millions of dollars. Borrowing ideas from those payloads, a new design was worked out for the

internal structure. Designed for a 2.5 cubic foot payload, the structure was built with eight I-shaped machined columns that bolted to the outermost holes in the GAS experimenter's mounting plate (EMP). The complete structure was created with a milling machine, requiring no welding or x-raying. The columns were formed by segments bolted between the shelves (not passing through the shelves), so assembly and disassembly were much more simple than with G-399. Constructed over a hectic eighteen week period, G-178 flew in September of 1994 aboard Discovery.

## **ARPA TRP Grant**

The decision to build G-178 as quickly as possible was brought about by the arrival of a higher priority project. After the flight of G-399, Michael Dobeck wrote a proposal for Sierra College for an ARPA/TRP grant in the area of manufacturing engineering education. The grant was awarded in November of 1993.

The ARPA grant, which is managed by the NASA management office at the Jet Propulsion Laboratory in Pasadena, California, has three major goals. The first of these goals is the creation of a multi-track Space Technology degree and transfer program. Students earning a heavily interdisciplinary Space Technology degree will use a project as the focus of their studies. The project forms the second goal of the grant: the design, implementation and flight of a microsatellite. The satellite will use a spectrograph to measure the ozone layer and take digital images to characterize the target area. The final goal of the grant is the subject of this paper: the creation of standard flight qualified GAS hardware including a support structure, computer, and battery box. This standard hardware will allow other schools or industry users to create Space Shuttle experiments with greatly reduced difficulty.

## **THE STANDARD STRUCTURE**

### **Design Goals**

The goals of the design for the standard structure were fairly simple: minimize weight, maximize usable volume, manufacture without welding, allow easy assembly and disassembly, and provide some flexibility in configurations. The design process was essentially an optimization of the G-178 structure.

### **Description**

The standard structure uses I-shaped columns like G-178, but the number of columns was reduced from eight to six. The columns were also reduced in weight by increasing their thickness slightly while changing their cross-section from a solid rectangle to an I-beam. A pictorial view of the standard structure is shown as figure two.



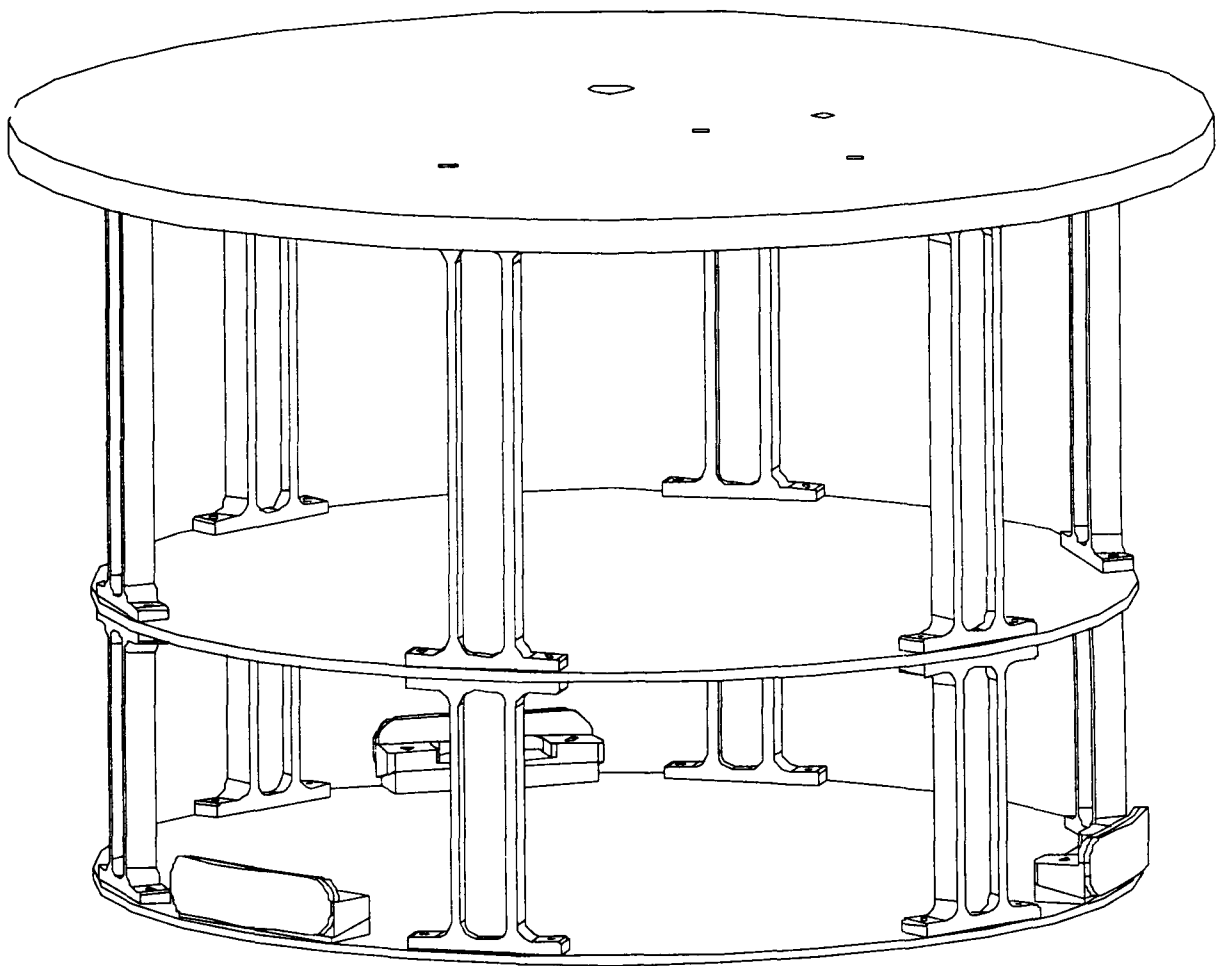


Figure 2: The standard 2.5 cubic foot GAS structure

The use of six columns also allowed for the easy placement of three snubbers. NASA requires the snubbers unless it can be proven through analysis that the structure will not deflect into the GAS canister. It was determined that a standard structure built with enough stiffness to eliminate snubbers would simply weigh too much. The optimal solution was to use the minimum number of snubbers, which is three.

The snubber design is shown pictorially in figure three. The design requirements were as follows: the contact area with the canister of each snubber be at least four square inches, the adjustment mechanism be accessible from below the structure, and a positive locking mechanism be used. Further design goals were to minimize the weight of the snubbers and their footprint. Minimizing the amount that the snubbers intrude into the shelf space maximizes the space available for experiments.

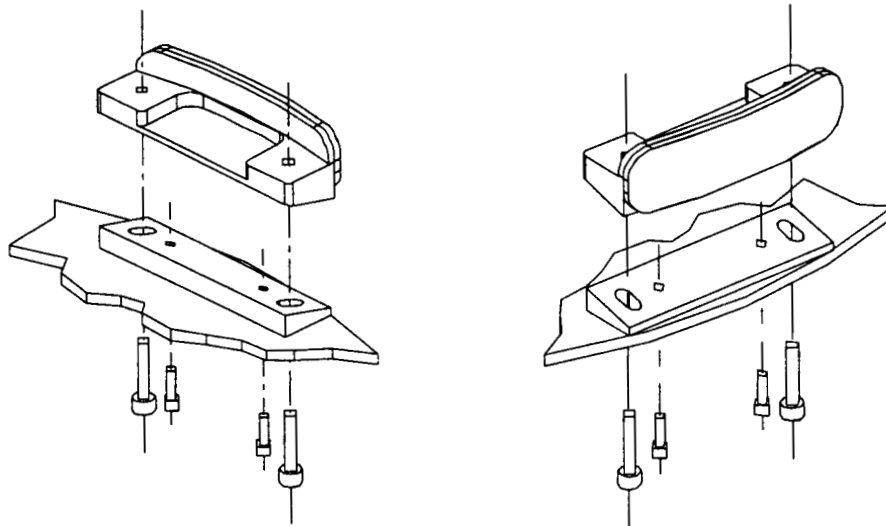


Figure 3: The standard GAS structure snubber -- two views

The design places the snubber on an inclined block that is first bolted to the shelf. The block and the shelf have two matching slots milled in them through which bolts pass from below the shelf up into threaded locking inserts in the snubber. As the bolts are tightened the snubber moves down the inclined plane of the block and out towards the wall of the GAS canister. Once the snubbers are adjusted out against the walls of the canister and the bolts are torqued, a positive lock is achieved because movement of the snubber inward would require movement up the inclined plane, which would stretch the torqued mounting bolts. The snubber design provides for an easy adjustment procedure from below, and, as can be seen in figure 4, a minimal amount of shelf space is used.

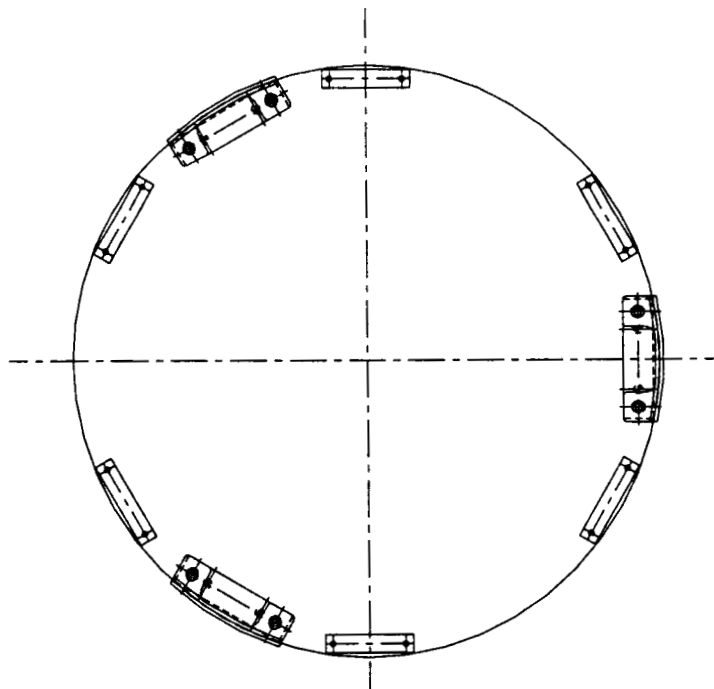


Figure 4: the layout of columns and snubbers on the bottom shelf

The standard GAS structure was also designed with modularity in mind. The goal was to be able to substitute different length columns within the GAS canister envelope to achieve different configurations with respect to the number of shelves and the spacing between them. Two prototype designs have been built for 2.5 cubic foot structures, as shown in figure five. Preliminary finite element analysis has indicated that these configurations are more than adequate under static loads, and dynamic modeling was in progress as this paper was being written. These configurations will be doubled in length and analyzed as potential five cubic foot structures. If the design passes dynamic analysis, a large number of configuration options will be available by selecting different length columns.

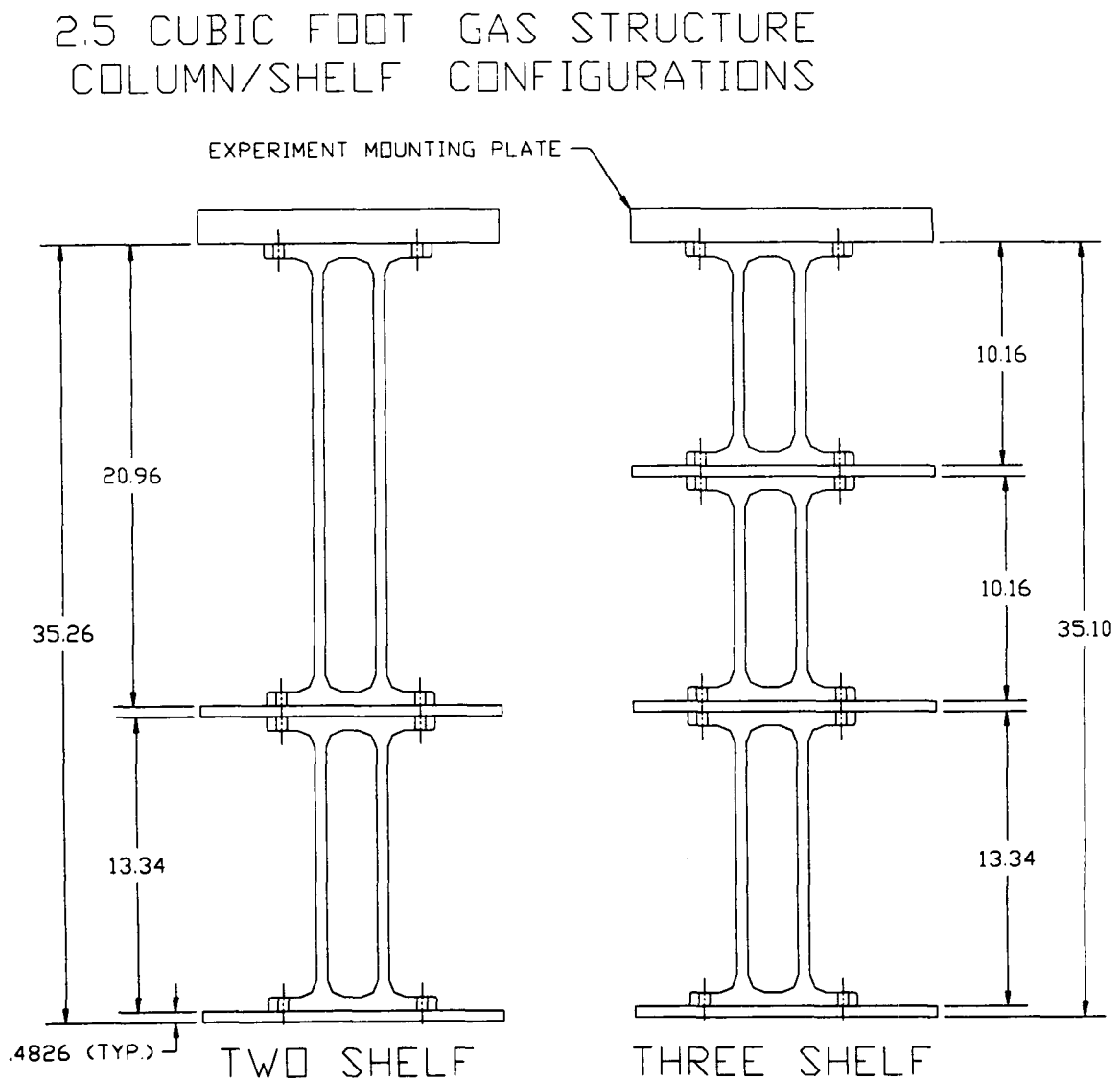


Figure 5: 2.5 cubic foot standard structure configurations (dimensions in centimeters)

## **OTHER STANDARD GAS COMPONENTS**

### **Standard GAS Computer**

Progress is also being made on the development of the other standard GAS components. The Sierra College space technology program was created by Michael Dobeck, who is a computer science professor at the school. Since the program is an outgrowth of the computer science department, the controllers for Sierra's GAS payloads have been viewed as the most easily developed subsystem of the experiments. G-399 used a controller designed and built by Sierra students based on an 8051 processor. G-178 used a commercially available 80386 single board computer. Designs have also been worked out for standard GAS computers based on low power 80x86 and 68xxx processors. The current plan, however, is to develop a standard GAS computer based on a very small, cheap, ultra-low-power RISC microcontroller. It was decided that this would be a more valuable contribution to the GAS community than duplicating other easily available single board computers. The RISC microcontroller has plenty of computing power for most GAS payloads, and has the advantage of very low consumption of both power and physical space. GAS experimenters who require more computing power have a number of readily available options in the commercial market.

### **Standard GAS Battery Box**

The standard GAS battery box, like the computer, is still in the developmental stage. The design will use commercial alkaline F cells, which are highly suitable for GAS payloads due to their long shelf life, relative low cost, easy availability, and minimal safety hazards. Several designs for the box have been considered, seeking a model that can be built without welding while providing maximum flexibility in use. The current idea is to develop a relatively small box, which will give the gas experimenter many options for placement on the structure while allowing the total power available to be a function of the number of boxes flown. Another advantage of small battery boxes is that devices attached to the structure that weigh less than five pounds do not require additional structural analysis.

## **CONCLUSION**

The GAS program provides a tremendous opportunity for low cost access to space based experimentation. Sadly, this program has not been taken advantage of to the fullest extent possible. Sierra College is developing standard GAS hardware to make the GAS opportunities more easily obtainable for potential experimenters. The availability of pre-approved GAS hardware should greatly simplify the development of a GAS payload, and hopefully will expand the use of the program.

## **G-399 AND G-178: LESSONS LEARNED**

Michael Dobeck  
Sierra College

### **ABSTRACT**

This paper outlines the lessons learned implementing GAS payloads G-399 and G-178 with regard to power systems, computer/data logger, structure and working with undergraduates<sup>1</sup>.

### **INTRODUCTION**

Sierra College has successfully flown two GAS payloads. The first of these payloads, G-399, flew in June of 1993 aboard the Shuttle Endeavour and the second payload, G-178, flew in September of 1994 aboard the Discovery. The experience gained on these two flights is being applied to a third GAS payload, G-744, that will fly in April of 1996.

Sierra's "space program" now spans more than five years. During this time over 200 students have been involved in the design, analysis, manufacturing and test of GAS payloads. We are currently working with students to create a small remote sensing satellite that is scheduled for launch in late 1997.

The high-points of the cumulative knowledge gathered in building two GAS payloads is presented in the following paragraphs.

### **POWER SYSTEM**

One of the major failure modes in GAS payloads is the power system. More than one payload has gone into orbit with a depleted battery pack. Power issues can be easily overcome with proper planning, design, and battery choice. The key in planning is to calculate realistic rates of energy consumption and run tests on the payload to determine the accuracy of the calculations. If energy is a critical issue, careful attention must be paid to low-power design techniques. The battery pack must be able to deliver the required power at worst-case payload thermal conditions.

The power source in GAS payloads is limited by safety considerations and cost factors to batteries. The battery of choice for both G-399 and G-178 was an alkaline F cell. Although one could argue for more exotic power sources, the time and effort required for flight approval is, in most cases, prohibitive. The F cell is a standard

---

<sup>1</sup> The work described in this paper is supported by an ARPA/TRP grant. The grant is managed through the NASA management office at the Jet Propulsion Laboratory in Pasadena, California. The grant number is NAG7-1.

commercial product, manufactured by a number of vendors, for use in 'lantern' batteries and a variety of other products. Each 1.5 V F cell delivers 20 amp-hours with a 0.5 amp load. This type of cell is available pre-packaged from several distributors in custom configurations. In both of our GAS payloads, the F cell batteries performed as expected.

## **Batteries**

There are a wide variety of battery types on the market, but all batteries fit into two basic categories-- primary cells and secondary cells. Primary cells are designed for a single discharge only-- i.e. primary cells cannot be recharged. Secondary cells (e.g. NiCd) are designed to be recharged several hundred times. (1)

The major considerations in choosing batteries are as follows:

- Safety concerns must be addressed-- i.e., explosion hazard.
- The batteries must provide sufficient energy at flight temperatures.
- The voltage and current availability must match your experiment.
- The batteries must have a shelf life of at least 3 months-- 6 months is more reasonable.

### Primary Cells and Secondary Cells

The standard dry-cell battery is made up of a central carbon rod surrounded by a cathode mixture of manganese dioxide, carbon, ammonium chloride and zinc chloride electrolytes. The cathode is separated from the zinc anode outer can by an insulating layer. The can is sealed with a wax and asphalt seal. If this sounds primitive, that's because it is primitive! This type of cell has low power density, a sloping discharge curve and its impedance rises as the cell is discharged. (2) The heavy duty dry cells offer improved delivery of their rated energy capacity, but still have a number of the standard cell drawbacks. The one advantage of these batteries is their low cost (see Table 1).

Alkaline dry-cell batteries offer far better performance than the standard and heavy duty dry-cell batteries. Alkalines have a shelf life of several years and perform well at temperatures ordinarily experienced in the GAS environment. The F type cells have a higher energy density than consumer D cells. Type F alkaline dry cells are also widely available at low cost.

Mercury and silver oxide cells perform better than alkaline cells, but they are expensive. Because of mercury's willingness to combine with other metals, mercury batteries are considered a severe safety hazard (2). If your program can afford silver oxide cells, they are worthy of further investigation.

Lithium batteries are nearly perfect for GAS payloads when using the categories listed in table one as the determining factors. Unfortunately, they constitute a major safety hazard because they have exploded on several occasions causing severe damage to equipment and personnel. The small button type lithium batteries embedded in real-time clocks generally do not pose a hazard (2).

Secondary batteries (rechargeable) have lower energy density than primary batteries and the secondary cells self discharge. A NiCd battery will lose 50% of its

charge in four months, and a lead-acid battery will lose one-third of its charge in eight months. The major feature of secondary batteries is that they can be recharged, but is this an important characteristic for a one-shot payload? On the positive side, both lead-acid and NiCd cells have low internal resistance, so current can be drawn from the cells at a high rate.

Battery Type	Energy Density (Wh/in <sup>3</sup> )	Performance				
		Discharge Curve	at 5 Degrees C	Shelf Life	Safety Hazard	Cost
Zinc-carbon (standard cell)	1-2	sloping	poor	?	minimal	low
Zinc-carbon (heavy duty)	2-2.5	sloping	poor	?	minimal	low
Alkaline	3.5	sloping	good	very good	flown	low
Mercury	7	flat	good	good	high	high
Silver oxide	6	flat	very good	excellent	?	high
Lithium	8	flat	excellent	excellent	high	high
NiCd	1	flat	good	poor (50% of charge lost in 4 months)	flown	low
Lead Acid	1	flat	good	acceptable (33% of charge lost in 8 months)	flown	low

Table 1: Battery characteristics.

## LOW POWER DESIGN

Low power design is a philosophy that must be embraced for most GAS payloads. Because of battery power limitations, mission success generally depends upon the designer's skill in minimizing power usage. The basic low-power design philosophy can be summed up as follows:

- Don't build in more computing power than you need (CPU speed, memory size).
- Use low power (i.e. CMOS) electronics whenever possible.
- If a device is not required during a certain time period, *turn it off*.

## Computer and Data Logging

The computer on most GAS payloads does not have to be very powerful in terms of processor speed and memory size. Typically the processor is used as an event sequencer and data logger. Although numerous 80x86 single board computers are available off-the-shelf, most are quite power hungry. There are numerous microcontroller

boards ( not based on the 80x86 architecture) available that use very little electrical energy and can be programmed using PC based tools. Microcontrollers are ideal for most GAS experiments.

On our first GAS payload, G-399, the students and staff built a custom 80C552 based microcontroller card. The major drawbacks to this approach were the long development time and the lack of a high-level language for programming. On our second GAS payload, G-178, we used an off the shelf 80x86 based single board computer. The major advantage of this approach was ease of programming using the 'C' language in a PC environment. The disadvantage of the single board computer was its high power consumption (>100 mA at 5 VDC).

Our current approach is to use an ultra low-power RISC microcontroller. The Microchip PIC<sup>TM</sup> consumes less than 1 mA at a clock speed of 4 Mhz (3). The PIC has between 12 and 20 general purpose I/O lines and it executes almost all of its 33 instructions in one clock cycle. By placing PICs in each instrument in the payload, and using an RS-485 bus in a simple network configuration, the wiring harness is cut to four wires daisy-chained between devices. This approach distributes the intelligence to the various devices in the payload and requires very little electrical power.

Another approach to saving energy is to power cycle the entire experiment. By using a real-time hardware clock with a time-out output, coupled to a solid-state power switching relay, the payload can be powered-up at appropriate time intervals. We have run a number of successful laboratory experiments on this approach. When using power cycling you must be careful to correctly program the time-out interval. A mistake in programming the clock can shut down the experiment for several years!

Recording experiment data is essential to most payloads. It is also useful to collect information on the operation of the experiment for later analysis. On our GAS payloads we collected primarily temperature data, but a number of other useful parameters such as valve status, current draw and battery pack voltage, can also be gathered. This data can be stored in battery backed SRAM, EEPROM, Flash memory or hard disk. On G-399 we used 8 kb of battery backed SRAM, but on G-178 the digital images required 50 kb each, so we flew a pair of laptop grade hard disks. The hard disks we flew could withstand a 100 G operating shock. The complete data set was recovered from both disks without error. Our next GAS payload will use Flash memory for data recording. Flash memory consumes less than 1 mA in stand-by mode and it can be power cycled.

## **STRUCTURE**

A number of different GAS structures have been designed and flown by a variety of educational users. Our advice is to use someone else's design and focus your attention on your experiment. Unless your requirements are very unique, it is easier to build a previously flown structure. We have designed and flown a standard 2.5 cubic foot GAS structure. The drawings and notes are available to all GAS users.



## WORKING WITH UNDERGRADUATES

Building Space Shuttle experiments can be a very effective learning experience for students who choose to participate in the process. GAS experiments require students to apply the knowledge acquired in physics, engineering and computer science. Students must analyze, design and manufacture the experiments. The following are a few guidelines for building GAS payloads with freshman and sophomore college students:

- Clearly define the objectives of the experiment you are building. What data do you hope to recover from the completed experiment?
- Divide the class into design teams for the various subsystems. Write a "contract" with each group so they know exactly what they are expected to produce during the quarter or semester. Limit the size of each group to four people.
- Design the group projects so the groups must interact with one another. This builds excellent communication and work skills.
- Have each team report its progress during weekly meetings.
- Have the students in each group grade one another's performance and use that grade as a portion of the students final grade.
- Have each team present formal midterm and final reports. The final report should include a demonstration of the product built by each team.
- Focus the teams on building the flight article. Most undergraduates do not understand the difference between analysis and design problems. Many students believe there is only one solution to a design problem-- theirs. Care must be taken to arrive at the best solution given the manufacturing environment available.

## CONCLUSION

Building GAS payloads with an experienced engineering team is a difficult task. Careful selection of batteries and use of low-power design techniques help to ensure mission success. Use of existing structures can dramatically reduce the work load.

Building GAS payloads with freshman and sophomore students is complicated by the need to help students to implement an appropriate solution to a given problem. The head of such a project must act as teacher, coach, mentor and cheerleader. The students who participate in a GAS project come away with deep knowledge of product design, analysis and manufacturing.

## References

1. Horowitz, P.; Hill, W.: The Art of Electronics, 2nd edition, Cambridge University Press, 1989.
2. \_\_\_\_\_: Manned Space Vehicle Battery Safety Handbook, NASA JSC-20793, 1985.
3. \_\_\_\_\_: Embedded Control Handbook 1994/1995, Microchip Technology Inc., 1994.

# Description of and Preliminary Tests Results for the Joint Damping Experiment (JDX)<sup>1</sup>

Jeffrey G. Bingham and Steven L. Folkman  
Utah State University

## ABSTRACT

An effort is currently underway to develop an experiment titled Joint Damping Experiment (JDX) to fly on the Space Shuttle as Get Away Special Payload G-726. This project is funded by NASA's IN-Space Technology Experiments Program and is scheduled to fly in July 1995 on STS-69. JDX will measure the influence of gravity on the structural damping of a three bay truss having clearance fit pinned joints. Structural damping is an important parameter in the dynamics of space structures. Future space structures will require more precise knowledge of structural damping than is currently available. The mission objectives are to develop a small-scale shuttle flight experiment that allows researchers to: 1) characterize the influence of gravity and joint gaps on structural damping and dynamic behavior of a small-scale truss model, and 2) evaluate the applicability of low-g aircraft test results for predicting on-orbit behavior. Completing the above objectives will allow a better understanding and/or prediction of structural damping occurring in a pin-jointed truss. Predicting damping in joints is quite difficult. One of the important variables influencing joint damping is gravity. Previous work has shown that gravity loads can influence damping in a pin-jointed truss structure. Flying this experiment as a GAS payload will allow testing in a micro-gravity environment. The on-orbit data (in micro-gravity) will be compared with ground test results. These data will be used to help develop improved models to predict damping due to pinned joints. Ground and low-g aircraft testing of this experiment has been completed. This paper describes the experiment and presents results of both ground and low-g aircraft tests which demonstrate that damping of the truss is dramatically influenced by gravity.

## INTRODUCTION

Utah State University is currently developing an experiment titled Joint Damping Experiment (JDX) to fly on the Space Shuttle as Get Away Special Payload G-726. This project is funded by NASA's IN-Space Technology Experiments Program and is scheduled to fly in late July 1995. The objectives of JDX include development of a small-scale shuttle flight experiment which allows researchers to characterize the influence of gravity and joint gaps on structural damping and dynamic behavior of a small-scale truss and application of nonlinear finite element modeling capability to simulate the measured behavior. This will allow a better understanding and/or prediction of the structural dynamics occurring in a pin-jointed truss.

## TRUSS DESIGN

A photograph of the JDX truss is given in Figure 1. The bottom of the truss is attached to a base plate which attaches to the GAS Experiment Mounting Plate (EMP) and thus provides a cantilevered boundary condition for that end of the truss. A rigid plate is attached to the top bay of the truss to provide a tip mass which lowers the natural frequencies. The excitation system can preferentially excite three modes in the truss; two bending modes and a torsional mode. The two bending modes are the two lowest frequency modes of the truss. These two bending modes are described as "bend 1" and "bend 2" modes. The lacing of the struts separates the two bending mode frequencies so each can be easily identified. The torsional mode consists of a rotational motion about the long axis of the truss. The small plates attached to the tip mass in Figure 1 are used by the excitation system. The damping and dynamic characteristics are observed by recording the free decay of the modes.

---

<sup>1</sup>This work was funded through NASA Langley Research Center (LaRC) under contract NAS1-19418. The support of Mark Lake at LaRC as technical monitor is gratefully acknowledged.

The strut and joint design for an “unlocked” joint is illustrated in Figure 2. The aluminum struts can be adjusted in length by turning the threaded strut tubes. The joints utilize press-fit hardened steel inserts to minimize joint wear. Hardened steel shoulder bolts are used for joint pins. The gap in the joints can be adjusted by using different diameter shoulder bolts. The JDX truss also uses “locked” joints which do not permit any deadband motion or rotations. The locked joint design is similar to Figure 2 except no inserts are used and the shoulder bolts are oversized such that they must be press fit into the joint. Additionally, shims are installed between the clevis and tang pieces and the shoulder bolt is tightened to apply a high preload across the joint interface. Impacting and macro-slip damping mechanisms are not present in the locked joints. By locking only a portion of the joints in the truss, a method of tailoring truss dynamics is obtained.

The initial tests of the JDX truss showed that with all the joints unlocked, the vibration modes were almost obscured with high frequency hash. The high frequency hash was caused by impacting of the numerous truss joint gaps. It was clearly shown that only a few unlocked joints in a truss would dramatically influence the dynamic behavior. The flight model configuration of the truss has only eight unlocked joints located at the top of the first bay as illustrated in Figure 3.

The nominal radial clearance between the pins and the strut inserts in the JDX flight mode truss design was

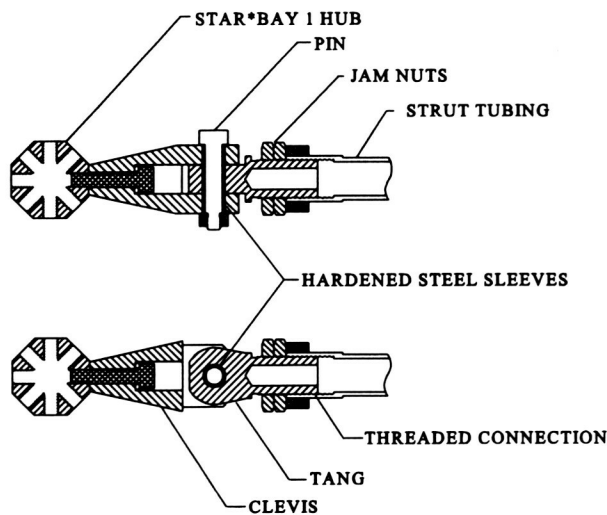


**Figure 2.** Illustration of the pinned joint design.

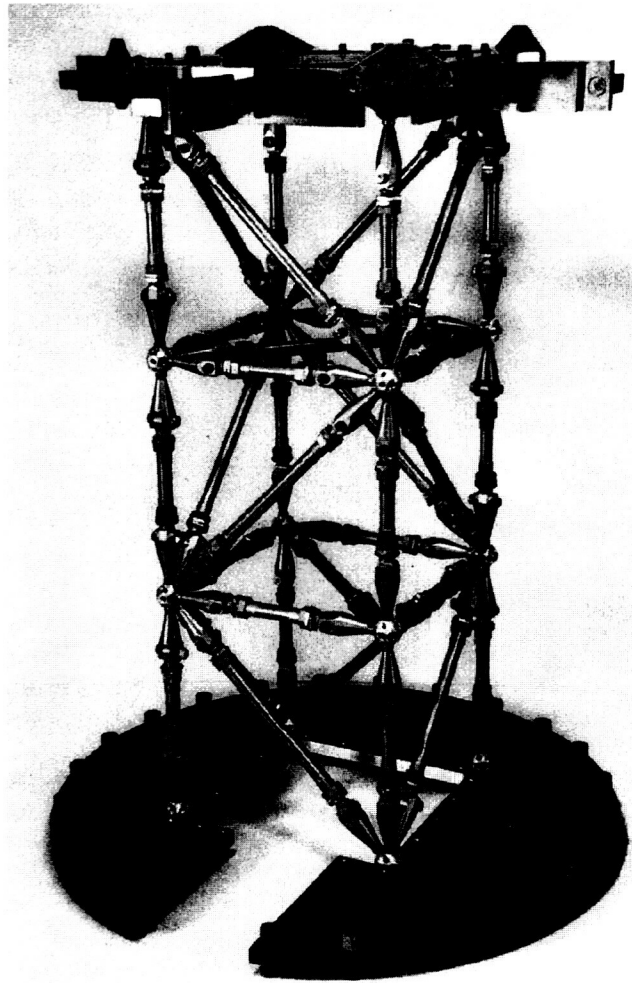


**Figure 1.** Photograph of the JDX truss.

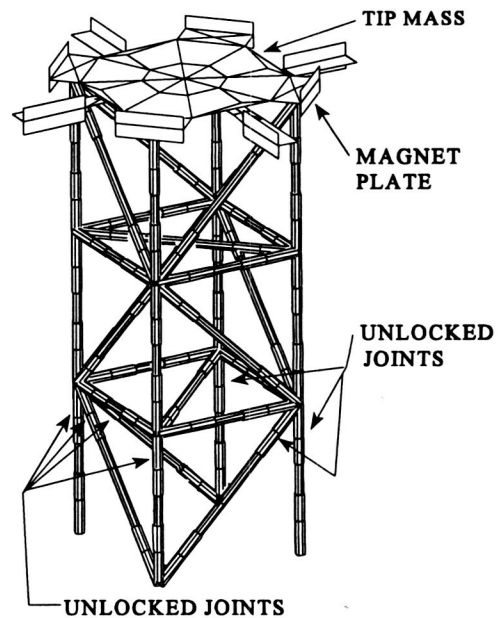


**Figure 3.** Location of unlocked joints.

0.0003 inch. This represents a very close fit for a 0.1875 inch pin. This is essentially the largest pin which could be freely inserted into the joint. Figure 4 illustrates quasi-static pull tests of a JDX strut which has a pinned joint on one end and a locked joint on the other. The hysteresis behavior of the strut with two different pin diameters are shown in Figure 4. The 0.00025 inch radial pin gap represents the class of fit used in the flight model truss. The quasi-static tests using the 0.00025 inch radial gap shows no clear display of deadband, but significant hysteresis due to friction. Imprecision in the assembly of the strut masks the deadband in these tests, as compared with the 0.00055 inch radial gap. Although the gap in the joint is small, the dynamic effects on the truss remain significant. The quasi-static tests in Figure 4 do not reflect the dynamic behavior. Ferney and Folkman<sup>1</sup> reported an initial series of force-state-map tests of the JDX struts which demonstrate that the joint gaps give rise to multiple rebounds during dynamic loading.

## EXPERIMENT DESCRIPTION

JDX consists of the three-bay truss shown in Figure 1 and associated hardware for truss excitation and measurement of oscillations. The experiment is located inside a 5 cubic foot GAS canister. Figure 5 is an illustration of the experiment which shows some of the major components which make up the experiment. Figure 5 is a sectional view such that some of the components "inside" the experiment are illustrated. Figure 6 is a photograph of the experiment.

Truss excitation system can preferentially excite two bending vibration modes and a torsional vibration mode. The excitation assembly consists of a framework which supports linear actuators, linkages, and electromagnets. Some of the framework is illustrated in Figure 5. The top plate and the vertical support posts are used to support most of the excitation hardware. A "box" placed inside the middle truss bay is also used to support linear actuators. This box is mounted to the battery box.

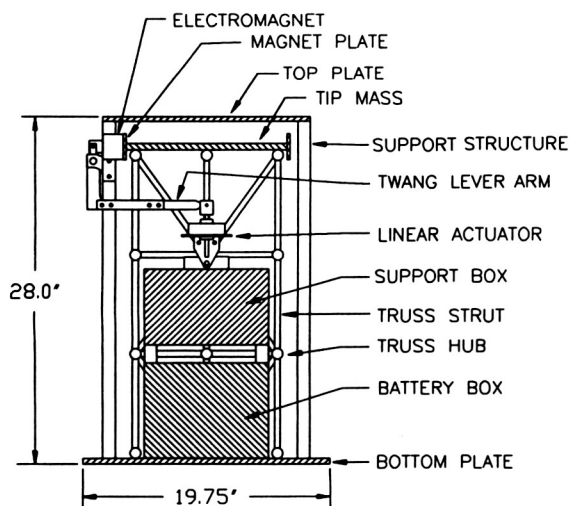


**Figure 5.** Illustration of major components of the JDX experiment.

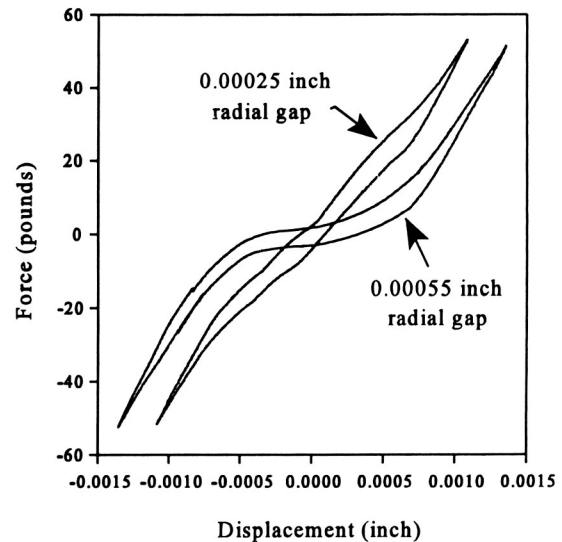


**Figure 4.** Hysteresis in quasi-static pull tests of a JDX strut.

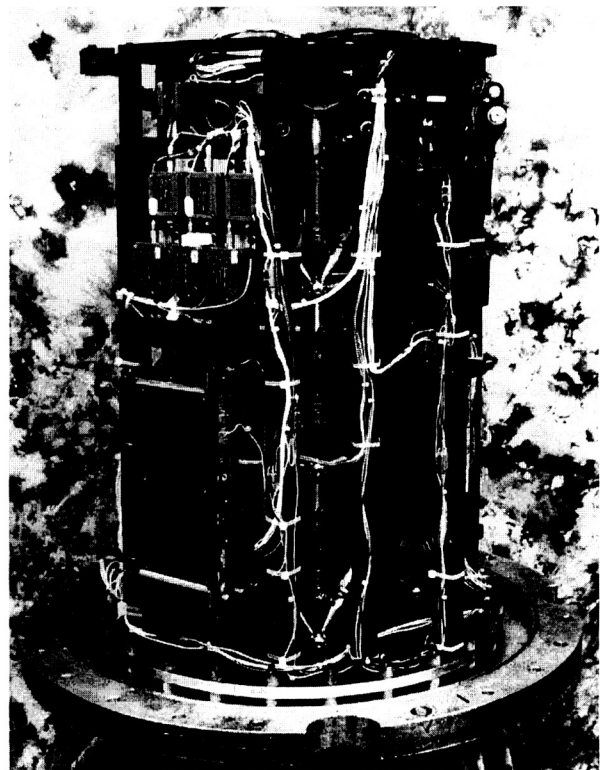


**Figure 6.** Illustration of the truss.

The linear actuator shown in Figure 5 is used to excite a "bending" mode. The actuator pushes on the lever arm which rotates about a pivot point. The lever arm is attached to the electromagnet. When the actuator pushes up on the lever arm, the electromagnet is displaced horizontally. The magnet is brought into contact with a plate attached to the tip mass and then power is applied to the magnet. Retracting the magnet will displace the truss in a shape resembling a bending mode. After displacing the truss, power to the electromagnet is removed which releases the tip mass and excites a vibration mode. This is described as a "twang" excitation method. The JDX experiment has other excitation system components similar to that shown in Figure 5 which will excite a bending mode in a direction perpendicular to the first and a torsional mode.

A mechanism for truss-tip support during launch and reentry is used to protect the truss from launch and reentry vibrations. The truss is locked by a one inch diameter stainless steel pin which can be inserted into a sleeve attached to the tip mass.

The controller/datalogger system controls the operation of the experiment by performing a set of preprogrammed instructions. These operations include the movement of linear actuators, energizing/de-energizing electromagnets, and measuring data. The experiment controller used is a Campbell Scientific CR10 Measurement and Control Module. This module has very low power consumption (0.7 mA quiescent) and can provide switching control and measurement operations. The CR10 when combined with Campbell Scientific SDM-CD16 Control Port Modules, can switch on and off the power for all the devices, including the five linear actuators and four magnets used in the experiment. The CR10 data acquisition rate is limited to about 1000 Hz. which is not adequate for recording the decays of the truss. For high speed data measurement, a Campbell Scientific CR9000 measurement module was utilized. The CR9000 has a measurement bandwidth of 100,000 samples per second with a resolution of 16 bits. The CR9000 contains 2 MBytes of EEPROM for program and data storage. The CR9000 has a high power consumption (0.5 A) and thus is only powered up during measurement operations. Accelerations of the tip mass are detected by the use of Kistler KBeam accelerometers, model 8302A10 with a 10 g full scale range. Three accelerometers are mounted to the tip mass to record the decay of the truss. Three additional accelerometers are attached to the base plate to monitor vibration or motion input to the experiment from the Space Shuttle. All the accelerometers are recorded at a rate of 3000 Hz. on each accelerometer channel.

Power for the experiment is provided by Gates sealed lead acid batteries. The batteries are contained in a sealed battery box that is vented using the standard GAS battery box vent system. Figure 5 shows that the battery box is located inside the first (or lowest) bay of the truss. The batteries consist of a combination of D and X cells which formed four, 12 volt battery packs.

## EXPERIMENT OPERATION

During the Shuttle flight, a baroswitch is attached to Relay A and will be activated at an altitude of 50,000 feet. The experiment controller will then be power up when the baroswitch closes. After a one hour time delay, the truss is unlocked. Then the controller then monitors its built-in clock, the GAS relay B, and the battery box temperature. It is desired to conduct the twang tests during a time period in which vehicle accelerations are minimized (an astronaut sleep period). The experiment is also limited in that if it gets too cold waiting for a sleep signal, it might not function properly. The experiment begins the twang test sequence when one of the three following events occur:

1. An astronaut low g signal has been received (closure of relay B at the beginning of a sleep period).
2. 18 hours has passed since the closure of the baroswitch.
3. The temperature of the experiment drops below a lower limit value.

When the controller determines it is time to start the experiment procedure, it will perform the following:

1. Move all electromagnets to their preset stop positions.
2. Perform approximately 10 twang tests for each mode shape.
3. Record experiment temperature during the tests.
4. Lock the truss by activating a linear actuator.

The experiment shall continue to monitor experiment temperatures during the flight. Prior to the end of a Shuttle mission, an astronaut shall set Relay A to latent. When Relay A becomes latent the controller will be powered

down.

## ORIENTATION FOR GROUND TESTING

Because gravity can influence the behavior of a pinned joint, ground tests of the JDX truss were conducted with the truss in two orientations with respect to the gravity vector. Figure 7 illustrates the  $0^\circ$  and  $90^\circ$  truss orientations. The  $0^\circ$  orientation minimizes the gravity preload in the struts. Although the preload in the truss is minimized in the  $0^\circ$  orientation, it is not zero since the joints must still support the weight of the truss. The  $90^\circ$  orientation provides the maximum gravity induced strut preloads. It is important that the truss was carefully assembled such the preloads due to imprecise strut lengths are virtually eliminated. That is, if gravity loads are removed, the deadband region is easily traversed. This turns out to be a difficult procedure in that the strut lengths must be set near the same level of accuracy as the joint pin gaps. In practice, this is difficult to obtain but can be closely approximated.

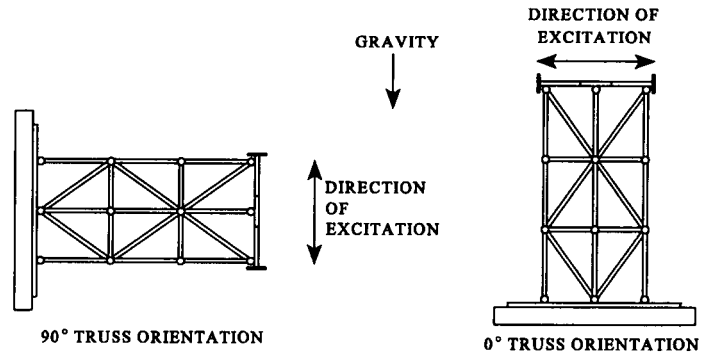


Figure 7. Illustration of  $0^\circ$  and  $90^\circ$  test orientations.

## TEST RESULTS

Ground tests of the flight model JDX tests are illustrated in Figures 8, 9, 10, and 11. These figures are plots of accelerations of the tip mass in the direction of the excitation. The free decay of the bend 1 mode with all joints locked is illustrated in Figure 8. Low damping and a typical exponential decay is observed. Figure 9 shows the initial decay over a 1 second time period. Because the JDX truss is displaced and released from rest, there is a small amount of higher mode content which quickly damps out. Figure 10 illustrates the decay of the bend 1 mode for a truss in the  $0^\circ$  orientation with eight unlocked joints. Note the rapid decay and the large amount of high frequency hash in the decay. Also the frequency is about 10% lower when compared with the truss with all locked joints. Figure 11 illustrates the decay of the bend 1 mode with the truss in the  $90^\circ$  orientation and with eight unlocked joints. Note that damping is decreased relative to the  $0^\circ$  orientation test but the damping is still much greater than that of a locked truss. Note how the initial decay is not symmetric about the equilibrium position. The accelerometers produce a DC output and since the accelerometer is oriented in the direction of the gravity vector, it reads approximately 1 g at equilibrium. An acceleration of 0 g's coincides with the position where the joints supporting the weight of the truss would traverse their deadband region. Clearly, when the highly loaded joints traverse the deadband region, the dynamics of the truss are greatly modified. The damping is reduced significantly when the amplitude of the peak accelerations drops below 1 g since the active joints remain under preload at all times. At small amplitudes, the damping approaches that of the truss with all joints locked. The bend 2 mode recorded similar behavior.

The results reported above are similar to those reported earlier for the JDX engineering model truss<sup>2</sup>. Damping of the truss can be inferred from the logarithmic decrement of the decay if we treat the truss as a single degree of freedom system and assuming energy is not transferred to other modes. Reference 2 reports the logarithmic decrement of the bend 1 mode for the locked,  $0^\circ$ , and  $90^\circ$  truss orientations as a function of acceleration amplitude. It was reported that:

- 1) damping rates can change by a factor of 2 to 5 as a result of simply changing the orientation of a truss;
- 2) the addition of a few unlocked joints to a truss structure can increase the damping by a factor as high as 40;
- 3) damping is amplitude dependent;
- 4) at low amplitudes the damping in the  $90^\circ$  orientation approaches that of the locked truss.

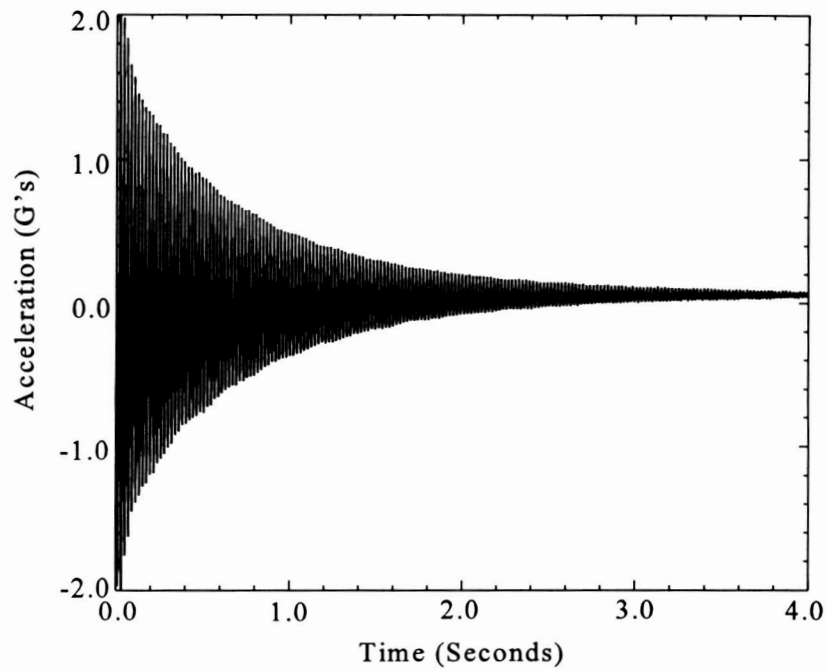


**Figure 8.** Decay of the bend 1 mode with the truss in a  $0^\circ$  orientation with all joints locked.

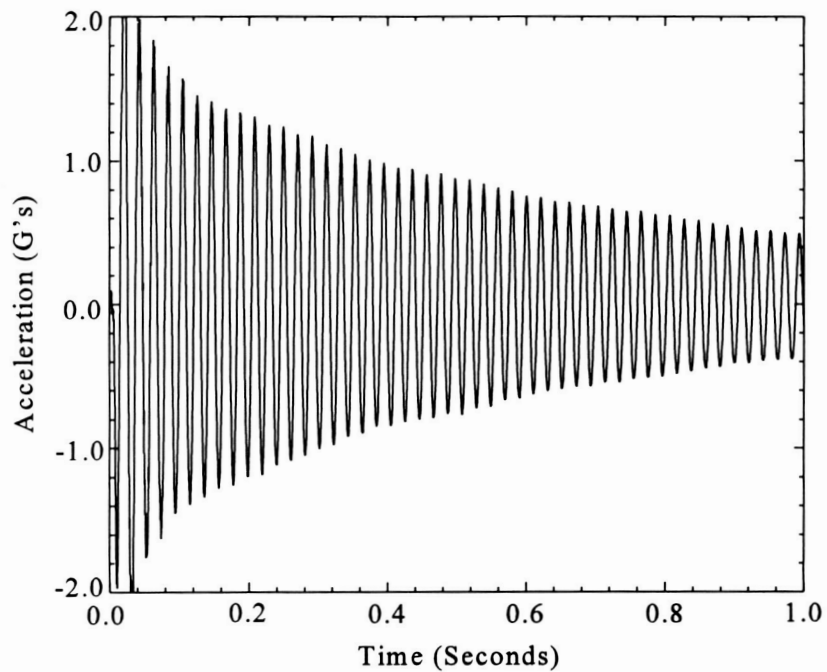


**Figure 9.** Initial decay of the bend 1 mode with the truss in a  $0^\circ$  orientation with all joints locked.

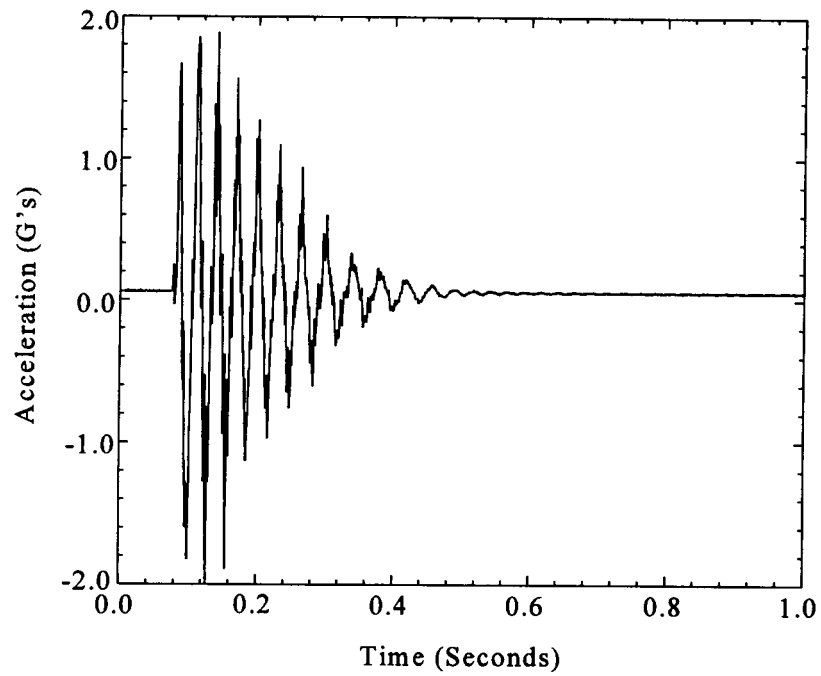


**Figure 10.** Decay of the bend 1 mode with the truss in a  $0^\circ$  orientation and 8 unlocked joints.

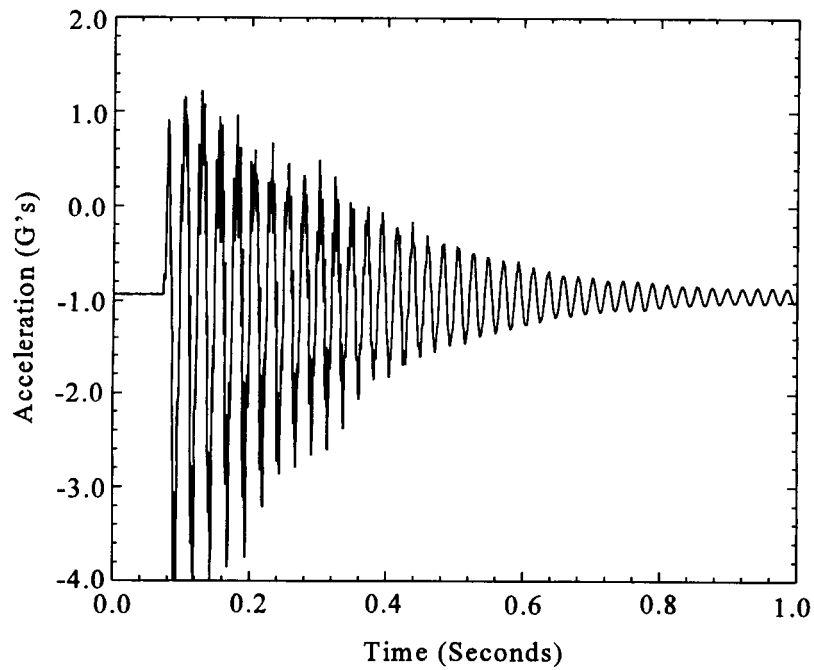


**Figure 11.** Decay of the bend 1 mode with the truss in a  $90^\circ$  orientation and 8 unlocked joints.



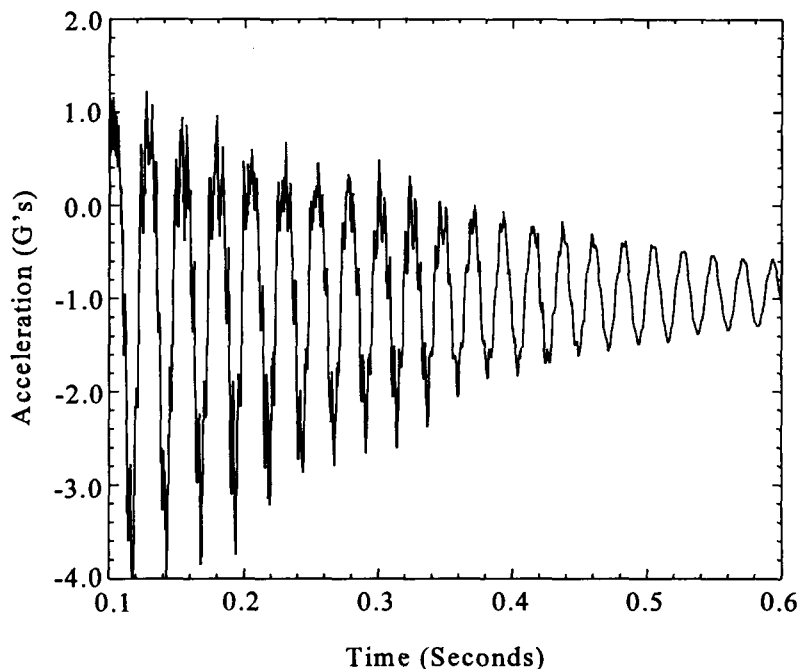


**Figure 12.** Initial decay of the truss in the 90° orientation with eight unlocked joints.

At low amplitudes, strut preloads may discourage a macroslip mode of friction damping as well as impacting. In this case, one would expect the damping to approach that of a locked joint. Although the damping becomes smaller at low amplitudes in the 0° truss orientation with unlocked joints, it is still significantly higher than the truss with locked joints.

The high frequency hash in Figures 10 and 11 is suspected to be caused by impacts occurring in the joints. This is more clearly shown in Figure 12 which shows the first 0.6 seconds of the decay in Figure 11 for the 90° truss orientation. Figure 12 shows that the occurrence of the high frequency hash corresponds to the traversal of the deadband region. After approximately 0.4 seconds, the highly loaded joints can no longer traverse the deadband region and the high frequency hash becomes greatly diminished.

Although the test results indicated that impacting is a significant source of damping in pinned joints, friction is also suspected to provide a significant source of energy dissipation. The joints which carry the majority of the load in the 90° orientation tests with unlocked joints should not be traversing the deadband zone after the amplitude drops below 1 g. Lightly loaded joints in the truss could still be traversing the deadband zone, but the magnitude of the impacts ought to be small. Thus, much of the damping from the 90° tests with unlocked joints is suspected to be predominately from a friction mechanism.

## LOW-G AIRCRAFT TESTS

Tests have been conducted with the JDX truss on NASA's KC-135 aircraft which can produce approximately 20 seconds of micro-gravity during its parabolic flight path. Tests were conducted with the experiment mounted to the aircraft and with it free floated in the aircraft. The aircraft floor is not very stiff and the vibrations transmitted to the experiment from the aircraft made tests with the experiment mount to the aircraft floor of little value. The free-float tests isolated the experiment from aircraft vibrations, but it is needed to approximately simulate the cantilever boundary condition of the truss at the base plate. This could be accomplished by attaching a large rigid mass to the base of the experiment. However, safety concerns limited free-float items to under 600 pounds. To that end, approximately 350 pounds of steel plates and framework were attached to the experiment base, and a canister simulating a GAS canister, bringing the total mass to about 550 pounds. This mass gives a reasonable approximation to a cantilevered boundary condition which allows comparison of free-float data with data from ground tests. Figure 13 is a photograph of a free-float test. Figure 14 illustrates the decay of the bend 1 mode

for the truss with eight unlocked joints in a free-float test. Comparing Figures 10 and 14 shows that damping is higher in microgravity than in 1-g with a  $0^\circ$  truss orientation. A close examination of Figure 10 shows that low amplitude vibrations continue until approximately 0.7 seconds. Figure 14 shows no observable accelerations after about 0.4 seconds. The low amplitude accelerations are very readily damped. In a  $0^\circ$  truss orientation test in 1-g, the truss has the lowest level of gravity induced preloads. These preloads prevent the traversal of the deadband region in the joints in 1-g tests. In the free-float tests, the struts have no preloads present even low amplitude oscillations traverse the deadband region of the joints. When the deadband region is traversed, damping is greatly increased.

### SHUTTLE FLIGHT STATUS

At the time this article was written, the experiment has been delivered to KSC for integration on the Space Shuttle Endeavor and is waiting for flight.

### CONCLUSIONS

An experiment to characterize the influence of gravity on damping of a truss using pinned joints has been constructed and delivered for flight testing on the Space Shuttle. The three bay truss is cantilevered from a mounting plate attached to the GAS EMP and has a tip mass attached to the free end to lower the resonant frequency. The damping of the truss is inferred from the measured free decay. The experiment contains a mechanism to excite two bending modes and a torsional mode.



Figure 13. Photograph of a free-float twang test.

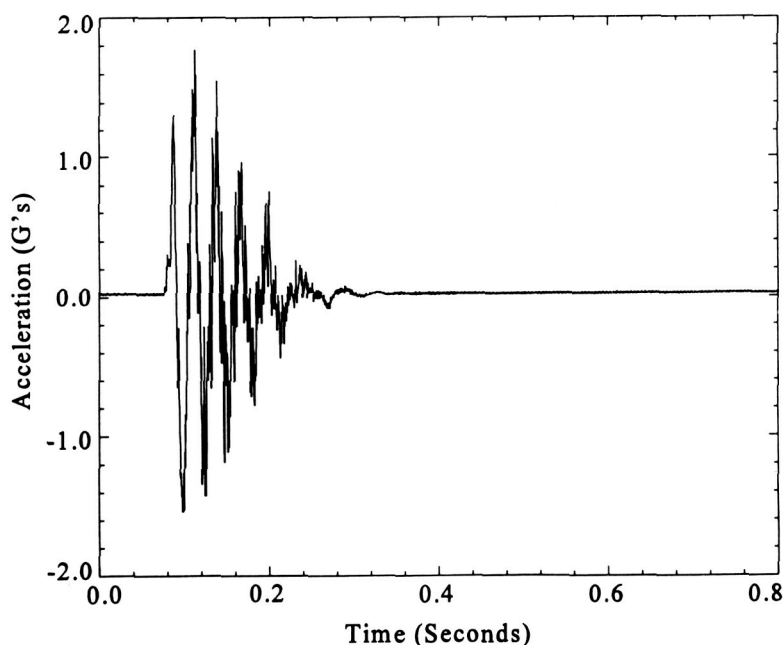


Figure 14. Decay of the bend 1 mode during a free-float tests with eight unlocked joints.

If a truss structure utilizes a pinned joints with clearance fit pins, the joints can become the primary source of damping in the structure. The resonant frequency and driving of higher modes are also significantly influenced. Measured data for a three bay truss containing eight pinned joints was presented. The measured data clearly shows that as gravity induced preloads are decreased, damping increases. Impacting is demonstrated by the observation of high frequency hash in the decay data. Driving of higher modes by impacting is suspected to be a significant source of damping. High preloads caused by gravity in the 90° truss orientation ground tests can prevent impacting in the joints carrying the majority of the loads (as long as the amplitude of the oscillations is smaller than 1 g). Damping in this time period should be dominated by friction losses. Measured data confirms that friction damping is a significant factor. Measurements during low-g aircraft tests show that damping is further increased as gravity loads are removed from the structure. The above conclusions assume the truss has been carefully assembled so that no preloads are induced during assembly so that as gravity loads are removed, strut preloads go to zero and joints can traverse their deadband zone.

## REFERENCES

1. B. D. Ferney and S. L. Folkman, "Results of Force-state Mapping Tests to Characterize Struts Using Pinned Joints," *Proceedings of the 36th AIAA/ASME/ASCE/AHS/ASC Structures, Structural Dynamics and Materials Conference*, April 1995, AIAA-95-1150.
2. S. L. Folkman, E. A. Rowsell and G. D. Ferney, "Gravity Effects on Damping of a Truss Using Pinned Joints," *Proceedings of the 35th AIAA Dynamics Specialists Conference*, April 1994, AIAA-94-1685.

# **The Growth of Solar Radiated Yeast**

**Tyrone Kraft**

**South Dakota School of Mines and Technology**

## ***Abstract***

This researcher plans to determine if solar radiation affects the growth of yeast. The irradiated yeast was obtained from a sample exposed in space during a Space Shuttle flight of September 9-20, 1994. Further, the control groups were held at: 1. Goddard Space Flight Center (GSFC) in Greenbelt, Maryland and 2. South Dakota School of Mines and Technology.

The procedure used was based on the fact that yeast is most often used in consumable baked goods. Therefore, the yeast was incorporated into a basic Betty Crocker bread recipe. Data was collected by placing measured amounts of dough into sample containers with fifteen minute growth in height measurements collected and recorded. This researcher assumed the viability of yeast to be relative to its ability to produce carbon dioxide gas and cause the dough to rise. As all ingredients and surroundings were equal, this researcher assumed the yeast will produce the only significant difference in data collected.

This researcher noted the approximate use date on all sample packages to be prior to arrival and experiment date. All dates equal, it was then assumed each would act in a similar manner of response. This assumption will allow for equally correct data collection.

## ***Introduction***

For the past 3 years I have been going to the Scientific Knowledge for Indian Learning and Leadership (SKILL) camp that is funded solely by NASA. It was the work of NASA that enabled me, and other students just like me, to send small payloads into space. It is to my knowledge that the Get Away Special (GAS) is the only small payload that has ever carried yeast.

## ***Purpose***

The purpose of this project was to find out whether or not solar radiation affects the growth of yeast in a bread dough mix.

## ***Hypothesis***

I believe that the yeast that was sent into space will have a reaction to the solar radiation, it will react in a way that it will not grow as rapidly or grow as much. The solar radiation affects things in ways that it harms it or even may mutate it in sense. In most cases, when living things are exposed to radiation they do not adapt to their own living environment, their growth rate is poor, and in some cases it even may die. This may also happen to the yeast when it is ready to make the dough rise.

## ***Procedure***

I obtained twelve packages of Red Star Quick Rise Yeast, four of which went into space, four that stayed at the GSFC as a control group and four that stayed at the South Dakota School of Mines and Technology, also as a control group. I then sent eight packages to NASA's GSFC. NASA kept four on the ground and sent four into space on the Space Shuttle Discovery, mission STS-64. The yeast was in flight for 11 days and was exposed at that time to the solar radiation.

After receiving the yeast back from space, I mixed up the two different batches of dough of the control yeast to find out whether or not keeping the yeast at different places would affect its growth. It did not affect the growth, so in my project I only used the yeast that was sent into space and the yeast that was kept by NASA. At that point I mixed up the two different batches of dough, the dough containing yeast that was in flight, and dough that contained yeast kept by NASA. After the dough was mixed, I weighed it into 4 ounce masses, 10 masses for each group. I then measured and recorded the growth of the yeast in all 20 beakers every fifteen minutes for two hours.

## **Results**

With the data collected in my results, I found that the yeast that was sent into flight grew less than my control yeast. The average growth differences among the 2 groups for every fifteen minutes were 0.5cm for the first fifteen minutes, 0.5cm, 0.2cm, 0.3cm, 0.3cm, 0.2cm, 0.3cm, and 0.4cm. The average final growth of the dough was 11.9cm for the flight yeast whereas it was 12.3 for the control yeast.

## **Conclusion**

I now conclude that flight yeast has a slight growth difference than the control yeast. The flight yeast did not grow as much or as fast as the control group did. So as you can see, the solar radiation had a slight affect on the growth of yeast in bread dough.

## **Flight**

The specimens were flown on Space Shuttle Discovery STS-64, from September 9-20, 1994. They were in a canister called the GAS. During this flight they were exposed to solar radiation. The yeast was also kept at a constant controlled pressure.

## **Material**

In my experiment I used 10,250 ml beakers a thermometer, that I read in Fahrenheit, a scale read in ounces, and a ruler read in centimeters. The yeast used was Red Star Quick Rise Yeast.

## **References**

1. *Principles of Micro Biology*, Alice Lorraine Smith, C V Mosby Co., St. Louis, MO 1981.
2. *The Microbial World*, Roger Y. Stanier, Michael Doudroff, Edward Adelberg, Prentice Hall, Inc., Englewood Cliffs, NJ 1970.
3. *Microbiology*, George Wistreich, Max Lechtman, Glencoe Publishing, Ecino, CA 1976.
4. *International Review of Cytology A Survey of Cell Biology*, Kwang Jeon, Jonathan Jarvick, Academic Press, San Diego, CA.

# **Non-gravitational Effects on Genus Penicillium**

**MacKenzie Loup  
Newell High School**

## ***Abstract***

In September 1994, Shuttle Orbiter Discovery, STS-64, launched into space. Aboard that shuttle was a payload containing Fungi spores, genus *Penicillium*.

With the over looking help of Dr. Audrey Gabel, Associate Professor of Biology at Black Hills State University, investigations on differing media types began. Basis for this experimentation was to determine if there was any differences between the space exposed spores and control spores. Studies concluded that there were differences and those differences were then recorded. It was hypothesized the spores may have been effected causing differences in growth rate, colony size, depth and margins, coloring, germination, and growth on different media.

## ***Introduction***

In 1928 Alexander Fleming discovered a strain of fungi that would eat away at the edges of bacteria. In 1929 it was given the name penicillin. This fungi would later be used to make thousands of vaccines for infectious diseases. Since Flemings' work in 1928 hundreds of different antibiotics have been discovered. Two well known scientists, Charles Thom and Thomas Raper, have continued studying strains of fungi. Their work in 1957 was the most recent studies since.

The present studies of space of exposed penicillin involve three various agars and a laboratory environment. The products of this experiment could be of great value to drug companies, people in the medical field, and animal husbandry.

The research studies involved three agars, potato dextrose, sodium acetate, and czapeks. Potato dextrose agar is a extremely starchy agar and most all penicillins grow very well on it. The sodium acetate agar is very acidic and few strains of the investigated fungi grow on it. The czapeks agar contains salt and growing capability depends on the strain of penicillin.

## ***Test Specimens***

The specimens used were obtained from Dr. Gabel on June 21, 1994. They were exposed to external atmospheric conditions for eleven days beginning on September 9, 1994 and ending on September 20, 1994. The fungi were placed in a GAS can and flown aboard the Shuttle Orbiter Discovery, STS-64. The flight environment is unknown.

## ***Test Environment***

All laboratory work was done at Black Hills State University. The inoculation, growing, and germination temperature for the media plates was room temperature. Observations were made daily and the data recorded.

## ***Final Results***

In January 1995, experimental processes began. I inoculated various media types prepared using standard agar recipes. I observed specimen under a compound microscope and recorded data for each part of the experiment. After about three weeks I recorded my final results. The colonies and

shape of two different groups varied as did the growth rate for the czapeks and the potato dextrose agars. The space exposed spores grew slower than the control group. Studies were made and recorded that the potato dextrose agar plates did not differ significantly. Studies also concluded that differences occurred among the czapeks medias. Control colonies for the czapeks grew faster showing brilliant coloration. Space specimens lagged behind control studies by approximately twelve hours.

Although not many differences were found in the plates of media, there were tremendous differences in the germination studies. The germination tubes on space exposed spore were narrow and longer while the control spores were shorter and thicker.

### **References**

1. Brock, Thomas D., *Biology of Microorganisms*, Edition two, 1974.
2. Chan, E.C.S., Noel Krieg, and Michael J. Pelczar, Jr., *Microbiology*, 1986.
3. Gabel, Dr. Audrey, Associate Professor of Biology at Black Hills State University, June 23, 1994 - March, 1995.
4. Jeon, Kwang W., *Intentional Review of Cytology: A Survey of Cell Biology*, Vol. 156, 1994.
5. Raper, Kenneth B., and Charles Thom, *A Manual of the Penicillia*, 1949.
6. Sakaguchi, Kin-Ichiro, *Atlas of Micro-organisms/The Penicillia*, 1957.

# THE EFFECTS OF SOLAR RADIATION ON PLANT GROWTH

Joslyn Agard  
Selfridge High School  
and  
SKILL/NASA Honors Program  
South Dakota School of Mines & Technology

## ABSTRACT

### Phase 1

#### Groups 1, 2, and 3

This phase of this continuing project was completed in April, 1994, using Dahlgren #855 hybrid sunflower seeds as **CONTROL** seeds. Data was recorded in a Data Log, and the results are included in this report.

### Phase 2

#### (a) Groups 1a, 2a, and 3a

Three groups (1a, 2a, 3a) of plants will be grown using Dahlgren #855 hybrid sunflower seeds as **TEST** seeds, which were exposed to solar radiation aboard Space Shuttle Discovery on Flight STS-60 in February, 1994. Data will be taken and recorded in a Data Log, and compared directly to data taken and recorded in Phase 1, and compared to the other data recorded in this experiment.

#### (b) Groups 4, 5, and 6

Three groups (4, 5, 6) of plants will be grown using Park Seed #0950 non-hybrid sunflower seeds as **CONTROL** seeds. Data will be taken and recorded in a Data Log, and compared directly to data taken and recorded in Phase 2 (c), and compared to the other data recorded in this experiment.

#### (c) Groups 4a, 5a, and 6a

Three groups (4a, 5a, 6a) of plants will be grown using Park Seed #0950 non-hybrid sunflower seeds as **TEST** seeds, which were exposed to solar radiation aboard Space Shuttle Discovery on Flight STS-64 in September, 1994. Data will be taken and recorded in a Data Log, and compared directly to data taken and recorded in Phase 2 (b), and compared to the other data recorded in this experiment.

### Phase 3

#### Groups 7a, 8a, and 9a

This phase will be undertaken, beginning in February 1996, to determine



the effects of solar radiation on second generation plant growth. Several radiated Park Seed #0950 seeds will be planted in the family garden this summer, and the seeds from producing plants will be used to make the determination, using the data recorded in this phase compared to the data recorded in the other phases of this experiment.

## INTRODUCTION

### Phase 1

Phase 1 of this project was completed in April, 1994, using Dahlgren #855 hybrid sunflower seeds as control seeds, Groups 1, 2, and 3. The Data Log and Written Report for Phase 1 are included as part of the current display.

### Phase 2

One-half of a one pound lot of Dahlgren #855 hybrid sunflower seeds were exposed to solar radiation aboard the Space Shuttle Discovery Flight STS-60 during the month of February, 1994.

One-half of a one pound lot of Park Seed #0950 non-hybrid sunflower seeds were exposed to solar radiation aboard the Space Shuttle Discovery Flight STS-64 during the month of September, 1994.

This phase of the project is performed using Dahlgren #855 hybrid sunflower seeds as test seeds, from the one-half lot which was exposed to solar radiation; Park Seed #0950 non-hybrid sunflower seeds as control seeds, from the one-half lot not exposed to solar radiation; and Park Seed #0950 non-hybrid sunflower seeds as test seeds, from the one-half lot which was exposed to solar radiation.

Dahlgren #855 was developed for rapid germination and growth, and high yield and oil content.

Park Seed #0950 sunflower seeds are *Helianthus* of the Large Flowered *Giganteus* genus.

The total time required for development of a sunflower plant and the time between the various stages of development depends on the genetic background of the plant and the growing environment.

Shortly after germination the plants enter the vegetative emergence stage, which is described as the stage after the seedlings have emerged and the first leaves are less than 4 cm long.

The various vegetative stages, or V(numbers), are determined by counting the number of true leaves, those leaves at least 4 cm in length, beginning with V1, V2, V3, V4, etc. Should the lower leaves wither and fall, the leaf scars are counted to determine the proper stage.

There are nine stages to the reproductive cycle beginning with R1, where the terminal bud forms a miniature floral head rather than a cluster of leaves. When viewed from directly above, the immature bracts form a

many-pointed star-like appearance. R2 is reached when the immature bud elongates 0.5 to 2.0 cm above the nearest leaf attached to the stem. Leaves that are attached directly to the back of the bud are to be disregarded. R3 is reached when the immature bud elongates more than 2.0 cm above the nearest bud. R4 is reached when the inflorescence begins to open, and ray flowers are visible. R5 is the beginning of flowering. The stage can be divided into substages dependent upon the percent of the head area that has completed or is in flowering. Example - R5.1 = (10%), R5.8 = (80%). R6 is reached when flowering is complete and the ray flowers are wilting. R7 is reached when the back of the head has started to turn a pale yellow color. R8 is reached when the back of the head is yellow but the bracts remain green. R9 is reached when the bracts become yellow and brown. this stage is regarded as physiological maturity.

### Hypothesis:

Through this experiment I expect to prove that there will be some significant adverse effects of solar radiation on seed germination, plant growth, or uniformity, or any combination of these.

## **THE EXPERIMENT**

### **Phase 1**

The procedures used in Phase 1 of this project are included in the Written Report for Groups 1, 2, and 3, which is a part of the current display.

### **Phase 2**

Groups 1a, 2a, and 3a: Dahlgren #855 hybrid sunflower seeds, as test seeds, with two seeds planted in a six inch planting pot for each group, with each group having a different soil type. Groups and plants will be identified as marked on their respective planting pots.

Groups 4, 5, and 6: Park Seed #0950 non-hybrid sunflower seeds as control seeds, with two seeds planted in a six inch planting pot for each group, with each group having a different soil type. Groups and plants will be identified as marked on their respective planting pots.

Groups 4a, 5a, and 6a: Park Seed #0950 non-hybrid sunflower seeds as test seeds, with two seeds planted in a six inch planting pot for each group, with each group having a different soil type. Groups and plants will be identified as marked on their respective planting pots.

Two seeds from each one-half lot will be placed in tissue and water to determine the germination time.

Tap water will be measured and added as needed.

Germination, vegetative stages, reproductive stages, and uniformity will be observed and recorded.

Measurements of height of each plant will be taken and recorded.

All data collected during this experiment will be compared.

Results and conclusions will be recorded.

All data collected and observations made will be kept in a Data Log, one for each group, according to the following schedule: Daily for the first twenty days; every second day beginning the twenty second day; every fourth day beginning the forty second day, until this phase of the experiment is completed.

## DISCUSSION

This portion of this report will be divided into two sections. The first section will discuss the results of the experiment, through the twenty sixth day. The second portion will discuss the conclusions based upon the results.

### Dahlgren #855 -- Germination

Group	Lot	Soil Type	Germination Time	** % Seeds	% Plants
1	Control	Potting	27 hours	100%	100%
2		Sandy			100%
3		Potting/Sandy			100%
1a	Test	Potting	68 hours	100%	100%
2a		Sandy			50%
3a		Potting/Sandy			100%

\*\* This column refers to the 2 seeds placed in tissue and water to determine germination time.

#### Rate

1. Control = 100%

2. Test = 87.5%

a. Seeds = 100%

b. Plants = 83.3% \*\*

\*\* Group 2a - Plant #2; seed did not germinate.

#### Time

Test seeds took 2.5 times longer to germinate than Control seeds.

Park Seed #0950 -- Germination

Group	Lot	Soil Type	Germination Time	** % Seeds	% Plants
4	Control	Potting	45 hours	100%	100%
5		Sandy			50%
6		Potting/Sandy			100%
4a	Test	Potting	45 hours	100%	100%
5a		Sandy			100%
6a		Potting/Sandy			100%

\*\* This column refers to the 2 seeds placed in tissue and water to determine germination time.

Rate

Control = 87.5%

a. Seeds = 100%

b. Plants = 83.3% \*\*

Test = 100%

\*\* Group 5 - Plant #2; seed did not germinate.

Time

Germination time was consistent between Control seeds and Test seeds.

Dahlgren #855 -- Growth

Group	Lot	Soil Type	Average Group Height	Vegetative Stage
1	Control	Potting	27.75 cm	V6
2		Sandy	24.50 cm	V3
3		Potting/Sandy	28.00 cm	V4
1a	Test	Potting	34.25 cm	V4 - V5
2a		Sandy	** 14.00 cm	V4
3a		Potting/Sandy	34.50 cm	V4

\*\* Group 2a - Plant #2; seed did not germinate.  
 Group 2a - Plant #1; growth rate very slow.

Average lot height

Control = 26.9 cm

Test = 27.6 cm

Vegetative stages

Fairly consistent between Control and Test plants with the exception of Group 2a - Plant #1 which did not reach true V1, V2 because the leaves for these two stages were thin and withered and never reached the required length of 4 cm.

**Park Seed #0950 -- Growth**

Group	Lot	Soil Type	Average Group Height	Vegetative Stage
4	Control	Potting	34.25 cm	V4 - V6
5		Sandy	** 34.00 cm	V4
6		Potting/Sandy	28.25 cm	V4
4a	Test	Potting	39.00 cm	V4 - V6
5a		Sandy	33.50 cm	V4
6a		Potting/Sandy	26.25 cm	V4

\*\* Group 5 - Plant #2; seed did not germinate.

Average plant height

Control = 32.2 cm

Test = 32.3 cm

Vegetative stages

Very consistent between Control plants and Test plants.

# **Dahlgren #855 -- Uniformity**

Group	Lot	Soil Type	Uniformity	
			Stems	Leaves
1	Control	Potting	Normal	* Abnormal
2		Sandy	Normal	* Abnormal
3		Potting/Sandy	Normal	* Abnormal
1a	Test	Potting	Normal	** Abnormal
2a		Sandy	Normal	*** Abnormal
3a		Potting/Sandy	Normal	**** Abnormal

\* The leaves on both plants in each group appeared to be abnormal at V1 and V2.

\*\* The leaves of this group appeared to be abnormal at V1 and V2.

\*\*\* The leaves on plant #1 appeared to be abnormal at V1 and V2.

\*\*\*\* The leaves in this group appeared to be abnormal at V1, V2, and V3.

**Abnormal** in appearance meaning that the leaves are very wide and have rounded and disfigured outer tips.

# **Park Seed #0950 -- Uniformity**

Group	Lot	Soil Type	Uniformity	
			Stems	Leaves
4	Control	Potting	* Abnormal	Normal
5		Sandy	Normal	Normal
6		Potting/Sandy	Normal	Normal
4a	Test	Potting	** Abnormal	Normal
5a		Sandy	Normal	Normal
6a		Potting/Sandy	Normal	Normal

\* Group 4 - Plant #1; stem is split from the soil level to the cotyledons.

\*\* Group 4a - Plant #1 and Plant #2; stems are split from the soil level to the cotyledons.

## Conclusions:

### Dahlgren #855

Germination rate -- Group 2a - Plant #2 not germinating could have been caused by the type of soil, or it could have been caused by solar radiation, or it could have been a natural germination failure.

Based upon the information and data available, I conclude that solar radiation did not cause this failure.

Germination time -- The difference in germination time between the Control seeds and Test seeds could be because the Test seeds were tested for germination a full year after the Control seeds were tested, or it could have been caused by solar radiation.

Based upon the information and data available, I conclude that solar radiation did not cause the longer germination time of the Test seeds.

Growth -- The slow rate of growth of Group 2a - Plant #2 could have been caused by the type of soil, or it could have been caused by solar radiation, or it could be a defect as a result of the hybrid cross.

The failure of Group 2a - Plant #1 to reach true V1, V2 could have been caused by the type of soil, or it could have been caused by solar radiation, or it could have been caused by a defect as a result of the hybrid cross.

Based upon the information and data available, I conclude that solar radiation has no significant adverse effects on plant growth.

Uniformity -- Since the leaves on the Control plants as well as the Test plants appeared to have abnormal leaf configuration, and the fact that this condition did not go beyond V3, it does not seem likely that this condition is significant.

Based upon the information and data available, I conclude that solar radiation has no significant effects on the uniformity of these plants.

### Park Seed #0950

Germination rate -- Group 5 - Plant #2 not germinating most likely was a natural germination failure.

Germination time -- Germination times were consistent.

Based upon the information and data available, I conclude that solar radiation had no significant adverse effects on the germination rate or germination time of these plants.

Growth -- The average growth rate and the vegetative stages reached were very consistent.

Based upon the information and data available, I conclude that solar radiation has no significant effect on the growth of these plants.

Uniformity -- The fact that stems of a Control plant as well as that of a Test plant were split would indicate that it may be a common occurrence with this type of plant.

Based upon the information and data available, I conclude that solar radiation has no significant effects on the uniformity of these plants.

## CONCLUSION

Based upon the results obtained through this experiment, and the conclusions reached based upon that data and other information available, I conclude that solar radiation has no significant adverse effects on seed germination, plant growth, or plant uniformity of either Dahlgren #855 hybrid sunflower seeds and plants or Park Seed #0950 non-hybrid sunflower seeds and plants, when the seeds used to determine germination time and grow Test plants are exposed to solar radiation.



## REFERENCES

Plant Science -- Growth, Development, and Utilization of Cultivated Plants. By: Hudson T. Hartmann, William J. Flocker, and Anton M. Kofranek.

An Introduction to Physical Science -- By: James T. Shipman, Jerry L. Adams, and Jerry D. Wilson.

Sunflower -- Production and Pest Management. North Dakota State University, Fargo, North Dakota.

Fundamentals of Plant Breeding and Genetics -- By: James R. Welsh.

Evolution of Crop Plants -- Edited by: N. W. Simmons.

Crop Production -- Principles and Practices. By: Stephen R. Chapman, and Lark P. Carter.

Mutations in Plant Breeding -- International Atomic Energy Agency, Vienna.

Mutations in Plant Breeding II -- International Atomic Energy Agency, Vienna.

Radiation -- Waves & Particles/Benefits & Risks. By: Laurence Pringle.

NOTE: Information was also obtained from Sioux County Extension Service, and Cenex/Land O'Lakes, Minot, ND.

## **Preliminary Results and Power Analysis of the UAH SEDS G503 GAS can**

**Lyle B. Jalbert, Steven Mustaikis II and Philip Nerren  
University of Alabama in Huntsville**

### **ABSTRACT**

The G-503 Get Away Special (GAS) Canister contained four experiments. A stainless steel corrosion experiment, an experiment to mix and cure concrete, a plant root growth chamber, and a group of 8 chambers to characterize diatom growth cycles in microgravity. As would be expected for this selection of experiments a significant amount of power was required to carry out these investigations over several days in a GAS environment. This was accomplished through the use of low power experiment control circuitry, heaters, and an estimated 3.6 kWh battery pack. The battery was designed around 120 standard Duracell Alkaline F cells. This pack weighed 29.5 kg (65 lbs) including a DC/DC converter and the power distribution bus for all of the experiments. Although not rechargeable, this configuration was a fraction of the cost of rechargeable systems and did not require venting to the outside of the can. Combining this with the long term storage performance, 85 percent of initial capacity after four years at 21°C (70°F), this guarantees sufficient power even with unexpected launch delays. This paper describes the experiments, their operation and initial results. Also, the performance of the power system during the STS-68 SRL2 mission will be addressed.

### **INTRODUCTION**

The G-503 payload was sponsored by the Students for the Exploration and Development of Space (SEDS) through the University of Alabama in Huntsville (UAH). The objective of the payload was to successfully complete the following experiments. Diatom growth and survivability in a cosmic radiation and microgravity environment, the mixing and curing of concrete, a study of microgravity influenced root growth, and a study of corrosive pitting in stainless steel. The first three were built by students at UAH while the last was done by students from the University of Alabama at Birmingham. Support for these experiments came from UAH, the Alabama Space Grant Consortium, Master Builders of Cleveland Ohio, and NASA Marshall Space Flight Center.

The Microgravity and Cosmic Radiation Effects on Diatoms (MCRED) was the first test of a concept for a bioregenerative life support system to be used on space station and Lunar/Mars expeditions. The experiment was designed to grow a series of diatom cultures in a controlled environment in low earth orbit.

The Concrete Cured In Microgravity (ConCIM) experiment was designed to give scientists and engineers valuable data about the characteristics of mixing and curing concrete in a microgravity environment. To gain accurate maximum strength of mixture data the concrete had to be cured for at least seven days in a microgravity environment. Once the experiment was recovered, the strength and chemistry of the space concrete was measured against the strength and chemistry of a ground based control sample.

The Root Growth In Space (RGIS) experiment was to study effects of microgravity on the early stages of germination of several seed types. The specific effects to have been examined included production of gases during germination and the development and distribution of chemicals and hormones affecting gravitropism.

The Microgravity Corrosion Experiment (COMET) was designed to examine the effects of microgravity on the initiation and growth of pitting in metals. Pitting is an extremely localized corrosion phenomenon which initiates on exposed surfaces and results in holes in the metal. Unlike many types of corrosion, pitting is difficult to predict. COMET induced pitting in a stainless steel sample in order to study it in the absence of gravity and determine what forces drive this type of corrosion. The experiment has applications on earth as well as in space for preventing pitting in corrosive material piping systems.

To make a complete study of the biological systems enough biomass had to be grown to allow for comparisons. This set the required time for operation of all environmental systems in the GAS can at 8 days. Three of the experiments

required positive thermal control and operating temperatures in the 21 to 25°C range. Hence activation of the payload was required as soon as possible so as to maintain the thermal environment of prelaunch for the experiments. This was achieved through the use of the baroswitch which turned on all experiment and thermal control circuitry at 18,300 m (60,000 feet). This also initiated a two hour timer which, at its completion provided main power to the experiments which started their nominal operations. In the event of a problem in the nominal operations a battery health monitoring circuit was provided which, at a set voltage initiated the proper shutdown of all experiments. These procedures allowed full control of all operations within the GAS can thus ensuring that the power pack would be at an optimal operating temperature at the start of the experiments.

## EXPERIMENT HARDWARE

G503 used an internal experiment support structure which consisted of a rectangular aluminum plate which divided the canister longitudinally. One end of this plate was bolted to the machined rib of a round plate which was bolted directly to the GAS standard experiment mounting plate.

The MCRED experiment (see figure 1) consisted of 8 acrylic growth chambers with dehydrated diatom cells in six chambers and aqueous algae cultures in the remaining two chambers. Each device was designed to function as a self contained, closed, environmental control chamber. At the onset of the experiment each chamber would be flooded with aqueous Guillard fresh water growth media with vitamins by 6 separate valves. A 1 Watt white fluorescent light source for photosynthesis was provided; 1 light for two chambers. The experiment had environmental sensors for monitoring the temperature, pressure, light intensity, and pH of each chamber. A heater operating at 25°C was mounted on the outside of all the chambers. The temperature was controlled by bimetallic switches located inside the experiment housing. An embedded electronic processor controlled the experiment. The processor began its preprogrammed timeline when it received main power. At that time, it was to flood each of the six growth chambers with nutrient solution. Once all chambers were flooded, the controller was to begin taking data from the 32 on-board sensors every 15 minutes. The lights would be on for 12 of every 24 hours allowing for light and dark phases of photosynthesis. Every 24 hours a chamber was to be flooded with 1.5 % glutaraldehyde in order to 'fix' the specimen. After two chambers were 'fixed' the light supporting those chambers was to be turned off to conserve power.

However, several problems occurred. First, a software problem caused the experiment lights to be turned on and remain in that position for the whole mission. Second, it has been determined post flight, that due to the one month launch delay the nutrient storage and delivery system had lost pressure. This loss of pressure was due to a leak in the nutrient interfaces to the valve assembly. The leak resulted in a pressure drop in the delivery system as well as loss of some fluid. Therefore there was not enough pressure to open an in line 13.79 kPa (2 psi) check valve. Third, there was a short in the sensor bundle which pulled all the data lines to ground resulting in a loss of data.

However some interesting results were found. These diatoms experienced some severe conditions. The aqueous cultures were loaded in the GAS experiment in June 1994. They sat in the sealed can (103.4 kPa (15 psi)), in the dark with no environment support except for external temperature control (20 °C) for 4 months. They were exposed to high g loads at lift off and then microgravity for several days at elevated temperatures in constant light and then freezing darkness. Upon landing in California they were in the dark at desert temperatures for 3 weeks. The cultures were finally collected and fresh water with growth media added. The cultures began to grow vigorously and continue to grow to this day. If these defined mixed cultures can survive all of this abuse, they can surely survive the conditions of space station and other similar systems.

The ConCIM experiment (see figure 2) was conducted inside a single mixing chamber (For a full description of the hardware see [1,2]). At launch the chamber was filled with a mortar mixture of 50/50 sand and Portland cement. A helical blade inside the chamber was driven by a motor/gearhead assembly after activation by the controller circuit. With the blade turning, a mixture of water and Polyheed (a water reducing admixture provided by Master Builders Inc. of Cleveland OH) was released into the chamber from an external nitrogen back-pressurized piston accumulator. To prevent pressurization when the water was injected the chamber was evacuated. At the end of the mix cycle an actuator was to release an internal false bottom in the chamber that was supposed to move up the chamber until an equilibrium position was reached at which point no free volume would remain within the mixing chamber. Since the curing of concrete is an exothermic reaction no insulation was required around the mixing chamber. However the water/admixture solution had to be kept from freezing thus a heater was

wrapped around the accumulator. The heater was controlled by bimetallic switches operating at a temperature of 15°C. A temperature monitor recorded the temperature of the concrete chamber via a thermocouple placed in the chamber.

The experiment had one failure; the false bottom did not release which resulted in some large voids in the unmixed portion and around the blade. The failure of the false bottom produced three different levels of hydration and a non mixed section. These samples are providing information on hydration products and mixing characteristics. Compressibility strength tests and petrographic analysis was performed on a central core sample. These measurements have revealed higher compressibility strengths and less entrained voids. Further results will be published as they become available.

The RGIS experiment (see figure 1) consisted of a single growth chamber in which seeds were placed prior to launch. Once in orbit a water/fertilizer solution was to be delivered to the seeds via a magnetically geared pump. The experiment required a temperature of  $25 \pm 5$  °C. This was accomplished by a sheet heater placed on the growth chamber. The whole experiment was insulated from the rest of the canister. At the end of the experiment a glutaraldehyde solution was to be used to stop further growth. Unfortunately due to some problems with the delivery system the seeds never received the water/nutrient solution and no growth was seen.

COMET (see figure 2) was conducted inside a 30.5 cm (12") acrylic tube that was 7.6 cm (3.0") in diameter. The tube was sectioned off into 3 separate chambers. At integration the chamber at the bottom of the tube contained the samples. The middle chamber contained a 6% ferric chloride solution designed to cause pitting on the stainless steel samples. The top chamber contained mineral oil to stop the pitting and preserve the pitting that occurred on-orbit. The experiment had a sheet heater coupled with bimetallic switches to maintain the temperature of the middle chamber at  $27 \pm 2$  °C. For insulation, a 0.64 cm (1/4") bat of Fiberfrax insulation was wrapped around the heater and the rest of the exposed acrylic chamber. When main power was received, the control circuit activated the motor/gearhead and retracted the sample from the lower chamber into the middle chamber where the pitting took place. At shutdown, the control logic once again started the motor/gearhead and the sample was pulled into the mineral oil chamber.

COMET worked as planned and produced pitting in the samples which showed some morphological differences. Typically a pit is a pinhole with subsurface degradation of the steel while the pits on the microgravity sample were spread more along the surface.

### **G503 BATTERY RESULTS**

The G503 payload had a Zinc-Manganese Dioxide battery pack. The pack contained 120 Duracell F-size batteries, configured for +29.6 VDC (after diode drop) and 120 Amp-Hours, yielding approximately 3.6 kilowatt hours. The battery pack consisted of 6 parallel strings of 20 cells in series to achieve the desired voltage and amperage. The cells were packed in an aluminum semicircular battery box on one side of the can (see figure 1). The base of the box contained spaces for the DC/DC converter and battery health monitoring circuit. A semicircular conduit located against the central plate provided access to the battery leads and DC/DC converter connections. Each cell of the pack was wrapped in a Kynar sheath to insure that the cells could not be shorted together. As well, all exposed battery surfaces and the battery box were coated with a conformal coating which was resistant to KOH. The series strings were separated by Pellon, an electrolyte absorbent material, in case of leakage. A combination of an acrylic sheet and Pellon was used between the battery layers and the battery box to electrically isolate the batteries from the battery box and also provide some insulation. With this choice of battery type it was possible to vent the battery to the inside of the GAS container. The complete battery and power distribution system (PDS) weighed approximately 29.5 kg (65 lbs). Similar rechargeable systems of the same mass have far less total power.

The G503 electrical subsystems comprised the PDS, thermal and experiment control circuitry and temperature recorders. The PDS had a 300 watt DC/DC converter powered by the experiment battery. Power was distributed through a 150 watt +5VDC power bus and a 150 watt +12VDC bus. There were 15 ampere fuses on both the positive and negative sides of the battery. The PDS was energized as planned at 60,000 feet by a baroswitch which set GCD A to HOT. At this time all heaters were energized to maintain a constant temperature in each experiment. The thermal control circuit consisted of bimetallic switches on both leads of the heaters. These switches provided a simple safe redundant system which required no external power. After a 2 hour onboard timer expired all experiments began their nominal operations. For mission success each experiment had its own micro controller. During the mission three temperature monitors recorded data, two on

experiments and one for the complete can. The monitors were +5VDC temperature loggers which stored there data in an EEPROM. The data were used to characterize the on-orbit thermal environment as seen by the experiments.

The battery provided experiment and thermal control power for 170.48 hours as calculated from the data of the temperature monitors(see figure 3). At that point the battery voltage had dropped to 17.2 volts which was pre-selected before launch as a cutoff voltage. This was set to insure that the batteries did not go below 16 volts which is the dead cell voltage for the packs. Below this value cell reversals can happen causing the reverse charging of single cells and there eventual explosion since F-cells do not have a vent to allow excess gases to escape. This occurrence was observed in ground tests when the packs reached 10 volts. Therefore at 17.2 volts the battery health circuit in the battery box sent an equivalent GCD C HOT signal to the three experiments which had procedures that needed to be carried out before shut down . 10 minutes after this signal the circuit disabled the DC/DC converter. From this point until the complete shut down of the G503 payload by the astronauts the battery only powered a single temperature monitor.

The power consumption data for the mission as calculated post flight are shown in table 1. The total power used was 3,543 watt hours. Almost exactly as expected from the battery data provided by Duracell. However the battery only lasted 170.48 hours. To understand why the battery did not last the required eight days let's examine what did and did not work on each experiment.

- The COMET experiment from UAB worked as planned with their heater cycling on and off throughout the mission (50% duty cycle)(see figure 3).

- The ConCIM experiment also worked as planned. However as evident from the temperature profiles(see figure 3) the large heater located on the outside of the accumulator which was set to turn on at 15°C cycled on and off for most of the mission (50% duty cycle assumed) maintaining the overall temperature of the can just below 15°C until the it was shut off when the health circuit disabled the DC/DC converter.

- The RGIS experiment did not work properly. The temperature monitor became disconnected and thus no temperature flight data was recorded. We have assumed a 50% duty cycle on the heater for calculation of total used power.

- The MCRED experiment also failed to operate correctly. An error in the program caused the onboard controller to lock up after 12 hours. At this point all 4 lights were on in this experiment. From ground tests before flight the amount of heat the lights produced was more than sufficient to keep the heater from turning on.

Hence with the lights staying on in MCRED this experiment drew more power than originally calculated. The battery health monitoring circuit performed correctly sending the shutdown signal to the experiments and allowing all experiments to be properly turned off. These results give us confidence that, had all experiments worked as originally programmed, the battery would have provided power for eight or more days.

## Summary

The G503 GAS can was a success. Two out of the four experiments worked well and are providing good data for analysis. A large disposable battery pack was built and flown which provided sufficient power and long life at a fraction of the cost of rechargeable systems. A compartmentalized approach for control of all experiments insured that a single failure would not destroy all of the science. The single battery pack provided an easy way to distribute power to all experiments while insuring sufficient power for proper sequencing of the experiments. All of the people involved in this payload were new to the process of flying shuttle payloads and have learned a great deal from this very enjoyable experience.

## References

- [1] Mark A. Bury et. al, *Concrete and Mortar Research Aboard the NASA Space Shuttle*, **Concrete International** September 1994, pp. 42-46.
- [2] Mark A. Bury, Lyle Jalbert and Steven Mustaikis II, *Taking Concrete to the Outer Limits*, **Concrete Construction** July 1995, to be published

Experiment	Volts	Amps	Watts	Hours Operated	Total Watt-Hours
<b>Experiment #1 (MCRED)</b>					
Lights (VAC)(4)	270.00	0.005	1.35	673.92	909.79
Inverter(2)	5.00	0.054	0.27	336.96	90.98
Controller	5.00	0.060	0.30	168.48	50.54
	12.00	0.013	0.16	168.48	26.28
	-12.00	0.004	0.05	168.48	8.09
Valves(16)	12.00	1.333	16.00	0.00	0.00
Heater	5.00	1.000	5.00	0.00	0.00
Signal Cond	12.00	0.333	2.00	168.48	336.96
Sensors	12.00	0.083	0.50	168.48	84.24
<b>Total MCRED</b>					<b>1,506.89</b>
<b>Experiment #2 (CONCIM)</b>					
Motor	12.00	6.700	80.40	0.17	13.40
Solenoid Valve	12.00	1.000	12.00	0.033	0.40
Actuator	12.00	0.146	1.75	0.017	0.03
Heater	12.00	0.500	6.00	85.24	511.44
Temp. Monitor	5.00	0.001	0.01	168.48	0.84
<b>Total CONCIM</b>					<b>526.11</b>
<b>Experiment #4 (RGIS)</b>					
Pumps(2)	12.00	0.170	2.04	0.20	0.41
Heater	5.00	1.000	5.00	85.24	426.20
Temp. Monitor	5.00	0.001	0.01	0.00	0.00
<b>Total RGIS</b>					<b>426.61</b>
<b>Experiment #5 (COMET)</b>					
Motor	12.00	0.083	1.00	0.020	0.02
Heater	5.00	1.000	5.00	85.24	426.20
Temp. Monitor	5.00	0.001	0.01	168.48	0.84
<b>Total COMET</b>					<b>427.06</b>
<b>System Interface</b>					
Interface Logic	5.00	0.050	0.25	257.44	64.36
Temp. Monitor	5.00	0.001	0.01	257.44	1.29
<b>Total</b>					<b>65.65</b>
<b>Total Experiment Power</b>					<b>2,952.31</b>
<b>DC/DC Converter Overhead</b>					<b>590.46</b>
<b>Total Power Required</b>					<b>3,542.78</b>

Table 1. G503 power usage during the STS-68 mission. Total power is calculated from assumptions based on temperature monitor data and post flight analysis of each experiment. The DC/DC converter is 80% efficient (calculated from preflight ground tests). Power lost to battery internal resistance and diode drop has been ignored for these calculations

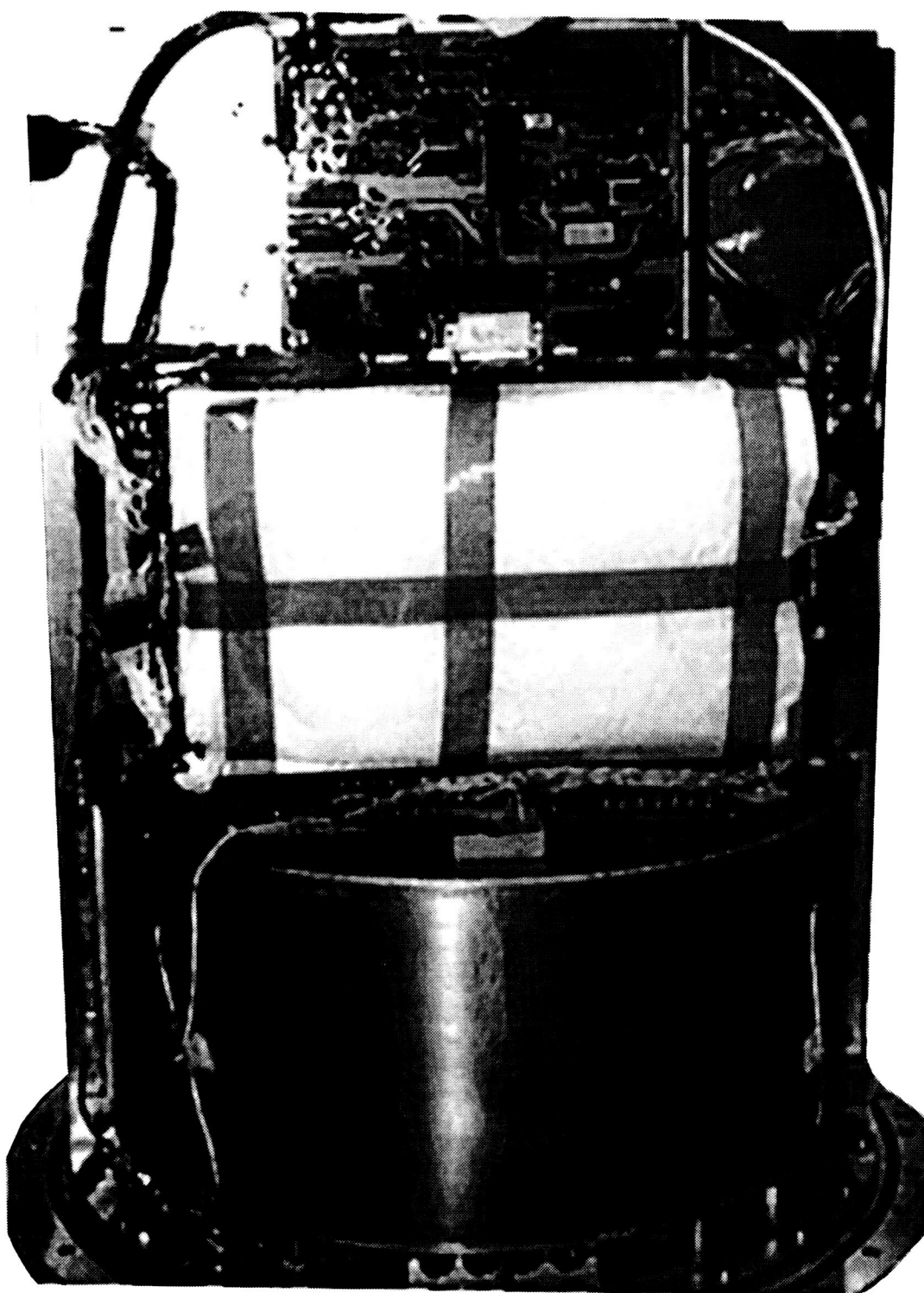


Figure 1. From Top to Bottom - the RGIS experiment with the MCRED electronics covering it, MCRED experiment chambers and plumbing (behind absorbent material), and then the battery pack with the power bus on top of it and the DC/DC converter underneath. The thermocouple for the can temperature monitor was placed at the top of the battery pack against the central plate.

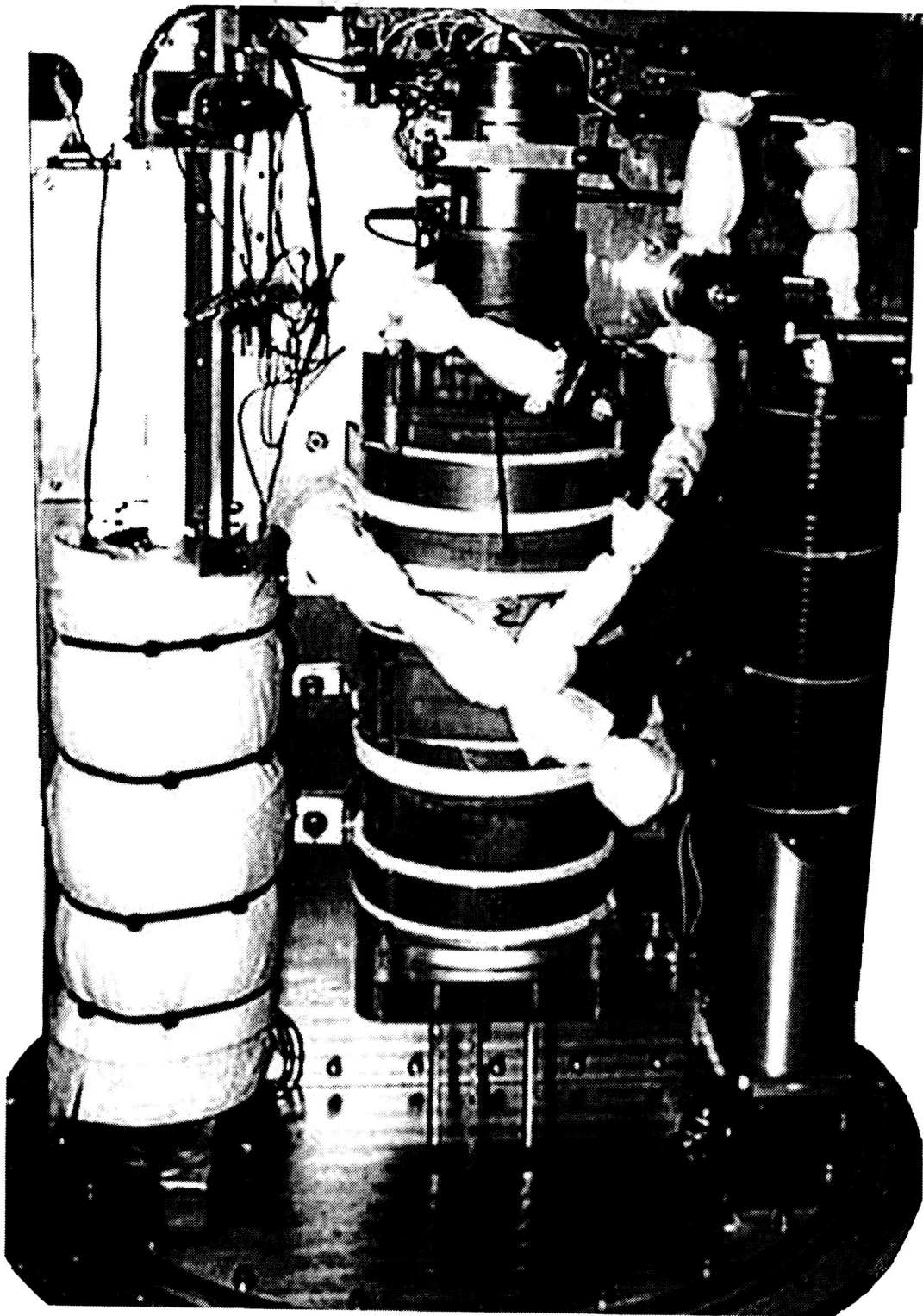


Figure 2. The other side of G503 had the COMET experiment on the far left, the ConCIM mixing chamber and motor in the center, and the accumulator with the heater (set to turn on at 15°C) wrapped around it on the far right. The thermocouple for COMET was placed in its central chamber (hidden by insulation) while ConCIM's thermocouple port is just visible above the "2" on the mixing chamber.



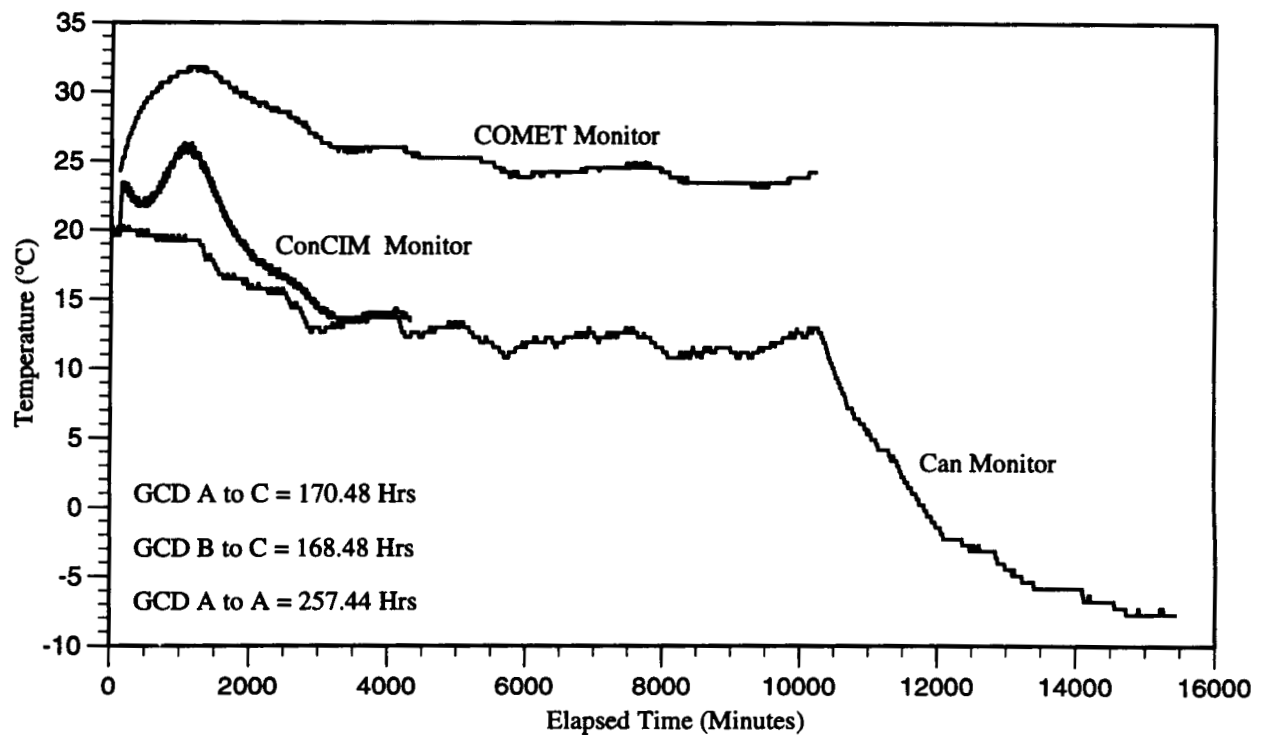


Figure 3. Temperature data from the 3 monitors in the can - The total time the experiments were powered is calculated from this data. The COMET monitor was on from GCD B to HOT, end of the two hour timer, until GCD C to HOT, when the battery health monitoring circuit shutdown disabled the DC/DC converter. The ConCIM monitor was on from GCD A to HOT and thereafter for 72 hours. The can monitor was on from GCD A to HOT (baroswitch) until GCD A to LATENT (astronauts).

## **G254: USU Student Payload Flown on STS-64 in September, 1994**

Tumkur Raghuram (Payload Manager),  
Oscar A. Monje, Brett Evans, Matt Droter, Mark Lemon, Kristen Redd, Tina Hubble, Mark Wilkinson,  
Michael Wilkinson, Dan Tebbs, and Casey Hatch

Student Experimenters, USU GAS Program,  
Department of Physics, Utah State University  
Logan, UT 84322-4415

Brandon Lobb, Kent Altsuler

ex-students of Kinkaid School,  
Houston, Texas

R. Gilbert Moore\* Jan J. Sojka

Faculty Advisors, USU GAS Program  
Department of Physics, Utah State University  
Logan, UT 84322-4415

Prent Klag

Director, Edith Bowen Lab School,  
Logan, UT

### **ABSTRACT**

G254 is the culmination of USU Get Away Special (GAS) students' efforts to get back into space. After a hiatus of a decade, the USU GAS program flew its sixth canister on STS-64 in September 1994. Like its predecessor payloads, this one contained a diverse set of experiments, six in all. Each experiment has its own lessons learned, which hopefully can be passed on to the next generation of GAS students. This presentation will give a balanced view of the successes and failures of G254. Emphasis will be placed on describing the stumbling blocks and the many lessons learned that come from experience rather than academic training. G254 has once again taken a team of about fifteen USU students, plus about one hundred fourth and fifth graders, and given them an immeasurable education.

---

\* Now at US Air Force Academy, Colorado Springs, Colorado.

## **INTRODUCTION**

The Get Away Special (GAS) program is an academic program at Utah State University (USU) which enables students and other educational organizations to participate by designing their own engineering and microgravity science experiments. Five of the experiments on this payload utilized the "spacepak" concept similar to G-008, G-004, and G-518. The sixth used the new "Isospacepak" concept. The external shape and dimensions of each experiment was standardized and each experiment was independently controlled (ref. 1).

The USU GAS program is heavily biased towards developing student skills associated with conducting individual experiments. Currently, the safety review has been completed for our next GAS payload, G200. G200 is a back-up GAS payload on STS-76 due to be launched in March 1996 and primary GAS payload on STS-77 in April 1996.

To start with, we will briefly talk about the experiments on G254 and later talk about the problems faced and the lessons learned on each of them.

## **BRIEF SUMMARY OF EXPERIMENTS**

A detailed description of the G254 experiments were presented at the 1992 Shuttle Small Payloads Symposium (ref. 1). The fully assembled structure is shown in figure 1.

### **Experiment 1: Distillation Experiment**

This experiment was proposed by the students of Kinkaid School in Texas. After working on the experiment for some time, Kinkaid School turned over the reservation to USU with USU completing their experiment in return for the rest of the space in the canister. The objective of this experiment was to distill a mixture of two fluids in microgravity using a temperature differential. The fluids used were trichloro-trifluoroethane and carbon tetrachloride. These fluids were contained in two different aluminum chambers with a solenoid valve in between. The chamber containing the mixture of the two fluids was heated to a temperature in between the boiling points of the two fluids. During the heating operation the solenoid valve was kept open. Since distillation is a gravity dependent process, it was an interesting way to see how the system would behave in microgravity conditions. A cut-out of the experiment is shown in figure 2.

### **Experiment 2: Float Zone Instability Experiment (FZIE)**

This is an experiment which aimed to investigate convective instabilities in float zone geometries. The primary goal of the experiment is to verify the Plateau Instability Limit, which states that in zero gravity a fluid cylinder is unstable when the ratio of length  $L$  to radius  $R$  exceeds  $2\pi$ . Three independent liquid wax bridges with varying lengths and radii were held between copper supports and the wax is melted by heating one of the copper supports by means of a heater. The liquid wax would be allowed to resolidify under "non-quiescent" conditions to qualitatively measure the background g-levels by looking at the common distortions in the resolidified float zones. A cut-out of the experiment is shown in figure 3.

### **Experiment 3: Pachamama**

The idea for this experiment was conceived by one of our students, who is from Bolivia and Pachamama means 'Mother Earth' in Bolivian.

The objective of this experiment was to study the effects of microgravity on the photosynthetic ability of a plant lichen with the help of chlorophyll fluorescence measurements. Due to the inherent harsh environment of the GAS can, the lichen was chosen for the experiment. A lichen can stay dormant for a period of time and then be rejuvenated with the help of water and light. The temperature in the sample chamber could be varied using heaters. Once the lichen is sufficiently rehydrated, data acquisition is done through a pair of photometric sensors. Measurements were made at five different temperatures in order to characterize the temperature response of the organism. A cut-out of the experiment is shown in figure 4.

### **Experiment 4: Bubble Interferometer Experiment**

The objectives of this experiment were to: (i) observe the formation of bubbles in a microgravity environment, (ii) look for interference bands due to bubble wall thickness gradients, and (iii) observe surface tension induced motions on the bubble surface.

Bubbles were formed using a mixture of diffusion pump oil and a surfactant. The bubble blowing sequences were recorded on an 8 mm movie camera and the temperature data was stored in an EPROM. The bubbles were blown with the help of two linear actuators and an air pump. A fluorescent lamp with a monochromatic filter served as the source for the interferometer. A small incandescent lamp was used to heat the bubble surface. The heating is not uniform and causes a gradient in the surface tension. This induced surface tension gradient will cause movement of the material on the bubble surface. A cut-out of the experiment is shown in figure 5.

### **Experiment 5 and 6: Elementary School Experiments**

One of the spacepaks contained popcorn kernels and radish seeds, in addition to the regular experiment. An experiment with these were conducted by the Edith Bowen Elementary School. After being flown in space, students popped the popcorn and tasted it. Similarly, the radishes will be grown and sampled. The scientific purpose of this experiment was to foster interest in the space sciences amongst the younger generation.

### **CHALLENGES ENROUTE**

Some of the errors we committed on this payload would seem very trivial and silly to the professional organizations that fly GAS payloads. But these are probably common to an amateur student group with the whole show being run by students. These are the results of inexperience and the education derived from them has proved to be invaluable to the concerned students.

Two years after work started on this payload, things came to a stand-still with the Challenger disaster. In the ensuing two years, it took a lot of ingenuity on the part of the concerned faculty to keep the program alive at USU. By the time the GAS queue was reopened, most of the original students had

graduated and new students had come in their places. The tendency of every new student is to redesign things that have been in existence up to that point. As a result, no progress was made for a long time. In addition, no one had a clear picture of the exact paper-work involved with NASA and the new safety regulations that were in place. The general morale was so low and none of the students had any idea about when their experiments would fly or what direction to proceed on the experiments. This was mostly the story till 1992 and was probably the biggest challenge that the program faced.

The item of priority was to pick up the paper work with NASA. A revised Payload Accommodations Requirements (PAR) was sent to NASA. Work was then started on the Safety Review. The Preliminary Safety took a long time to be put together due to lack of experience. With the wrong notion that this had to be the most comprehensive document, a lot of time was lost in pursuing unimportant issues. After all this effort, the first comment during the telecon with NASA was that we had the wrong format for our safety package. It was a pre-Challenger format!

The Final Safety was sent in with the proper format. But at this stage we learnt a few new things about our payload. The entire design for the payload was pre-Challenger. So we had different sets of batteries scattered all through the payload. NASA wanted us to either group all the batteries in one place or to build a box around each set of batteries. The second option was impossible since there was hardly any room in the spacepaks to accommodate separate battery boxes. The boxes had to be liquid-tight only and not air-tight. In order to satisfy NASA's requirement, we had to remove one of the proposed experiments in order to make room for batteries. In spite of accommodating 67 cells in this spacepak, 30 more cells had to be placed in half of another spacepak. Power was not allocated in a very efficient manner too. There was a lot of power available but the payload could have performed equally well with lesser batteries.

The original design of the payload included a USU GAS switch, which after receiving power from the NASA relays did the switching internal to the payload. But NASA requires that their relays be in direct control of the payload power. This opened up a new problem. The payload had 18 different power supplies and each of them was being turned on at different times. The only relays available to us were the three NASA relays A, B and C. Relays B and C do not handle more than 2 A of current. This necessitated 3 6-pole relays, which would provide us with a total of 18 different switches. With redundancy in mind, 2 sets of 3 relays were included.

With the introduction of two sets of batteries and a set of our own relays, more complications began to creep in. The relays and the half-pak of batteries were at the bottom of the payload. The other spacepak of batteries was located in the middle of the payload. The NASA control lines came into our own relays whose power was coming from the other pak. These relays in turn, switched power from the other pak to the different experiments. In short, this needed a very sophisticated wire harness running across the length of the payload.

Being conservative is useful when dealing with a lot of issues with NASA. But students often tend to get carried away in their quest to be conservative. The following is a prime example. On several circuits in the payload, the current being handled required the use of 12 gauge teflon wire. Students decided to use 10 gauge wire just to be on the safe side. After having committed to 10 gauge wire in the SDP, we were shocked to see what 10 gauge wire really meant. The wire thickness is very large and the wire itself is highly inflexible. Soldering the wire on to the pins of a D-connector turned out to be a

nightmare. Soldering a combination of 10 gauge and 16 gauge wire to the set of 6 USU relays was only worse.

A vibration testing of the payload was planned 2 months prior to the shipment date. The shaker table needed repairs and it was finally fixed only 10 days before the payload shipment date. With such a short time to ship, we could either test the payload and break it or ship it without testing and run the risk of it coming loose during launch. We chose the former option. Since the shaker table was operating at less than normal power, we could only test individual paks at a time and not the entire payload. The first payload we tested had been completed well in advance. It was a high precision mechanical truss and the objective of the experiment was to examine the vibration dampening characteristics of the truss-joints. The mounting plate was not bolted to the shaker table perfectly. During the test there were a couple of bad shocks. Upon inspection of the payload after the test, the locking mechanism had come loose and hence the truss had got bent out of shape. Since it was a high-precision mechanical truss, the bending ruled the experiment out of the flight. There was quiet feeling of gloom in the USU GAS lab after this.

The week before the shipping of the payload turned out to be hectic and chaotic. Some students had completed their experiments and were busy testing the different subsystems. But some students were still working on finishing up their experiments. Some were coding the final flight software into their controllers. When the time came for the payload to be put into the shipping container, there was no relief yet for the already exhausted students. The payload and the bumper system refused to fit snugly into the shipping container. Students battled hard trying to shave off material in the hope of getting a good fit. Tired as they were, no one was thinking. Only frustrations set in. Help from a professional machinist was summoned. The problem was fixed and the payload was shipped off to KSC. G254 had left USU on way to space finally after 10 years.

The travails for the USU GAS team were not over yet. They continued to the end till integration. On day 3 of integration, it was discovered the lid of the battery box in spacepak 1 was a little too tall and the pak would not fit into the canister. With the help of the GAS Integration team, this problem was solved and the last and most embarrassing of all mistakes was discovered. We found that instead of leaving the NASA connectors on the payload hanging, we had fixed them to the bottom of the payload. This was not a very serious problem, since NASA offered to give us another set of cables and connectors which would extend the length to reach the interface plate. We discovered to our utter shame we had the wrong connector on our end. So NASA had to cut two different connectors and Big Tom from the GAS Integration team spliced the two cables together with a cheerful smile on his face. The GAS Integration team saved the day for us with their professionalism. It was 11 PM when we left the GAS Facility in KSC after setting up the leak-test on our canister.

## **POST-FLIGHT RESULTS AND LESSONS LEARNED FROM INDIVIDUAL EXPERIMENTS**

### **Experiment 1**

After the flight, there were a few things that had gone wrong and a few others that had worked in ways different from expectations. Of the four circuits that were present in this payload, one of the circuits had been wired carelessly during integration. This resulted in a short and hence a blown fuse. This was the circuit which was doing the temperature control and timing. So the experiment was in a

run-away state with just the heaters on and the solenoid open. Upon opening the two chambers, it was found that the liquid was present in both chambers, contrary to expectations. The liquids were carefully extracted from the two containers. These two liquids and a sample of the original mixture have been sent for gas chromatography analysis. Results from this are eagerly awaited and will be presented at the symposium.

The controller on this experiment was a simple Schmitt trigger circuit which maintains the right temperature of the liquid mixture. A simple binary counter times the duration of the heating. During testing, we found that not having a micro-controller made of lot of things inflexible. Unconnected pins on digital chips caused a lot of problems with floating grounds. By tying these to ground, the outputs of the controller were consistent and noise-free. A little more thought in the designing of the chamber fittings would have saved time during the liquid filling and removal operations. The experiment testing procedure was designed without faculty input, often resulting in erroneous tests. Some of the wiring was done too late which resulted in an electrical short. The battery box was never assembled before hand and the problem with the excess height was discovered only during integration.

The hope is to resolve some of these problems and to build a better experiment for reflight sometime in the near future.

## **Experiment 2**

This was the only experiment which had visible indicators to show whether the payload worked while in space. Of the three wax columns, the shortest column had melted completely and formed a ball of wax around the heater. The other two columns had melted partially and resolidified. It is assumed that the power to the experiment was removed earlier than anticipated. The reasons for this have not been determined. No analysis has been done on the experiment results.

The lack of analysis on the part of students could be attributed to the long delay between the conception of the experiment idea and the flight of the experiment. The student who worked on the experiment in the end was not the student who started the experiment. The curiosity for the experiment results was lost and there was satisfaction with merely having the experiment work partially in space.

## **Experiment 3**

On deintegration of the experiment and the experiment memory storage module, it was found that 77 kilobytes of data was collected during flight. Initially this was reason to cheer about since we had a biology experiment that had collected some data. While doing a ground run of the experiment, a serious bug in the flight program was discovered which rendered the acquired data extremely difficult to interpret. Looking back, this does not come as a total surprise since the final flight program was written barely a day before shipment. A lot of time was spent in testing the experiment with power supplies which did not source enough amps and as a result, something always showed up as faulty, when in reality it was not.

The final phase of work on this experiment was started very late and with the complexity of the experiment, there was not enough time to do adequate testing. The complexity of the experiment itself could have been substantially reduced if help was sought from knowledgeable electrical engineers. But

on the positive side, the experiment has provided a biology major with a fairly good background in electronics and hardware. A simple lesson learnt from this experiment is that teflon wire is rigid, expensive, heavy and its positioning should be included in the blueprints wherever possible. Perhaps the best of all lessons learnt is as simple as START EARLY.

#### **Experiment 4**

The Bubble experiment was probably the most impressive experiment in the entire payload for several reasons. It had a very good experiment idea, the hardware was machined very well and it was the most tested experiment in the entire payload. But the saddest part was that the experiment never saw power turned on to it while in flight. This was the last experiment in the payload to be turned on during the mission. There is good reason to believe that the batteries had failed on the switching relays by this time and hence they failed to turn power on to the experiment. Upon return, when the experiment was powered up using power supplies, the experiment went through its sequences flawlessly. We had either seriously underestimated our power budget on the relays, or the batteries had behaved contrary to expectations while in flight. This experiment is a worthy candidate for reflight on a future GAS payload.

#### **Experiment 5**

This was probably the most successful of all experiments in terms of post-flight analysis. In December 1994, fourth and fifth grade students gathered in the school to conduct experiments on the space flown and ground samples of popcorn. A total of 120 students were involved in this massive experiment. The group was divided into 10 specialized research teams. They were:

Event Facilitators, Science Writers, Exhibit Committee, Science Illustrators, Popper personnel, Data Collectors, Data Analyzers, Space Futures Study Group, Seeds in Space Trainers (to educate primary students) and EBTV (school video news reporters).

Two specific trials were held to examine the popcorn which was flown in space and the popcorn which was maintained on earth. A lot of experimentation was done with these two trials. Some of them were the following:

The weight of the popcorn bags before and after popping, width and height of the popped bags, odor of the popcorn after popping, the number of popped kernels and the number of unpopped kernels from each trial, the size, color, odor, kernel weight, ingredients left in the bag, freshness/staleness, crunchiness, chewiness, saltiness and after-taste.

The whole process was carried out for almost two hours. The fourth and fifth graders collected data and worked in a very efficient and effective manner. Following data collection, students compiled their data into a consistent format and included illustrations and drawings that were taken on site. Following this, some data interpretation was held with some most interesting results. Some of them were:

1. Students found a 10 gram difference in the bag weight of the space popcorn as compared with the weight of the earth popcorn. The space popcorn being lighter.



2. Students found that the space popcorn had 779 kernels pop per bag compared to 545 kernels in the earth popcorn.
3. Students found that on a rating scale of 1-5 for crunchiness, the space popcorn rated 4.0 while the earth popcorn rated with 3.0 with 5 being most crunchy.
4. The students found that in terms of after-taste, the earth popcorn rated 5.0 and the space popcorn 3.0 - on a scale of 1-5, with 5 having the most after-taste.

The process had a few scientific deficiencies, but without a doubt, it exposed the fourth and fifth graders to the scientific process. It had a tremendous impact on all who were involved. It most certainly motivated students to become interested in space science and engineering. Students became real life investigators of real-life phenomena. It was an example of a tremendous STS related science experience which were all the primary objectives of this experiment.

### **Experiment 6**

This refers to the experiment pertaining to the space flown radish seeds. At this time, the school has acquired some growth chambers and the details of the experimentation are being worked out. This should also provide the elementary school children with a very unique experience related to space experimentation.

### **LOOKING INTO THE FUTURE**

The overall lessons learned from G254 have been invaluable for the USU GAS team on their subsequent payloads. G254 had stayed in the lab for so long, that students wanted to get it flown at any cost. That the experiments had partial successes on the flight seems like a bonus. But the total educational experience derived from it have more than compensated for the failures of the experiments.

The USU GAS team is currently working on G200 which is slated to fly on STS-77 in April 1996. The safety review for this payload has already been completed. The entire payload has been designed and drawn using CAD software. Materials have been chosen carefully. The structural analysis was completed before any metal was cut. After having been through some embarrassing moments, the students now want to build a professional looking payload which works according to its objectives. With the way things have gone so far, there is every reason to believe that the lessons from G254 were learned well and will be incorporated into G200.

## REFERENCES

1. *G-254 Undergraduate Experiment*. NASA Conference Publication 3171, October 1992, pp 151-163.

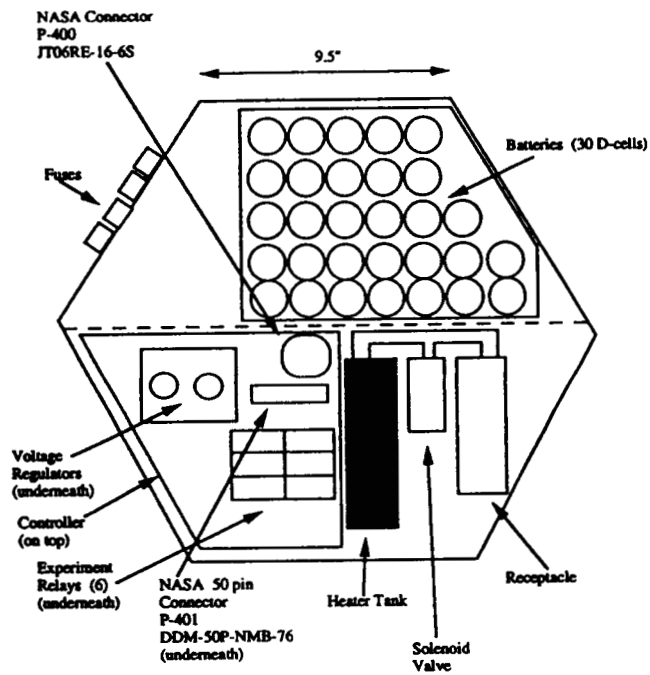


Figure 2 Cut-out of expt. 1

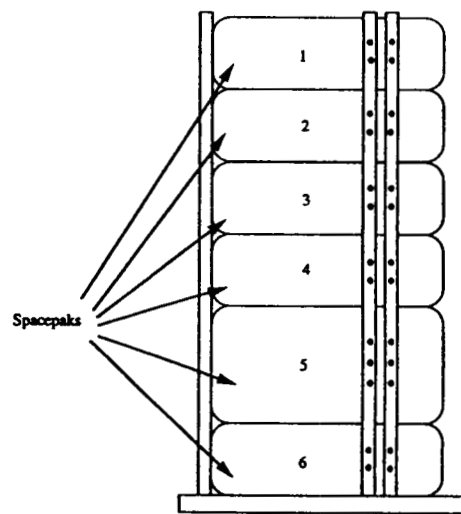


Figure 1 Fully assembled Structure

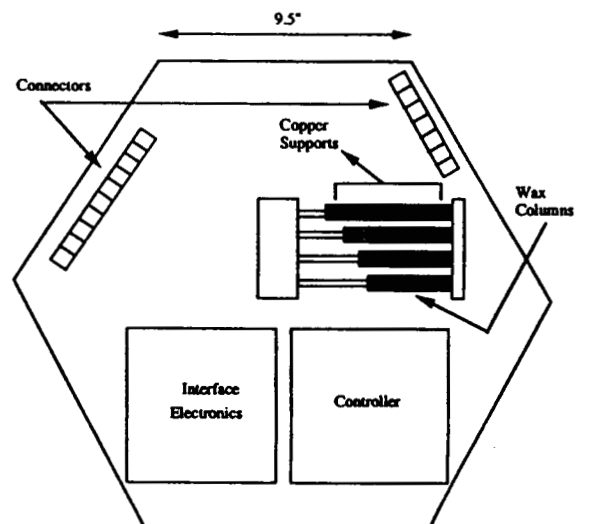


Figure 3 Cut-out of expt. 2

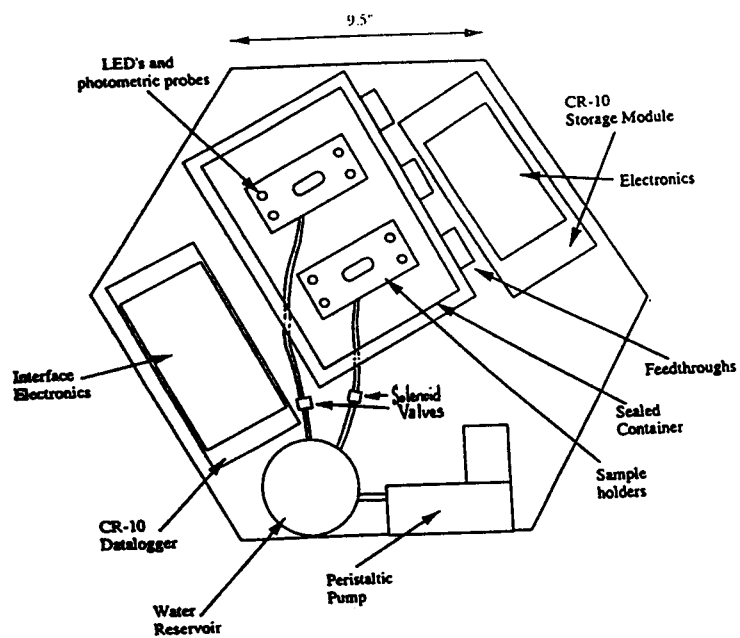


Figure 4 Cut-out of expt. 4

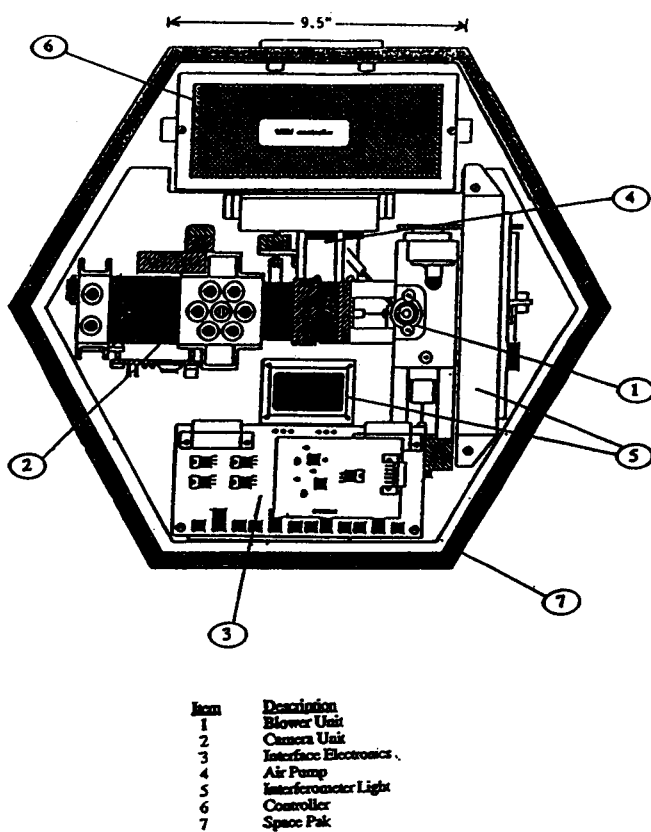


Figure 5 Cut-out of expt. 4

# MEASUREMENTS OF THE STS ORBITER'S ANGULAR STABILITY DURING IN-ORBIT OPERATIONS<sup>1</sup>

Werner M. Neupert<sup>2</sup>, Gabriel L. Epstein<sup>3</sup>, James Houston, and  
Andrew Zarechnak<sup>4</sup>

Laboratory for Astronomy and Solar Physics

NASA/Goddard Space Flight Center  
Greenbelt, MD 20771

## ABSTRACT

We report on measurements of the angular stability, commonly called "jitter", of the STS Orbiter during normal operations in space. Measurements were carried out by measuring optically the Orbiter's roll and pitch orientation relative to the solar vector as the Orbiter was held in a  $-Z_0$  solar inertial orientation (orbiter bay oriented toward the Sun). We also report observations of an interesting perturbation to the Orbiter's orientation noted by the crew during the STS-60 mission. These data may be useful in analyzing the in-orbit response of the Orbiter to thruster firings and other applied torques, and may aid in the planning of future experiments that require fine-pointed operations by the Orbiter.

## INTRODUCTION

The Orbiter Stability Experiment (OSE) is a "Get-Away Special" payload designed to characterize the angular stability ("jitter") of the STS Orbiter about its X-axis (pitch) and Y-axis (roll) when the Orbiter's  $-Z_0$  axis is pointed to the Sun during its operation in space (ref. 1). The original motivation for these observations was to obtain a database for designing an image motion compensation system for a solar extreme ultraviolet imaging instrument that would use the orbiter as a platform for solar observations during an STS mission. Although the solar instrument that was planned was never implemented and flown, the Get-Away Special was flown as the flight equipment had already been prepared. The observational results, which cover angular amplitudes of Orbiter motions from about two degrees to the sub-arc second range, may be of use to other STS users. The OSE was flown on two shuttle flights, STS-40 and STS-60, during which observations were made and on a third flight, STS-64, when the proper STS attitude for OSE observations was not scheduled.

## DESCRIPTION OF THE ORBITER STABILITY EXPERIMENT

Angular deviations from the solar vector were observed with two Lockheed Intermediate Sun Sensors (LISS) which can detect deviations about the two axes normal to the solar vector of as little as 0.1 arc sec. Each sensor therefore provided both Orbiter pitch and roll information, and one unit was rotated about the  $Z_0$  axis by 180 degrees relative to the other so that actual STS motions would result in opposite polarity signals from the two LISS sensor outputs, thereby distinguishing Orbiter motions from any possible in-phase electronic system noise. The four analog signals from the LISS were each sampled 58 times per second, filtered, multiplexed, processed by a 16 bit analog to digital converter, stored in shift registers, and recorded on a Lockheed Model 4200B tape recorder. Measurements were made over the frequency range of 0.01 to approximately 10 Hz, the high frequency cutoff of the 12 db/octave filter beginning at 11 Hz to avoid aliasing. Ancillary data channels provided calibration voltage levels, a nominally 100 Hz clock signal, and three temperature sensor outputs. These were interleaved with the primary data stream.

<sup>1</sup> This project was supported via the Director's Discretionary Fund of the Goddard Space Flight Center

<sup>2</sup> Present Address: Code R/E/SE, Space Environment Laboratory, NOAA, 325 Broadway, Boulder CO 80303

<sup>3</sup> Present Address: Code 410.0, NASA/Goddard Space Flight Center

<sup>4</sup> Virginia Polytechnic Institute, Blacksburg, VA 24060

## ANGULAR SENSITIVITY OF THE OSE SENSORS

The nominal angular field of view (FOV) of the Lockheed Intermediate Sun Sensor (LISS) used on OSE is  $\pm 2$  degrees, appropriate for its usual application as a Sun pointer on suborbital sounding rockets. On OSE, this FOV was subdivided with a 16-bit scalar to yield a sensitivity (the change in the offset of the solar vector corresponding to the least significant bit of the scalar output) of 0.23 arc sec. For the STS-40 mission, the FOV of one of the two LISS was increased (thereby reducing the sensitivity) to  $\pm 3$  degrees to increase the likelihood of obtaining data even if the offset of the instrument's line of sight (LOS) from the Sun, via the Orbiter's navigational base, were as great as three degrees. For the STS-60 flight, we increased the sensitivity of the second LISS by a factor of more than ten, yielding 0.036 arc sec per LSB, comparable to the noise level from the LISS itself. System electronic noise, introduced by the A/D circuitry, was typically 0.75 LSB. This noise level was measured during STS flight by operating the OSE in the absence of sunlight, i.e., during the nighttime portion of the orbit.

## OSE ALIGNMENT TO THE GAS BRIDGE AND THE STS STRUCTURE

Angular alignment to the STS navigational system was critical as the total FOV of the OSE sensors was never greater than  $\pm 3$  degrees. Prior to flight, we estimated the limits of potential misalignment of the LISS to the Orbiter's navigational base, based on the machining tolerances of the LISS sensors and their attachment to the GAS mounting plate, and the machining tolerances of GAS container, the GAS bridge, and the mounting points of the GAS bridge to the STS. The largest potential contributor to OSE-solar alignment was the alignment of the GAS bridge to the Orbiter structure and the deformation of that structure, relative to the guidance system mounted in the nose of the STS. Given published Orbiter tolerances (ref. 2), this misalignment could amount to several degrees. However, from earlier solar pointing measurements made on STS-3 during flight of the OSS-1 payload, it was known that experiment-Orbiter misalignments could be held to 0.1-0.2 degrees.

Each LISS's reference optical surface was optically aligned to a precisely machined mounting plate (the LISS Alignment Plate (LAP)) mounted externally on the sunward end plate of the GAS container. Optical co-alignment of the two LISS reference surfaces to 0.2 arc min in pitch and 2.8 arc min in roll was achieved. The LAP was then shimmed, using an inclinometer and precision bubble levels, to bring it into alignment with the GAS bridge structure and the trunnions by which the GAS bridge attaches to the STS Orbiter sills. Using these techniques, the total misalignment of the LISS to the GAS bridge was held to a few (5-10) arc min in both pitch and roll, based on alignment measurements carried out before and after flight of both STS-40 and STS-60.

No direct measurements of alignment of the LISS to the Orbiter X and Y axes were made. From the machining tolerances of the LISS mounting system to the GAS container, we estimated that the alignment errors of the GAS Bridge to the Orbiter Trunnion system were no greater than 1 degree and therefore acceptable for the observations to be made.

Overall alignment of the LISS LOS to the solar vector after establishing a  $-Z_0$  solar inertial attitude was extremely good on STS-40, amounting to offsets of at most 4 arc min in pitch and 5 arc min in roll. On STS-60, on the other hand, the alignment in roll was again about 5 arc min, but in pitch it was 35-38 arc min, which placed the solar LOS out of the FOV of the high-gain pitch channel. This significant misalignment is within the limits given in the ICD quoted above, but is inconsistent with the performance achieved on STS-40. We suggest that it may be due to a long-term drift in the STS inertial attitude control system, which is updated by reference to the inertial reference from bright stars. On STS-40, an IMU recalibration was carried out two hours before OSE operations and accurate alignment to the Sun was achieved. On the other hand, on STS-60, the most recent IMU alignment was carried out 67 hours before OSE operation and the Orbiter navigational base may have drifted by up to 0.6 degrees in pitch in that period of time.

## ON-ORBIT OBSERVATIONS

The OSE was operated for approximately two hours on STS-40 and for nearly one hour on STS-60. In this paper we incorporate results obtained on both of these mission, as neither data set has been fully analyzed and compared with

ancillary data on Orbiter operations. During the OSE observations on STS-60 the Orbiter was stabilized in the  $-Z_0$  solar inertial mode with a  $\pm 0.2$  degree deadband. Maintaining this deadband required firing of vernier thrusters, and the reversals of Orbiter motion produced by such firing are the most prominent feature in the OSE data stream. Figure 1 illustrates the overall motions of the Orbiter during the solar observing period on STS-60. A slow but steady drift of the mean pointing direction relative to the Sun during the observing period during both missions. On STS-60 this drift amounted to 9 arc min/hr in pitch (about the Orbiter  $Y_0$  axis) and 3 arc min/hr in roll (about the Orbiter  $X_0$  axis). The corresponding rates observed on STS-40 were 3.8 arc min/hr in pitch and 2.5 arc min/hr in roll.

A double differentiation of the LISS sensor data, which yields the angular acceleration of the Orbiter about its  $Y_0$  or  $X_0$  axis, clearly demonstrates the pitch or roll rate changes associated with each vernier thruster firing. A short interval of LISS pitch channel data analyzed for the STS-40 flight is shown in Figure 2. The times of vernier thruster firings are also marked (with a different symbol for each thruster) and combinations of such firings have repeatable results in the OSE pointing data. An unanticipated effect was the appearance of a pitch deviation when thrusters were commanded to accomplish an Orbiter roll maneuver. It is known that minor imbalances in thrust between pairs of thrusters can result in cross-coupling of movements about the roll and pitch axes and we apparently have observed the cross-coupled body motions of the vehicle that are the result.

We also detected perturbations that are not associated with thruster firings, but which may be due to crew activities or the operation of mechanical systems on the STS. No crew exercise activity was scheduled during the time period shown in Figure 3 (a sub-interval of that shown in Fig. 2) but angular accelerations (and decelerations) not related to thruster firings are clearly detectable. As the OSE was directly attached to the Orbiter sill via the rigid GAS Bridge, we believe that the observed angular rates truly represent the body motions of the Orbiter and are not vibrations of intermediate mechanical structures.

OSE was operated during an exercise period during the STS-60 mission, so that some of the smaller fluctuations in pointing shown in Fig. 1 may be attributable to torques on the vehicle as the crew operated the exercise equipment.

## OBSERVATION OF AN ANOMALOUS ATTITUDE PERTURBATION

We have detected an attitude perturbation, reported by the crew as a "shudder," just prior to shut down of the OSE on STS-60. Although barely detectable in comparison to the normal motion of the Orbiter within its specified deadband, this event is interesting in that it exhibits a spectrum of rotational (in pitch and roll) vibrations of the Orbiter that are characterized by sharp resonances and that are of longer duration in time than the duration of vernier thruster firings used to maintain the Orbiter's orientation (usually 1-2 sec long). The onset of the event, at MET 07/03:45.4  $\pm 1$  minute, coincides with small changes in Orbiter's pitch and roll rotation rates, suggesting that one or more thruster firings may have occurred. Rogers and Delombard have reported (ref. 3) that although this event has been ascribed by propulsion teams at the Johnson Space Center to three vernier engines firing simultaneously, data from the NASA/JSC Mission Evaluation Workstation System shows no such event at the time of the peak of a vibration recorded by the Shuttle Acceleration Measurement System (SAMS) and no significant vibration signature appeared in the SAMS data during several firings of three thrusters within six minutes of the event. Figures 4 and 5 illustrate those portions of the OSE data stream in during which this vibration event was observed in pitch and roll. The consistency of the OSE observations is demonstrated, in Figure 5, by the similarity of observations in our low gain (upper curve) and high gain (lower curve) roll channels, after applying the relevant sensitivity scaling and accounting for the rotation by 180 degrees of one LISS relative to the other on the LISS Alignment Plate. In this plot an electronic disturbance internal to the OSE would have produced out-of phase rather than in-phase variations of the two OSE signals.

The disturbance produced a modulation in the Orbiter's pitch rate for at least ten seconds, but a modulation of the roll rate could be detected for 20 seconds. The oscillatory motion superimposed on the Orbiter's slow rotational motion within its pointing deadband is best displayed by first subtracting a polynomial fit from the LISS data in each channel. The residual components, after suitable polynomial fits have been subtracted, are shown in Figures 6 and 7. The quality of the observations are clearly better in roll than in pitch, as the high gain pitch channel was saturated due to the pitch offset noted earlier.

## ANALYSIS OF THE ATTITUDE DISTURBANCE

Spectral analyses of the pitch and roll excursions were carried out in two second increments for the first twelve seconds of the event using an IDL Discrete Fast Fourier Transform defined by:

$$F(u) = \frac{1}{N} \sum_{x=0}^{N-1} f(x) \exp [-j2\pi ux/N]$$

This function differs by  $(N)^{-1/2}$  from the transform typically used in the analysis of Orbiter vibration data and in the microgravity requirements document for the space station, Space Station Freedom Microgravity Environment Definition-Rev B (ref. 4). Power Spectral Densities, in units of  $(\text{arcsec sec}^{-2}) \text{ Hz}^{-1}$ , are shown in Figure 8 for pitch and roll data taken during the first four seconds of the event.

Power is present at frequencies that are reasonably well correlated with the principal modes of vibration of the vehicle, as summarized by Bergemann (ref. 5). A vibration at 3.5-4 Hz observed in both pitch and roll channels may correspond to a fuselage torsional mode associated with wing and fin bending and another, at 5 Hz, may correspond to a fuselage first normal bending mode expected at 5.2 Hz. A rapidly damped oscillation at about 7 Hz in roll is matched most closely in Bergemann's tabulation by a fuselage first lateral bending mode at 7.4 Hz. Spectral power in both pitch and roll channels at 1-2 Hz and at 2-3 Hz in pitch at the onset of the event may correspond to structural frequencies of the Orbiter's radiators and cargo bay doors, but we have no way of discriminating among such possibilities.

The spectral power as a function of time at each significant frequency is shown in Figure 9 for both pitch and roll. These data enable us to estimate the damping constant associated with each major vibrational mode. The results are summarized in Table 1. We have not been able to identify the impulse which initiated the event, but changes in the pitch and roll rates of the vehicle at the beginning of the event suggest that on-orbit maneuvering jets were involved.

## REFERENCES

- (1) Neupert, W.M., Epstein, G.L., Houston, J., Meese, K.J., Muney, W.S., Plummer, T.B., and Russo, F.P., "The Orbiter Stability Experiment on STS-40," *1992 Shuttle Small Payloads Symposium*, NASA Conf. Publ. 3171, p. 1, 1992.
- (2) STS Interface Control Document, Vol. XIV, Paragraph 3.3.1.2.1 and Table 4.1.2-3, p. 3-27.
- (3) Rogers, M.J.B., and Delombard, R., "Summary Report of the Mission Acceleration Measurements for STS-60, Spacehab-2," NASA Lewis Research Center, Cleveland Ohio, 1994.
- (4) Johnson, T. and Holtz, T., "Techniques for Post Flight Data Processing of On-orbit Acceleration Data," *Minutes of Microgravity Measurements Group, Meeting No. 14*, March 21-23, 1995.
- (5) Bergemann, E., "HIRAP Data for Microgravity," *Minutes of Microgravity Measurements Meeting No. 6*, September 17-18, 1990.

Table 1. Damping Constants of Orbiter Pitch and Roll Vibrations (sec)

Pitch		Roll	
1-2 Hz	0.6	3.9 Hz	2.95
2-3 Hz	0.7	5.0 Hz	0.67
3.9 Hz	2.14	7.0 Hz	1.35
5.0 Hz	2.85		



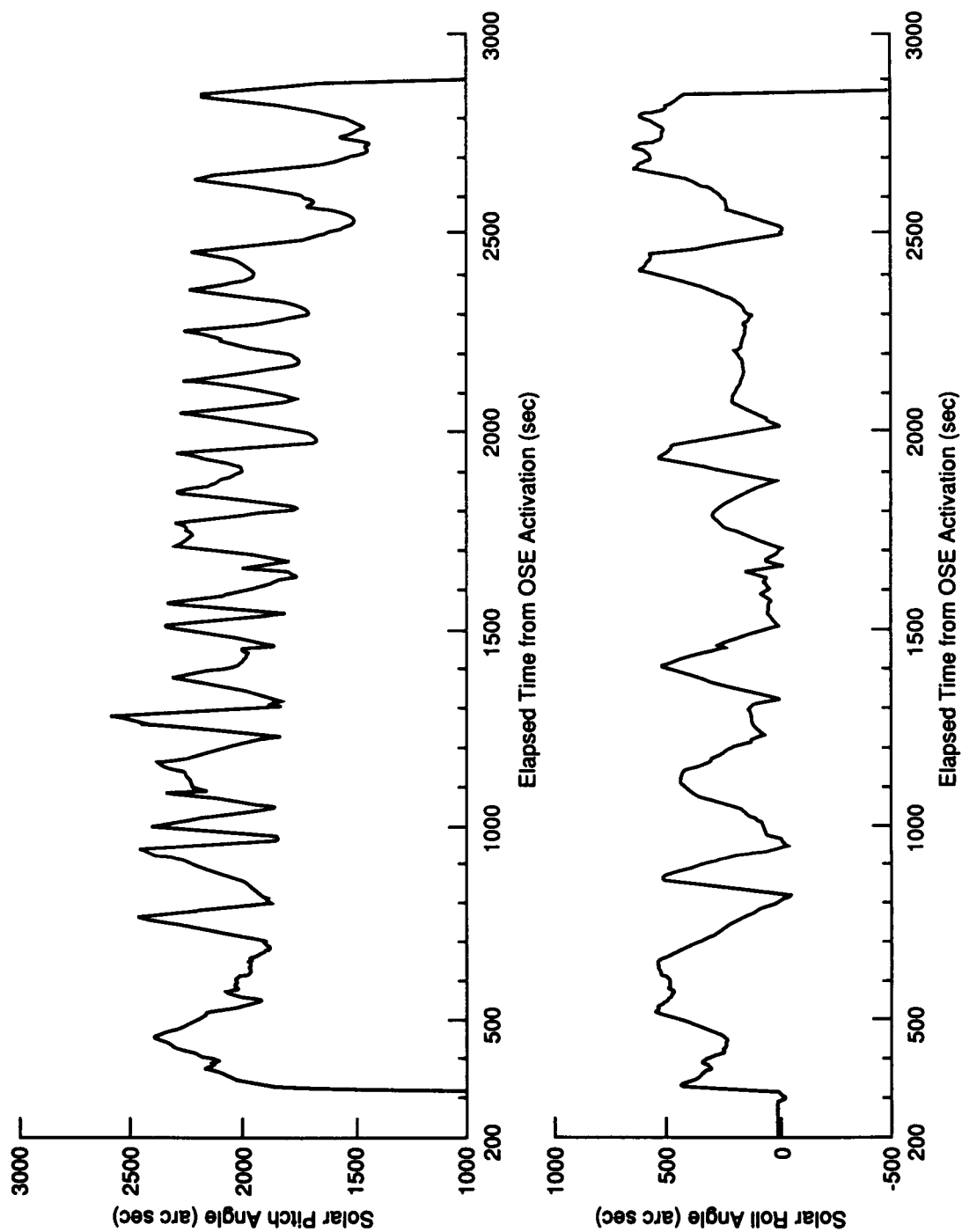


Figure 1. Angular deviations of the Sun's position relative to the reference directions of the Orbiter Stability Experiment's sun sensors as a function of time during operation of the instrument on STS-60. These deviations are interpreted as motions of the Orbiter in pitch and roll relative to a line between the Sun and the Orbiter.

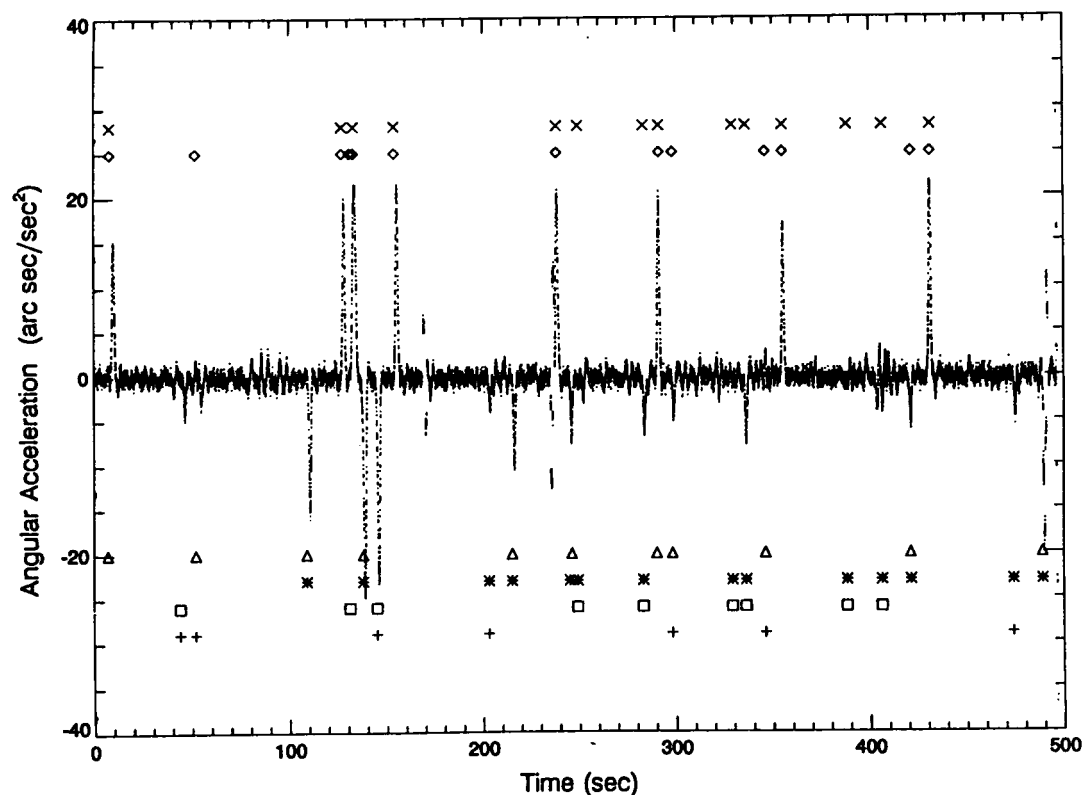


Figure 2. Angular accelerations of the STS in pitch in response to vernier thruster firings on STS-40. Coincidence of crosses and diamonds mark times of vernier thruster firings to accomplish pitch maneuvers.

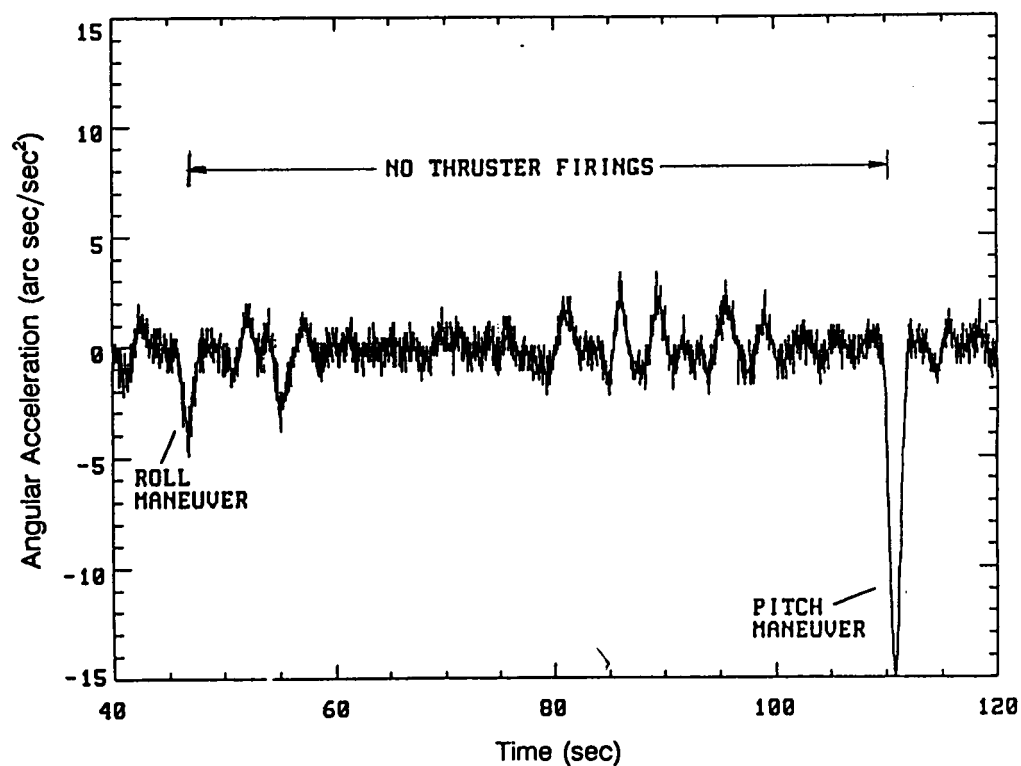


Figure 3. A short interval of data from the STS-40 mission illustrating perturbations in STS pitch orientation when no vernier jets were being fired. One pitch maneuver is obvious at the end of the data interval shown, and a roll maneuver at the beginning of the interval also produces a slight acceleration in pitch at the beginning of the data interval.

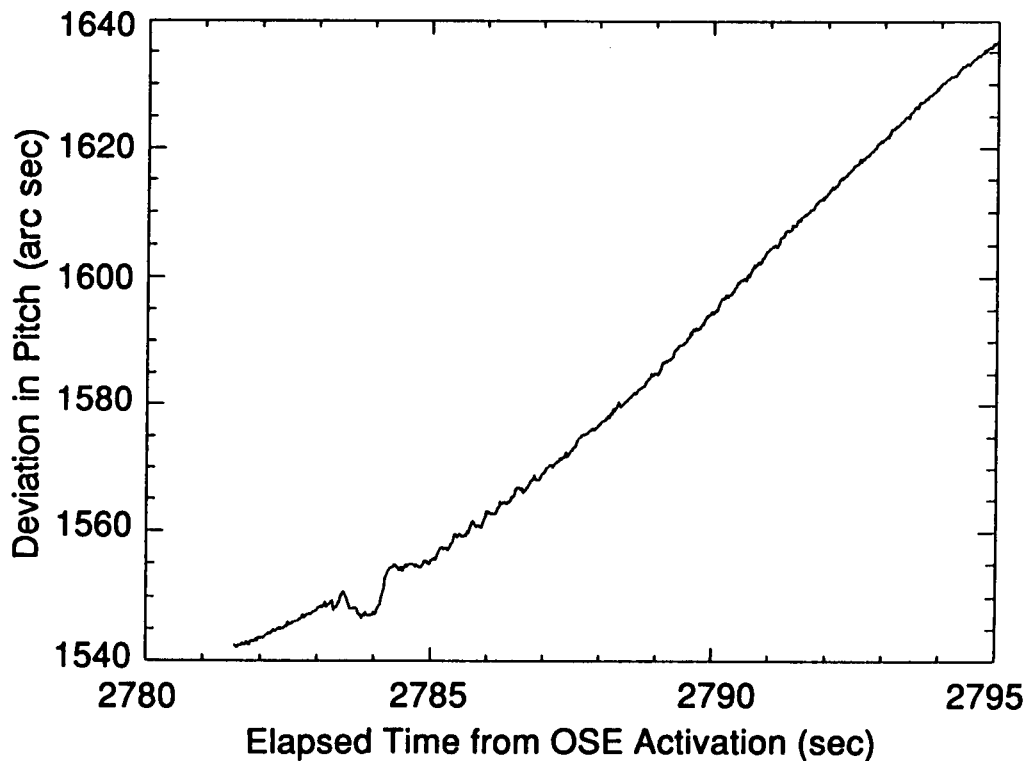


Figure 4. Detection of an anomalous attitude perturbation about the Orbiter's pitch axis at 2784 sec after initiation of OSE Operations on STS-60. This perturbation occurred near the end of OSE operations on that mission.

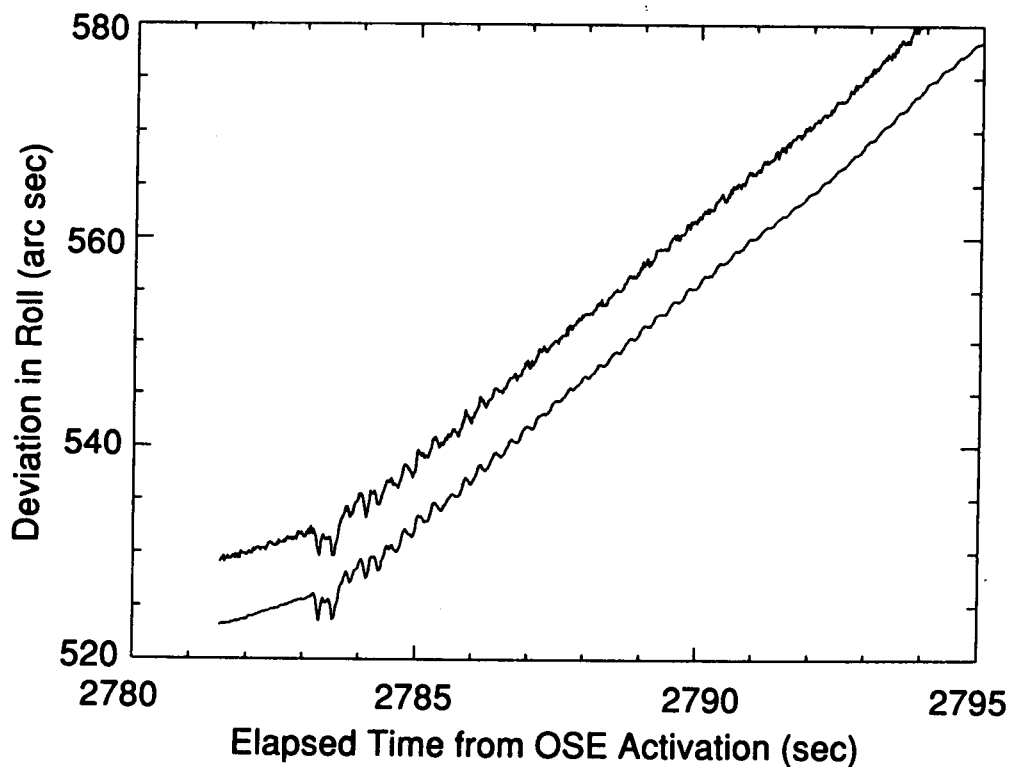


Figure 5. Detection of the same perturbation, in this case about the Orbiter's roll axis, as observed in the OSE's low-gain (upper curve) and high gain (lower curve) roll channels. Note the change in Orbiter roll rate at the beginning of the event, suggesting that a vernier thruster firing may be associated with this event.

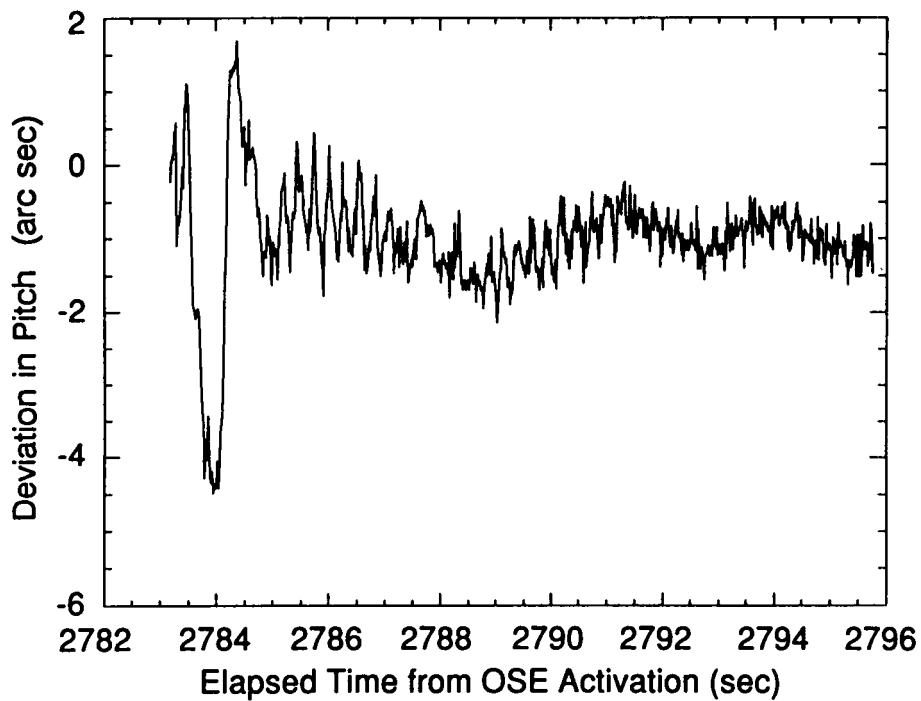


Figure 6. Pitch deviations from a polynomial fit to the OSE data at the beginning of the attitude perturbation shown in Figure 4.

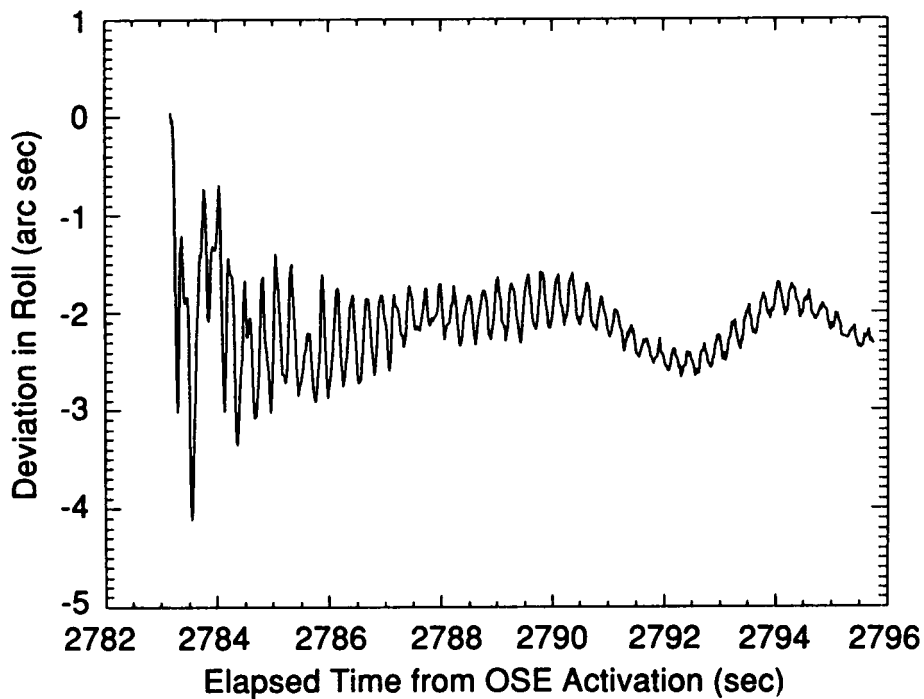


Figure 7. Roll deviations from a polynomial fit to the OSE high-sensitivity roll channel at the beginning of the attitude perturbation.

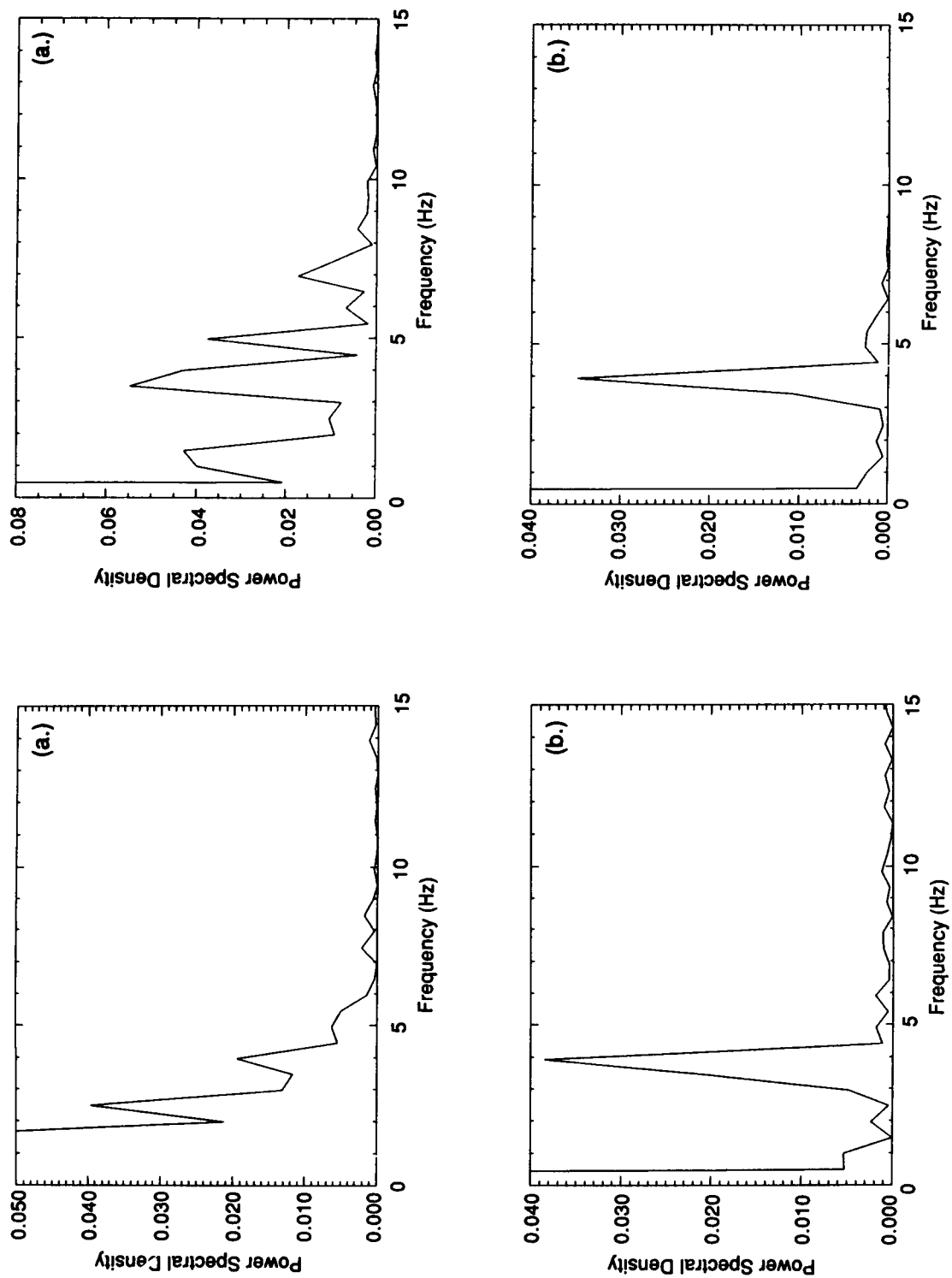


Figure 8. Power spectra of pitch deviations (left panel) and roll deviations (right panel) from polynomial fits to each data channel as a function of frequency at (a) 0.0-2.0 and (b) 2.0-4.0 sec after the beginning of an attitude perturbation on the STS-60 mission.

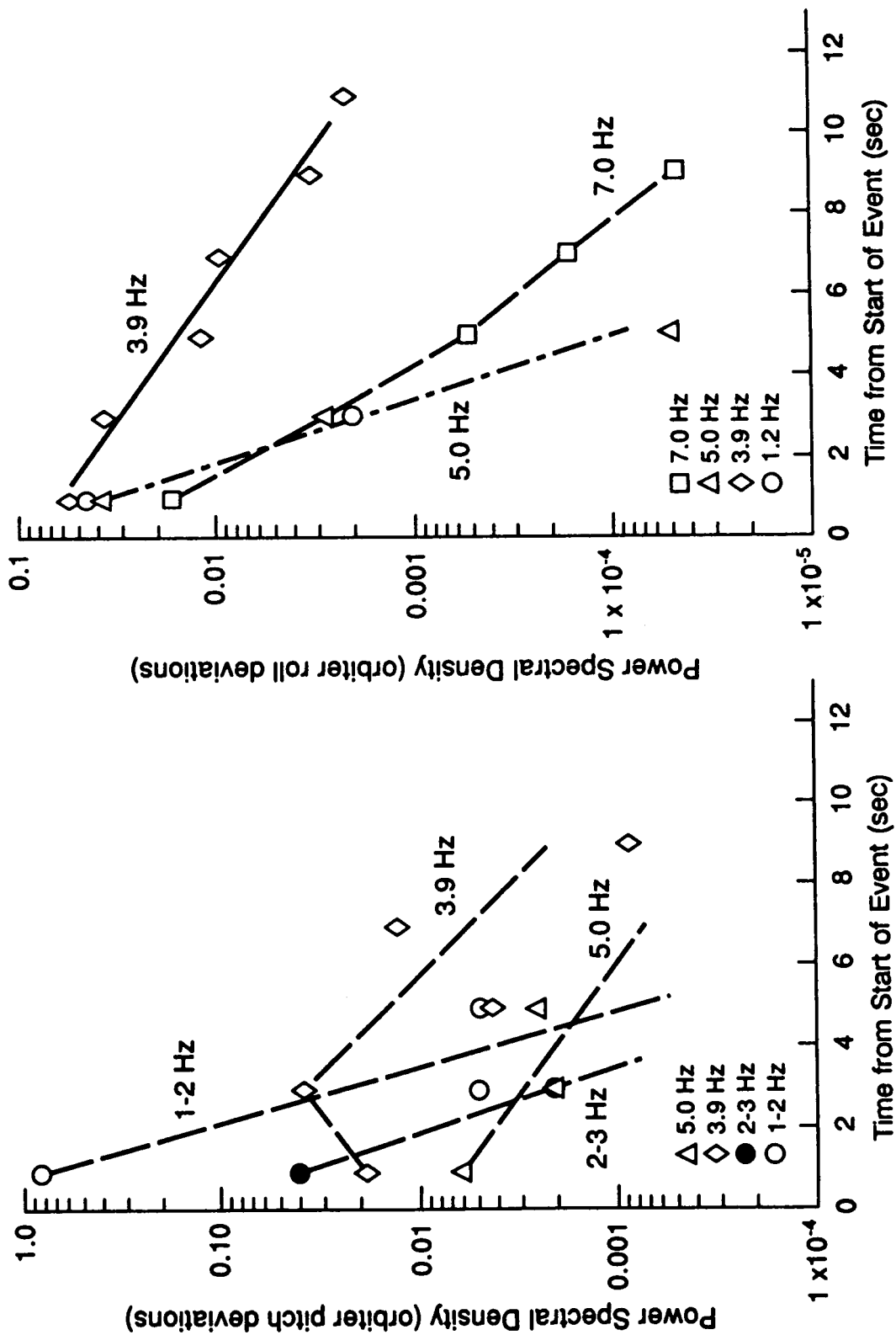


Figure 9. Spectral Power as a function of time for selected frequencies of Orbiter motions during the attitude perturbation shown in Figures 6 and 7.

## **ACOUSTIC MODAL PATTERNS AND STRIATIONS (AMPS) EXPERIMENT G-325, NORFOLK PUBLIC SCHOOLS**

Joy W. Young  
NORSTAR Project

Norfolk Public Schools Science and Technology Advanced Research Project

### **ABSTRACT**

This paper will describe how high school students with the guidance of volunteer mentors were able to successfully complete an acoustics space experiment. Some of the NORSTAR program strategies used to effectively accomplish this goal will be discussed. The experiment and present status of results will be explained.

### **INTRODUCTION**

The Norfolk Public Schools Science Technology Advanced Research (NORSTAR) experiment flew aboard Discovery, STS-64, during September of 1994. Several years ago a group of 9-12 graders in an extended day program for gifted students was awarded a GAS canister (G-325) by NASA Langley Research Center (NASA LaRC). NASA scientists, under the direction of Dr. Joseph Heyman, volunteered to act as mentors to the student group. This NASA commitment stimulated the formation of the NORSTAR project in Norfolk Public Schools and gave the impetus for development of this hands-on, real time, highly motivational, alternate model to the normal high school science program.

The main goal of the NORSTAR program includes both science objectives and broader educational objectives. The main science objective of G-325 was to explore the interaction of sound with particles in a closed microgravity environment. The educational objectives of the NORSTAR project include development of skills such as leadership, teamwork, oral and written communication, and critical and creative thinking. With the G-325 payload we wanted to involve and stimulate the students in a space investigation that had scientific significance and to educate the students in all aspects of carrying out scientific experiments (funding, design, manufacturing, testing, analysis). These objectives have been supported consistently by the skilled mentoring techniques of the NASA LaRC mentors and various other mentors from businesses, industries and universities nationwide. The primary G-325 experiment, Acoustic Modal Patterns and Striations (AMPS) was developed over a four year period by NORSTAR students. The idea for the experiment was initiated from students' studies of the Kundt tube and the recent work in acoustic modal visualization of Dr. Robert Apfel, Yale University. Also included in the G-325 payload were 50 small passive experiments from elementary and middle school students.

### **PROGRAM DESIGN**

The NORSTAR GAS-325 program was jointly designed by Norfolk Public Schools Gifted Program and volunteer mentors from NASA Langley Research Center. NORSTAR students are selected by standardized test scores, grades, teacher recommendations and interviews, and are bused each school day to the Norfolk Technical Vocational Center. Students also put in extra volunteer time on Saturdays and during school vacations. Students receive a 1/2 credit for every 75 hours of participation in the program with a semester limit of 1 1/2 credits.

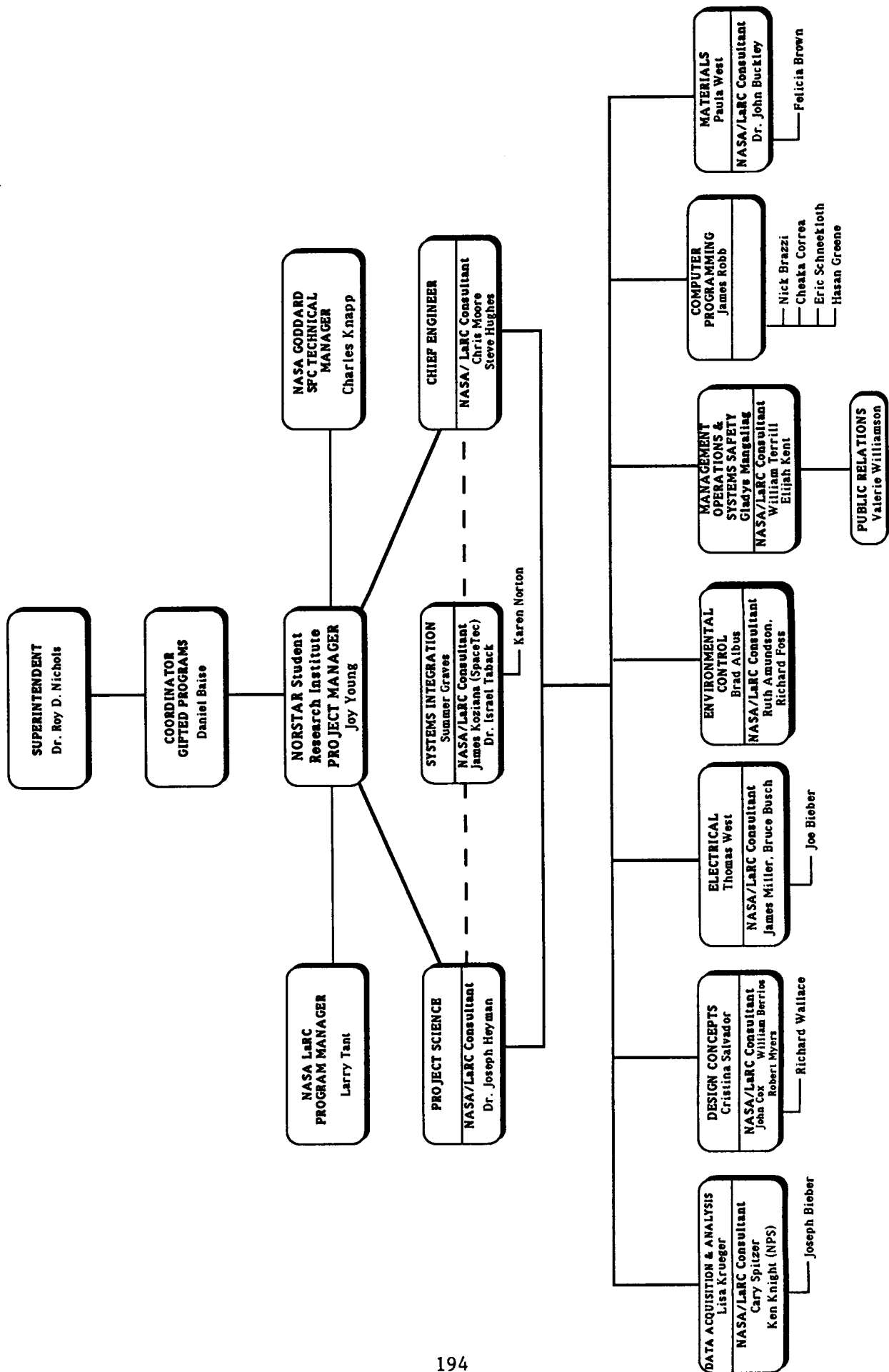


FIGURE 1. NORSTAR SUBSYSTEMS ORGANIZATIONAL CHART



Learning through 'real work' projects is the main objective of the NORSTAR program with teacher and mentors used as facilitators and guides. The students are allowed considerable freedom to design and carry out their ideas and develop projects in a small team setting. Each team is responsible to other teams and for the success of the main space experiment. Teams give regular status reports which detail projected weekly workloads and accomplishments made during the previous week. The student teams and their responsibilities in their subsystems are as follows:

- **Project Scientist:** leadership of the overall scientific validity of the project
- **Chief Engineer:** leadership of all the structural details of the space experiment
- **Systems Integration:** leadership of integration of all systems for the success of the project
- **Management Operations and System Safety:** documentation of the main experiment and safety data to NASA Goddard and NASA LaRC
- **Materials:** selection and assessment of all materials and documentation of materials for the main project
- **Electrical:** design and construction of the electrical circuits and power supply for the main experiment
- **Thermal:** monitoring of the thermal limits of all experimental apparatus and preparation of the Thermal Analysis and thermal safety of the main project
- **Data Acquisition:** design of the data acquisition apparatus and analysis of data obtained.

These teams approximate NASA guidelines for project teams each with its own volunteer mentor. The students and mentors communicate regularly by telephone, fax, and in face to face meetings either in the school or at the mentor's workplace.

The NORSTAR teacher and mentors focus on training students to be knowledgeable enough in science/technology/engineering to produce a project of real scientific significance. They encourage team work, individual learning, responsibility in self-directed learning and interactive and communication skills. To these ends the NORSTAR teachers and mentors encourage, design, and direct activities which will improve and give maximum opportunity to practice the following skills.

- knowledge of scientific principles and practices
- reading and comprehension
- writing papers to communicate facts and persuade points of view
- oral communication - one on one and presentation to groups
- computer literacy
- design of experiments and projects
- analysis of results of research and experiments
- planning of workload to achieve success - time management
- brainstorming and original thinking
- integration of 'think' time and 'production' time to produce results
- listening and questioning skills
- self confidence and self esteem
- intergroup and interpersonal working skills
- ability to work, despite frustration, to completion of a project deadline

These skills are encouraged and developed at slightly different rates for each student

depending on the number of hours of experience in the NORSTAR setting and the cognitive level of the student. The student is viewed in a holistic manner and encouraged to develop skills and knowledge independent of team/group setting as well as in a team/group setting. Specific methods to achieve these objectives are as follows:

- students are expected to read for research and write daily logs of their work
- students present Weekly Status Reports both written and oral to the group (stating progress made and projected work)
- students who are not currently engaged in work on the main project are assigned computer literacy, research, experiment or design tasks
- students are assigned peer seminar oral presentations
- students present status reports in the form of Design Reviews to a board of mentors at NASA Langley Research Center
- students work individually or as a team towards completion of the main experiment
- student/instructor interaction consists of questioning the student and leading the student to resources such as books, phone contacts, mentors, to discover answers
- students work in teams to achieve the success of the main experiment
- students are encouraged to ask questions, seek answers and be accountable for their progress at Weekly Status Report sessions, in conferences with their mentors and other 'outside the classroom' experts
- students are encouraged to seek many sources for information
- if the student becomes discouraged the teacher/mentor acts as an encouraging factor by giving direction
- outside speakers visit on a regular basis to extend student learning
- students give presentations on their ongoing work to interested adult and student groups which have included in state, out of state and visiting groups from other countries - Japan, England, South Africa

The NORSTAR program has evolved over the years, with NASA mentor guidance, into a student centered science/engineering experience which has produced highly motivated students in a cross section of Norfolk Public Schools population. On average, forty nine percent of the students are minorities, ninety percent of the NORSTAR graduates enter college programs in the science/technology fields. Whether in the areas of space, aeronautics, or other science, business and industrial fields, we feel that similar programs could only serve to enhance the understanding of science in the United States. This model could be adapted by business and industry to encourage learning and produce a scientifically literate, motivated core of leaders for future exploration of space, creative engineering, and problem solving in the twenty first Century.

Parent involvement has been a crucial part of the NORSTAR endeavor. Parents with technical skills have helped at every stage of the G-325 project. Our parent organization raised the money for all of our students to travel from Norfolk to Kennedy Space Center to watch the launch of the project.

Local and national businesses and industries were contacted by the parents and students, first by telephone and then follow up letters. All hardware and manufacturing used in the G-325 were donated by these businesses and industries who supported and were willing to mentor our project.

## SCIENCE DESIGN

### Amps Experiment

The G-325 acoustical experiment was conducted in a five cubic foot Get Away Special (GAS) canister. Two twenty-one inch clear acrylic tubes were suspended from a box containing two titanium tweeters. A separate function generator was connected to each tweeter to supply the sound and an amplifier amplified the sound. Inside each test chamber four grams of cork dust acted as a medium to visualize the modal patterns created by acoustic standing waves at resonances of the test chambers. Different patterns were expected to be formed as the frequency range was ramped up in each tube. Frequencies from 6000 to 7499 Hz ran through Test Chamber 1. A frequency range from 7500 to 9000 Hz was run through Test Chamber 2.

In the ground experiments, modal patterns formed at 45 of the ramped frequencies. Striations were evident in the cork particles at each node (see fig.2). We hoped to see if these striations would also occur in microgravity or if they were a phenomenon caused by gravity. In the microgravity environment of space, the cork particles should have been free to move without the constraints of gravity and form floating discs at the nodes of the standing waves.

The modal patterns at different frequencies were videotaped. The videotape data gathered is being used to determine:

1. The number of nodes and antinodes.
2. The types of modal patterns.
3. The effect microgravity has on striations seen in nodes on Earth

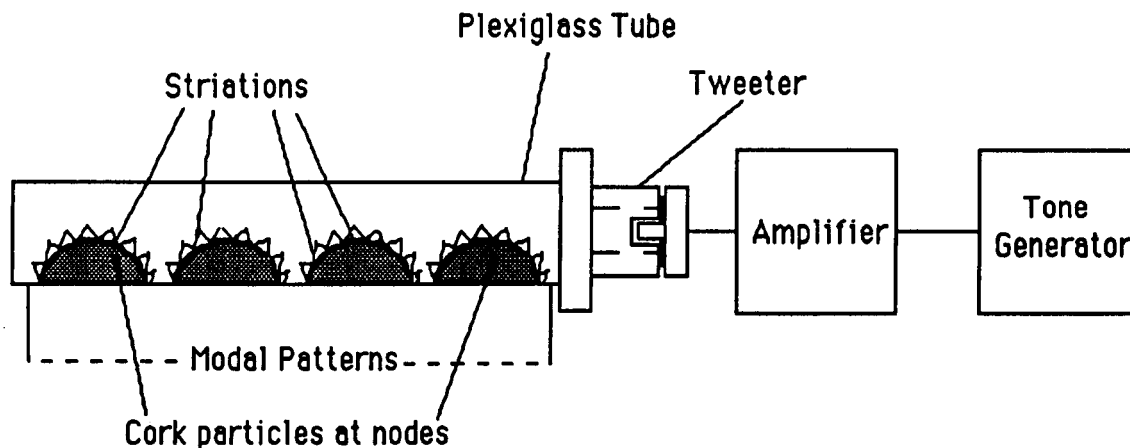


FIGURE 2. AMPS EXPERIMENT

### Passive Experiments

Although the primary objective of the NORSTAR GAS-325 project was to study acoustical standing wave modal patterns, on a space available basis, we included small,

passive, benign, experiments placed in a sealed container in the GAS canister. These were contributed by middle and elementary school classes in an effort to more widely share the excitement of space experimentation. The passive experiments fell primarily into the biological/physical sciences categories, and sought to discover and/or measure the effects of space and microgravity on prepared samples. Some examples are popcorn, marigold seeds, ink, paint, chalk, cooking oil, yeast, alum, and brine shrimp eggs.

## **EXPERIMENTAL RESULTS AND LESSONS LEARNED**

### **Science**

#### **AMPS Experiment**

All systems worked as projected. The videotapes show that lights, amplifier, tweeters and videocameras performed as expected. Sonograms from sound recordings showed the ramped frequencies in test chamber 2 (7500 - 9000 Hz) were completed but those in test chamber 1 (6000 - 7499 Hz) ceased at 57 minutes. The video footage on chamber 2 shows some promising visible activity from 17 minutes to 27 minutes. We do not at present have the technical expertise or equipment to sufficiently enhance the tapes for analysis but we are, at this time, seeking help from NASA, universities and industries to assist us in this final stage.

We learned that although ground experiments with four grams of cork dust showed definite patterns when the dust was dispersed in a microgravity environment the volume may not have been enough to produce results that were visible on video. We have since considered using greater amounts of cork dust or changing to larger or brighter particles as our medium to study acoustic modal patterns. We have also considered that we might have included a dispersal system for the cork dust after launch. There is some evidence of static cling inside the tube and a large deposit of cork dust on the end of the tube which may have resulted in fewer dust particles in free flow in the tubes and less resolution of modal patterns for the video recording. These are problems students will have to consider and resolve in their after flight analysis

#### **Passive Experiments**

Results of many of the seed experiments are not available at this time because students are awaiting seasonal growth of their plants. We are in the process of gathering all the student papers together and hope to have a list of results available for the September 1995 symposium.

### **Educational**

#### **AMPS Experiment**

The 9th - 12th grade NORSTAR students learned much from the process of developing the G-325 payload. We hope that they learned the skills that were previously listed and feel that their portfolios, presentations and the successful integration and flight of an experiment which was entirely accomplished by these students show the success of this educational project. When questioned about what they learned, the students expressed that the main lessons they learned were as follows:

- **perseverance:** the knowledge that all projects are not achieved without expenditure of time and personal involvement.
- **science:** the students felt that they had learned a considerable amount of physics.
- **group working skills:** all students felt that the NORSTAR experience had prepared them well for the teamwork situations found in most research labs, industry and businesses today. They stated that they have found these interpersonal skills of great value in other classes and in their daily lives.
- **responsibility:** seeing a project through to the end and being personally responsible for your part in the whole project.

Students said that this project has given them their first insight in to the real processes of the science/ engineering workplace. In one student's words " The NORSTAR experience educated me about science facts but more important, to me, is the way the program functions. It has given me independence to make decisions and then to learn to live with the consequences. In a normal textbook science experiment, if I got the wrong result I could modify or doctor data to satisfy what I knew would be the correct answer. At NORSTAR with the G-325 payload I learned that there was no fudging of results. I had to be responsible, it is a real project. I had to be honest, meet deadlines and really care about my work because my small part could affect the overall success of a 'real' experiment. This was exciting and tiring. I spent many extra hours repeating, revising and rethinking ideas. I was not working for a grade I was working for the project, the experiment, to discover. What I did was important and this was what meant most to me." This student is presently working a summer internship program at NASA LaRC.

Suffice it to say that the NORSTAR team believes that this 'real work' experience is beneficial to students beyond the normal high school experience. We feel that research and industry is looking for such prepared graduates.

### **Passive Experiments**

Teachers and students (2nd - 7th grades) were enthusiastic about the chance to participate in a space experiment. Five of these students and their parents were present at the launch of the project. We found that NORSTAR students benefited from activity as mentors to younger students. Although the experiments were at elementary levels, the students were enthused about space and sending up 'real' experiments whose result they could not exactly predict. We noticed that the younger students were more confident in their predictions than those who were older. Teachers told us that the process of developing the passive experiments taught students the importance of the scientific processes including: proposing a problem, research in books, hypothesizing, and planning the experiment with appropriate variables. The enthusiasm of these young students, both the initial contact and through later weeks of planning, resulted in increased parental and teacher interest in their learning as noted by parental and teacher calls asking for information about the NORSTAR project. The main problem has been that these young students have gone on to the next grade. We have learned that such projects should involve teachers in several grade levels so that youngsters can be monitored and mentored through these grades for the extended time it may take to complete the initial experiment and analysis of results. We must find some way to promote continuity. These young students began their space experiments in September of one year but the experiments did not fly until the following September and were returned to site in December. There must be some link between grade levels and teachers in a school system to ensure follow through and results. We are working on this problem to reach solution before our next attempted GAS project. Several ideas have been proposed, including:

- city wide training of teacher groups who will work together through several grade levels to provide follow up and closure
- selection of already existing cadres of teachers who are working in several grade levels
- working through guidance departments and elective programs particularly set up for such integrated experiments
- maintaining regular weekly contact with teachers and students

We encourage future GAS users to meet frequently with elementary and middle school students who are piggy backing on a main experiment. Enthusiasm generated during initial contact must be maintained (sometimes for a year or more through several grades) so that closure can produce meaningful results for these students.

## **FOLLOW UP**

The NORSTAR program is still, and probably always will be, changing and progressing. As new ideas and problems emerge and new contacts are made in business, industry and research, our ideas will continue to expand as they need to do in our rapidly changing technologic society. Flexibility, tempered by solid science processes, allows NORSTAR students to prepare for a future that will often present problems, that will call for both creative thinking and a solid grounding in reality. We hope in the future the NORSTAR program will present students with other real life challenges. We envision, after analysis of our first payload, a second GAS payload that will perfect our G-325 project, and present more tangible experimental results that will contribute significantly to the field of acoustic resonance research. We plan to include several other experiments in our payload of equal scientific significance in order to utilize the 5.00 cubic foot canister to its utmost efficiency.

In conclusion, the experience has been an exciting adventure for many K-12 graders. It has been a real working experience for students and teachers. Students have reacted positively and have stayed with the project through moments of deep despair, frustration and aggravation. They have, through mentor support and NASA commitment come through to an understanding of science principles and the knowledge that hard work, intuition, cooperation and vision can produce a tangible, fulfilling, life experience. We hope that this type of program will help many students to experience the freedom to touch the trail of a comet and be so lifted from the regular that they will want to persevere to significantly contribute to mankind's exciting and constantly changing future.

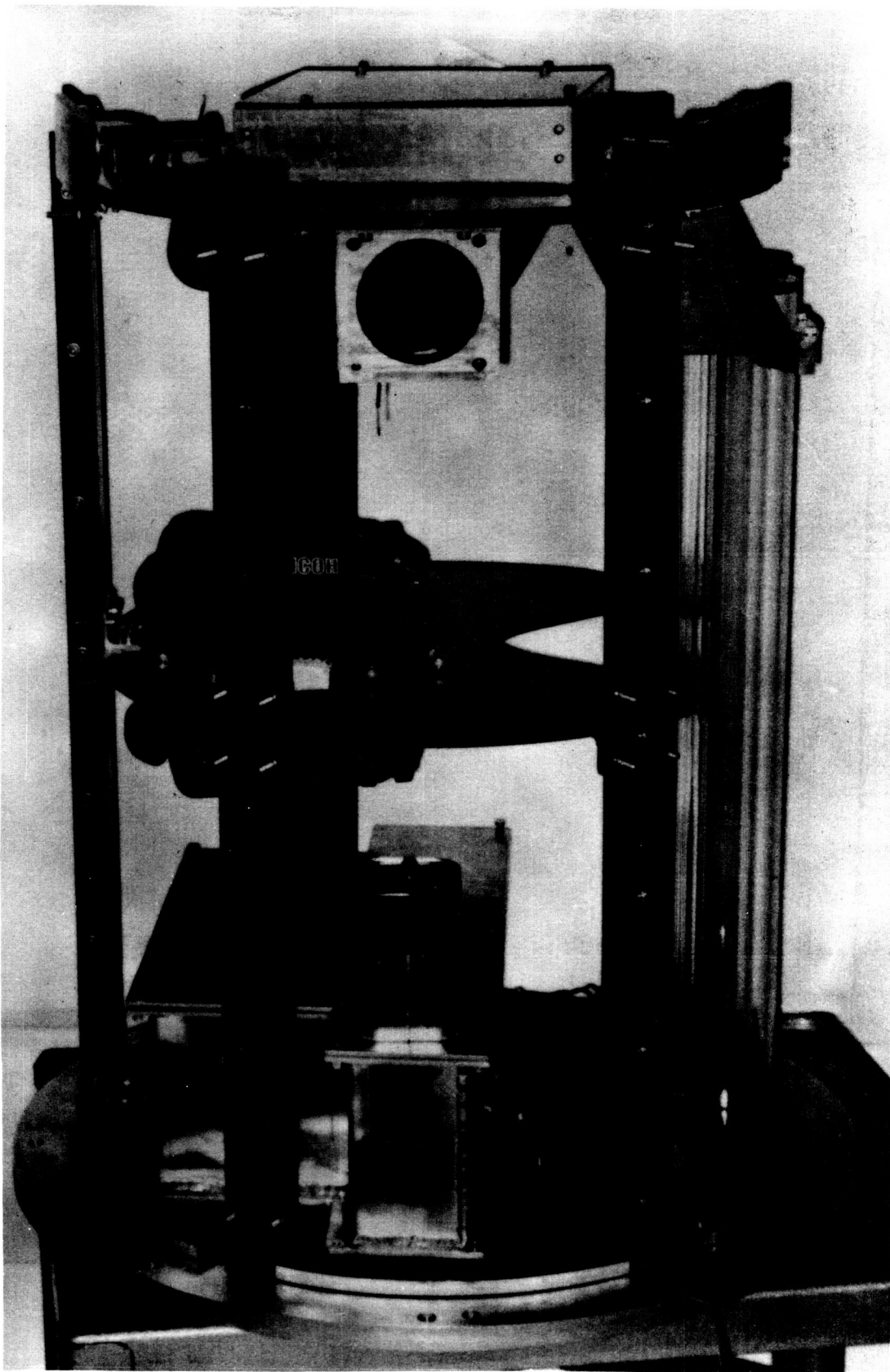


FIGURE 3. NORSTAR G-325 AMPS PAYLOAD

## CONSTRUCTION OF THE GAMCIT GAMMA-RAY BURST DETECTOR (G-056)

Michael H. Coward, John M. Grunsfeld\*, Benjamin J. McCall, Albert Ratner  
California Institute of Technology, Pasadena, California 91125

### ABSTRACT

The GAMCIT (Gamma-ray Astrophysics Mission, California Institute of Technology) payload is a Get-Away-Special payload designed to search for high-energy gamma-ray bursts and any associated optical transients. This paper presents details on the development and construction of the GAMCIT payload.

In addition, this paper will reflect upon the unique challenges involved in bringing the payload close to completion, as the project has been designed, constructed, and managed entirely by undergraduate members of the Caltech SEDS (Students for the Exploration and Development of Space). Our experience will definitely be valuable to other student groups interested in undertaking a challenge such as a Get-Away-Special payload.

### SCIENTIFIC MOTIVATION

The first report of gamma-ray bursts (GRBs) occurred in 1973 from earth orbiting satellites. GRBs are highly energetic events that are characterized by a rapid increase in the observed gamma-ray flux, at energies from tens of keV to several MeV's. The decline of such events may be a simple exponential or quite complex non-linear decay. Three gamma-ray bursts observed by the BATSE detector on the Compton Gamma Ray Observatory are depicted in Figure 1. [2]

It soon became evident that gamma-ray bursts represent one of the most energetic and violent events in the observable universe. Ever since the first detection of these phenomena, many experiments, including the BATSE experiment, have been designed to monitor them, yet their origin is still one of the great enigmas of modern astrophysics. The BATSE observations have yielded important data on the possible location of these events. By determining the coarse location of these bursts, BATSE researchers have observed an isotropic distribution of GRBs. Furthermore, from studies of the intensities of the bursts, researchers have deduced that the bursts are not distributed homogeneously, but have a definite boundary. [3] The distribution of a sample of gamma-ray bursts, observed by BATSE and showing their isotropy, is shown in Figure 2. These facts indicate that the bursts are either local to the solar system, distributed in a large halo around the galaxy, or at cosmological distances. One theory suggests that the neutron stars in binary systems are the cause. In this scenario, a normal companion star transfers material into an extremely strong gravitational potential well near the neutron star. The energy gained by this matter is converted into gamma-rays near the surface of the neutron star producing a gamma-ray burst. Other models predict that comets, or other material is accreted by an isolated neutron star or black hole producing a GRB. An interesting prediction of the former theory is that as the gamma-rays strike the atmosphere of the

---

\* NASA Johnson Space Center, Houston TX 77058



companion star, some of the gamma-ray energy may be converted to visible light. If these theories are correct, then a GRB may be accompanied by an optical transient. [4]

## **OVERALL SYSTEM DESIGN**

GAMCIT uses two standard NaI(Tl) scintillation gamma-ray detectors, combined with a 35mm film camera and film sensitive to visible light. GAMCIT is the first experiment to search for gamma-ray bursts and their associated optical transients truly simultaneously. An on-board computer triggers the camera when a burst is detected by the scintillators.

During the system design, the GAMCIT team decided to store the energy and arrival time for every gamma ray photon incident on the detectors during the mission. Most experiments to date have either stored the photon data only during gamma-ray bursts, or by the data into time and energy bins. Storing every incident photon does dramatically increase the amount of on board storage required by the payload, but it reduces the complexity of the hardware and software, and opens up the possibility of doing significant advanced post-flight data analysis.

## **STRUCTURAL DESIGN**

The three major structural components of the GAMCIT experiment are the user lid, the main supporting structure, and the battery enclosure. The GAS lid is the attachment interface between the can and the NASA mounting plate. Since we are using a Motorized Door Assembly (MDA), a major task was designing a space facing pressure vessel lid. The concerns that were dealt with during the design process were structural integrity, thermal insulation, and maximization of gamma-ray penetration.

These concerns were dealt with using a User Designed Mounting Disc (UDMD). The UDMD was machined out of a solid acrylic disc 53 cm in diameter and has three circular cutouts for the two photo-multiplier tubes and the quartz window for the camera. In addition, it has three small holes for mounting three vacuum rated electrical feedthroughs to carry signals and power to the top of the lid. One of the challenges of the structural design was to ensure that the lid would not leak despite the components mounted in it. To achieve this goal, each component mounted in the lid had an O-ring seal. An example of these O-ring seals can be seen in figure 3.

To thermally isolate the UDMD from the Experiment Mounting Plate provided by NASA, an Experiment Thermal Isolation (ETI) consisting of an acrylic ring 50 cm in diameter and 3.2 cm in thickness was used. To further reduce the thermal conductivity between the mounting plate and the UDMD, titanium bolts were used instead of traditional steel bolts to connect the EMP, ETI, and UDMD because of their lower thermal conductivity. Figures 4 and 5 provide two views of the EMP, ETI and UDMD.

The main supporting structure is composed of three aluminum sheets which divide the GAS compartment into three pieces. The three sheets meet in the center and run along the length of the can. The sheets fit into machined slots on the UDMD and another

acrylic disk on the bottom of the can. The UDMD and bottom disk are attached together by 10 rods that run the length of the can.

The battery enclosure is one of the more unusual aspects of the GAMCIT payload. In order to maximize the space available for the experiment hardware, a Tubular Battery Enclosure (TBE) was designed. Instead of the traditional battery box, the TBE consists of 21 PVC tubes, each of which holds 10 batteries. In flight configuration, only 19 of these tubes are filled due to weight considerations, but all of the tubes are identical. Each tube has a copper disk on the top and bottom, with a spring on one end, leading to a "flashlight" type of system. Figure 6 provides a view of the TBE.

## **DETECTOR DESIGN**

The GAMCIT detector system is composed of two major subsystems: the gamma-ray detector system and the optical transient detection system. The gamma-ray detector is composed of two NaI(Tl) scintillator crystals, 13 cm in diameter, and 2.5 cm in thickness. Each crystal is coupled to a 10 stage 13 cm photo-multiplier tube (PMT). The PMTs collect the photons emitted by the crystals and convert them into an amplified electrical signal. Because of the protective aluminum shell around the crystal, the lowest energy gamma-ray photons that can be detected is about 50 keV. To extend the range down into the hard x-ray region, two experimental avalanche photo-diodes provided by Dr. Desai of Goddard Space Flight Center will be flown. [4]

The other major system is the optical camera system. The system is comprised of a professional 35mm film camera with a 250 exposure data back. The lens system is a standard 50mm f/1.2 lens available from the camera manufacturer. Since the image is to be photographed at infinity, and the depth of field is unimportant, the lens may be stopped down to the lowest setting (f/1.2). The focus ring, however, must be fixed so that vibrational stress does not cause the camera to de-focus. The data back holds 250 exposures, and each burst triggers the camera for five exposures, giving us enough film for 50 bursts. This is an over-estimate of the number of real bursts that are statistically expected, however, false triggerings may significantly increase this number.

The film used is a standard ASA 3200 film which will be pushed during processing to ASA 50000. With our optical system, we can expect to see up to seventh magnitude astronomical objects.

## **ELECTRONICS DESIGN**

The core of the electronics is an embedded 486 single board CPU. Although the team considered building a custom microcontroller board for the experiment, the use of a standard board allowed for more rapid prototyping and development of the controller. This controller is responsible for all instrument control, data handling and system maintenance functions. Figure 6 shows a block diagram for the payload.

The primary function of the controller is to identify and record a gamma-ray burst. This is accomplished by having the output current from the PMT pass through the

amplification and detection electronics. The signal from the PMT passes through a charge sense amplifier that converts its current pulse into a voltage spike. This spike is then integrated to give a voltage proportional to the energy of the incident gamma ray photon. This voltage is digitized by a high-speed 12 bit analog to digital converter and is fed to the CPU.

The CPU examines the incoming photons and triggers the camera when it detects a burst. For the purposes of the payload, a burst is defined as an increase in the gamma-ray count of 5.5 sigma. When the burst is detected, the CPU will trigger the camera to take five successive frames.

The CPU also stores the incoming time and energy of every time to the data storage subsystem. It consists of an array of 5 800 megabyte hard disk drives. The drives were originally designed for use in laptops, and as a result, are both low power and rugged, with shock and vibration specifications well in excess of the Shuttle launch and landing specifications. To reduce power, the drives will be powered down for the majority of the flight, and will only be powered up for short intervals to write the accumulated data. To buffer the data, a 32 megabyte static ram array is attached to the processor to reduce the number of times that the drives must be powered up.

To achieve accurate time stamping of incoming gamma-ray photons and to allow for accurate position information, a Global Positioning unit (GPS) is used. Because of the doppler shifts caused by the speed of the Shuttle, traditional GPSs would be unable to acquire enough satellites to obtain a position and time fix, but the GPS manufacturer has provided special software to enable it to acquire in a low earth orbit. When the GPS acquires, it provides a pulse every second which is accurate to within a microsecond. The CPU uses this pulse to establish an accurate time of arrival for every photon that is seen by the PMTs.

## **POWER MANAGEMENT**

One of the primary concerns of the GAMCIT team was the power source selection, since all Get-Away-Special payloads must be totally autonomous from the Space Shuttle Orbiter except for the crew activated relays. Thus, upon drawing up a power budget, it was our task to determine which type of power source was the most appropriate to our application requirements. After a careful consideration of the products currently available on the market, and of those that fell within the NASA safety margins, we decided on standard commercially available alkaline D-size cells. The cells have a nominal voltage of 1.5 V with a rated capacity of 14.25 Amp-hours.

The major problem one encounters with alkaline cells is the less than ideal discharge characteristic. In general, such cells discharge linearly with time from their nominal voltage (1.5 V) to the rated cut-off voltage (0.8 V). In order to overcome this difficulty, we were forced to use a DC-DC converter. The DC-DC converter that we chose has an input voltage range from 7-35 VDC, and three output terminals: two at 12 VDC and 0.7 amperes maximum, and one terminal at 5.1 VDC and 5.0 amperes maximum.

The actual battery setup is configured as 19 packs of 10 batteries each, for a total of 190 batteries. Each pack of batteries provides 15 VDC nominally, discharging to the cut-off voltage of approximately 8 VDC. Each parallel leg of the total battery power supply is protected by a Schottky diode to prevent circulating currents which would lead to mission failure. In addition, the whole power supply is protected by a 6 Amp fuse, chosen in accordance with NASA regulations, on the ground leg.

The electronic system is fully powered through the DC-DC converter, expect for a two clocks, one on the GPS, and one on the CPU, powered by small watch type silver-zinc cells.

## **CONSTRUCTION**

GAMCIT has been under design and construction for about four years. In the summer of 1993, GAMCIT was able to offer stipends to five students to work for ten weeks on the project. During the summer, most of the design details were hammered out, and prototyping began. Construction continued during 1994, with the bulk of construction taking place during late 1994 and early 1995. As construction progressed, new ideas continued to surface, and the design slowly evolved. Some of the changes were driven by component availability, with the most notable being the crystal size and shape. Originally, GAMCIT was to have two pie shaped crystals with plastic light integration cones connecting them to the PMTs. When the crystals became unavailable, two standard cylindrical crystals were substituted and it was decided to directly couple the PMTs to the crystals. Other changes were driven by ideas for better ways to solve the problems presented by the experiment, with the best example being the substitution of the Tubular Battery Enclosure instead of a conventional battery box.

## **INTEGRATION**

In May 1995, the GAMCIT team brought the payload to Kennedy Space Center for integration onto STS-69. During a routine leak check, a vacuum was pulled inside the can and the resulting reverse pressure on the lid was enough to fracture it. A replacement lid could not be fabricated in time, and the payload was pulled from the flight. The GAMCIT team is currently machining a new lid, and we hope to fly the payload in late 1995 or early 1996.

## **CHALLENGES**

The GAMCIT project at Caltech has been driven entirely by undergraduate students since its beginning. GAMCIT is a spin-off of the Caltech Students for the Exploration and Development of Space (SEDS), a student group with over one hundred members (over 6% of the student body, graduate and undergraduate). The sponsorship of SEDS has been essential to the success of the project, in terms of drawing in interested students, facilitating support from Caltech's administration, and bringing in start-up funds from aerospace corporations.

While the sponsorship of a large student group is very beneficial, our experience has proven that projects such as ours cannot succeed without faculty and staff support. Dr. John M. Grunsfeld served as our first advisor for the GAMCIT project, and was instrumental in obtaining recognition and laboratory space for the project, as well as in the preliminary design work. After Dr. Grunsfeld left Caltech to become an astronaut, the students of GAMCIT approached Dr. Maarten Schmidt of the astronomy department to serve as a faculty advisor. Dr. Schmidt's assistance has proven invaluable in securing financial support from Caltech and outside organizations to continue the project. It is also worth noting that securing course credit for work on the project has been very helpful in recruiting new members to the project team.

However, the challenges involved in the GAMCIT project go far beyond those of politics. Because our "engineers" are all undergraduates, the project's participants have faced quite a learning curve in all areas of the science and engineering of the payload. While this makes for a much slower timetable than projects in industry might enjoy, it also serves to provide a hands-on experience for undergraduates that is seldom available in standard university curricula.

As in any other workgroup, leadership, responsibility, and personal relations are critical issues to the success of a project such as ours. However, these problems are exacerbated by having an all-undergraduate working group - students are students first and space experimenters only in their "spare time." Offering course credit can serve as a limited incentive to get things done, but ultimately the motivation must come from the students' own sense of involvement in the project, which is in turn dependent in large part on the leadership and group dynamics of the project.

The challenges and pitfalls involved in a project such as ours, staffed entirely by students, are indeed distinct from those faced in similar projects in industry or the military. While the pitfalls are many, the rewards of a student-run project are even more plentiful. We welcome correspondence from present, past, or potential student groups who are interested in Getaway Special projects.

## **CONCLUSION**

The GAMCIT experiment has been a rewarding experience for all involved in its design and construction. GAMCIT also provides an almost guaranteed return, because any gamma-ray data collected can be correlated with similar observatories currently on ULYSSES, the Pioneer Venus Orbiter and the Compton Gamma Ray Observatory. A single optical transient correlated with a gamma-ray burst would provide a stringent constraint on burst theories.

## REFERENCES

1. McCall, B.J. et al.: The GAMCIT Gamma-Ray Burst Detector. 1993 Shuttle Small Payloads Symposium, NASA CP-3233, 1993, pp. 47-56.
2. Fishman, G.J., Meegan, C.A., Wilson, R.B., Paciesasm, W.S., Pendelton, G.N., The BATSE Experiment on the Compton Gamma-Ray Observatory: Status and Some Early Results, NASA CP-3137, 1992, pp. 26-34.
3. Meegan, C.A., Fishman, G.J., Wilson, R.B., Paciesasm, W.S., Pendelton, G.N., Hornack, J.M., Brock, M.N., and Kouveliotou, C., Spatial Distribution of Gamma-ray Bursts Observed by BATSE, *Nature*, 1992, vol. 355, pp. 143-145.
4. Stewart, A.C., and Desai, U.D.: New Room Temperature High Resolution Solid-State Detector (CdZnTe) for Hard X-Rays and Gamma-Rays. 1993 Shuttle Small Payloads Symposium, NASA CP-3233, 1993, pp. 25-32.

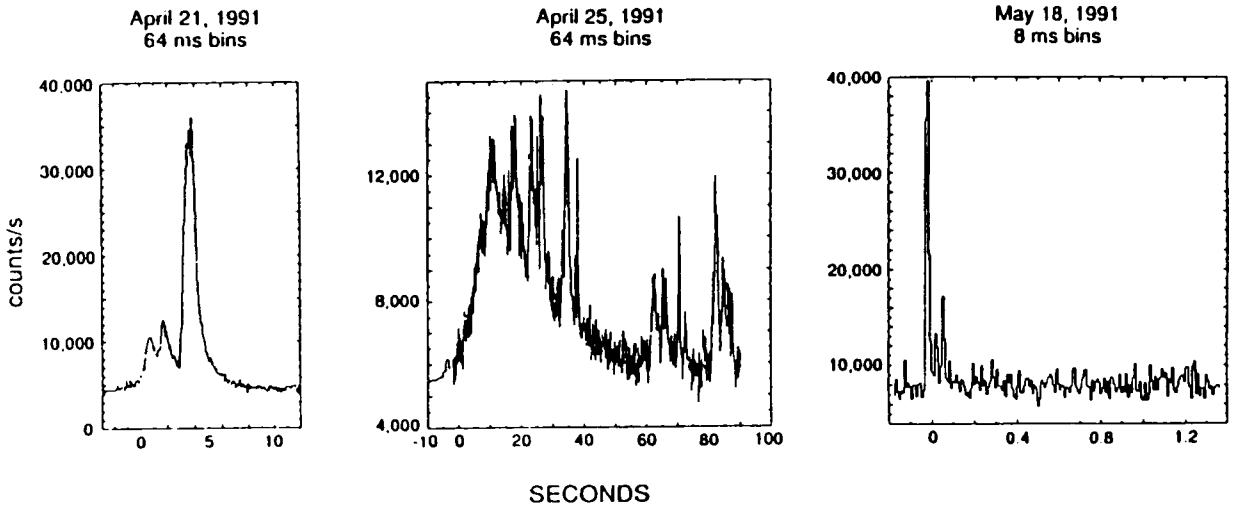


Figure 1 - A sample of gamma-ray bursts as observed by the BATSE instrument on the Compton Gamma Ray Observatory (reproduced from [2]). These burst profiles show the wide variety of structure and varying time durations of gamma-ray bursts, from milliseconds to 100s of seconds. The energies of the gamma-rays in these plots range from 60 keV to 300 keV.

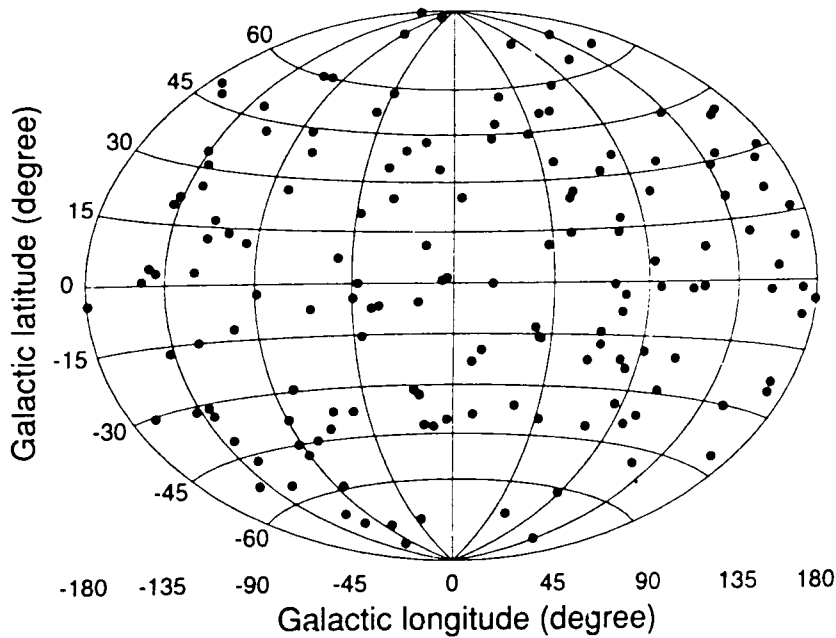


Figure 2 - The angular location of gamma-ray bursts in Galactic coordinates as observed by the BATSE instrument on the Compton Gamma Ray Observatory (reproduced from [3]). The observed distribution shows no significant deviation from isotropy. In particular, no enhancement along the Galactic plane (latitude=0) is seen, as would be expected if the sources of gamma-ray bursts had the same distribution as the stars in the Galaxy.

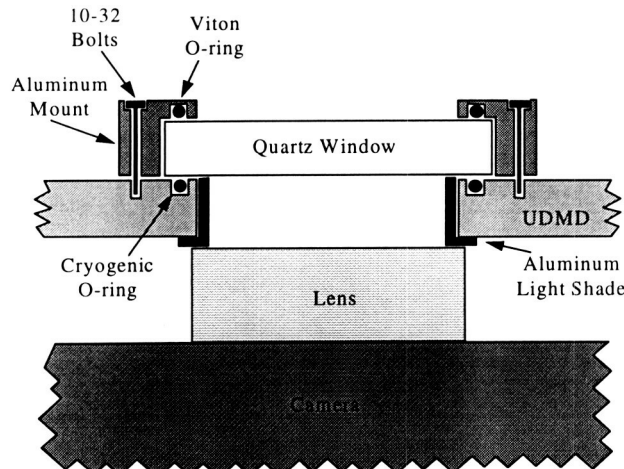


Figure 3 - O-ring seal on quartz window for Camera

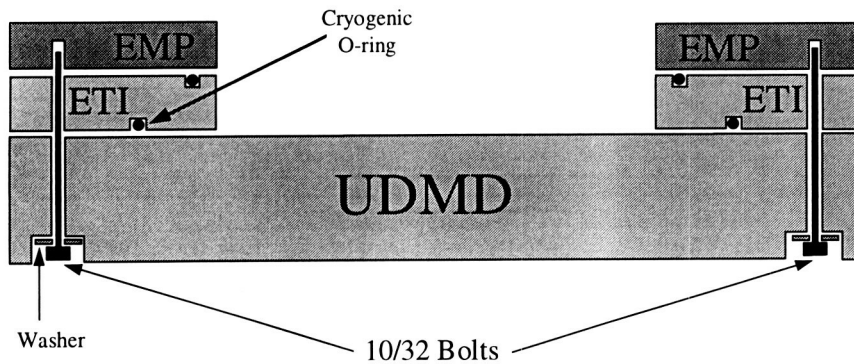


Figure 4 - Side view of UDMD (User Designed Mounting Disk), ETI (Experiment Thermal Isolator), and EMP (Experiment Mounting Plate)

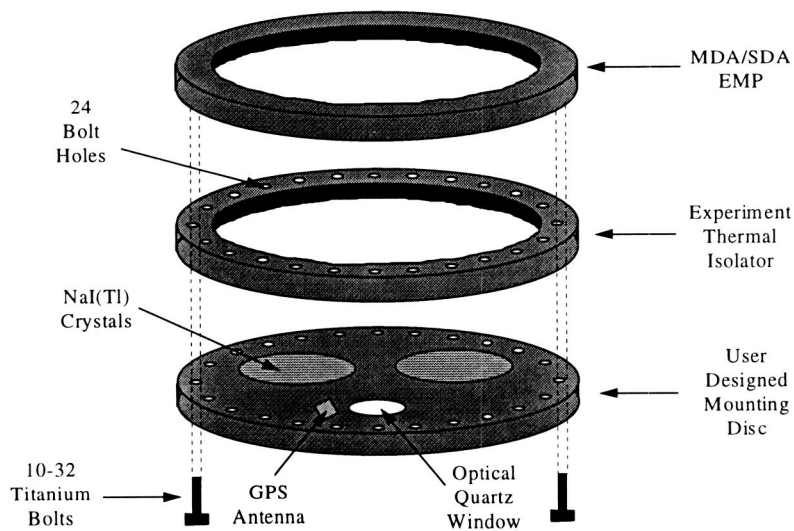


Figure 5 - Exploded view of EMP, ETI, and UDMD



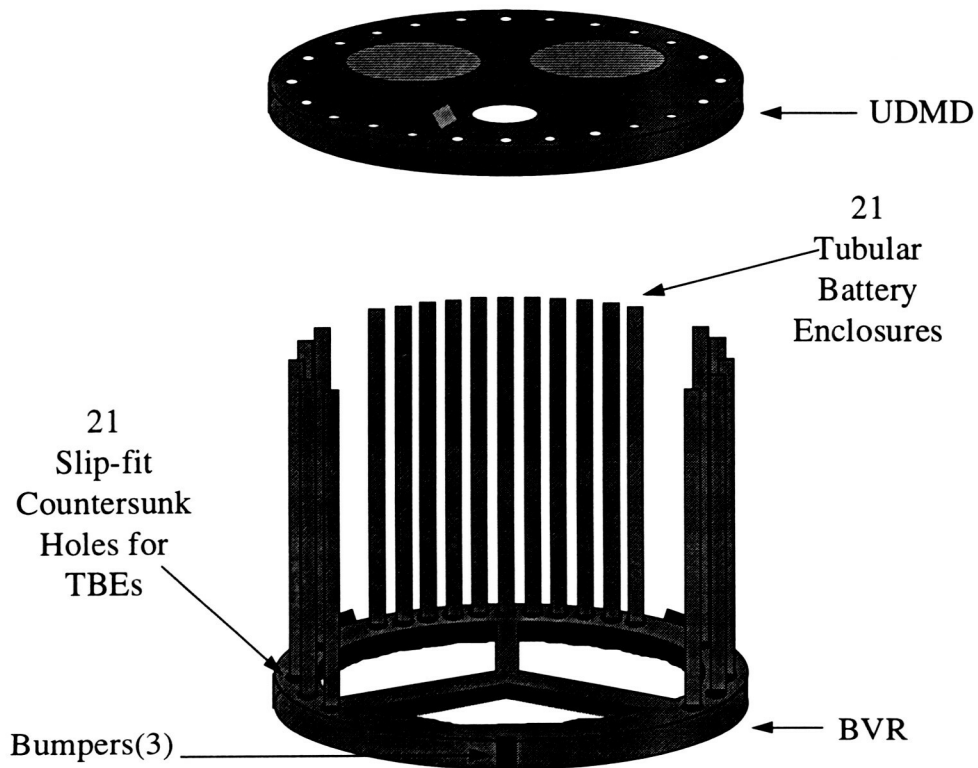


Figure 6 - Tubular Battery Enclosure

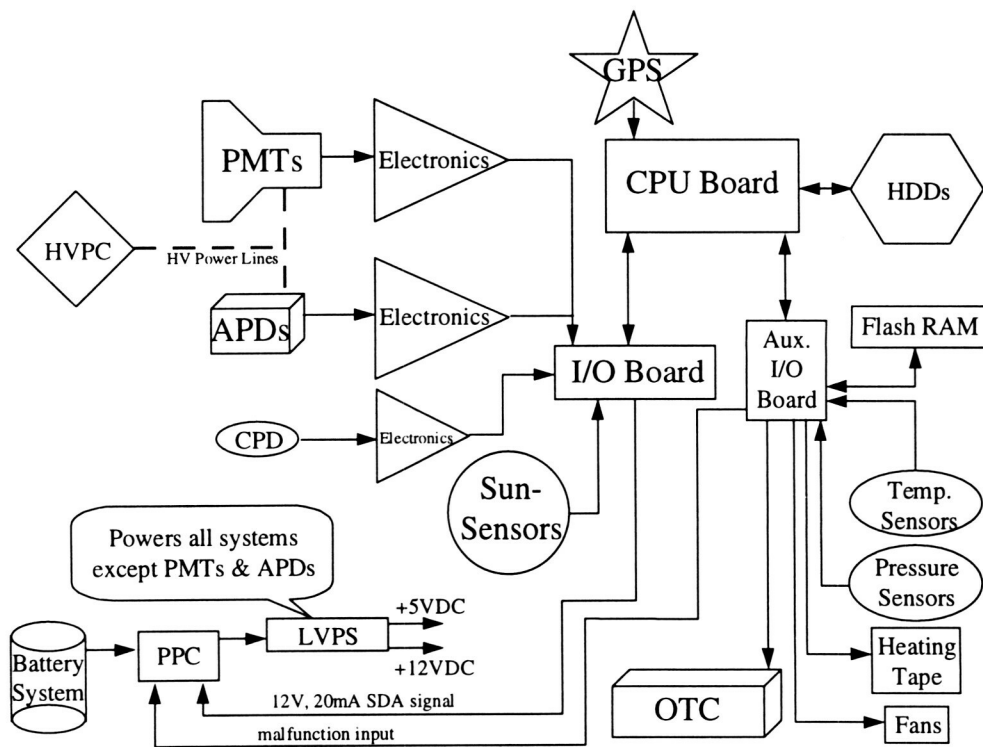
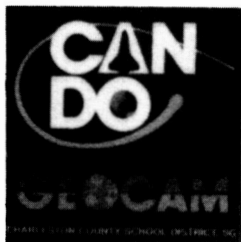


Figure 7 - Block Diagram of the Electronics Subsystem



## PHOTOGRAPHING THE EARTH G324, The CAN DO GeoCam Payload

James H. Nicholson and Thomas J. O'Brien  
Medical University of South Carolina  
Carol A. Tempel  
Charleston County School District



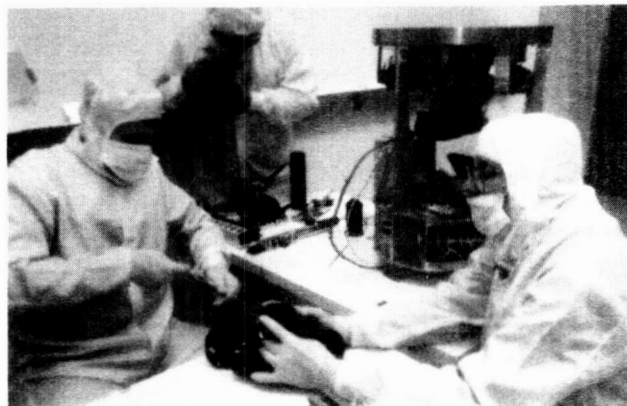
### ABSTRACT

The flight of the Charleston County School District **Can DO** Project **GeoCam** payload on STS-57 was the climax of a decade long endeavor to bring the promise and excitement of the space program directly into the classroom. The payload carried four cameras designed to take high resolution photographs of the Earth under the direction of children operating the first ever student control room. During the course of the flight, the students followed the Shuttle's orbital tract, satellite weather images and selected a target list that was sent up to the crew each night as part of the execute package. Targets from this list, as well as ones chosen by the crew visually, resulted in the successful collection of photographic runs at many interesting sites on three continents.

### EDUCATION AND EARTH OBSERVATION

Later this decade, earth sensing platforms will analyze Earth processes as part of a multi-national program, *Mission to Planet Earth*. By examining the past and monitoring the present it is possible to reach a deeper understanding of the Earth as a complex system. Photographic comparisons are powerful teaching tools, especially in the appreciation of change over time. By comparing transformation documented in earth viewing photographs, changes that occurred in our lifetime can be observed. Photographic documentation of global change makes it more immediate and real.

NASA and other agencies are concerned about the projected shortage of scientists and technicians able to understand and use complex global data. At the height of the *Mission to Planet Earth* program, approximately two terabytes of data per day will be generated. This staggering amount of data needs to be analyzed and assimilated to be of value. Students need training now to be able to understand and use this information in the future. An important goal of the *GeoCam* mission is to provide hands-on experience for students in visualizing and interpreting global environmental change. This training will better prepare them to make informed decisions that will determine the quality of life on the battered world that they will inherit.

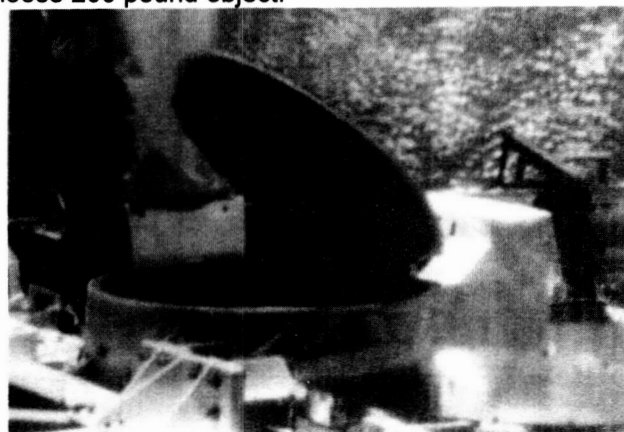


G324 Payload Integration

Can Do Photo

### TECHNICAL DESCRIPTION

G-324 flew as a five cubic foot payload contained behind a Standardized Door Assembly (SDA) fitted with a 0.92 inch by 19.25 inch fused silica window. An internal 0.625 inch aluminum faceplate, which supports four Nikon F3 cameras fitted with 250 exposure film backs, also provides impact isolation for the window as an integral part of the payload fracture control plan. This plan calls for the isolation of the window from debris weighing 0.25 pounds or more, a size that could conceivably scratch it. A nick or microscopic scratch on the window could propagate to catastrophic proportions, making this a failure point in the structure. A sealed five cubic foot flight canister itself is considered containment for a loose 200 pound object.

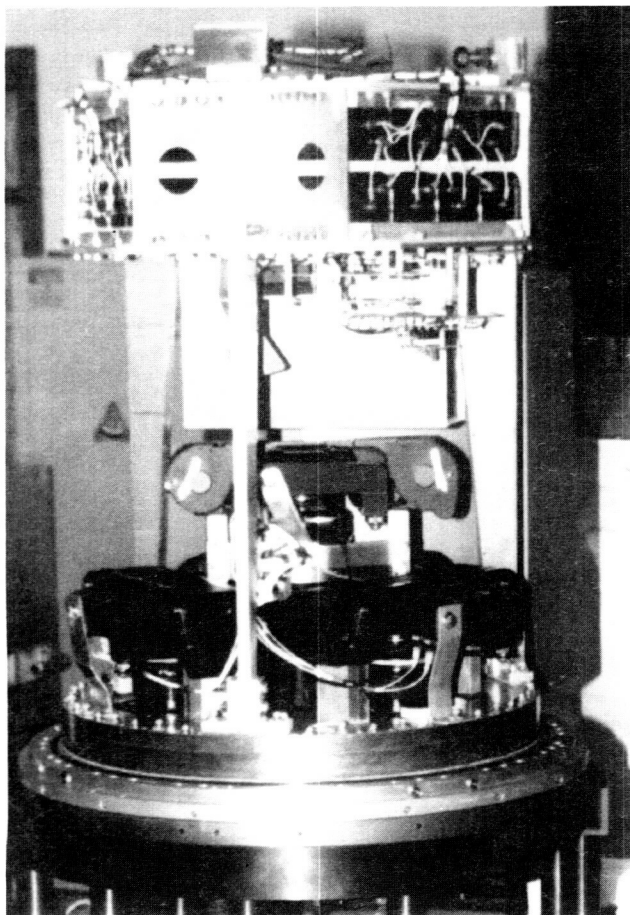


S.D.A. Opening

NASA TV

During ascent, a barometric pressure relief valve lowers the internal nitrogen pressure to 7.5 psia in an effort to further reduce the stress on the window. At payload activation - or during operation, a differential pressure switch monitors the internal pressure of the payload. If the internal pressure approaches the cargo bay pressure, there is a seal failure, and it must be assumed that there is a failure of the window. Upon detecting a failure, the differential pressure switch will inhibit SDA operation to protect the cargo bay and vehicle from debris damage. The SDA is further protected with an interlock from payload power which is controlled by GCD-A from several banks of 12-volt alkaline batteries.

In addition to the 1000 picture capacity of the cameras in the primary experiment, the G-324 flight contained 261 individual passive experiments, each in a 5.0ml cryogenic containment vial. The passive vials were further contained in an 11.5 x 7.5 x 4.5 inch aluminum box bolted to an internal structural plate. This method of containment, coupled with preselection guidelines, stringent materials examination, and full documentation, greatly simplified the safety procedures.



Can Do Photo

## **THE PAYLOAD POST FLIGHT**

Post flight inspection of the payload was carried out in two stages. A general inspection of the payload and canister was carried out during deintegration of the payload at the Cape, and a detailed examination was performed after returning to Charleston. The film magazines were quickly examined for mechanical failure as the canister was lifted off, and found to be intact with expended film. G-324 WORKED!

As the canister cleared the base (SDA deintegration takes place upside-down with the door in its jig), the rest of the payload appeared intact. At this point, loaded voltage readings were recorded on all batteries, and found to be well within the expected range. The environmental system was higher than expected, indicating minimal drain by the heaters, thanks in part to the earth viewing mission. All four cameras indicated a full mission profile run by the film counters, but two showed inconsistent values. Later examination showed the counters probably shifted due to vibration, since the film was expended. The payload was separated from the SDA by removing the 10-32 mounting ring bolts, and the payload was lifted free. An examination of the payload face and light baffles showed the flat black paint remained firmly bonded to all surfaces, the light baffles were intact, the baffle to lens seals were intact and all lenses were firmly locked to their respective cameras. An examination of the SDA window showed no visible scratches or damage to the interior window surface. Upon closer inspection of the SDA window, a slight greasy and somewhat crystalline blur about three inches in diameter was noticed in the center of the window. At the center of this blur was a slight buildup, translucent light brown in color, that resembled a slight bump or beginning of a drip. During the integration procedure, the window was meticulously cleaned and inspected by the GSFC integration crew and inspected and passed for assembly by both the G-324 PI and Chief Engineer. During the final test of the payload after integration, the door was opened and the cameras cycled for one complete nine exposure photo series. At that time, the window was again checked for contamination, and none was found. The spot had the appearance of a condensation deposit that resembled the Apiezon grease used on the sealing O-ring. A sample wipe was taken for later analysis by the integration crew.

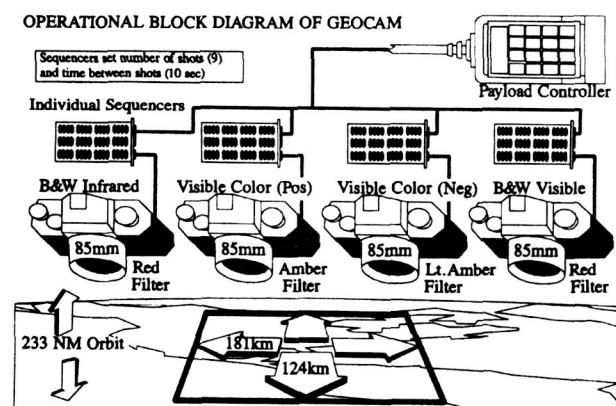
All cameras performed as expected, yielding outstanding photographs, with the exception of the center camera. Although a few photographs are relatively clear from this camera, analysis shows the blur was there from the beginning. The deposit is dynamic in nature, changing its brown translucent

density during the 125 orbit mission. GSFC will make further tests to determine the origin and mechanism of the deposit and determine the procedures necessary to prevent its recurrence on future flights of the window.

## CAMERA SYSTEM

The GeoCam camera system consisted of four 35mm single lens reflex cameras equipped with 250 exposure film backs. The lenses were chosen to specifically match the STS-57 planned altitude of 230 nm. With a 85 mm focal length lens, each photograph encompassed an area of approximately 180 km by 125 km (22,400 km<sup>2</sup>). This compares with 26,500 km<sup>2</sup> for the Skylab S190A multispectral camera system which GeoCam was designed to emulate.

The camera system lacked any positive motion compensation to prevent image blur so shutter speeds were selected to prevent motion degradation of the images. Using the orbital speed of 7.66 km/sec and calculating the limits of motion to prevent visible blurring, it was determined that a minimum shutter speed of 1/500th was required. By using 85 mm lenses with a maximum aperture of f1.4, this exposure was achieved while still permitting the use of high resolution slow speed films. The lenses were set at or near the maximum aperture of f1.4 because the Earth was always at infinity focus and depth of focus was not a consideration. This required careful prefocusing on an optical bench and positive securing of the focus mechanism to prevent slippage due to vibration.



## FILM AND FILTER SELECTION

To compensate for the relatively small 35 mm film size, the films selected were the finest grain, highest resolution available. The Skylab S190A camera system used four types of film; black-and-white visible, black-and-white infrared, color infrared and color visible. It was determined that the infrared color film would significantly deteriorate during the relatively long GAS payload storage period, so it was

reluctantly omitted from G324. An extra roll of color negative film was flown as a back up to the color transparency film instead. This turned out to be a fortunate choice.

All of the cameras were equipped with filters either to limit spectral range or to correct image quality. In all cases, the filter was used to eliminate the ultraviolet which is the wavelength most scattered by particulates and pollutants in the atmosphere.

FILM TYPE	FILM SPEED (iso)	FILTER TYPE	FILTER COLOR	WAVE-LENGTH (μm)
B&W Infrared	50	25	Red	0.7-0.9
Color (Slide)	64	85B	Amber	0.5-0.7
Color (Print)	25	81C	Light Amber	0.5-0.7
B&W Visible	25	21	Orange	0.6-0.7

## OPERATIONAL CAMERA CONTROL

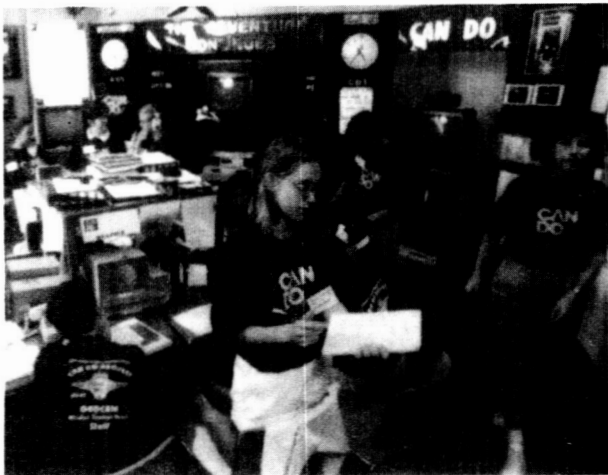
The shuttle crew initiated each camera activation. Each camera was controlled by an individual sequencer to control the number of individual shots for each activation and to set the interval between photographs. The interval was determined by the coverage of the lenses and the orbiter's speed over ground. On STS-57, a 10 second interval between shots provided an image overlap of 15 - 50% depending on the orientation of the rectangular film format to the direction of the orbiter's forward motion. Each photo sequence consisted of nine shots on each camera.

Exposure was controlled by the cameras standard automatic exposure meter. The film speed was determined by careful ground testing using actual lenses and filters and controlled lighting simulating in-flight conditions. This resulted in usable exposures on all shots with only minor variations caused by such artifacts as bright clouds in the center of the active meter. In no case were these variations beyond range of printing correction.

## THE CAN DO GeoCam CONTROL ROOM

To allow students to directly participate in the flight and to have active input in the Earth photography, a unique control room was set up at the Medical University of South Carolina. The functions were divided into four desks each operated by a team of four students with a teacher advisor.





Student Control Room

NGS Photo

### **OPERATIONS**

Students at the operations desk monitored crew activities by using the mission timeline. They updated the timeline as required by monitoring NASA Select Television and Shuttle radio transmissions. It was their responsibility to know when orbiter orientation and crew activities permitted use of the camera system.

### **WEATHER**

The weather desk staff monitored worldwide weather patterns to look for cloud conditions that would allow successful photography. They relied on satellite weather images relayed by the Earth Observation Lab at Johnson Space Center. Additional information was supplied by a student team working at the Charleston Air Force Base weather office. The students forecast weather and cloud conditions one day ahead since each day's target selections were made for the next day's execute package.

### **TARGETING**

The students at the targeting desk correlated the daily orbital path of the shuttle with potential targets of geological or environmental interest. Targeters had to have a thorough knowledge of geography, geology and maps. Candidate targets were checked through the weather and operations desks to determine if photographic coverage was possible.

### **COMMUNICATION**

The communications staff worked with targeting and operations to prepare the target list for the Johnson Space Center to uplink to the shuttle. They prepared daily updates on the flight for press and student briefing. This desk was also responsible for handling all public relations activities.

### **CONTROL ROOM EDUCATIONAL BENEFITS**

Far more than the production of the daily target list, the main value of the control room was as an educational tool of immense power. The opportunity to operate in a meaningful decision making position proved to be a powerful motivation for learning. Students learned geography, orbital physics, shuttle activities and many other disciplines. Often this learning was done on their personal initiative based on a desire to maximize this once in a lifetime experience. Knowing that this was no simulation, but rather an actual functioning payload operations control room produced a very high level of interest and excitement. A senior editor from the National Geographic Society, use to student geographic ignorance, was amazed at the level of knowledge achieved by the targeting teams. A newspaper reporter was startled when a first grade student explained how to tell infrared from visible light satellite images. His class spent several Saturdays at the Air Force Base Weather Office learning these skills.



Targeting Desk

NGS Photo

### STS-57 CREW INPUT

In addition to their commitment to execute the student list as much as possible, the crew obtained permission to freely activate the cameras on their own initiative. This fostered a true feeling of team effort with the students. The crew was also in a position to take targets of opportunity that might not have been included in the execute package. The value of this teamwork was illustrated by the superb and extremely rare photo sequence of the Congo basin. The Congo is almost always blanketed in clouds and nothing in the weather satellite images indicated a change. Consequently, it was never listed as a potential target. The alert crew, however, spotted an opening in time to fire the cameras. The result was unique enough to rate a fold-out display in the August 1994 *National Geographic Magazine*.

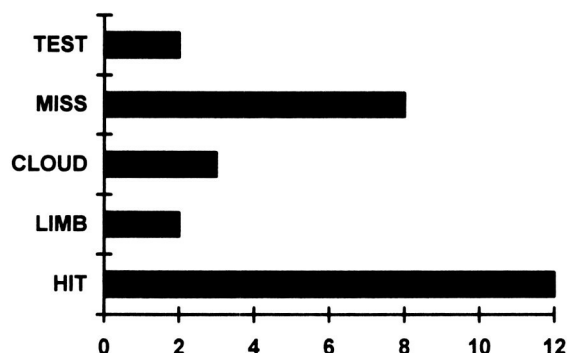


Astronaut Nancy Sherlock uses the A.P.C. NASA

### PHOTO LOG

All photo sequences activated by the STS-57 crew resulted in a full nine shot sequence on all four cameras. All cameras performed faultlessly until all available film was exposed. Not all activations resulted in successful photos of the ground however. The largest group of misses ( 30% of all shots ) were a result of the flight crew receiving inaccurate information from the ground concerning the angle of view of the camera system. This resulted in eight photo runs missing the Earth entirely. Aside from this mishap, the percentage of useful sequences on the remaining film was an outstanding 82%. The two runs showing the limb of the Earth proved both useful and popular although not originally planned.

### RESULT OF 27 RUNS



### LIST OF GROUND TARGETS

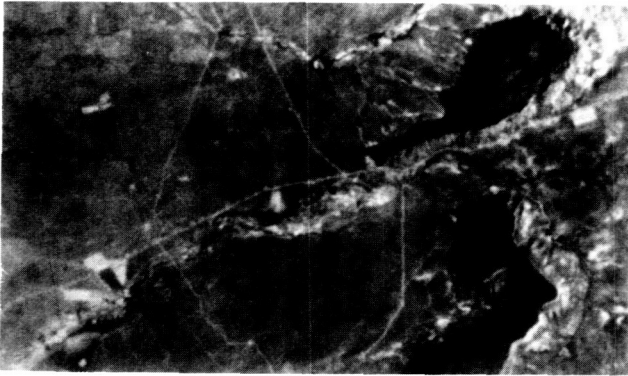
A list of the successful ground targets in the order in which they were taken:

1. Bahamas Islands
2. Skeleton Coast of Namibia (Africa)
3. Kalahari Desert (Africa)
4. Baja (Mexico)
5. Great Sand Sea of Namibia (Africa)
6. Hawaiian Islands
7. Atacam Desert of Chile (South America)
8. Chari River (Africa)
9. Lakes Albert and Kyoga (Africa)
10. Cape Verde on Senegal Coast (Africa)
11. Congo (Zaire) River Basin (Africa)
12. Katanga Plateau (Africa)



### SKYLAB TARGETS

One goal announced in the 1992 Symposium Proceedings was the attempt to rephotograph areas documented by the SkyLab S190A camera system. Technically, the GeoCam camera system did a good job of emulating the S190A. Unfortunately, in large part due to the time of launch, no matching areas were photographed.



Extreme Enlargement From a Photo of the Kalahari Desert to Show Clearly Resolved Roads and Trails.

GeoCam Photo

### **PHOTOGRAPHIC RESULTS**

Focus was consistently excellent validating the value of optical bench calibration. Enlargement of the negatives established that the 500th of a second exposure eliminated any evidence of image streaking from motion. The photographic experts at Johnson Space Center advised us not to expect resolution better than 30 meters at this image scale. This figure was based on results obtained with hand held cameras through the orbiter's multilayered safety windows. In fact, under ideal visibility conditions, resolutions under 10 meters were obtained. In the photos of the Kalahari Desert, individual trails and one lane roads were clearly resolved. In the dry air of the Atacam Desert, individual mining buildings and sheds are clearly seen. This extraordinary image quality was apparently the result of superb lenses, optical bench prefocusing, a top quality optical window and ultrafine grain film. On a later shuttle flight, the crew attempted to use the same black-and-white film. Because of the need to use a smaller aperture to compensate for manual focusing, the pictures were unsuccessful due to excessive motion.

### **PUBLICATION AND DISPLAY**

#### **Smithsonian Institution Air and Space Museum**

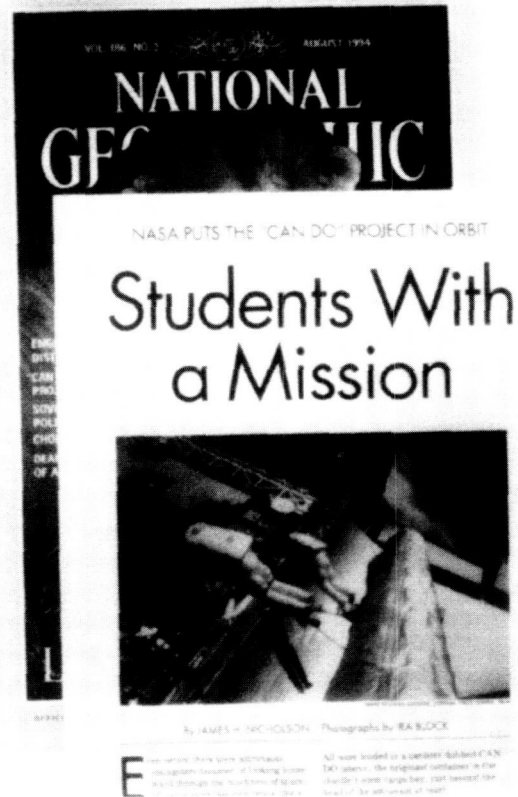
A black and white print of the Atacam Desert was selected for display in the "Looking at Earth Gallery" of the Air and Space Museum from Sept. 1994 to Sept. 1995. This museum is the most popular in the world with visitors.

#### **South Carolina State Museum**

The state museum in Columbia, South Carolina built a complete exhibit on the CAN DO Project. The exhibit includes color and black and white prints as well as a continuous video illustrating control room activities. Originally scheduled for one year, the display has been extended for another six months.

### **National Geographic Magazine**

A long time supporter of the project, the National Geographic Society became interested in an article as the flight became a reality. The result was a sixteen page article in the August 1994 issue. The article which covered the whole CAN DO Project, featured a centerfold with photographs of the Congo River and the Skeleton Coast of Namibia.



### **National Geographic WORLD Magazine**

As a companion to the article in the adult magazine, the National Geographic Society published an article in WORLD, their student publication. It also was published in August, 1994 and featured a photo of the shuttle above the Baja,

### **OWL Magazine**

OWL is a popular Canadian Children's magazine. It covered the CAN DO Project in a February 1995 article titled "Kids With a Mission". The article also covered some other student space activities.

### **SHUTTERBUG Magazine**

A photography magazine, *Shutterbug*, published an article in November 1994 titled "Space Photography - An Educational Experience". Written by freelance author Philip Chen, the article discussed the photographic design of the payload.

## EXPERIMENT MAGAZINE

In July of 1995, the Greek Magazine *Experiment* carried a 14 page article. The magazine is similar to National Geographic and carried a slightly modified version of the NGS article in Greek.



It's Greek to Us

### Η ΕΠΙΣΤΡΟΦΗ ΤΗΣ ΑΠΟΣΤΟΛΗΣ

Στο Διοσημικό Κέντρο Κένεντυ, ο μηχανικός Τζομ Ο'Μπράιεν κι ο συγγραφέας αυτού του άρθρου (απέναντι αριστερά) ανοίγουν τη σκευοθήκη της αποστολής CAN DO σμέως μετά την επιστροφή της. Η βοηθός της αποστολής Σάμερ Σπάρκμαν και ο μαθητής λυκείου Έιντριαν Νάιντα (αριστερά) επεξεργάζονται τους δοκιμαστικούς σωλήνες που έστειλαν οι μαθητές στο διάστημα. Η πεντακάθαρη φωτογραφία της Ακτής των Σκελετών (κάτω), στη νοτιοδυτική Αφρική, δείχνει τόσο πολλές λεπτομέρειες, που θα δώσει στοιχεία για πολλές γεωλογικές και γεωγραφικές μελέτες τα επόμενα χρόνια.

NGS/Experiment Photo

### South Carolina Educational Television

The entire project was superbly recorded in an hour long television documentary produced and regionally broadcast by South Carolina Educational Television. Television crews filmed every step of the payload construction and integration process. In addition, in-flight footage was provided through the courtesy of the television facilities at Johnson Space Center.

### POST FLIGHT EDUCATIONAL ACTIVITIES

Having obtained outstanding photographs of the Earth, the next step is to develop new and innovative ways to use them in the classroom. It has been discovered that excellent results are obtained through the use of very large prints which the students can examine in detail. Laminated 16 x 20 inch enlargements of the black and white photos have been produced for classroom use. The particular use depends on the grade level and interest of the class. One example is the use of the Atacam Desert photos to illustrate volcanism and mountain building. The run includes, dry lakes, new volcanoes and the edge of the Andes Mountains. The Katanga Plateau sequence has three major lakes all of which show obvious signs of loss of water level in recent years. They illustrate all too well the desertification afflicting so much of Africa. Photos can also be used in conjunction with other educational materials. The striking photo of the Skeleton Coast of Namibia shows many of the features described in the National Geographic television feature and magazine article on this desolate spot. Individual teachers develop curriculum based materials in their particular areas of interest which are then shared with other teachers.

## GROUND TRUTHING

In July 1995, 28 Charleston County Teachers sailed to the Bahamas as part of a special course in Tropical Marine Science. They were able to sail across and dive on some of the reefs shown in the beautiful photos taken of the Berry Islands. This unique ground truthing experience helped the teachers see close up the information contained in the GeoCam photos.



Teachers "Ground" Truth the Bahamas by Sailboat  
Can Do Photo

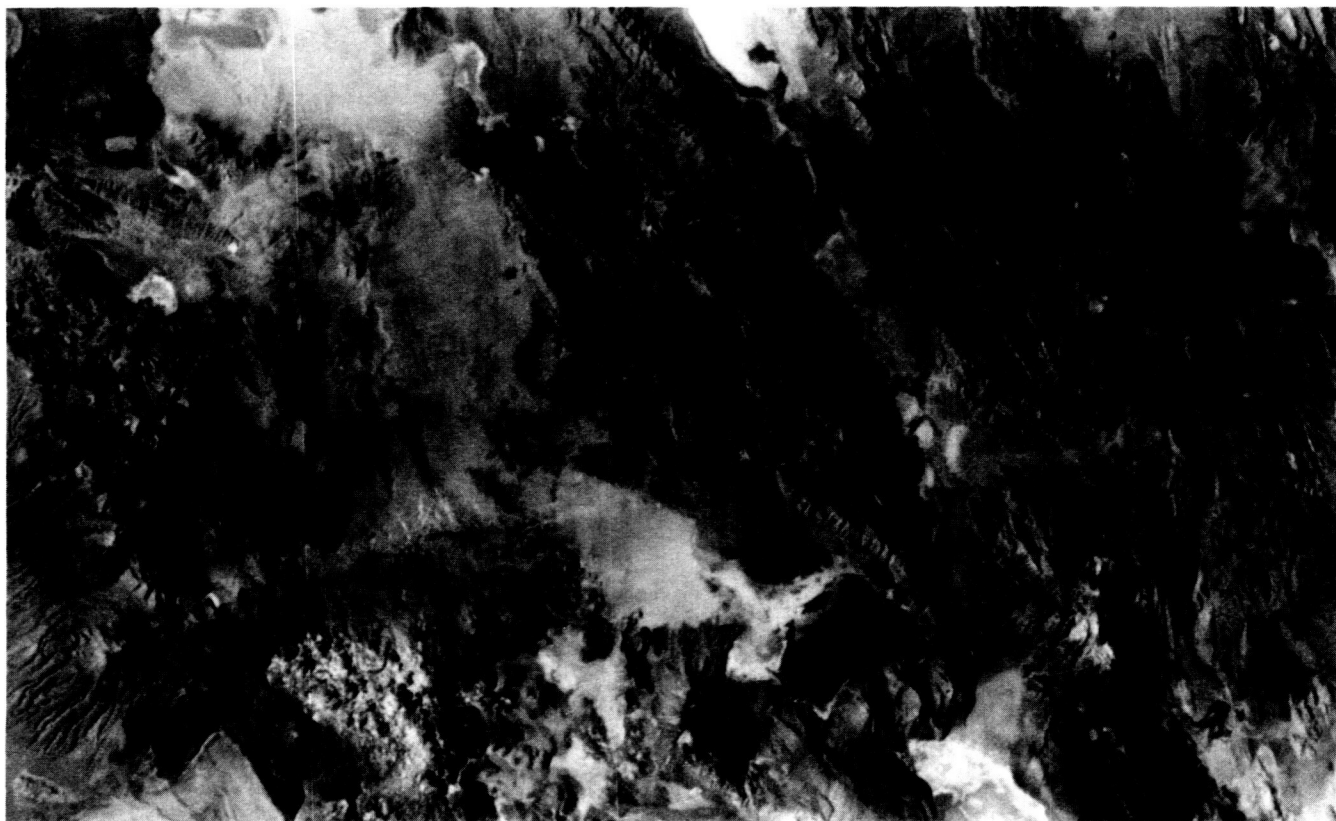
## FUTURE GOALS

The Can Do Project has a wide ranging program of activities underway. Last July, the program sent teachers to both Australia and the Hubble Space Telescope Institute in Baltimore. From these locations, the teachers were eye witnesses to the spectacular impact of Comet Shoemaker Levy 9 with Jupiter. The Australian team flew eight miles up into the stratosphere aboard the NASA Kuiper Airborne Observatory.

The program continues to enjoy the active support of the South Carolina Space Grant. This has produced a very productive working partnership. Can Do is also actively participating in the KidSat Program with J.P.L.

One dream that is very much alive is to fly GeoCam again. Using the lessons learned and the experiences gained, the Can Do team believes that it could be even better than the first time. Two innovations planned would be the use of digital cameras and an Internet Home Page to put the control room in touch with students everywhere. The flight of STS-57 completed part of the CAN DO goals, but it also represents one part of a work still in progress.





GeoCam Photograph of the Atacam Desert of Chile

GeoCam Photo

## **The VOrtex Ring Transit EXperiment (VORTEX) GAS Project**

Sven G. Bilén, Lynn S. Langenderfer, Rebecca D. Jardon,  
Hansford H. Cutlip, Alexander C. Kazerooni, Amber L. Thweatt,  
Joseph L. Lester, and Luis P. Bernal  
(for the VORTEX Project team)

University of Michigan Students for the Exploration and Development of Space  
François-Xavier Bagnoud Building  
1320 Beal Avenue  
Ann Arbor, MI 48109-2118

### **ABSTRACT**

Get Away Special (GAS) payload G-093, also called VORTEX (VOrtex Ring Transit EXperiment), is an investigation of the propagation of a vortex ring through a liquid-gas interface in microgravity. This process results in the formation of one or more liquid droplets similar to earth based liquid atomization systems. In the absence of gravity, surface tension effects dominate the drop formation process. The Shuttle's microgravity environment allows the study of the same fluid atomization processes as using a larger drop size than is possible on Earth. This enables detailed experimental studies of the complex flow processes encountered in liquid atomization systems. With VORTEX, deformations in both the vortex ring and the fluid surface will be measured closely for the first time in a parameters range that accurately resembles liquid atomization. The experimental apparatus will record images of the interactions for analysis after the payload has been returned to earth. The current design of the VORTEX payload consists of a fluid test cell with a vortex ring generator, digital imaging system, laser illumination system, computer based controller, batteries for payload power, and an array of housekeeping and payload monitoring sensors. It is a self-contained experiment and will be flown on board the Space Shuttle in a 5 cubic feet GAS canister. The VORTEX Project is entirely run by students at the University of Michigan but is overseen by a faculty advisor acting as the payload customer and the contact person with NASA. This paper summarizes both the technical and programmatic aspects of the VORTEX Project.

### **INTRODUCTION**

A group of students at the University of Michigan have begun the design and development of a Get Away Special (GAS) payload experiment called VORTEX (VOrtex Ring Transit EXperiment). The experiment will study the propagation of a vortex ring through a liquid-gas interface in microgravity. This process results in the formation of one or more liquid droplets similar to earth based liquid atomization systems. The limit of interest is when surface tension effects dominate the interaction and drop formation processes. The microgravity environment allows the study of these processes for a parameter range relevant to atomization systems but using a larger droplet size than is possible on Earth. This allows detailed experimental studies of the complex flow processes encountered in liquid atomization systems. Deformations in both the vortex ring and the fluid surface will be measured closely for the first time in a parameters range that accurately resembles liquid atomization. The experimental apparatus will record images of the interactions for analysis after the payload has been returned to earth.

The physics of liquid break-up and drop formation by a vortex ring flow in microgravity is a fundamental problem with application to manufacturing and systems development in space. It is also important in many Earth-based engineering systems. For example, fuel atomization—the break-up of a liquid stream into small droplets—is an important aspect of the design and operation of internal combustion engines. Another example is inert gas atomization used in powder metallurgy to produce metal powders of desired characteristics. Medical and biological applications are in the manufacture of encapsulated drops of complex structure for drug delivery.

VORTEX is a student-run project organized by the University of Michigan Students for the Exploration and Development of Space (UMSEDS). UMSEDS is a student engineering organization which brings together U of M students who have an interest in space and space exploration and helps them in exploring those interests by 1) providing its members

with information and opportunities helpful to careers in space-related fields; 2) being a forum for the discussion and exchange of ideas in space-related areas of interest; and 3) educating students and the general public about the benefits of space exploration and development. By designing, building, and flying a GAS payload experiment, UMSEDS members are able to apply their interest in space exploration to a real-world engineering problem which will advance scientific knowledge.

This paper summarizes both the technical and programmatic aspects of the VORTEX project. An overview of the scientific objectives and theoretical considerations is presented first. This is followed by a description of the experimental apparatus and how the experiment will be implemented. Following the technical aspects, a description of the VORTEX organization and educational aspects is presented.

## SCIENTIFIC OBJECTIVES AND THEORETICAL CONSIDERATIONS

### Scientific Objectives

The microgravity environment represents an opportunity to study surface tension dominated phenomena relevant to many earth-based engineering systems. This is particularly true for fluid interfaces with a large density change across the interface. On earth, the shape and dynamic evolution of the interface is dominated by the gravitational force. In the microgravity conditions of space, the shape and evolution of fluid interfaces is dominated by surface tension effects, and not gravitational effects.

The flow configuration is shown schematically in Figure 1. It consists of a vortex ring formed in the liquid below the interface propagating towards the interface (Figure 1a). If the vortex ring has sufficient impulse, then the collision of the vortex ring with the interface results in the formation of a droplet (Figure 1b). The volume of liquid moving with the vortex ring determines the size of the droplet. The vorticity distribution in the vortex ring determines the motion of the liquid inside the droplet. This relatively simple flow captures many important dynamical processes relevant to the evolution of fluid interfaces in microgravity and in other flow systems.

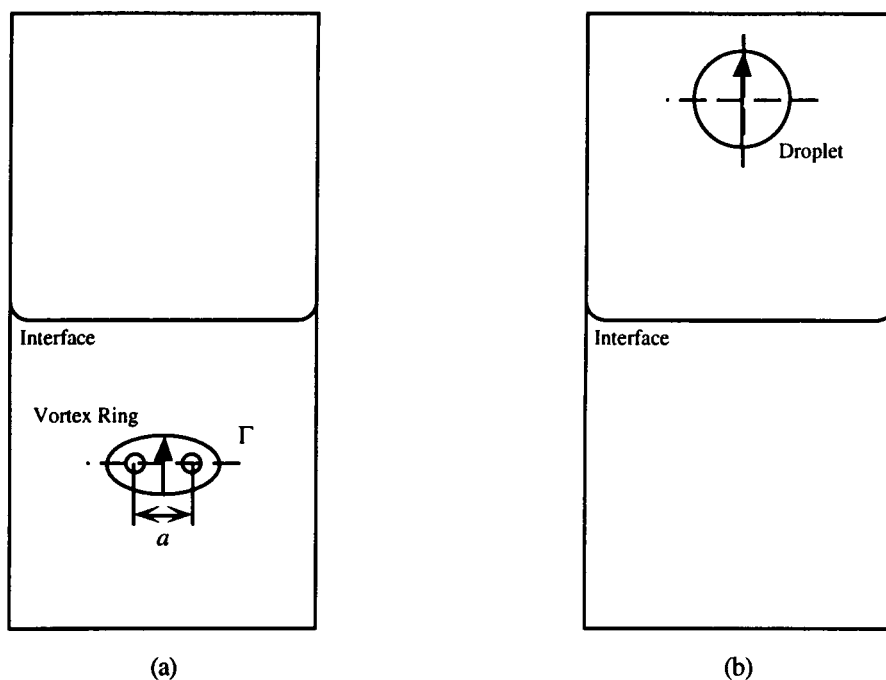


**Figure 1** Schematic diagram of the interaction of a vortex ring with a liquid-gas interface: (a) idealized diagram before the interaction; (b) idealized diagram after the interaction.

Figure 2 is a sequence of photographs of the interaction of a vortex ring with a fluid interface in simulated microgravity conditions [1]. These photographs illustrate the main features of the interaction. Simulated microgravity conditions were obtained by using liquids of similar densities. Initially the slightly heavier liquid is below the interface. A vortex ring is formed in the heavier liquid which then propagates towards the interface (Figure 2a). When the vortex ring penetrates the

interface it forms an elongated column of liquid from the lower layer into the upper layer. The interface breaks at the bottom of the column in Figure 2c forming a droplet. The droplet is highly elongated after breakup but subsequently evolves into a more spherical shape. The droplet motion is upwards initially but due to the larger density of the fluid inside it eventually moves downward toward the interface due to gravitational pull.

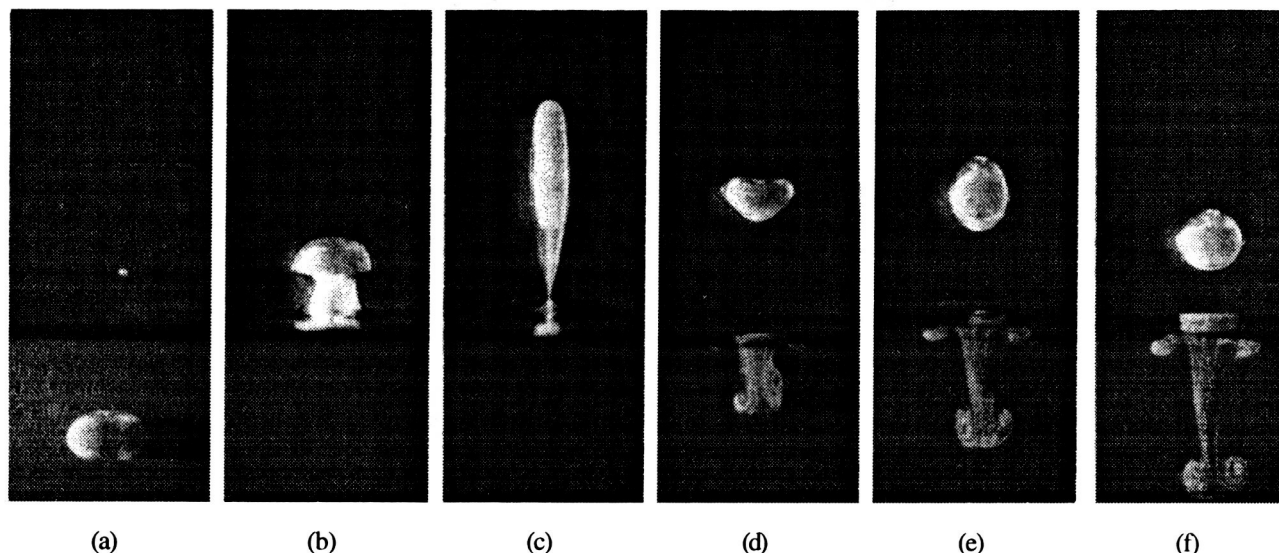


**Figure 2** Interaction of a vortex ring with a liquid interface in simulated microgravity conditions,  $\Gamma t/a^2$  (a) 0; (b) 14; (c) 29; (d) 43; (e) 57; (f) 72.

The major differences between VORTEX and the experiment described above and shown in Figure 2 is that VORTEX will examine the case of large density change across a liquid-gas interface, not a small change across a liquid-liquid interface. In addition, VORTEX will be dominated by surface tension effects and not gravitational effects. The flow evolution will be documented by visualization using a high speed camera. Typical images would be similar to the photographs shown in Figure 2. Several flow conditions will be studied each corresponding to a different strength of the vortex ring flow. The flow visualization data will be analyzed to determine the number and size of the drops formed, and the relation of these parameters to the vortex ring diameter and strength.

### Theoretical Considerations

To determine the relevant flow parameters for the experiment we follow the analysis of *Bernal et al.* [1]. The initial state before the interaction is characterized by the vortex ring diameter,  $a$ , and the circulation,  $\Gamma$ . The interface is characterized by the densities  $\rho_1$  and  $\rho_2$ , the viscosities  $\mu_1$  and  $\mu_2$ , and the surface tension  $\sigma$ . The ring moves toward the interface with speed  $V$  and collides with it. Generally, the collision and the subsequent evolution of the droplet depend on fluid inertia, viscosity and surface tension. Therefore, three nondimensional numbers define the problem: the Weber number, the Bond number, and the Reynolds number which are defined as

$$\text{We} = \frac{V}{\sqrt{\frac{\sigma}{\rho_1 a}}}, \quad \text{Bo} = a \sqrt{g \frac{\rho_1 - \rho_2}{\sigma}}, \quad \text{and} \quad \text{Re} = \frac{\rho V a}{\mu_1} \quad (1)$$

respectively. In addition, the density ratio  $r = \rho_2/\rho_1$  and the viscosity ratio  $\lambda = \mu_2/\mu_1$  must be specified. Here, subscript 1 denotes the liquid below the interface and inside the droplet and subscript 2 denotes the gas or liquid above the interface. The Bond number characterizes the relative magnitude of surface tension and gravitational acceleration in the dynamics of the interface. It is important to recognize that for a fixed liquid-gas interface the Bond number depends only on  $a\sqrt{g}$ , thus atomization phenomena in 1 g with droplet size of the order of a few microns can be examined in microgravity ( $10^{-5}$  g) at a much larger scale.

To illustrate the implications of this Bond number scaling, consider the case of a vortex ring in water with a diameter of 1 cm propagating through the water-air interface, which are typical of VORTEX. The density ratio is  $r = 10^{-3}$  and the Bond number is 0.01 at a microgravity level of  $10^{-5}$  g. This value of the Bond number corresponds to a droplet size of  $30\text{ }\mu\text{m}$  in a 1 g experiment. Clearly this droplet diameter is in the range found in typical fluid atomization systems [see for example ref. 2]. VORTEX will examine, for the first time, the details of interface breakup and droplet formation by a vortex ring at a range of parameters relevant to fluid atomization processes with a resolution that can not be obtained in ground based experiments.

## EXPERIMENTAL APPARATUS DESCRIPTION

The final design of the VORTEX payload has not yet been completed; however, the current payload design consists of a fluid test cell with a vortex ring generator, digital imaging system, laser illumination system, computer based controller, an array of housekeeping and payload monitoring sensors, and batteries for payload power. All equipment is mounted on an equipment support structure. VORTEX will be a self-contained experiment and will be flown onboard the Space Shuttle in a 5 cubic feet GAS canister.

### Experiment Instrumentation

The following is a brief description of the experimental instrumentation. A schematic of the instrumentation and the flow of information between subsystems can be seen in Figure 3.

The fluid test cell is a rectangular container 60.0 cm x 12.5 cm x 12.5 cm with transparent walls. In the initial state, before orbital insertion, a silicon liquid occupies the lower part of the container closed by an interface cover system. Once the experiment begins, the interface cover opens leaving a flat fluid interface. The experiments will then take place beginning with the higher velocity tests. The vortex rings are produced by a vortex ring generator at the bottom of the container. The upper part of the test container will be filled with a liquid absorbing foam material to collect the drops after each test. It is expected that after several tests, fluid droplets may accumulate in the middle of the test area hindering the flow visualization experiments. To avoid this the interface cover system will be closed after a number of experiments to force the free standing drops back into the original lower half of the tank.

The vortex ring generator is located at the bottom of the container and consists of a rapidly moving piston that is driven via a gear assembly by a stepper motor. Fluorescent dye is added above the piston by a positive displacement pump for the purpose of flow visualization of the vortex ring by laser induced fluorescence. The vortex ring generator and dye injection

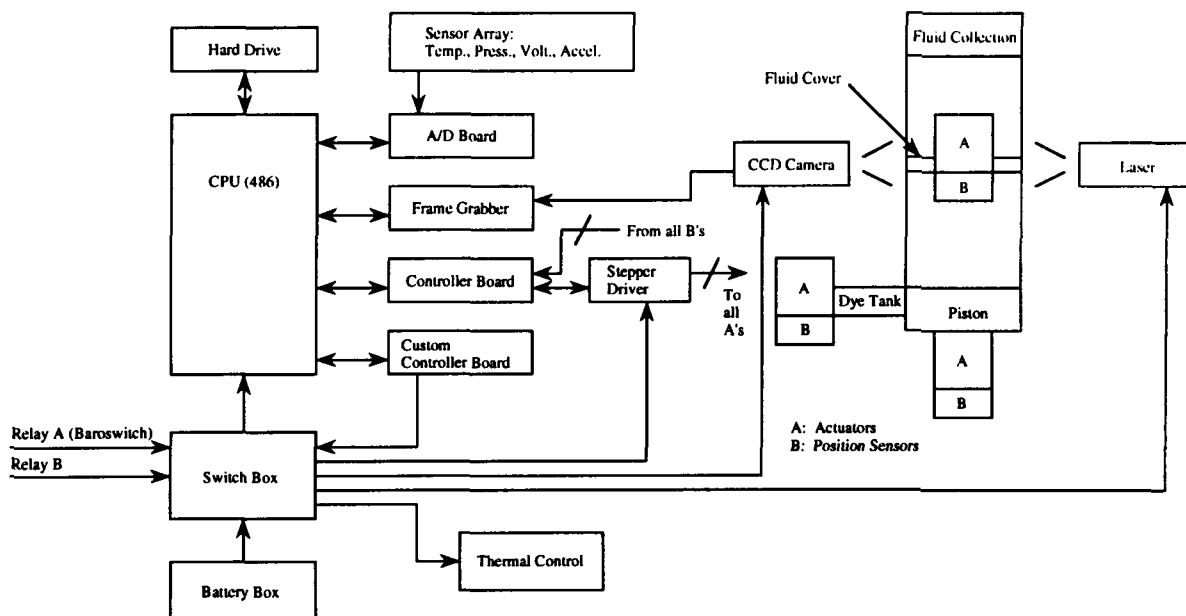


Figure 3 VORTEX instrumentation schematic and information flow diagram

system are under computer control. The experiments will be captured by a charged coupled device (CCD) digital camera with 128 x 512 pixel resolution that is capable of filming 100 frame bursts at speeds up to 300 frames per second. The laser illumination system will consist of a solid state visible green laser with output power of about 5-10 mW. An optical system will be used to generate a plane of laser light from the pencil beam output. This light plane will be used to illuminate a single plane in the fluid tank perpendicular to the camera plane. The laser will only be operated during camera data acquisition.

The computer system serves to control the entire experiment event sequence. The hardware consists of a 486 architecture microprocessor, a motherboard with eight expansion slots, a frame grabber to store photographic data, a 1 GB hard drive, and multiple controller cards for the sensor and stepper motors. The computer will collect and store sensor data such as acceleration, piston speed, temperature, pressure, and camera images, and will monitor failure modes for all subsystems.

Several sensors will also be included. The output of these sensors will be conditioned if necessary and then sampled via an A/D board attached to the computer. Data rate will depend on the temporal resolution required from the sensor. Temperature sensors will be placed on the battery box, computer, electronics boxes, laser, camera, and along the walls of the fluid container. Pressure sensors will be used to measure ambient pressure in the GAS canister as well as in the fluid test cell and on the motorized interface door. The accelerometer will measure the level of microgravity. The fluid level will be measured with a capacitive proximity sensor mounted on the fluid tank wall. The piston position will be measured with a linear encoder on the piston. The battery current and voltage will be monitored to determine power consumption.

### **Payload Power System**

The payload power system (PPS) is responsible for safely delivering the power to run all payload components for a total of eight hours. The design of the PPS has been broken down into smaller tasks which include battery selection, fusing, circuit design, and construction. Currently, payload power requirement estimates indicate that power will be supplied by nineteen Silver-Zinc cells with a capacity of 50-60 A-hr and a total output voltage of 28 V. From these batteries, power will be conditioned and transformed to fit the needs of the payload's various electrical components.

VORTEX will consume approximately 1 kW-hr during its estimated eight hours of operation. The estimated total battery capacity under worst case scenario is 1500 W, thereby leaving a 50% margin of error between the expected energy consumption and the energy available. Under nominal operating conditions the extra energy will be used to power the experiment beyond its intended minimum lifetime and to heat the payload before experiment activation.

### **Equipment Support Structure**

The components of the VORTEX payload will be supported by an equipment support structure (ESS), consisting of two complete shelves and one half shelf. The complete shelves are circular plates with a radius of 247.7 mm and a thickness of 9.525 mm. The half shelf has the same dimensions, but is a semicircle. The plates will be separated by six "I"-shaped support beams, which are 124.9 mm wide at the ends, 74.1 mm wide in the center, and 12.7 mm thick. These beams will be spaced equally around the perimeter of each plate as is illustrated in Figure 4. The beams will be bolted to the plate for easy removal and access to the components. The plates and beams are made of 6061T6 aluminum, and the entire shelving unit weighs approximately 23 kg.

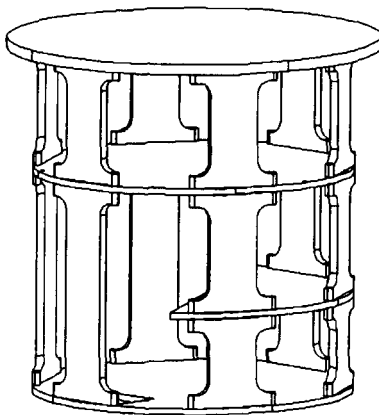


**Figure 4** Schematic of the VORTEX equipment support structure.

The major components will be arranged on the support plates as illustrated in Figure 5. Some of the components on the top level will be attached to the experiment mounting plate (EMP), instead of the support plate, in order to reduce the amount of weight, and consequently stress, on the shelving unit. There will also be ventilation and wiring holes in each of the plates (not shown in Figure 5).

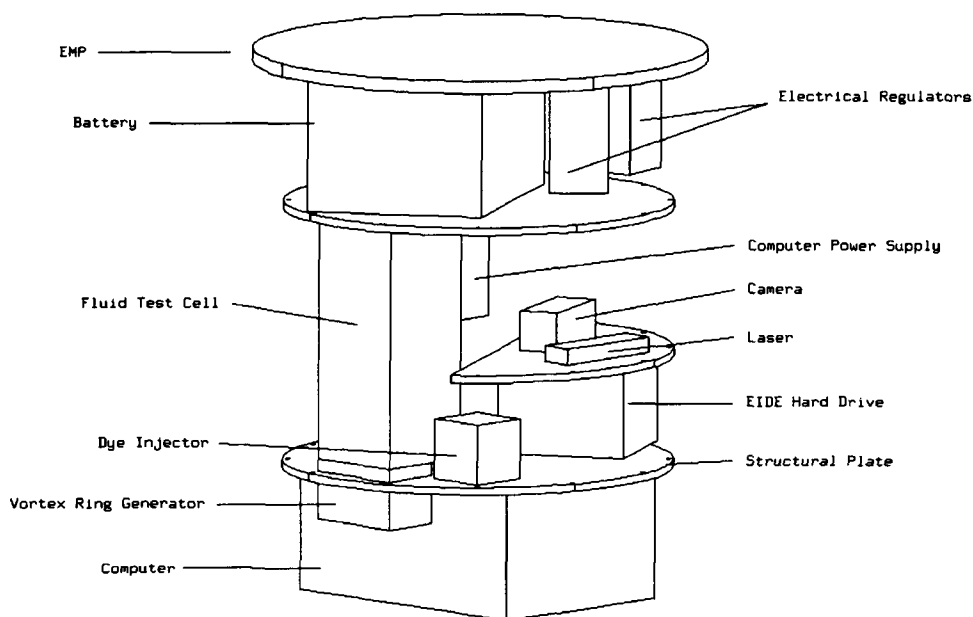


**Figure 5** Payload component placement on the equipment support structure.

## Systems Integration

Because it is essential that each subsystem understands what another subsystem may require of them, a systems engineer was designated to ensure communication and teamwork between the subsystems. A performance requirements document (PRD) was developed to facilitate this. In the PRD, each subsystem lists each piece of hardware and the requirements it imposes on another subsystem. In this manner the systems engineer becomes aware of all needs and requirements of the experiment. Subsystems designers must then work together to meet these requirements.

A VORTEX database system was also developed to aide in integrating the systems. This database encompasses all documents received and sent out by the VORTEX project members. Having all of these documents cataloged on-line and as hard copies further facilitates communication between subsystems. This is due to the fact that all project information is then available to all team members virtually anywhere on campus since almost all computers are networked. The on-line information system expedites any search for data and eliminates the chance that the data is already in use or unavailable. It is hoped that careful planning will allow all systems to be integrated successfully and with minimum hassle.

## EXPERIMENT IMPLEMENTATION

### Sequence of Events

The experiment sequence of events is outlined here. During ascent, the baroswitch will turn on the GAS payload power via relay A for thermal control within the canister. Relay B will be controlled by the astronauts. Once relay B is activated, the computer turns on and takes over the thermal control. The experiment operational procedure is then as follows:

- Baroswitch turns on Relay A, experiment thermal control begins, payload power is on;
- GCD Relay B enables experiment;
- Computer initializes;
- Computer performs diagnostics on all systems;
- Experiment sequence begins;

- Open interface door within fluid test cell;
- Wait for fluid stabilization;
- Inject fluorescent dye;
- Pull down piston;
- Turn on laser;
- Fire vortex ring, record piston position;
- Start image capture;
- Turn off laser;
- Transfer images to disk;
- After five experiments have been run, reset fluid interface by closing fluid test cell door and return to computer diagnostics of systems;
- Run experiments for up to eight hours.

## Implementation Issues

Although there are several issues regarding the payload implementation which must still be addressed, two are particularly important. The first has to do with ensuring that the microgravity experiments are truly run under microgravity conditions. Since astronaut movement and orbiter maneuvering system (OMS) firing will greatly affect the microgravity environment, VORTEX is requesting that the experiment be activated prior to a low g period lasting from 5-8 hours, such as a crew rest period, and that no OMS burns occur during experiment operation. In addition to this request, the VORTEX payload will use its accelerometer to monitor the level of microgravity during the experiments.

Another implementation issue yet to be resolved is how to maintain the fluid-gas interface in microgravity. It is anticipated that the cover mechanism will be sufficient to periodically re-establish the interface; however, there is no way to fully test the device before flight.

## VORTEX ORGANIZATION

The VORTEX project is entirely student run but is overseen by a faculty advisor acting as the payload customer and the contact person with NASA. The project has adopted a management structure that allows for the free flow of information between all levels. Day to day operations are run by a project and deputy project manager. Other groups, each with its leader, are responsible for a specific section of the payload. These groups are safety, systems engineering, sensors and controllers, fluid systems, electrical and power, computer systems, structures and integration, and science and theory. The VORTEX organizational structure is shown in Figure 6.

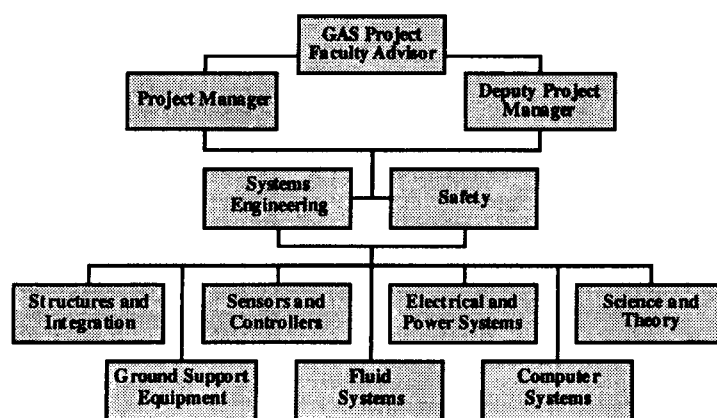


Figure 6 UMSEDS VORTEX organizational structure

Project management is responsible for the oversight of the GAS project. The management will consist of a faculty advisor and a project and deputy project manager. The faculty advisor acts as the GAS experiment customer; provides engineering support and guidance; and acts as the liaison between the students, NASA, and the University of Michigan administration. Before starting the VORTEX Project, UMSEDS felt that it was extremely important that the faculty advisor



acts as a customer, since he is keenly interested in seeing the project fly. The project teams are responsible for helping to define mission goals with the project management as well as specification of system requirements and components. Two of the project teams, systems engineering and safety, work together and with NASA to ensure that the project meets safety requirements. The remaining seven project teams are responsible for building and testing the GAS hardware. First-year students to Ph.D. candidates in majors ranging from engineering to business are involved with the project.

## **VORTEX PROJECT EDUCATIONAL ASPECTS**

As a project run by university students, the educational aspects of a project such as VORTEX are of utmost importance. There is considerable interest among engineering students in obtaining hands-on experience with "real-world" projects. To be challenging to the students, the projects must go beyond "cookie-cutter" laboratory experiments. Building and flying an experiment on the Space Shuttle is just such a "real-world" engineering project, and as such can motivate learning in engineering and science fields, as well as in other fields such as business. Space experimentation provides a medium where faculty and students can work together with industry and government toward a common goal. The knowledge and experience gained by participating in developing and flying GAS payloads can be significant and extremely beneficial to future careers [3, 4].

The VORTEX Project specifically provides students with essential experiences necessary for successful scientists, engineers, and businesspersons. Each student has the opportunity to be involved in the design, fabrication, integration, and testing of the GAS project. Therefore, each student is able to experience the design and development of an engineering project from its beginning through its completion. For the VORTEX Project, this involves such activities as writing progress reports emphasizing technical writing, preliminary design via computer aided design (CAD), structural analysis via finite element methods (FEM), systems integration, and the establishment of industry investors.

Although the nature of payload design is not like traditional laboratory classes, several opportunities for academic credit are available. For example, several students have taken directed studies for the design of a certain subsystem. Other students have taken the opportunity of using their design efforts for final projects in design classes. Still other students are satisfied with the engineering experience gained through their involvement in the project. In all cases, students are learning what it takes to design real engineering and science systems under external deadlines. They are also learning how to interact with industry, academia, and government.

One of the most vibrant and important activities UMSEDS engages in is educational outreach to K-12 schools near the U of M campus. UMSEDS has set up semester long programs in several schools to talk to K-12 students about space and related topics. In future semesters, UMSEDS will be talking to middle and high school students about what engineers do and how they develop space-flight hardware using VORTEX as an example.

Upon successful completion of the first GAS payload, UMSEDS plans to continue with future payloads. Much of the effort of this first project will involve setting up the infrastructure which can be immediately applied to subsequent projects. In this way, students can continue to learn through GAS experiment development.

## **CONCLUSION**

The technical and programmatic aspects of the VORTEX project have been summarized in this paper. VORTEX is an investigation of the propagation of a vortex ring through a liquid-gas interface in microgravity. The current design of the VORTEX payload consists of a fluid test cell with a vortex ring generator, digital imaging system, laser illumination system, computer based controller, batteries for payload power, and an array of housekeeping and payload monitoring sensors. It is a self-contained experiment and will be flown on board the Space Shuttle in a 5 cubic feet GAS canister. The VORTEX Project is entirely run by students at the University of Michigan but is overseen by a faculty advisor acting as the payload customer and the contact person with NASA.

It is felt that some of the experiences of the VORTEX Project, as outlined here, may prove beneficial to other GAS projects, especially student run projects at universities. With the wide-spread availability of the Internet and the World Wide Web (WWW), UMSEDS and VORTEX maintain a WWW homepage (<http://www.engin.umich.edu/societies/seds>), where information of a public and general nature about the project can be obtained.

## REFERENCES

1. Bernal, L.P., P. Maksimovic, F. Tounsi, and G. Tryggvason, "An experimental and numerical investigation of drop formation by vortical flows in microgravity," AIAA paper 94-0244, AIAA 32nd Aerospace Sciences Meeting, Reno, Nev., Jan. 10-13, 1994.
2. Wu, P.-K., and Faeth, G. M, "Aerodynamic effects on primary breakup of turbulent fluids," *Atomization and Sprays*, vol. 3, 265-289, 1993.
3. Gerondakis, G. G., "Get Away Special (GAS) educational applications of space flight," *IEEE Transactions on Education*, vol. 34, no. 1, 5-10, 1991.
4. Sacco, A., Jr., "The NASA GAS program: A stepping stone to education," *IEEE Transactions on Education*, vol. 34, no. 1, 27-30, 1991.



## **G 301: THE FLYING FALCON GEOLOGICAL REMOTE SENSING EXPERIMENT**

**Dr. Robert K. Vincent, Associate Professor**  
Department of Geology  
Bowling Green State University  
Bowling Green, Ohio 43403-0218

**Curtis Birnbach, President**  
Hudson Research Inc.  
P.O. Box C  
New Rochelle, N.Y. 10804-0122

**Arthur H. Mengel, President**  
Teltron Technologies Inc.  
2 Riga Lane  
Birdsboro, PA 19508

### **ABSTRACT**

Get-Away Special (GAS) G-301, named the Flying Falcon and scheduled for launch on the STS-77 Space Shuttle in April, 1996, is being prepared to perform an experiment designed by the Department of Geology, Bowling Green State University (BGSU). The experiment will employ a new type of infrared imager designed and built by a consortium of Teltron Technologies Inc., Hudson Research Inc., and BGSU that is an uncooled, quantum ferro-electric, infrared return beam vidicon (IRBV) camera capable of detecting thermal infrared radiation throughout the 2.0-50.0  $\mu\text{m}$  wavelength region, and to which an integral, tunable Fabry-Perot filter and a telescopic lens have been added. The primary objectives in the experiment include the mapping of methane plumes from solid waste landfills and wetlands in the midwestern U.S., the mapping of methane plumes offshore in the Gulf of Mexico and in the Middle East, brief monitoring for precursors of volcanoes or earthquakes in the South China Sea and the East Pacific Rise (about 300 km west of Easter Island), and the mapping of silica content in exposed outcrops and residual soils of the southwestern U.S. and Middle East.

The IRBV camera will be operated as a framing camera with a 512 x 512 pixel frame, due to GAS constraints. It is capable of collecting one frame each 1/30th of a second. The integrated tunable filter will switch spectral bands faster than the framing speed of the camera, and images of two consecutive spectral bands will be co-registered during ground-based image processing by

dropping an appropriate number of lines off the beginning of one image (band 1) and the end of the next image (band 2). The zoomed spatial resolution of the sensor will be 20 m, with a non-zoomed resolution of 200 m. The limitation on number of spectral bands that can be co-registered is limited by the speed of the Space Shuttle and the acceptable size of the resulting multispectrally co-registered image. For the imaging of methane plumes over land or water, three spectral bands in the 3.0-4.0  $\mu\text{m}$  wavelength region are sufficient. A different three spectral bands (in the 8-14  $\mu\text{m}$  wavelength region) will be used for mapping silica content in exposed rocks. Approximately 127 data collection opportunities (DCO) will be collected, each covering 1,356 x 512 pixels of non-overlapped area in three spectral bands, with about 2.36 megabytes per DCO. A computer program called FALCEYE, operating on a personal computer board, will use input from an on-board global positioning satellite (GPS) receiver and from a GIS data base to automatically tell the camera when to collect data, with which trio of spectral bands. A clone of the zoom version of the camera described below, aboard a geostationary platform, may be well suited for mapping precursors to earthquakes and volcanic eruptions.

## INTRODUCTION

Carbon dioxide and methane are both Greenhouse gases, because they are transparent in the visible wavelength region (passes visible sunlight) and opaque in parts of the thermal infrared wavelength region. A Greenhouse gas absorbs heat radiated by the Earth's surface and re-radiates it back down to the surface, thereby heating the surface. The global atmospheric concentration of carbon dioxide has increased from 280 parts per million by volume (ppm) to 353 ppm since 1800 AD, the beginning of the Industrial Revolution, and methane has increased from 0.8 ppm to 1.72 ppm in that same time period (ref. 1). Thus, methane has increased at almost twice the rate of carbon dioxide over the last 200 years. Most natural methane is thought to come from vegetative decay in wetlands, particularly tundra regions, though some comes from natural gas seeps and volcanic eruptions. Recent work (ref. 2, 3, and 4) has implicated methane as a precursor of earthquakes and volcanic eruptions, and thermal anomalies associated with the outflow of methane and charged particles from stressed rocks have reportedly been mapped from weather satellite images. Man-made sources of methane include pipeline/well leaks, solid waste landfills, sewage treatment plants, and livestock feedlots. Methane imaging has been proposed (ref. 5) by the use of three narrow spectral bands in the 3.0-4.0  $\mu\text{m}$  wavelength region, which could be performed on data collected during night-time or day-time.

The silica content of exposed silicate rock types can be mapped with two or more spectral bands in the 8.0-14.0  $\mu\text{m}$  (ref. 6). A hyperspectral thermal infrared sensor with narrow spectral bands in both the 3.0-4.0  $\mu\text{m}$  and the 8.0-14.0  $\mu\text{m}$  wavelength regions would be able to perform both of these tasks. In

the past, this would have required two different detector systems, one with a Hg:Cd: Te sensor and the other with an InSb sensor. The sensor that will be used in the Flying Falcon experiment is uniquely qualified for imaging differences in both methane content of the atmosphere and silica content of exposed rocks and soils on the ground.

The anomalies and areas selected for study include methane escape from solid waste landfills in the midwestern U.S., known methane seeps in the Gulf of Mexico (at the edge of the continental shelf), methane flares in the Middle East, methane anomalies associated with earthquake and volcanic eruptions in the South China Sea and the East Pacific Rise (about 300 km west of Easter Island), and exposed rocks in the southwestern U.S., the Middle East, and Australia.

## THE CAMERA

A new type of infrared sensor, called an infrared return beam vidicon (IRBV) camera, will be employed for the experiment. Fig. 1 shows a cross-sectional drawing of the camera. The IRBV camera is very similar to a return beam vidicon (RBV) camera that works in visible wavelength regions and has been employed on early satellites of the LANDSAT series, except that the electron "target" (photocathode) inside the video tube is a quantum ferroelectric (QFE) material that is sensitive to thermal infrared photons, instead of visible photons, and the IRBV camera lens is reflective instead of transmissive. Fig. 2 shows a cross-sectional drawing of the QFE video tube.

The camera was designed and build by a consortium of Teltron Technologies Inc, which supplied the unique QFE video tube; Hudson Research Inc., which supplied lens, optical and electro-optical design, tunable filter, low noise power supply, video electronics, and system integration; and the departments of geology and physics at Bowling Green State University, which supplied the multispectral design, custom circuit boards, and custom machined parts. The IRBV which has variable framing, but the constraints of a GAS experiment resulted in our choice of 512 pixel x 512 pixel frames, each collected in 1/30th of a second. The IRBV is uncooled and can detect single photons, owing to its noiseless signal amplification by a negative electron affinity dynode amplifier (ref. 7). A photon hits the QFE material inside the tube, kicking out several electrons, which are then multiplied  $10^{15}$  times by the photomultiplier tube, with no Johnson noise. The video tube integrates all incoming photons except during readout. The electrons are then counted in a scan sweep across the back of the QFE photocathode, which is converted to 512 pixels during the on-board analog to digital conversion. Except for the QFE photocathode, the telescope, and the tunable filter, other parts of this sensor package are almost identical to visible RBV cameras that have been flown in space on several occasions. The noiseless amplification feature is one of the principal ways of achieving low-light-level vision in the visible

wavelength region. With the new quantum ferro-electric coating, this same feature yields low-heat-level thermal vision in the thermal infrared wavelength region.

A tunable Fabry-Perot filter, which is integrated with the QFE video tube, is capable of restricting the input infrared radiation to selectable, narrow spectral bands anywhere in the 2.0-50.0  $\mu\text{m}$  wavelength region. The switching rate of the tunable filter is faster than the framing rate of the IRBV camera, which permits three spectral bands to be selected as three consecutive frames of data. To provide multispectral co-registration of the spectral bands, images of two consecutive spectral bands will be co-registered during ground-based image processing by dropping an appropriate number of lines off the beginning of one image (band 1) and the end of the next image (band 2). Currently, the spatial resolution of the sensor will be 20 meters in the zoom mode, which means that the Space Shuttle's velocity will cause approximately 15 lines to be dropped on each image of a two-band pair, for a total of 30 lines for the pair. If a third band is co-registered with the first two bands, a total of 60 lines must be dropped of the total of 512 lines per frame, leaving a  $452 \times 512$  pixel image with all three bands co-registered, yielding an area covered per frame of  $9.0 \text{ km} \times 10.2 \text{ km}$  in the zoom mode. In the non-zoom mode, the pixel size will be 200 m on a side, which will yield a total area covered per frame of  $90.4 \text{ km} \times 102.4 \text{ km}$ .

The number of spectral bands that can be co-registered is limited by the speed of the Space Shuttle and the acceptable size of the resulting multispectrally co-registered image. There will be two sets of three spectral filters used for this experiment, one trio for imaging methane plumes over land or water, and a second trio for imaging silica differences in exposed rocks and soil on land. Methane imaging will be performed with a trio of 0.032- $\mu\text{m}$ -wide spectral bands, one (called band 2) centered at 3.314  $\mu\text{m}$ , where methane absorption is greatest, and two bands centered near wavelengths of 3.116  $\mu\text{m}$  (band 1) and 3.516  $\mu\text{m}$  (band 3), respectively (ref. 5). Fig. 3 shows a three-band spectral ratio (the average of bands 1 and 3 divided by band 2) versus ppm of methane in a 10-m-thick plume of methane, as seen from space (ref. 5). Such a plume would be equivalent to one-thousandth as much methane concentration (in ppm by volume) for a 10-km-thick "plume" (ref. 5). The minimum difference in methane concentration for a 10-m-thick plume that is detectable from space by normal infrared sensors has been estimated by signal-to-noise calculations to be 16,000 ppm, which is considerably less than the lower explosive limit of methane in air (ref. 5). This is equivalent to saying that a 10-km-thick plume would have a minimum detectable methane concentration limit of 16 ppm. The proposed sensor will likely be substantially (more than a factor of 2) better. The trio of spectral bands for mapping silica content in exposed rocks will be approximately 0.10  $\mu\text{m}$  wide, centered at 8.95  $\mu\text{m}$ , 11.40, and 10.60  $\mu\text{m}$ , (labeled bands 4, 5, and 6), respectively.

The camera design is based on experience gained from a number of space and military applications. Teltron built the video imaging system on the Apollo landers, so their expertise in producing highly reliable hardware is well established. The camera contains the necessary support electronics. These include deflection circuitry, various high voltage DC power supplies (including those for the Fabry- Perot filter), synchronization circuitry, and signal amplifiers associated with the photocathode. The camera also has circuitry to support the anti-blooming, dynode amplifiers, self-adjusting pedestal, and electronic zoom and centering features. The self-adjusting pedestal, which effectively neutralizes the charge on the electron target when the shutter is closed, eliminates the need for an external chopper or shutter.

## **SUPPORT ELECTRONICS EXTERIOR TO THE CAMERA**

The camera analog output will be digitized with 10 bits per pixel and stored on a solid state memory device capable of holding approximately 300 megabytes of 10-bit digital data. Nine frames of data will be recorded for each data collection opportunity (DCO), overlapping just enough such that the total area covered by each DCO will be  $1,356 \times 512$  pixels, with 3 spectral bands of data. A DCO will be mapped either for methane or for silica content, but not both. Because of the along-track overlap, there will be  $3 \times 512 \times 512 \times 3 = 2.36$  megabytes of data stored for each DCO. Therefore, there will be enough data storage for approximately 127 DCOs.

An on-board GPS (Global Positioning Satellite) receiver and on-board computer will be used to determine the position of the Space Shuttle and to automatically tell the camera when it is time for a DCO. Study areas are being selected and digitized with a GIS system to determine the polygon outline of each study area. A study area will typically be much greater in size than a DCO. A computer program (FALCEYE) on a solid-state ROM, created at BGSU, will determine when the camera should start a DCO by automatically comparing the Shuttle's GPS position with the stored study area polygons. Any DCO within a study area will be deemed acceptable, day or night (this is a thermal infrared sensor). Rather than automatically detecting clouds, we will accept cloud cover as-is and spend most of the post-processing time on the cloud-free DCOs.

The final piece of support electronics is the Shuttle Motorized Door Assembly (MDA), which will be activated when the Shuttle bay is finally opened and pointed at Earth, and just before the Shuttle bay is closed.

## **POST PROCESSING**

The stored data will be brought to the BGSU Geology Department for downloading and image processing in our GIS/Remote Sensing computer

lab, which contains 5 Silicon Graphics Indigo computers and 3 Sun Microsystems (SPARC 10, SPARC 1000, and 470) workstations. KHOROS, ERMAPPER, and other image software will be used to spectrally co-register the images of each DCO. Spectral ratio images and other types of processed images will then be produced. Field work will be conducted, as travel support for graduate students becomes available in the post mission phase.

## CONCLUSION

The following "firsts" are expected, among others, to occur as the result of the Flying Falcon GAS experiment:

1. The first imaging attempt for a GAS experiment.
2. The highest spatial resolution of any civilian thermal infrared imaging system ever orbited.
3. The first space test for an IRBV camera.
4. The first attempt at imaging methane from space in the thermal IR.
5. The first attempt at imaging silica differences in exposed rocks and soils from space.

If this experiment is able to conclusively image methane, the IRBV camera would make an excellent addition to a geostationary platform, where the zoom capability would yield pixels of about 4.5 km spatial resolution and would cover an area about 2,300 km x 2,300 km, with a virtually unlimited number of narrow spectral bands available for use. Any gas with an infrared absorption band in an atmospheric window region could be imaged with such a system. If large-area methane anomalies are a precursor of earthquakes and volcanic eruptions, as some have claimed (ref. 2 and 3), this capability would be excellent for monitoring such precursors.

## REFERENCES

1. Harriss, R.C., "Tropospheric Chemistry," *Atlas of Satellite Observations Related to Global Change*, Editors R.J. Gurney, J.L. Foster, and C.L. Parkinson, Cambridge University Press, Cambridge, U.K., 1993, pp. 181-189.
2. Qiang Zuji and Dian Changgong, The Thermal Infrared Anomaly of METEOSAT - Precursor of Impending Earthquakes, *Proceedings of the Ninth Thematic Conference on Geologic Remote Sensing*, The Environmental Research Institute of Michigan, Ann Arbor, Michigan, 1993, Vol. II, pp. 1005-1013.
3. Qiang Zuji, Dian Changgong, Zhao Yong, and Guo Manhong, Satellite Thermal Infrared Temperature Increase Precursor -- Short Term and Impending Earthquake Prediction, *Environmental Assessment of Geological*



*Hazards, Proceedings of the Space Congress*, European Space Report, P.O. Box 140 280, 80452 Munich, Germany, 1995, pp. 53-57.

4. Zhao Gaoxiang and Wang Hongqi, The Possibility of Monitoring Increased CH<sub>4</sub> Concentration in the Atmosphere and Its Potential Use in Earthquake Prediction, *Environmental Assessment of Geological Hazards, Proceedings of the Space Congress*, European Space Report, P.O. Box 140 280, 80452 Munich, Germany, 1995, pp. 58-62.

5. Vincent, R.K., Flying Falcon: Multispectral Thermal IR Geological Imaging Experiment, *Remote Sensing for Oil Exploration and Environment, Proceedings of the Space Congress*, European Space Report, P.O. Box 140 280, 80452 Munich, Germany, 1995, pp. 139-146.

6. Vincent, R.K., and F. Thomson, Rock Type Discrimination from Ratioed Infrared Scanner Images of Pisgah Crater, California, *Science*, 1972, Vol. 175, pp. 986-988.

7. Dereniak, E.L, and D.G. Crowe, *Optical Radiation Detectors*, John Wiley & Sons, New York, NY, 1984, pp. 116-121.

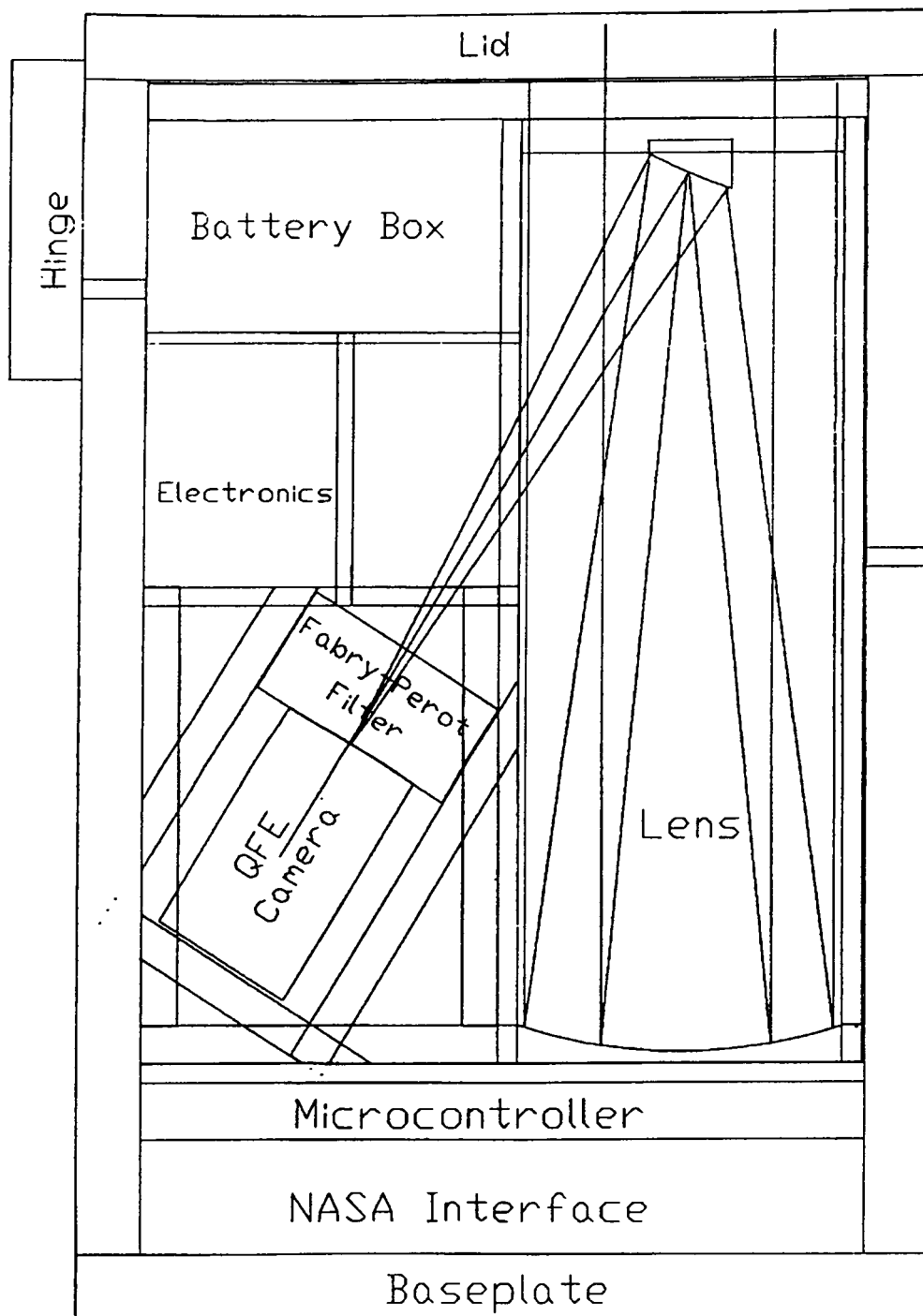


**Fig. 1. Drawing of the Flying Falcon experiment, showing the quantum ferro-electric (QFE) infrared return beam vidicon (IRBV) camera, to be flown as the Get-Away-Special G-301 package with the STS 77 Shuttle mission in April, 1996.**

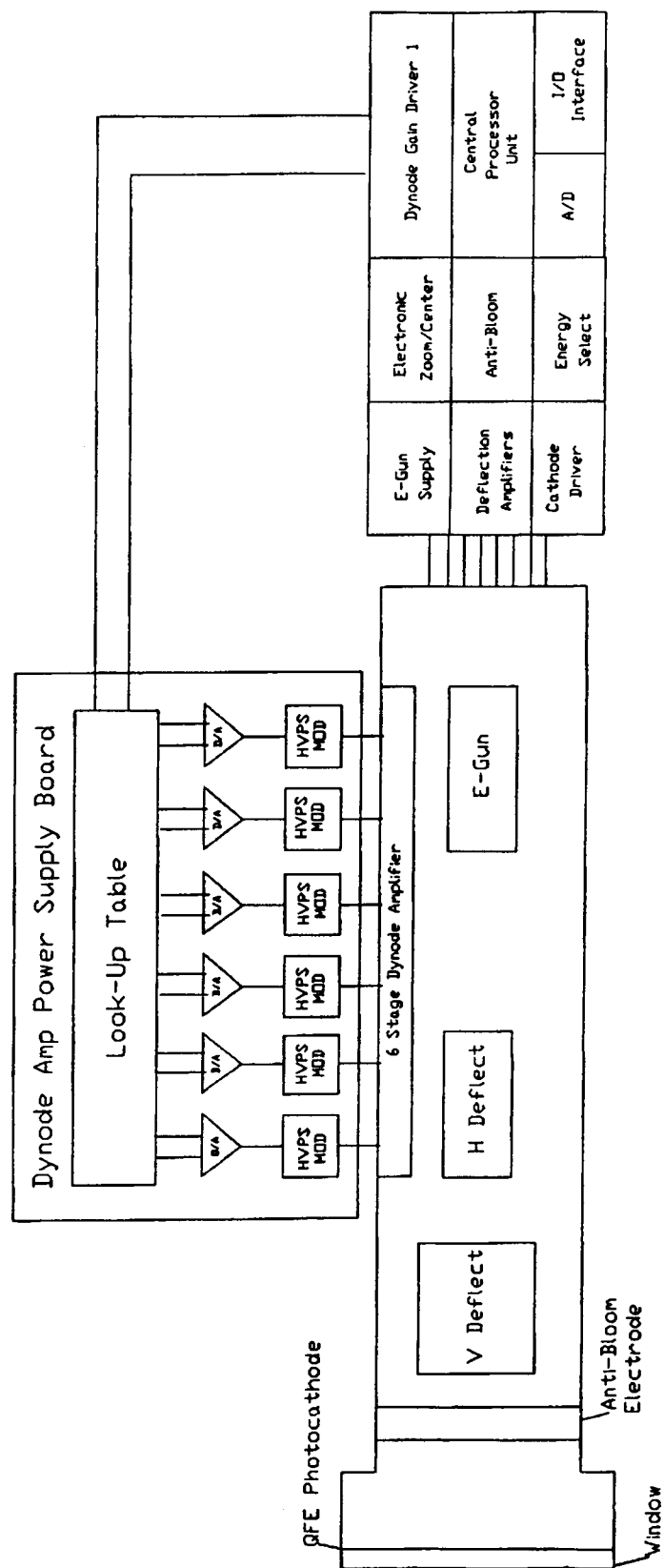
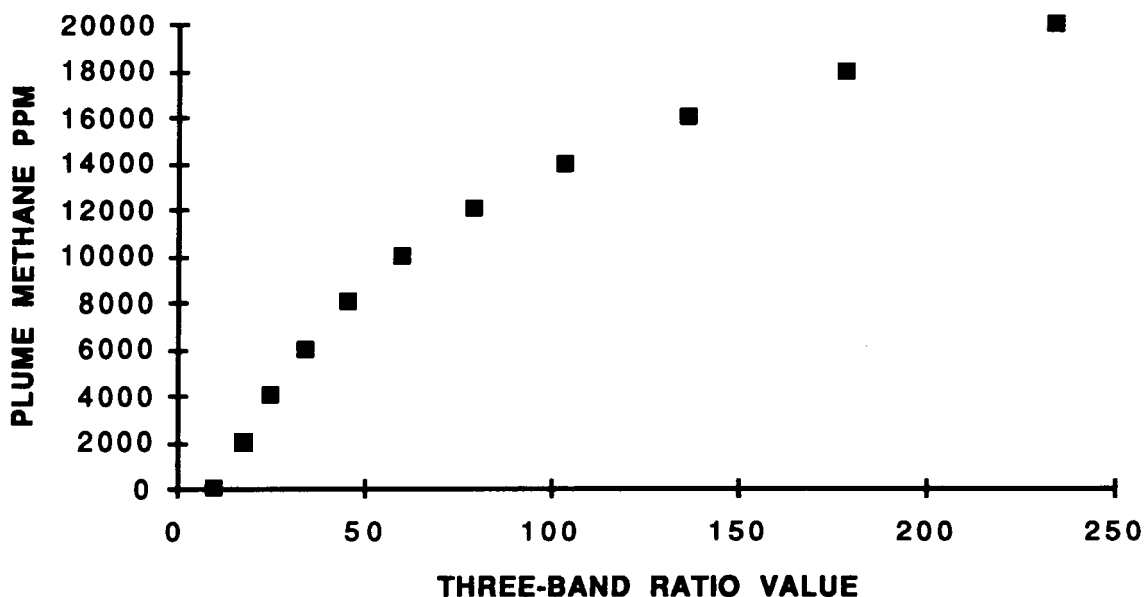


Fig. 2. Cross-sectional drawing of the quantum ferro-electric (QFE) video tube, which is the heart of the G-301 Flying Falcon infrared imaging experiment.

### METHANE PPM vs. THREE-BAND RATIO



**Fig. 3. Concentration of methane (in ppm by volume) in a methane/air plume of 10-meter thickness versus a three-band ratio ( $R_{1+3,2}$ ) as observed over the ocean by a three-band (3.100-3.132  $\mu\text{m}$ , 3.298-3.330  $\mu\text{m}$ , and 3.500-3.532  $\mu\text{m}$ ) thermal Infrared sensor from space, under conditions of the ocean surface temperature at 25°C and temperature of the plume (and sea-level atmosphere) at 5°C or less.**

# **CONSTRUCTION MATERIAL PROCESSED USING LUNAR SIMULANT IN VARIOUS ENVIRONMENTS**

Stan Chase, Bridget O'Callaghan-Hay, Ralph Housman, Michael Kindig, John King, Kevin Montegrande,  
Raymond Norris, Ryan Van Scotter, Jonathan Willenborg  
Orange Coast College (OCC)

Harry Staubs  
American Institute of Aeronautics and Astronautics (AIAA)  
Orange County Section

Michael Petran, Ed Tate, Tim Williams  
California State University, Long Beach (CSULB)

Phong Chen, Campbell Dinsmore, Lincoln Le, Gautam Shah, Phat Vu  
California State Polytechnic University, Pomona (CAL POLY)

## **ABSTRACT**

The manufacture of construction materials from locally available resources in space is an important first step in the establishment of lunar and planetary bases. The objective of the CoMPULSIVE (Construction Material Processed Using Lunar Simulant In Various Environments) experiment is to develop a procedure to produce construction materials by sintering or melting Johnson Space Center Simulant 1 (JSC-1) lunar soil simulant in both earth-based (1-g) and microgravity (~0-g) environments. The characteristics of the resultant materials will be tested to determine its physical and mechanical properties. The physical characteristics include: crystalline, thermal, and electrical properties. The mechanical properties include: compressive, tensile, and flexural strengths. The simulant, placed in a sealed graphite crucible, will be heated using a high temperature furnace. The crucible will then be cooled by radiative and forced convective means. The core furnace element consists of space qualified quartz-halogen incandescent lamps with focusing mirrors. Sample temperatures of up to 2200°C are attainable using this heating method.

## **INTRODUCTION**

The GAS-072 payload consists of an experiment designed and developed by the CoMPULSIVE team: student members of Orange Coast College Research Club (OCCRC), California State University, Long Beach Extension Program (CSULB), and California State Polytechnic University, Pomona (CAL POLY). Technical support is provided by a group of Orange County Section American Institute of Aeronautics and Astronautics (AIAA) engineers, scientists, and consultants.

The establishment of a long term human base on the moon presents many challenges. The production of suitable construction materials must meet several criteria. Due to the high transportation costs of raw materials from Earth, to be cost effective, any production method should utilize as much local lunar material as possible. To keep the production cost low the process should be simple and the required hardware and labor should be minimized. The final product should have the properties to withstand the harsh environmental conditions on the Moon. In the lunar environment there is a near absolute vacuum, a total lack of atmosphere and weather, and continuous exposure to galactic cosmic radiation and solar flares. The lunar surface temperature ranges from 127°C to -173°C. The lack of atmosphere means that there is no convection to help equalize temperatures between the sunlit and shaded sides of any construction. Thus for points in close contact very large temperature differences can exist. Also, any structure will be subjected to a constant bombardment of meteorites and micrometeorites.

It has been proposed (ref. 1) to use sintering or cast basalt manufacturing in the early stages of lunar base establishment. Both of these techniques heat the lunar soil to the melting temperature and then let it cool gradually. Among the heating methods proposed are concentrating solar energy, using electric (resistance) furnaces and microwave irradiation.

## EXPERIMENT OBJECTIVES

The lunar simulant prepared by both the University of Minnesota (MLS-1) and NASA Johnson Space Center (JSC-1) has been successfully sintered and melted. The resulting sample was tested as a construction material (ref. 2,3). In particular, McDonnell Douglas (ref. 4,5,6) investigated the feasibility of using a solar array to focus direct sunlight onto a sample of lunar soil. The prototype solar array produced columnar bricks possessing various degrees of structural integrity.

It has been proposed that samples produced by sintering or melting in microgravity may have a more homogenous distribution of basaltic components upon resolidification and could produce a material with a smaller grain size. Fine grain structures have greater compressive strength and ductility. Presently, no known material processing work has been conducted with lunar soil simulant in a microgravity environment.

The objective of the CoMPULSIVE experiment is to sinter or melt a sample of lunar soil simulant in a Shuttle Get-Away-Special (GAS) canister. The specimen obtained once the experiment has been flown will be tested to determine its compressive strength, ductility, density, crystalline structure, thermal, and electrical properties. This data can be compared to samples processed on earth to determine if there is any change in properties. If there is a change, the 1-g and near 0-g data can be interpolated to predict the properties of the material formed by heating and cooling lunar soil in the lunar environment.

## EXPERIMENT DESCRIPTION

The experiment will be housed in a NASA provided 0.142 cubic meters GAS canister. A schematic diagram of the test setup is shown in Figure 1. A cylindrical specimen (1.27 cm diameter, 3.81 cm height) of lunar soil simulant (JSC-1) in powder form will be encased in a pyrolytic graphite crucible. The crucible will be surrounded by six halogen bulbs positioned 60 degrees apart around the long axis of the sample. Each bulb has a gold-plated reflector to optimize heat transfer. The entire assembly will be placed in the pressurized vessel.

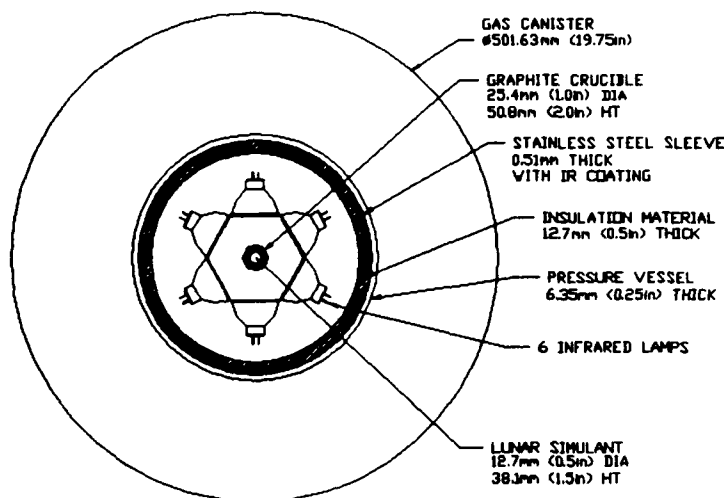


Figure 1. Schematic Diagram of the CoMPULSIVE Project

The power supply required to heat the sample may be provided by 32 Gates model BC 2 Volt batteries. An astronaut will start the experiment by switching on the GAS control decoder (GCD) system on the shuttle during a quiet period for the crew. Thermocouples will monitor the temperatures during the experiment. The temperature and other vital parameters will be monitored using an automated data acquisition system.

The post-flight ground control test will duplicate the entire flight experiment after the experiment is flown on the space shuttle and will be used as the control sample.

## TECHNICAL TASKS

The technical tasks have been divided into five categories: Thermal Analysis; Furnace Design; Power; Control, Monitoring, and Data Acquisition Systems; and Structure. The thermal analysis and furnace design are critical design elements, setting the requirements for the remaining components.

### Thermal Analysis

A thermal model of the furnace has been developed using the Systems Improved Numerical Differencing Analyzer (SINDA). It has been used to predict the temperature histories of the lunar soil simulant and furnace components. The SINDA model of the lunar soil simulant, crucible, and furnace is a transient (time-varying), one-dimensional radial system which is composed of multiple nodes. In addition to the furnace, a thermostatically controlled power source is also included. Figure 2 shows a discretized resistor network and the nodes used in modeling the system. Note that results presented do not include modeling of the insulated pressure vessel.

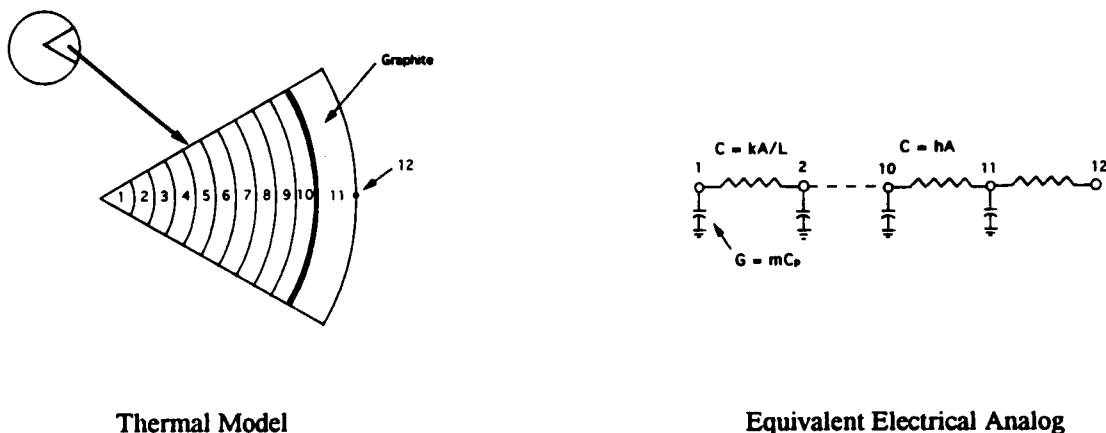


Figure 2. Resistor Network Schematic of SINDA Model

The assumptions used in the model are as follows:

1. Thermal conductivity and specific heat are constant with temperature.
2. Ideal bulk properties of the lunar soil simulant are used. In reality, density varies with porosity, compaction, and state (solid or molten).
3. The heat of fusion of lunar soil simulant is constant and is assumed to be 2337 J/kg.
4. Modeling of contact resistance between particles, flow of molten soil through pores, etc., are not considered.
5. The crucible does not decompose.

The following steps are being taken to update the SINDA model:

1. Modeling of the insulated pressure vessel and new furnace designs.

2. Using temperature dependent thermal conductivity and specific heat properties.
3. Modeling of the phase change in the JSC-1.

The SINDA model results have raised the following issues:

1. Processing of the JSC-1 currently takes too long and may exceed the time available in orbit.
2. Temperature gradients may cause thermal stresses and cracking during cool-down.

The issues and limitations of the SINDA thermal model indicate a need for testing to determine the feasibility of the JSC-1 melting experiment as currently specified.

### **Furnace Design**

The purpose of the furnace is to sinter or melt a sample of JSC-1 of a given size and shape. Additionally, the furnace must also be able to regulate the heat transfer rates during both the heating and cooling phases of the sample processing cycle. In order to achieve this, the furnace is comprised of four major components: Heating Elements, Simulant Containment, Heat Transfer Control, and Pressure Vessel.

First and foremost is the heating element. This device takes the energy stored in the batteries and transforms it into thermal energy in the sample. The heating elements will consist of six 15V, 150W lamps arrayed radially around the sample as shown in Figure 1. The radiated energy emitted from the bulbs is expected to raise the temperature of the JSC-1 from 289 K to 1513 K.

Second is the simulant container. This component is responsible for containing the sample during the entire processing cycle. The simulant will be processed in a pyrolytic graphite crucible. This material was chosen because of its high strength, high thermal conductivity, and superior dimensional stability at high temperature. Because of this dimensional stability, it is highly unlikely that the crucible will bind with sample when cooled from the processing temperature.

Third, there must be a method of controlling heat transfer from the various components of the furnace. First, there must be a controlled cooling of the sample. This is needed to prevent cracking due to thermal stresses, as well as to control the final properties of the processed simulant. Second, the furnace should be insulated. This would help minimize the amount of heat loss from the furnace and consequently minimize the electricity which is consumed in the experiment. This will also serve to protect the other components contained within the GAS canister.

Finally, a pressure vessel is required to maintain a vacuum within the furnace. The use of a pressure vessel will contain any outgassing byproducts, and serve to optimize the heat transfer environment within the furnace.

These four components will comprise a furnace system which will be able to accurately control both temperatures and heat transfer rates.

### **Power**

A controlled power system will provide electricity to the furnace and the data acquisition system. This power system will help prevent excessive temperatures in the heating components, thus minimizing the power being drawn from the batteries.

The power system consists of an active controller, batteries, battery case, and battery vent. Thirty-two Gates model BC batteries have been selected to provide the required power. Each battery has a mass of 1.58 kg and 2 V dc. Therefore, thirty-two batteries are needed to generate 3,121 W to sinter or melt the JSC-1.



## **Control, Monitoring, and Data Acquisition System**

Control, monitoring, and data acquisition systems are needed to control the heater duty cycle and to record data, the conditions under which the JSC-1 was processed. The components which comprise the system include: relays, switches, wiring, voltmeters, ammeters, thermocouples, pressure transducers, controller hardware and software.

### **Structure**

The structure holds the entire GAS project together and prevents Shuttle launch loads from affecting components. The experimental components will be held by the structure which will in turn be cantilevered from the NASA provided mounting plate. A vibration isolation system may be used to prevent damage to sensitive components. This system may also be used to protect the specimen from damage during shuttle operations and reentry. Finally, bumpers will prevent the experiment from hitting the sides of the canister.

## **PROJECT MANAGEMENT**

The Project faculty adviser is Dr. Ernest W. Maurer, the Dean of Technology at Orange Coast College (OCC). The main contingency of active participants is comprised of student members of the OCC Research Club. The key members of the research club include: Stan Chase, Michael Kindig, John King, Kevin Montegrando, Raymond Norris, Bridget O'Callaghan-Hay, Ryan Van Scotter, and Jonathan Willenborg. These members are concentrating on project management, budgeting, research, thermal analysis, safety, tooling, and manufacturing.

The GAS Project Committee Chair is Harry Staubs, the lead representative of the AIAA Orange County Section. Harry is serving as the NASA payload manager. Joseph Morano, the President of the AIAA Orange County Section, is the NASA customer contact.

The schools, CSULB and CAL POLY, have taken on the focuses of furnace design and support structural design, respectively. Members of the CSULB team include Michael Petran, Ed Tate, and Tim Williams. The CAL POLY team members are Phong Chen, Campbell Dinsmore, Lincoln Le, Gautam Shah, and Phat Vu.

Technical support has been provided by a team of consultants. This team includes: Aaron Ayotte, Brian Dubow, Ralph Housman, and Jim Perez.

## **TEST PROGRAM**

The test program is divided into four stages: Critical Technology Test, Ground Test, Flight Test, and Post Processing Test.

### **Critical Technology Test**

A test will be conducted to sinter or melt JSC-1 in a ground test configuration using a power supply to establish the power requirements. This will help to optimize the test sample size and the flight battery pack configuration. This test will be conducted to verify that the experimental apparatus functions correctly and ensure that the flight test can be successfully accomplished.

### **Flight Test**

Gas Payload G-072 will melt a specimen of JSC-1. The heater will be started by a power-up GAS Control Decoder relay 'A' command which will be activated by the Shuttle crew. A JSC-1 specimen will come to temperature equilibrium at 1240°C within 36 to 48 hours after power-up. This time is based on a preliminary thermal analysis from the SINDA thermal model. Power to the sample will be cycled on and off to optimize the use

of on-board available battery power. Once the target temperature is reached, the specimen will be allowed to cool in a controlled manner to avoid thermal stresses that could adversely affect structural integrity of the specimen.

### **Ground Test**

A ground test will be conducted using the actual flight hardware. This test will be conducted to obtain control data at 1-g which will be used in conjunction with near 0-g data to interpolate the results to the gravitational pull of the moon. Several specimens will be made for test controls.

### **Post Processing Tests**

Both the earth bound and the Shuttle borne sample sets will have their physical and mechanical properties evaluated. The physical tests to be performed will determine the density, thermal properties, electrical conductivity, and crystalline structure of the samples. The mechanical tests to be performed will determine the compressive strength, the tensile strength, the flexural strength, and modulus of the samples.

## **CONCLUSIONS**

A simple and economical method has been proposed to obtain data for the properties of sintered or melted lunar soil. The data accumulated from the near 0-g environment will be compared to the earth ground test. An interpolation will be made to determine the data for a lunar 1/6-g environment. These results are required by researchers and engineers who will be designing structures to be built on the lunar surface.

## **REFERENCES**

1. Binder, A. B., et al., "Lunar Derived Construction Materials; Cast Basalt", Proceedings of Space 90, ASCE 1990.
2. David S. McKay, James L. Carter, Walter W. Boles, Carlton C. Allen and Judith H. Alton, "JSC-1: A New Lunar Soil Simulant".
3. Carlton C. Allen, John C. Graf and David S. McKay, "Sintering Bricks on the Moon", Presented at Engineering, Construction and Operations in Space IV Conference, American Society of Civil Engineers, 1994.
4. Garvey, J. M. and Magoffin, M. A., "The Feasibility of Solar Energy for Lunar Resource Processing", 42nd Congress of the International Astronautical Federation, IAF-91-670, October 5-11, Montreal, Canada.
5. Garvey, J. M. and Magoffin, M. A., "Solar Concentrator Lunar Simulant Processing Project", Space Studies Institute, The High Frontier Newsletter, Volume XVI, Issue 5, September/October 1990.
6. Magoffin, M. A., and Garvey, J. M., "Lunar Resource Processing Using Concentrated Solar Energy, 1990 Final Report", MDC H6194, January 1991.

Neutrons, Gamma Rays, and Beta Particles Interactions with IlaO  
Films Flown on Astro I and Astro II and Comparison  
With IlaO Flown on the Get-Away- Special STS-7

Ernest C. Hammond, Jr., Kevein Peters, and Kevin Boone  
Morgan State University, Baltimore, Maryland

ABSTRACT

The current requirements for the Laboratory for Astronomy and Solar Physics, sends rocket satellites and in the near future will involve flights in the shuttle to the upper reaches of the earth's atmosphere where they will be subjected to the atomic particles and electromagnetic radiation produced by the sun and other cosmic radiation. It is therefore appropriate to examine the effect of neutrons, gamma rays, beta particles and X-rays on the film currently being used by the Laboratory for current and future research requirements. It is also hoped by examining these particles in their effect that we will have simulated the space environment of the rockets, satellites and shuttle. Several samples of the IlaO film were exposed to a neutron howitzer with a source energy of approximately 106 neutrons/steradians. We exposed several samples of the film to a 10 sec. blast of neutrons in both metal and plastic containers which were produced by Kodak. At the intensities mentioned, the film in the metal container exhibited higher density readings which indicated the possibility of some secondary nuclear interactions between neutrons and the aluminum container. The plastic container showed some variations at the higher densities. Exposure of the samples of IlaO film to a neutron beam of approximately 10 neutrons per steradians for 8 minutes produces approximately a thirteen percent difference in the density readings of the dark density grids. It is noticeable that at the lighter density grid the neutrons have minimal effects, but on a whole the trend of the 8 minute exposed IlaO film density grids at the darker end had a 7.1 percent difference than the control. Further analysis is anticipated by the increasing the exposure time. Two sets of film were exposed to a beta source in a plastic container. The beta source was placed at the bottom so that the cone of rays striking the film would be conical for a period of seven days. It is observed in the film designated 4a and 4b a dramatic increase in the densities of the grids occurred. One can observe the attenuation of beta particles due to the presence of air. The darker density grids since its position was furthest from the beta source displayed minimal fluctuations as compared with the control. It is suspected that the orientation of the film in the canister with the beta source is the key factor responsible for the dramatic increases of the lighter density grids. Emulsions #3a and 3b exposed for a period of six days with the grid orientation reserved produced substantial differences in the darker grids as shown in the graphs. There is a great deal of fluctuations in this sample between the beta exposed density grids and the control density grids. The lighter density grids whose orientations was reversed displays minimal fluctuations due to the presence of this beta source and the attenuation that is taking place.

## **Neutron Interaction**

Using Morgan State University Neutron Howitzer for varying lengths of exposure the H&D curve shows an increased fog level at the shoulder or is substantially fogged. The controls are relatively well behaved except for pronounced reciprocity failure for both the controls the neutron exposed film. In one sample set it was observed that the neutrons seemed to have some effect on the very transparent grains and small amount of fogging occurs.

## **Gamma Rays**

Examinations of the data using a gamma ray source seems to produce a remarkable separation of at the linear portion of the H&D curves. This separation is remarkable for both, at the toe and shoulder of the H&D curve. This separation is unobserved. But it is remarkable that at longer exposures of gamma rays from the gamma ray source, the lower densities of large grains seem to increase substantially at both the toe and shoulder of the H&D curves.

## **Beta Particles**

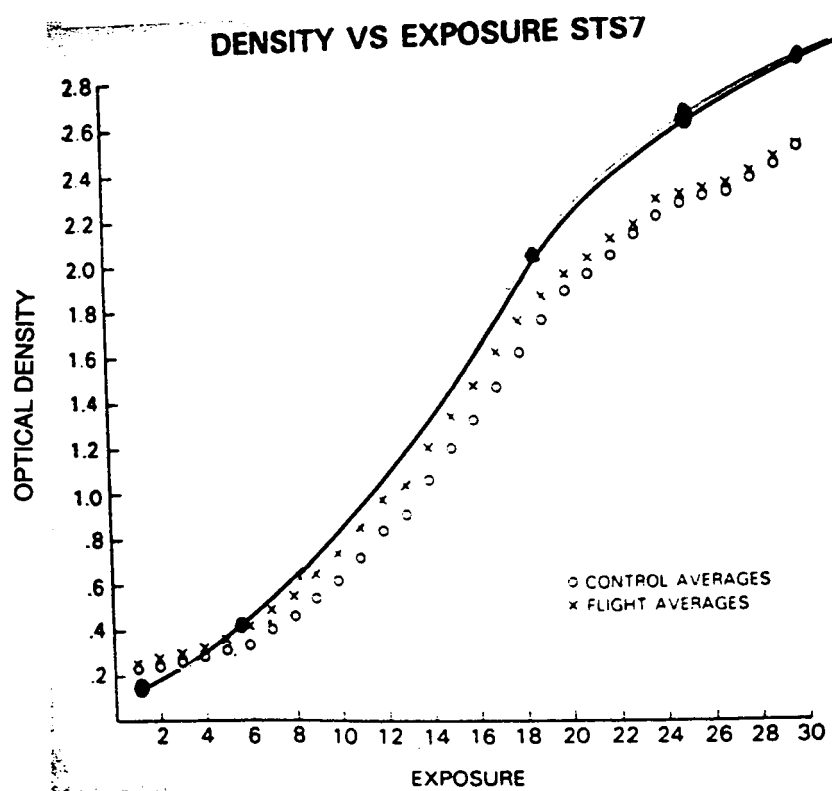
Looking at the effect of the beta particles over a period of six days. With the grid orientation reversed, differences can clearly be seen at the linear density wedges while the beta particles tend to effect the higher density of the film. Reversing the beta particles source within the plastic canister tend to effect the fogging levels for the lower density wedges. So in conclusion, the closer the source of the beta particles to the film will cause sensitometric fogging increases recorded on the film.

On STS7 the separation between the linear portion of the H&D curve is substantial and is reasonably comparable to the gamma ray effects. An STS50 averaging all the individual step wedges produced a substantial separation at the lower density wedges, while at the darker density wedges for the flight film produced reduced fogging or some type of reciprocity failure which was compared to both neutron and gamma ray. An examination of alpha particle interaction at three major energies seems to confirm that the higher energy particles produce greater damage at the low density wedges. Current data from the most recent flights on the shuttle are being analyzed.

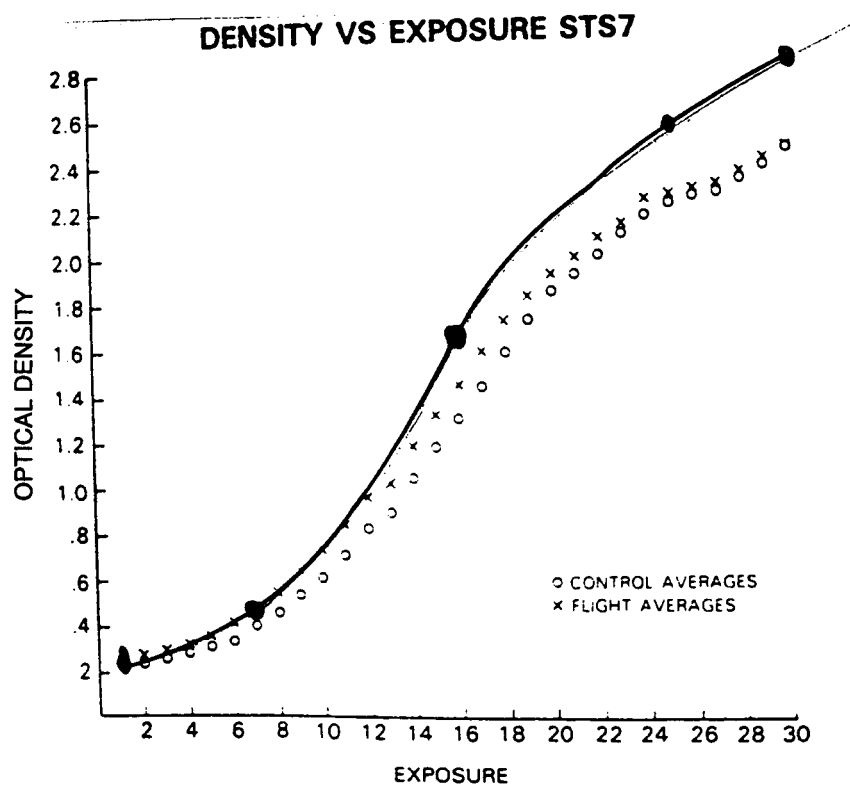
## Conclusion : Radiation Effects as Related to Flight Film

After the examination of neutron, gamma ray and beta particle interaction with the control film, let us compare these results to the density versus exposure for STS7 films flown on the Get-Away -Special. The neutrons show an increase in fogging at the shoulder of the H and D curve. There are no such increase observances on the films flown on STS7. The laboratory gamma ray exposure shows some slight statistical change between the control and the flight film. There is a slight similarity just above the toe of the H and D curve which can be clearly associated with some type of gamma or cosmic ray interaction. The beta particle interaction is extremely high at the shoulder and the toe of the H and D curve. We believe that the separation between the control and flight film are primarily due to gamma, cosmic, and thermal ray interaction at much higher density levels.

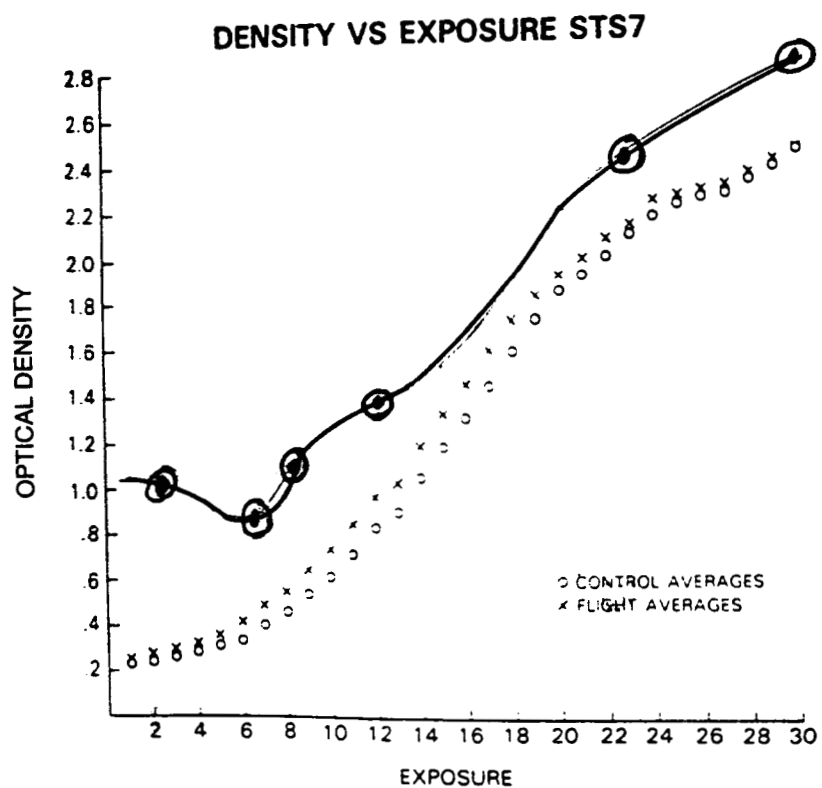
## Neutron Responses Compared to Flight Film



## Gamma Ray Responses Compared to Flight Film

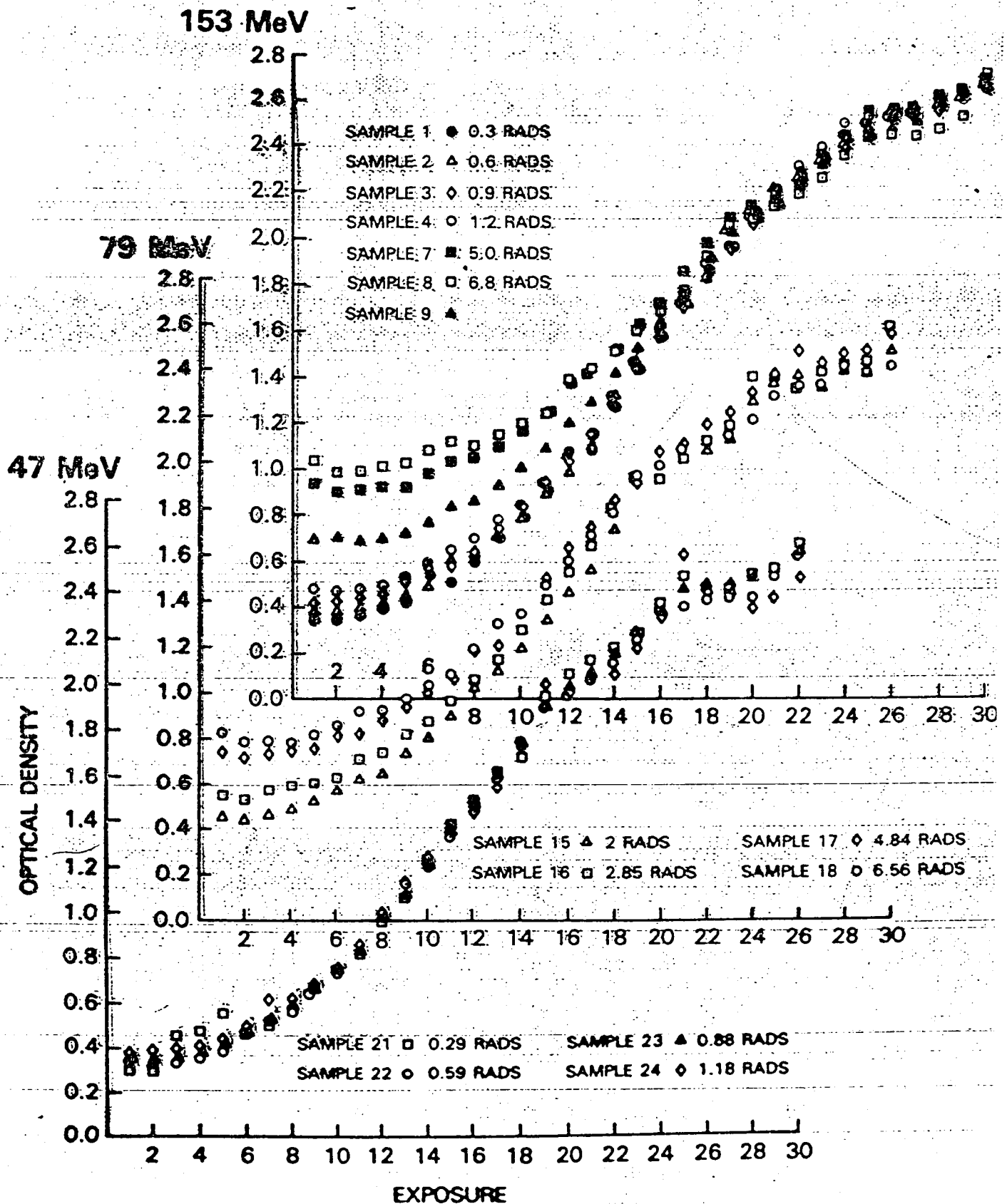


## Beta Particles Responses Compared to Flight IIaO Film





# MeV ENERGY VS. DOSAGE



## CHARACTERIZATION OF FLUID PHYSICS EFFECTS ON CARDIOVASCULAR RESPONSE TO MICROGRAVITY [G-572]

George M. Pantalos, Thomas E. Bennett\*, M. Keith Sharp,  
Stewart Woodruff, Sean O'Leary, Kevin Gillars, Mark Lemon†, and Jan Sojka†

University of Utah, Salt Lake City, Utah

\*Bellarmine College, Louisville, Kentucky

†Utah State University, Logan, Utah

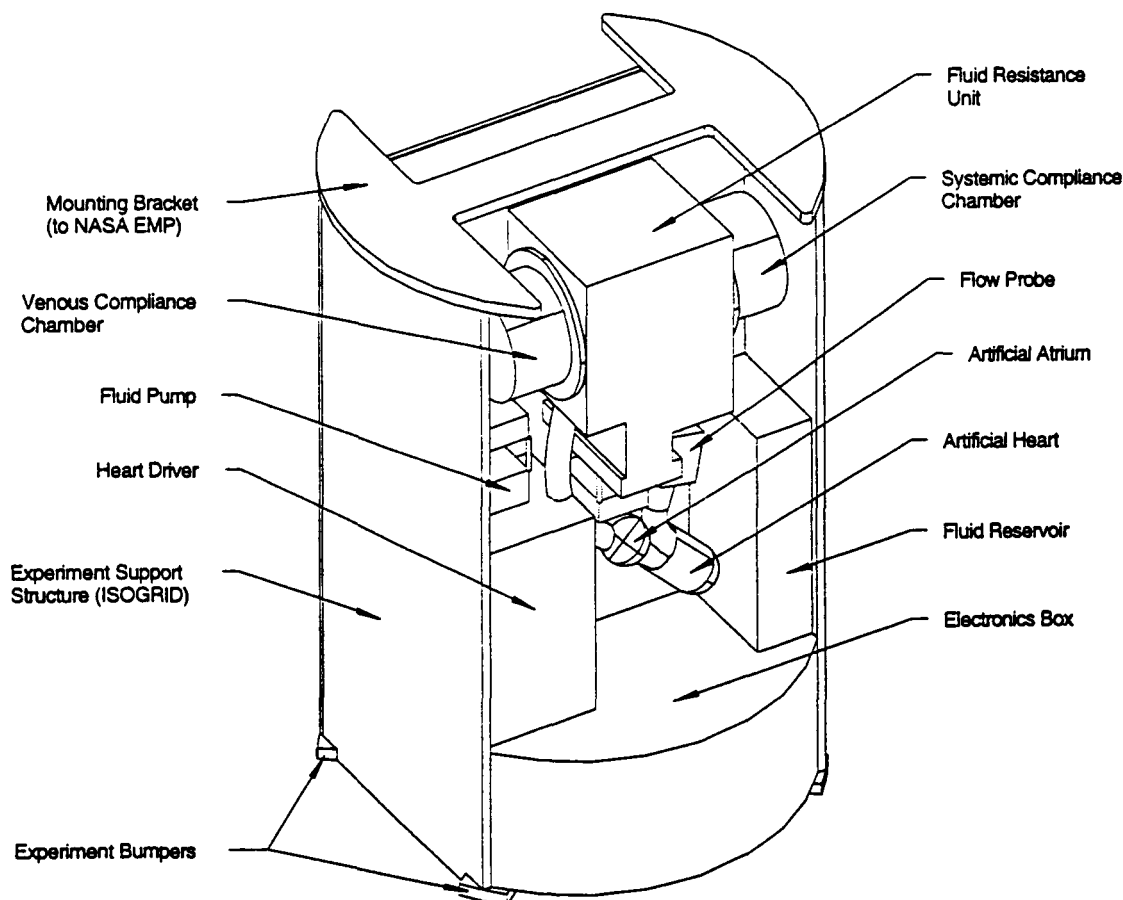
The investigation of cardiovascular adaptation to space flight has seen substantial advancement in the last several years. In-flight echocardiographic measurements of astronaut cardiac function on the Space Shuttle have documented an initial increase, followed by a progressive reduction in both left ventricular volume index and stroke volume with a compensatory increase in heart rate to maintain cardiac output. To date, the reduced cardiac size and stroke volume have been presumed to be the consequence of the reduction in circulating fluid volume within a few days after orbital insertion. However, no specific mechanism for the reduced stroke volume has been identified. The following investigation proposes the use of a hydraulic model of the cardiovascular system to examine the possibility that the observed reduction in stroke volume may, in part, be related to fluid physics effects on heart function. The automated model is being prepared to fly as a GAS payload within the next year.

Many factors influence the filling of the heart during diastole. These factors include (1) the atrial pressure, (2) the inertia of the blood as it enters the ventricle, (3) the transmural pressure difference, (4) the myocardial compliance including myofibril passive, elastic recoil, and (5) the gravitational acceleration-dependent hydrostatic pressure difference that exists in the ventricle due to its size and anatomic orientation. This pressure gradient, which can be estimated to be  $6660 \text{ dynes/cm}^2$  ( $\approx 5 \text{ mm Hg}$ ) in an average adult, acts to augment the diastolic filling of the heart. The investigators have hypothesized that the absence of this contribution to the ventricular filling process in the microgravity environment of space flight may account, in part, for physiological factors that would act to reduce cardiac filling and consequently result in a reduced stroke volume.

The experimental apparatus to investigate this issue consists of a pneumatically actuated, elliptical artificial ventricle (UTAH-100 human version left ventricle) connected to a closed-loop, hydraulic circuit (Penn State) with adjustable compliance and resistance elements to create physiologic pressure and flow conditions. A 40% glycerin in water solution is used in the hydraulic circuit to simulate the viscosity of blood. The ventricle is powered by a miniaturized controller (Symbion, Heimes® Portable Heart Driver) originally developed for use with clinical artificial heart recipients. Ventricular instrumentation includes high-fidelity, acceleration-insensitive, catheter-tip pressure transducers (Millar Instruments) in the apex and base to determine the instantaneous ventricular pressures and  $\Delta P_{LV}$  across the left ventricle ( $LVP_{\text{apex}} - LVP_{\text{base}}$ ). The ventricle is also instrumented with pressure transducers (Millar Instruments) immediately upstream of the inflow valve and downstream of the outflow valve, and an ultrasonic transit-time flow probe (Transonic Systems) downstream of the outflow valve. Acceleration of the experiment will be sensed by a miniature piezoresistive accelerometer (Endevco) and the temperature at three

locations in the experiment will be sensed and recorded by an ambient temperature recording unit (NASA/ARC ATR-4). Heating elements (Minco) are incorporated into the hydraulic circuit to establish and maintain the temperature in the operational range of 20° to 40° C. The experiment is thermally insulated by an external sleeve of multiple layers of aluminized Mylar with a Beta cloth cover (NASA/JSC). A bidirectional roller pump is used to inject or withdraw fluid from the hydraulic circuit to create different preload conditions for the artificial ventricle. The experiment is microprocessor controlled (Campbell Scientific, CR-10) with analog signals stored on a seven channel FM data tape recorder (TEAC, HR-30) which can provide up to three hours of continuous recording. Power for the experiment is provided by an array of alkaline batteries (Duracell) in a sealed battery box.

On-orbit performance of the experimental protocol will be initiated once the operational temperature range has been established. By experimentally varying the circulating fluid volume in the hydraulic circuit, ventricular function can be determined for varying preload pressures at a regulated, fixed afterload pressure of 95 mm Hg. This variation in preload condition will permit the construction of ventricular function curves for the microgravity environment for comparison to ventricular function curves constructed from data recorded in the 1-G environment. Eight developmental experiments on board the NASA KC-135 aircraft have demonstrated proof-of-concept and provided early support for the proposed hypothesis. Developmental progress on the GAS version of this experiment will be presented. The schematic layout of the experiment package is presented below.



# **Does Solar Radiation Affect the Growth of Tomato Seeds Relative to their Environment?**

**Kristi Holzer  
Timber Lake High School**

## ***Introduction***

Have you every thought that you might have the opportunity to send something up in to space? Receiving an opportunity like this has been a great experience for me. Recently I send tomato seeds up into space to see whether radiation affected the growth of the tomato seeds. I also wanted to see whether the tomato seeds will produce any fruit.

## ***Purpose***

The purpose of this experiment is to sequentially study and analyze the data collected from the germination and growth of irradiated Rutgers Supreme tomato seeds to adult producing plants. This experiment will not use irradiated seeds as a control as I plan to note growth in artificial verses natural environment as the basic experiment.

## ***Procedure***

Sequence is defined and divided into three phases. First as the process of germination, transplanting, and noting growth until the Regional ISEF on March 21, 1995. Secondly, when appropriate, selected seedlings will be transplanted to an outdoor garden allowing for natural growth within our regional climate for data collection. Third, to remove some selected plants prior to fall to an artificial indoors setting to continue the growth process and collect data.

In phase one, I will use an active control and experimental group of seeds (same flight, different package lot number) with the same approximate package date. Laboratory conditions will be such to afford the same for both groups to simulate a natural setting. I have considered the actual age of the seeds, being packaged and sent in the Shuttle Columbia on January 1990 as a possible problem to germination rate, but equal to all seeds used for experimentation. Phase one and two will employ growth after germination. This is outlined in the following paragraphs.

Phase two notes the movement of plants to an outdoors harden and creates the necessity of new data collection methods. This researcher will stop height measurements after the first table ripe tomato is removed and shall then begin to weigh and count all ripe tomatoes produced by each individual plant. Unripe tomatoes will be added to data at time of the plants' death. This outdoors method will assume all of natures activities will be equal as well as artificial methods of watering and fertilizing. This method will allow for control verses experimental group comparisons with some plants remaining indoors.

For all but six preselected plants data collection will conclude when plants die as a result of natural activities of the climate.

Phase three is to collect the preselected plants prior to frost relative to their natural death and reinstall them into an indoor artificial climate. This process will allow the continued collection of plant growth data. I will proceed with this last step until the plants die or no longer produce tomatoes.

## **Hypothesis**

Through this experiment I expect to prove that there will be significant adverse effects of solar radiation on the plant germination and growth.

## **Conclusions**

I have made the following conclusions, that the germination rate and germination time were not normal. The tomato seeds that went into space seemed to germinate faster than the regular seeds or the control group. The growth rate was normal, with the exception of Group B, which appeared to be slow in development. The germination time was half that of the common seeds.

## **Results**

The germination rate was 100%. Germination time was half that of the common seeds. The plant growth appeared to be normal except for Group B which appeared to be slow in development.

As of July 5, 1995, I have no recent results because on July 3, 1995 at 4:30 p.m. a thunderstorm that produced hail destroyed my tomato plants. The plants had just begun to have blossoms on the leaves.

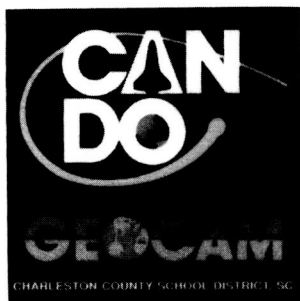
At the present time I am unaware of the possible results but will attempt through the above steps to determine the growth effects of artificial verses natural environment using irradiation Rutgers Supreme tomato seeds.

## **Bibliography**

J. W. Bracheer, *Seeds Dormancy and Germination*, New York: Chapman and Hall, 1988.

University of Minnesota, *The Plant Seed, Development, Preservation, and Germination*, New York: Academic Press, 1979.

Zilke, Samuel, *Effects of Environment on Seed Germination and Early Seedling Development of *Cirsium Arvense**, 1967.



## SMALL PASSIVE STUDENT EXPERIMENTS ON G324 261 INDIVIDUAL QUESTS FOR STUDENT KNOWLEDGE

James H. Nicholson -- Medical University of South Carolina

Carol A. Tempel -- Charleston County School District

Ruth Ashcraft-Truluck -- Wando High School

Robin Rutherford -- Goodwin Elementary School

### ABSTRACT

The Charleston County School District **CAN DO** Project payload on **STS-57** had a primary goal of photographing the Earth with the **GeoCam** camera system. In addition, the payload carried 261 passive student experiments representing the efforts of several thousand students throughout the district and in four other states. These experiments represented the individual concepts of teams ranging in age from pre-school to high school. Consequently, a tremendous variety of samples from collard green seeds to microscopic "water bears" were flown. Each prospective team was provided a simple kit equipped with five vials. Each student team submitted five coded samples, one for space flight and four control samples. The control samples were exposed to radiation, cold and centrifugation respectively while one negative control sample was passively stored. The students received the samples back still coded so that they were unaware of which samples were flown. They then investigated their samples according to their individual research protocols. The results were presented in poster and platform form at a student research symposium.

**Space Trees** grown from tree seeds flown in the payload have been planted at all district schools, and at many guest schools. These seeds represented another way in which to involve additional classes and students.

Both the passive experiments and the space trees were housed in what otherwise would have been wasted space within the payload. They extended the **GAS** programs worthwhile ballast concept to another level. The opportunity to fly an experiment in space is too precious not to be extended to the greatest number of students possible.

### EXPERIMENTAL RATIONALE

To be successful, a payload should actively involve many students working at their own level. This suggests some possible criteria in the design of a perfect experiment. One is that it should be applicable to as many grade levels as possible and require a minimal amount of expertise, equipment and expense. It also should require a small enough

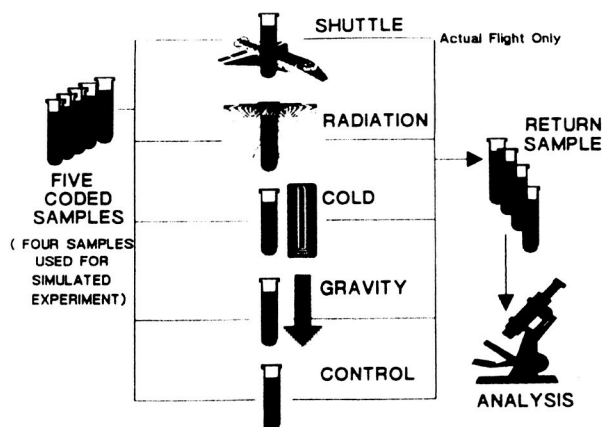
time commitment to allow it to fit into already crowded curriculum schedules. It is important that the experiment teaches some fundamental, solid scientific principles and uses sound scientific methodology. Most important, the activity should be as fail-proof as possible, provide active participation, and be fun.

A good example of an activity that comes very close to meeting these criteria is the inclusion of small passive student experiments in the G324 payload

### CONCEPT DEVELOPMENT

When the G324 payload was originally scheduled to fly in 1986, the criteria for student designed experiments was very open for both size and weight. In spite of this, almost all of the experiments submitted fit quite easily into small 5ml cryovials. These cryovials are designed to survive freezing in liquid nitrogen and provide a positive gasket seal. The vials are inexpensive and meet safety requirements for positive containment.

One problem with many of the materials that students might choose to fly in space is that they will be unaffected by the relatively benign environment aboard a vehicle designed to fly fragile humans. Also the normal handling procedures for GAS payloads include long storage times that preclude most living materials.



Our main goal was not to teach just the effects of low Earth orbit but to teach scientific methodology. It was apparent, especially to those who judged science fairs, that many students had a poor concept of what constitutes a valid scientific experiment. Fundamental principles, such as blind studies, and the use of controls were mostly unknown. It was decided to use the small passive student experiments as a vehicle to teach these important principles.

### **EXPERIMENTAL PROCEDURE**

Each student team was provided with a kit composed of an envelope and five color coded 5ml cryovials. The envelope also served as the experimental registration form and was filled out with all the information necessary to handle and track the sample. The students filled each vial with an identical sample of their material and wrote their experiment number on the vial with indelible pen.

One of the five vials was placed in a special aluminum housing inside the G324 payload and flown aboard STS-57. A second vial was exposed to extreme doses of radiation in a laboratory gammator. The third vial was frozen in two separate cycles in liquid nitrogen. The fourth vial was spun on a laboratory centrifuge to approximately 600g. The fifth vial was passively stored to serve as a negative control. At the completion of the flight, all five vials were returned to the student teams. The teams were not informed as to which color vial experienced which condition so that all research would be conducted "blind".

### **SAFETY**

Safety rules were developed both to protect the shuttle and the student experimenters. Forbidden items included: flammable, pyrotechnics, human pathogens, body fluids, disease causing organisms, corrosives, radioactive material, lithium batteries, oils, and soda. Students were not allowed to taste or consume any test material. Radiation safety officers at the Medical University of South Carolina confirmed the safety of the irradiated material. A volunteer pathologist reviewed all submissions for disease hazard. The cryovials performed well with no incidents of breakage or leakage in either space-flown or control material.

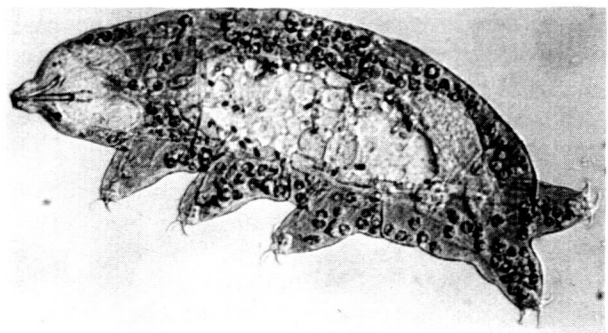


Bear Hunters

NGS Photo

### **WATER BEARS**

It is impossible to describe all 261 experiments in a short paper but one experiment serves as a model for all. Microscopic tardigrades (*water bears*) live on lichens. These unique little creatures can live for years in suspended animation when dried. They begin to re-animate in as little as 20 minutes if placed in water. Students in a biology class at Wando High School in Mt. Pleasant SC decided that this made *water bears* prime space candidates. At first they ordered specimens through a biological supply house, but discovered that they could collect them locally. Although Charleston has none of the limestone rock that tardigrades prefer, the students discovered that they could be found on old limestone tombstones. By flushing water through collected lichens, *water bears* could be concentrated under a microscope. Once carefully dried, the tardigrades were flight-ready having gone from a 19th century graveyard to an ultramodern spacecraft. Because the *water bears* were easy to see under a classroom microscope, other classes became interested. Wando High's "Bear Hunters" became mentors to first grade scientists at Goodwin Elementary School and supplied them with *bears* and training.



Water Bear

Can Do Photo



Planting Space Trees

Can Do Photo

### **SPACE TREES**

Smaller lenses and a reduced requirement for heating batteries brought G324 down in weight. This opened up the possibility of more secondary experiments. The Timberlands Division of the Westvaco Paper Company offered to supply seed for the first ever "space trees". With the forester's advice, students selected Loblolly Pine and Sycamore as representative South Carolina trees. The devastation to local forests from the August 1989 visit of Hurricane Hugo made this project even more appealing.

With the help of students enrolled in a forestry intern program, seeds were gathered from selected prize trees and carefully prepared for space flight. They were supplied in bulk packages for housing in the aluminum experiment box in the payload. In addition, Westvaco made seeds available to any classes who wished to use them for small passive experiments.

After the flight, the seeds were returned to the care of the foresters who grew them into seedlings suitable for transplantation.

On Arbor Day 1994, a pair of seedlings was supplied to all the schools in the district. Additional trees were supplied to guest schools in neighboring districts and four other states as far away as California. Several schools in the Houston, Texas area received trees to plant for the children of the STS-57 crew. Complete care instructions and classroom materials were enclosed with all of the trees. Most schools scheduled ceremonies to commemorate the planting of the Space trees. Many students wrote poems and songs for the occasion.

**Space trees spread your roots  
Reach to the far corners of the Earth  
Drink water  
Spread you limbs, grow your leaves  
Grow to touch the stars**

*Michael      Grade 4*

### **CAN DO RESEARCH SYMPOSIUM**

In April 1994, a research symposium was held at James Island High School with over 85 of the small passive experiment teams attending. Modeled after the format of scientific meetings, the results were presented as either platform or poster presentations. In addition to giving their experimental results, most students identified which vial had actually flown in space. At this symposium, the color codes were finally revealed. Interestingly, most teams correctly identified the space flown vial even though the sample rarely if ever showed significant change. As expected, the radiation and cold control samples were much more likely to show change due to the extreme nature of the treatments.



Research Symposium

Can Do Photo

### **THE PRESENT AND THE FUTURE**

As a method to develop the procedure, simulated experiments were conducted in the years leading up to the flight. The procedure is identical except that the fifth (space flight) vial is omitted. Teachers found this to be a useful tool for teaching the scientific method and a fun classroom activity. As a result they use the simulated experiments as a part of their regular curriculum in Earth Space Science.

Plans are underway to fly the Can Do payload again. In any future mission, these special little experiments will be an important part.



## **SMALL PASSIVE STUDENT EXPERIMENT MATERIALS**

Acrylic Paint  
Alka Seltzer  
Batteries (2)  
Beans, Navy  
Beans, Lima  
Biodegradable Bags  
Black Bread Mold  
Bread Mold (3)  
Brine Shrimp (7)  
Bubble Fluid  
Bubble Mixture  
Bubbles  
**CHEMICALS**  
Alum  
Baking Soda (3)  
Copper Sulfate Pentahydrate  
Cornstarch and Water  
Cornstarch and Coloring  
Fluorite  
Hexamethylenediamine  
Oil and Water  
Salt  
Vinegar  
Water, natural (2)  
Clinitest Tablets  
Clinitest Tape  
**COLLOIDAL MATERIALS**  
Mayonnaise  
Jell-O  
Gelatin  
Crystals, Cobalt Chloride  
Crystals, Copper Sulfate  
Detergents  
Dosimeters  
Enzyme, Thymosin Fraction 5  
Etafilicon-A  
Fertilizer (4)  
Fertilizer 10-10-10  
Film, Exposed  
Film, Negative (3)  
Food Cling Wrap  
Glue  
Hair, Human (2)  
Hot Dog Buns  
Ink Cartridges  
Insect Eggs, Spider  
Iron Fillings  
Killifish Eggs  
Latex Paint  
Lemon Juice

Lichens (3)  
Litmus paper  
M & M's  
Magnets (5)  
Magnets and Salt Water  
Metal Strips, Copper  
**MINERALS**  
Magnetite  
Feldspar crystals  
Quartz  
Quartz, Cubic Zirconia  
Sphalerite  
Mosses  
Paint, Poster  
Paper Clips  
Pluff Mud  
Popcorn (17)  
Rubber Bands (4)  
Sand Designs  
**SEEDS**  
Acorn  
Bermuda Grass  
Bird  
Brassica Rapa  
Camphor Weed  
Centipede Grass  
Chinese Tallow  
Cleome  
Collard Green  
Corn (2)  
Cosmos  
Cotton (2)  
Coxcomb  
Dandelion  
Dogwood (2)  
Dried Beans  
Four O'clock (2)  
Georgia Collard  
Golden Rod  
Grass  
Indian Popcorn  
Lemon  
Lettuce  
Lima Bean  
Loblolly Pine (39)  
Longleaf pine  
Magnolia  
Marigold (3)  
Mimosa (5)  
Mimosa & Brassica Rapa

**SEEDS (continued)**  
Okra (2)  
Palmetto (2)  
Pea  
Pine (2)  
Popcorn Tree (5)  
Pumpkin  
Radish (3)  
Red Pepper  
Strawberry  
Sunflower (2)  
Sweet Potato  
Sycamore (11)  
Tomato  
Turnip  
Virginia Pine  
Wild Flower  
Semi-permeable Membrane  
Silly Putty (2)  
Slime (3)  
Soil Samples (3)  
Spanish Moss (2)  
Spices, Cinnamon  
Spices, Old Bay  
Spores, Dry Penicillin  
Steeped Coffee  
Super Conductors  
Tea Leaves  
Teeth (2)  
Toothpaste (2)  
Trash Bags  
V-8 Juice  
Water Bears (5)  
Water, Ocean (4)  
Water, Pond (2)  
Water, Rain  
Wheat  
Yeast (7)  
YTLA Ceramics - Type II



261 Dreams      Can Do Photo

## CAN DO EXPERIMENT PACKAGE

School Burst Academy  
School Address 103 Calhoun Street  
Charleston S.C., 29403  
School Phone \_\_\_\_\_

### EXPERIMENT NAME

Charlotte Webb in Space

### EXPERIMENTAL QUESTION

Will space affect the way spiders make their web?

Experiment # **732**

Teacher Kelly R. Kelly Class 5-B  
Home Phone \_\_\_\_\_  
Student Team Michelle Paves,  
Nathaniel VanLandingham,  
Jonathan Brannon

Material Spider eggs in cases

Source of Material 8 spiders found around the hotel homes

How was material prepared?

We gathered untreated  
spider eggs and placed them  
in the test tubes

How will material be tested after treatment?

spiders will be grown in  
incubators

### RETURN TO:

Carol A. Tempel, Coordinator  
Charleston County School District  
Office of Math, Sciences & Technology  
3 Chisolm Street Charleston, S.C., 29401  
(803) 720-3020



A Standard Small Passive Student Experiment Envelope

Can Do Photo

# HITCHHIKER MISSION OPERATIONS

## Past, Present and Future

Kathryn Anderson  
Omitron, Inc.  
6411 Ivy Lane, Suite 600  
Greenbelt, Maryland 20770  
(301) 474-1700

Contributors: Agustin J. Alfonso, Georgeann Brophy, Victor Gehr, Brian Murphy, Francis Wasiak

---

### ABSTRACT:

*What is mission operations? Mission operations is an iterative process aimed at achieving the greatest possible mission success with the resources available. The process involves understanding of the science objectives, investigation of which system capabilities can best meet these objectives, integration of the objectives and resources into a cohesive mission operations plan, evaluation of the plan through simulations, and implementation of the plan in real-time.*

*In this paper, the authors present a comprehensive description of what the Hitchhiker mission operations approach is and why it is crucial to mission success. The authors describe the significance of operational considerations from the beginning and throughout the experiment ground and flight systems development. The authors also address the necessity of training and simulations. Finally, the authors cite several examples illustrating the benefits of understanding and utilizing the mission operations process.*

---

### INTRODUCTION

The mission operations process starts at the earliest stages of Hitchhiker Project and customer interaction and culminates in on-orbit operations. Experience has proven that an attention to operations is integral to the development and ultimate success of a Hitchhiker Payload.

Ideally, payload operations activity begins even before an experiment is manifested as a shuttle payload. At this stage, when experiments are still being conceptualized, mission operations plays a crucial role. A customer can design an experiment to maximize the possibility of mission success by understanding the capabilities and limitations of the Hitchhiker and Orbiter systems up front.

The Hitchhiker operations group aims to capitalize on the wide range of services and capabilities available to Hitchhiker customers. As the team investigates which capabilities can best meet science objectives, compatibility between payload requirements and Space Shuttle Program (SSP) resources is determined. Mission Operations is a driving factor in the definition of the Space Shuttle Manifest.

Once a payload is manifested on a compatible flight, requirements and resources are integrated into a cohesive

mission operations plan through an interactive dialogue between Hitchhiker, Orbiter, and experiment personnel. The resulting operations plan prepares and guides the Hitchhiker Flight Operations Team (FOT), consisting of both operations personnel and experiment teams, through both nominal and contingency flight situations.

### MISSION OPERATIONS PLANNING

Mission planning is a multi-faceted and interactive process, as illustrated in Figure 1. Early reviews are essential in the planning of flight timelines and procedures. Operations training, provided through all stages of payload development, plays a fundamental role by introducing the capabilities and constraints of the Hitchhiker and Orbiter systems. Knowledge of these constraints aids in the development of hardware, software, and mission operations documentation and plans. Once the flight activities and requirements have been documented and the Hitchhiker ground system has been verified, the Hitchhiker operations group prepares experimenters for real-time operations through further classroom training and interactive simulations.

The mission planning process involves years of preparation which culminate in a relatively brief period of flight. As the mission success of the payloads, not to mention the safety of the Orbiter and crew, are dependent upon the thorough

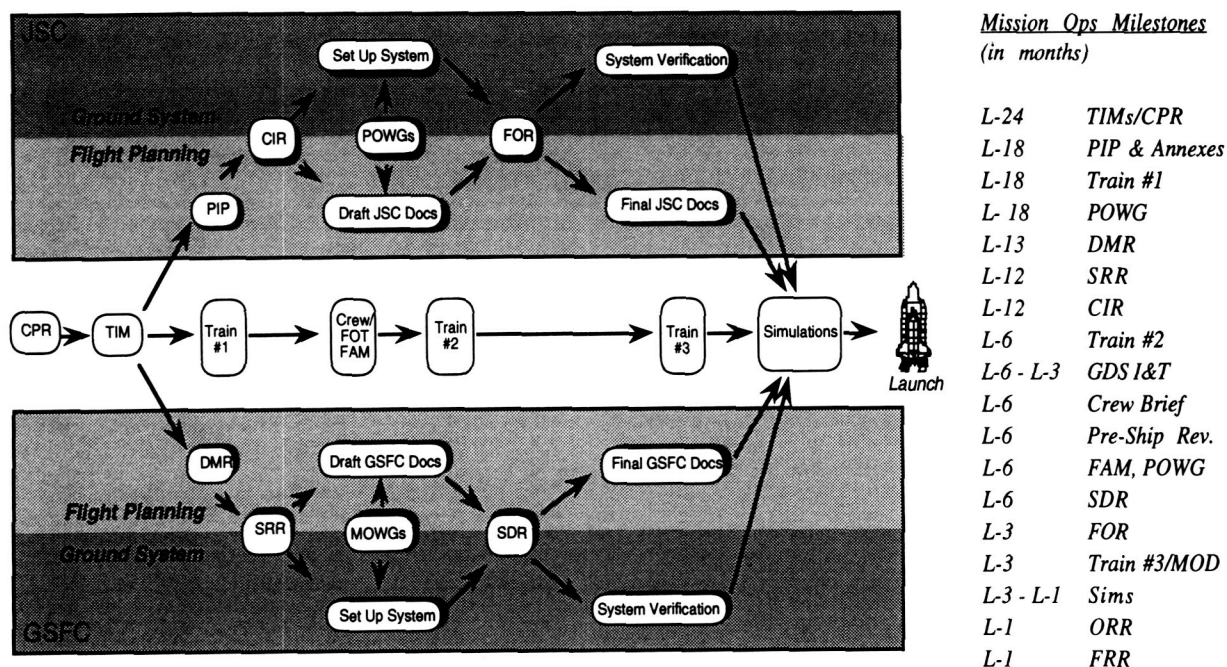


Figure 1: Mission Planning Process

Documentation/Event	Corresponding Review
• Customer Payload Requirements (CPR)	• Technical Interchange Meeting (TIM)
• Training #1/ Payload Integration Plan (PIP)	• Payload Operations Working Group (POWG)
• Detailed Mission Requirements (DMR)	• Cargo Integration Review (CIR)
	• System Requirements Review (SRR)
	• System Design Review (SDR)
	• Ground Data System I&T (GDS I&T)
• Ship to KSC	• Pre-Ship Review
• Document Publication/Training #2	• Payload Operations Working Group (POWG)
• Crew Brief/Familiarization Brief (FAM)	• Flight Operations Review (FOR)
• Simulations/Training #3	• Sim Debrief
• Mission Operations Document (MOD)	
• "GO" for Launch	• Operational Readiness Review (ORR )
	• Flight Readiness Review (FRR )

planning and preparation of the entire flight team, final simulations and reviews are held to verify the flight readiness status of all supporting elements, both human and mechanical.

### Flight Operations Documentation/Meetings

#### Payload Requirement Definition

The earliest stage of the mission operations planning process is concentrated about the generation of documentation within the customer's facilities and at the Goddard Space Flight Center (GSFC). Early technical interchange between the Hitchhiker team and the customer is crucial in the definition of payload requirements and the development of the

experiment flight and ground systems. These preliminary meetings, designated Technical Interchange Meetings (TIMs), are ideally scheduled approximately two years prior to flight. TIMs provide a forum for the discussion of payload requirements and goals as defined in the agreement between the Hitchhiker Project and the customer, the Customer Payload Requirements (CPR) Document. The CPR contains a myriad of detailed experiment information: operation cycles, crew involvement, command/telemetry requirements, power requirements, ground system requirements, Orbiter pointing restrictions, instrument field of view, descriptive material and mission objectives. The Mission Manager (MM) utilizes the CPR and information gathered at TIMs to oversee the integration of the customer's experiment with the Hitchhiker and Orbiter communities.

In preparation for the TIMs, the MM gathers lead personnel from various disciplines supporting Hitchhiker missions to discuss payload integration issues and payload operational requirements and constraints. The team leads are then responsible for generating and maintaining documentation of payload requirements and specifications for submittal to the Johnson Space Center (JSC). The Operations lead, designated the Operations Director (OD), maintains an ongoing dialogue with the customer point of contact throughout the mission operations planning process and verifies his/her work through customer feedback. The OD also supports payload status meetings to determine if payload development and integration issues could impact mission operations.

The OD supplements the TIMs with preliminary mission operations training sessions, providing the customer with an early awareness of the operational capabilities and constraints of the Orbiter and Hitchhiker systems. From these sessions, an expanded definition of payload requirements materializes and the OD begins to analyze customer requirements versus the wide range of services and capabilities available.

As payload development progresses, the OD integrates payload requirements into both joint (between the JSC and all payloads) and Hitchhiker specific documentation and support JSC in the final preparation of these documents. Hitchhiker specific documents are developed defining internal operations to be followed by the Hitchhiker FOT. The operations training provided throughout development aids in the definition and refinement of these requirements. Engineering and operations reviews are held throughout the mission planning process to analyze the compatibilities/conflicts between various payloads.

#### Joint Mission Documentation and Related Reviews

Utilizing the information in the CPR, the Hitchhiker team leads prepare the Payload Integration Plan (PIP) and its annexes. The PIP is the contract between the Hitchhiker Project, on behalf of the customer, and the SSP. General mission operations information relating to those requirements that affect the manifesting of the Hitchhiker payload with other payloads is contained within the PIP. Specific mission operations requirements and specifications between the Hitchhiker program and the JSC SSP are defined in the PIP annexes. The OD prepares annexes covering electrical and power requirements, flight activity planning, flight operations support, crew training, and Payload Operations Control Center (POCC) interfaces and aids the MM in the development of the PIP. These documents form the basis for detailed operations documentation by outlining specific Hitchhiker customer requirements and mission objectives. Payload Operations Working Group (POWG) meetings may be called to support the definition of payload

requirements and to resolve any issues during the development process.

After submittal of the PIP and Annexes to the JSC, payload representatives attend a Cargo Integration Review (CIR) at which the SSP assesses the compatibilities between the manifested payloads as well as the capabilities of the SSP to meet payload requirements. As stated earlier, mission operations requirements are a driving factor in the consideration of payload compatibility. Once the SSP feels confident that all mission requirements can be met, the shuttle manifest is formally solidified and the PIP and Annexes are baselined.

A basic version of all flight documentation products, including the Flight Data File (FDF), is then developed from the requirements in the baselined PIP and Annexes. The FDF is the total on-board complement of documentation and related aids available to the crew for execution of the flight, including operations plans, crew checklists, and reference data. The Flight Plan is the most significant component of the FDF as it is the control document for on-orbit operations, tying mission operations together by timelining the crew, Orbiter and payload activities. The Flight Plan is developed pre-mission and is updated daily during the flight. Various other documentation is developed to coordinate ground operations. These documents govern nominal procedures and define payload priorities and constraints for consideration in contingency scenarios.

All flight operations documentation is published in basic form approximately 6 months prior to launch. At this time the documents undergo extensive review by mission personnel. The OD involves the customer in this review after providing training on how to read and interpret flight documentation. The OD then submits any discrepancies to the published documentation to the SSP at the Flight Operations Review (FOR). The OD represents the customer at the FOR to ensure that all payload requirements are properly reflected in the final set of flight documentation products, which are used for both simulations and on-orbit operations.

The documentation process is fundamental to flight preparation and mission planning. The OD and the MM use the flight documentation to ensure that payload operational requirements and constraints are not intentionally violated during the flight. These documents facilitate mission operations by prioritizing and organizing on-orbit activities while also providing an assurance that all feasible efforts will be made to preserve and achieve payload goals.

#### GSFC Specific Documentation and Related Reviews

The overall objective of the Hitchhiker Project is to provide service to a variety of customers via standard interfaces as

defined in the Customer Accommodations and Requirements Specifications (CARS) document that can be used for experiment design and development, as well as mission operations. To this end, the Hitchhiker Ground Data System (GDS) utilizes standardized capabilities available at the GSFC. The OD provides training on these capabilities and works with the customer to define which services will best meet their needs.

Utilizing this information, the OD, in consultation with the Mission Support Manager (MSM), determines which GSFC elements are required to support the mission and outlines these requirements in the Detailed Mission Requirements (DMR) document. The MSM, who is responsible for the configuration of the GDS, then monitors the design and implementation of the requirements through a detailed review process.

As the DMR outlines the requirements of the Hitchhiker GDS, the Mission Operations Document (MOD) generated by the OD outlines the operational procedures to be utilized within the POCC. The MOD provides Hitchhiker operations personnel with guidelines to ensure an orderly and efficient operations center, as well as pre-planned decisions to minimize the response time to anomalous events.

The customer is responsible for developing detailed experiment operational documentation governing experiment flight procedures, such as console procedures, command plans, and contingency recovery plans. These procedures guide real-time experiment operations within the Hitchhiker POCC during simulations and flight. Many customers use the Hitchhiker Timeline System (HTS) product as a guideline in the preparation of operational plans and procedures. The HTS, developed exclusively for the Hitchhiker Project, provides operations personnel with communication availability predictions, Orbiter pointing predictions and payload activity timelines. The HTS product is based on the Flight Plan and supporting JSC documents. However, unlike the Flight Plan it is updated at the POCC in real-time. This proves a valuable tool through training, pre-mission planning, and flight by providing the POCC with a locally controlled operations timeline as well as with planning information not readily available from the JSC during a Shuttle flight.

Regardless of the time spent preparing nominal plans, actual on-orbit operations often bring rise to contingency situations in which nominal operational scenarios become unsuitable. Thus it is important that customers take into account all possible operating scenarios, regardless of improbability, in preparation for a mission. Unlike a world of free-flyers, where scientists have days, if not months, in which to troubleshoot a problem, shuttle flights offer a relatively short period for implementation of the experiment timeline.

Pre-mission contingency planning is critical for a successful flight. The OD aids the customer in the development of off-nominal scenarios pre-flight and facilitates the on-orbit execution of contingency resolution in a timely and efficient manner.

All internal GSFC documents and reviews are geared towards the creation of a functional and operational ground system. As the DMR outlines the resource and service requirements of the payload, the MOD guides the daily activities and duties of the operations personnel, and the experiment procedures govern the real-time operations of the payload. The procedures and protocols in the MOD foster an atmosphere geared to the success of real-time operations.

### **Mission Training**

In the early years of the Hitchhiker program, mission operations training was provided informally throughout payload development and presented in a formal session relatively close to flight. Although some experiments manifest as a Hitchhiker payload after system design is complete, some experiments manifest early enough in the development process for training to influence experiment design. Several customers have responded that an earlier insight into the resources of the Hitchhiker system would have helped them to design their experiments better by using more of the services available to them. Thus a new training approach has been adopted, one which offers formal training at at least three points through payload development and mission planning. This training is offered early and is repeated often throughout the development process.

### **Mission Operations Training**

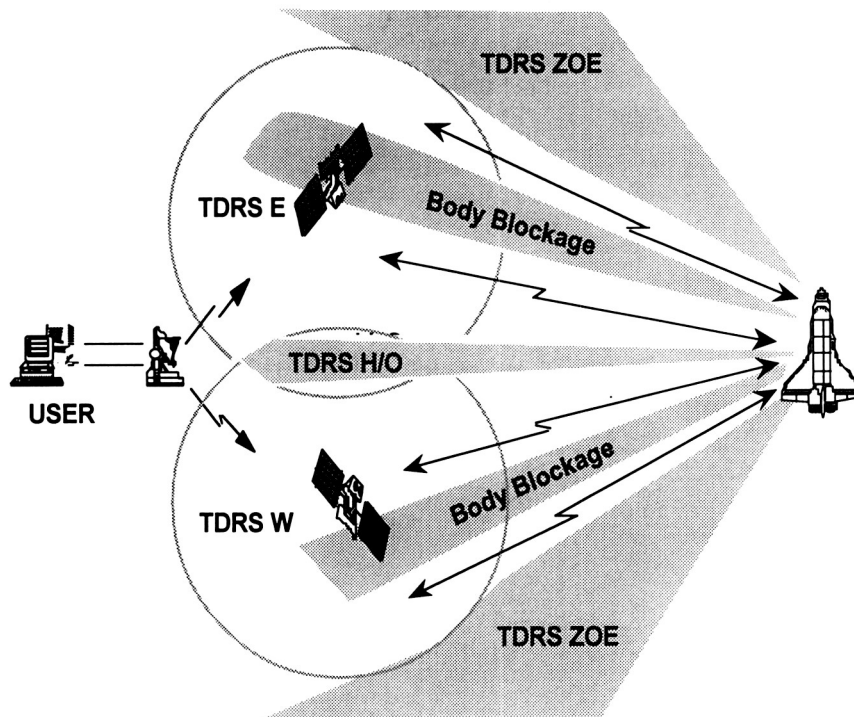
Payload Mission operations are driven by the capabilities and limitations of the resources at hand. Understanding the nature of Orbiter to ground communications, standard operational contamination factors, and GDS capabilities is imperative for maximizing science return during a mission. To provide this essential Hitchhiker education, a series of classroom training sessions is held to familiarize customers with Hitchhiker and Orbiter services, data systems configurations, and all aspects of mission operations as shown in Figure 1.

The first training session introduces the capabilities of the Orbiter telecommunications systems, addresses the concept and function of the Hitchhiker ground system, and summarizes contamination factors that may impact payload operations. This session plays an important role in payload development as experimenters can channel the design of their hardware and software both on-orbit and on-ground to the capabilities and constraints of the operational systems. For



*This diagram illustrates only a small portion of the operational systems and or factors which often enhance, and sometimes degrade, yet always dictate, Hitchhiker mission operations.*

*Hitchhiker experiments produce low rate (LR) and medium rate (MR) data which is transferred to the ground through the Orbiter S-Band and Ku-Band systems via the Tracking Data and Relay Satellite (TDRS) System (TDRSS). The Orbiter records LR data during Loss of Signal (LOS); MR data is not recorded. Communications via the TDRSS can be constrained by many factors, such as loss of sight to a TDRS due to the TDRS Zone of Exclusion (ZOE) or structural blockage, handovers of communications from one TDRS to the other, corrupted or weak communication signals due to interference, or conflicting Orbiter or payload requirements for dedicated satellite communications.*



*Shaded areas indicate a loss of communications between the Orbiter and the TDRSS.*

**Figure 2: TDRSS Communication Constraints**

example, experiments relying heavily on medium rate data may be influenced to add a recording device onto their payload to ensure that communication outages, some of which are illustrated in Figure 2, will have a minimum impact on their operations planning. Other experimenters may opt to design their command interface to allow serial commands in lieu of basic bi-level operations.

This initial training also plays an important role in the definition and requirement of system constraints. A flight constraint may sometimes be no stricter than a requirement that the Hitchhiker POCC be notified prior to a deviation from the planned contamination event or timeline. The reasons for this are two-fold: to safe instruments that may be wary of contamination yet who do not require an inhibit, or to enhance the science opportunities for payloads wishing to observe contamination events.

The most important function of this preliminary training session is to raise experimenter awareness of all of the factors that will dictate mission operations. The training provides the information necessary for the customer to levy informed requirements and constraints on the SSP through the operations documentation outlined before.

The second operations training session describes flight and ground documentation used during on-orbit operations. These documents form the basis for all payload operations and coordination. It is vital that experimenters can interpret and understand the flight documents which outline all mission operations. The OD instructs the customer on how to read the Flight Plan, Operations Timelines, Attitude Timelines and the HTS, with emphasis on all details which will prove critical in timing experiment operations. The customer learns how to use the HTS as a mission planning tool, above and beyond those provided by JSC. The OD presents this training as soon as the basic version of flight documents are published, facilitating customer participation in the FOR process.

The final mission training session is held immediately prior to the first simulation. This training focuses on real-time operations within the control center. The OD introduces many JSC-generated products which will be utilized in real-time during the mission and simulations, such as the Execute Package (Flight Plan). Additional Hitchhiker-specific products such as the HTS, contamination schedules, and status reports will also be distributed regularly to all users in the POCC during missions and simulations. The OD presents the MOD which outlines the important procedures that govern day-to-day operations within the POCC, such as shift handover guidelines, shift reports, and

voice protocol, and covers the distribution of products outlined above. The classroom session is supplemented with hands-on familiarization with POCC equipment.

The expansion of the training process through all stages of payload development offers more flexibility in customer support and involvement. Training sessions are often performed multiple times to train additional personnel or simply to reacquaint those previously trained with highlights from earlier sessions.

#### Crew/JSC Flight Operations Team Training

Approximately six months prior to launch, the MM, the OD, and the customer hold a Familiarization Briefing at the JSC to train the JSC FOT on the Hitchhiker payload. Around the same time, the crew visits the GSFC for the Crew Briefing at which the crew is briefed on the Hitchhiker payload goals and operations and views the payload hardware. Although crew involvement in the majority of Hitchhiker payloads operations has been generally limited to activation and deactivation of the payload and the possible establishment of observation attitudes, some payloads place significant responsibilities upon the crew. Thorough training provided by the JSC Training Team under the direction of the OD is essential in the success of crew-intensive payload operations.

#### **Ground Data System Development and Test**

The Hitchhiker Mission Readiness Manager (MRM) is responsible to the MSM for providing and verifying the Hitchhiker GDS ground system based on the DMR requirements. The Hitchhiker MRM verifies the functionality of the GDS with the payload and the JSC MCC through a series of tests beginning in conjunction with the payload integration activities and continuing until launch.

Customer experiments are delivered to the GSFC where they are electrically and mechanically integrated to the Hitchhiker carrier. After all experiments have been fully integrated, the MRM conducts a POCC Test to verify the end-to-end capability of the Customer Ground Support Equipment (CGSE), located at the Hitchhiker POCC, to communicate with the payload via the GDS. During these tests, telemetry from the payload is recorded for use in future interface tests and simulations in lieu of a real-time payload telemetry stream. The OD and the Sim Sup may script an operational scenario to run through during this test as a script allows for operational sequence evaluation and provides greater dynamics to data played back during the simulations. Following these activities, the payload is shipped to the Kennedy Space Center (KSC) where it is unpacked and readied for installation and flight.

Further tests using taped data are performed to verify all

interfaces and support elements that will comprise the operational GSFC GDS. Finally, the MRM schedules additional tests prior to each Joint Integrated Simulation (JIS) and launch to verify the command and LR telemetry interfaces between the JSC MCC and the GSFC.

#### **Simulations**

Once the Hitchhiker GDS has been verified and both joint and internal mission documents have been developed, operational simulations are conducted to verify operational procedures and exercise the communication between all operators. These simulations do not test how well experimenters know their systems; they evaluate whether the plans and procedures for real-time operations are satisfactory.

Simulations are supported by the entire Hitchhiker FOT, composed of all operators required for real-time support during the mission, including the Mission Manager, the experimenters, the Operations Directors and all supporting personnel within the POCC. Simulations allow the experimenters to apply the knowledge gained in the training sessions in a realistic environment. They provide familiarity with the control center environment, POCC operations and procedures, and both inter and intra-center coordination. Simulations also result in a diverse forum of FOT personnel who can benefit each other through the sharing of operational experience and lessons learned. 'Novice' Hitchhiker customers can learn from the experiences of flight 'veterans'; while experimenters with previous Hitchhiker experience can learn once again how to function within a diverse and intense team environment. The Hitchhiker operations group attempts to cultivate this team environment throughout the simulations with the aim of a cohesive and integrated FOT.

The Hitchhiker Program supports two kinds of simulations: Goddard Internal Simulations (GISs) and JISs. GISs exercise operational procedures and train personnel in POCC procedures. During GISs, the Hitchhiker ground system is configured using only GSFC facilities. Some supporting elements simulate the JSC by receiving commands from the POCC and playing back recorded payload telemetry to the experiments. These simulations test GSFC internal data, management, and operations interfaces and emphasize Hitchhiker POCC procedures.

JISs establish operability of the overall ground system including the links to the JSC Mission Control Center (MCC). During the JISs, the ground system is configured as for mission operations. The JSC MCC receives Hitchhiker commands and forwards a composite telemetry stream back to the GSFC except for the Hitchhiker data which is simulated via playback of Hitchhiker payload telemetry recorded during the POCC Command Test.



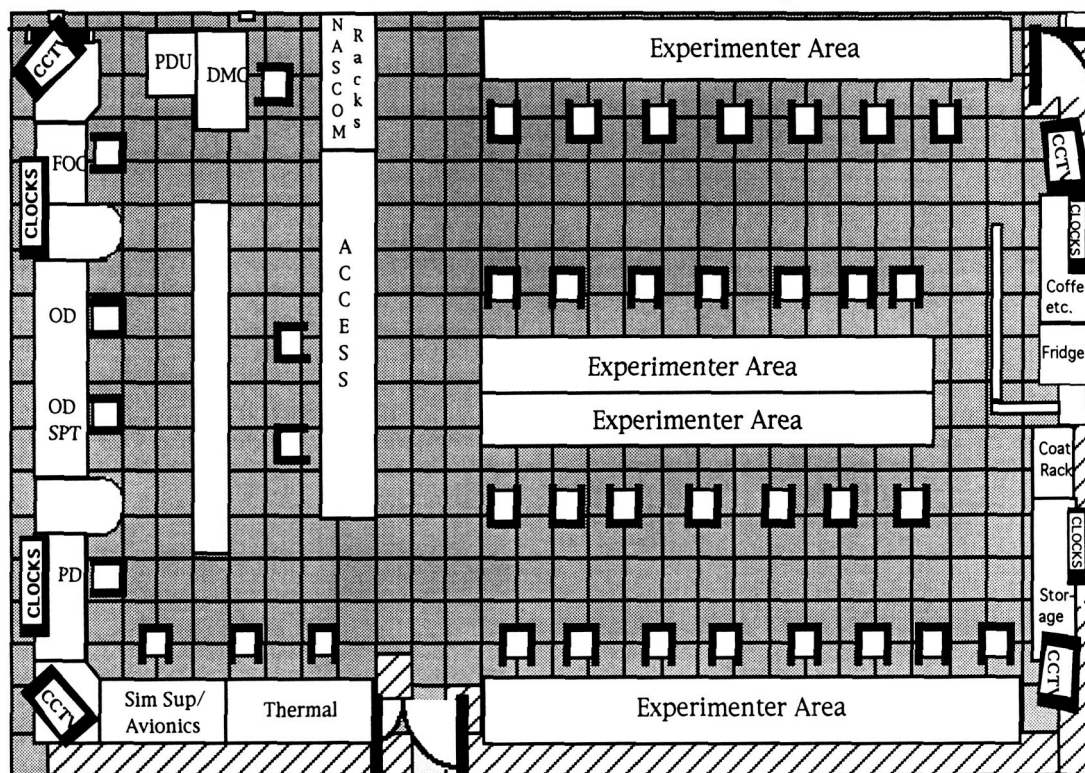


Figure 3: Hitchhiker POCC Layout

JISs are treated as an actual flight for the crew and all flight controllers and involve all facilities participating in the mission including the GSFC, the JSC and other remote POCCs. The crew participates from the Shuttle Mission Simulator (SMS) at the JSC which provides realistic shuttle subsystem data for the simulation. Coordination between the JSC MCC, the Hitchhiker POCC, and other payloads is emphasized during these exercises. System malfunctions are introduced which impact the mission community as a whole and require extensive inter-center coordination and replanning operations. These situations often require analysis of Orbiter resources and payload priorities and test the operational decisions outlined in the flight documentation.

Simulations provide a medium to evaluate the effectiveness of the operations plan and to develop both situational awareness and contingency resolution skills in an environment representative of the actual mission, thus providing the best available hands-on experience for experimenters about to launch into real-time operations.

#### REAL-TIME MISSION OPERATIONS

The mission operations process culminates in the real-time implementation of the comprehensively developed, thoroughly evaluated operations plan. The ultimate

responsibility of the OD is to guide and represent the customer, champion their interests, and coordinate real-time changes to the plan from launch through landing.

Hitchhiker operations are conducted in real-time based on overall plans prepared pre-mission. The Hitchhiker payload is assigned operating periods scheduled according to the requirements of all manifested payloads. Some payloads require dedicated Orbiter support such as attitude control or crew interaction. The assignment of dedicated periods to all payloads is made based on their priority and large resource requirements including crew-time and power. The Hitchhiker FOT often must strive to take advantage of all events in the flight plan and all available resources to accommodate Hitchhiker science objectives.

While higher priority payloads are being supported, the Hitchhiker may only be allowed sufficient power for maintenance of payload electronics and thermal conditioning. Low rate data and commanding may only be provided for periodic evaluation of payload health and safety. However, there may be opportunities for the Hitchhiker payload to operate in parallel with (piggyback) other payload operations. Piggyback operations are background operations, which take advantage of available Orbiter resources and gain science data on a non-interference basis with primary payload activity. Contingency operations are supported from the Hitchhiker ground system using available real-time command capability.

## **Payload Operations Control Center**

The focal point for Hitchhiker payload operations and management is the Hitchhiker POCC located at the GSFC in the Attached Shuttle Payload Center (ASPC). As a center part of the Hitchhiker GDS, the POCC provides efficient service to a variety of customers through simulations and real-time operations. It is designed for functionality with an attention to personnel comfort and can support several payloads and/or flights simultaneously.

The POCC is composed of a Mission Operations Area, an Experimenter Area and a Common Area, as illustrated in Figure 3, and accommodates all mission operations personnel and equipment. It also houses the Advanced Carrier Customer Equipment Support System (ACCESS): a PC-based, distributed network that provides the central interface between the CGSE and the outside world.

The POCC interfaces with the GSFC support facilities to provide telemetry and command for the Hitchhiker payloads. Additional GSFC supporting elements provide simulation support and attitude, orbit and data display generation. The POCC is equipped with a number of display devices, all with color capability, including large screen color monitors.

Real-time mission operations is the culmination of months, perhaps years, of careful preparation. An organized and efficient control center offering a complete set of tools for replanning and real-time operations is essential to mission success.

## **HITCHHIKER IN ACTION**

In the years since its inception, the Hitchhiker program has sponsored many payloads, of which the following examples are but a small sampling. Although all missions have seen their share of obstacles, the majority of Hitchhiker payloads have been a resounding success. Both the obstacles and victories alike have brought forth valuable insight that contribute to the success of following flights. The Hitchhiker operations group learns from all successes and failures and is thus able to continuously broaden and improve its scope of service.

### **Superfluid Helium On-Orbit Transfer**

The Superfluid Helium On-Orbit Transfer (SHOOT) payload which flew on STS-57 consisted of two vacuum insulated dewars (tanks) containing liquid helium connected by a transfer line, various instrument electronics, and control systems mounted on a Hitchhiker cross bay carrier. The objective of the SHOOT mission was to perform experiments demonstrating the technology and operations required to service payloads in space with liquid helium and to verify several cryogenic devices and procedures in the zero-g environment.

The majority of the operations involved the transfer of helium from one dewar to the other. Operations consisted of both ground-controlled and crew-controlled transfer of liquid helium. The crew used an Aft Flight Deck (AFD) computer for command and verification. These operations required real-time crew interaction and/or expert system software for diagnostic and control operations.

During payload development, the SHOOT customer was developing a high fidelity simulator to aid the crew in training with the AFD software. After discussions between the SHOOT customer, the MM, and the OD, the anticipated role of the simulator was expanded to include training of the entire FOT and use during all GISs and JISs. This resulted in very dynamic simulations that extensively exercised the coordination between the ground operators and the crew in a realistic environment. By providing realistic telemetry for both the ground and the crew, the simulator allowed the operations personnel to rigorously test both nominal and contingency SHOOT procedures. This SHOOT simulator provided an additional benefit: a critical failure in flight was simulated during one JIS, thus preparing the FOT for contingency resolution of the problem in real-time.

Despite some serious hardware problems on Flight Day 1, the SHOOT experimenters were able to accomplish all mission goals and milestones. They attributed this success to the great efforts of and coordination between the Goddard POCC, the MCC and the crew. They also attested to the value of the JISs in preparing the FOT to tackle real-time contingency resolution.

### **Robot Operated Materials Processing System**

Mission operations often entails striving for science under less than ideal conditions. Yet experience has shown that the means for accomplishment are available, often just waiting to be recognized and channeled in the right direction. During the STS-64 mission, the Robot Operated Materials Processing System (ROMPS) payload required low-g environments through several crew sleep periods for critical sample processing. In order to accomplish the task, a wide attitude deadband was programmed into the Digital Auto Pilot (DAP) settings of the Orbiter. However, despite the wide deadbands, predictions showed that the Orbiter would still often reach the deadband limits too fast for a sample to finish processing.

The OD prepared for this situation pre-flight by coordinating closely with the Guidance Navigation and Control (GNC) Officer at JSC to be cognizant of the signatures of the respective Orbiter Control System burns. Thorough procedures were developed and put to the test during the simulations. Several modifications were made, allowing direct contact between GNC and the OD, bypassing the normal flight protocol through the Houston Payloads Officer. During the flight, the GNC and the OD worked closely together to trend the timing between firings and give

ROMPS an emphatic "go" when sample processing times were assured. Several times the samples finished baking with only seconds to spare. This close coordination between the JSC and Hitchhiker FOTs helped achieve full mission success while operating under what could otherwise be seen as difficult circumstances.

### **Shuttle Glow Experiment**

The Shuttle Glow Experiment (GLO) has to date flown two times as a Hitchhiker payload, although several additional flights are currently manifested. The GLO payload consists of imagers and spectrograph assemblies and supporting electronics. The primary objective of the experiment is to observe and qualify both Orbiter and atmospheric glow in the 115 to 1150 nanometer spectral range. The GLO-I experiment aboard STS-53 experienced a combination of hardware problems and unlucky orbital conditions resulting from Orbiter and primary payload operations. As a result of primary payload requirements, the orbit trajectory was one in which the Orbiter did not have a night pass until the last day of the mission. Additionally, primary payload operations early in the flight led to propellant constraints, thus further limiting GLO observations. Due to these constraints the FOT had to restructure night observations originally scheduled throughout the flight to the last few orbits of the mission. This involved extensive prioritization, coordination, and replanning for both a nominal end to the mission and a sought for, yet ultimately denied, extension day.

The GLO-II instrument flew on STS-63, with upgraded hardware and a heightened insight into Orbiter operations that only a tough mission can bring. The GLO-II instrument experienced some hardware malfunctions which required much of the flight to troubleshoot. However, the FOT replanned GLO science operations and had an extremely successful flight, regardless of the difficulties encountered. STS-63 was a great learning experience for the entire FOT; several operational issues which arose during the flight and were resolved in real-time prepared operators for future flights of the GLO instrument.

The GLO-III experimenters have upgraded their instruments to add even more to their data ingestion capability; they have included an optical disk tape recorder which offers a great deal of data storage space. GLO recognizes the importance of an on-board recorder, as the experiment produces a large amount of medium rate science data that requires Ku-band for downlink. This addition to the GLO experiment adds an even greater flexibility to GLO operations.

The GLO experiment is the quintessential Hitchhiker: a prime example of taking advantage of all opportunities and resources at all times. The GLO payload operates almost continuously throughout the mission, sometimes eking significant scientific data out what could be considered trivial

Orbiter events. Through difficult flight and adverse operating conditions, the experimenters have continued to exhibit tremendous attention to experiment operations and replanning. This effort has rewarded the experimenters with success despite adversity.

### **Cryo Systems Experiment**

The Cryo Systems Experiment (CSE) which flew on STS-63 was designed to demonstrate and characterize the on-orbit performance of several cryogenic system components contained within a standard Get-Away Special (GAS) canister. These components include two Stirling cryocoolers, a passive reversible triple-point cryogen energy storage device, an oxygen diode heat pipe thermal switch, and additional supporting electronics. CSE was designed with the anticipation that payload commanding would be sporadic and greatly unavailable. Thus the experimenters designed a largely self-sufficient experiment with automated timelines. Although the CSE mission achieved total mission success, the experimenters noted that early insight into the resources available during payload development could have broadened the scope of their experiment.

### **HITCHHIKER 2000**

#### ***Future Trends In Mission Operations***

Both the human and technological factors within the Hitchhiker Project continuously evolve to new levels of mission preparedness and support. An important concept in mission operations is that there is no end in sight to this evolution of ideas and processes. Each success and each setback teaches valuable lessons for use in future flights.

Much like Hitchhiker operations, the POCC constantly evolves to best take advantage of technological capabilities of the Hitchhiker system. Hitchhiker plans to soon adopt a system of electronic flight documentation transfer. These documents are currently replanned and distributed daily via fax protocol. The adoption of electronic data transfer within the POCC will lessen the flow of paper products and decrease time-consuming practices such as faxing and photocopy. Hitchhiker is also currently investigating the possibility of increasing the capabilities of the various display systems in the POCC.

Technological advancements and the world-wide adoption of the information superhighway have made the concept of remote Hitchhiker Operations Centers both possible and practical alternatives to pursue. Travel of personnel and shipment of equipment consume a significant percentage of a customer's budget, thus limiting funding available for other pursuits. Remote POCCs make sense given current technology and today's fiscal reality.

During the STS-63 flight, the GLO experimenters forwarded near-real-time science data to their facilities at the University

of Arizona over the Internet. Hitchhiker will soon provide mission information and potentially real-time data on-line during flights.

Hitchhiker mission operations personnel continue to endeavor for continuous improvement, always through implementation of lessons learned. Mission operations responsibilities are not over after the payload deactivates or even once the Orbiter comes home. As scientists will spend months, perhaps years, analyzing their data with a fine tooth comb, the Hitchhiker operations group will review every success and shortcoming encountered during the flight, and strive to implement the lessons learned through all future operations.

As Hitchhiker Payloads become more complex, the requirements and operations become more demanding. Double Hitchhiker payload complements consisting of numerous experiments, two avionics, and two mounting structures, will be manifested on many coming flights. These payloads are comprised of a vast diversity of experiments, ranging from cryo-experiments, atmospheric spectrographs, and deployables, to Global Positioning System (GPS) systems and laser altimeters. Future Hitchhiker flights may also include Space Station based experiments and movable Hitchhiker carriers onboard the Orbiter. With mission goals becoming more ambitious, the importance of mission operations preparedness grows increasingly clear.

By coordinating a comprehensive approach to mission operations, with attention to all phases of payload development, from the initial definition of payload requirements, through the integration of the objectives into a cohesive mission operations plan, through simulations and testing, and finally through the implementation of the plan in real-time, the mission operations group plans to ensure the greatest possible mission success for increasingly demanding payloads.

# APPLICATION OF SPACE SHUTTLE PHOTOGRAPHY TO STUDIES OF UPPER OCEAN DYNAMICS

Quanan Zheng, Vic Klemas, Xiao-Hai Yan, and Zongming Wang  
Center for Remote Sensing, Graduate College of Marine Studies  
University of Delaware, Newark, DE 19716

## ABSTRACT

Three studies have been conducted using space shuttle imagery to explain the dynamics behavior of internal waves in the Atlantic and Indian Oceans and to derive tide-related parameters for Delaware Bay. By interpreting space shuttle photographs taken during mission STS-40, a total of 34 internal wave packets on the continental shelf of the Middle Atlantic Bight have been recognized. Using the finite-depth theory we derived that the maximum amplitude of solitons is 5.6 m, the phase speed 0.42 m/s, and the period 23.8 min. Deep-ocean internal waves in the western equatorial Indian Ocean on photographs taken during mission STS-44 were also interpreted and analyzed. The internal waves occurred in the form of a multisoliton packet in which there are about a dozen solitons. The average wavelength of the solitons is  $1.8 \pm 0.5$  km. The crest lines are mostly straight and reach as long as 100 km. The distance between two adjacent packets is about 66 km. Using the deepwater soliton theory, we derived that the mean amplitude of the solitons is 25 m, the nonlinear phase speed 1.7 m/s, and the average period 18 min. For both cases, the semidiurnal tides are the principal generating mechanism. The tide-related parameters of Delaware Bay were derived from space shuttle time-series photographs taken during mission STS-40. The water area in the bay were measured from interpretation maps of the photographs. The corresponding tidal levels were calculated using the exposure time. From these data, an approximate function relating the water area to the tidal level at a reference point was determined. Then, the water areas of the Delaware Bay at mean high water (MHW) and mean low water (MLW), below 0 m, for the tidal zone, and the tidal flux were inferred. All parameters derived were reasonable and compared well with results of previous investigations.

## INTRODUCTION

Since 1981 the United States has performed Space Shuttle missions. After 15 years of operations, a Space Shuttle Earth Observations Project (SSEOP) database has been set up. Among the photographs, about 75% represent the globally distributed coastal zone. The database has been made easily accessible to the research community (ref. 1).

Space shuttle photographs taken by the astronauts with hand-held cameras are suitable for the study of upper ocean dynamics due to the following advantages. The first is the visualization of the imagery of ocean features. The features were identified by human eyes then photographed with the camera adjusted for optimum performance. This method is unparalleled for other spaceborne remote sensing techniques, because it allows phenomena in the deep ocean far away from any satellite receiving station to be imaged with human intelligence. The second advantage is high spatial resolution, which is 20 - 30 m, much better than 1 km for NOAA/AVHRR images which are frequently used in oceanographic studies. The third is highly repeatable observation frequency, which can reach once a day for a short period. Sometimes a phenomenon might be photographed several times within a minute if the astronauts are interested in it. That provides a good opportunity for observation of time-dependent processes.

The Center for Remote Sensing at the University of Delaware has been engaged in the application of space shuttle photography to studies of upper ocean dynamics since 1991. We developed digitization, geometric correction, and image enhancement techniques for data processing, and applied spatial Fourier transforms to the spectral analysis of spatially periodical phenomena. We used space shuttle photographs for extracting parameters of internal waves on the continental shelf of the Middle Atlantic Bight and the western equatorial Indian Ocean, and for calculating tidal parameters of the Delaware Bay (ref. 2, 3, and 4). The major results are reviewed here.

---

\* This work is supported by the ONR Optics Program through grant N00014-95-1-0065; the NASA Space Shuttle Application Program and partly supported by the NOAA Global Change Program through grant NA26AP0257-01. The space shuttle photographs are provided by S. Ackleson, P. E. La Violette and K. Lulla.

## SPACE SHUTTLE PHOTOGRAPHS

The space shuttle photographs used in our studies were taken with the Aero Linhof Technika 45 camera for mission STS-40 and with the NASA-modified Hasseblad 500EL/M camera for mission STS-44. The specifications of photographs and the related information are summarized in Table 1.

Table 1. Specifications and Related Information of Space Shuttle Photographs Used in Our Studies

Item	Parameters or Description	
Mission	STS-40	STS-44
Platform		
Space shuttle	Columbia	Atlantis
Flight date	June 5 - 14, 1991	Nov. 24 - Dec. 1, 1991
Orbit altitude (km)	287	361
Inclination (degree)	39	28.46
Sensor		
Camera	Aero Linhof Technika 45	NASA-modified Hasseblad 500 EL/M
Lens	250 mm Tele-Arlon f/5.6	250 mm CF sonnar f/5.6
Incidence angle (degree)	0	0
Film		
Type	Kodak color transparency (QX 868)	Kodak Ektachrome 64 color transparency
Sensitive spectrum	Visible	Visible
Resolution (lines/mm)	50	50
Size of a scene (sq in.)	4 × 5	4 × 5
Photographing time	June 8 and 10, 1991	Nov. 28 - 30, 1991
Spatial Resolution (m)	23 (nadir)	23 (nadir)
Applications	Shallow water internal waves Delaware Bay	Deepwater internal waves

## OBSERVATIONS OF OCEAN INTERNAL WAVES

### Internal Waves on the Continental Shelf of Middle Atlantic Bight

The enlarged space shuttle photographs with a size of 30 × 40 square inches taken at 1518:24 and 1518:41 UT, or 1118:24 and 1118:41 EDST, June 8, 1991, were used for extracting the information of internal waves on the continental shelf of Middle Atlantic Bight. An interpretation map with geographic coordinates and sea bottom contours is shown in Figure 1. One can see that the total of 34 packets of internal waves are distributed over a huge area located from 38° to 40°N latitude and 72° to 75°W longitude, where water depth near the continental shelf break is from 50 to 150 m. The crest lines of internal waves are nearly parallel to local bottom contours, with the longest continuous length of 150 km. In this area, internal wave events have been observed with other satellites (ref. 5) and in situ investigations (ref. 6) many times in the last two decades. It is believed, therefore, that this is an active area for solitary internal waves.

The analysis of CTD data along the ship track AA shown in Figure 1 indicates that the case of interest satisfies the scale limits of the finite-depth theory. According to a steady state solitary solution given by Joseph (ref. 7), the amplitude of soliton has a form

$$A(\xi; a, b) = \frac{-\eta_0}{\cosh^2 a\xi + (\sinh^2 a\xi)/a^2 b^2} \quad (1)$$

where  $\xi = x - Ct$ , is a wavenumber like parameter ( $= 2\pi/\lambda$ ) satisfying the relationship,  $ab \tan(ah) = 1$ , and

$$b = \frac{4h^2}{3\eta_0} \quad (2)$$

and  $C$  is the nonlinear soliton speed given by

$$C = C_0 \left\{ 1 + \frac{H}{2H} \left[ 1 + \frac{H}{b} (1 - a^2 b^2) \right] \right\}, \quad (3)$$

where  $C_0$  is the phase speed of the lowest internal mode (ref. 8).

$$C_0 = \left( \frac{\delta \rho}{\rho} \frac{g}{k} \right)^{1/2} \left[ \coth kh + \coth k(H-h) \right]^{-1/2}, \quad (4)$$

where  $k$  is the wavenumber. The characteristic scale,  $L$ , is defined by the value of  $\xi$  at which  $A/\eta_0 = -1/2$ , and is given by

$$aL = \cosh^{-1} \left[ \frac{1 + 3(ab)^2}{1 + (ab)^2} \right].$$

We use equations (1)-(4) to calculate dynamic parameters of solitons.

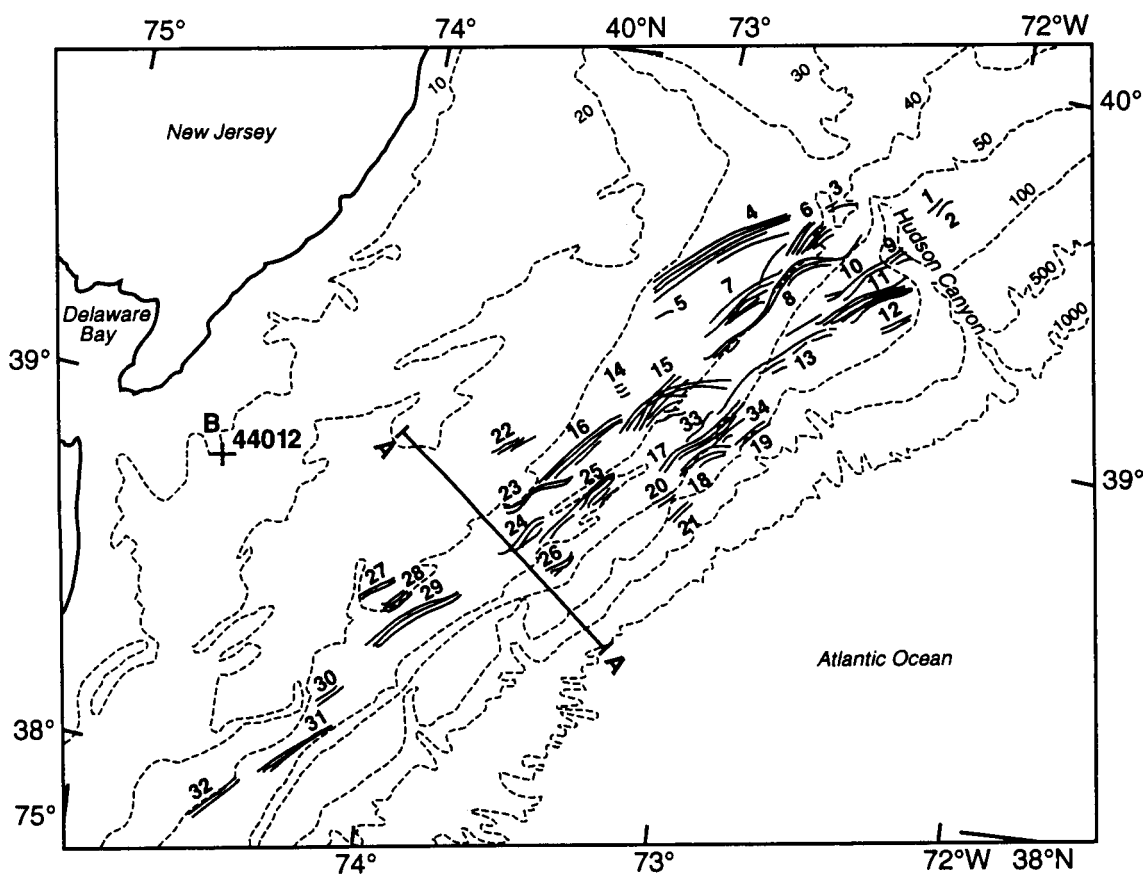


Figure 1. Internal wave interpretation map. The groups of solid lines coded with numbers are images of internal waves. The dashed lines are sea bottom contours with sounding in fathoms (1 fm = 1.8 m). Segment AA is the CTD data ship track; B marks the location of NOAA data buoy 44012.

*Maximum amplitude.* From (2) we have the maximum soliton amplitude  $\eta_0 = 5.6$  m.

*Soliton speed.* From (4) we have  $C_0 = 0.36$  m/s, and then from (3) we obtain the nonlinear soliton speed  $C = 0.42$  m/s.

*Period.* From the characteristic wavelength and the phase speed we derive the characteristic soliton period  $T = 23.8$  min.

*Horizontal velocities of water particles in the upper and lower layers.* For the upper layer,

$$U_1(x, t) = -U_{10} \operatorname{sech}^2[(x - ct)/L], \quad (5)$$

where  $U_{10} = C_0 \eta_0 / h$ . For the lower layer,

$$U_2(x, t) = -U_{20} \operatorname{sech}^2[(x - ct)/L], \quad (6)$$

where  $U_{20} = C_0 \eta_0 / (H - h)$  (ref. 9). For our case we have  $U_{10} = 0.13$  m/s, and  $U_{20} = 0.030$  m/s.

*Total energy per unit crest line.* An estimate of the total energy per unit crest length is (ref. 9)

$$E = \frac{4}{3} (\rho_2 - \rho_1) g \eta_0^2 L. \quad (7)$$

For our case, we have  $E = 6.8 \times 10^4$  J/m.

#### Deepwater Internal Waves in the Western Equatorial Indian Ocean

The space shuttle photographs taken during mission STS-44 were used for the study of deepwater internal waves in the western equatorial Indian Ocean. A map of the study area with space shuttle subtracks is shown in Figure 2. The isobaths

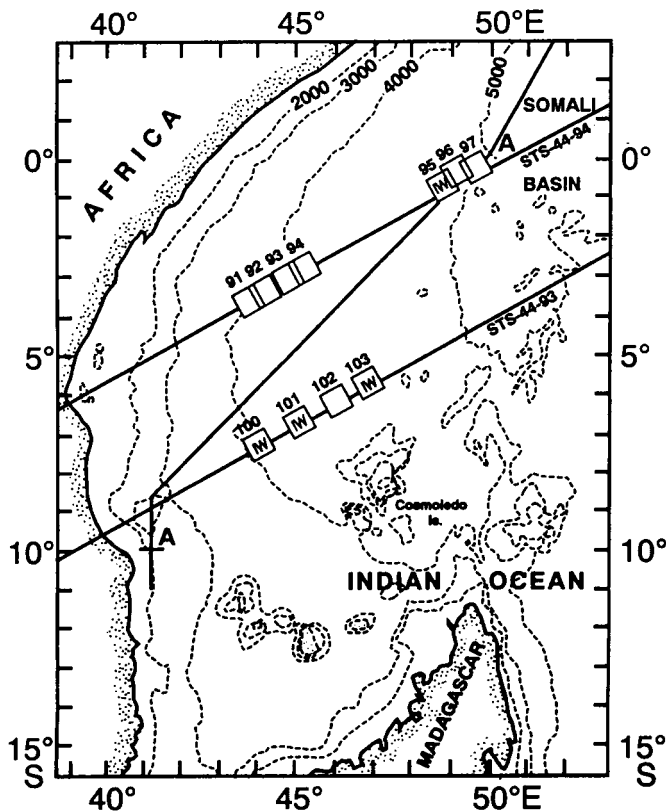


Figure 2. Map of the study area in the equatorial Indian Ocean. The parallel straight lines show subtracks of the space shuttle Atlantis during mission STS-44. Squares along subtracks show central locations and the coverage of space shuttle photographs. Numerals on the squares represent the number of each frame. IW in the squares denotes the photographs in which the internal waves are observed. Segment AA is the ship track for potential density measurements. Isobaths are in meters.



show that the depths of photographed locations range from 4000 to 5000 m, which are typical for the tropical deep ocean. Figure 3a shows one of the space shuttle photographs analyzed in this study coded STS 44-93-103. Its location and spatial coverage can be found in Figure 2. Figure 3b is an interpretation map of Figure 3a. One can clearly see the collision of two internal wave packets in the bottom center of the photograph. The images of the internal waves appear to be alternating bright and dark bands occurring in packets (see Figure 3a). The bands are nearly straight and have physical lengths as long as 100 km. The interpacket distance is 66.0 km. In a packet the number of waves may reach more than one dozen, and the wavelengths are distributed quite uniformly, unlike shallow-water internal wave packets in which the waves exhibit a general decrease in wavelength from the front to the rear of the packet (ref.10). The average wavelength is  $1.8 \pm 0.5$  km.

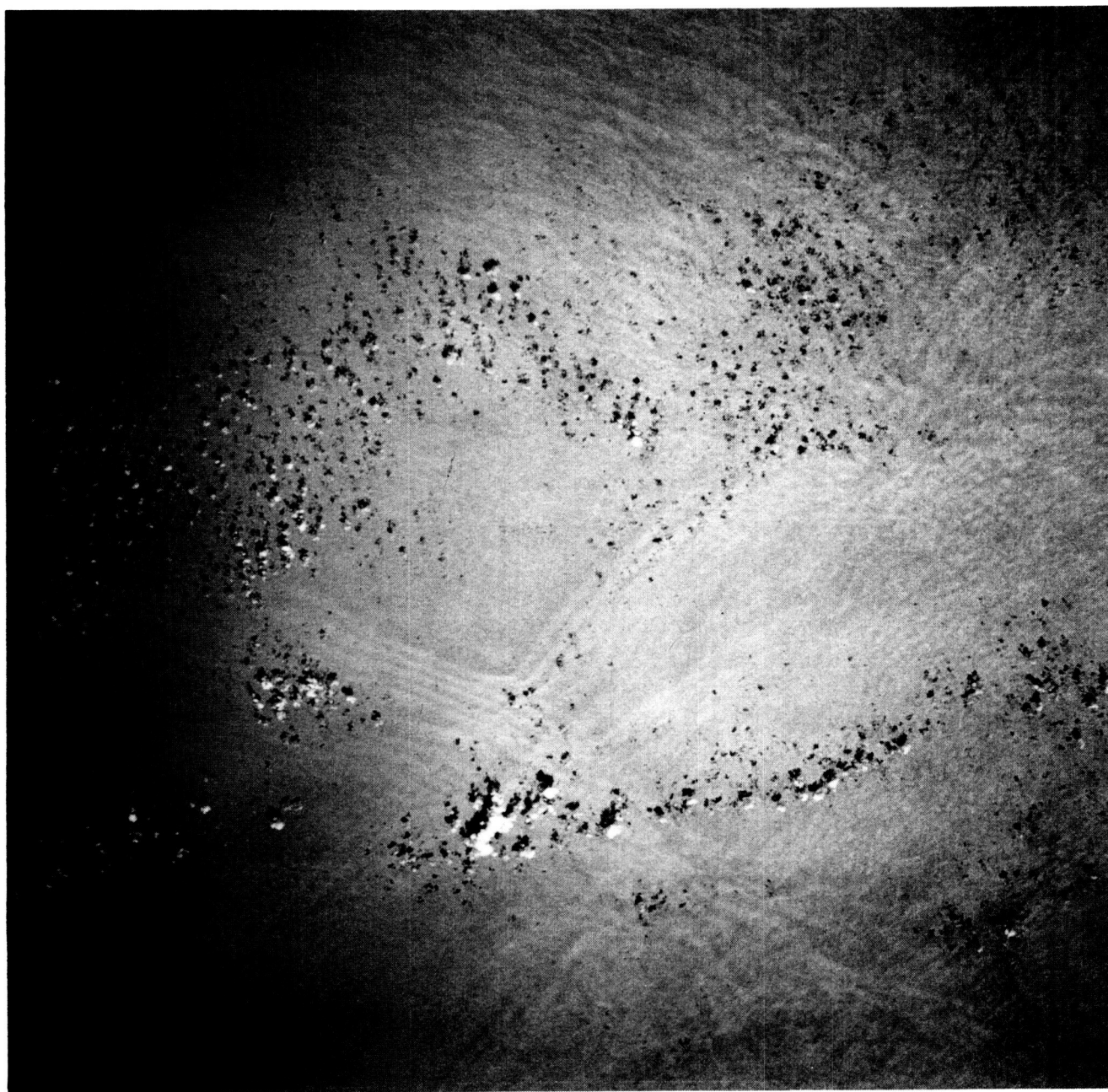


Figure 3a. Space shuttle photograph STS 44-93-103. Alternating bright and dark bands are surface manifestations of internal waves. The white and black spots are images of clouds and cloud shadows.

For the equatorial Indian Ocean, the vertical density structures can be quite accurately described by the two-layer model, with scale parameters:  $h = 75$  m and  $H = 4500$  m. Parameters  $L$  and  $\eta_0$  are not directly measured quantities, but the following estimations are reasonable, that is,  $L = O(0.3 \lambda) = O(5.4 \times 10^2 \text{ m})$ , and  $\eta_0 = O(20 \text{ m})$ . These scale parameters indicate that our case is close to the conditions of deepwater theory. Using the Benjamin-Ono equation (ref. 11 and 12) and measurement data, we can obtain dynamic parameters of the internal waves as follows (ref.4).

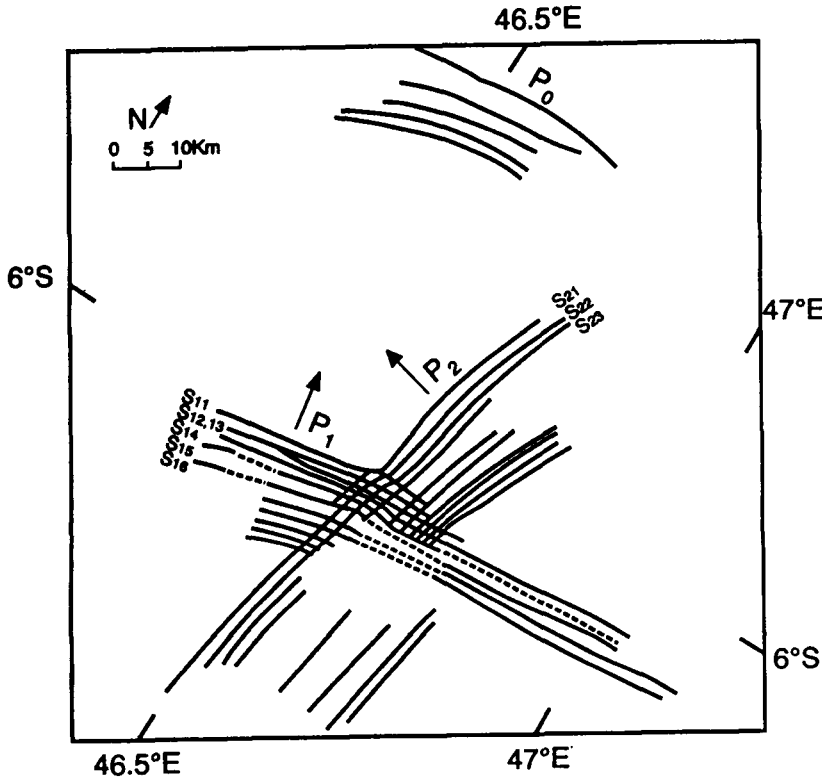


Figure 3b. Interpretation map of internal waves shown in Figure 3a.

**Characteristic length.** From space shuttle photographs, we have measured the average wavelength  $\lambda$  of  $1.8 \pm 0.5$  km. Reasonably assuming that  $\lambda$  is the soliton width at one tenth of the amplitude (i.e.,  $\eta/\eta_0 = 0.1$ ), from mean conditions we derive the characteristic half-width of solitons  $\Delta = 3.0 \times 10^2$  m. Therefore the characteristic length  $L = 2\Delta = 6.0 \times 10^2$  m.

**Amplitude.** The amplitude of the solitons  $\eta_0 = 25$  m.

**Nonlinear phase speed.** The average nonlinear phase speed of the solitons  $V = 1.7$  m/s.

**Period.** From the average wavelength and nonlinear phase speed we derive the average period of the solitons  $T = 18 \pm 5$  min.

**Horizontal velocities of the water particles.** Using the formula derived for the hyperbolic soliton (ref. 9), we can calculate the horizontal velocities of the water particles induced by the solitons. In the upper layer the average maximum horizontal velocity is

$$u_{10} = \frac{c\eta_0}{h} = 50 \text{ cm/s},$$

and in the lower layer

$$u_{20} = -\frac{c\eta_0}{H} = -0.85 \text{ cm/s}.$$

One can see that the velocity of the water particles in the upper layer is quite large, but in the lower layer it is negligibly

small.

*Total energy per unit crest length.* The total energy per unit crest length of internal waves is approximately (ref. 8)

$$E = (\rho_2 - \rho_1) g \overline{\eta^2}, \quad (8)$$

where

$$\overline{\eta^2} = \int_{-\infty}^{\infty} \eta^2(x, t) dx. \quad (9)$$

Calculating (9) and substituting the result into (8) yields the total energy per unit crest length

$$E = \frac{\pi}{2} (\rho_2 - \rho_1) g \eta_0^2 \Delta. \quad (10)$$

For our case,  $\rho_2 - \rho_1 = 3 \times 10^{-3} \text{ g/cm}^3$ ,  $\eta_0 = 25 \text{ m}$ , and  $\Delta = 3.0 \times 10^2 \text{ m}$ , so that  $E = 6.8 \times 10^6 \text{ J/m}$ . We measured the separation distance between two adjacent packets,  $P_0$  and  $P_1$ ,  $\Delta$ , as being 66.0 km. The group speed  $c_g = 1.5 \text{ m/s}$ . Hence we derive that the period of internal wave packets  $Tg = \Delta/c_g = 12.2 \text{ hours}$ . This result is close to the 12.5 hour average period of three most powerful modes of semidiurnal ( $M_2$ ) tides in the study area.

## DELAWARE BAY TIDAL PARAMETERS

The raw data used for this study are the positive color films with a size of  $4 \times 5 \text{ sq. in.}$ , which are dated June 8 and 10, 1991 during mission STS-40. The photographs are centered on Delaware Bay, and cover most of the coast of New Jersey, the Delmarva peninsula, and the Chesapeake Bay, as well as their adjacent continental shelf on the Middle Atlantic Bight. By enlarging the films into photographs with sizes  $30 \text{ in.} \times 40 \text{ in.}$  and  $16 \text{ in.} \times 20 \text{ in.}$ , the basic images for mapping and surveying are produced.

### Tidal Influx

According to the definition of the dynamics of a bay, the tidal influx,  $W_b$ , is calculated by

$$W_b = (S_1 + S_2) H / 2, \quad (11)$$

where  $S_1$  and  $S_2$  are the water areas corresponding to mean high water (MHW) and mean low water (MLW), respectively, and  $H$  is the mean tidal range, i.e. the difference in height between the two. This is a universal formula regardless of coastal geometry and bottom topography of the bay.

From (11), one can see that if  $S_1$ ,  $S_2$  and  $H$  are known, the tidal influx,  $W_b$ , can be calculated. Usually  $H$  can be found in the tide tables, and the areas  $S_1$  and  $S_2$ , must be measured either with a field survey or with remote sensing. Field surveys, however, hardly obtain synchronous data for a huge bay because of the changeable tide levels. Satellite remote sensing can provide synchronous imagery for a large bay, which can be used to map and to measure the water area. But the time of the satellite overpass rarely coincides with the required tide stage. In order to derive the water area at a given tide stage, it is necessary first to determine a function relating the water area to the tide level at a reference point. We assume that this function,  $A(h)$ , has the form of a power series:

$$A(h) = \sum_{n=0}^{\infty} k_n h^n, \quad (12)$$

where the variable  $h$  is the tide level at the reference point, and  $k_n$  the coefficient to be determined. Obviously, the water areas measured from satellite images, the exposure times and the tide tables can be used to obtain  $k_n$ , and the functional form of  $A(h)$  can be determined. Then the water area of the bay at any tide level can be simply calculated. The accuracy of  $A(h)$  determined by (12) depends on the highest order of  $h$ ,  $n$ . If we have two groups of data of the water area and their corresponding tide levels, the coefficients  $k_0$  and  $k_1$  are obtained by solving coupled equations, and a linear equation of  $A(h)$

can be determined as a first order approximation.

For this study, we chose two space shuttle photographs, which are coded 910608 151824 STS-40-LNHF-15 and 910610 135020 STS-40-LNHF-151-162, to determine the function of  $A(h)$  for Delaware Bay. In these two photographs, the Delaware Bay is located near the central parts, and the geometric distortion of the imagery of the bay is relatively small, therefore, the measurement error due to this distortion is not significant. With the enlarged photographs, we prepared interpretation maps of the water areas in the Delaware Bay. The definition of the bay is as follows. The line between Liston Point, Delaware, and Hope Creek, New Jersey, is defined as the upstream limit of the bay, while that between the tips of Cape Henlopen and Cape May as the downstream one. And the two sides of the bay are bounded by boundaries of the sea water at exposure time. The scales of interpretation maps are determined using four reference points distributed on the two coastal sides of the bay. The distance between two reference points across the bay is derived from the Atlantic Coast map with a scale of 1:1,200,000 at Lat. 40°00'N published by the NOAA National Ocean Survey in 1975. Then the water areas are measured from interpretation maps with a CALCOMP 9100 digitizer and ERDAS Image Processing System. The resolution of this system is 0.01 cm<sup>2</sup>, and measured areas in images are about 30 cm<sup>2</sup>, therefore, measurement errors are negligible. For each map we made measurements three times. The mean and the standard deviation are

$$A(h_1) = (1720 \pm 5) \text{ km}^2 \text{ for the 910608 photograph}$$

and

$$A(h_2) = (1776 \pm 3) \text{ km}^2 \text{ for the 910610 photograph.}$$

Breakwater Harbor, located at the inside of Cape Henlopen (38°47'N, 75°06'W), is chosen as a reference point for the tide level. It is the only station in the Delaware Bay listed in the Tide Tables. The height of tide at exposure time is calculated according to the method given in Table 3 of the Tide Tables (ref. 13). Before the calculation was performed, the exposure times annotated in GMT on the photographs, were first transformed into the local time which is used in the Tide Tables. For the 910608 image, the local exposure time is 10:18:24 ET, and the tide level,  $h_1$ , is 6 cm; for the 910610 image, 8:50:20 ET, and  $h_2$ , 99 cm.

Substituting the values of  $A(h_i)$  and  $h_i$  into (12), we obtain a linear function of the water area in the Delaware Bay versus the tide level at the Breakwater Harbor

$$A(h) = k_1 h + k_0 \text{ (km}^2\text{)} \quad (13)$$

where  $k_1 = 0.60 \text{ km}^2/\text{cm}$ , and  $k_0 = 1717 \text{ km}^2$ .

From the levels of high and low water at the Breakwater Harbor listed in the Tide Tables, we derive that the level of MLW is 3 cm, and that of MHW is 131 cm. Substituting these heights (levels) into (13), we have  $S_1 = 1796 \text{ km}^2$ , and  $S_2 = 1719 \text{ km}^2$ . The mean tidal range,  $H$ , in (11) can not be replaced directly with the values at Breakwater Harbor because it is variable along the coast. We chose 9 tidal stations which are generally uniformly distributed along both sides of the bay and coded by 1, 2, 3, 4, 9, 10, 11, 12 and Cape May Point shown in Figure 4 to take the average of the mean tidal ranges. We obtain the average  $H = 1.57 \text{ m}$ . Substituting  $S_1$ ,  $S_2$  and  $H$  into (11), the tidal influx into Delaware Bay,  $W_b$  is derived as  $2.76 \times 10^9 \text{ m}^3$ . The uncertainty or error of this value is dependent on the accuracies of  $S_1$ ,  $S_2$  and  $H$ . We believe that the error of this estimation is less than 3%, and is mainly caused by the interpretation error.

### Tidal Zone Area

As a first order approximation, (13) can be used to calculate the area of the bay at any tide stage. As an example, we calculate the area of the tidal zone in Delaware Bay. Checking the Tide Tables, we find that the highest high water and the lowest low water at Breakwater Harbor in a year are 174 cm and -27 cm, respectively. With (13) their corresponding water area is calculated as  $1821 \text{ km}^2$ , and  $1701 \text{ km}^2$ , respectively. Based on that, we obtain the area of the tidal zone in the Delaware Bay  $A_{int} = 120 \text{ km}^2$ .

### Area Below 0 m

If we let  $H$  in (13) be zero, we obtain the area below zero-meter depth for Delaware Bay, which is another important

parameter for a tidal bay  $A_0 = 1717 \text{ km}^2$ . This parameter characterizes the basic and stable part of the bay. If this parameter is getting smaller, that means that the bay is silting in.

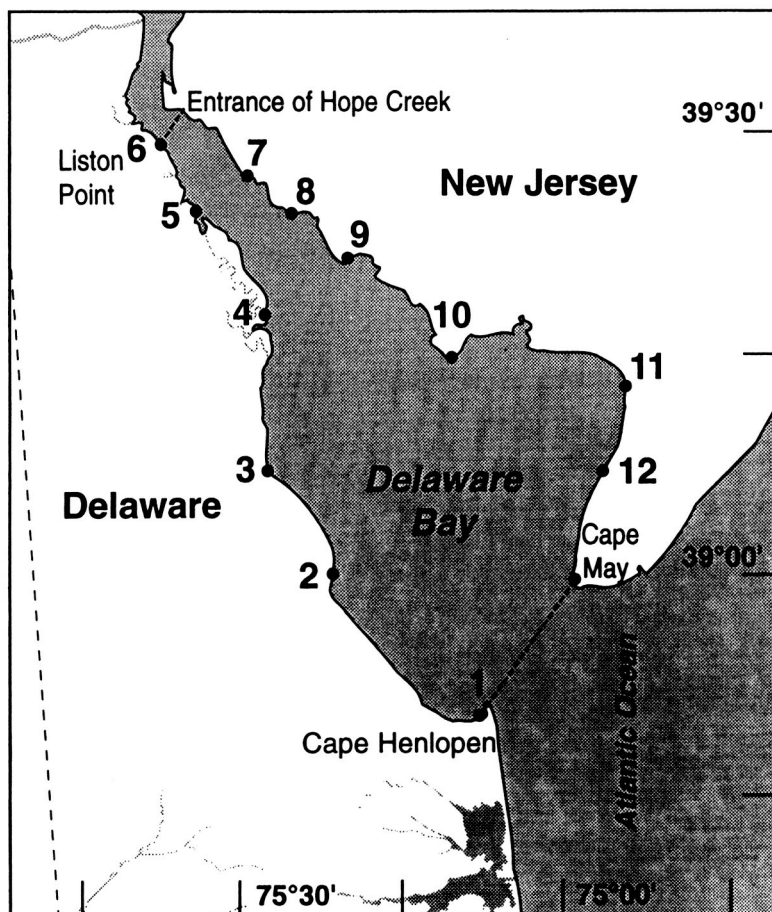


Figure 4. Interpretation map of the Delaware Bay drawn from the space shuttle photograph. The upstream and the downstream limits of the bay are drawn with the dashed and dotted lines. The solid circles coded along the coastal lines are the tide stations, for which historical data are available.

## DISCUSSION AND CONCLUSIONS

1. The internal wave field on the continental shelf of the Middle Atlantic Bight has a three level structure which consists of packet groups, packets, and solitons. From photographs we measured an average packet group wavelength of 17.5 km and an average soliton wavelength of 0.6 km. Using the finite-depth theory, we derived dynamic parameters of internal solitons: the maximum amplitude, 5.6 m; the phase speed, 0.42 m/s; the period, 23.8 min; the amplitude of the velocity of the water particles in the upper and lower layer, 0.13 m/s and 0.030 m/s, respectively; and the total energy per unit crest line,  $6.8 \times 10^4 \text{ J/m}$ .

2. Like in the shallow-water case, deepwater internal waves occur in packets or groups, but the average number of individual waves in a packet reaches 12, which is more than the average of the shallow-water internal wave packet, i.e. four to six (ref. 3 and 9). The amplitude of 25 m, the nonlinear phase speed of 1.7 m/s, the maximum horizontal velocity in the upper layer of 0.5 m/s, the crest length of 100 km, and the total energy per unit crest length of  $6.8 \times 10^6 \text{ J/m}$  indicate that deepwater internal waves are much stronger than those on continental shelves (ref. 3) and are similar to those in marginal seas, like the Andaman Sea (ref. 9).

3. The results of this study indicate that space shuttle photographs are valuable for studying bays and estuaries, not only qualitatively, but also quantitatively. High spatial resolution and small geometric distortion of the central parts of photographs provide a satisfactory accuracy for bay-scale mapping and measurement. Exposure time annotations on the photographs provide an important factor for calculating coincident tide levels which are a dominant forcing process in a bay originating

from the ocean. Combining these two directly measured parameters makes it possible to derive tide-related parameters of the bay, which are necessary for research and monitoring, but not easily obtained with traditional field surveys.

4. The water area at the Mean High Water (MHW) of the Delaware Bay is  $1796 \text{ km}^2$ , which is smaller than the historical value of the total surface area of  $1864 \text{ km}^2$  or 720 square miles (ref. 14). The reason is different definitions for the bay. We use the legal definition of the bay which takes Liston Point as the upstream limit, and the line between the tips of Cape Henlopen and Cape May as the downstream limit of the bay, because these two reference points are easily recognized on space shuttle photographs. The historical data was calculated with the Smyrna River as the upstream limit and a fold line between Cape Henlopen and the southwest tip of Cape May as the downstream limit (see Fig. 3, in ref. 14). The area of a tidal zone of  $120 \text{ km}^2$ , and the area below the zero-meter level of  $1717 \text{ km}^2$  obtained in our study are new results.

## REFERENCES AND NOTES

1. Ackleson, S.G., A summary of hand-held ocean and coastal photography taken during space shuttle missions: 1981-1991 (Abstract), *EOS* 72, 1992, pp. 69.
2. Zheng, Q., X.-H. Yan, and V. Klemas, Derivation of Delaware Bay tidal parameters from space shuttle photography, *Remote Sens. Environ.*, 45, 1993, pp. 51-59.
3. Zheng, Q., X.-H. Yan, and V. Klemas, Statistical and dynamical analysis of internal waves on the continental shelf of the Middle Atlantic Bight from space shuttle photographs, *J. Geophys. Res.*, 98, 1993, pp. 8495-8504.
4. Zheng, Q., V. Klemas, and X.-H. Yan, Dynamic interpretation of space shuttle photographs: Deepwater internal waves in the western equatorial Indian Ocean, *J. Geophys. Res.*, 100, 1994, pp. 2579-2589.
5. Sawyer, C., Tidal phase of internal-wave generation, *J. Geophys. Res.*, 88, 1983, pp. 2642-2648.
6. Burrage, D. M. and R. W. Garvine, Supertidal frequency internal waves on the continental shelf south of the New England, *J. Phys. Oceanogr.*, 17, 1987, pp. 808-819.
7. Joseph, R. I., Solitary waves in a finite depth fluid, *J. Phys. A math. Gen.*, 10, 1977, pp. L225-L227.
8. Phillips, O. M., The dynamics of the upper ocean, 2nd ed., *Cambridge University Press.*, New York, 1977, pp. 336.
9. Osborne, A. R. and T. L. Burch, Internal solitons in the Andaman Sea, *Science*, 208, 1980, pp. 451-460.
10. Apel, J. R. and F. I. Gonzalez, Nonlinear features of internal waves off Baja California as observed from the SEASAT imaging radar, *J. Geophys. Res.*, 88, 1983, pp. 4459-4466.
11. Benjamin, T. B., Internal wave of permanent form in fluids of great depth, *J. Fluid Mech.*, 29, 1967, pp. 559-592.
12. Ono, H., Algebraic solitary waves in stratified fluids, *J. Phys. Soc. Jpn.*, 39, 1975, pp. 1082-1091.
13. U.S. Department of Commerce, NOAA/NOS, *Tide Tables 1991*, East Coast of North and South America including Greenland, 1990, pp. 239-241.
14. Polis, D. F., and S. L. Kupferman, *Physical Oceanography*, Delaware Bay Report Series, Vol. 4, University of Delaware, Newark, 1973, pp. 1-143.

# COLLISION MANAGEMENT UTILIZING CCD AND REMOTE SENSING TECHNOLOGY

Harvey E. McDaniel Jr.  
Space Studies Institute at Princeton  
Tissue Engineering Society

## ABSTRACT

With the threat of damage to aerospace systems (space station, shuttle, hypersonic a/c, solar power satellites, loss of life, etc.) from collision with debris (manmade/artificial), there exists an opportunity for the design of a novel system (collision avoidance) to be incorporated into the overall design. While incorporating techniques from ccd and remote sensing technologies, an integrated system utilized in the infrared/visible spectrum for detection, tracking, localization, and maneuvering from doppler shift measurements is achievable.

Other analysis such as impact assessment, station keeping, chemical, and optical tracking/fire control solutions are possible through this system. Utilizing modified field programmable gated arrays (software reconfiguring the hardware) the mission and mission effectiveness can be varied.

This paper outlines the theoretical operation of a prototype system as it applies to collision avoidance (to be followed up by research).

## INTRODUCTION

Orbital debris travels in a wide variety of orbits used by earth orbiting satellites [1]. Orbital debris may orbit the earth for as long as centuries moving in many different direction and velocities (4-20 kps; see figure 1, and tables 1 and 2).

## DISCUSSION

With CCD technology the incident light is absorbed by the semiconductor substrate. An electric charge is released. The charge is collected and fixed by electrodes in the vicinity of the absorbing substrate. High resolution is achieved by smaller element-to-element spacing. The channel stop diffusion acts as a sink to prevent the photogenerated charge from spreading laterally (electrodes 5um depth within the semiconductor substrate).

The electrical signal is transferred via a multimode, stepped refracture index profile fiber optic wire (conventional image transfer and short distance data communications) to the analog to digital converter.

A parallel/flash type a/d converter will be used because:

- . single integrated circuit package
- . comparators can be referenced to a potential from equal resistors
- . massive parallelism
- . extremely fast

The conversion rate and time for optimum a/d converter performance is  $>3\text{mhz}$  and  $<330\text{ns}$  with a recovery setting time of  $<100\text{ns}$ . Once the signal has been quantized it is sent to the homomorphic

processors. Illumination (low frequency) and reflectance (high frequency) gains are applied through a linear shift invariant filter that gives simultaneous dynamic range reduction and contrast enhancement.

From the homomorphic processors the digital signal is sampled. The sampling rate is at least twice the sampling frequency [2]. The sampled signal is sent through a sequential grouping of digital filters/detectors combinations. The system utilizes massive parallelism (MIMD format throughout) along with artificial intelligence (neural networks) for target discrimination. Because the system uses an array format, each element in the array can be configured with 324, 648, or 1296 respectively equating to 1, .5, or .25 degrees of spacing respectively.

Once the signal is detected (range is mathematically determined by amplitude of the target signal), a bit stream is formulated. Triangulation is possible because each array element is hardwired to a specific sector. Because of triangulation high accuracy in tracking is achieved. With the initial detection of the target, the formulated bit stream (localization and range info) is sent to a specified memory location via a shift register. After several readings a doppler shift (rapid changes in target frequency amplitude) as well as velocity (determined by rapid changes in doppler shift) can be determined. The system can be configured to track multiple targets as well as different size and from different locations throughout the array special algorithms are under development). Bit representations for localization, range, doppler shift, and velocity (under development) make up the bit stream. The quantum cryptographic message [3] is sent via fiber optic wire to the main computer to determine collision probabilities. Quantum cryptography coupled with massive parallelism, and artificial intelligence allows for high speed transfer and processing to maintain a near real time format. The quantum cryptographic message that is sent to the main computer allows elements within the bit stream to be interrogated separately (algorithms under development). Various sections of the array have been mathematically determined to pose higher probabilities of collision. The embedded maneuvers (under development) in main memory will be activated by certain elements of the quantum cryptographic code. The maneuvers will encompass slide (left, right), attitude change, or roll about axis (as determined by the aerospace systems design or mission. Once the maneuver is initiated the systems memory repositions itself into the original position.

The data sent to the main computer is stored in memory to be accessed through telemetry monitoring by a ground station [4] or for systems adaptation (learning).

## CONCLUSION

The collision avoidance system allows solid state signal processing and imaging through a very basic approach. The three basic functions (CCD) sensing, storage, and transfer are conceptionally simple and allows for many configurations. With the CCD/Remote sensing approach higher element densities and better uniformity of response are obtainable.

Through the use of the array system quantum cryptography [3] and artificial intelligence (neural networks) the system can employ very high speed processing, secure communications, constant reconfiguration for mission purposes, constant telemetry data, and a learning capability (under development) for extended missions. Once the signal is digitized the entire processing can be done within the computer.

## REFERENCES

1. McDaniel, Harvey E. Jr. "Space Debris Collection System" Space Studies Institute (at Princeton) conference on Space Manufacturing (1993).
2. Oppenheim, Alan V. and Schafer, Ronald W. "Digital Signal Processing", Prentice Hall, Englewood Cliffs N.J. (1975).



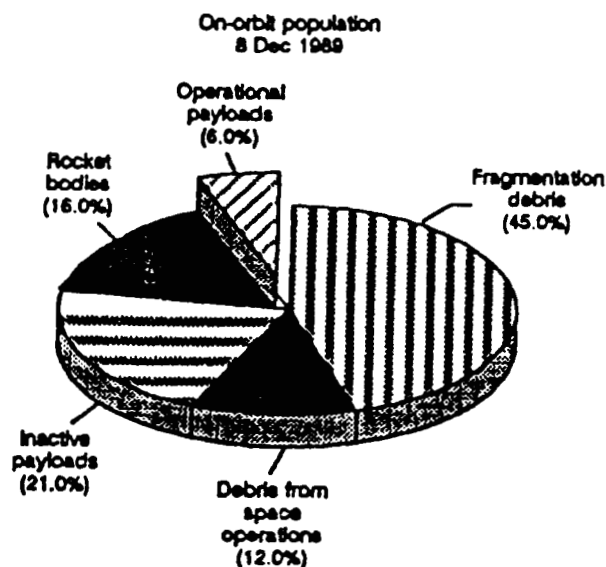
3. Bennett, Charles H., Brassard, Giles, and Ekert, Charles "Quantum Cryptography" Scientific American 1995 special issue.

4. Fortesque, Peter and Stark, John "Spacecraft Systems Engineering" Telecommunications and Telemetry section (1985).

Copyright ©1995 by Harvey E. McDaniel Jr., Space Studies Institute (at Princeton), and the American Institute of Aeronautics and Astronautics. All rights reserved.

## APPENDIX

Figure 1—Cataloged On-Orbit Population



SOURCE: Nicholas L. Johnson and David J. Newer, *History of On-Orbit Satellite Fragmentations*, 4th ed. (Colorado Springs: Teledyne Brown Engineering, January 1980), NASA Contract, NAS 9-18208.

Table 1—Elements of Orbital Debris

- deactivated spacecraft
- spent rocket stages
- fragments of rockets and spacecraft and their instruments
- paint flakes
- engine exhaust particles
- spacecraft rocket separation devices
- spacecraft coverings
- spent Soviet reactors

Office of Technology Assessment, 1980.

Table 2—Types of Hazardous Interference by Orbital Debris

1. Loss or damage to space assets through collision;
2. Accidental re-entry of space hardware;
3. Contamination by nuclear material of manned or unmanned spacecraft, both in space and on Earth;
4. Interference with astronomical observations, both from the ground and in space;
5. Interference with scientific and military experiments in space;
6. Potential military use.

SOURCE: Space Debris, European Space Agency, and Office of Technology Assessment.

## Optical Materials for infrared/visible with selected Properties

MATERIAL	R MIN um	R MAX um	Tm K*	Hk um 2/k <sub>g</sub> +
Quartz (SiO <sub>2</sub> )	0.12	5	174	740-460
Potassium Iodide (KI)	0.25	45	1000	
Cesium Bromide (CsBr)	0.25	80	900	20
Magnesium Fluoride (MgF <sub>2</sub> )	0.11	8		
Calcium Fluoride (CaF <sub>2</sub> )	0.13	12	163	160
Lithium Fluoride (LiF)	0.12	9	1140	100
Silicon (Si)	1.2	15	1690	1150
Germanium (Ge)	1.8	20	1210	
Potassium Chloride (KCl)	0.21	30	1060	

## SPARTNIK: ENGINEERING CATALYST FOR GOVERNMENT AND INDUSTRY

*James D. Prass*

*Structures Subsystem Engineer, Undergraduate, San Jose State University*

*Thomas C. Romano*

*Systems Engineer, Undergraduate, San Jose State University*

*Jeanine M. Hunter*

*Advising Professor, Aerospace Engineering, San Jose State University*

### ABSTRACT

Industrial demands for highly motivated and competent technical personnel to carry forward with the technological goals of the US has posed a significant challenge to graduating engineers. While curricula has improved and diversified over time to meet these industry demands, relevant industry experience is not always available to undergraduates.

The microsatellite development program at San Jose State University (SJSU) has allowed an entire undergraduate senior class to utilize a broad range of training and education to refine their engineering skills, bringing them closer to becoming engineering professionals. Close interaction with industry mentors and manufacturers on a real world project provides a significant advantage to educators and students alike. With support from companies and government agencies, the students have designed and manufactured a microsatellite, designed to be launched into a low Earth orbit. This satellite will gather telemetry for characterizing the state of the spacecraft. This will enable the students to have a physical check on their predicted values of spacecraft subsystem performance. Additional experiments will also be undertaken during the two year lifetime, including micro-meteorite impact sensing and capturing digital color images of the Earth.

This paper will detail the process whereby students designed, prototype and manufactured a small satellite in a large team environment, along with the experiments that will be performed on board. With the project's limited funds, it needed the support of many industry companies to help with technical issues and hardware acquisition. Among the many supporting companies, NASA's space shuttle small payloads program could be used for an affordable launch vehicle for the student project.

The paper address these collaborations between the student project and industry support, as well as explaining the benefits to both. The paper draws conclusion on how these types of student projects can be used by industry as a feasible resource for developing small platforms for space based experiments, as well as increasing the practical experience and engineering knowledge of graduating students. These benefits to industry and universities, can lead to a close working relationship between the two. These types of projects can facilitate the development of low-cost space rated parts to be used by the industry and university projects. It can also help with the understanding and use of acceptable risk non-space rated parts reducing the cost of the spacecraft. This will lead to the development of low cost platforms for space based experiments, providing research companies an inexpensive, long duration platform to conduct their in-space experiments, while better preparing engineering undergraduates for their transition into the work force.

### INTRODUCTION

The concept behind the SJSU microsatellite project is to provide an environment in which senior undergraduates can develop a better understanding of the design, manufacturing and operational process of a microsatellite. This practical knowledge that the students gain will become invaluable to them and to the companies that they will work for. The students have gone through the entire process in a large team environment with students managing and making important decisions for the design team. To help the students manage and address design issues properly, volunteer industry mentors interacted with each of the subsystem groups. The mentors gave constructive criticism of the students' design and helped each student understand the engineering concepts behind the design parameters. The industry mentors passed on their practical knowledge to the students, increasing the educational quality of graduating engineering students, and ensuring that the design was

reliable. This environment allowed the students to gain knowledge based on the extensive experience only available through long term industrial design.

SJSU is located in the heart of Silicon valley, a dense area of aerospace industries that have resources which are not generally available in academia, which include real world design, prototyping, manufacture and operation facilities. This allowed the SPARTNIK project to receive hardware and access to testing facilities through donations from the local companies. This also helped in developing and maintaining close working relationships with the industry mentors.

This type of project is not just for the benefit of the students, but for the aerospace industry and other research companies interested in space exploration. SPARTNIK is the initial design for a platform that industrial and research companies can use for inexpensive, extended-period space-based research. By funding a similar student project, the companies can employ senior undergraduate students to design the payload integration, manufacture and operate the satellite inexpensively compared to hiring one of the large aerospace companies.

The following will explain what senior aerospace engineers did at SJSU before the SPARTNIK project, the project process that the students went through to build SPARTNIK, and how the Space Shuttle Hitchhiker system can be one of the many lift systems that is used for launching the university built microsatellites, and the benefits to both the students and industry.

## **BACKGROUND**

In the past SJSU has offered an undergraduate senior design class which normally provides for a paper design of a complete spacecraft. In the fall of 1994 the spacecraft design instructor decided to take the concept further. Utilizing local industry support the class was given the opportunity to design on paper, then prototype, test and manufacture a spacecraft destined for orbit. By the end of the fall 1994 semester the SJSU micro-satellite development center was underway, with a completed paper design. Using industry collaboration during the early stages of the design, enabled the prototyping and manufacturing of the satellite to progress quickly. The collaboration continued through all stages of the project, which allow for the exchange of new ideas and experience between mentors and students.

## **DESIGN PROCESS**

The design process at SJSU has been consistent for a number of years. Students enrolled in the senior spacecraft design class are given general parameters from which they generate a mission plan, and then design hardware to satisfy that mission. The fall 1994 class was given a more specific mission--Build a microsatellite which will:

- Generate its own power.
- Maintain two-way communication.
- Carry at least one experimental payload.
- Fit as a secondary payload in any launch vehicle.

Given these general mission goals, the process took shape as follows.

Mission parameters were first determined after an extensive research on past university built microsatellites. These parameters gave the design team a basis from which to construct a preliminary mission plan. The research of past successful projects gave baseline design constraints on size, weight, power as well as payload considerations. With this baseline the design team formulated a mission plan for the SPARTNIK project, which is as follows;

- To manufacture and secure the launch of a reliable, low-cost satellite, which may be used for both scientific research and educational purposes.
- To provide practical design experience in a team environment for preparation of senior students to integrate into the industry work-force.
- To show the feasibility of a cooperative effort between academia and industrial sectors in space vehicle and mission design.
- To demonstrate the ease and low-cost of satellite imaging technology and how it can be used in our everyday lives.

- To provide a mobile and versatile platform from which to demonstrate scientific techniques and theory to encourage students and others to become involved in aerospace education and research.

Given the mission plan and the scope of the project, the class of 21 students formed subsystem design teams. These teams consisted of 3-4 students, one of which acted as the subsystem manager. Each team was required to solicit the help of at least one industry mentor, who was well versed in their particular subsystem. During the Preliminary Design phase of the project, these mentors provided invaluable insight into the design process. Mentors worked closely with students to guide them away from blind research, and towards mature designs. They were able to share 15+ years of experience and point out pitfalls which might have hampered speedy development.

Development fell into two phases; preliminary and critical design. At the end of the first semester (four months) the design team held a preliminary design review, where industry mentors were able to be briefed on the design status and give feedback to the student team. This also allowed the students to show consistent progress, while keeping the subsystems focused on the scale and integration into a larger design. The same was done for the critical design period at the end of the second semester.

The Preliminary design was the first decision point. This design was the product of academic research, mentor guidance, trade studies and subsystem design and integration meetings. These meetings were held throughout the entire project, insuring that the design of the different subsystems integrated properly. Students were allowed to formulate their preliminary designs, and based on those designs, choose the equipment and materials for each of their subsystems. The Preliminary Design Review (PDR) was the point at which funds were committed for the purchase of material. Specific hardware requirements were well documented by PDR, and those purchases were approved, while the design moved into the second phase.

The Critical Design Review (CDR) process began with the second of the two semester senior design project. The students returned to class with a PDR which required substantial refinement before manufacturing could begin. During the CDR phase, students began in-depth debugging of hardware and software. Detailed structural, thermal, and EM modeling began, with mission specific parameters being refined. Each subsystem made significant changes and improvements to accommodate integration requirements.

In parallel with the CDR progress, a payload launch adapter (PLA) team was formed, which went through an abbreviated PDR process. The PLA team continued initial research into launch environments and secondary payload systems on every commercial booster available, as well as the Hitchhiker platform offered by the Space Shuttle Small Payload Program. This team defined the ejection system hardware and process for launch from the payload bay of the launcher. Once this was well under way work began on launch verification testing and documentation.

The CDR process continued until the Final Design Review (FDR). At this point many of the subsystems had prototyped key components for testing. A design freeze was in effect, which prevented any major changes to the spacecraft and allowed integration. Subsystem fabrication began in earnest for all subsystems, including software development for the onboard computer.

Once the subsystems were substantially prototyped and the on-board computer built and programmed, the students began operational testing of the systems. By running each of the components through a rigorous testing scheme the students qualified each system as flight ready. If any anomaly was found the students assessed the problem and reevaluated their design and made changes where necessary. Structural testing was also conducted on the satellite bus. A aluminum prototype was built and tested on a shake table to qualify the general structure of the satellite in the various launch environments that it would encounter. With acceptable results on the prototype design, the team progressed to manufacture the flight structure and began to integrate the other subsystem components. Once the flight model was assembled with all the actual flight hardware installed, a second shake test was performed to qualify the flight structure and wash out any minor anomalies.

At the completion of the second shake test, a verification manual was compiled to report the readiness and reliability of the satellite to survive the launch environment of any launch vehicle. This document will be turned over to the launch vehicle company that SPARTNIK will be using, for their approval of flight readiness.

Students will also work closely with the launch vehicle company to ensure that the satellite will integrate properly with the launch vehicle, and convey the procedures for a successful launch. Once the satellite is in orbit the student team will

maintain and operate the various housekeeping and data collection procedures for the satellite via a ground station at SJSU. The students will compile experiment data and forward them to the respective research company for their use. The students will also maintain the satellite and deal with any anomalous contingencies that might arise while on orbit. The projected operational life time of SPARTNIK is a minimum of 2 years.

The collaboration that came about between NASA engineers, industry engineers and students is phenomenal. SJSU is located in downtown San Jose, within 20 miles of numerous aerospace companies that have extensive experience in the design and manufacture of all types of spacecraft. Industry mentors collaborated throughout the design process, and allowed their experience to fertilize the education of the student-engineers. This industry collaboration extended to hardware and financial donations for the different phases of the project, which allowed for prototyping of key systems with actual flight hardware. The commitment from local industry did not end with mentors, hardware and money. Systems engineers from several companies evaluated the design at PDR, CDR and FDR to act as a sounding board for the overall system, and evaluate the student project as if it were being manufactured in-house.

## HITCHHIKER

With the limited budget of the student project, a discounted or donated launch as a secondary payload is needed. There are many different launch vehicles that can be used by the student projects. Pegasus, Delta, Ariane IV, Lockheed Launch Vehicle and the Space Shuttle. The Space Shuttle program provides the Hitchhiker for experimental payloads, and offers this system to university programs for \$10,000. Although, the GAS can system normally ejected microsattellites from the Space Shuttle, this is no longer done and the size constraint of the GAS system is too small for SPARTNIK. The Hitchhiker, to date, has not launched any micro satellites, but the SPARTNIK team believes that it would be a good launching system. The team has developed a system to be used with the Hitchhiker and the other possible vehicles for launching student built microsattellites.

Figure 1 shows the possible locations where the microsattellite could be attached to the Hitchhiker. The spacecraft would attach to the various pallets by the payload adapter system, figure 2. The launch vehicle would supply a 28 V DC signal to the satellite to activate a release mechanism. A non-explosive separation nut and bolt system will be used for launching SPARTNIK. This assembly will be self-contained so that the separated parts will not float away and become a hazard to both the spacecraft and the astronauts. Once the main bolt is separated a spring will push the satellite away for the Hitchhiker, the resultant velocity of the satellite from the spring can be varied by installing different springs that have different spring constants before launch. This will enable the design team to ensure that the resulting orbit of the satellite will not come back around and hit the space shuttle. The base plate and stand-offs (figure 2) of the PLA will remain with the Space Shuttle after the launch, and will remain a rigid body throughout the entire mission.

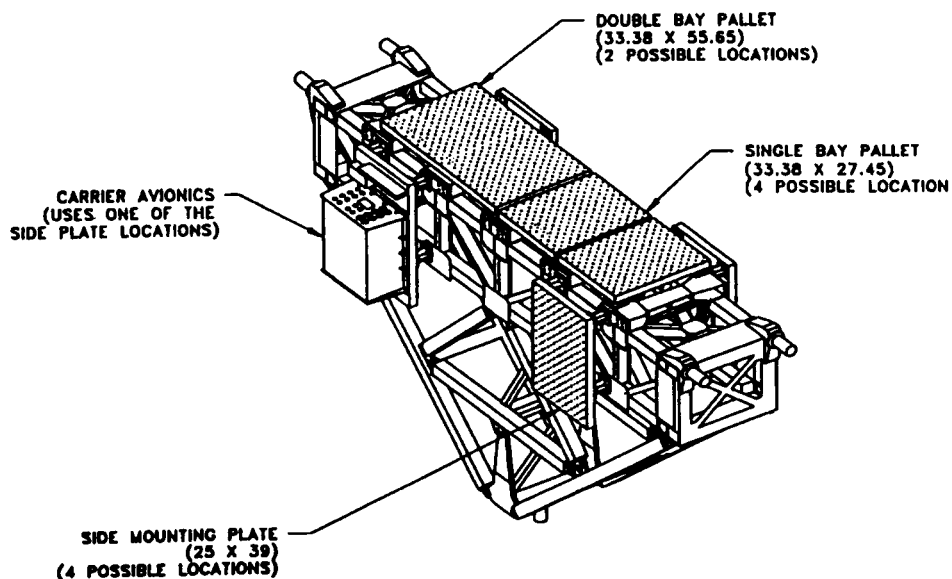


**Figure 1 - Hitchhiker Small Payload Attachment Locations<sup>1</sup>**

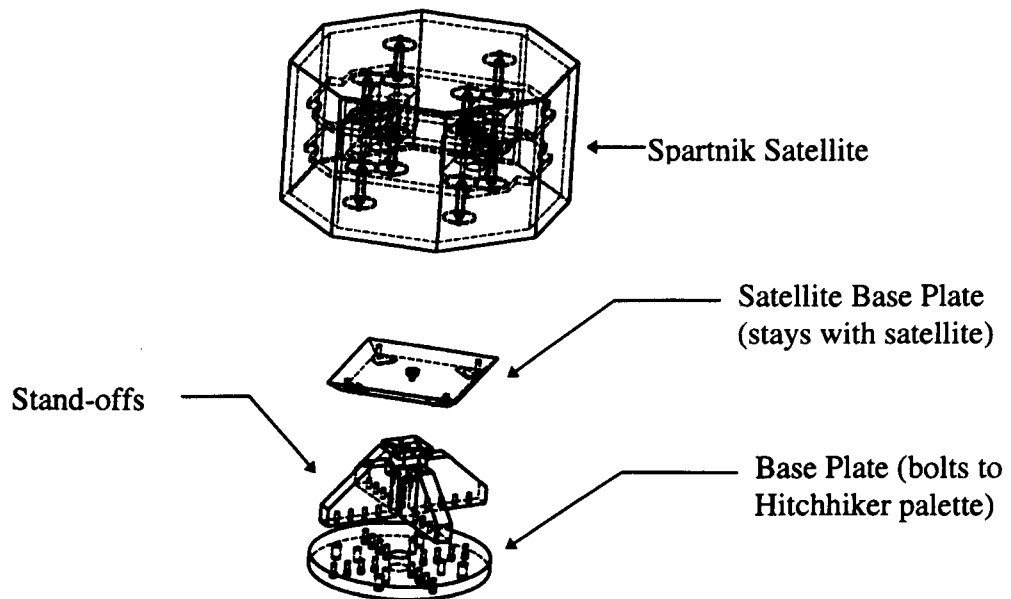


Figure 2 - SPARTNIK with Payload Adapter System

## **BENEFITS**

This type of collaboration is beneficial to both parties, and will continue to be so. The primary benefactors were the students of the class, who received direct exposure to engineering as it is practiced in industry. Approximately twenty percent of the AE students at SJSU get internships at local companies which specialize in the aerospace industries<sup>2</sup>. That is four students in a senior design class of 20 which can expect to work in some capacity on significant design project during their tenure as an AE student. This collaboration allowed 100% of the design class to have exposure to a large project, and work closely with mentors in their area of interest. Additionally, the collaboration allowed various companies to evaluate designers before they graduate in a project which tests engineering skills, documentation, and interpersonal communication abilities.

Beyond the potential personnel evaluation, companies have a platform to test new ideas and hardware effectively. New battery, solar cell or computer technology can easily be tested on a microsatellite. The small scale of the project allows for simplified testing on an actual orbiting spacecraft. The SPARTNIK project is testing commercial grade NiCd batteries in a space environment. In exchange for the donation of the cells, the SJSU Aerospace Engineering Department will document performance of the batteries over the lifetime of the spacecraft. This data will be downloaded as part of the normal housekeeping telemetry for the microsatellite, and forwarded to the donating company.

This type of collaboration should be encouraged by government and industry sponsors to entice university programs to develop their academic programs into a forum for new ideas and techniques for the entire aerospace industry.

## **CONCLUSION**

As SJSU becomes a development center for microsatellites, graduating engineers will be getting practical engineering knowledge that they will be able to use in industry. Thus, providing industry with better educated and prepared entry level engineers to contribute quickly to the aerospace industry. The industry mentorship will lead to a close working relationship between local industry companies and the universities, which will help with making the design more robust, the practical education of students, and the communication of industry needs to the university for trained engineers and direct the process in which this is done at the university level.

The student-run project will be an inexpensive way for research companies to perform space environment experiments for long durations and for the aerospace industry to test and qualify new satellite technologies for a low monetary risk. These projects can also be used to increase the understanding and use of acceptable risk non-space rated parts which lead to reliable, low-cost spacecraft.

The microsatellites will provide the research and industry companies with an orbiting test platform for a minimum of 2 years, inexpensively (\$10,000 for launch, plus hardware funding) compared to what they would normally get for launching permanently attached to the Space Shuttle bay for up to three weeks for several millions of dollars.

#### **REFERENCES**

<sup>1</sup>Space Shuttle Small Payloads Hitchhiker Users Guide, 1994

<sup>2</sup>Professor Hunter, Aerospace Engineering Department, San Jose State University

# **The Failure Analysis, Redesign, and Final Preparation of the Brilliant Eyes Thermal Storage Unit For Flight Testing**

T. Lamkin, Brian Whitney  
USAF Phillips Laboratory  
Kirtland AFB, NM

## **ABSTRACT**

This paper describes the engineering thought process behind the failure analysis, redesign, and rework of the flight hardware for the Brilliant Eyes Thermal Storage Unit (BETSU) experiment. This experiment was designed to study the zero-g performance of 2-methylpentane as a suitable phase change material. This hydrocarbon served as the cryogenic storage medium for the BETSU experiment which was flown 04 Mar 94 on board Shuttle STS-62. Ground testing had indicated satisfactory performance of the BETSU at the 120 Kelvin design temperature. However, questions remained as to the micro-gravity performance of this unit; potential deviations in ground (1 g) versus space flight (0 g) performance, and how the unit would operate in a realistic space environment undergoing cyclical operation. The preparations and rework performed on the BETSU unit, which failed initial flight qualification, give insight and lessons learned to successfully develop and qualify a space flight experiment.

## **INTRODUCTION**

After initial flight qualification vibration testing of the BETSU located inside the NASA Hitchhiker canister, significant damage was observed. Obviously, this experiment would not be allowed to fly until the cause of the failure was identified, corrected and the unit subsequently passed flight qualification testing. Following initial vibration testing, failures were identified and repaired, then the experiment was reintegrated and retested. Following the second vibration testing, less (but significant) damage was still observed. At this point a loose bracket was identified which was causing amplification during the vibration testing. Finally, the damage was repaired, the bracket was secured, and the experiment was vibration tested again. At this point, the BETSU was successfully qualified. Four months later the experiment was launched on STS-62 and performed exceptionally on orbit. This was only possible because of the intensive redesign and rework done during flight qualification.

## **INITIAL FAILURE ANALYSIS**

The BETSU was deintegrated from the HITCHHIKER can and then taken from Goddard Space Flight Center to Grumman Aerospace Corp. (builders of the BETSU) to undergo any and all necessary repairs. Due to NASA flight schedules, the unit would have only 48 hours before either a retest occurred, or the experiment would not be permitted to fly. However, at this time Grumman and the Air Force were involved in sensitive contractual negotiations. As a result, the Phillips Laboratory sent a flight hardware qualified technologist to investigate the BETSU, analyze, repair, re integrate and oversee the remaining tasks necessary to achieve flight on board the Shuttle. The existing contract was amended to allow this individual access to Grumman's facilities and also to initiate any repairs necessary to make the failed unit operational. To further complicate the task, the person who had built the original unit was no longer working at Grumman.

Disassembly showed three failures: S-glass straps broken, Q-meter frayed, and mounting post bent. Figure 1 shows the original design and figures 2 thru 4 show the damage.



### S-Glass

It was immediately apparent during disassembly at Grumman that the six S-glass straps, were completely destroyed. The straps are used to "suspend" the BETSU from the outside canister and to minimize thermal conductivity. The straps are about 1 1/2 " long, with a radius of about .140". Initial microscope examination indicated that the failure occurred at the apex of each radius. Analysis by the Phillips Laboratory representative on site, indicated the failure was consistent with the material "pulling apart" (Fig 2), and under the microscope one could see how the fiberglass was laid together and that it had delaminated at the apex of each S-glass strap radius. Later analysis indicated the vibration "modes" set up in the unit during testing were causing this delamination to occur.

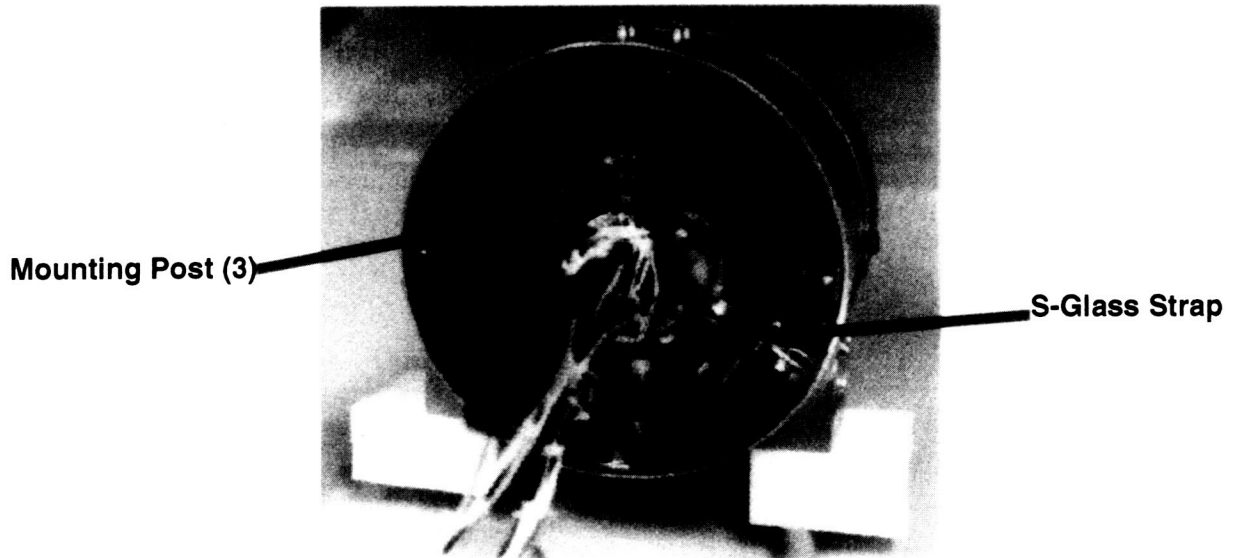


**Figure 1: Original BETSU Configuration**

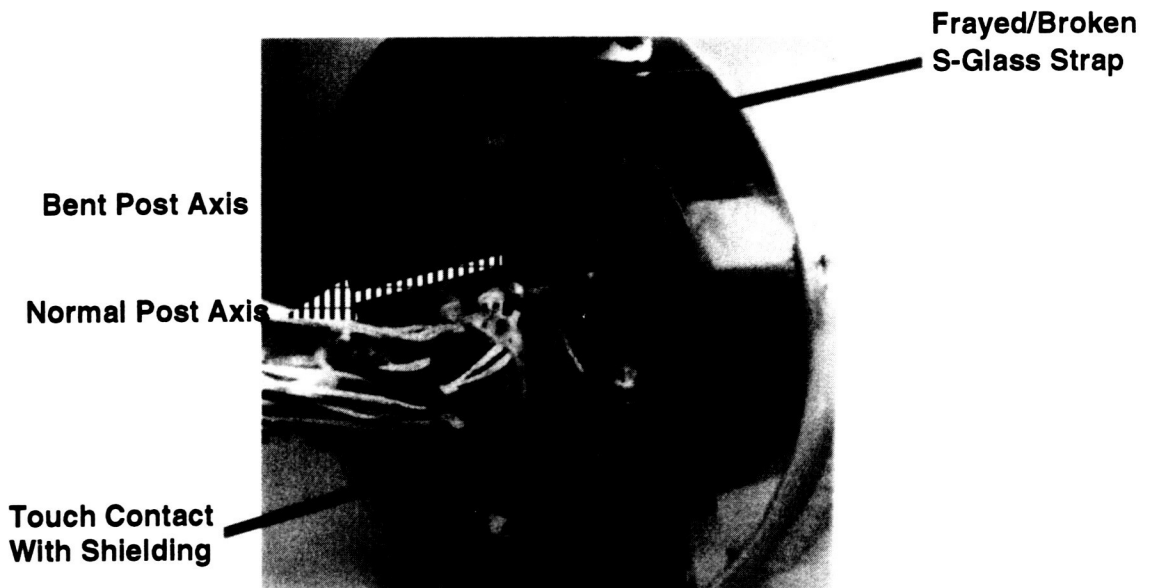


**Figure 2: BETSU Damage**

#### Mounting Post

After further disassembly and analysis, the cleavages on the three S-glass strap mounting posts (Fig 1) on the Q-meter side of the BETSU showed signs of failure. These three posts were integral parts machined into the top of the BETSU canister. It was discovered that two of the posts were cracked, about .150" up on the Q-meter side. The third post was bent almost completely over (40 deg) from normal. In addition, initial observation indicated one of the three posts on the opposite side of the BETSU (heater side) was also bent.

#### Q-Meter

Immediately after disassembly it was evident the Q-meter was frayed. The Q-meter is the calibrated mechanical link between the BETSU itself and the thermal shunt. It is braided steel (similar to a grounding strap), and the motion of the BETSU during vibration testing (postulated as a circular motion) had caused the attached Q-meter to literally fray apart. Since there was no Multi Layer Insulation on the unit for this test, this failure was identified by means of a bore-scope inspection.

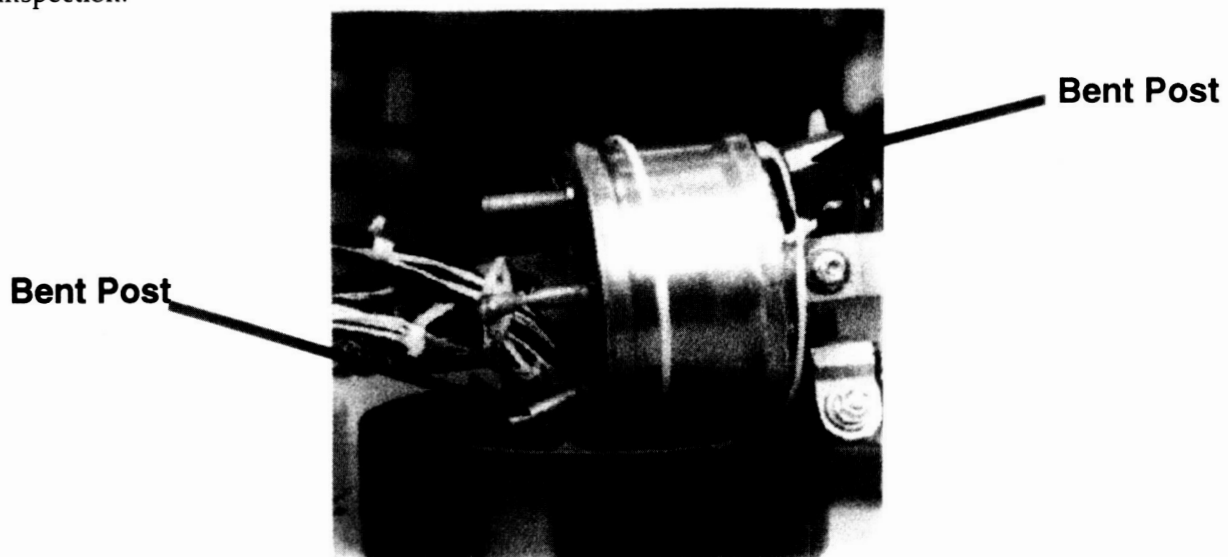


Figure 3: Mounting Post Damage

#### Sequence of Failure

After surveying the total damage to the unit, the Phillips Lab representative postulated that probably the front S-glass straps broke first. Since the Q-meter was bolted to the thermal shunt, with the other end attached to the "suspended" (but now free floating) BETSU, the "braided" portion of the Q-meter saw the brunt of the dynamic BETSU motion and this caused the massive fraying to occur (see figure 4). This also caused the Q-meter side posts to continually strike the outer canister and resulted in the bending and cracking noted in the post failure analysis. This hypothesis was confirmed when the inner gold shielding was examined and the "hit marks" discovered on the shielding were "reached" by physically seeing how much deflection the still attached BETSU would exhibit.

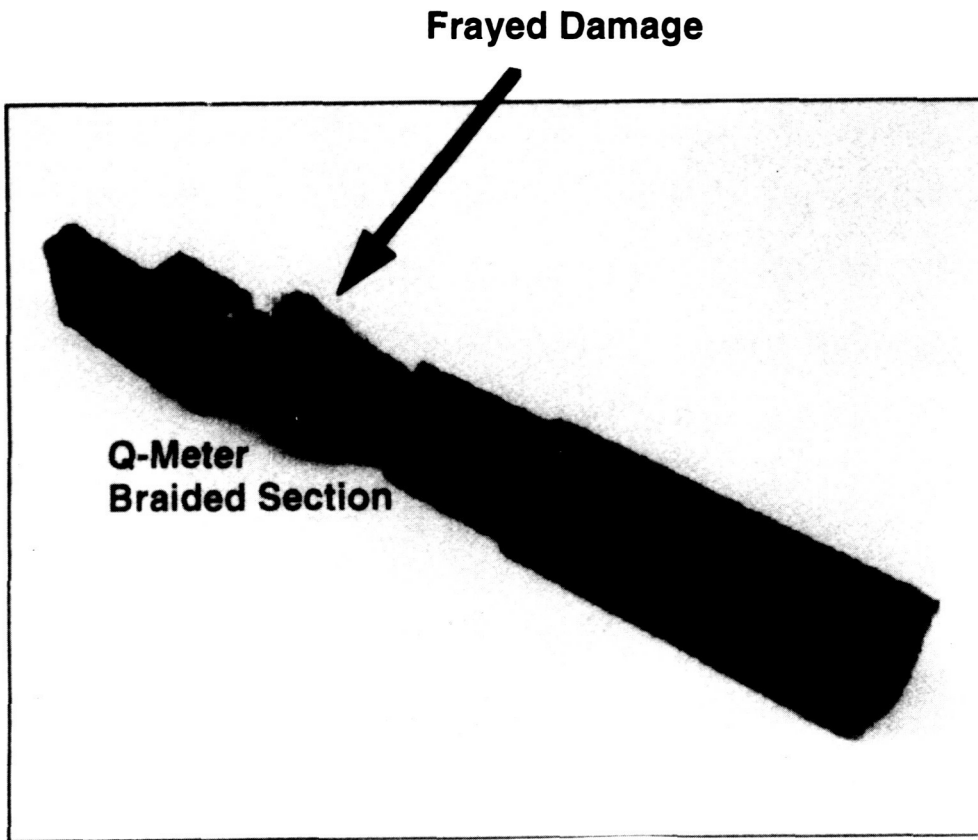


Figure 4: Q-Meter/Shunt Analysis

The "beat up" nature of the gold shielding confirmed that motion occurred at some point during the initial flight qualification testing, but whether it occurred during the 9.1g, 60 sec (each axis) random vibration test, or the 12.1g sine burst was unknowable. With only one unit in existence, this qualification unit was the actual flight unit. The qualification unit would need to be repaired and subjected to at least a repeat of the vibration testing before NASA safety would certify it flight worthy. Discussions with Grumman at this time centered on concerns with heat from any post welding operation being conducted into the BETSU canister with unknown consequences. The Phillips Laboratory tech suggested submersing the BETSU in water to keep it cold during the post welding operation and minimize thermal conductivity.

#### REPAIR/REINTEGRATION

##### S-Glass

As there was no way to repair the broken straps, they were replaced with flight spares.

##### Mounting Posts

A special tool was fabricated to straighten out the posts, but a penetrant test prior to straightening indicated more subtle problems existed with the two of the posts (see figure 3). These two posts exhibited numerous cracks, a typical crack being .050" long, with a .004 to .006" open gap and had a .020" to .060" depth. One post was on the heater side of the BETSU @ the 4 o'clock position, with the other one on the Q-meter side @ the 12 o'clock position.

The two posts which had multiple "cracks" were repaired in the following manner. Each crack was ground out about 1/4 of the post depth, and then welded by (TIG) process. Cold, wet rags were used as a heat sink, and finally the welds were ground and cleaned. However, the main, front Q-meter side post was a more challenging repair. This post was bent and cracked so bad that it

simply broke off about .070" from the bottom. After discussion with the Grumman machinist, the PL tech designed an L-shaped replacement post which utilized the main front Q-meter mounting point for stability. Figure 5 shows the redesigned post which replaced the broken one.

#### Q-Meter

As with the straps, the Q-meter was also non-repairable. consequently, it was replaced.

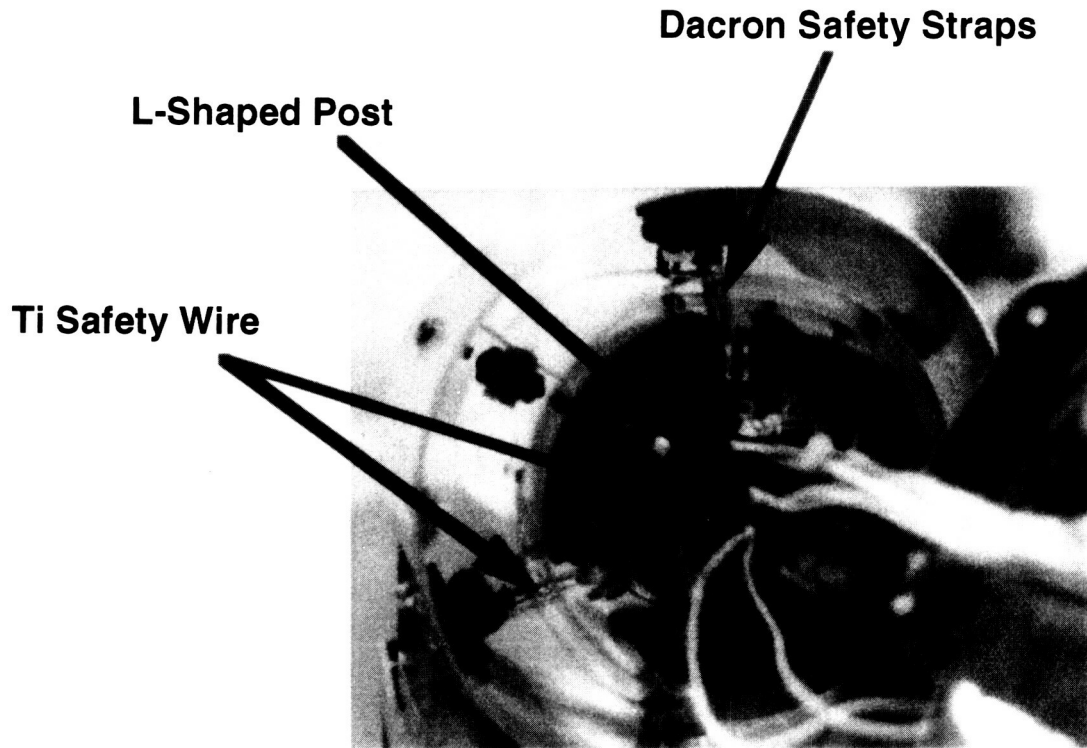


Figure 5: BETSU Repairs

As seen in figure 5, with the "base" of the L-shaped post was epoxied down, the "leg" inserted into the Q-meter mount, pinned and staked, all that was needed was to machine the vertical part to match the other existing posts. Most importantly, this solution involved no welding operations on the BETSU. At this point, repairs were basically complete on the BETSU, but still the "cause" of the failure was unknown, and thus the repaired unit would in all likelihood also fail if tested in it's present configuration. To attempt to strengthen the post "configuration" (since most of the posts had been through repeated welding and thus lost some tensile strength), the PL tech hand cut out a receiver groove (half round) in each post for use with flight safety wire. By "triangulating" safety wire around all three posts, any force was distributed across all three, and not potentially acting on only one post. This configuration was repeated on the three posts on the Q-meter end of the BETSU. Then all six posts had washers staked down on the can to give the clevice a little more strength. It was hoped that this would help the BETSU "survive" the qualification retest.

#### Additional Repairs/Reassembly

Besides the aforementioned mechanical/structural repairs, the qualification unit also needed to have the following repairs and/or replacements:

- a. Repair crushed heater wire near heater plate
- b. Repair Platinum Resistance Thermometer??? (PRT) #23 (on heater plate) wire in vicinity of Q-meter
- c. Install six new PRT's on Q-meter

- d. Rework daisy chain with six wires from new PRT's.
- e. Install aluminum tape over PRT #23 on heater plate
- f. Verification test the six thermocouples did indeed close when cooled (LN2 test)
- g. Re-epoxy one thermostat on inboard side of heater plate
- h. Replace one G-10 heater support angle from spares
- i. Clean gold plated thermal shields
- j. Re-stake hardware on heater plate and all other locations where appropriate.
- k. Replaced all fasteners per NASA flight hardware regulations

During BETSU reassembly, the PL tech discovered that although the unit was "secure" in a solely lateral or vertical direction, it was not as rigid when it comes to twisting or flexing about the unit's centerline. Since this was discovered during reassembly, and time was already running out, there was little to do except note the phenomenon. About this time, other players (namely people from the Aerospace Corp.) were beginning to work up models with the S-glass straps to see if they could really do the job. However, this was not finished in time for the reassembly timeline.

The unit was tightened "as solid" as the technologist felt was prudent, and this was greater than the original Grumman specifications called out.(12.72 lbs) However, tightening only to the Grumman specifications allowed too much torsional movement, and it was decided that this type of movement should be minimized if possible. The tech suggested that some sort of "safety strap" be used around the S-glass straps to minimize BETSU damage if another S-glass failure occurred during retest. This was purely a "damage mitigating" thought since it was felt the cause of the first failure was still unknown, and thus the same type of failure could occur. Safety strapping could thus help minimize internal damage and 1) reduce the amount of rework necessary and also 2) "protect" enough of the unit so that the "failure mechanism" may be more apparent. Thus, the tech added NASA flight certified Dacron as safety straps around the S-glass straps during reassembly.

#### **NASA FLIGHT QUALIFICATION RETESTING**

A little over 48 hours had passed when the repaired and reassembled unit was driven back to Goddard and reintegrated into the HITCHHIKER canister by the PL tech. The canister was vibrated again, and post-test inspection indicated another failure had occurred. The Q-meter was found to be loose, and the S-glass straps were broken again, the Q-meter was frayed, and the electronics were damaged. About this time, it looked as if an "amplification" was occurring inside the HITCHHIKER canister, and not just in the BETSU. This could be anything from a mass/location/inertia problem, to a faulty vibration test rig.

##### S-Glass

The straps had broken exactly as they had the first time the BETSU was shaken.

##### Q-Meter

The Q-meter was minimally damaged. It is believed that the safety straps had minimized the Q-meter damage

##### Electronics

The cryo electronic control module (CECM) package was found to be "broken.. Boards had come off their stand-offs, and even piece parts (chips, etc.) were "sheared" off the boards!

##### Loose Bracket

During disassembly/reassembly, the tech discovered a support structure mounting bracket for the CECM was loose. When this bracket was taken off, indications of motion was so severe that the plate it was attached to was gouged severely. This provided a possible explanation for the suspected amplification.

## REPAIR AND REINTEGRATION

### S-Glass

At this time, replacements for the S-glass straps were the number one priority. Various manufacturers and materials were tested for suitability. Kevlar was tested, but it was found that the elasticity characteristics were not suitable for the size and length of the attachment. In addition, the repaired posts would have to withstand whatever tension was necessary for the S-glass replacement material. It was later shown that the post redesign was three times stronger than the original, and had plenty of margin for the S-glass replacement material. In the end, the configuration tested and flown was titanium wire, with the "knot end" welded together and the Dacron safety wire as a backup. This necessitated additional repairs on the electronics control unit in addition to BETSU repairs and S-glass replacement testing.

### Q-Meter

Clipping frayed edges was the only repair task necessary to the Q-meter. The repaired Q-meter could be used in space, and then "recalibrated" on the ground.

### Electronics

The electronics were fully disassembled and inspected. All broken piece parts were repaired or replaced.

## NASA FLIGHT QUALIFICATION RETESTING

NASA safety agreed that at this point a component level vibration of the BETSU alone would be acceptable. It must be remembered that this GAS can had already gone through flight qualification testing, flown on the shuttle, and been subject to two more flight qualification vibration tests. It was strongly felt this bracket was shaking inside the canister and setting up the amplification which was destroying the internal components. This part of the structure was repaired and then NASA safety was called in to make a ruling on what the vibration retesting would consist of. It was felt the canister and all the components inside it had seen two vibration tests, and only the BETSU had never "passed".

The BETSU was bolted on a plate, re-vibrated, and it PASSED!

## CONCLUSIONS/LESSONS LEARNED

The entire BETSU failure analysis, redesign and flight acceptance highlights several important factors which anyone preparing to qualify hardware for space flight should consider.

First, NASA flight qualification standards are primarily geared towards preventing the unwanted, catastrophic failures of individual components which could damage/jeopardize the rest of the space vehicle. Proper operation of an individual subsystem after flight qualification testing is complete rests entirely with the manufacturer and/or hardware integrator. With this in mind, initial component design and analysis must ensure proper operation after flight qualification testing, not just enable the unit to "survive" this test. If the initial design is unable to operate after qualification testing, a redesign by personnel knowledgeable in the system/experiment, and familiar with the "host" spacecraft is essential. If that is not practical, the next best option, as demonstrated in this paper, is a flight hardware qualified technologist utilizing the best engineering practices in real time to rework the subsystem/experiment and enable the unit to complete the mission.

Second, a space hardware systems engineering thought process must enter into the initial design of any flight system/experiment. Without proper systems engineering design, a "black-box" which is designed to meet flight requirements may still experience failure when integrated into the rest of the spacecraft and tested as a complete unit. The structural rigidity of the spacecraft mounting, distributed power, thermal management, etc., are never fully certain until all the parts are fully assembled. As demonstrated by the BETSU failure, even a highly successful, seemingly well known environment like a NASA Hitchhiker canister can prove difficult to predict accurately. This highlights the fact that any piece of flight hardware must be treated as if it was being flown

for the first time and considered as a potential problem until proven acceptable. Thus, sufficient initial design margin and experienced hardware integrators can prevent a catastrophic failure which almost occurred with the BETSU.

Finally, failure analysis of any kind (not just during space flight qualification testing) should be considered from an overall systems perspective. Stopping a failure analysis just because the "broken" or "faulty" part is observed can cause you to zero in on the symptom and ignore or miss the cause of the failure. As observed with the BETSU, although it was expected that the original S-glass straps would have failed under normal vibration testing, this was not the only problem identified. Further inspection was required to identify the loose bracket which most likely was "amplifying" the vibration environment of the experiment. So, even if an obvious failure is identified, continue to completely examine the subsystem/experiment for other failures and also inspect the rest of the overall system for induced failure mechanisms.

## **AN ADAPTABLE PRODUCT FOR MATERIAL PROCESSING AND LIFE SCIENCE MISSIONS**

Gregory Wassick and Michael Dobbs  
Advanced Modular Power Systems, Inc.  
Ann Arbor, Michigan

### **ABSTRACT**

The Experiment Control System II (ECS-II®) is designed to make available to the microgravity research community the same tools and mode of automated experimentation that their ground-based counterparts have enjoyed for the last two decades. The design goal was accomplished by combining commercial automation tools familiar to the experimenter community with system control components that interface with the on-orbit platform in a distributed architecture. The architecture insulates the experimenter from the details of the on-orbit platform while providing the payload engineer with the tools necessary for managing a payload. By using commercial software and hardware components whenever possible, development costs were greatly reduced when compared to traditional space development projects. Using commercial-off-the-shelf (COTS) components also improved the usability of the system by providing familiar user interfaces, providing a wealth of readily available documentation, and reducing the need for training on system-specific details. The modularity of the distributed architecture makes it very amenable for modification to different on-orbit experiments requiring robotics-based automation.

### **INTRODUCTION**

Advanced Modular Power Systems, Inc. (AMPS), a small business, was incorporated in 1990 to conduct R&D and product development of advanced, efficient, cost-effective and reliable energy conversion systems for the production of electrical power in space and terrestrial applications. Similarly, the Space Resources Division (AMPS-SR) concentrates on the research, development, integration and manufacturing of cost-effective instruments, experiments, and complete systems (payloads) for terrestrial markets and space missions.

AMPS-SR objectives are the creation of a space automation supplier to industry. This industry is defined to include suppliers of laboratory automation equipment such as sample preparation and manipulation, sensors, process control, data acquisition and control, and data analysis systems. Technological and economic elements of these industries are well established, with suppliers providing automation-related products and services to terrestrial "customer" industries including electronic, pharmaceutical, chemical, and other consumer product areas (i.e., food and beverage). Many of these same industries, particularly those in the electronic and pharmaceutical areas, also have an active research and development (R&D) interest in the unique properties of the space environment (microgravity, ultrahigh vacuum, view of earth, etc.).

Recognizing the commercial potential of space-based experimentation and discovery as well as manufacturing, AMPS-SR is involved in several joint project activities with both public and private partners. While these projects focus on different niches, they all have a common goal to reduce the cost of space-based research and manufacturing through the development and deployment of technology that extends established terrestrial laboratory automation techniques to the space environment.

This paper examines the system architecture of the Experiment Control System (ECS), as used in the Robot Operated Materials Processing System (ROMPS), and its evolution into the private sector product the ECS-II, which will be used on Wake Shield Facility 3rd flight (WSF-3) as the control system for the Automated Wafer Cartridge System (AWCS). The ECS and ECS-II systems are built around two commercial off-the-shelf (COTS) technologies, Zymark's Zymate System V Controller and Interface and Control Systems' (ICS) Spacecraft Command Language (SCL).



Other ECS-2 missions include, the enhanced ROMPS-2, the large scale manufacturing mission on WSF-4, and a joint JPL-AMPS INSTEP payload that will demonstrate essential AMTEC power conversion technology for the Pluto Express program.

### **ROMPS MISSION OVERVIEW**

In 1991 a request was made by NASA's Goddard Space Flight Center (GSFC) to propose an alternative Experiment Control System (ECS) design for the ROMPS project. The ROMPS project is a Space Shuttle Hitchhiker mission centered around the rapid thermal processing (RTP) of semiconductor materials. The ROMPS mission's short-term objective is to develop commercially promising in-space processes by using a robot-based automation system to lower the cost of the material procedures. Figure 1 shows the payload configuration of the ROMPS Hitchhiker payload.

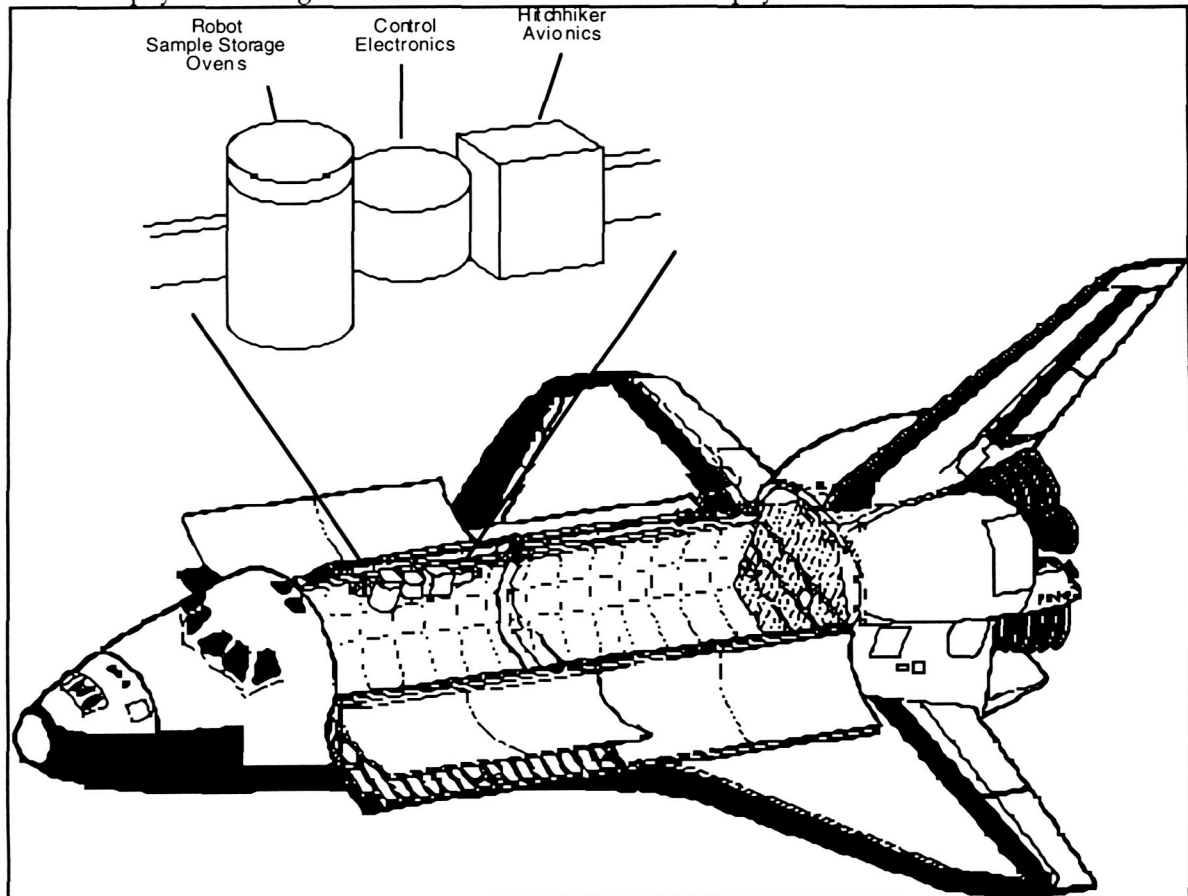


Figure 1. ROMPS Hitchhiker Payload Configuration

### **ROMPS AUTOMATED RAPID THERMAL PROCESSING**

Rapid thermal processing is a widely used industrial material processing procedure for two-dimensional semiconductor materials. In this process, a heat source capable of producing uniform surface area temperatures (usually a quartz halogen lamp) is used to melt semiconductor materials. The semiconductor materials are then allowed to cool and recrystallize. Semiconductor materials recrystallized in micro-gravity have larger and more uniform crystals that have better electrical properties.

ROMPS provides a robotic-based system capable of automating the RTP with up to 155 samples. In this system, a custom-built halogen lamp furnace provides the heat source for the RTP of the samples.

A robot designed by GSFC moves the semiconductor samples between their storage racks and the furnace. The ECS was developed to provide the computer, computer software, and electrical sub-systems for automatically controlling and monitoring the RTP of the semiconductor materials.

### WSF-3/AWCS MISSION OVERVIEW

Carried into space in the payload bay of the Space Shuttle, the Wake Shield Facility (WSF) presents a unique platform for the development of advanced semiconductor materials and devices through the use of the ultra-vacuum of space. The WSF is released into orbit by the Shuttle RMS robot arm. After the WSF maneuvers away from the Shuttle, it orients itself to shield out the residual atmosphere that remains in low earth orbit, thereby creating an ultra-pure vacuum in its wake, see Figure 2.

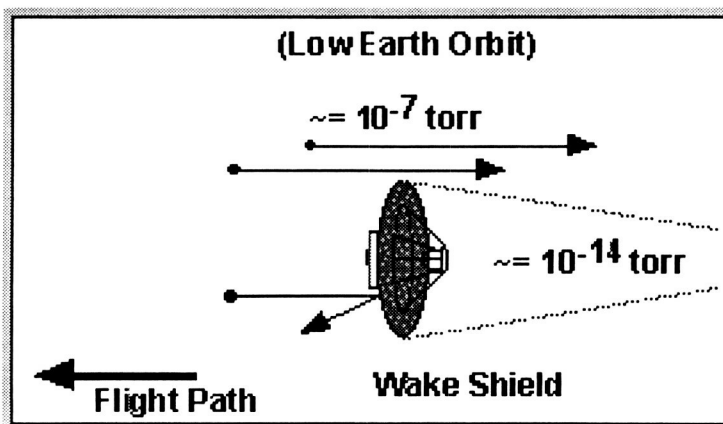


Figure 2 - Deployed Wake Shield Facility

This ultra-vacuum, nearly empty of all molecules, is then used to conduct a series of thin film growths by a process called molecular beam epitaxy (MBE) which produces exceptionally pure and atomically ordered thin films of semiconductor compounds such as gallium arsenide. Using this process, the WSF offers the potential of producing the next generation of semiconductor and superconductor thin film materials, and the devices they will make possible. After a several day period of free flight, the WSF platform is retrieved by the Space Shuttle and returned to Earth.

The first AWCS was designed to provide the WSF with a prototype manufacturing facility. In its current configuration, it will transport 100+ wafers to and from orbit, an increase of 15 times the present number of wafers processed. The AWCS design is readily scaleable to 1000+ wafers required by the WSF-4 mission. The AWCS utilizes a unique, patented 2 degree-of-freedom(dof) robot arm/gripper to move the wafers from the storage racks to the substrate rotator. The present system is designed to mount directly to the existing WSF carousel flange and to conform to ultra-high vacuum (UHV) practices regarding materials and mechanical systems.

### WSF-3/AWCS MBE PROCESSING

Epitaxy, a technique for controlled deposition of thin films in a vacuum, is the atomically ordered growth of a material on a substrate in an atom-by-atom, atomic-layer-by-atomic-layer manner. SVEC employs an epitaxial technique known as molecular beam epitaxy (MBE), whereby atoms or molecules emitted from heated crucibles impinge upon a substrate, condensing and forming a thin film, see Figure 3. The better the vacuum

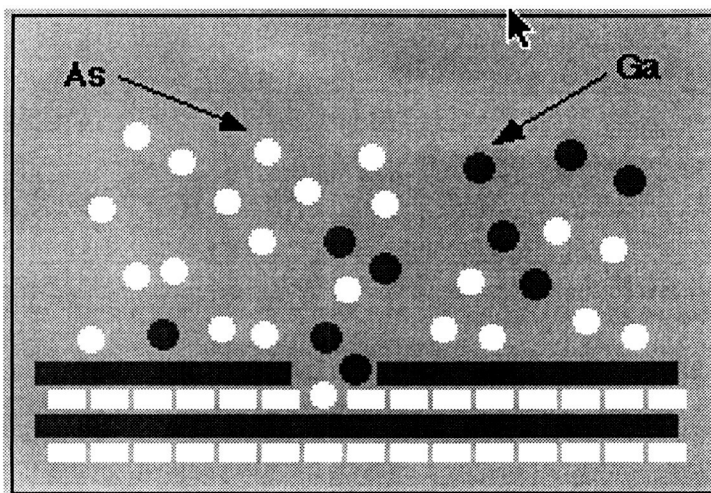


Figure 3 - MBE Processing

quality, the higher the quality of the thin film material grown. Scientists consider this technique to be one of the most powerful methods for synthesizing new and improved materials and devices.

## **MISSION REQUIREMENTS**

Table 1-Mission Requirements Matrix, provides a matrix of the mission requirements for both the ROMPS and WSF-3/AWCS missions. Also, included are the requirements for other upcoming missions.

**TABLE 1 - MISSION REQUIREMENTS MATRIX**

<b>FUNCTIONAL REQUIREMENTS</b>	<b>ROMPS</b>	<b>WSF-3</b>	<b>ROMPS-2</b>	<b>WSF-4</b>	<b>AMTEC</b>
<b>Robot Requirements</b>					
Motion Control Of N-Dof Robot Mechanisms	4	2	4	2	
End-Of-Travel (Eot) And Over-Force (Ovf)	X	X	X	X	
Calibration Of Home Position	X	X	X	X	
Stored Robot Move Sequences	X	X	X	X	
<b>Processing</b>					
<b>Furnace Controller</b>	X		X	X	
Power Or Temperature Setpoint	X		X	X	
Timed On/Off Sequences	X		X	X	
Multi-Step Time-Temperature Profiles	X		X	X	
<b>Process Sensors</b>					
Thermocouples, Thermistors	X	X	X	X	X
Video-Microscopy			X		
Non-Contact Temperature Measurement			X	X	
Reflected High Energy Electron Diffraction				X	
<b>Process Control</b>					
Closed Loop Temperature Control			X	X	X
Machine Vision Inspection Of Crystal Grain Boundaries			X	X	
<b>Payload Controller</b>					
Science/Engineering Data Collection And Transmission	X	X	X	X	X
Support Of Carrier CC&T Interfaces	X	X	X	X	X
Scripted Control Of Process Steps	X		X	X	X
Automated Health And Safety	X	X	X	X	X
Non-Volatile Storage Of In-Flight Mission Changes	X	X	X	X	X
<b>Ground Station</b>					
Archiving/Playback Of Telemetry	X	X	X	X	X
Command Generation	X	X	X	X	X
Display And Analysis Of Science/Engineering Data	X	X	X	X	X
Support NASA/Commercial Ground Station Interfaces	X	X	X	X	X
Configuration Control	X	X	X	X	X
Distribution Of Telemetry Via Internet			X	X	X

## **ECS/ECS-II DISTRIBUTED SYSTEM ARCHITECTURE**

The decision to use a distributed system architecture constructed of COTS components was driven by factors including:

- low cost
- use of commercial software packages
- 100% compatibility of software between ground development and flight systems
- parallel development capability on non-flight ground system
- established set of development tools

Both the ECS and ECS-II are designed using the same overall system architecture. The major difference is the use of COTS hardware to implement the servo subsystem in the ECS-II. Figure 4 shows the migration from the terrestrial architecture to the ECS-ROMPS architecture, then to the ECS-II/AWCS architecture.

## **USE OF COTS SINGLE-BOARD COMPUTERS AND PERIPHERALS**

First and foremost to meet our commercial customer objectives, the use of COTS components reduces the cost of experimental systems. Second, COTS components accelerate the space investigator's access to familiar or state-of-the-art technology.

### **Reduced Cost**

While it is difficult to compare the cost of conventional space "qualified" systems with space "ruggedized" systems, the following comparisons are of interest:

- An accepted estimate of developing full space qualified avionics systems (with the same mass as the ECS) ranges from \$1.1M to 7.6M.<sup>3</sup>
- Our approach, maximizing COTS content and accepting system reliability estimates of 97 percent versus 99.99 percent, reduced the actual cost (including mission support) to \$750K for ROMPS.

### **Acceleration of Technology Introduction**

As shown in Table 2, the introduction of computers to space missions has significantly lagged behind the same technology's commercial introduction. While a significant element of the lag is the lengthy and costly delay associated with radiation hardening, there are many missions that do not require this characteristic. One of our goals is to accelerate the introduction of a new computing capability where the need for high performance at low cost outweighs susceptibility to radiation.

In the upgrade of the ECS to the ECS-II one COTS module, a DSP based servo controller, allowed the replacement of three custom modules. This change increased the servo loop rate by a factor of 80, and also allows the use of both stepper and servo motors.

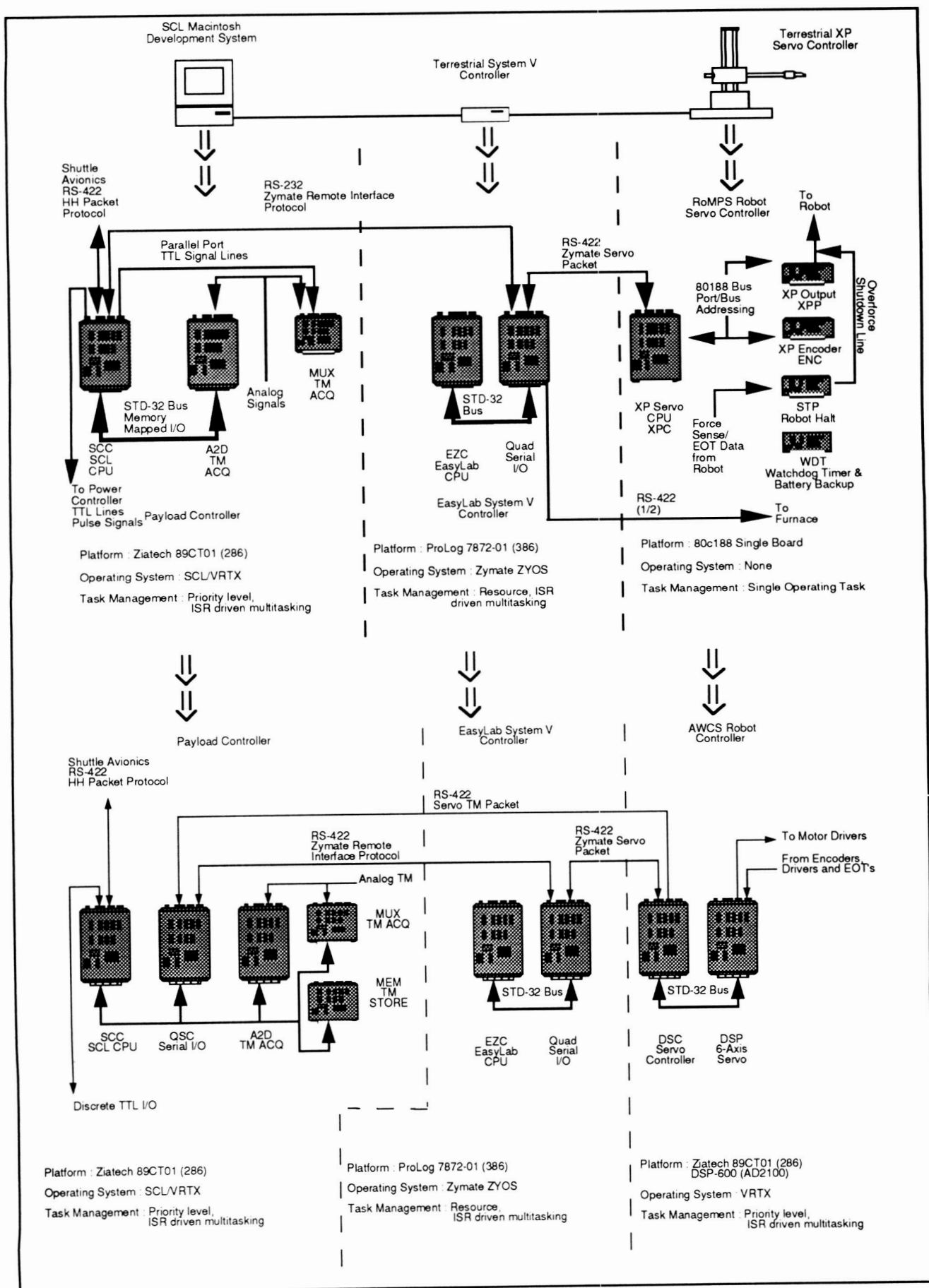


Figure 4. Migration of Terrestrial Architecture to a Space-Hardened Architecture

**Table 2. Technology Introduction Acceleration**

Computer Technology	Commercial Introduction	Space Mission Launch	Delay in Years
x186/188 also PC-XT	1983	1989	6
x286 also PC-AT	1984	1989 est	5
x386	1988	1993 est	5
x486	1989	1995 est	6
Pentium	1993	1996 est	3
PowerPC	1994	1996 est	2
R6000	1995	1996 est	1

### **Rapidly Increasing COTS Content**

In less than three years, we have gone from systems with no COTS content to systems with better than 60 percent COTS content (see Table 3). In 1992 we achieved 50 percent COTS contents; by 1996 we are planning systems with 80 percent COTS content. With each new customer and program, we continue to reduce the custom content of our systems while we improve performance.

**Table 3. COTS Content Increase**

	ARD 1992	ROMPS 1994	AWCS 1996	ROMPS-2 1997
Custom modules	4	4	2	2*
COTS modules	4	6	9	7
% COTS content	50 %	60 %	81%	78%

\*Both custom modules are reused designs.

### **THE FLIGHT SEGMENT ARCHITECTURE**

Figures 5 and 6 summarize the mapping of functional requirements onto the flight subsystems of the ECS and ECS-II systems. These figures also reveal the hierarchical levels of experiment control performed by the different subsystems. Moving from the SCL Experiment Supervisor on the far left to the Robot Servo Controller on the far right, the command interfaces become less abstract and more device-specific.

At the SCL Experiment Supervisor, the control of the experiment is at a very high abstraction level. This subsystem monitors the health and safety of the payload and halts the automation scripts if it detects an anomalous condition, such as temperature, of the motor drivers exceeding the safe operating limit.

During the ROMPS mission this subsystem executed the RTP processing scripts, which set sample processing parameters and initiated laboratory unit operations by sending commands to the Zymate System V Controller.

During the WSF-3/AWCS mission this subsystem will execute the Substrate Transfer scripts, which moves a specific wafer between its storage station, the rotator, a cooling station, and finally back to its storage station.

In both cases, the Zymate System V Controller executes the steps of the laboratory unit operations initiated by the SCL Experiment Supervisor. Device-specific commands are sent to the Robot Servo Controller to complete these laboratory unit operations.

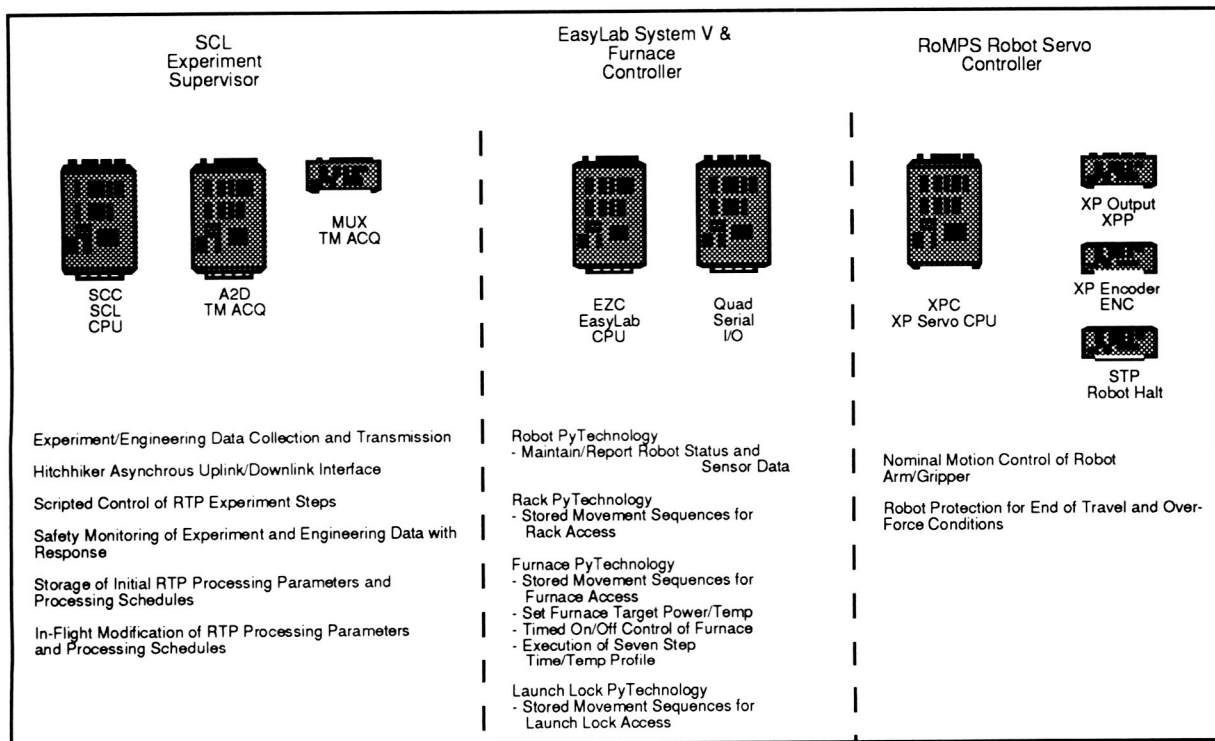


Figure 5 - Requirements Mapping of ROMPS Flight Subsystems

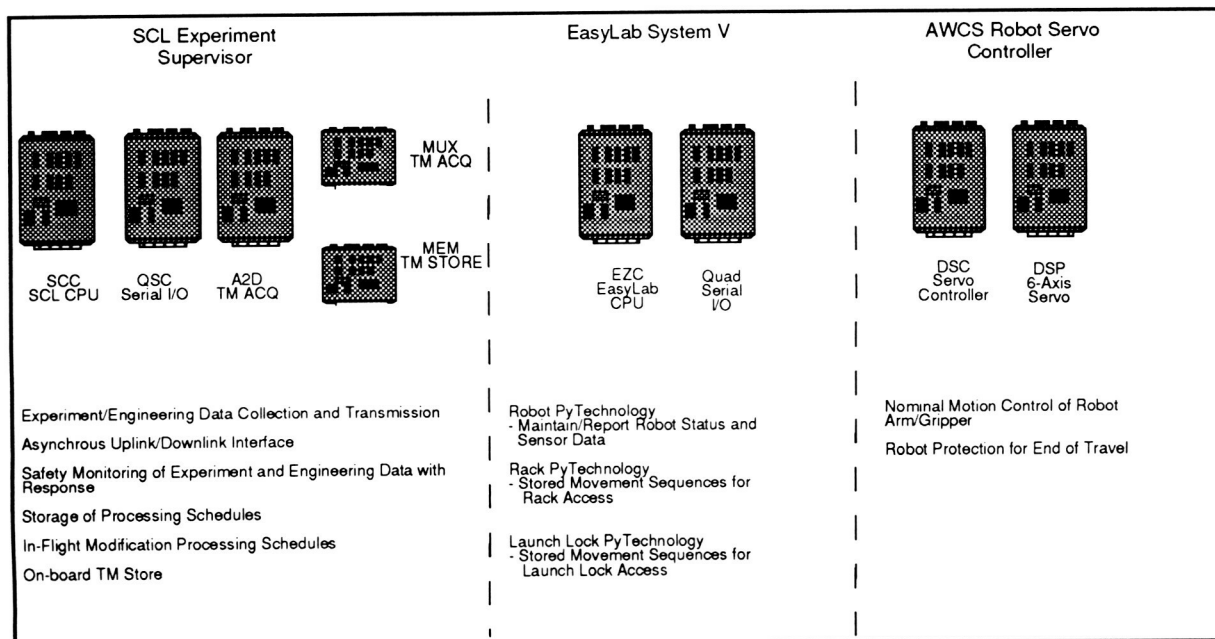
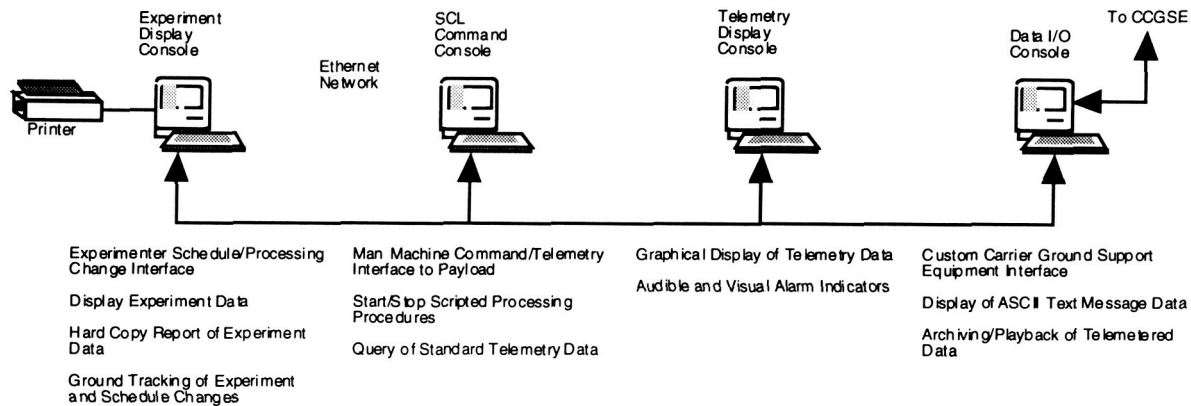


Figure 6 - Requirements Mapping of AWCS Flight Subsystems

Many of the disadvantages of a distributed architecture are eliminated in this system by the use of simple, robust, and well-tested communication protocols.

## THE GROUND SEGMENT ARCHITECTURE

The ground station architecture also makes use of a distributed architecture. Figure 7 summarizes the mapping of functional requirements onto the ground station subsystems of the Experiment Control System. Again, the hierarchical levels of command and control are shown. Decreasing levels of experiment control abstraction are shown as one proceeds from left to right across this figure.



**Figure 7. Requirement Mapping of Ground Station Subsystems**

At the far left, the Experiment Display Console allows the primary investigators to extract specific data from archived telemetry, allowing creation of reports. Additionally, the primary investigators use a set of spreadsheets to generate updated scripts to be executed against the on-board sample processing and schedule parameters. These updated scripts are then sent to the payload operator for preparation for upload to the payload.

The SCL Command Console is used by the payload operator to command the payload. Commands are processed by the SCL Command Console's compiler and transmitted to the Data I/O Console for upload to the payload. The SCL Command Console is also responsible for running ground side rules and scripts.

The Telemetry Display Console is a graphical display of the incoming telemetry. This graphical display is done using LabView®, see Figure 8 & Figure 9. The items being displayed are easily changed by opening another LabView Virtual Instrument® (VI). This allows an easy method to switch between engineering and science data displays. It is also possible to have more than one Telemetry Display Console.

At the Data Input/Output (I/O) Console, incoming telemetry from the payload is archived, and changed telemetry items are broadcast on the network for the other consoles. The Data I/O Console is also responsible for archiving incoming telemetry data, displaying text messages from the payload, and uploading the compiled command data sent from the attached SCL Command Console.

The Telemetry Display Console and the SCL Command Consoles receive updates for their local telemetry databases across the Ethernet network. These data are placed on the Ethernet network by the Data I/O Console.



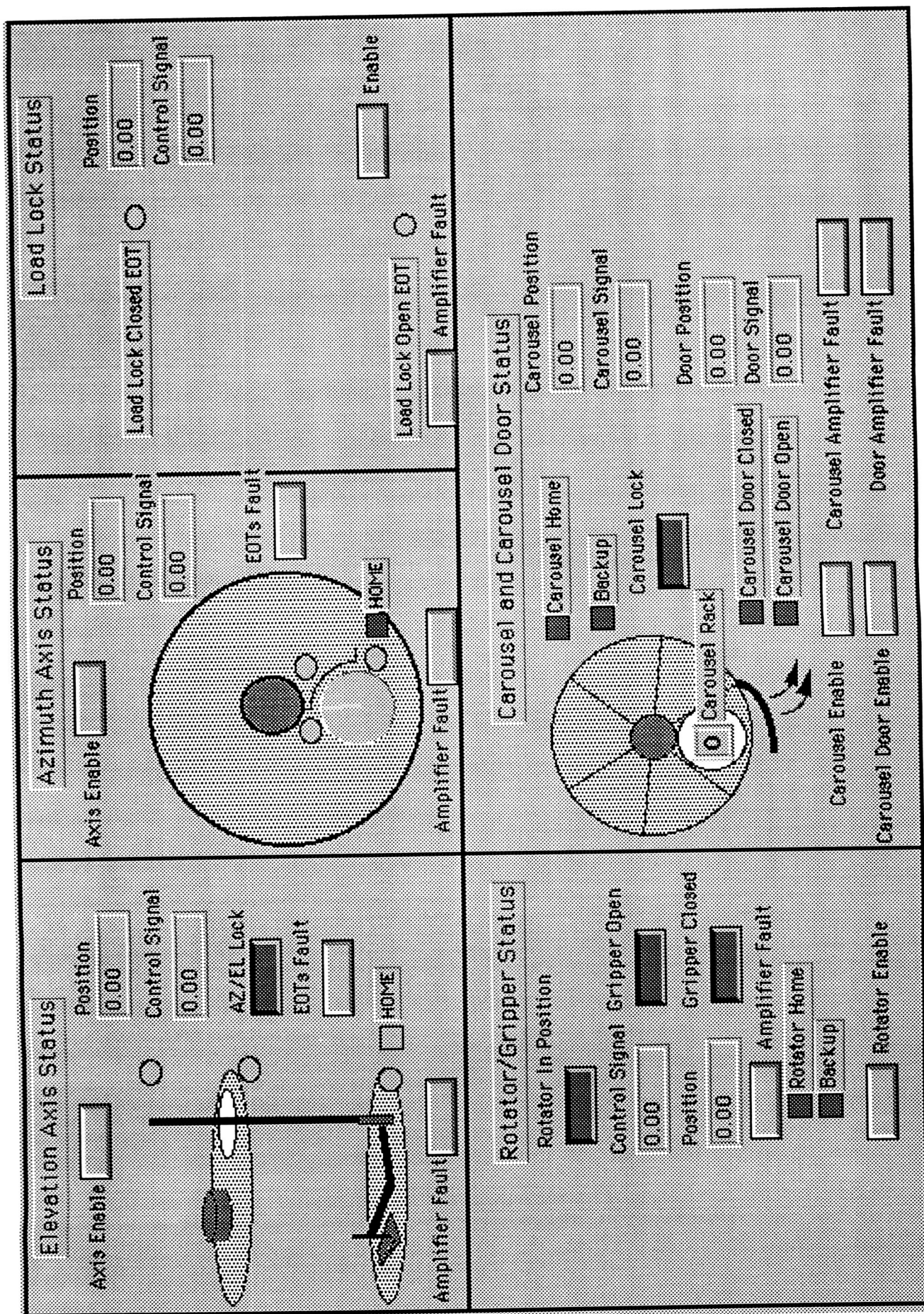


Figure 8 - Robot Telemetry LabView® Display



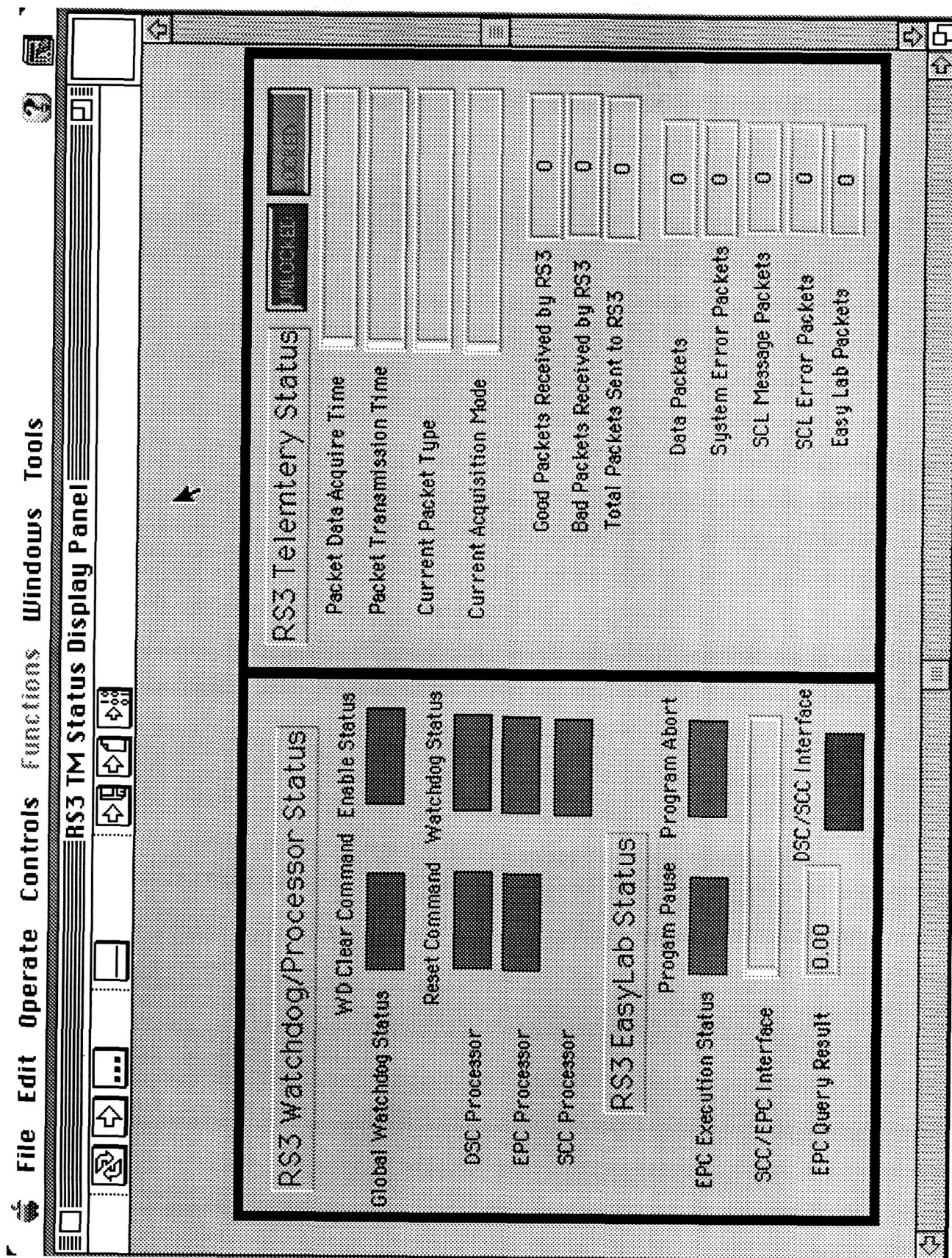


Figure 9 - Payload Processor Health LabView® Display

All of the application programs that make up the ground station use the standard Macintosh window/icon/pointer/mouse user interface paradigm. This allows users to concentrate on learning the functionality of the applications without worrying about the details of the human-machine interface.

### **MISSION OPERATIONS FOR MATERIAL PROCESSING PROCEDURES**

One of the driving philosophies of the ECS/ECS-II system architecture is to enable the PIs to interact with the payload in a meaningful way without the need of a payload operator to translate every command request into a set of payload directives. To meet this requirement, it was necessary to identify the operations the PIs would be interested in initiating and the telemetry data that would be of immediate value to them during mission operations. To accommodate this method of command and control, a set of on-board SCL mission scripts was implemented that would take as an input a list of samples to be processed. These scripts would then access a global table containing the processing parameters for all the samples aboard the payload.

To enable the PIs to interact with the payload, it was necessary to provide them with a data-entry mechanism for specifying a list of samples to be processed, and the processing parameters for these samples. It was decided that because this data was essentially tabular in nature, a spreadsheet could be used as the data input mechanism. Custom spreadsheet macros allow the user to generate lists of samples to be processed and to specify processing parameters. These macros create ASCII files to be compiled by SCL into scripts, which are uploaded and executed by the payload operator.

The ROMPS mission required that the PI's be able to specify up to seven time/temperature profiles for each sample. Additional, the PI's were able to specify which samples were to be processed during an operational period.

The upcoming WSF/AWCS missions contain very different requirements. The WSF3/AWCS mission is simpler than that of the ROMPS mission. During this mission SCL controls only the transfer of single substrates since all processing is controlled by the PI's on the ground. The PI's will indicate which substrate they want and the operator will execute the Substrate Transfer script using the substrate number as an argument.

It is expected that the WSF-4/AWCS mission requirements will be much more demanding. All factors of the MBE processing cycle will be controlled by the ECS-2. This includes substrate transfer, substrate heating, source cell heating, source cell shutter control and RHEED processing. SCL will be used for overall process control through the use of its script and rules. The RHEED processing will be done by a dedicated vision processing engine, which along with other sensors will provide SCL with the information needed to process the substrate. The PI's will again use a spreadsheet to enter the information regarding the process parameters.

### **POST-MISSION DATA ANALYSIS**

During the mission, data are archived by the DataIO application running on the data I/O console into playback files. These playback files archive the incoming telemetry packets and the outgoing command packets. The DataIO application can replay these play-back files and will drive all the attached processes as if the data were coming in real time. This allows the LabView application running on the Experiment Display Console to display archived data in order to review mission events. When playing back archive file, DataIO can preserve the relative time domain in which the telemetry occurred or at the maximum speed that the system is capable of performing.

In addition to the ability to drive attached telemetry display applications, the DataIO application can produce spreadsheet importable text files containing selected telemetry items. DataIO performs the necessary data translations so the telemetry items are presented in user units.

## **CONCLUSION**

The ECS for the ROMPS payload was completed in just 13 months with delivery of over 30,000 lines of source code, three space-hardened computer systems, and the electrical harnessing to connect them. The staffing of this project included two full-time software engineers, two software contractors, one full-time electrical engineer, one part-time mechanical engineer, one part-time assembly technician, and three co-op students. ROMPS flew on STS-64 where it successfully accomplished all of the primary and secondary objectives, well ahead of the mission schedule. The high level scripting and expert rule evaluation capability of the ECS was the key to achieving the early completion of all mission objectives.

AMPS has invested in the productization of the ECS and is offering the ECS-II system for sale as the first affordable off-the-shelf option for low cost missions. Ideal applications include the Hitchhiker and INSTEP programs.

AMPS-SR's ongoing challenge is to adapt the ECS-II to automate the MBE processing methods that will be performed by ground operators on WSF-3. This mission will extend the capabilities of the ECS with the addition of process control and process sensors. Keeping with the COTS philosophy, and modular architecture, this set of new capabilities will include pre-integrated add-on modules that perform real-time machine vision and indirect temperature sensing for the purpose of in-line process control.

All low earth orbit researchers can benefit from simple control of their experiments and faster turn-around of mission data.

## **REFERENCES**

1. L.J. Hansen and C.H. Pollock, *Space Mission Analysis and Design*, 2nd edition, Kluwer Academic Publishers, Boston, Chapter 16, p. 609, 1992.
2. L.J. Hansen and C.H. Pollock, *Space Mission Analysis and Design*, 2nd edition, Kluwer Academic Publishers, Boston, Chapter 16, p. 616, 1992.
3. R. Wong, *Space Mission Analysis and Design*, 2nd edition, Kluwer Academic Publishers, Boston, Chapter 20, p. 666, 1992.
4. L.D. Negron, Jr. and A. Chomas, *Space Mission Analysis and Design*, 2nd edition, Kluwer Academic Publishers, Boston, Chapter 14, p. 556, 1992.

## **ACKNOWLEDGMENTS**

AMPS would like to acknowledge the NASA Goddard Space Flight Center personnel who funded the ECS effort under NAGW-1198, NAG5-1517, and NAS5-32471. We deeply appreciated this research and development opportunity, and their willingness and support throughout this unorthodox and challenging effort. Similarly, this program could not have been accomplished without the tireless technical and financial support of the two commercial product vendors—the team at Interface and Control Systems for accomplishing many modifications and improvements to SCL, and the Zymark Corporation for their support in modifying the EasyLab and the XP servo software. Our thanks to the many unnamed individuals who contributed invaluable effort and advice when it was most needed.

### **TRADEMARK NOTICES**

Spacecraft Command Language is a registered trademark of Interface and Control Systems Inc. Zymate, Zymark, EasyLab, PyTechnology, and System V are registered trademarks of Zymark Corporation.

Apple, AppleTalk, and Macintosh are registered trademarks of Apple Corporation.

STD 32 is a registered trademark of Ziatech Corporation.

All other products mentioned are trademarks of their respective companies.

# **IJEMS**

## **Iowa Joint Experiment in Microgravity Solidification**

John R. Bendle and Steven J. Mashl, Ph.D.  
Iowa State University, Ames, Iowa

Richard A. Hardin, Ph.D.  
University of Iowa, Iowa City, Iowa

### **ABSTRACT**

The Iowa Joint Experiment in Microgravity Solidification (IJEMS) is a cooperative effort between Iowa State University and the University of Iowa to study the formation of metal-matrix composites in a microgravity environment. Of particular interest is the interaction between the solid/liquid interface and the particles in suspension. The experiment is scheduled to fly on STS-69, Space Shuttle Endeavor on August 3, 1995. This project is unique in its heavy student participation and cooperation between the universities involved.

### **INTRODUCTION**

The Iowa Satellite Project was formed at Iowa State University in 1991 with the single objective of designing and building a micro satellite, ISAT-1, to benefit the state of Iowa. ISAT-1 was designed and an engineering mock-up was built. The project was then put on hold until sufficient funding could be found to begin the construction phase. Then in October of 1994, the opportunity to fly an experiment presented itself. The experiment would be flown in a Smart Can with the Wake Shield Facility II under the Space Vacuum Epitaxy Center (SVEC) at the University of Houston. The necessary funds were available and the decision was made to modify the solidification experiment designed for ISAT-1 for flight in a Smart Can.

The final definition of the science objectives came in December of 1994. Because solidification is such an important part of the processing of composite metal parts it was selected as the focus of the experiment. The previous studies in this specific area are very limited and a great deal can be gained from the study of the solidification phase of metal matrix formation.

IJEMS is scheduled to run on Space Shuttle Endeavor, STS-69 on August 3, 1994. The experiment, consisting of four individual ingots of tin cadmium alloy with nickel particulate, will run over a 850 minute time span. The data and the ingots will be analyzed after the flight. Ground tests will also be performed after the flight to duplicate the conditions during flight. The two will then be compared to reveal what effect the absence of gravity has on the solidification process.

### **MANAGEMENT APPROACH**

From the beginning, one of the goals of the IJEMS project was to promote student involvement. This provided the students with the hands on experience that the classroom lacks while keeping project costs low with the increased participation. The IJEMS team consisted of 2 postdoctorates, 3 graduate students and 15 undergraduate students. The academic backgrounds included aerospace engineering, computer engineering, electrical engineering, mechanical engineering and metallurgical engineering.

One of the most difficult and most beneficial aspects of the project was the multiple university involvement. The majority of the of the systems work was done at Iowa State University (ISU) while the science was done at both the University of Iowa and ISU. Constant communication and frequent meetings were essential to the successful completion of the project. Ultimately, the most encouraging aspect of the cooperative effort was the ability to utilize the strongest attributes of the two universities thereby increasing the teams overall abilities.

## IJEMS SCIENTIFIC GOALS

Solidification is an important part of the processing scheme for many materials, and for cast parts, the solidification process can represent the final stage in which the structure and therefore the mechanical properties of a part are determined. As most materials contain particulates, either unintentionally in the form of inclusions, or intentionally as in the case of particle reinforced composites, the interaction between the moving solid-liquid interface and particulates suspended within the liquid is of particular significance. In the processing of metal-matrix composite (MMC) materials a uniform distribution of the reinforcing particles properly incorporated within the metal is critical to the mechanical soundness of the final product. Understanding the interaction of the particles with the solidification front is critical to the production of high quality MMC materials. An interested reader will find that the review by Lloyd (ref. 1) gives an overview of the state of MMC process technology using Al and Mg (aluminum and magnesium) alloys.

The scientific objective of the Iowa Joint Experiment in Microgravity Solidification (IJEMS) is to provide experimental data on the interactions between the solid/liquid (S/L) interface and suspended particulates during the directional solidification (DS) of Sn-Cd alloys under microgravity conditions. These microgravity (or space-based) experiments will then be compared with ground-based experiments. It is envisioned that these experiments will provide data for particle S/L interface interaction models (both for comparison with existing models, and perhaps development of new ones), insight into the effect of convection and buoyancy forces on the particle interface interaction, and should provide data for verification for numerical models of the process currently being developed at the University of Iowa.

A primary goal of this study will be to quantitatively evaluate the phenomena of particle pushing and entrapment. Depending on the conditions of the solidification process, a particle may be pushed or engulfed by the advancing S/L interface. When engulfment occurs, the particle is incorporated directly into the solid. If particles are pushed (as is often the case in multidirectional solidification), they will segregate into the last liquid to freeze. If this occurs, the locally high concentration of small particles behaves as a single large defect which can serve as a site for crack nucleation, potentially leading to failure.

Multiple, dissenting theories exist on the causes for pushing/entrapment behavior. A review of eight of these theoretical models is given by Asthana and Tewari (ref. 2), and compilations of papers on the field can be found in references 3 and 4. It is hoped that the data gathered through this research will provide insight into the pushing/entrapment phenomena, and clarify the accuracy of these existing theories.

### Basics of the Theory for Particle S/L Interface Interaction

Central to the theoretical models of particle S/L interface models is the concept of a critical velocity  $V_c$  which is the velocity at which the transition from pushing to entrapment occurs. Of particular interest in this work, will be the variation in  $V_c$  which may occur as the experimental conditions are varied. Additionally, any preferential location of the particles within the individual phases present will be worthy of note. Also, the experimental evidence suggests several modes of particle-front interaction (ref. 2) such as no entrapment at all, entrapment only after a period of pushing, and instant engulfment. Past experimental evidence shows that higher solidification front velocities are necessary to capture finer particles. Also, evidence to date suggests that  $V_c$  is dependent not only on the physical properties of the liquid melt, but also on the geometric and physical properties of the particle. The interested reader is directed to ref. 2 for the details. A summarized list of specific factors which have been proposed and shown to effect pushing/entrapment behavior is given below:

- solid-liquid, solid-particle and particle-liquid interfacial surface energies
- the solid/liquid interface velocity, the value of  $V_c$
- buoyancy forces acting upon the particle
- thermal conductivity of the particle and the liquid
- convective flow within the liquid
- particle size
- temperature gradient at the interface

## · interface morphology

Two of these factors, buoyancy effects and convective flow will be eliminated or at least greatly reduced in the microgravity environment aboard the space shuttle. The minimization of these factors should allow a more accurate determination of the role of the remaining parameters in particle S/L interface interactions. Ultimately, the results of the space based experiments will be compared to identical ground based experiments in order to quantify the effects of microgravity. Generally, a clear transition between pushing and engulfment is blurred somewhat by these many influences on the process, making this a research area where additional work can make technological improvements possible if these many effects can be properly accounted for and predicted.

In the IJEMS experiments, four ingots will be melted and directionally solidified. There will be two rates of solidification used by varying thermal boundary conditions, and the ingots will be (two each) of a eutectic and off-eutectic composition. Two samples of each composition will undergo a given rate of solidification to give the four experimental runs to be made by the IJEMS payload. By varying both alloy composition and thermal boundary conditions, the particle interaction with different interface morphologies can be explored. Another possible variation not explored in the current IJEMS experiment is to examine the effect of interfacial energy through varying the type of particles used. Only Ni particles were used in the IJEMS tests. In the IJEMS a combination of a range of particle sizes, along with the variation in interface velocity which will occur as the fraction of metal solidified increases, and should provide data on pushing versus entrapment over a range of conditions.

### Experimental Apparatus and Procedures

The space-based portion of this work will be performed within a canister aboard the space shuttle in which four directional solidification modules will be mounted. Each module holds a cylindrical crucible containing an ingot of Tin-Cadmium (Sn-Cd) alloy + particles as shown in Figure 1. Foil heaters (MINCO model HK5450) act to both melt the ingot and control the thermal conditions during solidification. As noted from Figure 1, there is a heater in the base used to both melt and control solidification. Also note the large "Melt Heater" wrapped about the bulk of the crucible; it is employed only in the melt cycle of the testing. Finally there is a narrow foil heater wrapped around the crucible opposite the base heater which is used to control the rate of solidification along the length of the sample and also to melt it.

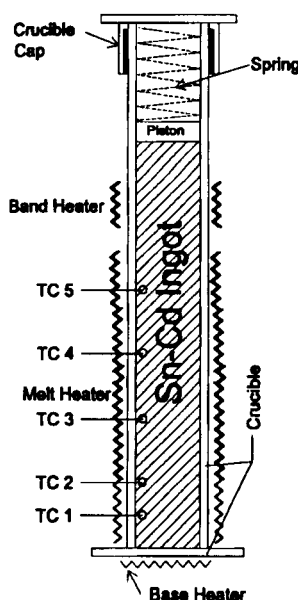


Figure 1 Schematic of the IJEMS experiment crucible



Thermocouples are placed on the "Base" and "Band" heaters to directly monitor and control them using on-off control, and the large "Melt Heater" is controlled using a thermocouple (TC 4) in the ingot. Five sheathed thermocouples (TC 1 through 5) are inserted through the crucible to approximately 1 to 2 mm into the sample, and sealed and fastened there using Omega high temperature epoxy. TC 1 through 5 serve to monitor conditions during solidification, and to track the position of the S/L interface over time. These thermocouples make up the primary experimental data recorded by the on-board computer, and can be used (following some corrections for heat loss) to determine the speed of the S/L interface. Following solidification on one of the samples, the heaters are turned off but temperature data is taken as the crucible cools. This "cool down" data will provide additional data for the heat loss corrections. During solidification, the thermal conditions in all modules are maintained so that solidification occurs directionally along the axis of the crucible as shown in Figure 2.

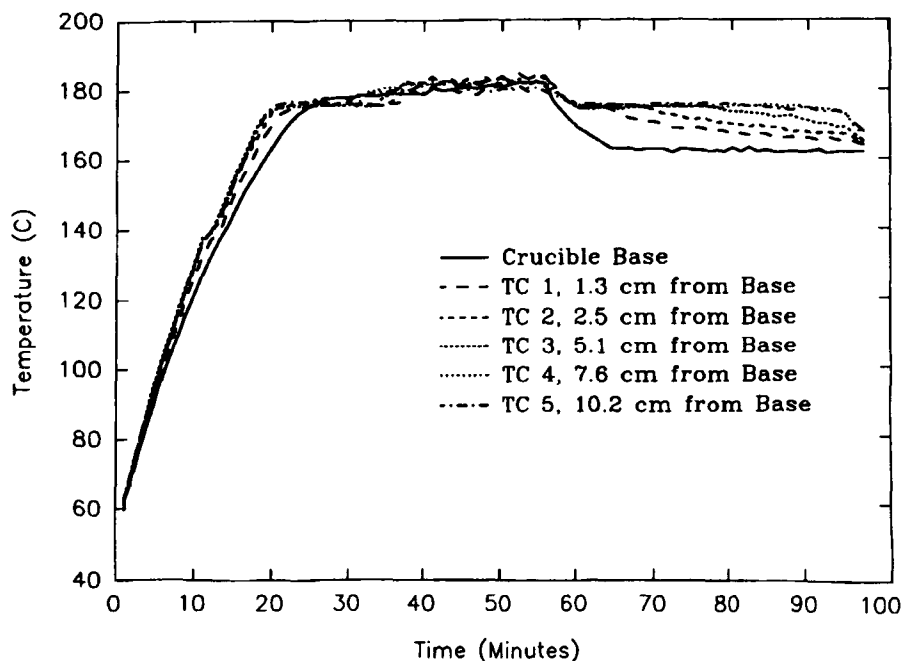


Figure 2 Temperature versus time for a mock-up test of the IJEMS experiment (refer to Figure 1 for positions of thermocouples, TCs)

Alloys of Sn and Cd were chosen for these tests because of their relatively low melting temperature (eutectic liquidus temperature  $T_L$  of 176 C, and the off-eutectic  $T_L$  used was 179 C). One reason for this is that the heaters used have a maximum temperature rating of 200 C, and other considerations were limitations on power, number of tests desired, and time constraints for the total duration of the experiment during the mission. Two of the ingots will be of the eutectic composition (67 wt.% Sn - 33 wt.% Cd) containing Nickel particles (from 1  $\mu$ m to 100  $\mu$ m in size). The thermal conditions are controlled in order to cause the solidification front to be planar in nature, characterized by alternating Cd and  $\beta$ -phase lamellae oriented normal to the growth front. The two remaining modules hold ingots having a slightly tin-rich, off-eutectic composition (70 wt.% Sn- 30 wt.% Cd) which also contain Nickel particles. Solidification of these ingots will be characterized by the growth of proeutectic  $\beta$  dendrites the remaining interdendritic liquid freezing to form eutectic.

Referring to Figure 1, the crucibles (made of 304 stainless steel tubes) were assembled under a vacuum with an undersized ingot being slid into the crucible with care taken not to damage the protruding thermocouples. The spring loaded piston was then assembled and the screw cap fastened down. Assembly under a vacuum eliminated air from being trapped inside the crucible (this may have led to Marangoni convection), and the spring loaded piston was carefully designed to accommodate the change in shape of the sample during melting or the metal floating about.

Given in Figure 2 is representative data for the IJEMS experiment for a laboratory mock-up with a eutectic sample. The two stages (melt and solidify) of the experiment are shown in Figure 2. First the melt stage (from 0 to 55 minutes) consists of a heat up period (0 to 20 minutes), the melting period (20 to about 35 minutes), and the hold period (shown here from 35 to 55 minutes to allow the sample to reach a superheated temperature  $\approx 183$  C that is adequately uniform prior to solidification). The second major stage is the solidification stage which is shown in Figure 2 from 55 to 95 minutes. Note that from 55 to 65 minutes the base heater is off as its set point is switched to 161 C, and the base heater kicks in again as its temperature hits 161 C. An improved control system would have eliminated oscillations in the base heater temperature. Fortunately, the observable effects of this were damped out to below the random variations and accuracy of the measurement system used. By setting the on-off band of the control system to a very small number some of this can be alleviated through rapid on-off cycling of the heaters.

Note that in the test case presented in Figure 2, TC 1, TC 2, and TC 3 break away from the eutectic temperature (indicating the passing of the S/L front) in a clearly directional fashion. Also, in this case, note that TC 4 and 5 drop below the eutectic temperature together which means the far end of the ingot is solidifying in an omnidirectional manner. This difficulty was overcome by using the "Band Heater" shown in Figure 1, and picking its set point carefully. In doing so, the rate of solidification and its directionality can be controlled better. As mentioned previously, there will be two rates of solidification used in the IJEMS; a relatively fast rate and a fairly slow one. The set points (temperatures) and duration times for the stages for the IJEMS experiments are given below:

Stage and Duration	Melt Heater	Base Heater	Band Heater
Melt (all tests), 70 min	183 C	183 C	183 C
Solidify (fast), 65 min	Off	163 C	177 C
Solidify (slow), 200 min	Off	167 C	192 C

These stages will then be duplicated in the matching ground-based experiments to acquire comparative data.

### Smart Can INTERFACE

The Smart Can that IJEMS is flown in is modeled after the Get Away Special Can but has a few additional features. The aluminum can has an inside diameter of 20.0 inches and an inside height of 31.25 inches resulting in a 5.68 cubic foot internal volume. It will hold a maximum payload mass of 200 pounds. The can has a power feed capable of supplying a constant 20 amps at 28 volts to the experiment contained within. The can is rated to supply nominal power of 400 watts with a 1,400 watt maximum. It is also capable of supplying command and real-time telemetry via the Shuttle downlink. The can is fixed to the cross bay carrier that supports the Wake Shield Facility II.

IJEMS takes advantage of the power feed, making an internal power source unnecessary. The real-time data line is not used but the associated connector in the can lid is used for ground testing. The IJEMS structure is bolted to the top of the can with 24 bolts while the other end is supported in the can by 3 rubber bumpers. The environment in the can is a half an atmosphere of dry nitrogen.

### IJEMS SYSTEMS

The systems portion of the project can be broken up into three major parts; structure, power and command and data handling. The systems had to be designed around the Smart Can and its environment while still making the science objectives possible.

#### Structure

The structure went through numerous iterations before the final design was reached. The factors under consideration were packing configuration, weight, and strength. The experiment had to fit in a manner that kept

the ingot heating elements away from the more sensitive electronics such as the computer. This also meant minimizing the conductive paths between the heaters and the electronics. The weight of the structure was not minimized but it was a contributing design factor to ensure that the maximum payload mass was not exceeded. The structure also had to be designed to withstand a 17g load factor, a 3 axis, 1 minute per axis, 9g rms random vibration test and a 2000 Hz swept sine vibration test. Once the design was finalized, its behavior was modeled using the ANSYS finite element program. The model showed a more than adequate ability to withstand the 17g load factor and the vibration test.

Next, the hardware phase began. All of the major components of the structure are made of 6061 aluminum, chosen for its light weight and high strength. The structure is made of two end plates. The top plate is 1/4 inch thick and has the 24 mounting holes milled in it. The bottom plate is 1/8 inch thick and has 3 rubber bumpers fixed to it. The top and bottom plate are connected by a plus shaped divider made of two intersecting plates, also 1/8 inch thick (figure 3). One of the dividers has a hole in it for the electronics box to pass through. All of these parts are connected to one another by 1 inch angle aluminum. Originally the angles were to be fastened using rivets but a miscalculation occurred and the holes were milled 1/16 of an inch larger than they should have been. There were no rivets the right size to fit the new holes. This led to the use of bolts with locking nuts at the fasteners. This increased the already conservative factor of safety.

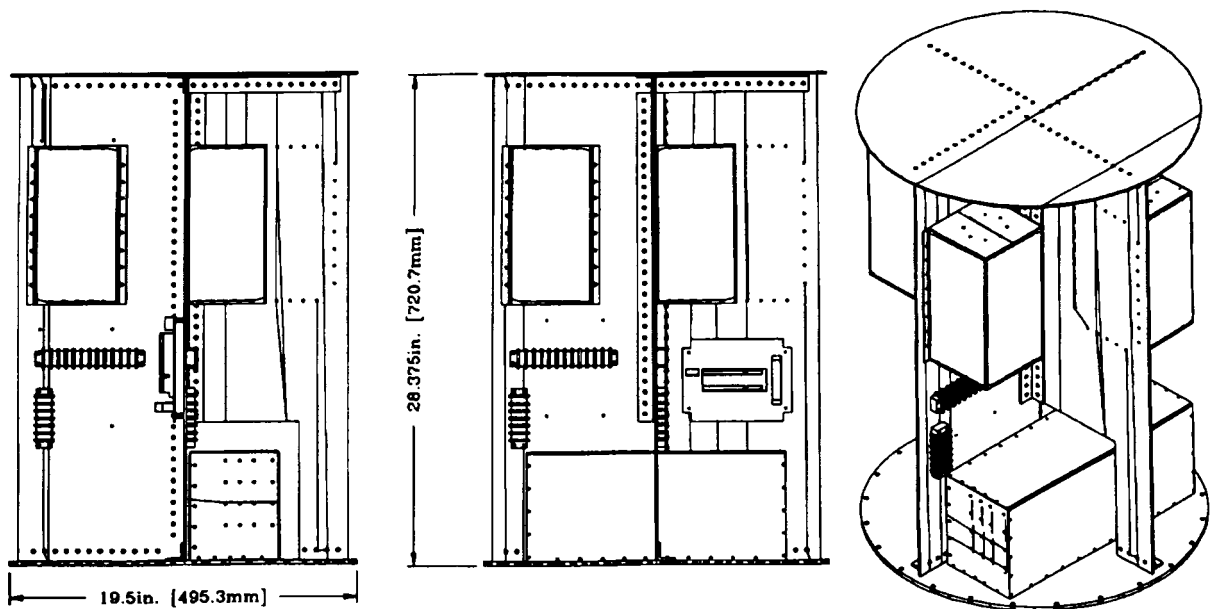


Figure 3 AutoCad Generated Assembly of IJEMS

Once completed, the structure underwent numerous tests to prove its integrity. The bare structure was first fitted with accelerometers and then spot tested with an impact hammer. The results yielded resonant frequencies almost exactly the same as those predicted in the finite element model. Next the fully loaded structure was tested on a shake table in all 3 axes for 1 minute per axis at 9g rms. The structure survived the test with only a minor complication. A few of the bolts that hold the experiment to the structure shook loose because no lock-tite had been applied. The structure fared well in the swept sine vibration test. Finally, once integrated into the Smart Can another set of vibration tests was run to determine if the characteristics of the combined modes would be problematic. A 3 axis, 30 second per axis, 7g rms vibration test was run along with a swept sine vibration test. Again the only problem was that 10 screws that fasten the experiment to the structure shook free during the vibration test because no lock tite was applied. Lock tite was applied after the test so the problem should not reoccur.

## Power

The power supplied to the can from the cross bay carrier is in the form of four separately fused lines, each

at 5 amps and 28 volts. A custom power distribution was designed and built. Two of the lines pass through emi filters before the power distribution board and the other two and go directly to the board. On the board each line has triple redundant 120 C thermal fuses. The filtered lines then combine go into a DC to DC converter which outputs +5 and +/-12 volts to supply power to the electronics. The unfiltered lines combine and lead into a solid state relay backplane which supplies power to the heaters at 28 volts. that melt the ingots.

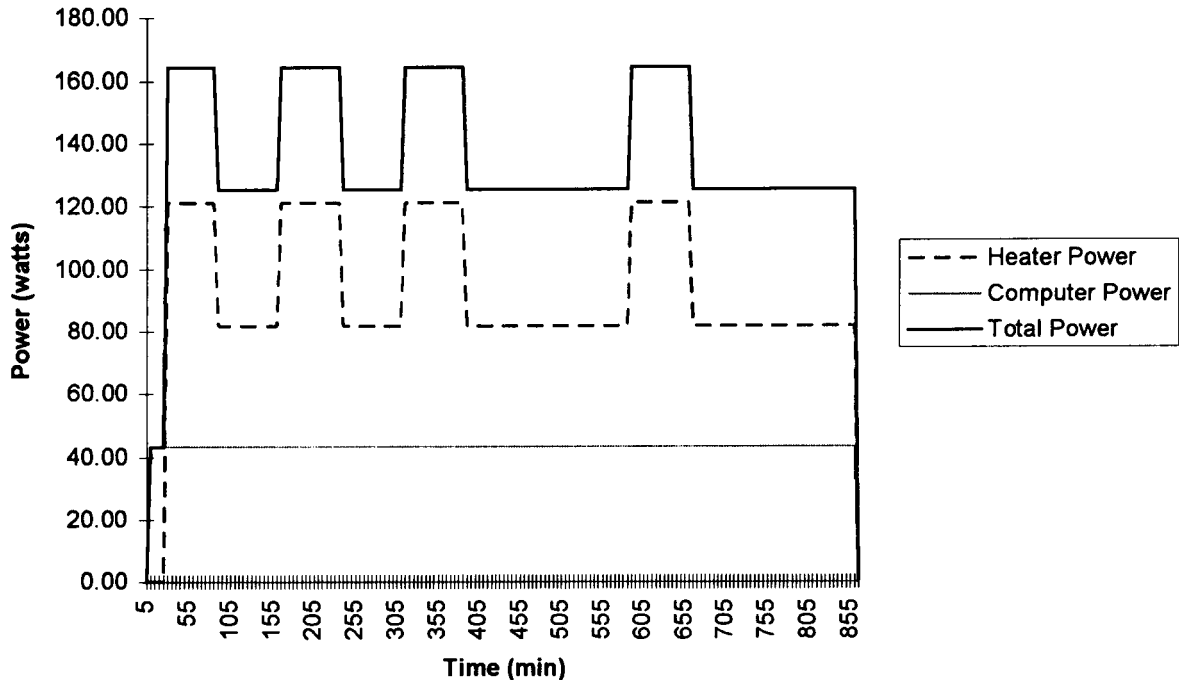


Figure 4 IJEMS Power Budget

Because IJEMS uses an external power source it was necessary to carefully budget the amount of power it consumed throughout the experiment. The power draw not only affects the experiment but also the Wake Shield Facility II because the power is drawn from the Wake Shield buss. It was therefore necessary to carefully schedule the operation of the experiment components and come up with a time dependent power budget (figure 4). The most critical concern was the operation of the heaters because they draw far more power than the electronics. The electronics draw 44 watts of power while the heaters draw as much as 122 watts of power. With a maximum combined power draw of 166 watts, the experiment draws far less power than the cross bay carrier is capable of supplying. The total power drawn over the 850 minutes is 1,941 watts.

### Command and Data Handling

The command and data handling (CDH) system was the most complex of all the systems. The CDH system is comprised of a computer, a digital I/O board, two A/D boards, a four slot backplane, a solid state relay backplane and two screw terminals. The computer is a 486SLC single board with 2 MB of ram and 3 MB of onboard flash RAM. The digital I/O board is a 24 channel TTL compatible board. The A/D boards are 16 channel, 15 bit boards with built in cold junction compensators. The solid state relay backplane is a buffered 24 position backplane. The screw terminals are standard 16 position terminals.

The system was designed to be completely autonomous. When the power is turned on the computer boots up. The first action the computer does is a system test. The computer checks for open thermocouples and makes a record of any openings. Then the computer performs a controlled melt of each cell as described earlier, storing the critical thermocouple data in the flash drive. Once the four cells have melted and solidified the computer shuts itself down. In the event of a power interrupt or shut down at some point during the experiment the computer resets to its initial state. If power is reapplied, the system will run as before, thus remelting any ingots that have already

been melted. There for it becomes necessary to determine whether it is beneficial to reapply power or not. This is a time based decision so it is required that someone be present to make that decision during the entire time that the experiment is running.

The CDH system encountered a problem. All of the data from the experiment is stored in the 3Mb flash memory drive. The 3Mb was a sufficient amount of storage for the for experiment data so capacity was not thought to be a problem. Unfortunately, the single board computer had a bios chip that could not effectively use the 3Mb. Instead, the computer could only store 0.9Mb in the flash drive. If any more than 0.9Mb was stored in the flash drive it locks up and the information cannot be retrieved. The computer manufacturer was able to provide a new bios chip but not until 1 week after the experiment was delivered to Houston for integration. Therefore, thermocouple sampling rates had to be reduced to compensate for the reduced storage capacity.

## **PREFLIGHT HEALTH TEST**

It is essential to have the ability to check the health of the system after it is installed into the Smart Can so that any problems can be revealed and remedied. A test apparatus was made so that anyone can check the health of the experiment, even if they know nothing about the experiment. All that is needed is a voltmeter and the single page of instructions. The test box interfaces with the experiment via the Bendix connector in the top of the can that was intended to be used for the real-time data link. The box has 6 electrical contacts and 3 LEDs.

The test box is important for three reasons. First, it allows for the testing of the power system. The 6 electrical contacts are +5 volts, -12 volts, +12 volts, +28 volts and two grounds. As long as each contact measures the voltage it is marked, the power system is healthy. Secondly, the LEDs indicate any open thermocouples. The number of times that the lights flash corresponds to a specific thermocouple that is not functioning. Finally, the LEDs also indicate when the test period is nearing the end. The experiment will begin to run once it has been on for 20 minutes. If the experiment began to run will still on Earth it could ruin the results. Therefore, after the payload has been on for fifteen minutes, the LEDs flash indicating that shutdown must occur within the next five minutes. The experiment can be turned on and off without concern as long as the 20 minute time limit is not exceeded.

## **CONCLUSION**

The Iowa Joint Experiment in Microgravity solidification has thus far been a successful venture. The few minor problems that occurred seem insignificant when compared to the rest of the project. The entire endeavor took less than 6 months from its October 1994 inception to the delivery of hardware on March 25, 1995. The final configuration weight at delivery was 83 pound. The photographs below (figure 5) show the experiment in its final configuration.

Still in store for project is a successful flight and subsequent data retrieval. The ground base tests also have to be performed after the data is retrieved. Only after the data has been analyzed and the ingots have been examined can the project be deemed a complete success.

## **ACKNOWLEDGMENTS**

It is with gratitude that the authors acknowledge the direction and guidance of Professor Christoph Beckermann of the University of Iowa and Professor Rohit Trivedi of Iowa State University. Without their leadership this project could not have been so expeditiously executed. The authors would like to acknowledge the Iowa Space Grant Consortium for their strong financial support. Also, this project would not have been possible without the financial support of the Institute for Physical Research and Technology at Iowa State University. Additional thanks goes to the Engineering Research Institute at Iowa State University for their expert help in milling and other metal work. Thank you to Toronto MicroElectronics for their donation of the computers and the accompanying technical support. A final and most sincere thank you goes to Space Industries, Inc. without whose help this project would not have been possible.

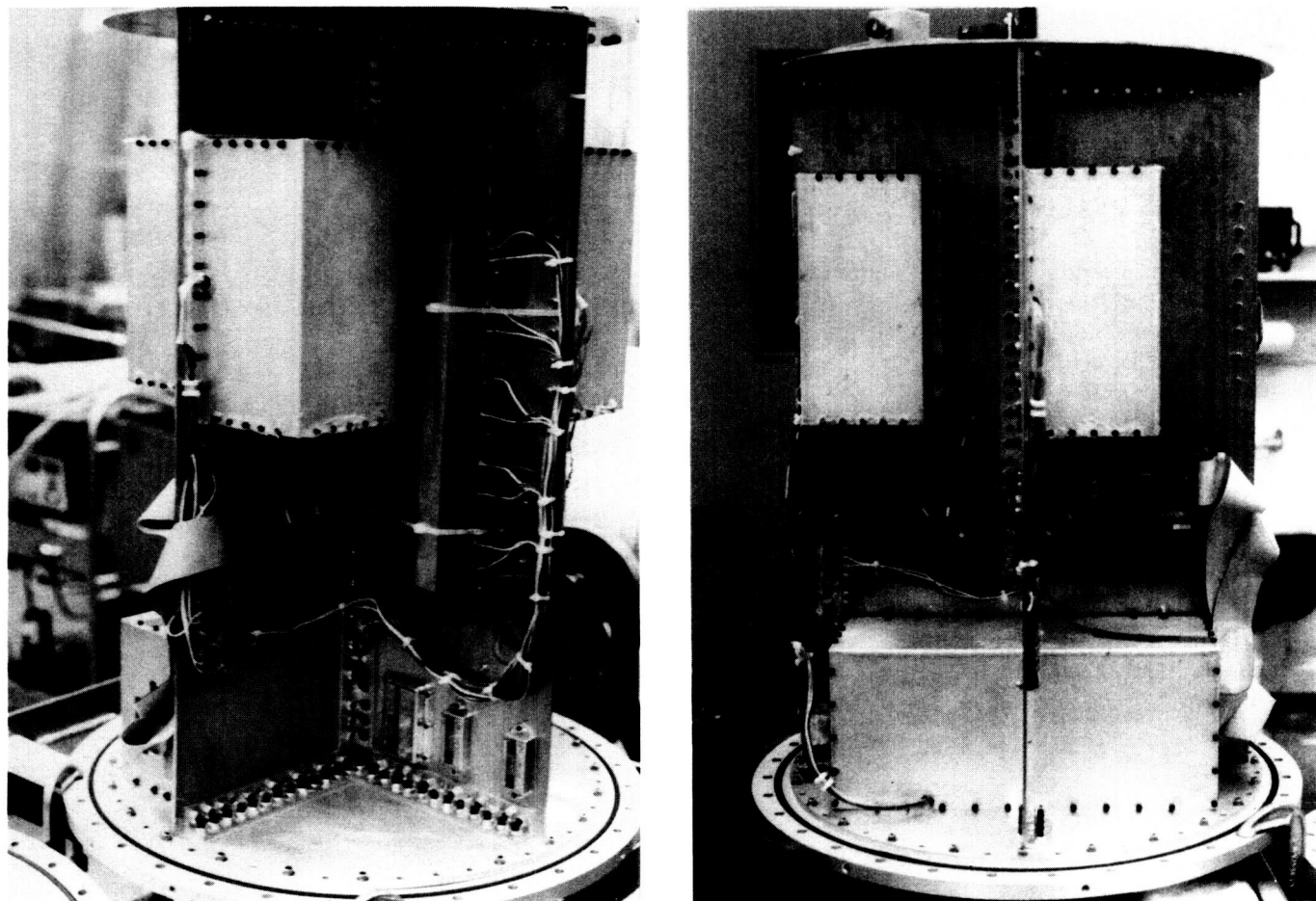


Figure 5 Photographs of IJEMS in Final Configuration

#### REFERENCES

1. Lloyd, D. J., "Particle reinforced aluminum and magnesium matrix composites," *International Materials Reviews*, Vol. 39, No.1, 1994, pp. 1-23.
2. Asthana, R., and Tewari, S. N., "Second phase particle-solidification front interactions: an evaluation of theoretical models," *Processing of Advance Materials*, Vol. 3, 1993, pp. 163-180.
3. *Solidification of Metal Matrix Composites*, edited by Pradeep Rohatgi, TMS, 1990.
4. *Processing of Semi-Solid Alloys and Composites*, Proceedings of the Second International Conference, edited by S.B. Brown and M.C. Flemings, TMS, 1993.

**REPORT DOCUMENTATION PAGE**Form Approved  
OMB No. 0704-0188

Public reporting burden for this collection of information is estimated to average 1 hour per response, including the time for reviewing instructions, searching existing data sources, gathering and maintaining the data needed, and completing and reviewing the collection of information. Send comments regarding this burden estimate or any other aspect of this collection of information, including suggestions for reducing this burden, to Washington Headquarters Services, Directorate for Information Operations and Reports, 1215 Jefferson Davis Highway, Suite 1204, Arlington, VA 22202-4302, and to the Office of Management and Budget, Paperwork Reduction Project (0704-0188), Washington, DC 20503.

<b>1. AGENCY USE ONLY (Leave blank)</b>		<b>2. REPORT DATE</b> September 1995	<b>3. REPORT TYPE AND DATES COVERED</b> Conference Publication	
<b>4. TITLE AND SUBTITLE</b>  1995 Shuttle Small Payloads Symposium			<b>5. FUNDING NUMBERS</b>  Code 740	
<b>6. AUTHOR(S)</b>  Frann Goldsmith and Frances L. Mosier, Editors				
<b>7. PERFORMING ORGANIZATION NAME(S) AND ADDRESS(ES)</b>  Goddard Space Flight Center Greenbelt, Maryland 20771			<b>8. PERFORMING ORGANIZATION REPORT NUMBER</b>  95B00118	
<b>9. SPONSORING/MONITORING AGENCY NAME(S) AND ADDRESS(ES)</b>  NASA Aeronautics and Space Administration Washington, D.C. 20546-0001			<b>10. SPONSORING/MONITORING AGENCY REPORT NUMBER</b>  NASA CP-3310	
<b>11. SUPPLEMENTARY NOTES</b>  Frances L. Mosier: Interstel, Inc., Beltsville, Maryland 20705				
<b>12a. DISTRIBUTION/AVAILABILITY STATEMENT</b>  Unclassified-Unlimited Subject Category: 12 Report is available from the Center for Aerospace Information (CASI), 800 Elkridge Landing Road, Linthicum Heights, MD 21090; (301) 621-0390.			<b>12b. DISTRIBUTION CODE</b>	
<b>13. ABSTRACT (Maximum 200 words)</b>  The 1995 Shuttle Small Payloads Symposium is a combined symposia of the Get Away Special (GAS) and Hitchhiker programs, and is proposed to continue as an annual conference. The focus of this conference is to educate potential Space Shuttle Payload Bay users as to the types of carrier systems provided and for current users to share experiment concepts.				
<b>14. SUBJECT TERMS</b>  Space Shuttle Small Payloads, Carrier Systems and Experiments—Past, Present, and Future			<b>15. NUMBER OF PAGES</b>  330	
			<b>16. PRICE CODE</b>	
<b>17. SECURITY CLASSIFICATION OF REPORT</b>  Unclassified	<b>18. SECURITY CLASSIFICATION OF THIS PAGE</b>  Unclassified	<b>19. SECURITY CLASSIFICATION OF ABSTRACT</b>  Unclassified	<b>20. LIMITATION OF ABSTRACT</b>  Unlimited	